GLOBAL FRONTIERS IN HEART VALVE INTERVENTIONS

EDITED BY: Peter Zilla, Vinod H. Thourani and Tsuyoshi Kaneko
PUBLISHED IN: Frontiers in Cardiovascular Medicine

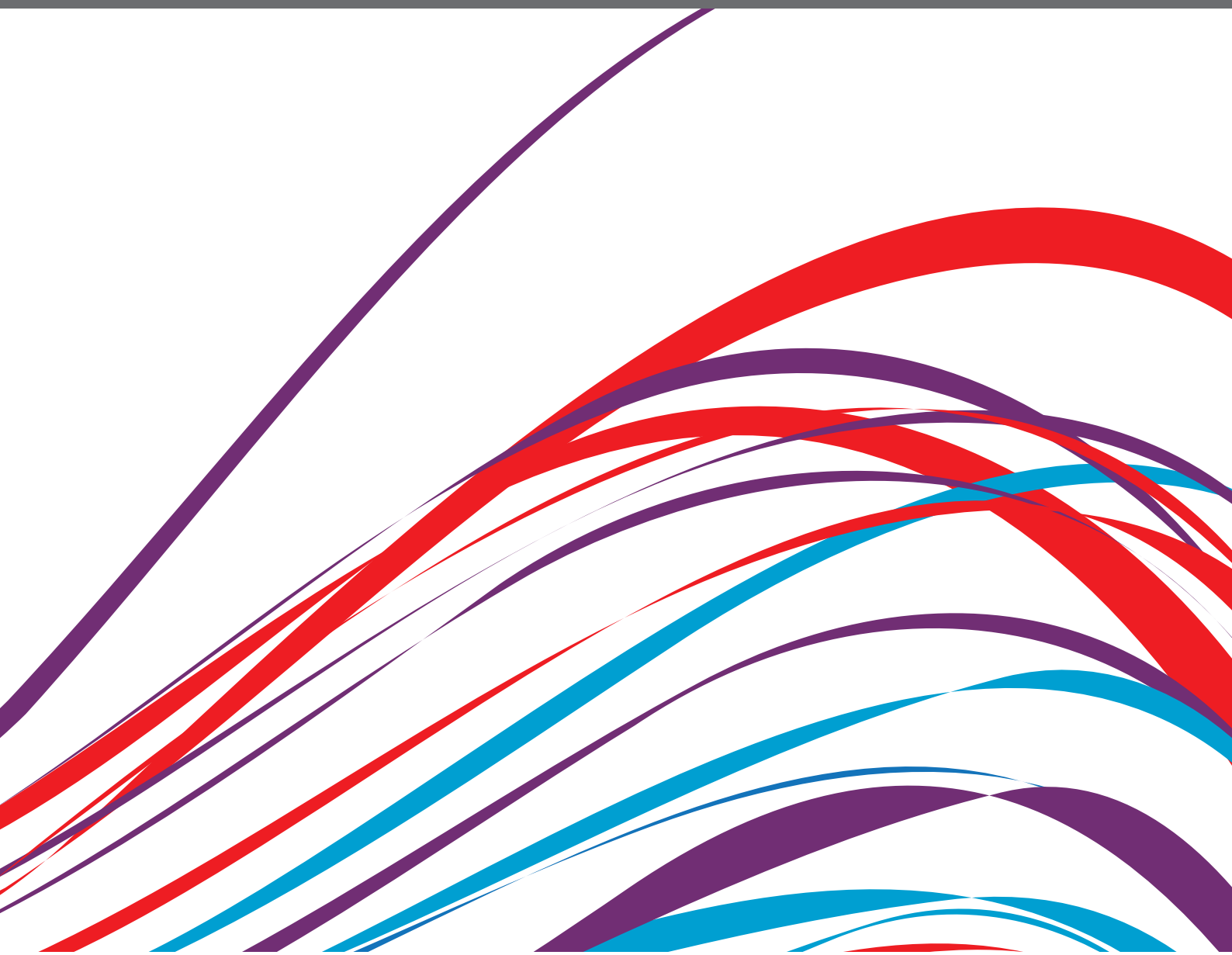

frontiers Research Topics

frontiers

ISSN 1664-8714
ISBN 978-2-88976-557-7
DOI 10.3389/978-2-88976-557-7

About Frontiers

Frontiers is more than just an open-access publisher of scholarly articles: it is a pioneering approach to the world of academia, radically improving the way scholarly research is managed. The grand vision of Frontiers is a world where all people have an equal opportunity to seek, share and generate knowledge. Frontiers provides immediate and permanent online open access to all its publications, but this alone is not enough to realize our grand goals.

Frontiers Journal Series

The Frontiers Journal Series is a multi-tier and interdisciplinary set of open-access, online journals, promising a paradigm shift from the current review, selection and dissemination processes in academic publishing. All Frontiers journals are driven by researchers for researchers; therefore, they constitute a service to the scholarly community. At the same time, the Frontiers Journal Series operates on a revolutionary invention, the tiered publishing system, initially addressing specific communities of scholars, and gradually climbing up to broader public understanding, thus serving the interests of the lay society, too.

Dedication to Quality

Each Frontiers article is a landmark of the highest quality, thanks to genuinely collaborative interactions between authors and review editors, who include some of the world's best academicians. Research must be certified by peers before entering a stream of knowledge that may eventually reach the public - and shape society; therefore, Frontiers only applies the most rigorous and unbiased reviews.
Frontiers revolutionizes research publishing by freely delivering the most outstanding research, evaluated with no bias from both the academic and social point of view. By applying the most advanced information technologies, Frontiers is catapulting scholarly publishing into a new generation.

What are Frontiers Research Topics?

Frontiers Research Topics are very popular trademarks of the Frontiers Journals Series: they are collections of at least ten articles, all centered on a particular subject. With their unique mix of varied contributions from Original Research to Review Articles, Frontiers Research Topics unify the most influential researchers, the latest key findings and historical advances in a hot research area! Find out more on how to host your own Frontiers Research Topic or contribute to one as an author by contacting the Frontiers Editorial Office: frontiersin.org/about/contact

GLOBAL FRONTIERS IN HEART VALVE INTERVENTIONS

Topic Editors:
Peter Zilla, University of Cape Town, South Africa
Vinod H. Thourani, Piedmont Heart Institute, United States
Tsuyoshi Kaneko, Brigham and Women's Hospital, Harvard Medical School, United States

Citation: Zilla, P., Thourani, V. H., Kaneko, T., eds. (2022). Global Frontiers in Heart Valve Interventions. Lausanne: Frontiers Media SA. doi: 10.3389/978-2-88976-557-7

Table of Contents

frontiers in Cardiovascular Medicine

ORIGINAL RESEARCH
published: 12 August 2021
doi: 10.3389/fcvm.2021.688396

Integration of Functional Imaging, Cytometry, and Unbiased Proteomics Reveals New Features of Endothelial-to-Mesenchymal Transition in Ischemic Mitral Valve Regurgitation in Human Patients

Adrien Lupieri[1], Yasufumi Nagata[2], Livia S. A. Passos[1], Dakota Beker-Greene[1], Katherine A. Kirkwood[3], Jill Wylie-Sears[4], Zahra Alvandi[4], Hideyuki Higashi[5], Judy W. Hung[6], Sasha A. Singh[5], Joyce Bischoff[4], Robert A. Levine[2] and Elena Aikawa[1,5,7]**

[1] Division of Cardiovascular Medicine, Center for Excellence in Vascular Biology and Harvard Medical School, Brigham and Women's Hospital, Boston, MA, United States, [2] Cardiac Ultrasound Laboratory and Harvard Medical School, Massachusetts General Hospital, Boston, MA, United States, [3] Department of Population Health Science and Policy, Icahn School of Medicine, International Center for Health Outcomes and Innovation Research, New York, NY, United States, [4] Vascular Biology Program and Department of Surgery, Boston Children's Hospital and Department of Surgery and Harvard Medical School, Boston, MA, United States, [5] Division of Cardiovascular Medicine, Center for Interdisciplinary Cardiovascular Sciences and Harvard Medical School, Brigham and Women's Hospital, Boston, MA, United States, [6] Echocardiography Laboratory, Division of Cardiology and Harvard Medical School, Massachusetts General Hospital, Boston, MA, United States, [7] Department of Human Pathology, Sechenov First Moscow State Medical University, Moscow, Russia

OPEN ACCESS

Edited by:
Jordan D. Miller,
Mayo Clinic and Foundation,
United States

Reviewed by:
Gretchen Mahler,
Binghamton University, United States
Kartik Balachandran,
University of Arkansas, United States

***Correspondence:**
Adrien Lupieri
alupieri@bwh.harvard.edu
Elena Aikawa
eaikawa@bwh.harvard.edu

Specialty section:
This article was submitted to Heart Valve Disease, a section of the journal Frontiers in Cardiovascular Medicine

Received: 30 March 2021
Accepted: 19 July 2021
Published: 12 August 2021

Citation:
Lupieri A, Nagata Y, Passos LSA, Beker-Greene D, Kirkwood KA, Wylie-Sears J, Alvandi Z, Higashi H, Hung JW, Singh SA, Bischoff J, Levine RA and Aikawa E (2021) Integration of Functional Imaging, Cytometry, and Unbiased Proteomics Reveals New Features of Endothelial-to-Mesenchymal Transition in Ischemic Mitral Valve Regurgitation in Human Patients. Front. Cardiovasc. Med. 8:688396. doi: 10.3389/fcvm.2021.688396

Background: Following myocardial infarction, mitral regurgitation (MR) is a common complication. Previous animal studies demonstrated the association of endothelial-to-mesenchymal transition (EndMT) with mitral valve (MV) remodeling. Nevertheless, little is known about how MV tissue responds to ischemic heart changes in humans.

Methods: MVs were obtained by the Cardiothoracic Surgical Trials Network from 17 patients with ischemic mitral regurgitation (IMR). Echo-doppler imaging assessed MV function at time of resection. Cryosections of MVs were analyzed using a multi-faceted histology and immunofluorescence examination of cell populations. MVs were further analyzed using unbiased label-free proteomics. Echo-Doppler imaging, histo-cytometry measures and proteomic analysis were then integrated.

Results: MVs from patients with greater MR exhibited proteomic changes associated with proteolysis-, inflammatory- and oxidative stress-related processes compared to MVs with less MR. Cryosections of MVs from patients with IMR displayed activated valvular interstitial cells (aVICs) and double positive CD31+ αSMA+ cells, a hallmark of EndMT. Univariable and multivariable association with echocardiography measures revealed a positive correlation of MR severity with both cellular and geometric changes (e.g., aVICs, EndMT, leaflet thickness, leaflet tenting). Finally, proteomic changes associated with EndMT showed gene-ontology enrichment in vesicle-, inflammatory- and oxidative

stress-related processes. This discovery approach indicated new candidate proteins associated with EndMT regulation in IMR.

Conclusion: We describe an atypical cellular composition and distinctive proteome of human MVs from patients with IMR, which highlighted new candidate proteins implicated in EndMT-related processes, associated with maladaptive MV fibrotic remodeling.

Keywords: ischemic mitral regurgitation, mitral valve, endothelial-to-mesenchymal transition, proteomics, echocardiography, histo-cytometry

INTRODUCTION

Ischemic mitral regurgitation (IMR) is a common complication after myocardial infarction (MI), and results from modification of the left ventricle (LV) architecture and papillary muscle (PM) displacement. It has been established that IMR is associated with an increase of heart failure and mortality post-MI (1, 2). IMR is a complex disease characterized by systolic blood flow from the LV to the left atrium, resulting from underlying geometric changes, such as limitations of mitral valve (MV) closure by PM tethering and a mismatch between annulus and valve size (3).

Little is known about the biological processes that can lead to adaptation of the MV. Different mechanisms have been proposed; first, that mechanical stress imposed by PM tethering promotes the increase of leaflet area and thickness associated with cellular changes, suggesting an active process of remodeling (4). In addition, it has been suggested that a modulation of leaflet distensibility associates with a change in collagen fiber orientation because of the anisotropic property of collagen fibers, which increases non-aligned fibers in the MV, thereby, increasing extensibility (5–7). However, the role of passive stretching, extracellular matrix (ECM) remodeling, matrix synthesis, and cell growth during MV adaptation remains unclear.

At the cellular level, changes in mitral leaflets during IMR have been associated with endothelial-to-mesenchymal transition (EndMT). During this process, MV endothelial cells (VECs) undergo a transformation of their phenotype toward a mesenchymal-like phenotype, expressing myofibroblastic markers, such as alpha-smooth muscle actin (αSMA) (8, 9). Both transforming growth factor β (TGFβ) and hydrogen peroxide-related oxidative stress primarily contribute to EndMT (10). EndMT within the MV is associated with leaflet extensibility and flexibility leading to MR due to tethering stress that can then be aggravated by MI, as demonstrated in a large animal model (8). Furthermore, angiotensin II pathway inhibition by losartan, which is known to decrease TGFβ signaling, resulted in a significant reduction of leaflet thickness and EndMT, without modification of the adaptive increase of leaflet area (9). Taken together, this suggests a major role of EndMT and TGFβ in the maladaptation of the MV to IMR.

Nevertheless, in human IMR, the effects of ECM remodeling and cellular changes, such as EndMT, are still largely unknown. This gap in knowledge is primarily due to a lack of available human biological material. In this study, we assessed alterations in MV leaflets and performed a comprehensive analysis on a cohort of surgical MV specimens from 17 patients with IMR by corroborating histo-cytometry with functional echocardiographic measurement and unbiased proteomics analyses. Based on this discovery approach, we aimed to bring new insights to the understanding of structural remodeling and cellular changes within the MV.

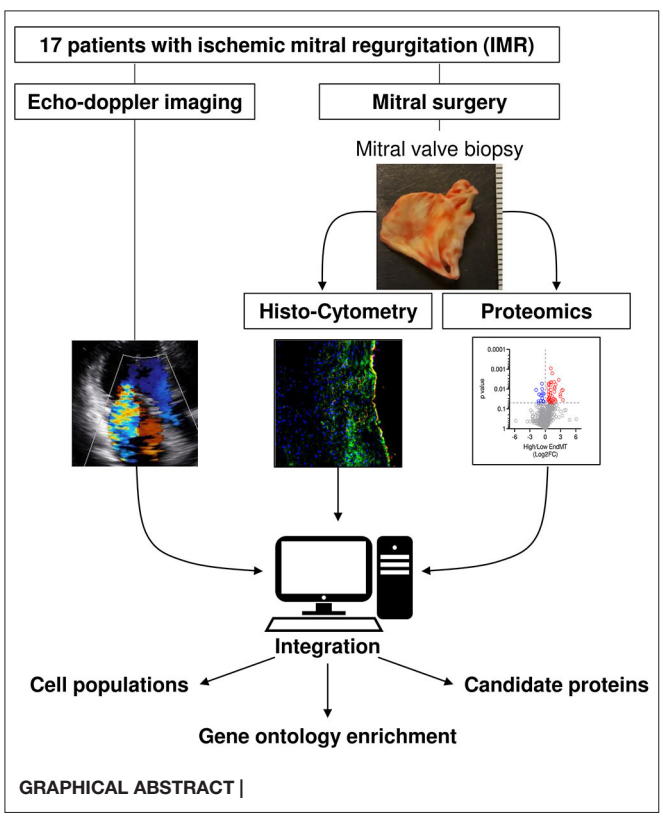

GRAPHICAL ABSTRACT |

MATERIALS AND METHODS

Mitral Valves

Adult patients with IMR defined by integrated approach, eligible for MV replacement were enrolled in the National Institutes of Health (NIH) / Canadian Institutes of Health Research (CIHR)-supported Cardiac Thoracic Surgery Network. MV biopsies were collected from subjects undergoing valve replacement, $\geq$ 1 cm^2 were excised from the anterior leaflet (A2) region. We excluded any evidence of structural MV disease (chordal or leaflet), ruptured papillary muscle prior MV repair, severe irreversible

pulmonary hypertension, contraindication to cardiopulmonary bypass, incapacity to measure the effective regurgitant orifice (ERO) and end-systolic volume index (ESVI), concomitant intra-operative procedure (with the exception of tricuspid valve repair, closure of patent *foramen ovale*, atrial septal defect and Maze procedure), cardiogenic shock, intravenous inotropic treatment, ST segment elevation MI within 7 days, congenital heart disease, evidence of cirrhosis or hepatic synthetic failure, excessive surgical risk, recent history of psychiatric disease, any concurrent disease with life expectance <2 years, and pregnancy at the time of randomization.

Histopathology

MV pieces from the anterior leaflet (A2) region obtained from 20 patients were snap frozen immediately after excision, then long-term stored at −80°C. Half-part of the frozen MVs were isolated using a razor cut at −20°C for proteomic analysis. The middle portion of frozen MVs were razor cut at −20°C and immediately embedded into Optimum Cutting Temperature compound (OCT, Sakura Finetek, USA). Then, MVs were sectioned into 6 μm slices using a cryostat (Leica CM3050S) followed by histological or immunohistochemical staining.

Hematoxylin and Eosin Staining

MV sections were fixed for 20 min in 10% formalin, then stained with successive bath of Harris hematoxylin for 1 min and alcoholic eosin for 1 min. MV thickness was evaluated by the average of 10 measures distributed over the whole leaflet section and analyzed using ImageJ software (NIH).

Masson Trichrome Staining

MV sections were fixed 30 min in Bouin solution, then stained with successive baths of Weigert iron hematoxylin for 5 min, Biebrich Scarlet fuchsin for 10 min, phosphomolybdic acid for 30 s, aniline blue for 3 min and acetic acid for 30 s.

Picrosirius Red

MV sections were fixed 10 min in 10% formalin, then dipped in a solution of Picric acid 0.1% Sirius red for 3 h, then 1 min in HCl 0.01 N solution. Collagen fibers were observed using polarized light microscope (Nikon), and measure of collagen composition was done from the whole section of MV leaflet by ImageJ software (NIH).

Immunohistochemistry

MV cryosections were first fixed 10 min in cold acetone −20°C and secondly fixed for 5 min in 4% paraformaldehyde solution. Sections were incubated for 1 h in blocking solution (PBS, 0.1%; Tween 20, 3% serum) at room temperature. We then incubated primary antibodies (see table below) overnight at 4°C. After 3 repeats of a 5 min wash in PBS, 0.1% Tween 20, sections were incubated with fluorescent-conjugated secondary antibodies (see Table below) for 2 h at room temperature. Slides were washed 3 times for 5 min in PBS containing 0.1% Tween 20 and nuclei were stained with DAPI (4,6-diamidino-2-phenylindole, R37606, Invitrogen), cover slipped, and examined with a Nikon Eclipse Confocal microscope (Nikon, USA).

Primary Ab	Reference	Dilution	Secondary Ab	Reference	Dilution
Anti-CD31	ab28364	1/50	Anti-rabbit IgG AF647	A21245	1/500
Anti-CD45	MA5-17687	1/500	Anti-rat IgG AF594	A11007	1/500
Anti-αSMA	M0851	1/500	Anti-mouse IgG AF488	A11001	1/500

Cell Population Analysis

Confocal microscopy images were analyzed by ImageJ software (NIH). Two methods of measure were performed using the average of 3 independent high power fields (640 × 640 μm) per sample. First, we performed unbiased assessment of the positive area for each staining: CD31+; CD45+ and αSMA+. We then measured the colocalization area for each pair of staining: CD31+ CD45+; CD31+ αSMA+ and CD45+ αSMA+. The single positive areas were calculated by subtraction of double positive areas from the total: CD31+ = (total CD31+)-[(CD31+; CD45+)+(CD31+ αSMA+)]; αSMA+ =(total αSMA+)-[(CD31+ αSMA+)+(CD45+ αSMA+)]; CD45+ = (total CD45+)-[(CD31+ CD45+)+(CD45+ αSMA+)]. The second method was a manual counting of nuclei (DAPI staining) colocalized with single or double positive staining determined by the first analysis, enabling to exclude the non-cellular staining.

Echocardiography

Comprehensive Two-Dimensional Transthoracic Echocardiography

Comprehensive two-dimensional transthoracic echocardiography was performed before the surgical procedure including MV replacement with MV excision with or without coronary-artery bypass grafting. Basic echocardiographic parameters were measured in the core laboratory (Massachusetts General Hospital, Boston, Massachusetts). MV-specific parameters were additionally measured blinded to any clinical and biological information. Left ventricular end-diastolic/end-systolic volumes and ejection fraction were measured by the biplane method of disks summation. The volumes were indexed by body surface area. *Vena contracta* width (VC) was measured to quantify MR severity (11). MV-specific parameters, open anterior and posterior leaflet lengths were measured from the leaflet insertion to the tip in the apical three chambers view during diastasis. Leaflet thickness was measured in the middle portion of the leaflet in the parasternal long-axis view to minimize the impact of stretch. Closure leaflet length was measured as the tissue length between anterior and posterior annuluses and the tenting area was measured as the area surrounded by leaflets and the line between annuluses on apical 3 chambers-view in mid-systole. The patients were categorized into two groups according to quantitative MR severity with VC to eliminate assumption error and hemodynamic factors in MR

classification, patients displaying VC $\leqq$ 7 mm were defined as moderately severe MR (MSMR), patients displaying VC > 7 mm were classified as severe MR (SMR).

Proteomics

Label-Free Proteomics Preparation for Human MV Samples

A total of 27 samples were processed together for proteomics analysis. Out of those, 7 samples were not included in the final proteomic analysis due to the unavailability of the echocardiography measures and the tissue cryosections. Each piece of frozen MV was pulverized in liquid nitrogen, then sonicated in RIPA buffer (Pierce, 89900) complemented with 1% protease inhibitor cocktail. Protein precipitation was performed with chloroform:methanol (2:1) method and redissolve using a solution of urea 6M/thiourea 2M/TEAB 100 mM (pH 8). 15μg of protein were cleaved using trypsin/LysC cocktail at 37°C overnight. The peptides were desalted using Oasis HLB column (Waters, USA) and dried with a Speed Vacuum concentrator (SPD1010, Thermo Fisher Scientific, USA). After re-suspension in 40 μl of 5% mass spectrometry grade acetonitrile (Thermo Fisher Scientific, USA) and 5% formic acid (Sigma-Aldrich, USA).

Data-Dependent Acquisition

The peptides were analyzed using the Orbitrap Fusion Lumos Tribrid mass spectrometer (Thermo Fisher Scientific) fronted with an Easy-Spray ion source and coupled to an Easy-nLC1000 HPLC pump (Thermo Fisher Scientific). The peptides were separated using a dual column set-up: An Acclaim PepMap RSLC C18 trap column, 75 μm X 20 mm; and an EASY-Spray LC heated (45°C) column, 75 μm × 250 mm (Thermo Fisher Scientific). The gradient flow rate was 300 nl/min from 5 to 21% solvent B (acetonitrile/0.1% formic acid) for 75 min, 21 to 30 % Solvent B for 15 min, followed by 10 min of a 'jigsaw wash', alternating between 5 and 95 % Solvent B. Solvent A was 0.1% formic acid. The instrument was set to 120 K resolution, and the top N precursor ions in a 3 second cycle time (within a scan range of 375–1,500 m/z; isolation window, 1.6 m/z; ion trap scan rate, normal) were subjected to collision induced dissociation (collision energy 30%) for peptide sequencing (or MS/MS). Dynamic exclusion was enabled (60 s).

Mass Spectrometric Data Analysis

The MS/MS spectra were queried against the human UniProt database (downloaded on August 1, 2018; 155, 133 sequencing) using the HT-SEQUEST search algorithm, *via* the Proteome Discoverer (PD) Package (version 2.2, Thermo Fisher Scientific). Methionine oxidation and n-terminal acetylation were set as a variable modification, and carbamidomethylation of cysteine was set as a fixed modification. The enzyme was set to trypsin (full), with a maximum of four missed cleavages, using a 10 ppm precursor tolerance window and a 0.02 Da fragment tolerance window. Peptides were filtered based on a 1% FDR based on the reverse database (decoy) results (12, 13). In order to quantify peptide precursors detected in the MS1 but not sequenced from sample to sample, we enabled the "Feature Mapper" node. Chromatographic alignment was done with a maximum retention time (RT) shift of 10 min and a mass tolerance of 10 ppm. Feature linking and mapping settings were, RT tolerance minimum of 0 min, mass tolerance of 10 ppm and signal-to-noise minimum of five. Precursor peptide abundances were based on their chromatographic intensities and total peptide amount was used for normalization. Peptides assigned to a given protein group, and not present in any other protein group, were considered as unique. Consequently, each protein group is represented by a single master protein (PD Grouping feature). We used unique and razor peptides per protein for quantification and filtered for proteins with two or more unique peptides.

The mass spectrometry proteomics data have been deposited to the ProteomeXchange Consortium via the PRIDE (14) partner repository with the dataset identifier PXD025096 and 10.6019/PXD025096.

Statistical Analysis

Non-parametric unpaired *T*-test were calculated using Excel to compare the protein abundance between subgroups of patients.

Simple linear correlation from proteomics data were calculated with Excel functions. For each protein we determined the correlation R = CORREL([array 1], [array 2]); T statistic was calculated by T = ([R]*SQRT([number of pairs of data]-2)/SQRT(1-[R]^2)); *p*-value was determined by p = TDIST([T], [degrees of freedom], [number of tails]).

Simple linear regression using echocardiography, histology or cytometry parameters were calculated using GraphPad Prism 8.4 software.

Gene ontology enrichment were identified using g:Profiler Homo sapiens database (https:/biit.cs.ut.ee/gprofiler) using g:GOSt (15). Functional enrichment was assessed from ordered list of protein (ascending *p*-value). Benjamini-Hochberg False Discovery Rate correction was applied to calculate the adjusted *p*-value.

Univariable linear regression models were used to explore the relationships between echocardiographic measures of mitral valve disease including mid-systole tenting area, *vena contracta* (VC), clinical characteristics including age and sex, and histo-cytometry measurements of CD45+/CD31+/αSMA+ immunostainings from excised mitral valve tissue samples. Logarithmic transformations were used as appropriate for non-normally distributed continuous variables. Variables showing a nominal association with the independent variable ($\alpha = 0.10$) were considered for inclusion in a multivariable model of VC, chosen as the echocardiographic measure most representative of mitral regurgitation. For all models, statistical significance was considered at the $\alpha = 0.05$ level; as these were hypothesis-generating analyses, no adjustment was made for multiple comparisons. All these analyses were conducted using SAS v9.4.

RESULTS

Echocardiography Analysis

Two-dimensional transthoracic echocardiography was performed before the surgical procedure to evaluate MV

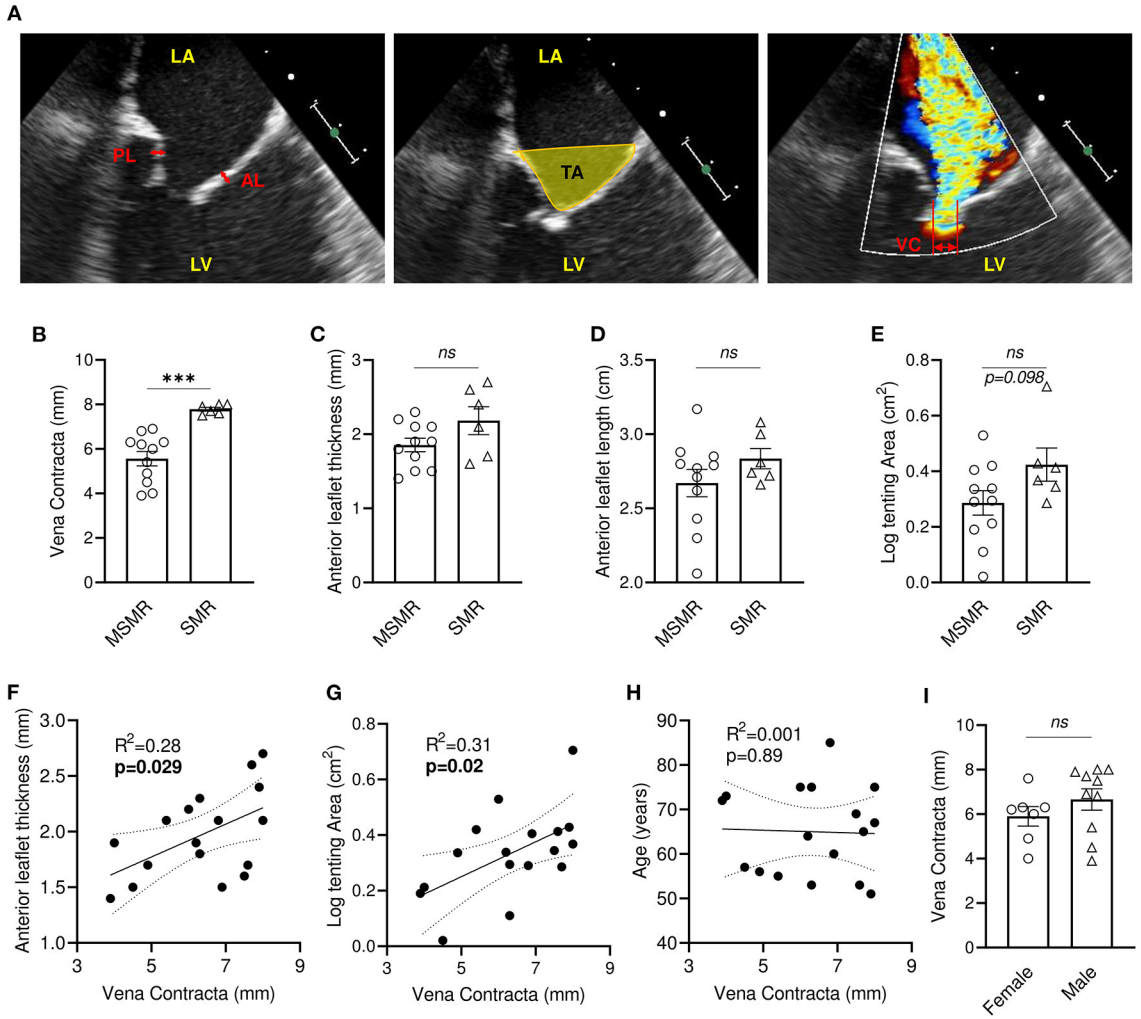

FIGURE 1 | Mitral regurgitation is associated with leaflet thickening and increased tenting area in patients with IMR. **(A)** Anterior and posterior mitral valve leaflet thickness were measured in the middle portion of the leaflet (left: bidirectional red arrows). Tenting area was measured as the area surrounded by leaflets and the line between annuluses on apical 3ch-view in mid-systole (middle: yellow area). Vena contracta (VC) width was measured as the narrowest width of mitral regurgitation jet (right: bidirectional yellow arrow). Comparison of VC **(B)**, anterior leaflet thickness **(C)**, anterior leaflet length **(D)**, tenting area **(E)** between patients presenting moderately severe MR (MSMR) ($n = 11$) and severe MR (SMR) ($n = 6$). Linear correlation between VC and anterior leaflet thickness **(F)**, tenting area **(G)**, anterior leaflet length **(D)** and age **(H)**. **(I)** VC in female ($n = 7$) and male ($n = 10$). LA, left atrium; LV, left ventricle; AL, anterior mitral valve leaflet; PL, posterior mitral valve leaflet. ns, no-significant, ***$p < 0.001$. Thin dotted line shows the 95% confidence interval.

function (**Figure 1A**). Echocardiographic evaluation of mitral regurgitation has been assessed by *vena contracta* (VC) measurement. All patients displayed a VC $\geq$ 4 mm (4–8 mm, $n = 17$), among which 11 patients presented moderately severe MR (MSMR) (VC between 4 and 7 mm) (16) and six patients exhibited severe MR (SMR) (VC > 7 mm) (16) (**Figure 1B**). Patients with MSMR or SMR did not present significant variation of anterior mitral leaflet (AL) thickness and length (**Figures 1C,D**). Nevertheless, simple linear regression model showed a significant positive correlation between AL thickness and VC ($R^2 = 0.28$, $p = 0.029$) (**Figure 1F**). Measurement of the MV tenting area at mid-systole displayed a non-normal distribution (Shapiro-Wilk test, $p = 0.012$), which required a logarithmic transformation. Patients with SMR tends to have large tenting area than those with MSMR ($p = 0.098$) (**Figure 1E**), and there was a significant positive correlation between VC and the tenting area ($R^2 = 0.31$, $p = 0.019$) (**Figure 1G**). Conversely, the linear regression model did not show an association of VC with anterior leaflet length ($R^2 = 0.002$, $p = 0.86$) (**Supplementary Figure 1A**). VC, AL thickness, and tenting area showed large heterogeneity (**Supplementary Table 1**), suggesting that in our cohort, tethering stress and left ventricle architecture modification had differing effects after MI. In our cohort, VC is not significantly associated with the age of the patient ($R^2 = 0.001$, $p = 0.89$) and does not vary significantly by gender ($p = 0.184$) (**Figures 1H,I**).

Histological Analysis

All samples used in this study were obtained from patients undergoing surgical excision of the anterior MV after IMR. Procedures were performed and registered with the Cardiothoracic Surgical Trial Network (CTSN). We obtained 20 tissue specimens from which two were excluded based on the histological appearance (samples designated Ex1, Ex2), due to their predominant myocardial composition, as presented in **Supplementary Figure 2A**. An additional sample was excluded based on the mean protein abundance, as determined by proteomics criteria (Ex1, Ex2, Ex3, in **Supplementary Figure 2B**).

Masson's trichrome staining of the mitral leaflet sections showed a large heterogeneity in size, morphology, and configuration of the different layers (**Figure 2A** and **Supplementary Table 2**). We observed three major groups of histological patterns: thin leaflets with high fibrotic content (sample #7, **Figure 2A** top), an intermediate phenotype with organized layers (sample #4, **Figure 2A** middle), and samples with largely disorganized structures and heterogeneous fibrotic composition (sample #11, **Figure 2A** bottom). The observed thickness variability was not related to gender ($n = 7$–10; $p = 0.54$) (**Figure 2B**), and was not correlated with the age of patients at time of surgery ($R^2 = 0.1$, $p = 0.21$) (**Figure 2C**). These results suggest that different processes, independently of gender and age, are linked to MV post-MI adaptation, leading to IMR.

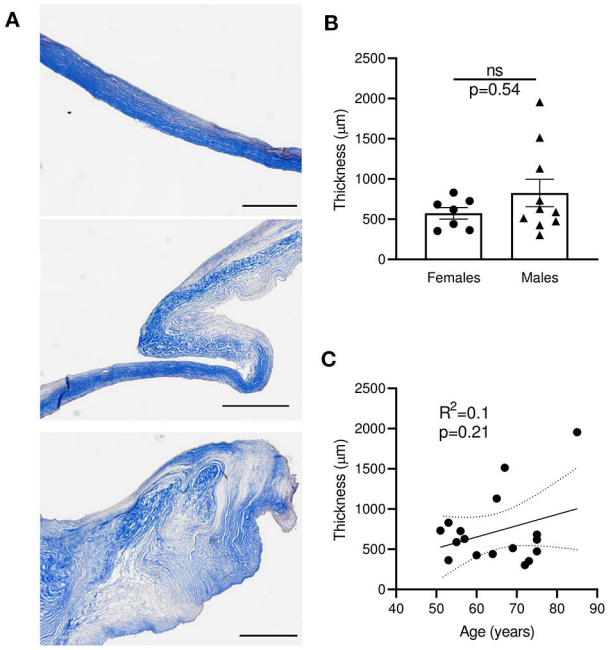

FIGURE 2 | Sections of human MV with MR display large heterogeneity of thickness, independently of age and gender. **(A)** Histological sections of human mitral valves representative of three different grades of histological remodeling (patients #7, #4, #11, **Supplementary Table 2**), stained with Masson trichrome (scale bar represents 1 mm). **(B)** Thickness of MV leaflet section from male vs. female samples. **(C)** Correlation between the age of donor and the MV thickness for each donor. Thin dotted line shows the 95% confidence interval. ns, no significant.

Echocardiography/Proteomic Integration

Proteome composition of the MVs from 11 patients displaying MSMR (VC $\leqq$ 7 mm) was compared to the MV's proteome from the six patients displaying SMR (VC $>$ 7 mm). From the 845 proteins identified in these samples, 20 showed a significant difference in protein abundance (6 increased and 14 decreased) (**Figure 3A**). To corroborate these results, we performed a second analysis using a linear regression model between the abundance of each protein and the MR severity of each patient, as assessed by echo-doppler measurement of the VC. From the 845 proteins identified in our sample group, 26 showed a significant correlation to protein abundance (8 increased and 18 decreased) (**Figure 3B**). A total of 39 proteins were found related to MR (**Figures 3C,D** and **Supplementary Table 3**), with 7 proteins significantly changed in both approaches (**Figures 3C,D**; black).

Next, we compared the main biological processes enriched in the group of significantly modulated proteins from both methods: comparison of MSMR vs. SMR groups and linear correlation to MR (**Figures 3C,D**). The analysis of biological process enrichment revealed an extensive implication of glutathione derivative metabolism (GO:1901685, GO:1901687) (**Figure 3E**), related to ESD (Esterase D) and GSTP1 (Glutathione S-Transferase Pi 1) decreased with the increase of MR. We also observed involvement of several inflammatory processes, such as regulation of the acute inflammatory response (GO:0002673, GO:0002526), blood coagulation (GO:0007597, GO:0072378), innate immune response (GO:0045087), and response to interleukin-12 (GO:0035722, GO:0071349, GO:0070671) and−1 (GO:0032612) (**Figure 3E**). 11 proteins matched with inflammatory-related GO:BP, including A2M (Alpha-2-Macroglobulin), C3 (Complement C3) were increased in samples with more severe MR, which were opposite to CAPZA1 (CapZ Alpha-1), CFL1 (Cofilin 1), CD44, F12 (Coagulation Factor XII), GSTP1, HMGB1 (High Mobility Group Box 1), PRDX5 (Peroxiredoxin 5), PSME1 (Proteasome Activator Subunit 1), S100A13 (S100 Calcium Binding Protein A13), which were decreased. We also found an enrichment of response to reactive oxygen species (GO:0000302) (**Figure 3E**), linked to GSTP1 and PRDX5, both decreased in samples with higher MR. Additionally, we observed an enrichment of the proteolysis-related process named regulation of peptidase activity (GO:0052547) (**Figure 3E**) connected to the reduction of CD44, HMGB1, PSME1, RCN3 (Reticulocalbin 3), and the induction of TIMP3 (Tissue Inhibitor of Metalloproteinases 3) in MVs with superior MR.

MV Cell Composition

The quadruple immunofluorescent staining (CD31, αSMA, CD45 and DAPI) associated with sub-analysis of single positive and double positive areas identified different cell populations within the MV leaflet is presented in **Figures 4A,B**. Average areas of each staining are included in **Figure 4B** and quantification by counting of each cell type is presented in **Supplementary Figure 3A**.

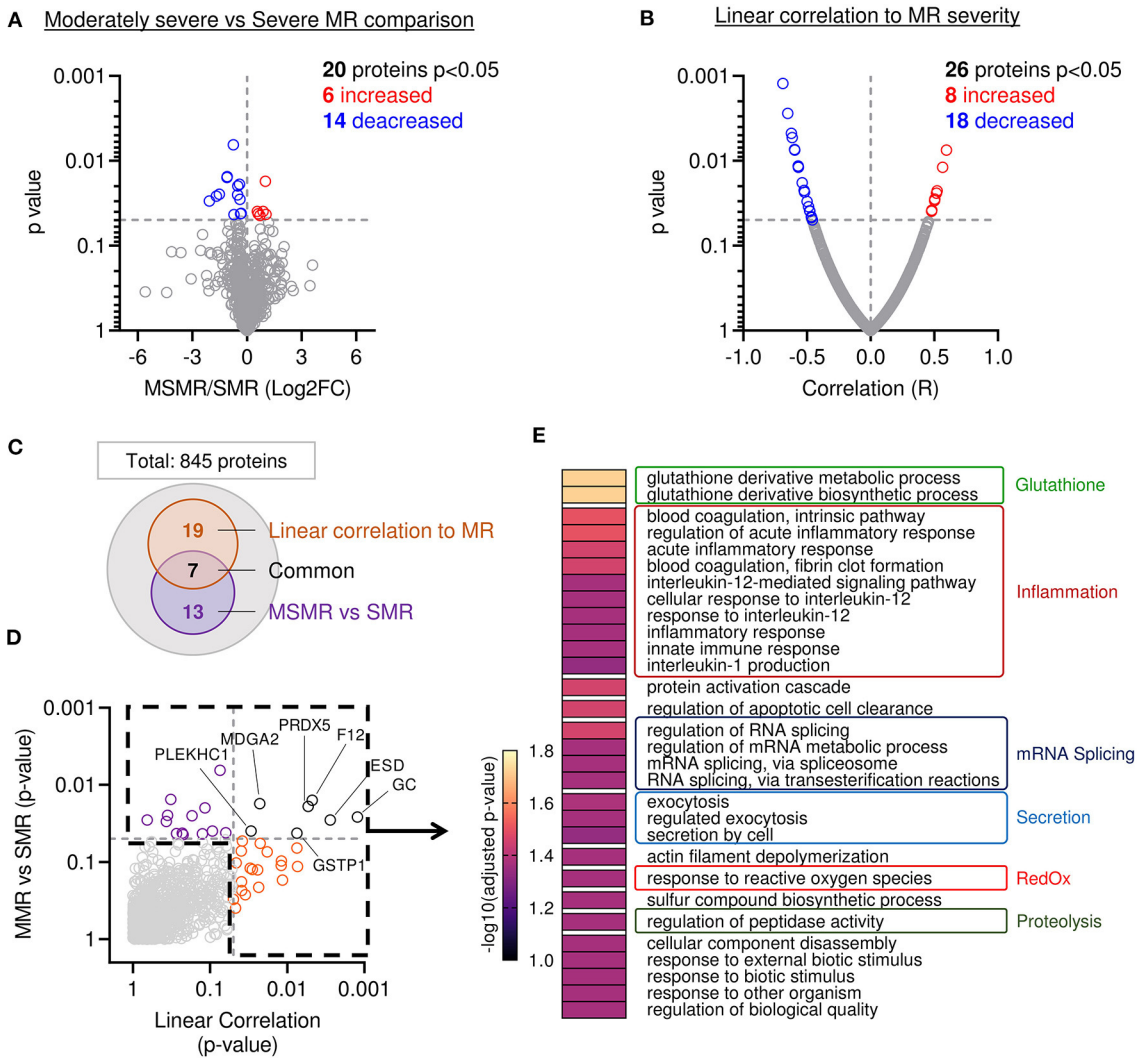

FIGURE 3 | Mitral leaflets from patients with higher MR display proteomic change associated to proteolysis-, inflammatory-, and oxidative stress-related processes. **(A)** Comparison of proteome composition from the samples having moderately severe MR (MSMR $n = 1$) vs. the samples with severe MR (SMR $n = 6$) Volcano plot displaying the log2 fold-change (x-axis) against the statistical p-value (log scale) for all 845 proteins detected. Proteins with significantly increased expression (Log2FC > 0, $p < 0.05$) in SMR group are shown in red, while the proteins with significantly decreased expression (Log2FC > 0, $p < 0.05$) are expressed in blue. **(B)** Comparison of proteomic composition using linear correlation with MR level quantification (vena contracta). Dot plot displaying the R (x-axis) against the statistical p-value (log scale) for all 845 patients detected. Proteins with the significant and positive correlation (R > 0, $p < 0.05$) to MR are shown in red, while the proteins with significant and negative correlation (R < 0, $p < 0.05$) are presented in blue. **(C)** Venn diagram displaying modulated proteins obtain from the linear correlation to MR (orange) and MSMR vs. SMR comparison (purple), common proteins were identified in black. **(D)** Dot plot exhibiting p-value 845 patients identified from both analyses presented linear correlation to MR (orange), MSMR vs. MR comparison (purple), common proteins (black). **(E)** Heatmap of gene ontology biological process (GO:BP) enriched from protein significantly modulated.

We assessed an αSMA as a marker of activated valvular interstitial cells (aVICs), also known as valvular myofibroblast-like cells. αSMA single positive (αSMA+) cells were heterogeneously present in the different MV donors and showed a strong negative correlation with collagen content detected by picrosirius red staining ($R^2 = 0.37$, $p = 0.009$) (**Supplementary Figure 3B**), but did not significantly correlate with leaflet thickness ($R^2 = 0.186$, $p = 0.08$) (**Supplementary Figure 3C**).

The population of CD45 single positive cells (CD45+) indicates leukocytes infiltrated the MV. We observed low levels of leukocyte infiltration (<10 CD45+ cells per high power field [HPF]) except in four samples (#3, #5, #12 and #17), which displayed >18 CD45+ cells per HPF (35.3; 20; 18.7; 21.3, respectively) (**Supplementary Figure 3A**). Furthermore, there was a significant negative correlation between CD45+ cells and collagen content ($R^2 = 0.42$, $p = 0.0046$) (**Supplementary Figure 3D**), but not with leaflet thickness

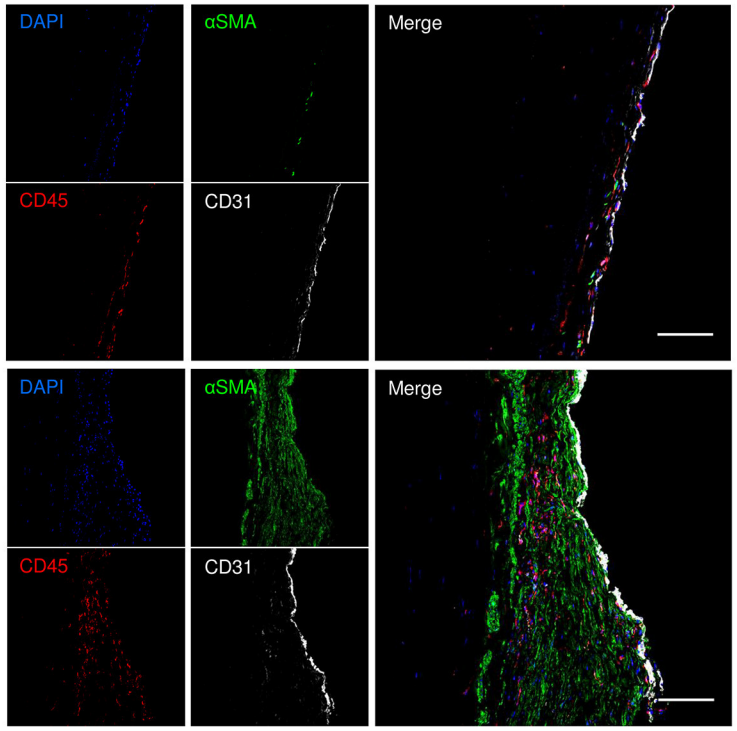

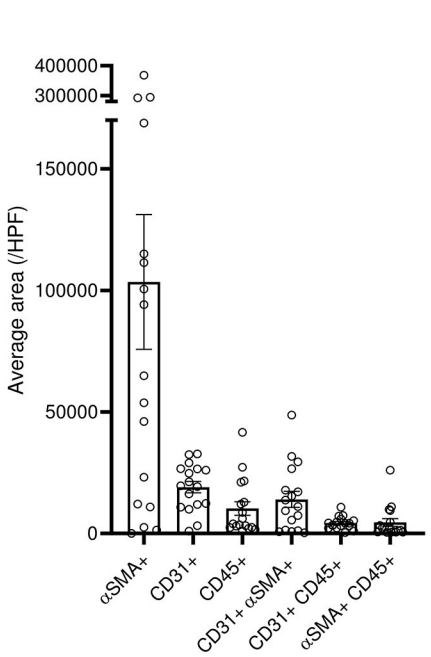

C

Shapiro-Wilk test

	p value
Echocardiography	
VC	ns
AL thickness	ns
PL thickness	ns
AL length	ns
PL length	ns
Tenting area	**0.012**
Cytometry	
CD31+	ns
CD45+	**0.0011**
αSMA+	**0.0044**
CD31+ CD45+	ns
CD31+ αSMA+	**0.0359**
αSMA+ CD45+	**<0.0001**

D

univariable linear regression for MR severity

	R^2	p value
Echocardiography		
AL thickness	**0.28**	**0.029**
PL thickness	0.13	0.16
AL length	0.0021	0.86
PL length	0.097	0.22
Tenting area (log)	**0.31**	**0.02**
Cytometry		
CD31+	0.016	0.63
CD45+ (log)	0.1	0.21
αSMA+ (log)	0.23	0.062
CD31+ CD45+	0.0086	0.72
CD31+ αSMA+ (log)	0.23	0.052
αSMA+ CD45+ (log)	0.031	0.5

E

multivariable linear regression for MR severity

	Adjusted R^2	Standard β	p value
AL thickness	0.47	0.42	0.057
Tenting area (log)		0.45	**0.04**
CD31+ αSMA+ (log)	0.58	0.52	**0.0095**
Tenting area (log)		0.59	**0.0041**
αSMA+ (log)	0.53	0.42	**0.046**
Tenting area (log)		0.55	**0.012**
CD31+ αSMA+ (log)	0.46	0.43	**0.027**
AL thickness		0.49	**0.047**
αSMA+ (log)	0.4	0.32	0.18
AL thickness		0.44	0.076

FIGURE 4 | Histo-cytometry assessment of MV cell composition correlated with echocardiography measures revealed that MR is concomitantly associated to EndMT and leaflet's thickness or tenting. **(A)** Representative MV section from patient with different range of cellular composition, (patients #14 upper and #12 bottom) stained with immunofluorescent co-staining of DAPI (blue), αSMA (green), CD45 (red), and CD31 (white), merge on the left panel (scale bar represents 100 μm). **(B)** Cell count per high power field (HPF) for αSMA single positive cells (αSMA+), CD45 single positive cells (CD45+), CD31 single positive cells (CD31+), along with CD31/αSMA double positive (CD31+ αSMA+) and CD31/CD45 double positive (CD31+ CD45+). **(C)** Shapiro-Wilk test of data distribution. **(D)** Univariable linear regression with VC. **(E)** Multivariable linear regression with VC. MV, mitral valves; VC, vena contracta; PL, posterior mitral leaflet; AL, anterior mitral leaflet; SP, single positive.

(**Supplementary Figure 3E**). On the other hand, the number of leukocytes (CD45+) and aVIC (αSMA+) was correlated significantly ($R^2 = 0.26$, $p = 0.037$) (**Supplementary Figure 3F**).

Endothelial cell population is characterized by CD31 single positive (CD31+) staining and the number of this cell type was consistent in all samples (**Figure 4B**), and associated with the endothelial layer surface measurements per field. These results suggest that endothelial cell content is not altered during post-MI IMR progression. However, we identified two additional CD31+ populations, including double positive CD31+ αSMA+

and CD31+ CD45+ cells. The CD31+ αSMA+ subpopulation demonstrated a wide variability between MVs (**Figures 4A,B** and **Supplementary Figure 3A**).

Previous preclinical studies in a large animal model reported the presence of endothelial cells undergoing EndMT, characterized by the co-expression of endothelial markers (e.g., CD31, VE-Cadherin, NOS 3) and mesenchymal markers (e.g., αSMA, calponin, SM22a, versican) (9, 10, 17). Similarly, we observed the presence of cells co-expressing CD31 and αSMA (CD31+ αSMA+) in the MVs from patients with severe IMR. Quantitative analysis of confocal fluorescent microscopy images applying two complementary methods (**Supplementary Figures 4A,B**), demonstrated significantly correlated values ($R^2 = 0.463$, $p = 0.0026$) (**Supplementary Figure 4A**). The assessment of EndMT cells' sub-localization within the leaflet layer showed CD31+ αSMA+ DAPI+ cells in the endothelial layer, as well as in the sub-endothelium and in valve interstitium (**Figure 5A**). The number of cells in each compartment was positively correlated ($R^2 = 0.58$, $p = 0.0004$), supporting the hypothesis of cell migration from the endothelium to the interstitium during EndMT (**Figure 5B**).

Echocardiography/Histo-Cytometry Integration

Various models of linear regression were applied to study the possible relationship between cell populations observed within the MV and clinical parameters measured by echocardiography. The variables with non-normal distribution including tenting area, CD45+, αSMA+, CD31+αSMA+ and αSMA+CD45+ cells (**Figure 4C**), were then transformed by logarithmic function for univariable and multivariable linear regression analysis (**Figures 4D,E**). *Vena contracta* (VC) was used as a numeral parameter representative of MR severity. Univariable and multivariable regression models were used to assess the relationship between clinical echocardiographic parameters measured at the time of surgery and histo-cytology parameters determined from tissue samples.

Univariable linear regression to MR with other echocardiography measurements demonstrated a significant association with anterior leaflet (AL) thickening and tenting area ($R^2 = 0.28$, $p = 0.029$ and $R^2 = 0.31$, $p = 0.02$, respectively) but no other echocardiography measurements (**Figure 4D**). Univariable linear regression demonstrated a trend toward an association between MR and cytometry measurements, including aVICs (αSMA+) ($R^2 = 0.23$, $p = 0.062$) and cells undergoing EndMT (CD31+αSMA+) ($R^2 = 0.23$, $p = 0.052$) (**Figure 4D**). Multivariable linear regression analysis was used to test which combination of parameter was the best model to predict MR severity by including variables selected in univariable analyses. Two variables were included in models according to the limited number of our cohort. Multivariable linear regression modeling MR dependent variables did not show a significant concomitant association with AL thickness and tenting area (**Figure 4E**); even though the relationship was close to significant ($R^2 = 0.47$, AL thickness $p = 0.057$, tenting area $p = 0.04$). However, when utilizing a multivariable linear regression model that incorporates MR dependent variables, we observed that MV tenting area and aVICs (αSMA+) ($R^2 = 0.53$), as well as tenting area and cells undergoing EndMT (CD31+αSMA+) ($R^2 = 0.58$), are significantly associated with MR severity (**Figure 4E**). Additionally, a multivariable linear regression model for MR severity displayed association with AL thickness and EndMT cells (CD31+αSMA+), but not with AL thickness and aVICs (αSMA+) (**Figure 4E**). These findings suggest MR severity is determined by the combination of geometric and histopathologic changes.

Histo-Cytometry/Proteomic Integration

The four samples displaying lower EndMT rate (**Supplementary Figure 4A**; white dots) were used as an internal control to investigate the proteomic changes specifically related to the EndMT process in the MV. From the 845 proteins identified in our samples, 60 showed a significant difference in protein abundance (46 increased and 14 decreased) (**Figure 5C** and **Supplementary Table 4**).

To support these results, we performed a second analysis using a linear regression model that considered the abundance of each protein and the EndMT level from each sample. For this, we used an unbiased measure of CD31+ αSMA+ area normalized as percent of the total CD31+ area. From the 845 proteins identified in our sample group, 51 showed a significant difference in protein abundance (15 increased and 36 decreased) (**Figure 5D** and **Supplementary Table 4**). Among them, 15 proteins were found significantly changed in both analyses (**Figures 5E,F** and **Supplementary Table 4**).

Furthermore, we found a significant difference in the abundance of proteins previously reported to be involved in the EndMT process (COL1A, CAST, TAGLN2, CAT, APOA1, BLVRB), or described in a comparable biological process of epithelial-to-mesenchymal transition (EMT) (HRG, EHD2, FGL2, FBN1, CA2, LASP1, HMGB1, LMCD1, NID1, FTH1, TGFB1I1, PRDX2, SRPX, LRP1, PLA2G2A, MAOA, TTN, IQGAP1) (**Supplementary Table 5**), which enhanced the confidence in our hypothesis that EndMT is highly involved in MV pathology. Moreover, 73 other proteins that were significantly altered, but have not been associated with EMT or EndMT, comprise new candidate proteins that might have key functional roles or work as biomarkers (**Supplementary Table 4**).

Next, we compared the main GO:BP enriched in the list of significantly modulated proteins from the various methods of analysis: comparison of high vs. low EndMT groups, the EndMT linear correlation, as well as the proteins common to both analyses (**Figures 5E–G** and **Supplementary Table 4**). The analysis focused on the 50 more significant GO:BP and selected the ones shared in the 3 approaches of analysis (**Figure 5G**).

The analysis of biological process enrichment revealed an extensive effect of several oxidative stress-related processes enriched in MV displaying high EndMT, including hydrogen peroxide metabolic processes (GO:0042744, GO:0042743), response to hydrogen peroxide (GO:0042542) and reactive oxygen species metabolic process (GO:0072593) (**Figure 5G**) subsequently to the upregulation of CAT, HBA2, HBB, HBD, PRDX2 and SNCA, as well as the downregulation of ARF4

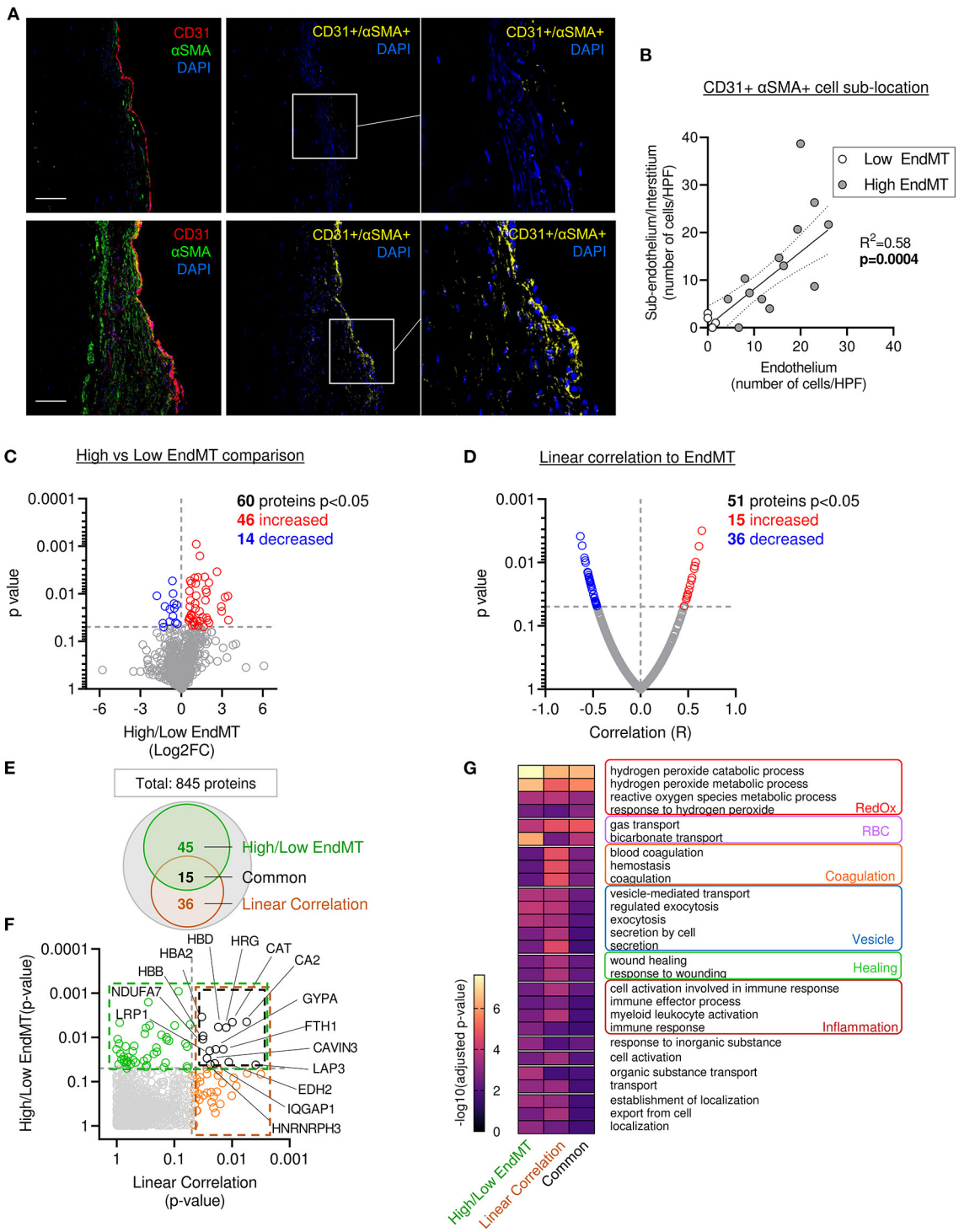

FIGURE 5 | Mitral leaflets displaying EndMT are associated with proteomic change associated to, oxidative stress-, inflammatory- and vesicle-related processes. **(A)** Representative mitral valve section from patient with different range of cellular composition, (patients #10 upper panel and #12 bottom panel) stained for DAPI (blue), CD31 (red), αSMA (green) merge on the left panel (scale bar represent 100 μm). CD31 and αSMA double positive areas are represented in yellow (two right panels). **(B)** Sub localization of EndMT cells (CD 31+αSMA + DAPI+) between endothelium layer (x axis) and sub endothelium and interstitium area (y axis). **(C)** Comparison of proteomic composition from the four samples having low level of EndMT (white dots in **B**) vs. the 13 other samples with higher level of EndMT (gray dots in **B**). Volcano plot displaying the Log2 fold change (x axis) against the statistical *p*-value (log scale) for all 845 proteins detected. Proteins with significantly increased expression (Log2FC > 0, $p < 0.05$) in sample with high level of EndMT are shown in red, while the proteins with significantly decreased expression (Log2FC > 0, $p < 0.05$) are

(Continued)

FIGURE 5 | presented in blue. **(D)** Comparison of proteomic using linear correlation with EndMT quantification (CD31+αSMA+ area normalized to total CD31+). Dot plot displaying R^2 (x axis) against the statistical *p*-value (Log scale) for all 845 patients detected. Proteins with significant and positive correlation ($R > 0$, $p < 0.05$) to EndMT are shown in red, while the proteins with significant and negative correlation ($R > 0$, $p < 0.05$) are presented in blue. **(E)** Venn diagram displaying the significantly modulated proteins obtain from the linear correlation to EndMT (dark orange) and Low vs. High EndMT comparison (green) and common proteins (black). **(F)** Dot plot exhibiting *p*-value of 845 patients identified from both analyses. Common proteins are indicated in black. **(G)** Gene ontology biological process (GO:BP) from protein significantly modulated in the low vs. high EndMT comparison, linear correlation to EndMT, or only in the common proteins.

and BST1 (**Supplementary Table 4**). CAT has been previously implicated in EndMT, PRDX2 has shown involvement in EMT (**Supplementary Table 5**), whereas SNCA and erythrocyte-associated proteins HBA2, HBB, HBD have not been linked to either processes.

In addition, we observed an involvement of inflammatory processes, which included cell activation in the immune response (GO:0002263), immune response (GO:0006955), immune effector process (GO:0002252) and myeloid leukocyte activation (GO:0002274) (**Figure 5G**). Proteins associated with these inflammatory processes revealed proteins previously associated with EndMT, including APOA1, CAT, COL1A1, as well as proteins previously connected to EMT, including FGL2, FTH1, HMGB1, HRG, IQGAP1, LRP1 and PLA2G2A. However, 15 of them have never been related to EMT or EndMT, including APCS, BST1, FTL, HBB, HSPD1, JCHAIN, PPBP, SERPINB6, and SNCA (**Supplementary Tables 4, 5**) suggesting potentially new players in this biological process.

Assessment of gene ontology enrichment also revealed the association of vesicle-mediated processes, such as vesicle-mediated transport (GO:0016192), regulated exocytosis (GO:0045055), endocytosis (GO:0006897), secretion (GO:0046903), and secretion by cell (GO:0032940) (**Figure 5G**). Among proteins connected to these biological processes, 3 have been related to EndMT (APOA1, CAT, TAGLN2), 7 have been associated to EMT (EHD2, FGL2, FTH1, HMGB1, HRG, TTN) (**Supplementary Table 5**), while 12 of them have never been linked to either process (ARF4, BST1, ERP70, F13A1, FTL, HBA2, HBB, JCHAIN, PPBP, SCARB2, SERPINB6, SNCA, SPTB) (**Supplementary Table 4**), indicating potential new members of this biological function.

DISCUSSION

In this study, we used MVs from patients with IMR to explore histologic and cellular characteristics of the MV leaflet, which were then corroborated with functional echocardiographic measurements and proteome composition. Our results indicate a multifactorial disease mediated by alterations in MV thickening and architecture related to changes in the cellular composition, such as EndMT and VIC activation.

In our cohort of patients displaying IMR, all *vena contracta* measurements were $\geq$ 4 mm (average 6.34 $\pm$ 1.39 mm), confirming diagnosis of severe MR (16). We observed a large discrepancy in leaflet thickness (from 1.4 to 2.7 mm based on echo-guided measurements), which revealed a variety of responses to IMR. The standard value for both anterior and posterior leaflet thickness established via echocardiography measurement was approximately 1.6 mm (4), indicating that not all patients with IMR displayed thickening of their mitral leaflets. However, we observed that anterior leaflet thickness is positively and significantly correlated with the regurgitation severity, confirming previous observations that leaflets tend to thicken following MR (18). Conversely, severity of MR was not correlated to mitral leaflet length variation.

Mitral tenting is the geometric feature characterized by insufficient systolic leaflet displacement toward the annulus with restricting leaflet coaptation, which is reflected by increased tethering forces on the MV and reduced closing forces. Tethering forces are increased by regional and global LV dilatating remodeling through chordae and papillary muscles with increased tenting area, resulting in MR deterioration (3, 19). We observed in our cohort a positive linear association between MR severity measured as *vena contracta* and tenting area (**Figure 1G**), which is consistent with previous reports demonstrating an important relationship between the MR severity in patients and morphological changes in the coordination of MV complex and LV (3).

Proteome Changes Related to MR

Our cohort presented a large discrepancy of MR severity. Comparison of the MV proteome from patients displaying different levels of MR allowed us to identify candidate proteins and the main biological processes related to MR. First, we compared protein abundance between MVs from patients displaying MSMR and SMR assessed by *vena contracta* measurement, where 20 proteins were found significantly changed. Secondly, we applied a linear correlation relationship between protein abundance in MVs and MR severity, where 26 proteins were found significantly modulated. A total of 39 proteins were found related to MR severity.

Assessment of gene ontology (GO) enrichment associated to these proteins showed biological processes were involved, including glutathione- and reactive oxygen species-related processes. Proteins related to glutathione metabolism (GSTP1 and ESD) are less abundant with the increase of MR severity, suggesting a reduction of glutathione metabolism in the MV as a response to MR. Glutathione metabolism participates in antioxidant defense of the cell. At the same time, we observed an enrichment of the GO "response to reactive oxygen species," associated with a decrease of PRDX5 in conjunction with MR severity. Altogether, this suggests a reduction of the antioxidant defense system in the MV associated with MR severity.

Assessment of gene ontology enrichment also showed that various inflammatory processes, such as blood coagulation, acute inflammation, IL-1 and IL-12 related processes. Proteins associated with the innate immune response were also found decreased (F12, CAPZA1, A2M, PSME1, HMGB1, CD44),

except C3, which was elevated in association with MR severity. Regarding the proteins linked to regulation of coagulation, we detected a decrease of F12, a major member of the coagulation cascade, in combination with an increase of A2M, an inhibitor of thrombin, suggesting a global inhibition of coagulation in the MVs in patients with more severe MR. Enriched inflammatory processes were also associated with decreased protein abundance, suggesting a subside of these pathways, along with MR severity. For instance, proteins linked to the inflammatory response (F12, PRDX, GSTP1), IL-1 production (GSTP1, S100A13, HMGB1), IL-12 response (CFL1 and CAPZA1) were found less abundant in MVs associated with high levels of MR.

Moreover, we observed a decrease of proteins linked to the modulation of peptidase activity (CD44, HMGB1, PSME1, RCN3), as well as an upregulation of an inhibitor of protease (TIMP3) in patients displaying higher MR. Altogether, this suggests a reduction of the proteolytic processes, which could be associated with a late stage of disease. Moreover, our observation linked CD44 to both immune response (GO:0045087) and proteolytic processes (GO:0052547) in the MV. Previous reports showed that CD44 deletion promotes inflammation and reduces collagen degradation during the early phase of cutaneous wound healing, leading to accumulation of collagen even after wound closure (20). We suggest a similar relationship in the MV, leading to the promotion of inflammation and fibrosis.

Overall, our findings indicate that the severity of MR is associated with a decrease of antioxidant defense, proteolysis, coagulation and inflammation modulation.

Activated Valvular Interstitial Cells

We found a large αSMA+ cell population in IMR MVs. Expression of myofibroblast markers such as αSMA by VICs implies that cells underwent phenotypic modulation from quiescent fibroblasts to activated myofibroblast-like cells (21). The activation of VICs is induced by various stimuli, including abnormal hemodynamic/mechanical forces or soluble factors (22). In our cohort of patients, we observed within the MV samples a strong association between the number of αSMA+ and CD45+ cells, suggesting a relationship between inflammatory cell infiltration and VIC activation. We also noticed a positive correlation of aVIC (αSMA+) numbers with MR severity ($p = 0.062$), albeit insignificant, suggesting an association between these two parameters in IMR. Nevertheless, using a multivariable linear regression model to investigate parameters regulating MR and aVICs showed a significant association with tenting area, but not AL thickness. Mitral tenting area is mainly determined by changes of heart architecture following myocardial infarction (23), suggesting that a myofibroblast-like phenotypic modulation of VICs is regulated by mechanical forces applied on mitral leaflets.

The myofibroblast αSMA+ cell population in the MV could be derived from quiescent VICs, but could also originate from endothelial cells undergoing EndMT by gaining mesenchymal phenotype (24). Further investigations are necessary to determinate the lineage of the aVICs population during IMR.

Leukocytes

CD45+ cell infiltration within the MV is associated with post-MI remodeling, but in our cohort of patients, we did not observe a correlation of leukocyte infiltration with MR or leaflet thickening. Surgically induced MR in sheep showed that CD45+ cell infiltration was independent of tethering stress, but dependent on occurrence of MI (8). Variation of CD45+ cell infiltration observed in this cohort of post-MI MR could be related to the size of infarcted territory or post-MI time.

CD45 was first shown to be expressed by all hematopoietic lineages, except for erythrocyte and platelets. In MVs, the origin of CD45+ cells co-expressing CD31 or αSMA is not clearly established. One hypothesis suggests bone marrow-derived circulating cells as precursors for different lineages, such as fibrocytes (CD45+ αSMA+) (25) or endothelial progenitor cells (CD45+ CD31+) (26). Nevertheless, the involvement of bone marrow-derived endothelial cells has been associated in humans with vascular endothelial repair or post-ischemia neovascularization (26), but has never been reported in cardiac valve diseases. Secondly, studies from our group showed that primary culture of MV endothelial cells undergoing EndMT after TGFβ treatment was a source of CD45+ cells co-expressing endothelial marker (VE-cadherin) and myofibroblast marker (αSMA) (27). This work demonstrated that CD45 could be a marker of EndMT. Nevertheless, in our study, CD31+ CD45+ and αSMA+ CD45+ cells correspond to a minor portion of mitral cell populations, and do not correlate with MR severity. Biological materials available for this study made it impossible to trace the cell lineage.

Endothelial-to-Mesenchymal Transition

Previous studies from our group introduced mitral EndMT in a sheep model of MR (8, 9). Here, we demonstrated the presence of CD31+ αSMA+ cells in human MVs with severe IMR, suggesting the occurrence of EndMT. We also examined the association of functional echocardiographic measurement with the rates of EndMT observed in IMR. We detected a close to statistical significance ($p = 0.052$) trend for positive linear correlation of EndMT levels with MR severity. This suggests an association between occurrence of EndMT and MR in humans, as previously described in experimental animal IMR (8, 9, 27). To investigate the parameters regulating MR associated with EndMT, we generated multivariable linear regression models. We observed a significant association between MR severity and combination of EndMT (CD31+ αSMA+) and tenting area or anterior leaflet thickness, indicating a strong relationship affecting MR between the geometric changes induced by mechanical stress applied on the MVs and occurrence of EndMT in humans, as was previously observed in an ovine model (8, 17).

Prospective New Members Involved in Mitral Valve Endothelial-to-Mesenchymal Transition

A proteomic discovery approach has been used to explore new possible players and biomarkers of EndMT during MR. First, we compared protein abundance between MVs displaying

low and high levels of EndMT detected by histo-cytometry. Second, we applied a linear correlation relationship between protein abundance in MVs and EndMT levels. Here, we propose different candidate proteins related to homologous biological processes, such as EMT or EndMT from other vascular beds. The candidate proteins that were not previously associated with EndMT and their hypothetical relationships are presented below.

EndMT is mainly regulated by TGFβ signaling (10). Furthermore, hydrogen peroxide-related oxidative stress potentiates TGFβ-mediated EndMT (28). Analysis of proteomic enrichment associated with EndMT demonstrated an overexpression of proteins implicated in hydrogen peroxide catabolism, including catalase (CAT; high vs. low EndMT, $p = 0.0045$ FC = 2.35; linear correlation to EndMT, $p = 0.016$ $R^2 = 0.335$), an enzyme responsible for hydrogen peroxide decomposition. Catalase has been described as a critical player in SIRT3-Foxo3a-mediated EndMT in hypertensive renal disease (29). Another enzyme catalyzing the reduction of hydrogen peroxide, Peroxiredoxin-2, was also found increased in correlation with EndMT levels in the MV (PRDX2, linear correlation to EndMT, $p = 0.038$ $R^2 = 0.26$). Peroxiredoxin-2 was previously described as a potent regulator of TGFβ-mediated EMT (30). We also observed downregulation of an enzyme producing hydrogen peroxide, Monoamine Oxidase A (MAOA, linear correlation to EndMT, $p = 0.015$ $R^2 = 0.34$), previously shown to be associated with EMT (31). In the context of atherosclerosis, hydrogen peroxide potentiates EndMT and TGFβ-mediated EndMT (28). Conversely, our observations from human MVs showed an increase of hydrogen peroxide catabolism and decrease of its synthesis associated with higher levels of EndMT. This divergence could be attributed to oxidative stress resolution processes or an advanced phase of remodeling.

In addition, we found other proteins related to TGFβ signaling. First, fibrillin 1 (FBN1) was significantly decreased in our samples with high levels of EndMT. Fibrilin 1 is a matrix protein, which forms microfibrils associated with elastic fibers, but also enables them to segregate TGFβ, reducing its bioavailability (32). Fibrilin 1-deficient mice exhibited MV alterations, such as increased length and thickness associated with an increased cell proliferation, decreased apoptosis, and excess TGFβ activation, rescued by TGFβ antagonism (33). This may suggest that the decrease of fibrilin 1 expression is associated with extracellular matrix (ECM) change alongside an increase of TGFβ signaling, increasing EndMT.

Furthermore, we showed a decrease in the abundance of Low-density lipoprotein Receptor Related Protein (LRP1), also called Transforming Growth Factor-β Receptor Type V. LRP1 mediates anti-proliferative effects of TGFβ *in vitro* on various cell types (34, 35). In addition, LRP1 has been shown to promote EMT in prostate cancer cells (36). LRP1-deficient mice presented a Marfan-like syndrome with perturbation of vascular ECM and overactivation of TGFβ signaling (37). While no study focused on cardiac valves in this model, it is reasonable to suggest that decreased levels of LRP1 in human MV could promote cell proliferation and affect the TGFβ pathway.

Some groups already provide hypotheses on extracellular vesicle (EV)-mediated EMT, predominantly in the context of cancer (38, 39), but this regulation has never been established in valve EndMT. Nevertheless, human endothelial cells that underwent EndMT secreted three-times more EVs than control endothelial cells (40). Proteomic analysis of EV content showed enrichment in inflammatory and immune-related proteins (40). These results could partially explain the similar profile of biological process enrichment we observed in leaflets with a high rate of EndMT. This suggests that EndMT, in addition to being induced by inflammatory factors (40), should play a major function in inflammatory progression.

IQGAP1 (IQ motif containing GTPase activating protein 1) was found decreased in MV displaying high level of EndMT and negatively correlated to EndMT level. In endothelial cells, IQGAP1 has been largely described as a key regulator of cell-cell adhesion and cell polarization leading the cell migration (41). EndMT required loss of cell-cell by endothelial cells (42), which is coherent with the downregulation of IQGAP1 related to EndMT observed in MV. Nevertheless, the reduction of IQGAP1 has been associated to an inhibition of EMT in gastric cancer (43), and the clear role of IQGAP1 in EndMT has not been clearly established yet.

Conversely to proteins presented above, which has been observed as actor of EMT or EndMT, some proteins highlighted from proteomics have never been described in mesenchymal-like phenotype transitioning process. These new candidate proteins may reveal hypothetical mechanism implicated in EndMT regulation in MR.

Erythrocyte's proteins HBA2, HBB, HBD (respectively hemoglobin alpha2, beta, delta) and GYPA (glycophorin A), were found overexpress in MVs displaying high level of EndMT, as well as linearly correlated to EndMT level. In the context of atherosclerosis, studies have demonstrated an infiltration of erythrocytes within the atheromatous lesion (44), promoting oxidative processes by the release of Redox-active ferrous iron (Fe++) (45, 46). In calcified aortic valve, Morvan et al. observed erythrocytes and iron deposits into the fibrosa related to endothelial fissure *in vivo,* leading to change of VICs differentiation into a pro-inflammatory and osteogenic phenotype (47). Occurrence of endothelial fissure and erythrocyte infiltration have not been shown in MR. Nevertheless, endothelial dysfunctions post-MR have been described, such as reduction of antioxidant ability, increase of osteoprogerin secretion and higher level of circulating microparticle (48). Altogether, these data suggest a plausible endothelial dysfunction associated to an erythrocyte infiltration, leading to an increase of oxidative stress within mitral leaflets. Furthermore, FTL (ferritin light chain) is decreased in mitral leaflets presenting high level of EndMT. This protein is an iron storage protein and critical for the protection again iron-mediated oxidative damage as well as inflammation (49). The decrease of FTL observed here imply a positive relationship between iron toxicity and level of EndMT. Nevertheless, no direct evidence has been established so far.

PPBP (pro-platelet basic protein), also called CXCL7, has been found positively correlated to EndMT level in mitral leaflets ($R = 0.64$, $p = 0.0057$). It is a chemokine released by alpha granule platelets, which signals through binding to its receptor CXCR2. Other chemokine, such as CXCL5 has been described to promote EMT of nasopharyngeal carcinoma cells by activating ERK/GSK-3β/snail signaling (50), and previous report mentioned that PPBP is able to promote proliferation and invasion of carcinoma cells (51), suggesting the possibility of an PPBP-regulated mesenchymal transition. Additionally, Grande et al. observed in platelet-derived microparticles from obese patients an enhanced capacity to induce EMT and EndMT marker genes *in vitro*. In addition, they found in these platelet-derived microparticles an overexpression of a few proteins, including PPBP (52). However, direct implication of PPBP in EndMT has not yet be determined.

TTN (titin) was found overexpressed in MV presenting high levels of EndMT. TTN is important for sarcomere contraction of muscle cells but were also described in smooth muscle cell and non-muscle cells in stress fibers (53). In addition, a nuclear form of titin has described in non-muscle cell as a key factor in laminin adhesion for nuclear organization (54). Subsequently, possible implication of TTN in EndMT might involve cytoskeleton reorganization through the stress fiber or epigenetic regulation through its nuclear form.

CD55, also known as complement decay-accelerating factor, was found decreased in mitral leaflet displaying high level of EndMT. Primary function of CD55 is to prevent the complement system through inhibition of C3 and C5 convertase, responsible of proteolytic cleavage of C3 into C3a and C3b and C5 into C5a and C5b. Interestingly, it has been shown that activation of C3aR is important for EMT in renal epithelium as well as in ovarian cancer cells (55). Furthermore, endothelial cells express C3aR and C5aR, leading to proliferation, actin cytoskeleton response or chemotaxis (55, 56).

Assessment of proteomic regulation corroborated with histo-cytomety measurement in mitral leaflets allowed to established gene ontology (GO) enrichment associated to EndMT, including oxidative stress, inflammation as well as vesicle-related processes. Furthermore, identification of new candidate proteins associated with EndMT permitted to present plausible new biological processes involved in MV's EndMT, such as iron-mediated oxidative process, platelets-derived vesicles or complement system. Nevertheless, further investigations are required to validate candidate proteins and establish their direct implication in EndMT during MR.

LIMITATIONS

For our study, patients' clinical history is unknown and could represent confounding factors such as medication history, co-morbidities, or proximity to initial MI. For instance, ACEi/ARB medications are likely to affect the histological characteristics of the valves and the severity of mitral regurgitation (9, 57). In addition, location and size of the primary cardiac infarction is unknown, which could also be a confounding factor regulating heart architecture post-MI. Furthermore, the small size of our cohort limited the statistical analysis and generation of univariable and multivariable regression model. However, gender representation is close to parity (Male: 58.8%; Female: 41.2%). Finally, the use of snap frozen human samples limited our cell phenotyping strategy for the identification of cell populations through immunofluorescence, including cells undergoing EndMT. Nevertheless, this study has provided us with a rare opportunity to analyze mitral valves from a unique population of patient with IMR.

CONCLUSION

Little is known about the mechanism of MV adaptation to ischemic heart remodeling in humans. Our investigation on a small cohort of patients with IMR provides an overall comprehension of general biological processes implicated as well as new cell population correlated with the severity of the regurgitation. For the first time in human MVs, we highlight the presence of EndMT during IMR, and its close relationship with MR severity, leaflet thickening and tenting. Moreover, our study corroborated observations from animal models of IMR and opens now the perspective of validation of candidate proteins for key functional actor or biomarker with *in vitro* approach and an independent cohort.

DATA AVAILABILITY STATEMENT

The datasets presented in this study can be found in online repositories. The names of the repository/repositories and accession number(s) can be found at: https://www.ebi.ac.uk/pride/archive/, PXD025096.

AUTHOR CONTRIBUTIONS

AL, YN, KK, EA, JB, and RL contributed to conception and design of the study. AL, YN, and KK performed the statistical analysis. HH and SS performed mass spectrometry and organized the proteomic database. AL wrote the manuscript. YN wrote sections of the manuscript. EA, JB, and RL edited and critically revised manuscript and contributed to overall project supervision and funding. All authors contributed to manuscript revision, read, and approved the submitted version.

FUNDING

This work was supported by National Institutes of Health grants R01HL141917 (to RL, JB, and EA) and R01HL136431 and R01HL147095 to EA. Biospecimens were acquired as part of clinical research conducted by the Cardiothoracic Surgical Trials Network (CTSN). This CTSN trial was supported by a cooperative agreement (U01 HL088942) funded by the National Heart, Lung, and Blood Institute and the National Institute of Neurological Disorders and Stroke of the National Institutes of

Health (NIH), Bethesda, MD, and the Canadian Institutes for Health Research (CIHR), Ottawa, ON, Canada.

ACKNOWLEDGMENTS

The authors wish to acknowledge the National Institutes of Health (NIH)/Canadian Institutes of Health Research (CIHR)-supported Cardiac Thoracic Surgery Network for giving us the opportunity to work with these samples. We thank Shiori Kuraoka for helping to organize the proteomic dataset.

SUPPLEMENTARY MATERIAL

The Supplementary Material for this article can be found online at: https://www.frontiersin.org/articles/10.3389/fcvm.2021.688396/full#supplementary-material

REFERENCES

1. Grigioni F, Enriquez-Sarano M, Zehr KJ, Bailey KR, Tajik AJ. Ischemic mitral regurgitation: long-term outcome and prognostic implications with quantitative Doppler assessment. *Circulation.* (2001) 103:1759–64. doi: 10.1161/01.CIR.103.13.1759
2. Bursi F, Enriquez-Sarano M, Nkomo VT, Jacobsen SJ, Weston SA, Meverden RA, et al. Heart failure and death after myocardial infarction in the community: the emerging role of mitral regurgitation. *Circulation.* (2005) 111:295–301. doi: 10.1161/01.CIR.0000151097.30779.04
3. Levine RA, Hagege AA, Judge DP, Padala M, Dal-Bianco JP, Aikawa E, et al. Leducq Mitral Transatlantic, Mitral valve disease–morphology and mechanisms. *Nat Rev Cardiol.* (2015) 12:689–710. doi: 10.1038/nrcardio.2015.161
4. Chaput M, Handschumacher MD, Tournoux F, Hua L, Guerrero JL, Vlahakes GJ, et al. Mitral leaflet adaptation to ventricular remodeling: occurrence and adequacy in patients with functional mitral regurgitation. *Circulation.* (2008) 118:845–52. doi: 10.1161/CIRCULATIONAHA.107.749440
5. Kunzelman KS, Cochran RP. Stress/strain characteristics of porcine mitral valve tissue: parallel versus perpendicular collagen orientation. *J Card Surg.* (1992) 7:71–8. doi: 10.1111/j.1540-8191.1992.tb00777.x
6. May-Newman K, Yin FC. Biaxial mechanical behavior of excised porcine mitral valve leaflets. *Am J Physiol.* (1995) 269:H1319–27. doi: 10.1152/ajpheart.1995.269.4.H1319
7. Lee CH, Zhang W, Liao J, Carruthers CA, Sacks JI, Sacks MS. On the presence of affine fibril and fiber kinematics in the mitral valve anterior leaflet. *Biophys J.* (2015) 108:2074–87. doi: 10.1016/j.bpj.2015.03.019
8. Dal-Bianco JP, Aikawa E, Bischoff J, Guerrero JL, Hjortnaes J, Beaudoin J, et al. Leducq Transatlantic Mitral, Myocardial Infarction Alters Adaptation of the Tethered Mitral Valve. *J Am Coll Cardiol.* (2016) 67:275–87. doi: 10.1016/j.jacc.2015.10.092
9. Bartko PE, Dal-Bianco JP, Guerrero JL, Beaudoin J, Szymanski C, Kim DH, et al. Leducq Transatlantic Mitral, Effect of Losartan on Mitral Valve Changes After Myocardial Infarction. *J Am Coll Cardiol.* (2017) 70:1232–44. doi: 10.1016/j.jacc.2017.07.734
10. Kovacic JC, Dimmeler S, Harvey RP, Finkel T, Aikawa E, Krenning G, et al. Endothelial to Mesenchymal Transition in Cardiovascular Disease: JACC State-of-the-Art Review. *J Am Coll Cardiol.* (2019) 73:190–209. doi: 10.1016/j.jacc.2018.09.089
11. Zoghbi WA, Adams D, Bonow RO, Enriquez-Sarano M, Foster E, Grayburn PA, et al. Recommendations for Noninvasive Evaluation of Native Valvular Regurgitation: A Report from the American Society of Echocardiography Developed in Collaboration with the Society for Cardiovascular Magnetic Resonance. *J Am Soc Echocardiogr.* (2017) 30:303–71. doi: 10.1016/j.echo.2017.01.007
12. Elias JE, Gygi SP. Target-decoy search strategy for increased confidence in large-scale protein identifications by mass spectrometry. *Nat Methods.* (2007) 4:207–14. doi: 10.1038/nmeth1019
13. Kall L, Storey JD, MacCoss MJ, Noble WS. Assigning significance to peptides identified by tandem mass spectrometry using decoy databases. *J Proteome Res.* (2008) 7:29–34. doi: 10.1021/pr700600n
14. Perez-Riverol Y, Csordas A, Bai J, Bernal-Llinares M, Hewapathirana S, Kundu DJ, et al. The PRIDE database and related tools and resources in 2019: improving support for quantification data. *Nucleic Acids Res.* (2019) 47:D442–D450. doi: 10.1093/nar/gky1106
15. Raudvere U, Kolberg L, Kuzmin I, Arak T, Adler P, Peterson H, et al. g:Profiler: a web server for functional enrichment analysis and conversions of gene lists (2019 update). *Nucleic Acids Res.* (2019) 47:W191–W198. doi: 10.1093/nar/gkz369
16. Bonow RO, O'Gara PT, Adams DH, Badhwar V, Bavaria JE, Elmariah S, et al. 2020 Focused update of the 2017 ACC expert consensus decision pathway on the management of mitral regurgitation: a report of the american college of cardiology solution set oversight committee. *J Am Coll Cardiol.* (2020) 75:2236–70. doi: 10.1016/j.jacc.2020.02.005
17. Dal-Bianco JP, Aikawa E, Bischoff J, Guerrero JL, Handschumacher MD, Sullivan S, et al. Active adaptation of the tethered mitral valve: insights into a compensatory mechanism for functional mitral regurgitation. *Circulation.* (2009) 120:334–42. doi: 10.1161/CIRCULATIONAHA.108.846782
18. Beaudoin J, Dal-Bianco JP, Aikawa E, Bischoff J, Guerrero JL, Sullivan S, et al. Mitral leaflet changes following myocardial infarction: clinical evidence for maladaptive valvular remodeling. *Circ Cardiovasc Imaging.* (2017) 10:e006512. doi: 10.1161/CIRCIMAGING.117.006512
19. Otsuji Y, Handschumacher MD, Liel-Cohen N, Tanabe H, Jiang L, Schwammenthal E, et al. Mechanism of ischemic mitral regurgitation with segmental left ventricular dysfunction: three-dimensional echocardiographic studies in models of acute and chronic progressive regurgitation. *J Am Coll Cardiol.* (2001) 37:641–8. doi: 10.1016/S0735-1097(00)01134-7
20. Govindaraju P, Todd L, Shetye S, Monslow J, Pure E. CD44-dependent inflammation, fibrogenesis, and collagenolysis regulates extracellular matrix remodeling and tensile strength during cutaneous wound healing. *Matrix Biol.* (2019) 76:314–30. doi: 10.1016/j.matbio.2018.06.004
21. Rabkin E, Aikawa M, Stone JR, Fukumoto Y, Libby P, Schoen FJ. Activated interstitial myofibroblasts express catabolic enzymes and mediate matrix remodeling in myxomatous heart valves. *Circulation.* (2001) 104:2525–32. doi: 10.1161/hc4601.099489
22. Shapero K, Wylie-Sears J, Levine RA, Mayer JE Jr, Bischoff J. Reciprocal interactions between mitral valve endothelial and interstitial cells reduce endothelial-to-mesenchymal transition and myofibroblastic activation. *J Mol Cell Cardiol.* (2015) 80:175–85. doi: 10.1016/j.yjmcc.2015.01.006
23. Dudzinski DM, Hung J. Echocardiographic assessment of ischemic mitral regurgitation. *Cardiovasc Ultrasound.* (2014) 12:46. doi: 10.1186/1476-7120-12-46
24. Bischoff J, Endothelial-to-mesenchymal transition. *Circ Res.* (2019) 124:1163–5. doi: 10.1161/CIRCRESAHA.119.314813
25. Haudek SB, Xia Y, Huebener P, Lee JM, Carlson S, Crawford JR, et al. Bone marrow-derived fibroblast precursors mediate ischemic cardiomyopathy in mice. *Proc Natl Acad Sci USA.* (2006) 103:18284–9. doi: 10.1073/pnas.0608799103
26. Urbich C, Dimmeler S. Endothelial progenitor cells: characterization and role in vascular biology. *Circ Res.* (2004) 95:343–53. doi: 10.1161/01.RES.0000137877.89448.78
27. Bischoff J, Casanovas G, Wylie-Sears J, Kim DH, Bartko PE, Guerrero JL, et al. CD45 Expression in mitral valve endothelial cells after myocardial infarction. *Circ Res.* (2016) 119:1215–25. doi: 10.1161/CIRCRESAHA.116.309598
28. Evrard SM, Lecce L, Michelis KC, Nomura-Kitabayashi A, Pandey G, Purushothaman KR, et al. Corrigendum: endothelial to mesenchymal transition is common in atherosclerotic lesions and is associated with plaque instability. *Nat Commun.* (2017) 8:14710. doi: 10.1038/ncomms14710
29. Lin JR, Zheng YJ, Zhang ZB, Shen WL, Li XD, Wei T, et al. Suppression of endothelial-to-mesenchymal transition by SIRT (Sirtuin) 3 alleviated the

development of hypertensive renal injury. *Hypertension.* (2018) 72:350–60. doi: 10.1161/HYPERTENSIONAHA.118.10482
30. Feng J, Fu Z, Guo J, Lu W, Wen K, Chen W, et al. Overexpression of peroxiredoxin 2 inhibits TGF-beta1-induced epithelial-mesenchymal transition and cell migration in colorectal cancer. *Mol Med Rep.* (2014) 10:867–73. doi: 10.3892/mmr.2014.2316
31. Liu F, Hu L, Ma Y, Huang B, Xiu Z, Zhang P, et al. Increased expression of monoamine oxidase A is associated with epithelial to mesenchymal transition and clinicopathological features in non-small cell lung cancer. *Oncol Lett.* (2018) 15:3245–51. doi: 10.3892/ol.2017.7683
32. Chaudhry SS, Cain SA, Morgan A, Dallas SL, Shuttleworth CA, Kielty CM. Fibrillin-1 regulates the bioavailability of TGFbeta1. *J Cell Biol.* (2007) 176:355–67. doi: 10.1083/jcb.200608167
33. Ng CM, Cheng A, Myers LA, Martinez-Murillo F, Jie C, Bedja D, et al. TGF-beta-dependent pathogenesis of mitral valve prolapse in a mouse model of Marfan syndrome. *J Clin Invest.* (2004) 114:1586–92. doi: 10.1172/JCI200422715
34. Huang SS, Ling TY, Tseng WF, Huang YH, Tang FM, Leal SM, et al. Cellular growth inhibition by IGFBP-3 and TGF-beta1 requires LRP-1. *FASEB J.* (2003) 17:2068–81. doi: 10.1096/fj.03-0256com
35. Tseng WF, Huang SS, Huang JS. LRP-1/TbetaR-V mediates TGF-beta1-induced growth inhibition in CHO cells. *FEBS Lett.* (2004) 562:71–8. doi: 10.1016/S0014-5793(04)00185-1
36. Hance MW, Dole K, Gopal U, Bohonowych JE, Jezierska-Drutel A, Neumann CA, et al. Secreted Hsp90 is a novel regulator of the epithelial to mesenchymal transition (EMT) in prostate cancer. *J Biol Chem.* (2012) 287:37732–44. doi: 10.1074/jbc.M112.389015
37. Zhou L, Takayama Y, Boucher P, Tallquist MD, Herz J. LRP1 regulates architecture of the vascular wall by controlling PDGFRbeta-dependent phosphatidylinositol 3-kinase activation. *PLoS ONE.* (2009) 4:e6922. doi: 10.1371/journal.pone.0006922
38. Conigliaro A, Cicchini C. Exosome-mediated signaling in epithelial to mesenchymal transition and tumor progression. *J Clin Med.* (2018) 8:26. doi: 10.3390/jcm8010026
39. Kletukhina S, Neustroeva O, James V, Rizvanov A, Gomzikova M. Role of mesenchymal stem cell-derived extracellular vesicles in epithelial-mesenchymal transition. *Int J Mol Sci.* (2019) 20:4813. doi: 10.3390/ijms20194813
40. Haynes BA, Yang LF, Huyck RW, Lehrer EJ, Turner JM, Barabutis N, et al. Endothelial-to-mesenchymal transition in human adipose tissue vasculature alters the particulate secretome and induces endothelial dysfunction. *Arterioscler Thromb Vasc Biol.* (2019) 39:2168–91. doi: 10.1161/ATVBAHA.119.312826
41. Noritake J, Watanabe T, Sato K, Wang S, Kaibuchi K. IQGAP1: a key regulator of adhesion and migration. *J Cell Sci.* (2005) 118:2085–92. doi: 10.1242/jcs.02379
42. Arciniegas E, Frid MG, Douglas IS, Stenmark KR. Perspectives on endothelial-to-mesenchymal transition: potential contribution to vascular remodeling in chronic pulmonary hypertension. *Am J Physiol Lung Cell Mol Physiol.* (2007) 293:L1–8. doi: 10.1152/ajplung.00378.2006
43. Liu J, Ni X, Li Y, Chen M, Chen W, Wu Y, et al. Downregulation of IQGAP1 inhibits epithelial-mesenchymal transition via the HIF1alpha/VEGF-A signaling pathway in gastric cancer. *J Cell Biochem.* (2019) 120:15790–9. doi: 10.1002/jcb.28849
44. Kolodgie FD, Gold HK, Burke AP, Fowler DR, Kruth HS, Weber DK, et al. Intraplaque hemorrhage and progression of coronary atheroma. *N Engl J Med.* (2003) 349:2316–25. doi: 10.1056/NEJMoa035655
45. Michel JB, Martin-Ventura JL. Red blood cells and hemoglobin in human atherosclerosis and related arterial diseases. *Int J Mol Sci.* (2020) 21: doi: 10.3390/ijms21186756
46. Delbosc S, Bayles RG, Laschet J, Ollivier V, Ho-Tin-Noe B, Touat Z, et al. Erythrocyte efferocytosis by the arterial wall promotes oxidation in early-stage atheroma in humans. *Front Cardiovasc Med.* (2017) 4:43. doi: 10.3389/fcvm.2017.00043
47. Morvan M, Arangalage D, Franck G, Perez F, Cattan-Levy L, Codogno I, et al. Relationship of iron deposition to calcium deposition in human aortic valve leaflets. *J Am Coll Cardiol.* (2019) 73:1043–54. doi: 10.1016/j.jacc.2018.12.042
48. Porro B, Songia P, Myasoedova VA, Valerio V, Moschetta D, Gripari P, et al. Endothelial dysfunction in patients with severe mitral regurgitation. *J Clin Med.* (2019) 8:835. doi: 10.3390/jcm8060835
49. Knovich MA, Storey JA, Coffman LG, Torti SV, Torti FM. Ferritin for the clinician. *Blood Rev.* (2009) 23:95–104. doi: 10.1016/j.blre.2008.08.001
50. Qiu WZ, Zhang HB, Xia WX, Ke LR, Yang J, Yu YH, et al. The CXCL5/CXCR2 axis contributes to the epithelial-mesenchymal transition of nasopharyngeal carcinoma cells by activating ERK/GSK-3beta/snail signalling. *J Exp Clin Cancer Res.* (2018) 37:85. doi: 10.1186/s13046-018-0722-6
51. Guo Q, Jian Z, Jia B, Chang L. CXCL7 promotes proliferation and invasion of cholangiocarcinoma cells. *Oncol Rep.* (2017) 37:1114–22. doi: 10.3892/or.2016.5312
52. Grande R, Dovizio M, Marcone S, Szklanna PB, Bruno A, Ebhardt HA, et al. Platelet-derived microparticles from obese individuals: characterization of number, size, proteomics, and crosstalk with cancer and endothelial cells. *Front Pharmacol.* (2019) 10:7. doi: 10.3389/fphar.2019.00007
53. Eilertsen KJ, Kazmierski ST, Keller TC 3rd. Cellular titin localization in stress fibers and interaction with myosin II filaments in vitro. *J Cell Biol.* (1994) 126:1201–10. doi: 10.1083/jcb.126.5.1201
54. Zastrow MS, Flaherty DB, Benian GM, Wilson KL. Nuclear titin interacts with A- and B-type lamins in vitro and in vivo. *J Cell Sci.* (2006) 119:239–49. doi: 10.1242/jcs.02728
55. Afshar-Kharghan V. The role of the complement system in cancer. *J Clin Invest.* (2017) 127:780–9. doi: 10.1172/JCI90962
56. Schraufstatter IU, Trieu K, Sikora L, Sriramarao P, DiScipio R. Complement c3a and c5a induce different signal transduction cascades in endothelial cells. *J Immunol.* (2002) 169:2102–10. doi: 10.4049/jimmunol.169.4.2102
57. Kim K, Kaji S, Kasamoto M, Murai R, Sasaki Y, Kitai T, et al. Renin-angiotensin system inhibitors in patients with or without ischaemic mitral regurgitation after acute myocardial infarction. *Open Heart.* (2017) 4:e000637. doi: 10.1136/openhrt-2017-000637

Author Disclaimer: The views expressed in this article are those of the authors and do not necessarily represent the views of the National Heart, Lung and Blood Institute, the National Institute of Neurological Disorders and Stroke, the National Institutes of Health, or the US Department of Health and Human Services.

Conflict of Interest: The authors declare that the research was conducted in the absence of any commercial or financial relationships that could be construed as a potential conflict of interest.

Publisher's Note: All claims expressed in this article are solely those of the authors and do not necessarily represent those of their affiliated organizations, or those of the publisher, the editors and the reviewers. Any product that may be evaluated in this article, or claim that may be made by its manufacturer, is not guaranteed or endorsed by the publisher.

frontiers in Cardiovascular Medicine

ORIGINAL RESEARCH
published: 19 August 2021
doi: 10.3389/fcvm.2021.707892

Preclinical Testing of Living Tissue-Engineered Heart Valves for Pediatric Patients, Challenges and Opportunities

Ionela Movileanu[1,2†], Marius Harpa[1,2*†], Hussam Al Hussein[1,2], Lucian Harceaga[1], Alexandru Chertes[1], Hamida Al Hussein[1], Georg Lutter[3], Thomas Puehler[3], Terezia Preda[1], Carmen Sircuta[1], Ovidiu Cotoi[1], Dan Nistor[1,2], Adrian Man[1], Bogdan Cordos[1], Radu Deac[1], Horatiu Suciu[1,2], Klara Brinzaniuc[1,2], Megan Casco[4], Leslie Sierad[5], Margarita Bruce[4], Dan Simionescu[1,4‡] and Agneta Simionescu[6‡]*

[1] Regenerative Medicine Laboratory, University of Medicine, Pharmacy, Science and Technology "George Emil Palade", Târgu Mureş, Romania, [2] Institute of Cardiovascular Diseases and Transplant, Târgu Mureş, Romania, [3] Department for Experimental Cardiac Surgery and Heart Valve Replacement, School of Medicine, University of Kiel, Kiel, Germany, [4] Biocompatibility and Tissue Regeneration Laboratory, Department of Bioengineering, Clemson University, Clemson, SC, United States, [5] Aptus Bioreactors, LLC, Clemson, SC, United States, [6] Tissue Engineering Laboratory, Department of Bioengineering, Clemson University, Clemson, SC, United States

Introduction: Pediatric patients with cardiac congenital diseases require heart valve implants that can grow with their natural somatic increase in size. Current artificial valves perform poorly in children and cannot grow; thus, living-tissue-engineered valves capable of sustaining matrix homeostasis could overcome the current drawbacks of artificial prostheses and minimize the need for repeat surgeries.

Materials and Methods: To prepare living-tissue-engineered valves, we produced completely acellular ovine pulmonary valves by perfusion. We then collected autologous adipose tissue, isolated stem cells, and differentiated them into fibroblasts and separately into endothelial cells. We seeded the fibroblasts in the cusp interstitium and onto the root adventitia and the endothelial cells inside the lumen, conditioned the living valves in dedicated pulmonary heart valve bioreactors, and pursued orthotopic implantation of autologous cell-seeded valves with 6 months follow-up. Unseeded valves served as controls.

Results: Perfusion decellularization yielded acellular pulmonary valves that were stable, no degradable *in vivo*, cell friendly and biocompatible, had excellent hemodynamics, were not immunogenic or inflammatory, non thrombogenic, did not calcify in juvenile sheep, and served as substrates for cell repopulation. Autologous adipose-derived stem cells were easy to isolate and differentiate into fibroblasts and endothelial-like cells. Cell-seeded valves exhibited preserved viability after progressive bioreactor conditioning and functioned well *in vivo* for 6 months. At explantation, the implants and anastomoses were intact, and the valve root was well integrated into host tissues; valve leaflets were unchanged in size, non fibrotic, supple, and functional. Numerous cells positive for a-smooth muscle cell actin were found mostly in the sinus, base, and the fibrosa of the

OPEN ACCESS

Edited by:
Peter Zilla,
University of Cape Town, South Africa

Reviewed by:
Laura Iop,
University of Padua, Italy
Christoph Schmitz,
Ludwig Maximilian University of Munich, Germany

***Correspondence:**
Ionela Movileanu
movileanu.ionela@yahoo.com
Marius Harpa
marius_harpa@yahoo.com

†*These authors have contributed equally to this work and share first authorship*

‡*These authors share last authorship*

Specialty section:
This article was submitted to Heart Valve Disease, a section of the journal Frontiers in Cardiovascular Medicine

Received: *10 May 2021*
Accepted: *05 July 2021*
Published: *19 August 2021*

Citation:
Movileanu I, Harpa M, Al Hussein H, Harceaga L, Chertes A, Al Hussein H, Lutter G, Puehler T, Preda T, Sircuta C, Cotoi O, Nistor D, Man A, Cordos B, Deac R, Suciu H, Brinzaniuc K, Casco M, Sierad L, Bruce M, Simionescu D and Simionescu A (2021) Preclinical Testing of Living Tissue-Engineered Heart Valves for Pediatric Patients, Challenges and Opportunities. Front. Cardiovasc. Med. 8:707892. doi: 10.3389/fcvm.2021.707892

leaflets, and most surfaces were covered by endothelial cells, indicating a strong potential for repopulation of the scaffold.

Conclusions: Tissue-engineered living valves can be generated *in vitro* using the approach described here. The technology is not trivial and can provide numerous challenges and opportunities, which are discussed in detail in this paper. Overall, we concluded that cell seeding did not negatively affect tissue-engineered heart valve (TEHV) performance as they exhibited as good hemodynamic performance as acellular valves in this model. Further understanding of cell fate after implantation and the timeline of repopulation of acellular scaffolds will help us evaluate the translational potential of this technology.

Keywords: acellular scaffolds, autologous cells, bioreactor conditioning, orthotopic implantation, cell seeding

INTRODUCTION

The most frequent pathology in the pediatric population is represented by congenital involvement of the right ventricular outflow tract, accounting for 20% of the total number of cardiac congenital malformations (1). Present alone or associated with other tissues, pulmonary valve stenosis is ranked third in the list of most frequent congenital cardiac conditions (2). For pulmonary valve replacement in this age category group, biological prostheses are preferred, those including the classical glutaraldehyde fixed, cryopreserved homograft bioprostheses, decellularized homografts, or mechanical valves (3). Artificial mechanical valves have the downside of requiring lifelong anticoagulation, whereas the biological valves are characterized by a limited lifespan and functionality, especially in children (4). Heart valve replacement in pediatric patients is a challenging endeavor; in addition to the technical surgical complexity, current valve prosthesis models cannot grow with the somatic growth of the patient and thus require multiple open-heart reinterventions until adulthood (5).

The field of regenerative medicine and tissue engineering strives to develop the next generation of heart valve substitutes, i.e., living-tissue-engineered heart valves (living TEHVs), which could overcome the current available drawbacks of artificial prostheses. Having their own metabolism, TEHVs are expected to have the capacity to grow and develop simultaneously with the body, with no need for anticoagulation and minimal long-term degeneration (6). Essentially composed of scaffolds and cells (7), manufacturing this new type of heart valve substitute represents a research task involving multidisciplinary teams and several challenges. Studies of synthetic (polymeric) scaffolds seeded with endothelial cells and myofibroblasts (8) showed that the presence of repopulating cells was associated with valvular insufficiency secondary to cusps remodeling and retraction. Scaffolds seeded with autologous stem cells (9), or just endothelial cells (10), also revealed multiple drawbacks, a major one being the fibrosis and contraction of the cusps, induced by the seeded cells (9, 11).

Recently, a switch in the traditional paradigm has occurred, where scientists implanted degradable or no degradable scaffolds and used the host body as a living bioreactor, repopulating the scaffold with autologous cells after implantation. In animal models, these scaffolds performed well for 4–6 months, fulfilling their mechanical function. Currently, ongoing clinical trials investigating the behavior of decellularized pulmonary valves implanted in humans are ongoing (12), as well as heart valve replacements with other acellular scaffolds (13). These scaffolds are developed by removal of all antigenic cells, using detergents. They are based on an extracellular matrix composed of collagen and elastin fibers, which are not entirely intact (collagen peptides are released); therefore, after implantation, they could be a target for proteases from infiltrating cells, especially under adverse mechanical and biochemical conditions. In order to create a living heart valve, able to not only accomplish the critical mechanical function but also maintain the matrix homeostasis and respond to stimuli in physiological and/or pathological environments, we developed a pulmonary valve based on a decellularized scaffold seeded with fibroblasts and endothelial cells (ECs) derived from autologous adipose tissue-derived stem cells. Our hypothesis is that a living-TEHV with a controlled composition at cellular and extracellular level will accomplish its mechanical function similarly to the native valve. Our TEHV technology includes three elements: (1) decellularized valve scaffolds as the most suitable biological, structural, and functional component; (2) autologous cells seeded in the appropriate tissue layers for matrix homeostasis; (3) dynamic conditioning in bioreactors before implantation for cell adaptation to physiologic stress.

To test our hypothesis, we proposed the preclinical validation of a scenario with significant translational potential (**Figure 1**). Briefly, this involves *in vitro* repopulation of decellularized pulmonary valves by seeding with autologous fibroblasts (FBs) and ECs derived from adipose tissue-derived stem cells, preconditioning of the living valves in dedicated pulmonary heart valve bioreactors, and orthotopic implantation in sheep with 6 months follow-up. Each step of this scenario is described in detail, documented by results, and complemented by discussion of the challenges encountered and opportunities offered by the study.

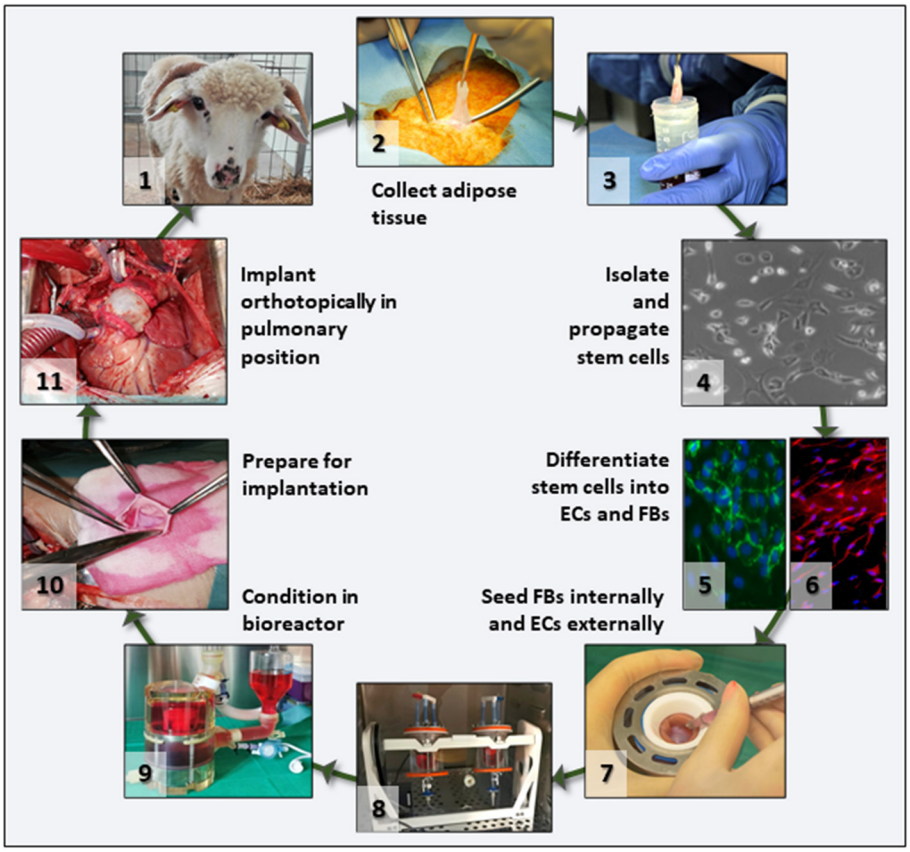

FIGURE 1 | Project overview. Flowchart depicting the main translational scenario steps that were tested in this study. After animal selection **(1)**, adipose tissue was collected under aseptic conditions **(2)**, the tissue transported to the lab in culture medium **(3)**, and stem cells isolated and propagated **(4)**. For differentiation, cells were split in two batches and separately differentiated into ECs **(5)** and FBs **(6)**. Then FBs and ECs were used to seed the acellular valve scaffolds **(7)** by injection and rotation **(8)**. Seeded valves were subjected to BR conditioning in sterile media **(9)** and transported to the operating theater where they were prepared **(10)** and then implanted orthotopically as autologous implants **(11)** in the same animal from which the stem cells had been collected.

MATERIALS AND METHODS

Scaffolds

Ovine hearts were collected immediately after euthanasia at a local abattoir. Animals were represented by mature sheep (male and female, aged 1.5–2.0 years, weighing 50–60 kg). The harvesting technique consisted in maintaining the pericardial sack, ascending aorta, and the pulmonary trunk intact. Following harvesting, hearts were transported on ice to the laboratory for dissection.

The ovine pulmonary valves ($n = 15$) were dissected and extracted with sterile basic surgical tools, preserving 3–4 cm of the circumferentially oriented myocardium at the valve base. Distally, the arterial tissue was sectioned at the level of the pulmonary trunk bifurcation (about 5–6 cm height from the cusps commissure). After rinsing, valve roots were placed in the MechAnnulus^{TM} mounting rings by clamping the myocardium between interlocking metal rings and set in the decellularization system (PDCell^{TM} Aptus Bioreactors, LLC, Clemson, SC, USA) in batches of five roots per system. The pulmonary trunk was cannulated with Luer-barbed adaptors and connected to the perfusion system. The mounting rings are unique in the fact that they provide a no-touch mounting system for valve roots, which does not affect cusp or artery integrity. The decellularization system was perfused by a peristaltic pump with a 30-s off/3-min on cycle over 12 days under a pressure gradient of 4 mmHg (between the intraluminal and the external environment), the last step ending in sterile conditions. Studies performed previously pointed to improved cell removal from the valve roots when using perfusion methods in comparison to only immersion of the heart valves (14, 15). The decellularization procedure started with 24 h of 0.02% NaN_3 in H_2O (Sigma-Aldrich Chemistry, St. Louis, MO, USA) followed by 1 h perfusion of 0.05M NaOH (Lach-Ner, Neratovice, Czech Republic) and rising with H_2O. Three batches of freshly prepared decellularization solution containing 0.05% sodium dodecyl sulfate (Sigma-Aldrich Chemistry, St. Louis, MO, USA), 0.5% TRITON X-100 (PanReac AppliChem, Castellar del Vallès, Spain), 0.5% sodium deoxycholate (Sigma-Aldrich Chemistry, St. Louis, MO, USA), 0.2% ethylenediaminetetraacetic acid (PanReac AppliChem, Spain) in 10 mM hydroxymethyl aminomethane TRIS (Sigma-Aldrich Chemistry, St. Louis, MO, USA) were circulated for

48 h each, followed by enzymatic treatments with 720 mU/ml deoxyribonuclease (PanReac AppliChem, Spain) and 720 mU/ml ribonuclease (PanReac AppliChem, Spain) for 48 h, at 37°C, applied twice. In the last day of the protocol, valves were treated with 70% ethanol and then 2 h with 0.2% peracetic acid for sterilization (Merck KgaA, Darmstadt, Germany) and storage in sterile phosphate-buffered saline (PBS) at 4°C. Further details can be found in our previous publication (14, 15).

To validate the extent of cell removal, the scaffolds underwent quality tests as follows. Histology with 4′,6-diamidino-2-fenilindol (DAPI) nuclear staining on cryosections (Thermo Fisher, Waltham, MA, USA) and hematoxylin/eosin assessed the extracellular matrix architecture and integrity and the absence of cells nuclei. DNA was also extracted from $n = 6$ tissue samples from each decellularization batch, quantified by NanoDrop spectrophotometry and analyzed by EthBr agarose gel electrophoresis, as described before (15). All valves underwent sterility testing as follows: decellularized valve fragments were collected in aseptic conditions, immersed in approximately 3 ml sterile saline, in sterile 15-ml tubes, and transported to the Microbiology Department of UMFST for further processing. Culture-based methods were used for testing the sterility of the valve fragments. For this, each sample was thoroughly vortexed in 0.5 ml sterile saline, and 10 μl was dispersed on blood agar plates (Oxoid, Hampshire, UK) to isolate the potential colonizers. Afterwards, each fragment was immersed in 4 ml Muller–Hinton broth (Oxoid, Hampshire, UK) for enrichment of potentially viable bacteria. The inoculated culture media were incubated at 37°C for 18–24 h in normal atmosphere. The development of colonies and cloudy appearance of the broth followed, respectively, which indicated bacterial colonization. For each batch of valve fragments, the saline solution used for transportation was also tested for potential bacterial contamination, after mixing in 1:1 proportion with 2 × Muller–Hinton broth and incubation at 37°C. A negative control consisting of Muller–Hinton broth only was also used. The eventual colonies that grew on blood agar were isolated. If the broth presented cloudiness, 1 μl was dispersed on blood agar, to isolate the enriched bacteria. The genus or species of the isolated bacteria was identified using routine bacteriological methods (microscopy and biochemical tests). Antibiograms were performed according to EUCAST standards, for epidemiological and infection control purposes.

Cells

Adipose-Derived Stem Cells

Subdermal ovine adipose tissue of about 2 cm^3 was harvested from each sheep from the paravertebral region in an aseptic environment and sterile conditions, in the experimental station of the university. The tissue was quickly immersed in sterile cell culture media composed of Dulbecco's modified Eagle's medium (DMEM) (Sigma-Aldrich Chemistry, St. Louis, MO, USA), 10% fetal bovine serum (Biowest, Nuaille, France), and 1% antibiotic and antimycotic (Sigma-Aldrich Chemistry, St. Louis, USA) at 37°C. Using chemical, enzymatic, and mechanical agents, stem cells were isolated using a method previously described (16). Adipose-derived stem cells (ADSCs) were cultivated in flasks with culture media, in an incubator (37°C, 5% CO_2), and propagated up to passage 3. To extend their usage and availability, the cells underwent cryopreservation in 10% dimethyl sulfoxide in 70% DMEM/20% FBS media cryotubes, at a ratio of 2×10^6 cells/vial, first frozen at 2–3°C/h down to −80°C in a Corning CoolCell™ device, followed by storage at −140°C in a dedicated freezer. Thawing tests followed by cell culture revealed over 85% viability of ADSCs after cryopreservation (17). After thawing, the stem cells were divided into two equal batches and differentiated toward ECs and separately toward FBs before seeding.

Differentiation Toward Endothelial Cell Lineage

To recreate the endothelium, the ADSCs obtained from each animal underwent a chemical and mechanical protocol with minor modifications (18). The ADSCs were cultured on gelatin-coated culture flasks and fed with differentiation media composed of Media 199 (Sigma-Aldrich, St. Louis, MO, USA), 13% fetal bovine serum, 12 ml/L antibiotics, 0.1 g/L L-glutamine (Fisher Scientific, Waltham, MA, USA), and 7.5 U/ml heparin (Sigma-Aldrich, St. Louis, MO, USA) for 1 week at 37°C, 5% CO_2. At the beginning of the second week, the media were supplemented with Endothelial Cell Growth Supplement (ECGS, from EMD Millipore, Burlington, NA, USA), at a concentration of 50 μg/ml and cells fed for an additional 3 weeks, with passaging of the cells at a ratio of 1:3, when 80% confluence was reached. The last week of the differentiation protocol consisted in applying shear forces to the cells by positioning the plates on an orbital shaker at 200 rpm (approximately 12 dynes) in a 37°C, 5% CO_2 incubator (19). Cell culture media were replaced every 3–4 days throughout the experiment. The evaluation of differentiation was assessed by immunofluorescent microscopy for specific EC markers: CD 31 (rabbit polyclonal, Abcam, Cambridge, UK), eNOS (rat polyclonal, Abcam, Cambridge, UK), and von Willebrand factor (rabbit polyclonal, Abcam, Cambridge, UK) at dilutions recommend by the antibody supplier. After differentiation, ECs were frozen in dimethyl sulfoxide (DMSO) and stored at −140°C until ready to seed.

Differentiation Toward Fibroblast Cell Lineage

ADSCs differentiation toward FBs was achieved by supplementing the culture media with 2 ng/ml transforming growth factor-beta1 (Sigma-Aldrich, St. Louis, MO, USA) (20). The protocol took place for 3 weeks with media exchange every 3–4 days and passaging of cells at a confluence of 80%. The assessment of differentiation was performed by immunofluorescent microscopy and Western blotting for specific fibroblast cell epitopes: vimentin, Pro-4-hydroxylase, and collagen type I at dilutions recommend by the antibody supplier. After differentiation, FBs were frozen in DMSO in medium and stored at −140°C until ready to seed.

Seeding

FBs Seeding

To reconstitute the main layers of the valve root, FBs were seeded internally at the cusps base and externally in the adventitia layer (**Figure 4**). First, using a 1-ml syringe, 4×10^6 cells were suspended in 1 ml of culture media, and by injection, the quantity was equally distributed and introduced at the bases of the three cusps. After a period of static immersion in culture media for

4 h, the intraluminal content was separated from the external volume by placing a plastic plug at the distal arterial end of the valve (**Figure 4**). Then, the valve root, while still in the MechAnnulus^{TM} mounting rings, was placed into an acrylic jar, and 16×10^6 cells were suspended in the culture media surrounding the adventitia; the jar containing the TEHV was rotated for 48 h with one rotation per minute (RPM) in a cell culture incubator to facilitate FB adherence to the adventitia.

ECs Seeding

ECs seeding consisted likewise of a static and a dynamic phase. First, 4×10^6 cells suspended in 0.9 ml of culture media were placed in the valve cusps "pockets," distributed equally in 0.3 ml for each cusp, followed by 4 h of static incubation. After plugging the lumen with a sterile plug, 16×10^6 cells were suspended intraluminally in the valve root, and the valves were rotated at 1 rpm for 48 h in a cell culture incubator. For both steps of dynamic seeding, an air pump was attached to the rotator jars *via* a sterile inline filter, continuously enriching the culture media with air from the CO_2 incubator.

Bioreactor Conditioning

The *in vivo* hemodynamic conditions were replicated in the laboratory using a dedicated heart valve bioreactor (Aptus Bioreactors, Clemson, SC, USA). The TEHVs were exposed cyclically to increasing systolic and diastolic pressures and frequency over a period of 5 days, until reaching the physiological pulmonary hemodynamic regimen, as follows. After EC seeding, the plug was removed, and the distal arterial segment was sutured to the cylindrical support, stabilizing the pulmonary artery component of the valve and maintaining it in the anatomical position. The sterile bioreactor components were assembled in the sterile hood, containing the seeded valve. After introducing the culture medium, the bioreactor was placed in the cell culture incubator (37°C, 5% CO_2), attaching the air pump to the system as described above with the rotator. The Aptus Physio^{TM} software was initiated, and the starting systolic pressure was set to 10 mmHg at 17 beats per minute (BPM). On the second day, the pressure was elevated to 15 mmHg at 30 BPM followed by a pressure of 19 mmHg with 45 BPM on the third day. On the last day of conditioning, the pressure was 24 mmHg at a rate of 60 BPM and maintained overnight until surgical implantation. Two additional TEHV were prepared, following identical decellularization, seeding, and preconditioning protocols. These served as cell-seeded, non-implanted controls.

Implantation

The animal study had obtained the approval of the University Ethics Committee of UMFST "George Emil Palade" under number 131/21.10.2016. Details of the pre- and postoperative care of the sheep implanted with TEHV have been described in detail in a recent publication (21).

Experimental animals for this study were sheep, from a local breed "Tsigai metis" produced at the Reghin Research and Development Station for Sheep and Goats, Romania.

The female sheep aged between 14 and 18 months were brought to the Experimental Station of the UMFST, and after 3 weeks of quarantine, while they were examined clinically, they were treated with ivermectin and randomly divided into two groups: Group 1, implanted with unseeded, cell-free acellular pulmonary valve scaffolds ($n = 6$), and Group 2, implanted with autologous cells-seeded pulmonary valve scaffolds ($n = 6$). The sheep in Group 2 were first used to obtain adipose tissue, as described above, and while the cells were isolated, differentiated, and seeded onto scaffolds, the animals were allowed to recover for about 3 weeks. Just before surgery, the sheep were approximately 17–19 months old and weighed around 53 ± 11 kg. Under general, inhalation anesthesia, in extracorporeal circulation, the right ventricle ejection tract was exposed through a lateral thoracotomy in the left third intercostal space. The TEHV was removed from its holder, trimmed to size, and prepared for implantation. After removal of the native pulmonary valve, the TEHV was implanted in an orthotopic pulmonary position. Its functionality was evaluated with transesophageal and epicardial ultrasound at the time of implantation and at explantation using a Mindray DC-N6 echocardiograph (Mindray, Shenzhen, China). For the transthoracic approach, the P7-3 transducer was utilized, respectively, P7-3T, for the transesophageal ultrasound examination. By two-dimensional examination, the morphology and movement of the valve components were examined, in addition to the opening and closing mechanisms. By Doppler, the competence was evaluated along with the presence of stenosis. After surgical implantation, the animals were followed up over a period of 6 months. Clinical signs were observed and recorded along with their somatic development. Periodic transthoracic ultrasound examinations were performed under mild animal intravenous sedation. At the end of the follow-up period, the sheep weighing about 70 ± 9 kg underwent transesophageal and epicardial ultrasound under general anesthesia with orotracheal intubation followed by explantation of the valves. Explants were macroscopically examined and immersed in 10% neutral buffered formaldehyde (Sigma-Aldrich, St. Louis, MO, USA) followed by embedding in paraffin. Standard histological sections were performed, and subsequently, mounting on glass slides and hematoxylin/eosin staining were realized. For immunohistochemistry, we utilized a Dako mouse antismooth muscle actin antibody clone 1A4 (M0851) at 1:100 dilution and a horseradish peroxidase (HRP) detection kit as recommended by the manufacturer (Dako, Glostrup, Hovedstaden, Denmark). For quantitative analysis, nine random images were taken at 40× magnification from a-SMA IHC-stained slides from each group (three from the valve base, three from the mid leaflet area, and three from the tip), and the number of positive (brown) cells per high power field (HPF) was calculated and compared between groups.

Statistics

Single-factor analysis of variance (ANOVA) was used to compare infiltrating cell numbers and echocardiographic measurements between the two TEHV groups.

RESULTS

Scaffold Decellularization and Sterilization

For this study, we performed nine perfusion decellularization procedures, yielding a total of 45 decellularized valves. One valve from each batch of five was randomly selected for quality control. Macroscopic evaluation of each valve at the end of the decellularization protocol did not reveal any signs of mechanical tears in any of the valve components. Decellularized valves acquired the "snow-white" color typical of acellular tissues. The sterility tests performed at the protocol finale revealed the absence of microbial contamination of all valves and of the storage media, except for four valves, which were removed from the study. Histological assessment by fluorescent staining for nuclei (DAPI) and classic optical microscopy (H&E stain) revealed preserved tissue matrix architecture and the three layers in the valve cusps, sinuses, and arterial walls along with complete absence of cell nuclei (**Figure 2**). These histological findings were confirmed by DNA extraction and quantitation, showing >98% reduction of DNA content and total absence of nucleic material detected by ethidium bromide agarose electrophoresis (**Figure 2**).

Scaffold Revitalization With Cells

Fourteen ADSCs cultures were obtained from $n = 14$ sheep, generating a total of over 100×10^6 cells. Each batch of cells was carefully labeled with the sheep number before freezing, to allow for autologous use later. To extend their availability and usability, all cells underwent cryopreservation in DMSO followed by thawing when needed for differentiation. ADSCs multipotency was confirmed earlier using specific histological stains after differentiating them toward osteogenic, adipogenic, and chondrogenic lineages using special kits (17).

ECs Differentiation

Twelve batches of ADSCs were differentiated into ECs in this study, using cell culture on gelatin-coated flasks in the presence of ECGS and shear. ADSCs exposed to these conditions displayed the ability to uptake DiI-AcLDL and were positive for CD31, vWF, and eNOS markers (**Figure 3**), while undifferentiated ADSCs exhibited very little reactivity for these markers and essentially did not uptake any DiI-LDL. Overall, about 68% of human ADSCs (hADSCs) stained positive for EC markers after differentiation.

FBs Differentiation

Twelve batches of FBs were prepared during this study, generating over 300×10^6 cells. To evaluate the effectiveness of differentiation, we stained the cells for vimentin, prolyl-4-hydroxylase (P4H), and collagen type I and analyzed them by immunofluorescence (**Figure 3**). In addition, cells were extracted for protein and analyzed for the presence of the same markers by Western blotting. ADSCs differentiated into FBs expressed slightly upregulated levels of vimentin and significantly upregulated expression of P4H and type I collagen, while undifferentiated ADSCs expressed very low or undetectable levels of these FBs markers. Overall, about 75% of hADSCs stained positive for HSP47, P4H, and COL I.

Cell Seeding and Bioreactor Conditioning

The goal of seeding was to place cells in the appropriate anatomical areas and revitalize the scaffold before implantation (**Figure 4**). To achieve this goal, we first injected FBs in the valve cusp interstitium, then used solid plugs to separate the lumen from the adventitia, and rotated the valve in an FBs suspension for adventitial seeding. Finally, we seeded the valve lumen with a suspension of ECs on a rotator. The valves functioned well in the bioreactor, with wide opening (mean geometrical orifice area of $\sim$1.4 cm^2 for valves of mean external diameters of approximately 16 mm) and perfect closure (**Figure 4**). The control TEHVs, i.e., the seeded, conditioned but not implanted valves, were assessed by histology, which revealed the presence of FBs at the cusps base and the adventitia and ECs on the luminal surface of the valve cusps (**Figure 4**). Finally, seeded valves were exposed to a gradual increase in the frequency and pressure until reaching the hemodynamic regimes of pulmonary circulation. Central closure with complete opening of the three cusps was observed along with fluid movement of the sinuses and arterial walls of the valve, synchronically with the cardiac cycle's phases—systole and diastole. No signs of tears or laceration of tissue were documented during the conditioning protocol.

Surgical Implantation and Follow-Up of TEHV

All animals included ($n = 12$) in the study successfully underwent the surgical implantation procedure. Animals were randomly divided into Group 1 ($n = 6$) implanted with acellular scaffolds, not seeded with cells, and Group 2 ($n = 6$) acellular scaffolds seeded with autologous FBs and ECs derived from ADSCs and conditioned in bioreactors (**Figure 5**). The first two valves from Group 1 were explanted early due to infective endocarditis. These were replaced by two new animals for Group 1. All surgeries were successful, with an average of 3.5 h of surgery time and with an average of 70 min of cardiopulmonary bypass, without any associated intraoperative death. In the immediate postoperative period, animals presented proper clinical status and evolution. Limited secretions were presented on the pericardial drain before removal of the tubing. Surgical incisions healed without any signs of infections or pathological accumulations. No fever or signs of acute heart failure were recorded. Restoration of vital organ function was present immediately after extubating.

Functionality evaluation of the TEHVs was periodically assessed using ultrasound for up to 6 months (**Table 1**). The initial evaluation was performed intraoperative using the transesophageal probe and epicardial access. The two-dimensional morphological assessment presented physiological movement of the three cusps with central cooptation and good opening.

Echocardiography in Group 1, control TEHVs, pointed to the presence of mediastinal collections in two out of the six animals and a pericardial effusion that was drained. Animals presented with preserved ventricular ejection fraction along with no changes in the cardiac cavities dimension excepting one animal with light dilatation of the right cardiac cavities resulting

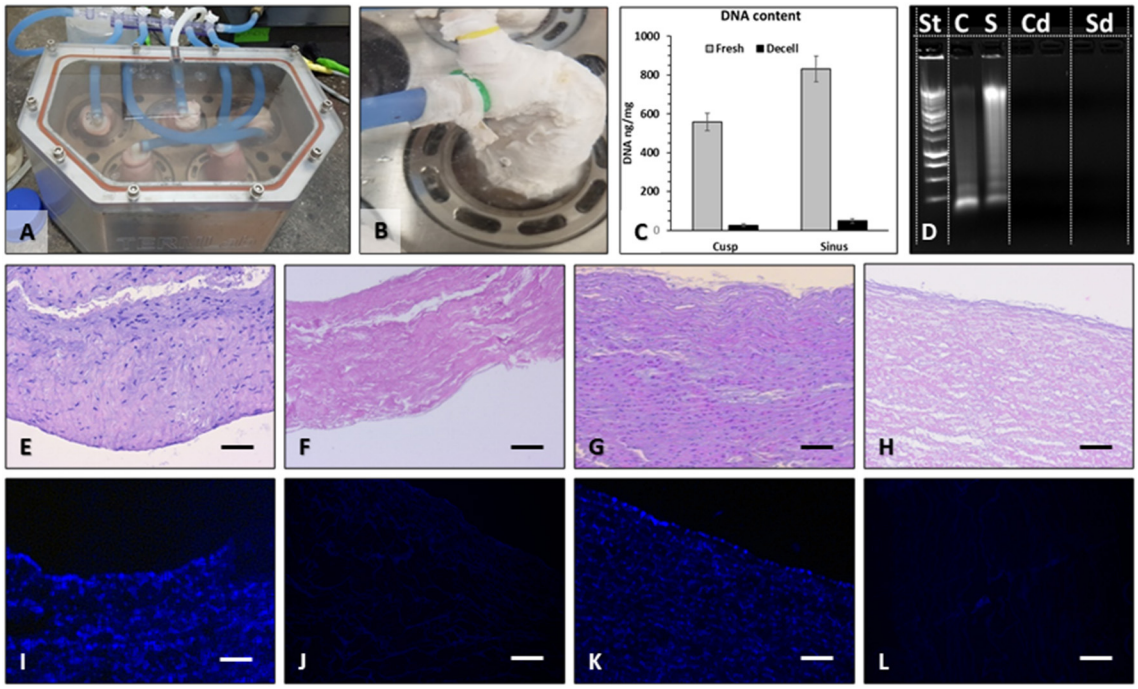

FIGURE 2 | Pulmonary valve decellularization. Valves were mounted onto purpose-designed external supports and inserted into the pressurized system **(A)**, which perfused each valve individually **(B)** with detergents and enzymes. For decellularization validation, DNA was extracted from the sinus and cusp tissues and quantified by NanoDrop **(C)**, using fresh tissues as controls. Extracted DNA was also run on ethidium bromide agarose gels by electrophoresis and imaged in UV light **(D)**. St, molecular weight DNA standard ladder; C, fresh cusp; S, fresh sinus; Cd, decellularized cusp, two lanes; Sd, decellularized sinus, two lanes. Histology using H&E stain of fresh cusp **(E)**, decellularized cusp **(F)**, fresh sinus **(G)**, and decellularized sinus **(H)** and using DAPI stain for nuclei (blue) in fresh cusp **(I)**, decellularized cusp **(J)**, fresh sinus **(K)**, and decellularized sinus **(L)**. Bars in all histology images are 200 μm.

from an important valvular regurgitation. Moderate insufficiency was observed in one animal and trivial in another.

In Group 2 of cell-seeded TEHVs, five out of six animals developed non-hemodynamically significant circumferential pericardial collections, with no indication for surgical drainage. On consecutive exams in two animals, resorption of the liquid was noted. At repeated exams, two animals presented enlarged right cavities. One of these two animals additionally developed valve stenosis with a planimetric measured area of 1.2 cm^2. In terms of regurgitation, one valve presented a moderate degree of insufficiency but with no impact on the right heart cavities. Due to technically surgical malposition (higher suture on the TEHV basis) of one TEHV, it presented mild central regurgitation. TEHV cusps revealed to be thin, supple, and mobile, with complete opening on echocardiography. Prior to the animal's euthanasia, TEHVs were examined by epicardial ultrasound.

TEHV Explants and Their Analysis

At 6 months after implantation, animals were prepared for euthanasia and explantation of the TEHV. At explantation, the implants and anastomoses were intact, and the valve root was well integrated into the host tissues, with a shiny endothelium covering the whole implant and the anastomoses, with no evidence of thrombi. The tubular implants looked unaltered and could hold saline if added distally, pointing to competent valves. The implants were then sectioned longitudinally, and opened roots were photographed. The valve leaflets were unchanged in size or thickness and were non-fibrotic, thin, supple, and semitransparent. Numerous cells positive for a-smooth muscle cell actin were found mostly in the sinus, base, and the fibrosa of the leaflets, indicating a strong potential for repopulation of the scaffold. Flat monolayers of endothelial cells were found on the surfaces of the valve leaflets, the sinus walls, and the pulmonary artery (**Figure 6**). No major differences were noted in performance or cell repopulation of cell-seeded vs. non-cell-seeded valves in the sheep study.

DISCUSSIONS

Key Findings

In this project, we proposed a translational scenario (**Figure 1**) based on our previous experience with acellular valve scaffolds, which performed very well hemodynamically in the right ventricular outflow tract (RVOT) in sheep (22, 23). The decellularization protocol proved to be effective in removing all nucleic materials while preserving the integrity and architecture of the ECM, as reported earlier in pilot studies (15). Acellular valve scaffolds have several advantages: they preserve the natural 3D architecture, have excellent hemodynamics and biomechanics, are highly biocompatible, are not antigenic,

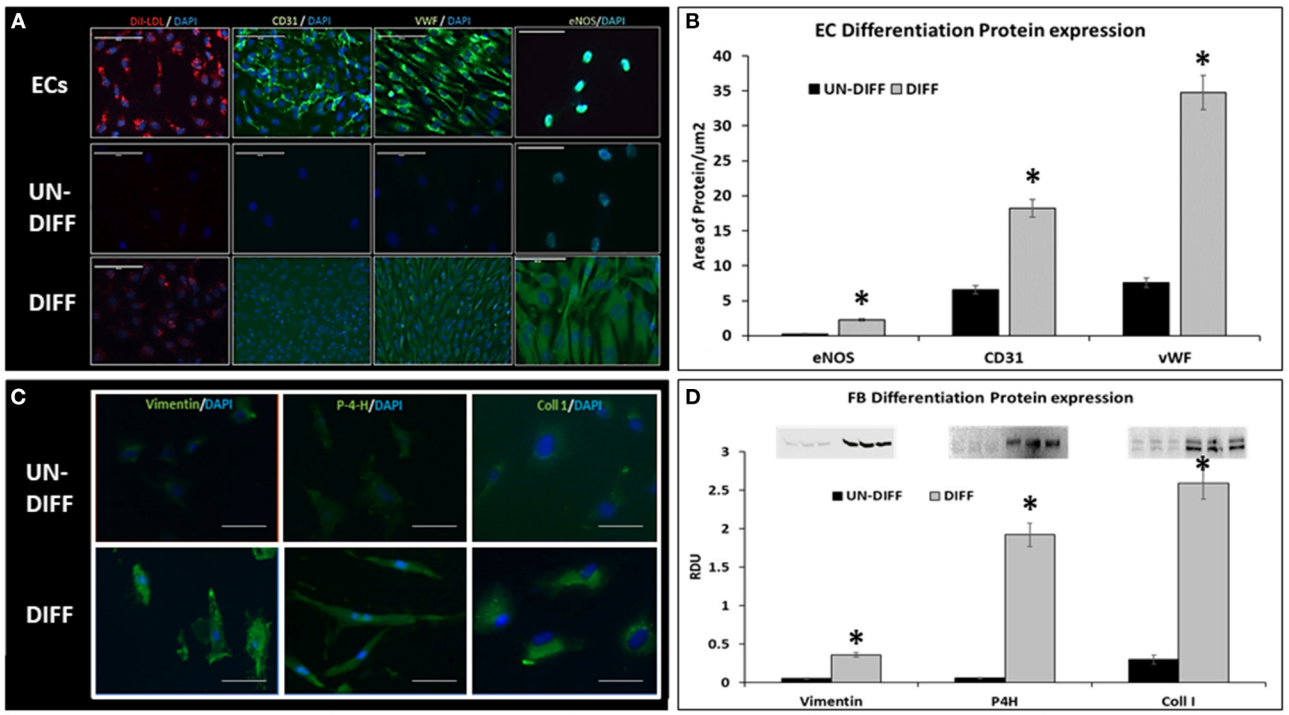

E Human Cells	Ac-LDL uptake	eNOS	CD31	vWF
ECs (HUVECs)	+++	+++	++	+++
UN-DIFF	-	+	+/-	+
DIFF	++	+++	++	+++

FIGURE 3 | Differentiation of adipose-derived stem cells. **(A)** For differentiation into ECs, ADSCs were subjected to ECGS media followed by dynamic shear. HUVECs (ECs) served as controls. For validation, cells were incubated with DiI-labeled LDL (DiI-LDL) and imaged by fluorescence microscopy (intracellular red particles). Cells were also immunostained for CD31, VWF, and eNOS (green, positive). Nuclei were stained with DAPI. Bars are 100 μm. **(B)** amounts of positive eNOS, CD31, and VWF proteins in immunofluorescent images were assessed by semiquantitative image analysis normalized to area. For differentiation into FBs, ADSCs were exposed to low doses of TGF and stained for **(C)** vimentin, prolyl-4-hydroxylase (P-4-H), and collagen type I (Coll 1). Cells were also analyzed by Western blotting for same antigens and band intensity measured in the BioRad imager **(D)**. A semiquantitative analysis of cell differentiation is shown in **(E)**. Asterisk in Panels **(B,D)** designate statistically significant differences when compared to UN-DIFF. In all panels, UN-DIFF, undifferentiated stem cells; DIFF, stem cells that have been exposed to EC or FB differentiation conditions.

maintain integrity for extended periods of time, and serve as excellent porous substrates for cell adhesion and repopulation (24, 25). Despite exposing bare collagen surfaces to flowing blood, we could not detect any thrombus structures in any of the explants, and there was no need for systemic anticoagulation. Notably, TEHVs can be considered tissue-derived bioprostheses heart valves, which, according to current clinical guidelines, require oral anticoagulation with Vitamin K antagonists for 3 months postoperation (9). In pilot studies, we explanted two acellular valves: one was explanted early (after 48 h) and a second after 7 days, both due to non-valve-related issues. As seen by histology, the valve at 48 h showed a thin layer of fibrin on the surfaces, which disappeared after 7 days (data not shown) and clearly was not present on any of the explanted valves at 6 months. This was not investigated systematically in the current study but confirms results published earlier by us and others (8, 26). Similarly to other investigators using decellularized valves (12, 27), in our hands, there was no inflammatory or immune reaction to the implant, no calcification was noted, and no pannus or tissue overgrowth was found in any of the valves analyzed in this study, indicating high biocompatibility and lack of antigenicity.

Earlier, we seeded acellular valve scaffolds with freshly isolated autologous stem cells (ADSCs) and immediately implanted them in sheep, without any stem cell differentiation or any dynamic bioreactor preconditioning; as most of the cells died within 3–4 days after implantation, we noted that stem cells were very vulnerable to dynamic functional pressures and flow (22), which was also confirmed *in vitro* using cell-seeded scaffolds tested in bioreactors (28). To overcome these issues, we hypothesized

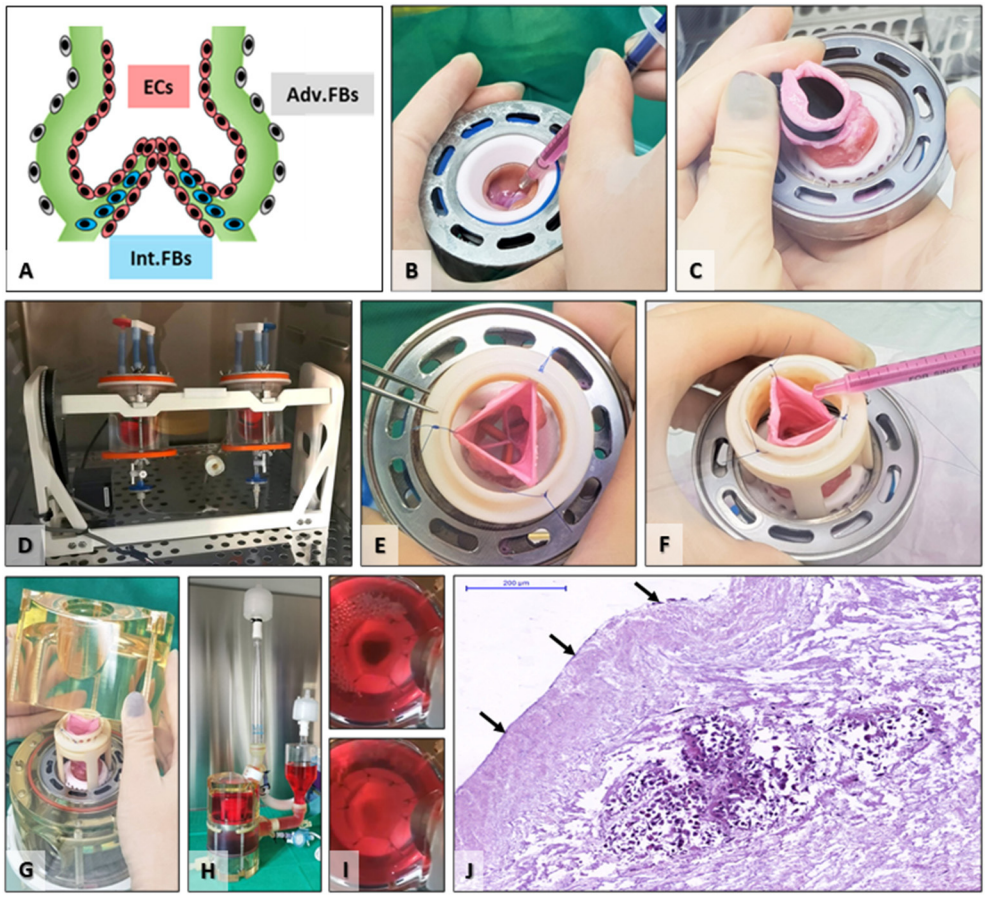

FIGURE 4 | Scaffold seeding and bioreactor preconditioning. **(A)** Schematic depicting the targeted cell distribution by seeding FBs internally (Int.FBs, blue) as well as adventitially (Adv.FBs, gray) and ECs in the root lumen, on cusps, sinus, and artery surfaces (ECs, red). **(B)** FBs seeding by injection in the base of each cusp. **(C)** Placing of an aortic plug to separate the lumen from the exterior environment. **(D)** TEHVs with aortic plugs placed in FBs suspension in the acrylic seeding cups on the rotator for adventitial seeding. **(E)** After removal of the plug, the pulmonary artery was temporarily maintained open using three or more single sutures, **(E)** for intraluminal seeding of ECs **(F)**. **(G)** Positioning the seeded valve in the bioreactor, **(H)** fully assembled heart valve bioreactor just before insertion in the incubator. **(I)** still shots saved from video recordings taken during valve conditioning in the bioreactor showing open (top) and closed (bottom) positions. **(J)** H&E staining of control TEHV (seeded and preconditioned, not implanted); arrows point to ECs surface coverage, while the cell-rich island in the middle is representative of interstitially injected FBs.

that seeding with mature cells and implementing progressive dynamic conditioning would enhance the viability of cells after implantation. Therefore, in current study, we decided to isolate the stem cells, differentiate them *in vitro* into more robust FBs and ECs, and use those cells for scaffold seeding; in addition, we subjected seeded scaffolds to progressive adaptation in heart valve bioreactors, by slowly increasing flow, frequency, and pressures so that within 5 days, the constructs reached pulmonary valve conditions. Endothelialization is a fundamental target for researchers and clinicians involved in vascular and valvular replacements (29, 30). Varied modalities to differentiate and to promote ADSCs commitment toward ECs were described, including genomic manipulation (31), immune modulation (32), induced hypoxia (33), and specific growth factors (34, 35). Comparative studies of differentiation of ADSCs toward ECs lineage revealed improved results when combinations of ECGS and shear were used (36, 37) pointing to the importance of recreating the *in vivo* conditions. Finally, in previous works, we mounted valve scaffolds in acellular pericardial tubes and implanted them as a shunt in the RVOT, which did not fully mimic the appropriate clinical application of such valves (22, 23). In the current study, we implanted the revitalized valves orthotopically using open-heart surgery under cardiopulmonary bypass (CPB), which better approximates the clinical use of such valve implants. Cell-seeded valves maintained their viability after progressive bioreactor conditioning and functioned well *in vivo* for 6 months. Cells positive for a-smooth muscle cell actin were found in the valves interstitium flat monolayers of endothelial cells were found on the surfaces indicating a strong potential for repopulation of the scaffolds.

Conclusions

To our knowledge, this is the first study to document preclinical validation of decellularized valvular scaffolds repopulated with heart-valve-specific cells differentiated from autologous

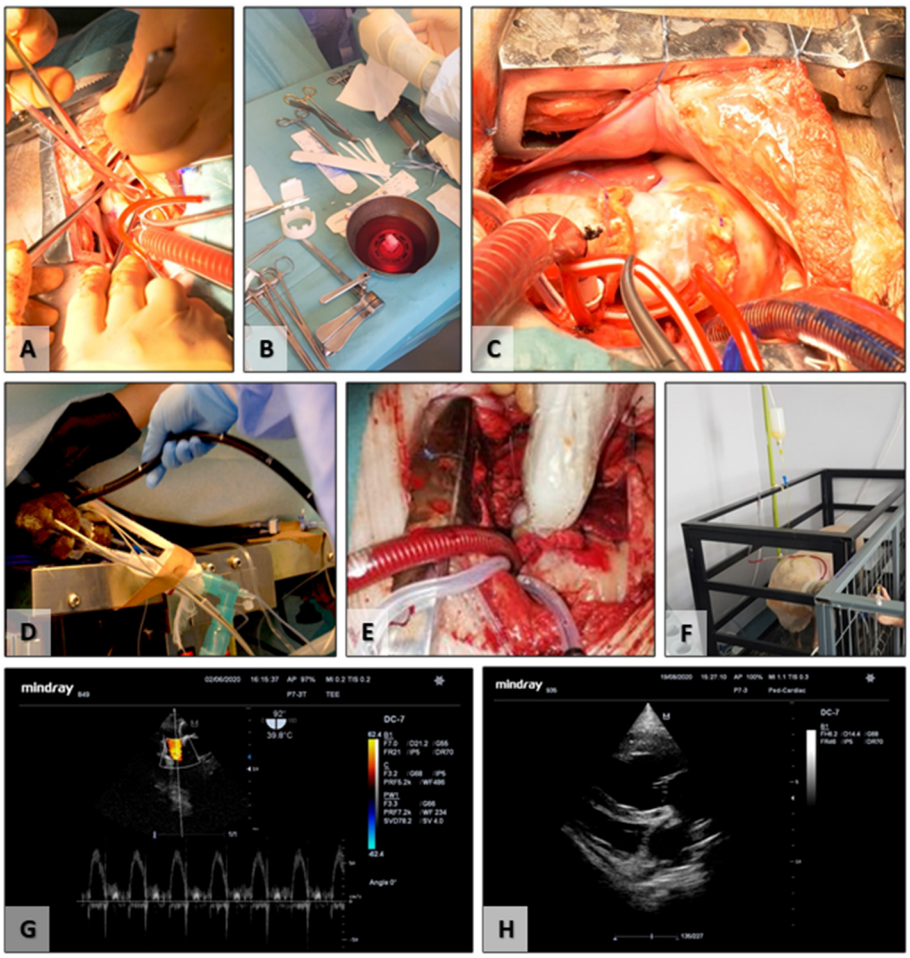

FIGURE 5 | Surgical implantation and follow-up. **(A)** Removal of the native pulmonary valve; **(B)** preparation of the TEHV before implantation; **(C)** final surgical aspect, postimplantation; **(D)** insertion of the transesophageal ultrasound probe; **(E)** intraoperative epicardial ultrasound; **(F)** postoperative experimental animal transthoracic ultrasound; **(G)** transesophageal ultrasound evaluation of the TEHV; **(H)** postoperative transthoracic evaluation of the cardiac cavities and TEHV.

stem cells and preconditioned before implantation using a dedicated bioreactor.

Our decellularization protocol resulted in acellular and sterile heart valve scaffolds, confirmed by histological assessment, DNA quantitation, and sterility tests. Preserved valve geometry and structure were documented along with conserved matrix architecture. Scaffold functionality was further assessed by ultrasound evaluation while functioning in a bioreactor, revealing absence of valvular regurgitation (data not shown here). Ovine ADSCs proved to be a convenient source of stem cells, their cryopreservation after propagation proving to be a good option for increasing their availability. Their differentiation toward heart-valve-specific cell lineages was successful, with upregulation of major markers, albeit not reaching expressions of adult mature target cells. Seeding efficacy was not wide ranging, with areas of scaffolds remaining cell free interstitially; however, cell viability was maintained during the seeding protocol. Bioreactor preconditioning did not change the integrity of the scaffold or the seeded cells. Surgical implantation in pulmonary position was successful, with no major incidents or complications, while the animal's follow-up proved challenging due to poor transthoracic ultrasound windows and their rapid somatic growth. Notably, host cells were found populating the implanted scaffolds in large numbers, with preference for the cusp base, fibrosa, and spongiosa layers of the valve cusps. Cells were distributed homogeneously, resembling regeneration processes more that hyperplasia. Overall, we concluded that cell seeding did not negatively affect TEHV performance, as they exhibited as good hemodynamic performance as acellular valves in this model.

Challenges and Opportunities

Scaffolds

Minimizing mismatch in the size of implanted valves is very important clinically (38). Initially, we worked with adult porcine valves (22), but they were too large for orthotopic implantation in the ovine pulmonary position; we tested a few valves from juvenile pigs that matched in size, but it was very difficult for us to

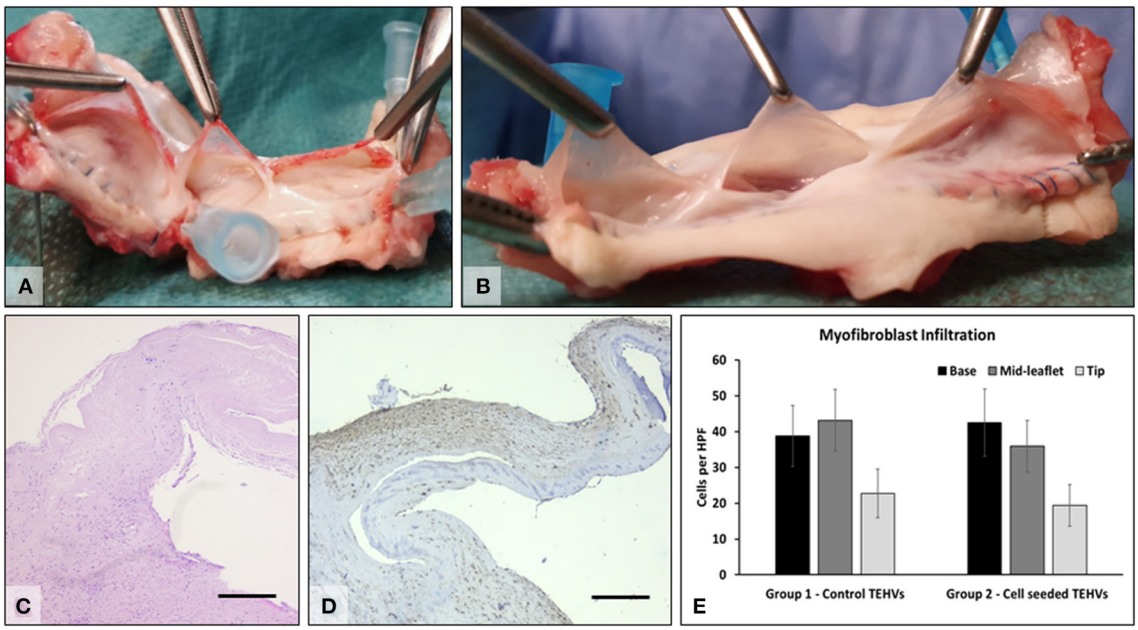

FIGURE 6 | Explant analysis. **(A)** Representative macroscopic images of freshly explanted TEHV and **(B)** cell-seeded TEHV. **(C)** Representative H&E stain of cells found within the valve interstitium; **(D)** immunohistochemistry for alpha-smooth muscle actin (brown, positive). Bar is 200 μm. **(E)** Quantitative data on alpha-smooth muscle actin positive cells infiltrated in the base, middle, and tip areas of the TEHVs. Statistical analysis revealed no significant differences in the number of infiltrated cells between the two valve groups.

ensure a constant supply of juvenile pigs for this study. Thus, we decided to pursue ovine tissue sources, which were a much better size match.

Decellularization

Removing all the cells was easily achieved using the perfusion system utilized before for aortic valve roots, with minor modifications in procedures (14), including adaptation of the mounting rings and a diminution of working pressures to less than physiological 20 mmHg. Sterility and long-term storage are a major challenge in TEHV. It is paramount that decellularization protocols efficiently remove all cells from cusps, muscle, and artery. In earlier phases of the project, we utilized peracetic acid sterilization of the valves while they were still mounted in the support rings, inside the perfusion system. We realized later that certain areas of the root tissues (clamped in the support rings) were not sterile because of lack of access to the sterilant. A few of these valves that were implanted had to be explanted early due to endocarditis. To solve this issue, we decided to take out the valves from the rings after decellularization, sterilize the entire root by immersion, and then remount them in a new set of sterile rings for further seeding and conditioning. Routine sterility testing of tissues and storage solutions is highly recommended throughout the process of manufacturing TEHV.

Cells

ADSCs are relatively easy to isolate and culture from subdermal adipose tissue samples. In a pilot study, we collected adipose tissue from several anatomical areas to determine the optimal source for ADSCs and found the interscapular area as most favorable (39). When needed, ADSCs can be safely cryopreserved for later use. Differentiated stem cells expressed some, but not all, specific markers for FBs or ECs; it is not clear whether this affects cell behavior after implantation. Furthermore, it is not clear if cryopreservation could be applied after ADSC differentiation into FBs and ECs. More detailed studies on ADSC-derived FBs and ECs are warranted.

Seeding

Manual injection in the cusp interstitium was limited to just a few sites, and it is not clear if cell migration took place later from the cell bolus. We do not know at this point if the cells found in the 6-month explants were the same cells that were seeded initially, or they were host-derived infiltrated cells. More studies with cell tracers on a discrete timeline are needed to answer this question. In addition, improved interstitial seeding methods are needed to address the need to distribute cells in specific anatomic areas more homogeneously.

Bioreactor

The ramping-up profile was not optimized but rather designed rationally. A time-dependent study looking at effects of different adaptation regimes on cell attachment and viability is needed. We do know that the bioreactor can maintain cell viability for up to 2 weeks (40). Maintaining valves alive in the bioreactor could be useful especially if implantation cannot occur as scheduled. Assembly of the bioreactor and mounting of the valve in sterile conditions are not trivial and require extensive preparation

TABLE 1 | Echocardiographic evaluation of the TEHVs.

Timeline	Initial evaluation—at implantation			End of the follow-up evaluation		
Animal #	**Right and left heart morphology and function**	**TEHV morphology and function**	**Trans- TEHV maximum velocity (m/s)**	**Right and left heart morphology and function**	**TEHV morphology and function**	**Trans- TEHV maximum velocity (m/s)**
Group 1 - control TEHVs						
#1	Normal size and function	Normal function	0.5	Normal size and function	Trivial regurgitation	0.7
#2	Normal size and function	Normal function	0.8	Normal size and function	Moderate regurgitation	0.5
#3	Normal size and function	Normal function	0.7	Dilatation of right ventricle	Important regurgitation	0.7
#4	Normal size and function	Normal function	0.6	Normal size and function	Normal function	0.6
#5	Normal size and function	Normal function	0.5	Normal size and function	Normal function	0.7
#6	Normal size and function	Normal function	0.8	Normal size and function	Normal function	0.7
	Mean +/– SEM		**0.65+/– 0.13**	**Mean +/– SEM**		**0.65+/−0.08**
Group 2 - cell seeded TEHVs						
#1	Normal size and function	Normal function	0.7	Dilated right ventricle	Important regurgitation	0.5
#2	Normal size and function	Normal function	0.8	Normal size and function	Normal function	0.7
#3	Normal size and function	Normal function	0.5	Normal size and function	Moderate regurgitation	0.6
#4	Normal size and function	Normal function	0.6	Normal size and function	Normal function	0.6
#5	Normal size and function	Normal function	0.7	Dilated right ventricle and pulmonary artery trunk	Hyper-echogenic aspect of the TEHV with impaired opening of the cusps	2.4
#6	Normal size and function	Mild regurgitation	0.7	Normal size and function	Mild regurgitation	0.7
	Mean +/– SEM		**0.66 +/– 0.10**	**Mean +/– SEM**		**0.91 +/−0.73**

Statistical analysis revealed no significant difference between the mean maximum trans-TEHV velocity between the two groups at all time points ($p = 0.06$).

and attention to detail. Preassembly of the major bioreactor components (reservoirs, connecting tubes, transducers, and atrial and ventricular chambers) in the sterile hood was instrumental in reducing the time it took for rapid mounting of the living valves. In our hands, no signs of microbial contamination of the valves or the culture media were observed during bioreactor conditioning.

Implantation

Despite timely coordination between the tissue engineering lab and the operating room, valve preparation in the operating theater can sometimes take longer than expected, or the patient could require extra care before implantation. This raises the question of how to maintain valve viability while in the operating room, using cold storage, a temporary warm storage solution, or even a transportation bioreactor. In the current study, the lab was in the vicinity of the animal facility, which reduced transportation time to a minimum. Echocardiography in sheep was found difficult unless in the open chest, where transepicardial access allowed for excellent imaging. The heart and its structures were periodically examined through non-standard transthoracic echocardiography windows given the brisk animal's somatic development in the postoperative period and emerging distortions in the mediastinal anatomy; these aspects represented significant limitations for an adequate ultrasound evaluation. Additionally, in the immediate postoperative period, examinations were limited by postsurgical inflammation processes. Considering the above stated constraints, the transthoracic examinations were restricted to evaluation of mediastinal collections. Visualization of TEHV proceeded with morphological evaluation of valve components, interrogation with both color and pulse Doppler, and evaluation of the existence of any degree of regurgitation, stenosis, or both. Regarding the TEHVs, when they could not be visualized directly, appearance of indirect signs of valvular dysfunction such as dimension and functionality of the right and left ventricles and atria was assessed.

Post Explant Analysis

Histology on unimplanted decellularized tissues is sometimes tricky. The classical stains do not always bind efficiently to

decellularized tissue components, and elastin autofluoresces intensely after decellularization. We found that washing of detergent-decellularized tissues with 70% ethanol before histological processing improved outcomes of histological analysis. Histology on explanted tissue, however, worked out much better, presumably because of host cells and protein infiltration. Immunohistochemistry was also found difficult at times because of paucity of antisheep antibodies and, at times, the diaminobenzidine reagent bound to collagen in decellularized tissues in the absence of any antibodies.

Future Directions for Research

Further work needs to be performed to fine-tune the different aspects of this translational scenario. Stem cells could be obtained from other sources, including induced pluripotent stem cells (iPSCs), and these could be differentiated *in vitro* into the desired target cells. Seeding devices capable of inserting cells in the appropriate sites are currently being designed and tested in our group. Seeded cells should be labeled by a permanent tag that would be stable and transmissible to daughter cells and monitored *via* a convenient imaging technique. This type of study should be implemented together with a more detailed long-term investigation with more numerous time points, looking at the fate of TEHV implanted in juvenile sheep and how they adapt to somatic growth. This should be accompanied by more reliable imaging follow-up; investigation of blood parameters of inflammation, immune reactions, and coagulation; and precise assessment of the ability of the TEHV to grow with the somatic growth of the patient. To assess growth, markers should be placed strategically in different areas of the implant, and tissue thickness should be measured at all time points. A comparison of cell-seeded scaffolds with cell-free scaffolds will allow to draw important conclusions relative to the need for *in vitro* repopulation before implantation, currently a topic of controversy. Several groups are investigating cell-free approaches, relying on the body's ability to repopulate or regenerate scaffolds with the appropriate cells (41, 42); however, it is not clear at the moment whether this response is a true regenerative process or a fibrotic healing reaction. We also do not know if implantation of a cell-seeded TEHV would stimulate or suppress local regenerative and/or fibrotic processes. Overall, we believe that with our approach, we are getting closer to the target, and with further interrogation, successful implementation of TEHV will benefit pediatric patients and young adults.

DATA AVAILABILITY STATEMENT

The raw data supporting the conclusions of this article will be made available by the authors, without undue reservation.

ETHICS STATEMENT

The animal study was reviewed and approved by University Ethics Committee of UMFST George Emil Palade under number 131/21.10.2016.

AUTHOR CONTRIBUTIONS

KB, GL, ThP, AS, and DS: concept, data analysis, and manuscript. IM, TeP, AM, MC, LS, MB, and AC: scaffold development, cell culture, and bioreactors. MH, HuA, LH, HaA, CS, DN, BC, RD, HS, and OC: animal surgery and explant analysis. All authors contributed to the article and approved the submitted version.

FUNDING

This paper was financed by a grant from the Competitiveness Operational Programme 2014–2020, tissue engineering technologies for cardiac valve regeneration, valve-regen, id P_37_673, Mysmis code 103431, contract 50/05.09.2016 (to DS); by NIH grant 1P30GM131959 from NIGMS (to DS); NIH grant 1R01HL133303 (to AS); and funding from the Harriet and Jerry Dempsey Endowment (to DS).

ACKNOWLEDGMENTS

We would like to acknowledge the excellent technical support of the veterinary technicians from the Experimental Station at the University of Medicine, Pharmacy, Science and Technology (UMFST) George Emil Palade, in Targu Mures, Romania, where the animal studies have been performed. These include Dr. Gabriela Marcus, Popeiu Teodora, Kinda Csilla, and Popeiu Ana. We would also like to thank Negru Bianca Catalina, Bartha Zsolt Mihaly, Veres Mihaly, and Oana Moldovan for surgical support. Finally, we acknowledge the outstanding logistical and financial support from the UMFST leadership including Prof Dr. Leonard Azamfirei, university rector, Conf Dr. Olah Peter, university scientific prorector, and Nicoleta Suciu, director of the Research Programme office.

REFERENCES

1. Kogon BE, Rosenblum JM, Mori M. Current readings: issues surrounding pulmonary valve replacement in repaired tetralogy of fallot. *Semin Thorac Cardiovasc Surg.* (2015) 27:57–64. doi: 10.1053/j.semtcvs.2015.02.010
2. Schwedler G, Lindinger A, Lange PE, Sax U, Olchvary J, Peters B, et al. Frequency and spectrum of congenital heart defects among live births in Germany: a study of the Competence Network for Congenital Heart Defects. *Clin Res Cardiol.* (2011) 100:1111–7. doi: 10.1007/s00392-011-0355-7
3. Protopapas AD, Athanasiou T. Contegra conduit for reconstruction of the right ventricular outflow tract: a review of published early and mid-time results. *J Cardiothorac Surg.* (2008) 3:62. doi: 10.1186/1749-8090-3-62
4. Zhang BL, Bianco RW, Schoen FJ. Preclinical assessment of cardiac valve substitutes: current status and considerations for engineered tissue heart valves. *Front Cardiovasc Med.* (2019) 6:72. doi: 10.3389/fcvm.2019.00072
5. Jacobs JP, Mavroudis C, Quintessenza JA, Chai PJ, Pasquali SK, Hill KD, et al. Reoperations for pediatric and congenital heart disease: an analysis of the Society of Thoracic Surgeons (STS) congenital heart surgery database. *Semin Thorac Cardiovasc Surg Pediatr Card Surg Annu.* (2014) 17:2–8. doi: 10.1053/j.pcsu.2014.01.006

6. Kheradvar A, Groves EM, Dasi LP, Alavi SH, Tranquillo R, Grande-Allen KJ, et al. Emerging trends in heart valve engineering: Part I. Solutions for future. *Ann Biomed Eng.* (2015) 43:833–43. doi: 10.1007/s10439-014-1209-z
7. Kluin J, Talacua H, Smits AI, Emmert MY, Brugmans MC, Fioretta ES, et al. In situ heart valve tissue engineering using a bioresorbable elastomeric implant - From material design to 12 months follow-up in sheep. *Biomaterials.* (2017) 125:101–17. doi: 10.1016/j.biomaterials.2017.02.007
8. Hoerstrup SP, Sodian R, Daebritz S, Wang J, Bacha EA, Martin DP, et al. Functional living trileaflet heart valves grown in vitro. *Circulation.* (2000) 102:III44–9. doi: 10.1161/01.CIR.102.suppl_3.III-44
9. Harpa MM MI, Sierad LN, Cotoi OS, Suciu H, Sircuta C, Preda T, et al. Pulmonary heart valve replacement using stabilized acellular xenogeneic scaffolds; effects of seeding with autologous stem cells. *Rev Romana Med Lab.* (2015) 23:415–29. doi: 10.1515/rrlm-2015-0046
10. Lichtenberg A, Tudorache I, Cebotari S, Ringes-Lichtenberg S, Sturz G, Hoeffler K, et al. In vitro re-endothelialization of detergent decellularized heart valves under simulated physiological dynamic conditions. *Biomaterials.* (2006) 27:4221–9. doi: 10.1016/j.biomaterials.2006.03.047
11. Driessen-Mol A, Emmert MY, Dijkman PE, Frese L, Sanders B, Weber B, et al. Transcatheter implantation of homologous "off-the-shelf" tissue-engineered heart valves with self-repair capacity: long-term functionality and rapid in vivo remodeling in sheep. *J Am Coll Cardiol.* (2014) 63:1320–9. doi: 10.1016/j.jacc.2013.09.082
12. Boethig D, Horke A, Hazekamp M, Meyns B, Rega F, Van Puyvelde J, et al. A European study on decellularized homografts for pulmonary valve replacement: initial results from the prospective ESPOIR Trial and ESPOIR Registry datadagger. *Eur J Cardiothorac Surg.* (2019) 56:503–9. doi: 10.1093/ejcts/ezz054
13. Hopkins RA, Jones AL, Wolfinbarger L, Moore MA, Bert AA, Lofland GK. Decellularization reduces calcification while improving both durability and 1-year functional results of pulmonary homograft valves in juvenile sheep. *J Thorac Cardiovasc Surg.* (2009) 137:907–13. doi: 10.1016/j.jtcvs.2008.12.009
14. Sierad LN, Shaw EL, Bina A, Brazile B, Rierson N, Patnaik SS, et al. Functional Heart Valve scaffolds obtained by complete decellularization of porcine aortic roots in a novel differential pressure gradient perfusion system. *Tissue Eng Part C Methods.* (2015) 21:1284–96. doi: 10.1089/ten.tec.2015.0170
15. Movileanu I, Branzaniuc K, Harpa M, Nistor D, Cotoi O, Preda T, et al. Pressurized perfusion system for obtaining completely acellular pulmonary valve scaffolds for tissue engineering. *ARS Medica Tomitana.* (2019) 25:149–56. doi: 10.2478/arsm-2019-0030
16. Zuk PA, Zhu M, Ashjian P, De Ugarte DA, Huang JI, Mizuno H, et al. Human adipose tissue is a source of multipotent stem cells. *Mol Biol Cell.* (2002) 13:4279–95. doi: 10.1091/mbc.e02-02-0105
17. Movileanu I, Brinzaniuc K, Harpa M, Cotoi O, Preda T, Al Hussein H, et al. Cryopreservation increases availability and usability of ovine adipose-tissue derived stem cells for regenerative medicine research. *Rev Chim.* (2019) 71:178–84. doi: 10.37358/RC.20.3.7986
18. Fischer LJ, McIlhenny S, Tulenko T, Golesorkhi N, Zhang P, Larson R, et al. Endothelial differentiation of adipose-derived stem cells: effects of endothelial cell growth supplement and shear force. *J Surg Res.* (2009) 152:157–66. doi: 10.1016/j.jss.2008.06.029
19. Movileanu I, Branzaniuc K, Chertes A, Preda T, Cotoi O, Harpa M, et al. A novel manufactured system designed to ensure consistent conditions in mechanical preconditioning of ovine adipose derived stem cells differentiation toward endothelial cell lineage. *Acta Medica Transilvanica.* (2019) 24:18-21.
20. Lee CH, Shah B, Moioli EK, Mao JJ, CTGF. directs fibroblast differentiation from human mesenchymal stem/stromal cells and defines connective tissue healing in a rodent injury model. *J Clin Invest.* (2010) 120:3340–9. doi: 10.1172/JCI43230
21. Al Hussein H, Al Hussein H, Sircuta C, Cotoi OS, Movileanu I, Nistor D, et al. Challenges in perioperative animal care for orthotopic implantation of tissue-engineered pulmonary valves in the ovine model. *Tissue Eng Regen Med.* (2020) 17:847–62. doi: 10.1007/s13770-020-00285-1
22. Harpa M, Movileanu I, Sierad L, Cotoi O, Suciu H, Preda T, et al. In Vivo Testing of xenogeneic acellular aortic valves seeded with stem cells. *Rev Rom Med Lab.* (2016) 24:343–6. doi: 10.1515/rrlm-2016-0031
23. Harpa M, Branzaniuc K, Movileanu I, Cotoi O, Suciu H, Deac R, et al. Implantation of valvular collagen biomaterials seeded with autologous stem cells – intraoperative hemodynamic measurements in an animal model. *Acta Medica Transilvanica.* (2015) 20:38–9.
24. Badylak SF. The extracellular matrix as a scaffold for tissue reconstruction. *Semin Cell Dev Biol.* (2002) 13:377–83. doi: 10.1016/S1084952102000940
25. Badylak SF, Freytes DO, Gilbert TW. Extracellular matrix as a biological scaffold material: Structure and function. *Acta Biomater.* (2009) 5:1–13. doi: 10.1016/j.actbio.2008.09.013
26. Lichtenberg A, Tudorache I, Cebotari S, Suprunov M, Tudorache G, Goerler H, et al. Preclinical testing of tissue-engineered heart valves re-endothelialized under simulated physiological conditions. *Circulation.* (2006) 114:I559–65. doi: 10.1161/CIRCULATIONAHA.105.001206
27. Cebotari S, Lichtenberg A, Tudorache I, Hilfiker A, Mertsching H, Leyh R, et al. Clinical application of tissue engineered human heart valves using autologous progenitor cells. *Circulation.* (2006) 114:I132–7. doi: 10.1161/CIRCULATIONAHA.105.001065
28. Kennamer A, Sierad L, Pascal R, Rierson N, Albers C, Harpa M, et al. Bioreactor conditioning of valve scaffolds seeded internally with adult stem cells. *Tissue Eng Regen Med.* (2016) 13:507–15. doi: 10.1007/s13770-016-9114-1
29. Deutsch M, Meinhart J, Zilla P, Howanietz N, Gorlitzer M, Froeschl A, et al. Long-term experience in autologous in vitro endothelialization of infrainguinal ePTFE grafts. *J Vasc Surg.* (2009) 49:352–62. doi: 10.1016/j.jvs.2008.08.101
30. Eberl T, Siedler S, Schumacher B, Zilla P, Schlaudraff K, Fasol R. Experimental in vitro endothelialization of cardiac valve leaflets. *Ann Thorac Surg.* (1992) 53:487–92. doi: 10.1016/0003-4975(92)90275-9
31. Arderiu G, Pena E, Aledo R, Juan-Babot O, Crespo J, Vilahur G, et al. MicroRNA-145 regulates the differentiation of adipose stem cells toward microvascular endothelial cells and promotes angiogenesis. *Circ Res.* (2019) 125:74–89. doi: 10.1161/CIRCRESAHA.118.314290
32. Sun Y, Lu B, Deng J, Jiang Z, Cao W, Dai T, et al. IL-7 enhances the differentiation of adipose-derived stem cells toward lymphatic endothelial cells through AKT signaling. *Cell Biol Int.* (2019) 43:394–401. doi: 10.1002/cbin.11093
33. Shang T, Li S, Zhang Y, Lu L, Cui L, Guo FF. Hypoxia promotes differentiation of adipose-derived stem cells into endothelial cells through demethylation of ephrinB2. *Stem Cell Res Ther.* (2019) 10:133. doi: 10.1186/s13287-019-1233-x
34. Khan S, Villalobos MA, Choron RL, Chang S, Brown SA, Carpenter JP, et al. Fibroblast growth factor and vascular endothelial growth factor play a critical role in endotheliogenesis from human adipose-derived stem cells. *J Vasc Surg.* (2017) 65:1483–92. doi: 10.1016/j.jvs.2016.04.034
35. Delaine-Smith RM, Reilly GC. The effects of mechanical loading on mesenchymal stem cell differentiation and matrix production. *Vitam Horm.* (2011) 87:417–80. doi: 10.1016/B978-0-12-386015-6.00039-1
36. Paul NE, Denecke B, Kim BS, Dreser A, Bernhagen J, Pallua N. The effect of mechanical stress on the proliferation, adipogenic differentiation and gene expression of human adipose-derived stem cells. *J Tissue Eng Regen Med.* (2018) 12:276–84. doi: 10.1002/term.2411
37. La A, Tranquillo RT. Shear Conditioning of Adipose Stem Cells for Reduced Platelet Binding to Engineered Vascular Grafts. *Tissue Eng Part A.* (2018) 24:1242–50. doi: 10.1089/ten.tea.2017.0475
38. Catalano MA, Rutkin B, Koss E, Maurer G, Berg J, Hartman A, et al. Accuracy of predicted effective orifice area in determining incidence of patient-prosthesis mismatch after transcatheter aortic valve replacement. *J Card Surg.* (2021) 36:191–6. doi: 10.1111/jocs.15148
39. Al Hussein H, Harpa M, Movileanu I, Al Hussein H, Suciu H, Branzaniuc K, et al. "Minimally invasive surgical protocol for adipose derived stem cells collection and isolation - ovine model". *Revista de Chimie.* (2019) 70:1826–8. doi: 10.37358/RC.19.5.7224
40. Sierad LN, Simionescu A, Albers C, Chen J, Maivelett J, Tedder ME, et al. Design and testing of a pulsatile conditioning system for dynamic endothelialization of polyphenol-stabilized tissue engineered heart valves. *Cardiovasc Eng Technol.* (2010) 1:138–53. doi: 10.1007/s13239-010-0014-6

41. Motta SE, Lintas V, Fioretta ES, Dijkman PE, Putti M, Caliskan E, et al. Human cell-derived tissue-engineered heart valve with integrated Valsalva sinuses: toward native-like transcatheter pulmonary valve replacements. *NPJ Regen Med.* (2019) 4:14. doi: 10.1038/s41536-019-0077-4
42. Huygens SA. Rutten-van Molken M, Noruzi A, Etnel JRG, Corro Ramos I, Bouten CVC, et al. What Is the Potential of Tissue-Engineered Pulmonary Valves in Children? *Ann Thorac Surg.* (2019) 107:1845–53. doi: 10.1016/j.athoracsur.2018.11.066

Conflict of Interest: LS was employed by the company Aptus Bioreactors.

The remaining authors declare that the research was conducted in the absence of any commercial or financial relationships that could be construed as a potential conflict of interest.

Publisher's Note: All claims expressed in this article are solely those of the authors and do not necessarily represent those of their affiliated organizations, or those of the publisher, the editors and the reviewers. Any product that may be evaluated in this article, or claim that may be made by its manufacturer, is not guaranteed or endorsed by the publisher.

frontiers in Cardiovascular Medicine

REVIEW
published: 13 September 2021
doi: 10.3389/fcvm.2021.728577

Long-Term Stability and Biocompatibility of Pericardial Bioprosthetic Heart Valves

David F. Williams[1,2]*, *Deon Bezuidenhout*[1,3], *Jandre de Villiers*[1], *Paul Human*[4] and *Peter Zilla*[1,3,4]

[1] Strait Access Technologies Ltd. Pty., Cape Town, South Africa, [2] Wake Forest Institute of Regenerative Medicine, Wake Forest School of Medicine, Winston-Salem, NC, United States, [3] Cardiovascular Research Unit, Cape Heart Institute, University of Cape Town, Cape Town, South Africa, [4] Christiaan Barnard Department of Cardiothoracic Surgery, University of Cape Town, Cape Town, South Africa

OPEN ACCESS

Edited by:
Frederick Schoen,
Brigham and Women's Hospital and Harvard Medical School, United States

Reviewed by:
Theodor Fischlein,
Nürnberg Hospital, Germany
Najma Latif,
The Magdi Yacoub Institute, United Kingdom

***Correspondence:**
David F. Williams
dfwillia@wakehealth.edu

Specialty section:
This article was submitted to Heart Valve Disease, a section of the journal Frontiers in Cardiovascular Medicine

Received: 21 June 2021
Accepted: 19 August 2021
Published: 13 September 2021

Citation:
Williams DF, Bezuidenhout D, de Villiers J, Human P and Zilla P (2021) Long-Term Stability and Biocompatibility of Pericardial Bioprosthetic Heart Valves. Front. Cardiovasc. Med. 8:728577. doi: 10.3389/fcvm.2021.728577

The use of bioprostheses for heart valve therapy has gradually evolved over several decades and both surgical and transcatheter devices are now highly successful. The rapid expansion of the transcatheter concept has clearly placed a significant onus on the need for improved production methods, particularly the pre-treatment of bovine pericardium. Two of the difficulties associated with the biocompatibility of bioprosthetic valves are the possibilities of immune responses and calcification, which have led to either catastrophic failure or slow dystrophic changes. These have been addressed by evolutionary trends in cross-linking and decellularization techniques and, over the last two decades, the improvements have resulted in somewhat greater durability. However, as the need to consider the use of bioprosthetic valves in younger patients has become an important clinical and sociological issue, the requirement for even greater longevity and safety is now paramount. This is especially true with respect to potential therapies for young people who are afflicted by rheumatic heart disease, mostly in low- to middle-income countries, for whom no clinically acceptable and cost-effective treatments currently exist. To extend longevity to this new level, it has been necessary to evaluate the mechanisms of pericardium biocompatibility, with special emphasis on the interplay between cross-linking, decellularization and anti-immunogenicity processes. These mechanisms are reviewed in this paper. On the basis of a better understanding of these mechanisms, a few alternative treatment protocols have been developed in the last few years. The most promising protocol here is based on a carefully designed combination of phases of tissue-protective decellularization with a finely-titrated cross-linking sequence. Such refined protocols offer considerable potential in the progress toward superior longevity of pericardial heart valves and introduce a scientific dimension beyond the largely disappointing 'anti-calcification' treatments of past decades.

Keywords: pericardium, biocompatibility, calcification, immunogenicity, crosslink

INTRODUCTION

Valvular Heart Disease (VHD) affects large numbers of individuals, perhaps as many as 100 million diagnosed annually, world-wide (1). Almost half of the cases involve the aortic valve (Aortic Valve Disease, AVD), the preferred treatment in those patients with advanced AVD being valve replacement (AVR); globally some 290,000 patients receive such replacements each year (2) the vast majority of them being in elderly patients of industrialized countries. The unmet needs for the largely young to middle-aged patients of low to middle income countries are estimated to be more than 1.2 million heart valve replacements each year (3, 4).

Several decades ago, the standard of care with respect to AVR involved an open-heart surgical procedure using either a mechanical prosthesis, where pyrolytic carbon gradually replaced other materials, or "tissue valves" where the shortage of human cadaver valves has led to the use of crosslinked xenograft valves from the late 1960 onwards (5, 6). Whilst very successful in general, these procedures presented some drawbacks, including the invasiveness of the surgery, the difficulties associated with the very elderly that have co-morbidities (7, 8), the tendency for thrombus formation, the necessity for life-long anticoagulation therapy (9), the occasional failure of mechanical prostheses (10) and the premature, age-dependent largely calcific degeneration of bioprostheses (11, 12).

Several factors have altered this position related to the prevalence of surgically implanted heart valves. The first was the general trend toward greater use of bioprosthetic compared to mechanical valves. The second was associated with the development of transcatheter techniques for valve replacement (TAVR) (13, 14), which obviated the need for open-heart surgery. The third concerned the market potential for valve replacement in low – to – middle income countries, where a majority of patients are young and suffer from rheumatic heart disease (RHD) (3, 4, 15).

Progress with, and indeed the very existence of, the latter two developments has been predicated on the evolution of the bioprosthetic concept. Clearly it is impossible to collapse a rigid mechanical prosthesis into a catheter for delivery to the heart, the only options, therefore, being flexible "soft" leaflets of either a tissue or synthetic polymer. Since an appropriate polymer had not been developed at the time Cribier was introducing his TAVR system (16), he had to rely on some form of tissue, and the obvious choice was one of the forms of pericardium used in surgical replacement valves. With respect to the RHD patients in poorer countries, the greater clinical convenience of a simplified, affordable TAVR approach relative to an open-heart procedure is pivotal, so that pericardium was always likely to be the first choice.

Whichever way the heart valve scenario is examined, it will be the pericardial leaflet that dominates materials selection. These leaflets have the mechanical characteristics to offer good hemodynamic function in a valve (17) and they pose a low risk of thromboembolic complications (18). However, they have one significant drawback, or to be more accurate, a collection of related drawbacks. These concern the specific mechanisms of the biocompatibility of the pericardium, including aspects of structural degradation, calcification and immune responses. These can lead to profound and rapid effects, involving lymphocytic inflammation and calcification with fatal consequences (19), and to long-term slow changes that eventually lead to structural or non-structural dysfunction, requiring replacement (20).

The mechanisms and kinetics of pericardial degradation are therefore of crucial significance in the management of VHD. Various algorithms have been published that may inform the selection of prostheses by clinicians (21, 22), one of the most important factors being the patient's age as a marker of their chances of death (by non-valve-related causes) before pericardium dysfunction. This is enshrined in the ESC/EACTS 2017 guidelines on the management of VHD (23) which states that "*A bioprosthesis should be considered in patients > 65 years of age for a prosthesis in the aortic position, or > 70 years of age in a mitral position, or those with a life expectancy lower than the presumed durability of the bioprosthesis.*"

For the elderly patients who are considered for TAVR rather than surgical procedures, any effects of altered valve design and mechanical function, and of the crimping procedure/deployment technique on pericardium longevity should, if known, be taken into account. Of crucial significance in the use of TAVR bioprosthetic valves in young RHD patients will be the anticipated leaflet durability, which should be included as a factor alongside the expected patient longevity.

This paper attempts to review, and critically analyze, the mechanisms of biocompatibility, degeneration and degradation of bioprosthetic heart valves and the evidence regarding the performance of pericardial leaflets that impacts on the decisions about prosthetic heart valve usage. It concludes with a discussion of optimal protocols for the modification of pericardium that yield the best clinical outcomes in bioprosthetic valves, especially TAVR valves. Emphasis is given to the ability to use TAVR valves in the low- to middle-income countries mentioned above, where valve longevity in young RHD patients is a critical factor.

THE STRUCTURE AND PROPERTIES OF NATURAL PERICARDIUM

The pericardium is a sac-like structure that envelops the heart and the roots of the major blood vessels (24) as shown in **Figure 1**. It consists of two sheets of tissue, the outer fibrous pericardium (the parietal sheet) and the inner serous pericardium, which is also known as the epicardium when it is in contact with the myocardium. The fibrous pericardium consists of connective tissue with a loose arrangement of collagen and other, elastic fibers such as elastin and fibrillin. The collagen is mostly Type I, although Types III, VI, and XII are also present. These fibers are embedded in an amorphous matrix of proteoglycans and glycosaminoglycans, including hyaluronic acid. This matrix acts as a reservoir for signaling molecules such as cytokines and growth factors. The predominant cell is the pericardial fibroblast. The serous pericardium is composed of mesothelium (epithelial-like cells) with its basal lamina overlying

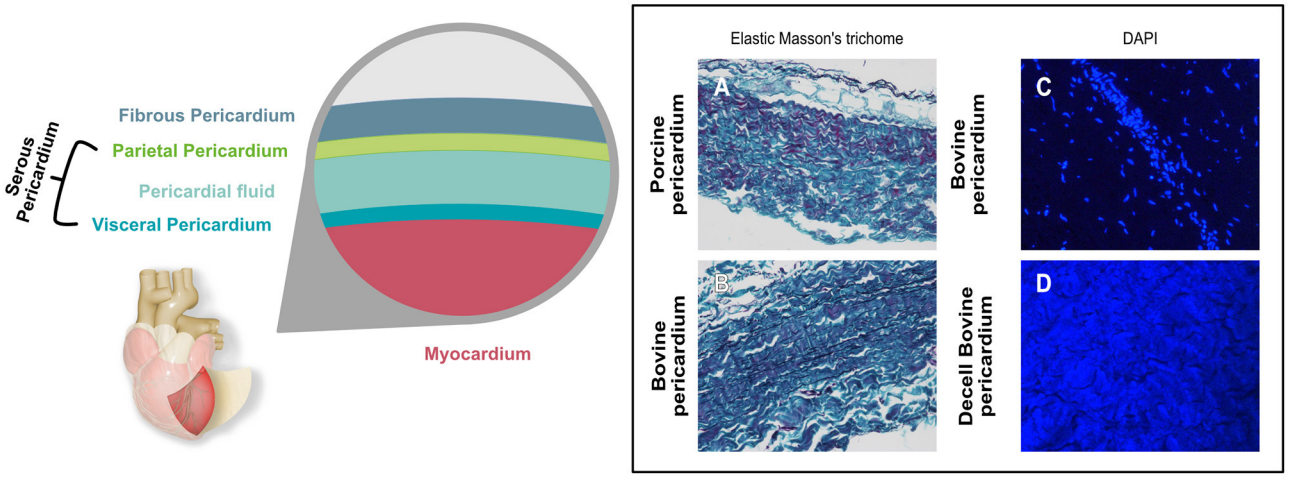

FIGURE 1 | Graphical representation showing the different layers of the pericardial sac. Histological micrographs **(A,B)** with Elastic Masson's trichrome stain shows the different components contained in the pericardium and how they differ between bovine and porcine. Keratin and muscle fibers are shown in red, collagen in blue or green, cytoplasm in light red or pink and cell nuclei are dark brown to black and elastic fibers in black. **(C,D)** show the DAPI stain of bovine pericardium before **(C)** and after decellularization **(D)**. Nuclei that show as bright blue dots in **(C)** are absent in **(D)**, where blue background results from autofluorescence.

a thin layer of loose connective tissue (25). The mesothelial cells form a monolayer lining in the visceral pericardium (26), which plays an important role in inflammation and tissue repair (27).

The thickness of the pericardium varies with species, and indeed can vary quite widely within species. Adult human pericardium is typically up to 2 mm thick, with the parietal sheet being several times thicker than the serous layer (28). Of the species that are most widely used in bioprosthetic components, bovine pericardium thickness is typically in the range 400-500 μm, and porcine, 100-200 μm (29).

Natural pericardium is anisotropic. In early studies, Xi et al. (30) showed that the ultimate tensile strength of fresh bovine pericardium was 9.9 MPa in a vertical direction and 14.5 in a horizontal direction. The collagen fibers dominate the stress-strain behavior and the orientation and general architectural features significantly influence both static and fatigue strength (31, 32). The mechanical properties of natural pericardium are complex; as discussed by Soares et al. (33), uniaxial tensile behavior of pericardial tissues is generally non-linear. The exponential behavior commonly observed in biological tissues is attributed to collagen fiber undulation and de-crimping/engagement upon extension. Simple mechanical properties such as Young's modulus are not able to characterize the inherently non-linear response, and are not suited because they entail the application of the linearized theory of isotropic elasticity to biomaterials undergoing large deformations.

BIOCOMPATIBILITY ISSUES WITH XENOGENEIC PERICARDIUM AND BIOPROSTHETIC HEART VALVES

General Overview

Biocompatibility, defined as "*the ability of a material to perform with an appropriate host response in a specific application*" (34), refers to all aspects of the interactions between biomaterials and host systems. This includes both the effects of the host on the biomaterial and of the biomaterial on the host, the mechanisms of these apparently separate entities clearly being entwinned. Mechanisms of biocompatibility have been discussed for decades, a detailed review being published in 2008 (35). A very thorough analysis of potential mechanisms that relate to clinical experiences (36), especially focusing on molecular pathways, showed that, for implanted devices, two types of mechanism predominate; these are the phenomena of mechanotransduction and sterile inflammation.

With bioprosthetic heart valve leaflets, there is an unusual characteristic for an implanted device, which contributes to the overall biocompatibility scenario; the leaflets are usually attached to mechanical frames, in the form of sewing rings or stents, which provide attachment to tissues. The leaflets do not normally contact host tissues other than flowing blood. Parenthetically, this ignores the possibility of coronary ostial obstruction, described by Webb and Dvir (37), where it is possible for the displaced native leaflets to come into contact with the coronary ostia or the overlying sinotubular junction (38), which is not a factor in valve biocompatibility.

The interface between valve leaflets and the host primarily involves the treatment-modified pericardium and flowing blood, although in some cases could also involve the sinotubular junction and annulus. Depending on the pre-treatment protocol, the composition of pericardial extracellular matrix will be altered (39), with the collagen cross-linked to varying extents within a proteoglycan/hyaluronan matrix. Since all contemporary commercial xenograft bioprostheses have been crosslinked and stored in fixative, there are certainly no living cells in this structure. In some of the commercial products today this step is additionally preceded by extracting cell membranes either through alcohol wash-outs or detergents such as SDS (40, 41).

There are no living resident inflammatory cells, at least initially, nor are there any accessible biologically-active macromolecules. Yet, remnant alkaline-phosphatase has long been suspected of contributing to the calcification process (42). Host inflammatory cells, however, are still able to invade crosslinked pericardial valves in non-clinical situations. Khorramirouz et al. showed the presence of a variety of CD+ inflammatory cells in decellularized porcine pericardium implanted subcutaneously in rats (43), which is a widely used animal model for the study of calcification (44), but obviously this does not represent a clinically realistic situation related to heart valves. Trantina-Yates et al. (45) demonstrated the infiltration of inflammatory cells into fixed porcine aortic roots when implanted in ovine aortic arches, but this does not replicate the bioprosthetic heart valve situation since there was direct communication between the host aortic wall with the implanted pericardium, which is obviated by the use of a frame in clinical valves. Interestingly, Skowasch et al. (46) demonstrated the presence of endothelial progenitor cells and dendritic cells in native aortic valves that have experienced degeneration, and similar cells were found in some GA-treated porcine valve replacements. Nair et al. (47) also reported a chronic inflammatory response in an explanted, deteriorating porcine prosthesis, with significant damage to the porcine aortic wall. Thus, inflammatory cells may be present in treated porcine aortic valves, and could be associated with structural dysfunction. In explanted bovine pericardial valves, macrophages were found invading and degrading implant-collagen leading cellular infiltrates and collagen disruption (48).

In most situations, bioprosthetic valves are stored in a glutaraldehyde (GA)—formaldehyde saline solution and then extensively rinsed in phosphate buffered saline before clinical implantation. The fluid phase of the cross-linked pericardium will largely comprise of water, with very low levels of processing residues, including some free GA, and possibly some cellular fragments following decellularization. Bezuidenhout *et al* reported values in the literature for the water content of pericardial leaflets ranging from 83 to 84%; they also reported overall collagen levels at 72-76% and elastin, 4-5% (44) (**Figure 2**). The hydration state is likely to vary with the processing conditions (50, 51); the formation of collagen-GA cross-links causes an increase in the total water content. Paradoxically, Suesca et al. indicate that cross-linked collagen type I scaffolds are more hydrophobic than non-cross-linked ones (52).

Little is known about the processes of adsorption and diffusion that take place at this interface. As noted by Meyer (53), the tight fibrous structure of cross-linked pericardium is a massive obstacle for molecular diffusion, and the hydrodynamic volume of molecules in this tissue structure will correspond to their molecular weights and hydrophobicity. At blood temperature and pH there should be rapid exchange of anions and cations between the fluid phases of the blood and pericardium, but matrix proteins in the latter, such as hyaluronic acid and serum proteins such as albumin in the former, would be essentially excluded from diffusion. It would also be expected that some of these proteins would be adsorbed on the pericardium surface, but the relevance is uncertain. Decades ago, several studies were able to monitor serum protein adsorption on "fixed" (54) or "preserved" (55) pericardium in *in vitro* and subcutaneous implantation studies, respectively, but could not demonstrate any clinical consequences. This is in agreement with the observations of Williams referenced above (36) who could find little evidence

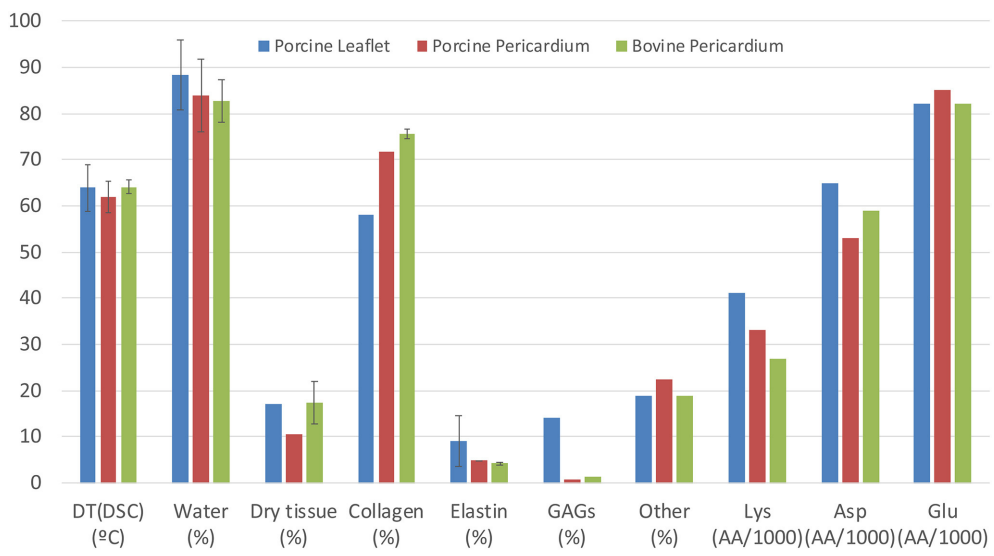

FIGURE 2 | Comparison of composition and properties of porcine and bovine pericardium with those of porcine aortic leaflets, including denaturation temperature (by differential scanning calorimetry), water content and dry tissue content. Collagen, elastin and other constituents are expressed as percentage of dry content, while amino acid content for Lys, Asp, and Glu are in amino acids per 1,000 residues [compiled from Bezuidenhout et al. (44); Zouhair et al. (49)].

of the relevance of protein adsorption on implanted devices in spite of a wealth of *in vitro* data.

The difficulty of diffusion of all-but low molecular weight species from blood through the surfaces of pericardial leaflets is not surprising in view of the performance of hemodialysis membranes (56), where permeability to natural medium- to -high molecular weight molecules, including plasma proteins, has been a significant challenge (57, 58). Cellulosic structures, with some similarities to pericardium, had great difficulty in controlling diffusion properties, even with a high degree of porosity. Since many biocompatibility pathways require significant molecular mobility, the performance of cross-linked pericardium is unlikely to follow normal paradigms.

In view of the above considerations, the biocompatibility phenomena associated with modified pericardium heart valves in clinical practice could involve the following;

- Interactions between leaflets and blood, leading to clinically-relevant effects on the blood, including toxicological effects of components of the processed tissue that are released from the surface,
- Structural changes in the proteinaceous components of the pericardial tissues that may lead to valve dysfunction over time,
- Calcification of the pericardial tissues, also potentially leading to valve dysfunction,
- Immunological responses to the pericardial tissues, which are, by definition, xenogeneic and therefore, potentially antigenic.

The first two of these can be dealt with briefly; parenthetically, this analysis does not include endocarditis, which is a risk factor with all prosthetic heart valves but is not directly biomaterials related.

It has been recognized for many years that replacement heart valves carry a risk of thrombo-embolic complications, ranging from non-obstructive thrombus formation to stroke, and that bioprosthetic valves carry a much lower risk than mechanical valves (59). There is an increasing recognition that the incidence of early thrombus with biological valves is not insignificant (60) and that risk factors may vary with age and conditions such as atrial fibrillation (61, 62). Tian et al. (63) have discussed the relationship between hemodynamic stability and risk of adverse cerebrovascular events with bioprosthetic valves. Many cases are of a sub-clinical nature, and the presence of subclinical thrombus may be considered as an almost ubiquitous finding (64), even if associated with a small increase in rates of transient ischemic attacks with bioprosthetic valves (65); moreover, management of non-obstructive thrombus is primarily achieved by optimization of anti-coagulation (59). As far as biomaterials-associated biocompatibility is concerned, it is hemodynamic rather them materials characteristics that dominate susceptibility to thrombosis. Vranckx et al. (66) noted that the underlying principles of clinical thrombosis relate to perturbations to blood flow which lead to activation of hemostatic factors, so that risk factors include incomplete expansion or apposition of the frame to the aortic wall. Midha et al. (67) specifically cited the valve design and geometry in relation to the prevalence of stagnation zone sizes and susceptibility to thrombosis.

There have always been concerns about the potential toxicity of the GA that is widely used in the treatment of pericardium (68, 69); since any released residual GA would be taken into the systemic circulation, these concerns are usually focused on risks of genetic toxicity rather than overt cytotoxicity (70). Tests for biological safety of commercial products address all potential mechanisms (71). In practice, the evidence would indicate that these are theoretical concerns with commercial products, with no indication of adverse clinical effects. The July 2017 report on the Toxicological Profile for Glutaraldehyde of ATSDR (72) indicate the NOAEL (No Observed Adverse Effects Level) for chronic ingestion exposure to GA in rats is 4 mg/kg/day, which is far higher than the levels expected to be released from biologic valves. The report also indicates that after intravenous injection of GA, more than 70% is rapidly eliminated in expired CO_2 and the majority of the remainder within the urine or feces.

Denaturation and Degradation

The main structural material of pericardium is collagen; this is a very stable material. Natural collagen within tissues does undergo some changes over time within the mechanisms of tissue remodeling and it would be expected that a collagen-based component such as pericardium would also undergo some change. The main driver for collagen denaturation is heat (73) but it can occur at ambient temperatures. Physical and chemical factors can synergistically interact in denaturation processes (74).

More significant changes to properties take place through degradation. Proteolysis is the breakdown of proteins through the hydrolysis of peptide bonds. Without catalysis, this is an extremely slow process that is physiologically irrelevant. Proteins are normally degraded by enzymatic activity, which can occur extracellularly or intracellularly. Because of its hierarchical helical structure, collagen is not susceptible to enzymatic degradation under most circumstances, especially those involving a normal extracellular matrix. Different collagen isotypes may vary in their susceptibility and various degradation pathways have been identified (75). There are a few exceptions, as described by Sabelman (76); notably they relate to the activity of type-specific collagenases, which bind to recognition sites on the three polypeptide chains. Collagenases are activated by proteases and activity is inhibited by alpha-macroglobulin, platelet factor and some tissue specific factors; of considerable significance to the use of pericardium in implantable devices, the activity is also inhibited by cross-linking of the substrate, which is discussed later.

The enzymatic degradation of pericardial collagen is influenced by mechanical forces, especially dynamic strain. Ellsmere et al. (77) demonstrated the synergistic effects of tensile stress and proteolysis on the degeneration of untreated bovine pericardium *in vitro*. Tensile loading accelerated degradation by collagenase but also dynamic loading was more damaging than equivalent static loading. Under dynamic loading, even a non-specific proteolytic enzyme such as trypsin could damage bovine pericardium. It is likely that collagen molecules undergo conformational changes under application of stress, making available new enzyme binding sites. The realignment of collagen fibers may allow exogenous enzyme penetrating faster and deeper

into the tissue, influenced by the pumping action of changing internal hydrostatic pressure during dynamic loading. Since there is considerable interplay between collagen fiber orientation and enzymatic degradation with respect to the influence of strain (78), the potential significance of cross-linking characteristics resulting from pre-treatment of bioprosthetic valves is apparent.

Collagenases may not be the only enzymes involved in pericardium degradation. Simionescu et al., in 1996, demonstrated that matrix metalloproteinases (MMPs) may also play a role (79), noting increased levels of MMP9, high levels of ß-glucuronidase and constant levels of active collagenase and MMP2 in explanted valve leaflets. This possibility was further discussed in 2001 (80). Much more has since been learned about MMPs and their influence as the main extracellular matrix enzymes involved in morphogenesis and tissue remodeling (81). Also oxidative stress, especially mediated via hydroxyl radical and tyrosyl radical mediated pathways, can influence the *in vivo* degradation of the pericardial valves (82).

Kataruka and Otto (83), have speculated that some unique mechanisms contribute to TAVR degeneration, including valve crimping, balloon expansion and stent under-expansion, but these are technique-related processes and not those of *in vivo* stability. While changes to collagen remain a theoretical cause for concern with respect to structural valve dysfunction, the clinical performance with pericardial TAVR is such that the deterioration of GA-treated materials has not been associated with clinically significant rates of failure when trans-catheter valves were confined to older recipients (84, 85).

When examining explanted, failed, bioprostheses, it may be difficult to identify separate roles for collagen degradation and calcification, and the involvement of the immune system (86). One recent study casts some light on some of the questions that arise (87). Explanted devices, of both porcine aortic valve and bovine pericardium origin, derived from over 30 years clinical experience, were examined. The specific focus was on valves that had failed for reasons of intrinsic structural valve deterioration and patients were stratified according to their blood group. With porcine valves, patients of blood group A were rare among early failures; with longevity up to 6 years, 9% were of Group A and 14.9% were non-group A ($p = 0.011$), with no statistical significance for valves which lasted longer than 6 years. With bovine pericardial valves, the difference was much stronger; no type A patient had a valve that failed before 6 years, but 27.5% of non-A patients failed in this time. It was suggested that cross-reactivity of alloantibodies, because of shared carbohydrate antigens between humans and animals, could explain these differences. The differences between porcine valves and bovine pericardial leaflet valves appears to be important in view of earlier comments about different access of cells and molecules to these different structures.

Calcification

Although only 1% of the human body's calcium content is found within fluids, which include extracellular fluids, cellular fluids and blood, this calcium has extremely important functions, involving muscle contraction, nerve impulses and cell metabolism. It should not be surprising that, depending on local and systemic conditions, this calcium may have a tendency to precipitate in some tissues, especially those of the cardiovascular system. It has been known for a century that equilibrium conditions relating to calcium salts such as calcium carbonate and various calcium phosphates and blood or serum are complex (88) and that their deposition in some tissues is of considerable clinical significance. This deposition in tissues, usually referred to as mineralization or calcification, is frequently seen in heart valves, and is a major factor in the etiology of AVD (89).

Lerman et al. (90) have summarized the molecular mechanisms of native valve calcification, which they state are similar to those involved in atherosclerosis. Activation of valvular interstitial cells (VICs) and the pathways of calcific stenosis are the result of shear stresses, endothelial damage and deposition of low density lipoproteins, which trigger inflammatory events. Monocytes, macrophages and T cells produce cytokines, including TGF-ß, that regulates cell proliferation and differentiation, TNF-α that regulates immune cells, and IL-2. Under these circumstances, the activated VICs become myofibroblasts, which develop angiogenic activity, and may transform into osteoblasts.

There are significant differences, of course, between natural and bioprosthetic valve leaflets, but there are sufficient similarities to allow for some extrapolation between AVD calcification and effects in pericardial valves (91); indeed, in his essay on biocompatibility pathways already mentioned (36), it was made clear that the molecular pathways proposed for biocompatibility phenomena, are not "new biological entities" but are variations on pathways seen within relevant tissues and disease states.

Each cusp of the human aortic valve (AV) is a few hundred microns thick and has three layers, the fibrosa, the spongiosa and the ventricularis, which encompass a complex microstructure which has a layered architectural pattern, optimally addressing the biomechanical needs. While the spongiosa acts as a sliding-plane between two layers bent at different radii, it also gives the valve its compressive properties and allows it to absorb high forces during coaptation. The ventricularis is located on the outer circumference of the leaflet and composed of circumferentially aligned collagen fibers that provide it with the necessary tensile strength to open and transmit forces during coaptation while closed (92). The ECM consists of collagen, elastin, proteoglycans and glycosaminoglycans (GAGs); the fibrosa is rich in collagen, the spongiosa with GAGs and the ventricularis with elastin. Valvular endothelial cells (VECs) occur at the blood-contacting surfaces and VICs are present throughout the layers, especially in the deeper layers. The VECs comprise a single layer on the cuspal surface. The VICs have, variously, characteristics of fibroblasts, myofibroblasts and smooth muscle cells; they can change their phenotype with age and mechanical stimulus.

AVD appears to be initiated with the formation of nodules of calcific material, particularly hydroxyapatite-like calcium phosphate, primarily and most significantly in the fibrosa (93). The deposits usually occur at the attachment of the cusps in regions of highest functional stress, initiated predominantly in VICs. One potential mechanism here, referred to as dystrophic calcification, involves reaction between the calcium-containing

extracellular fluid and the phosphorus-containing membranes of non-functional cells. An alternative mechanism is ossification, where there is osteogenic differentiation of VICs. In both cases, either mechanical or biochemical factors can be considered as potential regulators.

As discussed by Schoen (94–96) and by Bonetti et al. (97), calcification of biomaterials such as pericardium is determined by a combination of host metabolism, material characteristics and mechanical factors. Cells and extracellular matrix of dead tissue are the principal sites of pathologic calcification, occurring within the material (intrinsic calcification) or associated with attached cells and proteins at the surface (extrinsic). With bovine pericardium, intrinsic calcification is dominant, occurring in deep cells. Dynamic stress promotes but is not a prerequisite for pericardial calcification. A substantial calcium ion gradient across a cell membrane will cause an influx of calcium when that membrane is damaged, the phosphorus naturally present in that membrane allowing nucleation of calcium phosphate.

Two other important factors have to be mentioned here. First, questions have arisen over the role of the immune system. Although Schoen (95) was not convinced that the immune response and inflammation were significantly involved, with suggestions that the detection of antibodies in failed pericardial tissue valves could reflect a secondary response to valve damage rather than a cause of failure, evidence does indicate some involvement. Dahm et al. showed that glutaraldehyde-fixed bovine pericardium provoked cellular and humoral immunological reactions in rats and in humans (48). Human and Zilla (98–100) have addressed this issue and have shown a role of circulating antibodies in calcification. Similar conclusions were reached by Jeong et al. (101), who were able to demonstrate the beneficial effect of decellularization processes on this effect.

The other factor is the role of the fixation process. It was obvious that xenogeneic tissues, derived from porcine or bovine origins, would have to be treated in some way to render them sterile and minimally immunogenic. With bovine pericardium, this meant using some fixative which is both anti-bacterial and anti-fungal while also reacting with proteins to eliminate their antigenicity. The standard fixative used in the preservation of tissues for pathological purposes is 10% neutral buffered formalin (102). For fixation of pericardial valves, GA is preferred, partly because of its aqueous solubility and partly because of its more versatile cross-linking performance (103). However, although GA-fixed bioprosthetic valves have good mechanical and hemocompatibility properties, it became clear that collagen degeneration and calcification could take place. Carpentier noted that there were several cases of valve dysfunction with GA preserved heterografts within a few years (104) and went on to develop methods to minimize this calcification, including blocking calcification binding sites using Mg^{++} and decreasing the phosphorus content of the tissue (105). Schoen et al. (95) examined early structural failures of Ionescu-Shiley bovine pericardial bioprostheses and showed that this was due to calcific tissue degeneration and design-related cuspal tears and commissural perforations.

Immunogenicity

As noted above, the immune response (and inflammation) has been controversially associated with general biocompatibility and calcification of pericardial heart valve prostheses. Early studies were contradictory. Skinner et al. (106) published a case report that showed a dense epicardial reaction to processed bovine pericardium, which histology confirmed was associated with the presence of a severe inflammatory response. Dahm et al. (107) concluded from an animal study that GA-tanned bovine pericardium induces immunologic responses *in vivo* consistent with a host vs. graft reaction. Moczar et al. (108) examined explanted Mitroflow pericardial heart valves and found IgG, complement fragments and macrophages in the valves. The complement activation was associated with the pericardium itself and the peptides generated in the process stimulated monocyte migration, phagocytosis and exocytosis of proteases which were able to degrade the GA cross-linked matrix, leading to structural deterioration. On the other hand, Gong et al. deduced from an animal study (109) that there was no obvious relationship between bioprosthetic calcification and immunogenicity. Wong et al. (110) have shown that, whatever route of fixation and decellularization is used, the residual antigenicity and the degree of ECM architecture modification are very influential in modulating the recipient immune response. Dalgliesh et al. have discussed graft-specific immune tolerance and its relationship to residual antigenicity in xenogeneic scaffolds (111).

The mixed messages from early experimental and clinical studies reinforce the complexity of the immune response to xenogeneic bioprosthetic heart valves, with respect both to the involvement of processing agents and the clinical outcomes. As implied above, there are two areas of concern, the potential immunological rejection of clinical valves and the role of pre-treatments in calcification. This complexity was discussed by Luo et al. (112); the paper was directed toward the use of xenogeneic biomaterials in potential tissue-engineered valves but addressed the broad immunogenicity aspects. As noted in the Introduction to this paper, a major clinical disaster was encountered when porcine pulmonary valves were treated by a proprietary technique intended to substantially reduce leaflet cellularity, but residual cellular components initiated severe inflammation and total structural failure. This was not the only failure. The Matrix P device was also an acellular porcine pulmonary valve, which was supported by a GA-fixed equine pericardial patch. Although some early results seemed good, there were soon observations of other early obstructive failures, with very clear involvement of inflammatory and fibroproliferative processes (113, 114). Interestingly, work on the potential molecular mechanisms has suggested that canonical Wnt/ß-catenin signaling processes are involved in epicardial fibrosis, particularly in promoting epithelial-mesenchymal transition (115).

A schematic of the immune response is given in **Figure 3**.

As shown by Manji et al. (116) in 2006, it became increasingly clear that GA fixed xenogeneic valves can provoke cellular-humoral rejection, with subsequent secondary calcification. Ten years later, the same author (117) reviewed the status of the controversy, recognizing that the most important antigen that

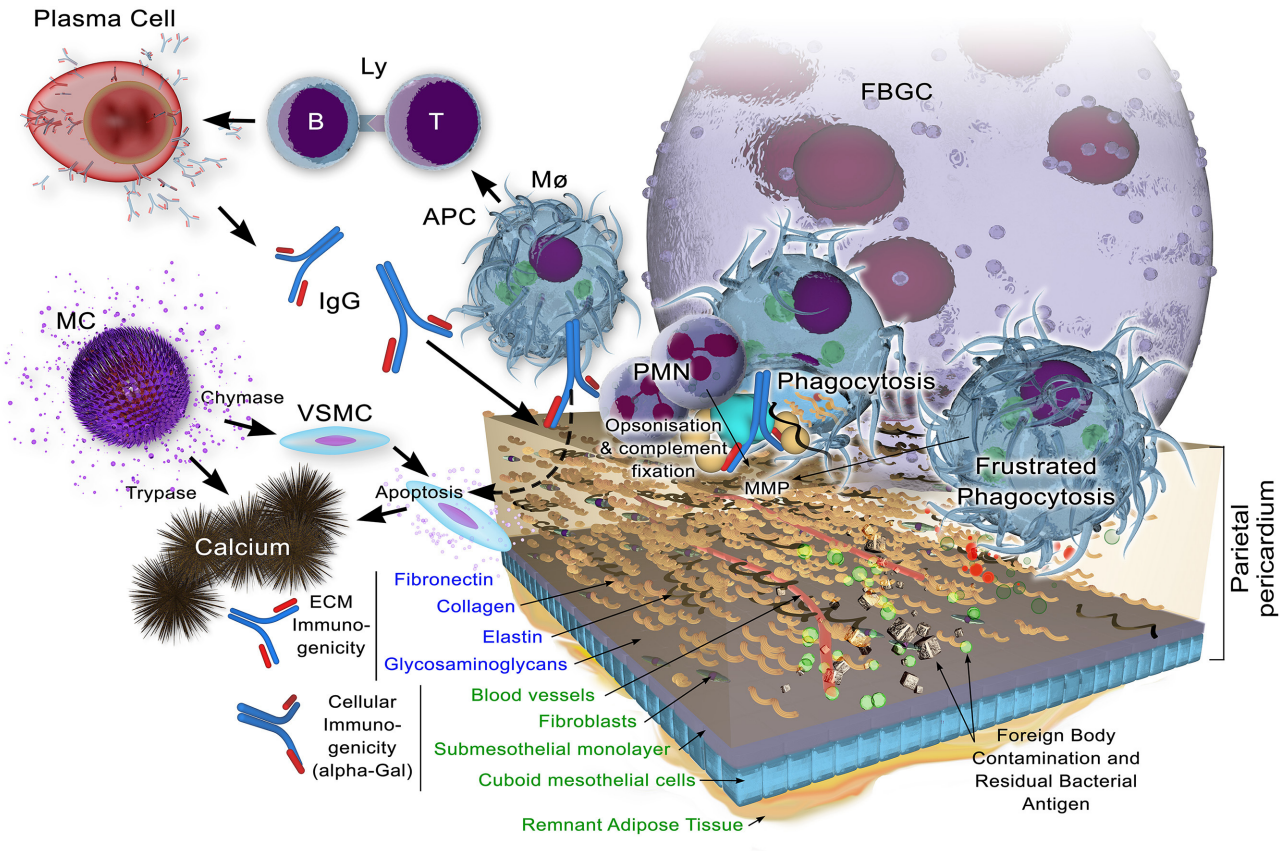

FIGURE 3 | Potential immune responses to xenogeneic pericardial tissue. While decellularization may remove the bulk of cellular components, including their highly immunogenic galactose-α1,3 galactose (α-Gal) antigen against which preformed natural antibody exists in the human recipient, remnant cellular antigens may yet persist. Structural extracellular components, apart from glycosaminoglycans which may be lost to some extent, are known immunogens which, when insufficiently masked through cross-linking, will bind immunoglobulin as a component of the adaptive immune response. Antigen is presented by antigen presenting cells (Macrophags, Mø, B-lymphocytes, B-Ly and dendritic cells) to T lymphocytes (Ly) with ensuing immunoglobulin production by plasma cells. This potentially opsonises the tissue for subsequent infiltration by Mø and polymorphonuclear neutrophils (PMNs). Matrix metalloproteinases (MMPs) contribute to the bioprosthesis digestion.

stimulates xenograft rejection of tissues and organs from pigs and cows by humans is the galactose-α1,3 galactose (Gal) antigen; the status of knowledge about immunological aspects of xenotransplantation at that time was published by Griesemer et al. (118). Gal antigens were present on commercially-available GA bovine heart valves and studies showed that Gal antigens were important in the structural deterioration of some valves. Several animal studies using α1,3-galactosyltransferase gene-knockout pigs (GTKO), which do not produce Gal, have supported this relationship (119). As Gates et al. (120) clearly point out, however, α-gal is not the only source of xenoantigenicity with bovine pericardium; they point out that antigenic proteins are not only of cellular origin but can be intimately associated with the matrix itself, leading to the concept of "antigen removal" rather than "decellularization."

The respective roles of GA fixation and decellularization on the immunogenicity of porcine valves was demonstrated in a clinical study by Bloch et al. (121). They showed that although antibody titers for collagen type I were the same in fixed only and decellularized valves, a considerable anti-α-Gal antibody response was observed with GA treated valves; in particular it was noted that IgG antibodies were considerably increased with GA treated porcine valves but with no response from decellularized valves. Using an *in vitro* model, Rieder et al. determined that neither cross-linking nor decellularization could eliminate human immune responses to xenogeneic biomaterials (122).

TREATMENT OF XENOGENEIC PERICARDIUM BEFORE CLINICAL IMPLANTATION

Ever since bioprostheses were considered as alternatives to mechanical heart valves, and the need for both sterility and non-immunogenicity was recognized, GA was considered as a principal candidate for valve pre-treatment (123). Manufacturers world-wide adopted such treatment and early clinical applications appeared to be acceptable (124). It was soon realized, however, that this simple treatment was insufficient to achieve long-term performance (125); specifically,

as alluded to before, it was demonstrated that GA played a role in calcification phenomena (126). In the subsequent 3-4 decades, there have been many attempts to understand the processes that occur during the pre-treatment of pericardium and to optimize these processes in order to maximize longevity. It has become clear that there are several different factors that contribute to effects of chemicals on the pericardium, and that these effects are interactive. It is convenient to consider these under the headings of fixation/crosslinking and decellularization whilst recognizing the impact of synergistic effects. This review does not address the anti-bacterial activity of GA, which has been well-documented from the early days of use in implant sterilization (127).

Crosslinking, Fixation, and Post-fixation

Natural collagen is cross-linked both intra- and inter-molecularly, involving two different mechanisms (53). One is by enzymatic control of the formation of specific divalent products that react spontaneously to form stable, complex, cross-links. The second process comprises several non-specific interactions that involve glucose and its oxidation products, leading to advanced glycation end products. As collagen matures, these enzymatic and non-enzymatic induced cross-links provide for very low solubility and stability against enzymatic and chemical changes. The concept of the pre-treatment of collagen products for medical use, including pericardium for heart valves, involves enhancing and strengthening these cross-links (128, 129); there are both physical and chemical techniques for this, the latter primarily using a number of different types of agents that react with specific amino acid residues on the collagen molecules.

Reactions with the ε-amino groups constitute the most widely used approach with chemical cross-linking. Specifically, primary aldehydes react with the ε-amino groups of lysine residues, with minor contribution from links to hydroxylysine, guanidine, phenolic and thiol groups. Formaldehyde may be used, but the reactions are largely reversible; they are also relatively inefficient and it is converted into paraformaldehyde on storage.

GA is the most commonly used aldehyde cross-linking agent and is discussed in a separate section below.

Isocyanates react readily with ε-amino groups; di-isocyanates can react with two amino groups to form cross-links. This has been used in products to cross-link collagen (130) and considered for use with bovine pericardium (131), but this has not been taken up seriously with heart valve technology. In addition, quinones or quininoid complexes react with the ε-amino groups of lysine groups of collagen; this has been used to cross-link collagen in experimental tendon tissue engineering (132), but again not with heart valve pericardium.

After the focus on amino groups, carboxyl groups have been targeted in some cross-linking techniques, especially those relying on the activation of carboxyl groups on the polypeptide chain that can react with the amino groups on other chains. These have tended to involve either the use of carbodiimides or acyl azides. Ethyl-3(3dimethylamino) propyl carbodiimide (EDC) reacts with carboxy groups, initially to form O-acylisourea groups which then combine with diamines to form amide bonds. These produce cross-linked collagens with very good mechanical properties, under consideration for tissue engineering scaffolds (133). Other EDC-facilitated crosslinking regimes include subsequent reaction with activated dicarboxylic acids to additionally crosslink the tissue amines, or pre-blocking the amines (with monoaldehydes) to prevent intramolecular crosslinking (134) has also been reported (135).

Epoxides, such as epichlorhydrin, and the conversion of the carboxylic acid side chains to acyl azides followed by reaction with tissue amines, are also used in cross-linking collagen (136). Cyclic ether rings can be opened by the nucleophilic attack of bases and acids, cross-links being formed between carboxyl and amino groups. The use of polyphenols, e.g., pentagalloyl glucose, PGG, (136), and genepin, a natural substance extracted from gardenias and purported to have lower toxicity, have been described (137).

Figure 4 provides a schematic that shows the essential chemistry of pericardium cross-linking.

Collagen can also be cross-linked by physical methods, for example by irradiation, including gamma rays and ultraviolet light, and dehydrothermal treatments, but these do not appear relevant to bovine pericardium.

Glutaraldehyde

GA is highly soluble in aqueous media, where the solution typically consists of mixtures of free aldehyde, mono- and di-hydrated monomeric GA, monomeric and polymeric hemiacetals and various unsaturated polymers (103). The free GA, cyclic hemiacetal and oligomers are in equilibrium with each other, with the amount of free GA usually being not more than 4% (138). As noted by Jones (139), GA solution at the pH of fixation also contains polymerized GA, the level of which will depend on conditions and age of the solution. Both the free GA and the unsaturated polymer take part in the polymerization process, and both have other biological effects, including cytotoxicity (140); it has been suggested that the biochemical processes and cytotoxicity of GA-fixed bioprostheses are dependent on the stability of GA polymers (141).

It seems likely that cross-linking occurs by the combined effects of Schiff base linkages formed by reactions between an aldehyde group on monomeric GA with an amino group, for example of lysine or hydroxylysine, and the polymerization of the GA *via* aldol condensation between adjacent aldehydes. There is variable stability between these resulting linkages and, of course, other amino groups and others such as carboxy groups may also be involved.

With this outline of the cross-linking process in mind, two of the more important characteristics of GA treated pericardium will be the density of the cross-links and the precise molecular structure of the links, and these in turn will be controlled by the concentration of the GA in the fixative solution and the nature of any other chemicals, especially amino acids, that are present in the solution (44, 142–144). These are not trivial issues since, as noted in an earlier section, the characteristics of the cross-linked pericardium strongly influence both mechanical properties and susceptibility to calcification (144–147).

Different manufacturers of bioprosthetic valves use somewhat different regimes of GA treatment. Typically there will be one

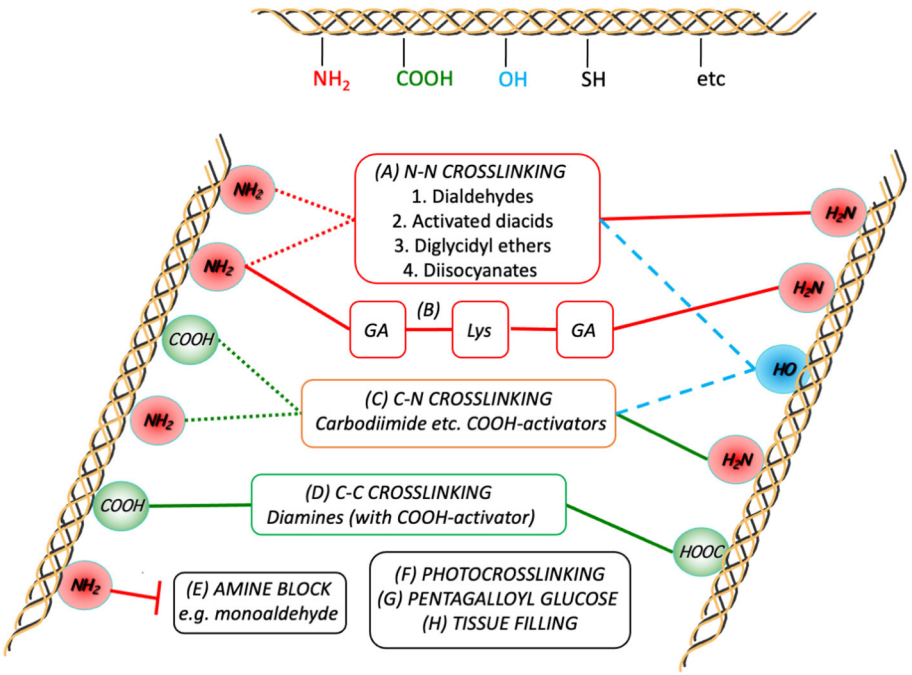

FIGURE 4 | Schematic representation of the crosslink chemistries as they relate to the major participating functional groups on the collagen chains. Although GA crosslinking **(A)** is complex, it is generally agreed to form inter- (and intramolecular; dotted red lines) links predominantly between the ε-amino groups of the lysines present in the peptide. Combining GA crosslinking with addition of lysine is also shown in **(B)**. Diamines are typically used to form intermolecular crosslinks between carboxylic acid groups (from Glu and Asp) after activation of the latter toward nucleophilic attack **(D)**. Some treatments use activated diacids to crosslink between the amines **(A2)**, sometimes in combination with **(D)**. In either **(A2)** or **(D)**, subject to sufficient proximity, activated tissue COOH-groups can also react with tissue NH_2-groups on the same or other chains **(C)**. In order to prevent the participation of tissue amines in the crosslinking process, they can be pre-blocked **(E)**. The potential for participation of hydroxyl groups with the activated COOH or other electrophiles is also indicated (dashed blue lines).

or more initial GA fixation processes, using concentrations of 0.2-0.8%, followed by storage, typically in 0.2% GA, sometimes in an organic solvent such as ethanol / octanol. Some processes involve post-fixation phases with lysine (44) or glycine (140). There have also been suggestions that dynamic rather than static conditions for fixation yield products with better mechanical properties (148), but this does not appear to be widely used. There have also been attempts to avoid prolonged storage in solutions, for example by freeze-drying, but too much damage to collagen fibrils takes place (149). Valves are thoroughly rinsed in saline, several times, before clinical application.

Decellularization

In 1984, Malone et al. took carotid arteries from a group of donor dogs and treated them with detergents before reimplanting them in recipient dogs (150). Two different detergents were used, sequentially, first Triton X-100, a non-denaturing detergent, used with a protease inhibitor, followed by sodium dodecylsulfate (SDS), a denaturing detergent; the tissues were rinsed with ethanol before reimplantation. This sequence essentially eliminated cells within the arteries and there was minimal immunogenicity after 90 days. This was the first example of decellularization used for the preparation of allogeneic/xenogeneic bioprostheses (151).

Naso et al. (152) reviewed attempts to produce alternative decellularization protocols in subsequent years, as follows. Wilson *et al* followed the Malone procedure with the introduction of a digestion step with nuclease enzymes, with both hypo- and hypertonic solutions, used for canine arteries (153). Bader et al. only used a 1% Triton X-100 solution together with a nuclease enzyme digestion step, with porcine heart valves (154). Steinhoff et al. (155) used a single extractive step with 0.05% trypsin for lamb pulmonary heart valve. Korossis et al. (156) used a single SDS detergent solution, with both hypo- and hypertonic conditions, for porcine heart valve leaflets. Kim et al. (157) used one exposure to 1% Triton X-100, followed by digestion with endonuclease, washing using hypertonic solution, then exposure to 0.5% SDS, for porcine heart valve leaflets. Meyer et al. (158) used one detergent, 0.5% Triton X-100, with protease inhibitor and both hypo- and hypertonic solutions, in rat aortic valves Erdbrugger et al. (159) used a single detergent step with sodium deoxycholate (DOC) with porcine pulmonary heart valves. Dainese et al. (160) used a single extraction step with 0.5% trypsin for pulmonary human heart valves.

Gallo et al. (161) first used a 1% Triton X-100 detergent step, then a protease inhibitor step, a further detergent step with 0.4% sodium cholate, using both hypo- and hypertonic solutions, washing with isopropanol and a final digestion step with endonuclease, for porcine aortic heart

TABLE 1 | Summary of decellularization techniques, their modes of action and effects on the extracellular matrix (ECM) Includes data from Gilbert et al. (162) and Crapo et al. (163).

Method	Mode of action	Effect on ECM
Techniques employed		
Agitation	Exposure to chemicals and removal of cellular material. Severe agitation can cause cell lysis	Aggressive agitation or sonication can disrupt ECM
Pressure	Exposure to chemicals and removal of cellular material. Pressure can also burst cells	Pressure gradient can cause damage or disruption to the ECM
Perfusion	Provides for exposure to chemicals and removal of cellular material.	Perfusion will create a pressure differential which can damage the ECM
Supercritical fluid	Provides for exposure to chemicals and removal of cellular material. The pressure associated with supercritical fluid can burst cells.	Pressure gradient can cause damage or disruption to the ECM
Physical methods		
Freeze/thaw cycles	Cells are burst by formation of intracellular ice crystals.	Ice crystals can also damage or disrupt ECM
Force	Tissue removed through direct force eliminates cells. Can also burst cells	Direct force can also damage the ECM
Electroporation	Cells are disrupted or burst by the pulsing electrical field	Can also damage the ECM
Biological methods		
Trypsin	Facilitates cleavage of peptide bonds at C-terminal of Arg and Lys amino acids	Prolonged exposure damages ECM ultrastructure, specifically GAG, fibronectin, collagen, laminin and elastin. However, removal of GAG slower compared to detergents
Nucleases	Catalyzes the hydrolysis of both ribonucleotide and deoxyribonucleotide chains	Removal is difficult. Remaining remnants could provoke an immune response
Dispase	Cleaves specific peptides, mainly fibronectin and collagen IV	Prolonged exposure can also remove the collagen and fibronectin.
Chemical methods		
Acids/Bases	Denatures proteins, disrupts nucleic acids and solubilizes cytoplasmic components of cells	Possible removal or damage of GAGs, collagen and growth factors
Hypo- and hypertonic solutions	Osmotic shock causes lysis of cells and disruption of DNA-protein interactions	Effective lyses of cells but does not remove the cellular debris
Non-ionic detergents (Triton X-100)	Effective in disruption of lipid-lipid, lipid-protein and DNA-protein interactions. Protein-protein interaction not affected	Efficacy dependent on tissue, some removal of GAGs and damage to ultrastructure
Ionic detergents (SDS, DOC, Triton X-200)	Both nuclear and cytoplasmic membranes are solubilized, some denaturing of proteins	SDS: Removes cytoplasmic proteins and nuclear remnants effectively, but disrupts ultrastructure, damages collagen and removes GAGs. DOC: Some disruption of ultrastructure and removal of GAG, but with mixed efficacy Triton X-200: Effective at removal of cells, but also causes greater disruption of ultrastructure
Solvents		
Acetone	Achieves cell lysis by dehydration, also solubilizes and removes proteins	Effective removal of cells from very dense tissue, inactivation of pyrogens but does crosslink and precipitate proteins including collagen
Alcohols	Achieves cell lysis by dehydration, also solubilizes and removes proteins	Effective removal of cells from very dense tissue, inactivation of pyrogens but does crosslink and precipitate proteins including collagen
Tributyl phosphate (TBP)	Forms stable complexes with metals and disrupts protein-protein interactions	Tissue determines efficacy, some loss of collagen in dense tissue, mechanical properties affected minimally.
Chelating agents (EDTA, EGTA)	They bind metallic ions facilitating the disruption of cell adhesion to the ECM	Ineffective when used alone, but effective when used with enzymatic methods

valve They observed that trypsin achieves only incomplete decellularization, and it is not included in currently used decellularization agents. They also noted that SDS, while being very effective in removing cellular components does cause some ECM damage.

Further details on different methods used for decellularization, their modes of action and effects on the ECM are given in **Table 1**.

Current Strategies

In the light of the above experiences, the trends in decellularization techniques in very recent years have been toward complexities in solutions and sequences. Three recent papers stand out as leaders in the formulation of these procedures which are leading toward optimization of techniques that provide calcification-resistant, non-immunogenic bovine pericardial heart valves.

The work of Collatusso et al. in Brazil (164) discusses the use of a proprietary 0.1% SDS solution, at 24 h at room temperature, followed by immersion in 70% ethanol for 24 h, then sequential washing in PBS for 10 days. This is followed by fixation in low concentration 0.1% GA for 7 days, with final storing of the manufactured valve in paraben. In a sheep model, after 180 days in the mitral position, the decellularized valve showed pliable leaflets without macroscopic signs of calcification and with a quantitative 89% reduction in calcium levels compared to non-decellularized controls.

Zouhair et al., with a largely Italian group, reported on what they described as the TRICOL process (49). Fresh native bovine pericardium was first stored in PBS; the decellularization protocol involved protease inhibitors, with alternated hypo/hypertonic solutions and "detergents such as 0.1-1% Triton X-100 and 10 mM sodium cholate." Residual nucleic acids were digested using non-specific endonucleases, and stored in antibiotic/antimycotic cold saline solution. No specific mention was made of cross-linking, although this appears to be consistent with their ultimate objectives of tissue engineering scaffolds rather than bioprosthetic heart valves. The importance of perfusion pressure gradients during decellularization was emphasized in the work of the Simionescu group (165).

On the other hand, the authors of the present paper (166) have directed the development of a combined decellularization and cross-linking protocol specifically for bioprosthetic valves. Pericardial sacs are initially exposed to hypotonic shock by placement in cold sterile, reverse osmosis, water containing sodium azide. The tissue are then decellularized with detergent solution containing 0.15% Triton X-100, 0.25% sodium deoxycholate, with 50 mM Tris, 0.1% EDTA and 0.02% sodium azide; this step takes place under agitation for 3-4 days at 18-25°C. Sterile rinsing takes places, successively in water, 70% ethanol and water for 20 min. There are then two identical repeat cycles of decellularization and rinsing. Tissue is then placed in DNAse / RNAse solution for 48 h, then placed in 0.7% GA in PBS before transfer to L-Lysine solution (0.1 M in PBS) for 48 h, followed by further rinsing, then a repeat of the GA cycle for 96 h. Free aldehyde and Schiff base reduction is achieved with 0.1 M sodium borohydride in PBS. Following rinsing, storage is undertaken in 0.2% GA.

It should be noted that in a very recent paper, Laker et al. (167) reinforce the concept of synergy achieved with combinations of detergents for decellularization.

Overview and Conclusions

The use of bioprostheses for heart valve therapy has evolved over four decades to a point where both surgical and TAVI devices are highly successful. The rapid expansion of the TAVI concept has clearly placed a significant onus on the need for improved production methods, especially in relation to the pre-treatment of bovine pericardium. Two of the major difficulties associated with the biocompatibility of bioprosthetic valves, that is the possibilities of immune responses and calcification, which have led to either catastrophic failure or slow dystrophic changes, have been addressed by evolutionary trends in cross-linking and decellularization techniques. Over the last two decades, these improvements have resulted in somewhat greater longevity.

However, as the need to consider the use of bioprosthetic valves in younger patients has become an important clinical and sociological issue, the requirement for even greater longevity and safety is now paramount. This is especially true with respect to potential therapies for young people who are afflicted by RHD, and for whom no clinically acceptable and cost-effective treatments currently exist (11).

To extend longevity to this new level, it has been necessary to evaluate the mechanisms of pericardium biocompatibility, with special emphasis on the interplay between cross-linking, decellularization and anti-immunogenicity processes. These mechanisms are reviewed in this paper.

On the basis of a better understanding of these mechanisms, a few alternative treatment protocols have been developed in the last few years. The most promising protocol here is based on a carefully designed combination of phases of tissue-protective decellularization with a finely-titrated GA-lysine cross-linking sequence. Such refined protocols offer considerable potential in the progress toward superior longevity of pericardial heart valves. It should also be noted that fully biostable synthetic polymers, such as some polyurethanes, could compete with pericardium as the construction materials for flexible leaflet valves, either surgical or TAVR.

AUTHOR CONTRIBUTIONS

DW wrote first draft and finalized the manuscript. DB and PZ contributed sections and edited the manuscript. JV and PH contributed data and artwork. All authors contributed to the article and approved the submitted version.

REFERENCES

1. Musumeci L, Jacques N, Hego A, Nchimi A, Lancellotti P, Oury C. Prosthetic aortic valves: challenges and solutions. *Front Cardiovasc Med*. (2018) 5:46. doi: 10.3389/fcvm.2018.00046
2. Naso F, Gandaglia A. Different approaches to heart valve decellularization: a comprehensive overview of the past 30 years. *Xenotransplantation*. (2017) 25:e12354. doi: 10.1111/xen.12354
3. Zilla P, Yacoub M, Zuhlke L, Beyersdorf F, Silva K, Khubulava G, et al. Global unmet needs in cardiac surgery. *Global Heart*. (2018) 13:293–303. doi: 10.1016/j.gheart.2018.08.002
4. Zilla P, Bolman RM, Boateng P, Silwa K. A glimpse of hope: cardiac surgery in low- to middle-income countries. *Cardiovasc Diagn Ther*. (2020) 10:336–49. doi: 10.21037/cdt.2019.11.03
5. Carpentier A, Lemaigre G, Robert L, Carpentier S, Dubost C. Biological factors affecting long-term results of valvular heterografts. *J Thorac Cardiovasc Surg*. (1969) 58:467–83. doi: 10.1016/S0022-5223(19)42561-0
6. Cohn LH, Collins JJ, Disesa VJ, Couper GS, Peigh PS, Kowalker W, et al. Fifteen-year experience with 1678 Hancock porcine bioprosthetic heart valve replacements. *Ann Surg*. (1989) 210:436–43. doi: 10.1097/00000658-198910000-00003

7. Elayda MA, Hall RJ, Reul RM, Alonzo DM, Gillette N, Reul GJ, et al. Aortic valve replacement in patients 80 years and older: Operative risks and long-term results, *Circulation.* (1993) 88:11–6.
8. Rostagno C. Heart valve disease in elderly. *World J Cardiol*. (2019) 11:71–83. doi: 10.4330/wjc.v11.i2.71
9. Dangas GD, Weitz JI, Giustino G, Makkar R, Mehran R. Prosthetic heart valve thrombosis. *J Am Coll Cardiol*. (2016) 68:2670–89. doi: 10.1016/j.jacc.2016.09.958
10. Omar RZ, Morton LS, Beirne M, Blot WJ, Lawford PV, Hose R, et al. Outlet strut fracture of Björk-Shiley convexo-concave valves: can valve-manufacturing characteristics explain the risk? *J Thorac Cardiovasc Surg*. (2001) 121:1143–9. doi: 10.1067/mtc.2001.113937
11. Zilla P, Brink J, Human P, Bezuidenhout D. Prosthetic heart valves: catering for the few. *Biomaterials.* (2008) 29:385–406. doi: 10.1016/j.biomaterials.2007.09.033
12. Scherman J, Zilla P. Poorly suited heart valve prostheses heighten the plight of patients with rheumatic heart disease *Intern J Cardiol*. (2020) 318:104–14. doi: 10.1016/j.ijcard.2020.05.073
13. Cribier A. The development of transcatheter aortic valve replacement. (TAVR). *Glob Cardiol Sci Pract.* (2016) 4:e201632. doi: 10.21542/gcsp.2016.32
14. Figulla HR, Franz M, Lauten A. The history of transcatheter aortic valve implantation. (TAVI): a personal view over 25 years of development. *Cardiovasc Revasc Med*. (2019) 21:398–403. doi: 10.1016/j.carrev.2019.05.024
15. Scherman J, Bezuidenhout D, Williams DF, Ofoegbu C, Zilla, P. TAVI for low and middle income countries. *Eur Heart J.* (2017) 38:1182–4. doi: 10.1093/eurheartj/ehx169
16. Bezuidenhout D, Williams DF, Zilla P. Polymeric heart valves for surgical implantation, catheter-based technologies and heart assist devices. *Biomaterials*. (2015) 36:6–25. doi: 10.1016/j.biomaterials.2014.09.013
17. Sotiropoulos F, Le TB, Gilmanov A. Fluid mechanics of heart valves and their replacements. *Ann Rev Fluid Mech.* (2016) 48:259–83. doi: 10.1146/annurev-fluid-122414-034314
18. Roudout R, Servbri K, Lafitte S. Thrombosis of prosthetic heart valves: diagnosis and therapeutic considerations. *Heart*. (2007) 93:137–42. doi: 10.1136/hrt.2005.071183
19. Simon P, Kasimir MT, Seebacher G, Weigel G, Ullrich R, Salzer-Muhar U, et al. Early failure of the tissue engineered porcine heart valve SYNERGRAFT in pediatric patients. *Eur J Cardiothorac Surg*. (2003) 23:1002–6. doi: 10.1016/S1010-7940(03)00094-0
20. Koziarz A, Makhdoum A, Butany J, Ouzounian M, Chung J. Modes of bioprosthetic valve failure: a narrative review. *Curr Opin Cardiol*. (2020) 35:123–32. doi: 10.1097/HCO.0000000000000711
21. Pibarot P, Dumesnil JG. Prosthetic heart valves: selection of the optimal prosthesis and ling-term management. *Circulation*. (2009) 119:1034–48. doi: 10.1161/CIRCULATIONAHA.108.778886
22. Rahimtoola RH. Choice of prosthetic heart valves in adults: an update. *J Am Coll Cardiol.* (2010) 55:2413–26. doi: 10.1016/j.jacc.2009.10.085
23. Baumgartner H, Falk V, Bax JJ, De Bonis M, Hamm C, Holm Per J, et al. 2017 ESC/EACTS Guidelines for the management of valvular heart disease. *Eur Heart J*. (2017) 38:2739–91. doi: 10.1093/eurheartj/ehx391
24. Grebenik EA, Gafarova ER, Istranov LP, Instranov EV, Ma X, Xu J, et al. Mammalian pericardium-based bioprosthetic materials in xenotransplantation and tissue engineering. *Biotechnol J*. (2020) 15:1900334. doi: 10.1002/biot.201900334
25. Shklover J, McMasters J, Alfonso-Garcia A, Lopera Higuita M, Panitch A, Marcu L, et al. Bovine pericardial extracellular matrix niche modulates human aortic endothelial cell phenotype and function. *Sci Rep*. (2019) 9:16688–700. doi: 10.1038/s41598-019-53230-1
26. Jaworska-Wilczynska M, Trzaskoma P, Szczepankiewicz AA, Hryniewiecki T, Pericardium: structure and function in health and disease. *Folia Histochem Cyto.* (2016) 54:121–5. doi: 10.5603/FHC.a2016.0014
27. Mutsaers SE. The mesothelial cell. *Int J Biochem Cell Biol*. (2004) 36:9–16. doi: 10.1016/S1357-2725(03)00242-5
28. Rodriguez ER, Tan CD. Structure and anatomy of the human pericardium. *Prog Cardiovasc Dis*. (2017) 59:327–40. doi: 10.1016/j.pcad.2016.12.010
29. Murdock K, Martin C, Sun W. Characterization of mechanical properties of pericardium tissue using planar biaxial tension and flexural deformation. *J Mech Behav Biomed Mat*. (2018) 77:148–56. doi: 10.1016/j.jmbbm.2017.08.039
30. Xi T, Liu F, Xi B. Effect of pretreatment with epoxy compounds on the mechanical properties of bovine pericardial bioprosthetic materials. *J Biomat Appl.* (1992) 7:61–72. doi: 10.1177/088532829200700104
31. Sacks MS, Mirnajafi A, Sun W, Schmidt P. Bioprosthetic heart valve heterograft biomaterials: structure, mechanical behavior and computer simulation. *Expert Rev Med Devices.* (2006) 3:817–34. doi: 10.1586/17434440.3.6.817
32. Whelan A, Duffy J, Gaul RT, O'Reilly D, Nolan PR, Gunning P, et al. Collagen fiber orientation and dispersion govern ultimate tensile strength and fatigue properties of bovine pericardium. *J Mech Behav Biomed Mater*. (2019) 90:54–60. doi: 10.1016/j.jmbbm.2018.09.038
33. Soares JS, Feaver KR, Zhang W, Kamensky D, Aggarwal A, Sacks MS. Biomechanical behavior of bioprosthetic heart valve heterograft tissues: characterization, simulation, and performance. *Cardiovasc Eng Technol*. (2016) 7:309–51. doi: 10.1007/s13239-016-0276-8
34. Zhang X, Williams DF. *Definitions of Biomaterials for the Twenty-First Century*. Oxford: Elsevier (2019).
35. Williams DF. On the mechanisms of biocompatibility. *Biomaterials.* (2008) 29:2941–53. doi: 10.1016/j.biomaterials.2008.04.023
36. Williams DF. Biocompatibility pathways: biomaterials-induced sterile inflammation, mechanotransduction and principles of biocompatibility control. *ACS Biomater Sci Eng.* (2017) 3:2–35. doi: 10.1021/acsbiomaterials.6b00607
37. Webb JG, Dvir D. Transcatheter aortic valve replacement for bioprosthetic aortic valve failure: the valve-in-valve procedure. *Circulation.* (2013) 127:2542–50. doi: 10.1161/CIRCULATIONAHA.113.000631
38. Lederman RJ, Babaliaros VC, Rogers T, Khan JM, Kamioka N, Dvir D, et al. Preventing coronary obstruction during transcatheter aortic valve replacement: from computed tomography to BASILICA. *JACC Cardiovasc Intervent.* (2019) 12:1197–216. doi: 10.1016/j.jcin.2019.04.052
39. Mercuri JJ, Lovekamp JJ, Simionescu DT, Vyavahare NR. Glycosaminoglycan-targeted fixation for improved bioprosthetic heart valve stabilization. *Biomaterials*. (2007) 28:496–503. doi: 10.1016/j.biomaterials.2006.09.005
40. Bottio T, Thiene G, Pettenazzo E, Ius P, Bartolotti U, Rizzoli G, et al. Hancock II bioprosthesis: a glance at the microscope in mid-long term explants. *J Thorac Cardiovasc Surg*. (2003) 126:99–105. doi: 10.1016/S0022-5223(03)00131-4
41. Arbustini E, Jones M, Moses RD, Eidbo EE, Carroll RJ, Ferrans VJ. Modification by the Hancock T6 process of calcification of bioprosthetic cardiac valves implanted in sheep. *Am J Cardiol*. (1984) 53:1388–96. doi: 10.1016/0002-9149(84)90099-7
42. Maranto AR, Schoen FJ. Alkaline phosphatase activity of glutaraldehyde-treated bovine pericardium used in bioprosthetic cardiac valves. *Circ Res.* (1988) 63:844–8. doi: 10.1161/01.RES.63.4.844
43. Khorramirouz R, Go JL, Noble C, Morse D, Lerman A, Young MD. *In vivo* response of acellular porcine pericardial for tissue engineered transcatheter aortic valves. *Sci Rep.* (2019) 9:1094. doi: 10.1038/s41598-018-37550-2
44. Bezuidenhout D, Oosthuysen A, Human P, Weissenstein C, Zilla P. The effects of cross-link density and chemistry on the calcification potential of glutaraldehyde-fixed bioprosthetic heart valves. *Biotechnol Appl Biochem*. (2009) 54:133–40. doi: 10.1042/BA20090101
45. Trantina-Yates AE, Human P, Bracher M, Zilla P. Mitigation of bioprosthetic heart valve degeneration through biocompatibility: *in vitro* versus spontaneous endothelialization. *Biomaterials*. (2001) 22:1837–46. doi: 10.1016/S0142-9612(00)00365-3
46. Skowasch D, Schrempf S, Wernert N, Steinmetx M, Jabs A, Tuleta I, et al. Cells of primary extravalvular origin in degenerative aortic valves and bioprostheses. *Eur Heart J*. (2005) 26:2576–80. doi: 10.1093/eurheartj/ehi458
47. Nair V, Law KB, Li AY, Phillips KRB, David TE, Butany J. Characterizing the inflammatory reaction in explanted Medtronic Freestyle stentless porcine aortic bioprosthesis over a 6-year period. *Cardiovasc Path.* (2012) 21:158–68. doi: 10.1016/j.carpath.2011.05.003
48. Dahm M, Husmann M, Mayer E, Prüfer D, Groh E, Oelert H. Relevance of immunological reactions for tissue failure of bioprosthetic

heart valves. *Ann Thorac Surg.* (1995) 60(Suppl 2):S348–52. doi: 10.1016/0003-4975(95)00291-R
49. Zouhair S, Sasso ED, Tuladhar SR, Fidalgo C, Vedovelli L, Filippi A, et al. A comprehensive comparison of bovine and porcine decellularized pericardia: new insights for surgical applications. *Biomolecules.* (2020) 10:371. doi: 10.3390/biom10030371
50. Jastrzebska M, Wrzalik R, Kocot A, Zalewska-Rejdak J, Cwalina B. Hydration of glutaraldehyde-fixed pericardium tissue: Raman spectroscopic study. *J Raman Spectrosc*. (2003) 34:424–31. doi: 10.1002/jrs.1016
51. Jastrzebska M, Mroz I, Barwinski B, Zalewska-Rejdak J, Turek A, Cwalina B. Supramolecular structure of human aortic valve and pericardial xenograft material; Atomic force microscopy study. *J Mater Sci Mater Med.* (2008) 19:249–56. doi: 10.1007/s10856-006-0049-2
52. Suesca E, Dias AMA, Braga MEM, de Sousa HC, Fontanilla MR. Multifactor analysis on the effect of collagen concentration, cross-linking and fiber/pore orientation on chemical, microstructural, mechanical and biological properties of collagen type I scaffolds. *Mat Sci Eng C*. (2017) 77:333–41. doi: 10.1016/j.msec.2017.03.243
53. Meyer M. Processing of collagen based biomaterials and the resulting materials properties. *BioMed Eng Online*. (2019) 18:24. doi: 10.1186/s12938-019-0647-0
54. Setiawan T, Dewanjee MK, Gross DR. Quantitation of adsorption and conjugation of plasma proteins by residual glutaraldehyde in fixed collagenous tissue with radio-iodinated plasma proteins. *ASAIO J.* (1998) 44:M445–8. doi: 10.1097/00002480-199809000-00024
55. Shen M, Carpentier SM, Cambillau M, Chen L, Martinet B, Carpentier A. Protein adsorption in glutaraldehyde-preserved bovine pericardium and porcine valve tissues. *Ann Thorac Surg.* (2001) 71:S408–9. doi: 10.1016/S0003-4975(01)02506-1
56. Williams DF. A systems engineering approach to restoring kidney structure and function. In: Orlando G, Remuzzi G, Williams DF, editors. *Kidney Transplantation, Bioengineering and Regeneration*. London: Elsevier (2017) p. 769–86.
57. Van Gelder MK, Abrahams AC, Joles JA, Kaysen GA, Gerritsen KGF. Albumin handling in different hemodialysis membranes. *Nephrol Dialysis Transplant*. (2018) 33:906–13. doi: 10.1093/ndt/gfx191
58. Eloot S, Ledebo I, Ward RA. Extracorporeal removal of uremic toxins: can we still do better? *Sem Nephrol*. (2014) 34:209–27. doi: 10.1016/j.semnephrol.2014.02.011
59. Lim WY, Lloyd G, Bhattacharyya S. Mechanical and surgical bioprosthetic valve thrombosis. *Heart*. (2017) 103:1934–41. doi: 10.1136/heartjnl-2017-311856
60. Brown ML, Park SJ, Sundt TM, Schaff HV. Early thrombus risk in patients with biologic valves in the aortic position. *J Thorac Cardiovasc Surg.* (2012) 144:108–11. doi: 10.1016/j.jtcvs.2011.05.032
61. Poli D, Antonucci E, Pengo V, Grifoni E, Maggini N, Twsta S, et al. Risk of reoperation in bioprosthetic valve patients with indication for long-term anticoagulation. Results from the observations retrospective multicenter PLECTRUM study. *Open Heart*. (2018) 5:e000837. doi: 10.1136/openhrt-2018-000837
62. Izumi C, Miyake M, Amano M, Kitai T, Obayashi Y, Takegami M. Registry of antithrombotic therapy in atrial fibrillation patients with bioprosthetic valves: a retrospective observational study. *J Cardiol.* (2020) 76:44–50. doi: 10.1016/j.jjcc.2020.02.006
63. Tian Z, Li T, Ma S. Impact of leaflet thrombosis on hemodynamics and clinical outcomes after bioprosthetic aortic valve replacement: a meta-analysis. *Clin Cardiol.* (2020) 43:468–74. doi: 10.1002/clc.23331
64. Jewgenow P, Schneider H, Bokenkamp R, Horer J, Cleuziou J, Foth R, et al. Subclinical thrombus formation in bioprosthetic pulmonary valve conduits. *Int J Cardiol*. (2019) 281:113–8. doi: 10.1016/j.ijcard.2019.01.095
65. Chakravarty T, Sondergaard L, Friedman J, De Beckar O, Berman D, Kofoed KF, et al. Subclinical leaflet thrombosis in surgical and transcatheter bioprosthetic aortic valves: an observational study. *Lancet.* (2017) 389:2383–92. doi: 10.1016/S0140-6736(17)30757-2
66. Vranckx P, Windecker S, Welsh RC, Valimigli M, Mehran R, Dangas G. Thrombo-embolic prevention after transcatheter aortic valve implantation. *Eur Heart J*. (2017) 38:3341–50. doi: 10.1093/eurheartj/ehx390
67. Midha PA, Raghav R, Sharma R, Condado JF, Okafor IU, Rami T, et al. The fluid mechanics of transcatheter heart valve leaflet thrombosis in the neosinus. *Circulation*. (2017) 136:1598–609. doi: 10.1161/CIRCULATIONAHA.117.029479
68. Gendler E, Gendler S, Nimni ME. Toxic reactions evoked by glutaraldehyde-fixed pericardium and cardiac valve tissue bioprostheses. *J Biomed Mater Res.* (1984) 18:727–36. doi: 10.1002/jbm.820180703
69. Umashankar PR, Mohanan PV, Kumari TV. Glutaraldehyde treatment elicits toxic response compared to decellularization in bovine pericardium. *Toxicol Internat.* (2012) 19:51–8. doi: 10.4103/0971-6580.94513
70. Zeiger E, Gollapudi B, Spencer P. Genetic toxicity and carcinogenicity studies of glutaraldehyde – a review. *Rev Mut Res*. (2005) 589:136–51. doi: 10.1016/j.mrrev.2005.01.001
71. International Standards Organization, ISO 10993. *Biological Evaluation of Medical Devices.* Geneva: International Standards Organization.
72. Agency for Toxic Substances and Disease Registry. *(USDHHS), Toxicological Profile for Glutaraldehyde.* Washington, DC: Agency for Toxic Substances and Disease Registry (2017).
73. Bozec L, Odlyha M. Thermal denaturation studies of collagen by microthermal analysis and atomic force microscopy. *Biophys J*. (2011) 101:229–36. doi: 10.1016/j.bpj.2011.04.033
74. Ivankin A, Boldirev V, Fadeev G, Baburina M, Kulikovskii A, Vostrikove N. Denaturation of collagen structures and their transformation under the physical and chemical effects. *J Phys Conf Ser*. (2017) 918:012010. doi: 10.1088/1742-6596/918/1/012010
75. Laurent GJ. Dynamic state of collagen: pathways of collagen degradation *in vivo* and their possible role in regulation of collagen mass. *Am J Physiol Cell Physiol.* (1987) 21:C1–C9. doi: 10.1152/ajpcell.1987.252.1.C1
76. Sabelman EE. Biology, biotechnology and biocompatibility of collagen. In: Williams DF. editor. *Biocompatibility of Tissue Analogs.* Boca Raton, FL:CRC Press. vol 1 (1985). p. 27–59.
77. Ellsmere JC, Khanna RA, Lee JM. Mechanical loading of bovine pericardium accelerates enzymatic degradation. *Biomaterials*. (1999) 20:1143–50. doi: 10.1016/S0142-9612(99)00013-7
78. Ghazanfari A, Driessen-Mol A, Bouten CVC, Baaijens FPT. Modulation of collagen fiber orientation by strain-controlled enzymatic degradation. *Acta Biomater*. (2016) 35:118–26. doi: 10.1016/j.actbio.2016.02.033
79. Simionescu A, Simionescu D, Deac R. Biochemical pathways of tissue degeneration in bioprosthetic cardiac valves: the role of matrix metalloproteinases. *ASAIO J.* (1996) 42:M561–7. doi: 10.1097/00002480-199609000-00049
80. Bracher M, Simionescu D, Simionescu A, Davies N, Human P, Zilla P. Matrix metalloproteinases and tissue valve degeneration. *J Long Term Eff Med Implants*. (2001) 11:221–30. doi: 10.1615/JLongTermEffMedImplants.v11.i34.90
81. Jablonska-Trypuc A, Matejczyk M, Rosochacki S. Matrix metalloproteinases (MMPs), the main extracellular matrix (ECM) enzymes in collagen degradation, as a target for anticancer drugs. *J Enzyme Inhib Med Chem.* (2016) 31:177–83. doi: 10.3109/14756366.2016.1161620
82. Christian AJ, Lin H, Alferiev IS, Connolly JM, Ferrari G, Hazen SL, et al. The susceptibility of bioprosthetic heart valve leaflets to oxidation. *Biomaterials.* (2014) 35:2097–102. doi: 10.1016/j.biomaterials.2013.11.045
83. Kataruka A, Otto CN. Valve durability after transcatheter aortic valve implantation. *J Thorac Dis*. (2018) 10:S3629–36. doi: 10.21037/jtd.2018.07.38
84. Hamm CW, Arsalan M, Mack MJ. The future of transcatheter aortic valve implantation. *Eur Heart J*. (2016) 37:803–10. doi: 10.1093/eurheartj/ehv574
85. Li KYC. Bioprosthetic heart valves: upgrading a 50-year old technology. *Front Cardiovasc Med.* (2019) 6:47. doi: 10.3389/fcvm.2019.00047
86. Cote N, Pibarot, Clavel M-A. Incidence, risk factors, clinical impact, and management of bioprosthesis structural valve degeneration. *Curr Opin Cardiol*. (2017) 32:123–9. doi: 10.1097/HCO.0000000000000372
87. Schussler O, Lila N, Perneger T, Mootoosamy P, Grau J, Francois A, et al. Recipients with blood group A associated with longer survival rates in cardiac valvular bioprostheses. *EBioMedicine*. (2019) 42:54–63. doi: 10.1016/j.ebiom.2019.02.047
88. Sendroy J, Hastings AB. Studies of the solubility of calcium salts: III. The solubility of calcium carbonate and tertiary calcium

phosphates under various conditions. *J Biol Chem*. (1927) 71:797–846. doi: 10.1016/S0021-9258(18)84410-6
89. Merryman WD, Schoen FJ. Mechanisms of calcification in aortic valve disease: role of mechanokinetics and mechanodynamics. *Curr Cardiol Rep*. (2013) 15:355. doi: 10.1007/s11886-013-0355-5
90. Lerman DA, Prasad S, Alotti N. Calcific aortic valve disease: molecular mechanisms and therapeutic approaches. *Eur Cardiol Rev*. (2015) 10:108–12. doi: 10.15420/ecr.2015.10.2.108
91. Schoen FJ. Mechanisms of function and disease of natural and replacement heart valves, *Annu Rev Path.* (2012) 7:161–83. doi: 10.1146/annurev-pathol-011110-130257
92. Ayoub S, Ferrari G, Gorman RC, Gorman III JH, Schoen FJ, Sacks MS. Heart valve biomechanics and underlying mechanobiology. *Compr Physiol*. (2017) 6:1743–80. doi: 10.1002/cphy.c150048
93. Mohler ER, Chawla MK, Chang AW, Yyavahare N, Levy RJ, Graham L, et al. Identification and characterization of calcifying valve cells from human and canine aortic valves, *J Heart Valve Dis*. (1999) 8:254–60.
94. Schoen FJ, Levy RJ. Calcification of tissue heart valve substitutes: progress towards understanding and prevention. *Ann Thorac Surg*. (2005) 79:1072–80. doi: 10.1016/j.athoracsur.2004.06.033
95. Schoen FJ. Pathological calcification of biomaterials. In: Ratner BD et al., *Biomaterials Science: An Introduction to Materials in Medicine*. Amsterdam: Elsevier (2013) p. 739–54.
96. Schoen FJ, Fernandez J, Gonzalez-Lavin L, Cernaianu A. Causes of failure and pathologic findings in surgically removed Ionescu-Shiley standard bovine pericardial heart valve bioprostheses: emphasis on progressive structural deterioration. *Circulation.* (1987) 76:618–27. doi: 10.1161/01.CIR.76.3.618
97. Bonetti A, Marchini M, Ortolani F. Ectopic mineralization in heart valves: new insights from *in vivo* and *in vitro* pro-calcific models and promising perspectives on non-calcifiable bioengineered valves. *J Thorac Dis.* (2019) 11:2126–43. doi: 10.21037/jtd.2019.04.78
98. Human P, Zilla P. The possible role of immune responses in bioprosthetic heart valve failure. *J Heart Valve Dis*. (2001) 10:460–66.
99. Human P, Zilla P. Characterization of the immune response to valve bioprostheses and its role in primary tissue failure. *Ann Thorac Surg*. (2001) 71(Suppl 5):S385–8. doi: 10.1016/S0003-4975(01)02492-4
100. Human P, Zilla P. The neglected villain of bioprosthetic degeneration: inflammatory and immune processes. *J Long Term Eff Med Implants.* (2017) 27:143–61. doi: 10.1615/JLongTermEffMedImplants.v27.i2-4.50
101. Jeong WS, Kim YJ, Lim H-G, Jung S, Lee JR. The immune responses and calcification of bioprostheses in the α 1,3-galactosyltransferase knockout mouse. *J Heart Valve Dis.* (2016) 25:253–61.
102. Grizzle WE. Models of fixation and tissue processing. *Biotech Histochem*. (2009) 84:185–93. doi: 10.3109/10520290903039052
103. Jayakrishnan A, Jameela SR. Glutaraldehyde as a fixative in bioprostheses and drug delivery matrices. *Biomaterials*. (1996) 17:471–84. doi: 10.1016/0142-9612(96)82721-9
104. Carpentier A, Deloche A, Relland J, Fabian JN, Forman J, Camilleri JP, et al. Six year follow up of glutaraldehyde preserved heterografts, with particular reference to the treatment of congenital valve malformations. *J Thorac Cardiovasc Surg*. (1974) 68:771–82. doi: 10.1016/S0022-5223(19)41639-5
105. Carpentier A, Nashef A, Carpentier S, Ahmed A, Goussef N. Techniques for prevention of calcification of valvular bioprostheses. *Circulation.* (1984) 70:165–8.
106. Skinner JR, Kim H, Toon RS, Kongtahworn C, Phillips SJ, Zeff RH. Inflammatory epicardial reaction to processed bovine pericardium: case report. *J Thorac Cardiovasc Surg*. (1984) 88:789–91. doi: 10.1016/S0022-5223(19)35451-0
107. Dahm M, Lyman WD, Schwell AB, Factor SM, Frater RW. Immunogenicity of glutaraldehyde-tanned bovine pericardium. *J Thorac Cardiovasc Surg*. (1990) 99:1082–90. doi: 10.1016/S0022-5223(20)31465-3
108. Moczar M, Lecerf L, Mazzucotelli J-P, Loisance D. Immunoglobulins and complement deposits in Mitroflow pericardial bioprosthetic heart valves: a contributing factor to structural deterioration. *J Heart Valve Dis*. (1996) 5(Suppl 3):5276–83.
109. Gong G, Seifter E, Lyman WD, Factor WD, Blau S, Frater RW. Bioprosthetic cardiac valve degeneration: role of inflammatory and immune reactions. *J Heart Valve Dis*. (1993) 2:684–93.
110. Wong ML, Wong JL, Vapniarsky N, Griffiths LG. *In vivo* xenogeneic scaffold fate is determined by residual antigenicity and extracellular matrix preservation. *Biomaterials.* (2016) 92:1–12. doi: 10.1016/j.biomaterials.2016.03.024
111. Dalgliesh AJ, Parvizi M, Lopera-Higuita M, Shklover J, Griffiths LG. Graft-specific immune tolerance is determined by residual antigenicity of xenogeneic extracellular matrix scaffolds. *Acta Biomater*. (2018) 79:253–64. doi: 10.1016/j.actbio.2018.08.016
112. Luo J, Korossis SA, Wilshaw S-P, Jennings LM, Fisher J, Ingham E. Development and characterization of acellular porcine pulmonary valve scaffolds for tissue engineering. *Tissue Eng Part A*. (2014) 20:2963–74. doi: 10.1089/ten.tea.2013.0573
113. Perri G, Polito A, Esposito C, Albanese SB, Francalanci P, Pongiglione G, et al. Early and late failure of tissue-engineered pulmonary valve conduits used for right ventricular outflow tract reconstruction in patients with congenital heart disease. *Eur J Cardiothorac Surg*. (2012) 41:1320–5. doi: 10.1093/ejcts/ezr221
114. Cicha I, Ruffer A, Cesnjevar R, Glockler M, Agaimy A, Daniel WG, et al. Early obstruction of decellularized xenogeneic valves in pediatric patients: involvement of inflammatory and fibroproliferative processes. *Cardiovasc Pathol*. (2011) 20:222–31. doi: 10.1016/j.carpath.2010.04.006
115. Ye B, Ge Y, Perens G, Hong L, Xu H, Fishbein MC, et al. Canonical Wnt/ß-catenin signaling in epicardial fibrosis of failed pediatric heart allografts with diastolic dysfunction. *Cardiovasc Pathol.* (2013) 22:54–7. doi: 10.1016/j.carpath.2012.03.004
116. Manji RA, Zhu LF, Nijar NK, Rayner DC, Korbutt GS, Churchill TA, et al. Glutaraldehyde-fixed bioprosthetic heart valve conduits calcify and fail from xenograft rejection. *Circulation.* (2006) 114:318–27. doi: 10.1161/CIRCULATIONAHA.105.549311
117. Manji RA, Lee W, Cooper DKC. Xenograft bioprosthetic heart valves: past, present and future. *Int J Surg.* (2015) 23:280–4. doi: 10.1016/j.ijsu.2015.07.009
118. Griesemer A, Yamada K, Sykes M. Xenotransplantation: immunological hurdles and progress towards tolerance. *Immunol Rev*. (2014) 258:241–58. doi: 10.1111/imr.12152
119. Cooper DK. How important is the anti-Gal antibody response following the implantation of a porcine bioprosthesis. *J Heart Valve Dis.* (2009) 19:671–2.
120. Gates KV, Dalgliesh AJ, Griffiths LG. Antigenicity of bovine pericardium determined by a novel immunoproteomic approach. *Sci Rep.* (2017) 7:2446. doi: 10.1038/s41598-017-02719-8
121. Bloch O, Golde P, Dohmen PM, Posner S, Konertz W, Erdbrugger W. Immune response in patients receiving a bioprosthetic heart valve: lack of response with decellularized valves. *Tissue Eng.* (2011) 17:2399–405. doi: 10.1089/ten.tea.2011.0046
122. Rieder E, Steinacher-Nigisch A, Weigel G. Human immune-cell response towards diverse xenogeneic and allogeneic decellularized biomaterials. *Int J Surg*. (2016) 36:347–51. doi: 10.1016/j.ijsu.2016.06.042
123. Rygg IH, Westengaard E, Frederiksen T, Morkeberg C, Poulsen A. A new method for fixation of prosthetic cardiac valves and closure. *J Cardiovasc Surg.* (1963) 4:467–72.
124. Nishiyama H. Glutaraldehyde preserved porcine pericardium in cardiovascular surgery: clinical application to forty-eight patients. *Jpn J Thorac Surg.* (1980) 33:755–60.
125. Wallace RB. Tissue valves. *Am J Cardiol.* (1975) 35:866–71. doi: 10.1016/0002-9149(75)90123-X
126. Golomb G, Schoen FJ, Smith MS, Linden J, Dixon M, Levy RJ. The role of glutaraldehyde-induced cross-links in calcification of bovine pericardium used in cardiac valve bioprostheses. *Am J Pathol*. (1987) 127:122–30.
127. Thomas S, Russell AD. Studies on the mechanism of the sporicidal action of glutaraldehyde. *J Appl Bacteriol*. (1974) 37:83–92. doi: 10.1111/j.1365-2672.1974.tb00417.x
128. Paul RG, Bailey AJ. Chemical stabilization of collagen as a biomimetic. *Sci World J*. (2003) 3:138–55. doi: 10.1100/tsw.2003.13
129. Adamiak K, Sionkowska A. Current methods of collagen cross-kinking: review. *Int J Biol Macromol*. (2020) 161:550–60. doi: 10.1016/j.ijbiomac.2020.06.075

130. Mosler E, Dieringer H, Fietzek PP, Folkhard W, Knorzer W, Koch M, et al. Structural dynamic of collagen fibers cross-linked with isocyanates: application of synchrotron radiation in macromolecular chemistry. *Angew Chemie Int Ed Eng.* (1987) 26:551–2. doi: 10.1002/anie.198705511
131. Vasudev SC, Chandy T, Sharma CP. The anti-calcification effect of polyethylene glycol – immobilized on hexamethylene diisocyanate treated pericardium. *Artif Cells Blood Substit Immob Biotechnol.* (2000) 28:79–94. doi: 10.3109/10731190009119787
132. Koob TJ, Hernandez DJ. Material properties of polymerized NDG-collagen composite fibers: development of biologically based tendon constructs. *Biomaterials*. (2001) 23:203–12. doi: 10.1016/S0142-9612(01)00096-5
133. Li J, Ren N, Qiu J, Jiang H, Zhao H, Wang G, et al. Carbodiimide crosslinked collagen from porcine dermal matrix for high-strength tissue engineering scaffold. *Int J Biol Macromol.* (2013) 61:69–74. doi: 10.1016/j.ijbiomac.2013.06.038
134. Everaerts F, Torriani M, Hendriks M, Feijen J. Biomechanical properties of carbodiimide crosslinked collagen: influence of the formation of ester crosslinks. *J Biomed Mater Res A*. (2008) 85:547–55. doi: 10.1002/jbm.a.31524
135. Zeeman R, Dijkstra PJ, van Wachem PB, van Luyn MJA, Hendriks M, Cahalan PT, et al. Successive epoxy and carbodiimide cross-linking of dermal sheep collagen. *Biomaterials.* (1999) 20:921–31. doi: 10.1016/S0142-9612(98)00242-7
136. Tedder ME, Liao J, Weed B, Stabler C, Zhang H, Simionescu A, et al. Stabilized collagen scaffolds for heart valve tissue engineering. *Tissue Eng Part A*. (2009) 15:1257–68. doi: 10.1089/ten.tea.2008.0263
137. Chang Y, Tsai C-C, Liang H-C, Sung H-W. *In vivo* evaluation of cellular and acellular bovine pericardia fixed with a naturally occurring crosslinking agent (genipin). *Biomaterials*. (2002) 23:2447–57. doi: 10.1016/S0142-9612(01)00379-9
138. Whipple EB, Ruta M. Structure of aqueous glutaraldehyde. *J Org Chem*. (1974) 39:1666–8. doi: 10.1021/jo00925a015
139. Jones GJ. Polymerization of glutaraldehyde at fixative pH. *J Histochem Cyto*. (1974) 22:911–3. doi: 10.1177/22.9.911
140. Lee C, Kim SH, Choi S-H, Kim YJ. High concentration glutaraldehyde fixation of bovine pericardium in organic solvent and post-fixation glycine treatment: *in vitro* material assessment and *in vivo* anti-calcification effect. *Eur J Cardiothorac Surg*. (2011) 39:381–7. doi: 10.1016/j.ejcts.2010.07.015
141. Huang-Lee LLH, Cheung DT, Nimmi ME. Biochemical changes and cytotoxicity associated with the degradation of polymeric glutaraldehyde derived crosslinks. *J Biomed Mater Res*. (1990) 24:1185–201. doi: 10.1002/jbm.820240905
142. Cheung DT, Nimni ME. Mechanism of cross-linking of proteins by glutaraldehyde: II reaction with monomeric and polymeric collagen. *Connect Tissue Res*. (1982) 10:201–16. doi: 10.3109/03008208209034419
143. Zilla P, Bezuidenhout D, Weissenstein C, van der Walt A, Human P. Diamine extension of glutaraldehyde crosslinks mitigates bioprosthetic aortic wall calcification in the sheep model. *J Biomed Mater Res*. (2001) 56:56–64. doi: 10.1002/1097-4636(200107)56:1<56::aid-jbm1068>3.0.co;2-3
144. Zillla P, Bezuidenhout D, Torrianni M, Hendricks M, Human P. Diamine-extended glutaraldehyde and carbodiimide act synergistically in mitigating bioprosthetic aortic wall calcification. *J Heart Valve Dis*. (2005) 14:538–45.
145. Zilla P, Weissenstein C, Bracher M, Human P. The anti-calcification effect of glutaraldehyde detoxification on bioprosthetic aortic wall tissue in the sheep model. *J Card Surg*. (2001) 16:467–72. doi: 10.1111/j.1540-8191.2001.tb00551.x
146. Weissenstein C, Human P, Bezuidenhout D, Zilla P. Glutaraldehyde detoxification in addition to enhanced amine cross-linking dramatically reduces bioprosthetic tissue calcification in the rat model. *J Heart Valve Dis*. (2000) 9:230–40.
147. Zilla P, Weissenstein C, Human P, Dower T, von Oppell U. High glutaraldehyde concentrations mitigate bioprosthetic root calcification in the sheep model. *Ann Thorac Surg*. (2000) 70:2091–5. doi: 10.1016/S0003-4975(00)02011-7
148. Duncan AC, Bougher D. Effect of dynamic glutaraldehyde fixation on the viscoelastic properties of bovine pericardial tissue. *Biomaterials.* (1998) 19:777–83. doi: 10.1016/S0142-9612(97)00215-9
149. Polak R, Pitombo RNM. Care during freeze drying of bovine pericardium tissue to be used as a biomaterial: a comparative study. *Cryobiology*. (2011) 63:61–6. doi: 10.1016/j.cryobiol.2011.05.001
150. Malone JM, Brendel K, Duhamel RC, Reinhert RL. Detergent-extracted small-diameter vascular prostheses. *J Vasc Surg*. (1984) 1:181–91. doi: 10.1016/0741-5214(84)90197-6
151. Wright J, Eberhardt C, Gibbs M, Saul M, Gilpin CB. Hancock II—an improved bioprosthesis. In: Cohn L, Gallucci V, editors. *Cardiac Bioprostheses*. New York, NY: Yorke Medical Books (1982) p. 425–44.
152. Naso F, Stefanelli U, Buratto E, Lazzari G, Perota A, Galli C, et al. Alpha-gal inactivated heart valve bioprostheses exhibit an anti-calcification propensity similar to knockout tissues. *Tissue Eng*. (2017) 23:19–20. doi: 10.1089/ten.tea.2016.0474
153. Wilson GJ, Courtman DW, Klement P, Lee JM, Yeger H. Acellular matrix: a biomaterials approach for coronary artery bypass and heart valve replacement. *Ann Thorac Surg*. (1995) 60:353–8. doi: 10.1016/0003-4975(95)98967-Y
154. Bader A, Schilling T, Teebken OE, Brandes G, Herden T, Steinhoff G, et al. Tissue engineering of heart valves - human endothelial cell seeding of detergent acellularized porcine valves. *Eur J Cardiothorac Surg*. (1998) 14:279–84. doi: 10.1016/S1010-7940(98)00171-7
155. Steinhoff G, Stock U, Karim N, Mertsching H, Timke A, Meliss RR, et al. Tissue engineering of pulmonary heart valves on allogenic matrix conduits: *in vivo* restoration of heart valves. *Circulation.* (2000) 102(19 Suppl 3):50–5. doi: 10.1161/01.CIR.102.suppl_3.III-50
156. Korossis SA, Booth C, Wilcox HE, Watterson KG, Kearney JN, Fisher J, et al. Tissue engineering of cardiac valve prostheses: II Biomechanical characteristics of decellularized porcine aortic heart valves. *J Heart Valve Dis*. (2005) 11:463–71.
157. Kim WG, Park JK, Lee WY. Tissue-engineered heart valve leaflets: an effective method of obtaining acellularized valve xenografts. *Int J Artif Organs*. (2002) 25:797–7. doi: 10.1177/039139880202500807
158. Meyer SR, Nagendran J, Desai LS, Rayat GR, Churchill TA, Anderson CC, et al. Decellularization reduces the immune response to aortic valve allografts in the rat. *J Cardiothorac Surg*. (2005) 130:469–76. doi: 10.1016/j.jtcvs.2005.03.021
159. Erdbrugger W, Konertz W, Dohmen PM, Posner S, Ellerbrok H, Brodde O-E, et al. Decellularized xenogeneic heart valves reveal remodeling and growth potential *in vivo*. *Tissue Eng*. (2006) 12:2059–68. doi: 10.1089/ten.2006.12.2059
160. Dainese L, Guarino A, Burba I, Esposito G, Pompilio G, Polvani G, et al. Heart valve engineering: decellularized aortic homograft seeded with human cardiac stromal cells. *J Heart Valve Dis*. (2012) 21:125–34.
161. Gallo M, Naso F, Poser H, Rossi A, Franci P, Bianco R, et al. Physiological performance of a detergent decellularized heart valve implanted for 15 months in Vietnamese pigs: surgical procedure, follow-up and explant inspection. *Artif Organs*. (2012) 36:E138–50. doi: 10.1111/j.1525-1594.2012.01447.x
162. Gilbert TW, Sellaro TL, Badylak SF. Decellularization of tissues and organs. *Biomaterials*. (2006) 27:3675–83. doi: 10.1016/j.biomaterials.2006.02.014
163. Crapo PM, Gilbert TW, Badylak SF. An overview of tissue and whole organ decellularization processes. *Biomaterials*. (2011) 32:3233–43. doi: 10.1016/j.biomaterials.2011.01.057
164. Collatusso C, Roderjan JG, de Noronha L, Klosowski A, Suss PH, Guarita-Souza LC, et al. Decellularization as a method to reduce calcification in bovine pericardium bioprosthetic valves. *Interact Cardiovasc Thorac Surg.* (2019) 29:302–11. doi: 10.1093/icvts/ivz041
165. Sierad LN, Shaw EL, Bina A, Brazile B, Rierson N Patnaik SS, et al. Functional heart valve scaffolds obtained by complete decellularization of porcine aortic roots in a novel differential pressure gradient perfusion system. *Tissue Eng Part C Methods*. (2015) 21:1284–96. doi: 10.1089/ten.tec.2015.0170
166. Human P, Ofoegbu C, Ilsley H, Bezuidenhout D, de Villiers J, Williams DF, et al. Decellularization and engineered crosslinking: a promising dual approach towards bioprosthetic heart valve longevity.

Eur J Cardiothorac Surg. (2020) 58:1192–200. doi: 10.1093/ejcts/ezaa257

167. Laker L, Dohmen PM, Smit FE. Synergy in a detergent combination results in superior decellularized bovine pericardial extracellular matrix scaffolds. *J Biomed Mater Res B.* (2020) 108:2571–8. doi: 10.1002/jbm.b.34588

Conflict of Interest: DW, DB, and PZ are Founding Directors of Strait Access Technologies Ltd. Pty. JV is an employee of Strait Access Technologies Ltd Pty.

The remaining author declares that the research was conducted in the absence of any commercial or financial relationships that could be construed as a potential conflict of interest.

Publisher's Note: All claims expressed in this article are solely those of the authors and do not necessarily represent those of their affiliated organizations, or those of the publisher, the editors and the reviewers. Any product that may be evaluated in this article, or claim that may be made by its manufacturer, is not guaranteed or endorsed by the publisher.

frontiers in Cardiovascular Medicine

REVIEW
published: 29 September 2021
doi: 10.3389/fcvm.2021.722693

How Transcatheter Aortic Valve Implantation (TAVI) Was Born: The Struggle for a New Invention

*Henning Rud Andersen**

Department of Cardiology, Research Unit, Aarhus University Hospital, Aarhus, Denmark

This story is about the invention of transcatheter aortic valve implantation (TAVI), and the people who transformed it from a concept and primitive device to a breakthrough lifesaving treatment for hundreds of thousands of patients with aortic valve stenosis. It is an inspirational example of a new disruptive technology that began with an idea most dismissed. The story describes the ups and downs from idea, design, construction, animal testing, proof-of-concept, scientific publication hurdles, a patent, license agreement, cooperation with several companies, fighting in patent courts in Europe and USA and finally how multinational companies financially bypassed the inventor. It is also a story about the struggles and battles the inventor experienced when injected into a world of lawyers and patent fights. I hope my personal story and journey can provide an inspiration and word of caution for new inventors.

Keywords: transcatheter, aortic stenosis, invention, development, history, patent, TAVI, TAVR

OPEN ACCESS

Edited by:
Peter Zilla,
University of Cape Town, South Africa

Reviewed by:
Theodor Fischlein,
Nürnberg Hospital, Germany
Max Emmert,
University of Zurich, Switzerland

***Correspondence:**
Henning Rud Andersen
henning.rud.andersen@dadlnet.dk

Specialty section:
This article was submitted to Heart Valve Disease, a section of the journal Frontiers in Cardiovascular Medicine

Received: *09 June 2021*
Accepted: *23 August 2021*
Published: *29 September 2021*

Citation:
Andersen HR (2021) How Transcatheter Aortic Valve Implantation (TAVI) Was Born: The Struggle for a New Invention. Front. Cardiovasc. Med. 8:722693. doi: 10.3389/fcvm.2021.722693

BACKGROUND AND HISTORY

This history leads back to Dr. Charles Dotter, the "Father of Interventional Radiology." He invented percutaneous transluminal angioplasty and treated the first patient with a tight arterial stenosis in a leg by dilating it with tapered 8 and 12 Fr. catheters. It was in 1964 in Oregon, USA. Later that year, Dotter conducted a lecture on angioplasty in Frankfurt, Germany which was attended by Dr. Andreas Grüntzig. He was inspired by Dotter and Grüntzig conceptualized constructing the new balloon dilatation catheter and he became a pioneering inventor of Percutaneous Transluminal Coronary Angioplasty (PTCA). Grüntzig performed the first-in-man (FIM) PTCA in 1977 in Zurich, Switzerland. Both Charles Dotter and Andreas Grüntzig received a nomination for the Nobel Prize in Physiology or Medicine in 1978 for one of the most successful examples of translational medicine in the twentieth century. Shortly thereafter, Dr. Julio Palmaz was inspired by Andreas Grüntzig during a lecture in New Orleans in 1978 and went on to invent the first balloon expandable coronary stent.

THE IDEA

TAVI sprang to life in February 1989 when I concepted implanting heart valves percutaneously by catheter technique without surgery. I got my inspiration from listening to Julio Palmaz during a 1989 conference in Scottsdale, Arizona, USA. Palmaz was lecturing about how he invented and implanted balloon expandable coronary stents in animals. While I was listening, I suddenly got the idea of making the stent diameter much bigger and insert a collapsible biological valve inside the big stent. This should enable me to implant artificial heart valves using the same balloon technique

described by Grüntzig and Palmaz without surgery. I was very exhilarated with my new idea. I wanted to be the first in the world to implant heart valves without heart surgery. And so, on my flight back to Denmark I formulated five requirements for the method. It should be:

- performed by retrograde catheterization
- a closed chest procedure
- a closed heart procedure
- a beating heart procedure
- performed without cardiopulmonary bypass.

FIRST PROTOTYPES

Back in Denmark I immediately wanted to get to work, so there was no time to seek support from industry, engineers, or funding. To build stents, I bought different wires made of iron and steel from the local hardware store and procured surgical stainless-steel wires from the hospital. Initially, the various wires were bent into 15–16 loops and formed into a circle ∼25 mm in diameter which was closed end-to-end by soldering. Several wires with varying thickness and stiffness were tested. The thicker wires were too stiff for balloon dilatation and the thinner too soft to maintain architectural integrity of the device. The evaluation of these mechanical parameters was done by simple visual observation and gentle finger compressions without exact measurements. I found that the surgical steel monofilament wires with a diameter of 0.55 mm fulfilled my criteria which were minimum 90% stent diameter after balloon dilatation compared to maximum balloon diameter and <10% recoil after balloon deflation followed by gentle finger compression. I soon learned that one ring did not adequately support the valve. Therefore, I tested two and three rings tied together on top of each other and found that three rings were best. Consequently, in the first-in-animal (FIA) implantation on May 18, 1989 I used three rings (**Figure 1**, top row). It turned out however that three rings were a bit too stiff when the valve was mounted inside as it created a small waist on the middle of the balloon during balloon dilatation. Therefore, for the succeeding experiments in 1989–1992, two rings were used. Initially, these early first-generation stents were finger folded using simple handheld tools from the hardware shop. This resulted in rather irregular bending of the loops. Afterwards, in the second-generation stents, an iron bar with holes and pins was used to make the folding much more regular (**Figure 1**, middle row). The first-generation stents were not constructed with three high loops for the trileaflet valves' commissure posts. Later, a young doctor under training for cardiac surgery, J. Michael Hasenkam, recommended making the stent with three high loops for the commissure posts (**Figure 1**, middle row and **Figure 2**). The biological valves were obtained from pig hearts which I bought from the local slaughterhouse. The aortic valve was carefully cut out and mounted inside the stent (**Figure 2**).

Also, I was assisted by a medical student, Lars Lyhne Knudsen, to build the stents and mount the valves inside the stents. Both assisted me with the experiments and animal implantations. Therefore, I granted 25% of my patent to them to share, so we were three patent owners (**Figure 3**).

In the animal laboratory, I also got help from an anesthesiologist and a doctor specialized in echocardiography. Thus, the multidisciplinary TAVI heart team approach was established in the animal laboratory already when TAVI was born in 1989.

Next a 75 cm long, 41 Fr. introducer sheath with an external diameter of 13.6 mm was constructed from two flexible plastic tubes telescoping one into the other (**Figure 1**, bottom row, left). A reused 12 Fr. three-foiled balloon aortic valvuloplasty (BAV) dilatation catheter telescoped inside the inner plastic tube. At the tip of the sheath, a stiff plastic tube was glued which housed the balloon and the finger crimped valve during vascular introduction (**Figure 2**). The inner plastic tube was used to push the balloon with the crimped valve out from the stiff plastic tube.

Due to my economic constraints, only a limited number of balloon catheters of random diameters were available after being used in patients. Unfortunately, they did not always match the size of the aortic annulus in the animal. They also contained X-ray contrast from their previous clinical use, which made the catheter and the balloon stiff and fragile. Furthermore, the catheters were not constructed with one circular balloon. Instead, the balloon catheters used in my institution were built with three individual longitudinal balloons (**Figure 1**, bottom row, right). Each of the three balloons were 70 mm long and had a diameter of 12–15 mm. Thus, the TAVI valves were not completely circular when dilated and implanted, but somewhat tri-angular in shape (**Figure 4**) reflecting the three small balloons. This resulted in increased paravalvular leak but they were the only balloon catheters available to me.

FIRST IMPLANTATION. PROOF-OF-CONCEPT

We used adult pigs for implantations (**Figure 5**, top). Since the femoral arteries of the pigs were only 3–4 mm in diameter, retroperitoneal access to the abdominal aorta was established (**Figure 5**, bottom) and a large vascular graft was sewn end-to-side to the aorta at a 45° angle. Then, the 75 cm long introducer sheath was inserted retrogradely *via* the graft into the aorta. The first implantation was performed in an 80 kg pig on May 1, 1989 (**Figure 1**). Luck was with us and it was a success. The time from conception of the idea in Scottsdale to initial proof-of-concept took only 2½ months.

REFINING THE TECHNIQUE

After the first successful procedure, we performed a series of implantations. All procedures were acute feasibility studies with animals euthanized after completion of the procedure and the heart explanted to allow inspection. Initially, not all attempts

Abbreviations: BAV, balloon aortic valvuloplasty; FIA, first-in-animal; FIM, first-in-man; JACC, Journal of the American College of Cardiology; PTCA, percutaneous transluminal coronary angioplasty; TAVI, transcatheter aortic valve implantation; DTI, Danish Technology Institute; Edwards, Edwards Lifesciences; J&J, Johnson & Johnson; SST, Stanford Surgical Technologies; PVT, Percutaneous Valve Technologies.

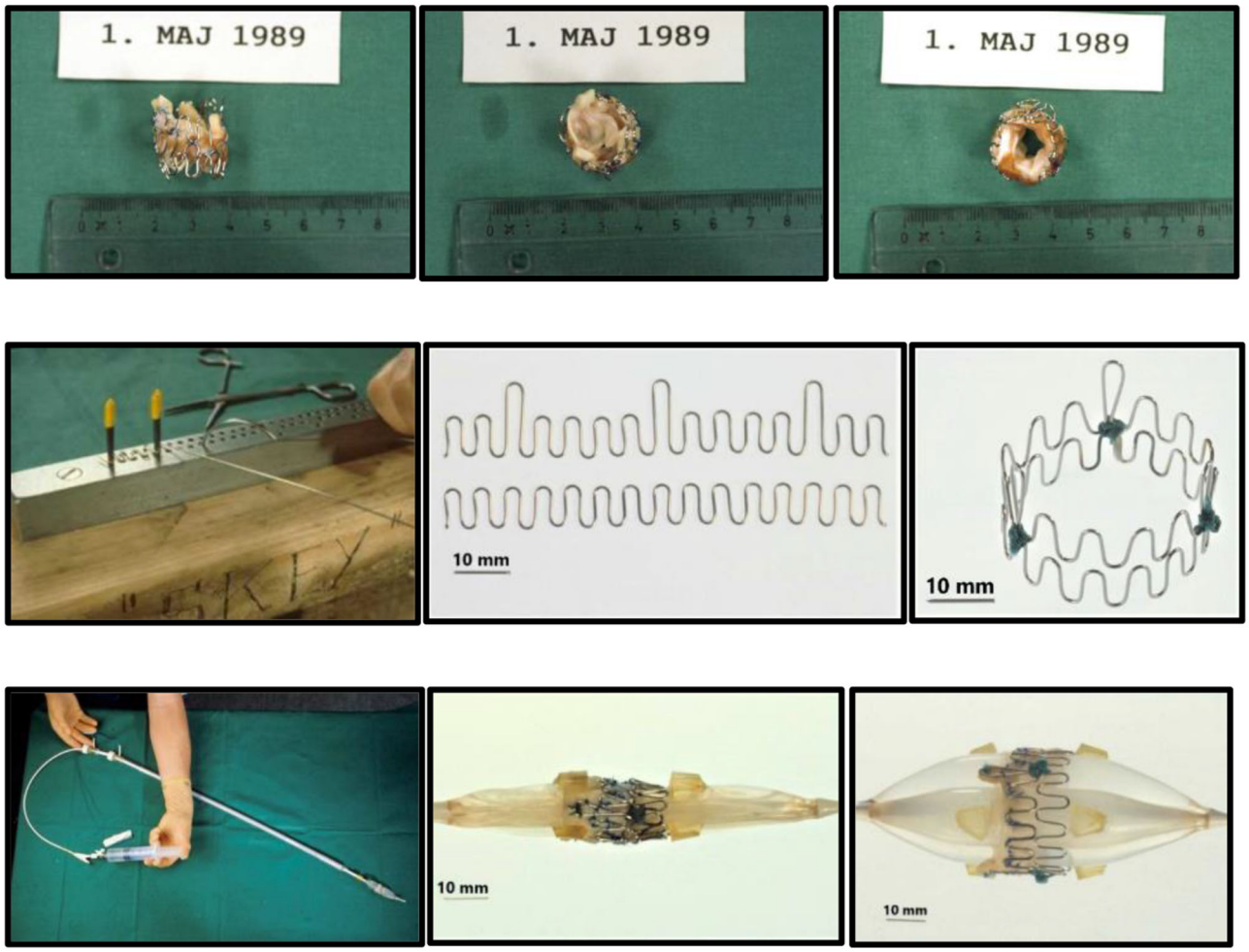

FIGURE 1 | Prototype of TAVI valve and catheter technology. **Top:** The first-in-animal (FIA) valve implanted May 1. 1989. **Middle:** Later refinement of stent construction. **Bottom:** The 75 cm long, 41 Fr. introducer sheath with crimped and dilated TAVI valve on a three-foiled balloon aortic valvuloplasty dilatation catheter.

met with success. Sometimes the pig died before catheterization was initiated because of fatal bleeding caused by the extensive abdominal surgery (**Figure 5**, bottom). Occasionally the stiff secondhand balloons ruptured before full inflation. Sometimes, the coronary ostia were occluded. Other times the valve dislodged and embolized because the available balloons were smaller than the pig's aortic annulus. On occasion the inflated balloon with the dilated valve was pushed downstream into the ascending aorta by the blood flow. Indeed, we learned the hard way that we had to buy smaller pigs if we only had 25 mm balloons available that day. The lesson being "one size of pig does not fit all secondhand balloon catheters"! In one case, the assisting medical student mounted the valve upside down. This valve was implanted successfully in the correct location under the coronary ostia. Initially we were happy with the implantation based on the aortic angiogram which showed brisk flow into both coronary arteries. Yet happiness did not last long as we soon discovered that the valve completely blocked the blood flow from the heart. I learned that I had to double-check the valve's orientation on the balloon myself, and the young medical student was seriously advised not to turn the valve upside down again!

I also realized that we had to temporarily stop the blood flow through the left ventricle to reduce risk of distal embolization with the blood flow during deployment. Therefore, a new experimental catheter technique was developed. Two soft 12 Fr. urine bladder catheters with a 40 mm inflatable balloon at the tip were spliced together. Then, using right heart catheterization and Swan-Ganz catheter technique, this catheter was inserted and floated into the common pulmonary trunk with the balloon inflated to only a small diameter. By inflating the balloon further to 40 mm, it blocked the pulmonary trunk preventing the blood flow toward the lungs and heart. After few seconds, the pig had a beating heart in sinus rhythm but without blood flow. We could then implant the valve without risk of distal embolization (**Figure 6**).

Ultimately, all of these various implantation challenges were encountered, understood and mitigated. These are still relevant concerns even today, all of which were seen in our early work.

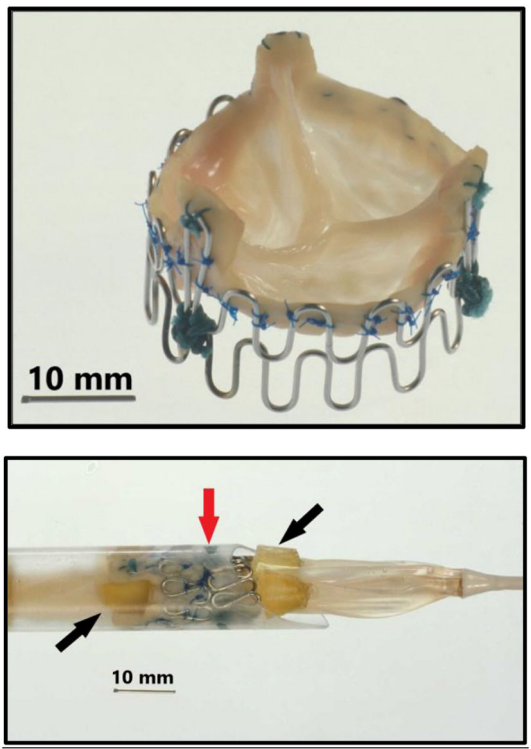

FIGURE 2 | Top: Second generation three-leaflet handmade porcine TAVI valve with high loops for the commissure posts. **Bottom:** Tip of the 41 Fr. introducer sheath with balloon catheter inside and a crimped TAVI valve (vertical red arrow) on the middle of the balloon. Two soft silicone blocks (skewed black arrows) with a height of 3 mm were glued on each of the three balloons on the three-foiled balloon catheter. They were separated by a distance of 18 mm. The soft silicone blocks prevented the valve from sliding from the middle of the balloon during intravascular advancement and implantation.

Most of the implantations were performed in the experimental animal laboratory, but sometimes we snuck into the clinical cardiology catheterization laboratory in the evening when the patients had left because the X-ray quality there was much better (**Figure 7**).

AORTIC INSUFFICIENCY EXPERIMENTS

In addition to the work regarding aortic valve stenosis, a new experimental model for aortic insufficiency was developed. The purpose was to study how the TAVI valve could protect the left ventricle when it was implanted in the proximal descending thoracic aorta in pigs with severe aortic insufficiency. It mimicked the very first human surgical heart valve implantations dating back to 1952 when Dr. Charles Hufnagel performed the first insertion of caged-ball valves in the proximal descending thoracic aorta in patients with native aortic valve insufficiency (1, 2). First, the pigs were opened through a long laparotomy (**Figure 5**) which continued through a long sternum split which nearly divided the animal into two halves. An electromagnetic flow probe was then mounted on the ascending aorta, and pigtail

TABLE 1 | Left ventricular blood pressure (median values, $n = 6$).

Baseline	120/8 mmHg
Aortic insufficiency with intact TAVI valve function	88/29 mmHg
Aortic insufficiency with eliminated TAVI valve function	88/41 mmHg

catheters were inserted from the carotid arteries into the left ventricle and aorta. Baseline hemodynamic and angiographic measurements were performed. Then, the huge 75 cm long 41 Fr. introducer sheath was inserted retrograde *via* the graft into the abdominal aorta, and the TAVI valve was implanted in the proximal part of the descending thoracic aorta. To create aortic incompetence, a plastic tube with an inner cross-sectional area of 100 mm^2 and with multiple side holes was inserted retrograde in the ascending aorta and placed across the native aortic valve. It created severe acute aortic valve regurgitation. New measurements and angiograms were then performed. Initially, the TAVI valve in the proximal descending thoracic aorta blocked the blood volume from the lower part of the body, 80–85% of total blood volume, to regurgitate. Then, only the blood from the head and the front legs, 15–20% of total blood volume, could regurgitate. Thereby, the TAVI valve partially "protected" the heart with the acutely insufficient native valve and resulted in only moderate aortic insufficiency. Afterwards, a special homemade catheter was inserted from the carotid artery into the TAVI valve. The catheter could push aside the three leaflets eliminating the function of the TAVI valve. It allowed the blood volume from the lower part of the body to regurgitate back through the TAVI valve toward the heart, thus creating acute, severe aortic insufficiency. Measurements were performed again showing increased end-diastolic pressure in the severely insufficient, "unprotected" left ventricle (**Table 1**).

The study confirmed the clinical results obtained by Dr. Hufnagel (1, 2). The difference was that he used classical thoracic surgery whereas we used catheter-based techniques. The study protocol was very extensive and physiologically challenging for the animals. Most pigs died from complications before all measurements were finished. Out of 24 experiments with aortic insufficiency, only 6 completed the study protocol. The complications were fatal bleeding from the extensive surgical procedures ($n = 8$), malignant arrhythmia ($n = 6$), thrombosis of the implanted TAVI valve ($n = 3$) and malignant hyperthermia ($n = 1$). These results have never been published before because we believed that the model introduced too much selection bias given the high mortality rates and variety of failure modes. But for historical information and documentation, the data are now revealed.

IN-VITRO EXPERIMENTS

At the same time, simple *in-vitro* testing was performed (**Figure 8**). A total of 36 valves were implanted in isolated pig aortas using 25 mm ($n = 18$) and 31 mm balloons ($n = 18$), respectively.

In six valves dilated with 25 mm balloons and in six valves dilated with 31 mm balloons, transvalvular pressure

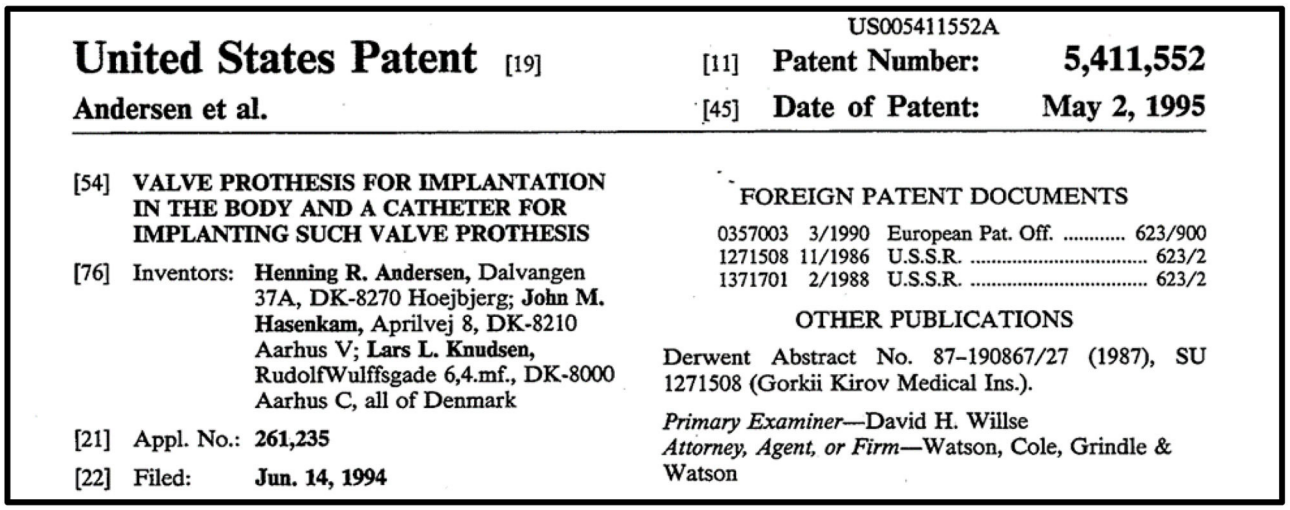

US005411552A

United States Patent [19]

Andersen et al.

[11] **Patent Number: 5,411,552**

[45] **Date of Patent: May 2, 1995**

[54] **VALVE PROTHESIS FOR IMPLANTATION IN THE BODY AND A CATHETER FOR IMPLANTING SUCH VALVE PROTHESIS**

[76] Inventors: **Henning R. Andersen,** Dalvangen 37A, DK-8270 Hoejbjerg; **John M. Hasenkam,** Aprilvej 8, DK-8210 Aarhus V; **Lars L. Knudsen,** RudolfWulffsgade 6,4.mf., DK-8000 Aarhus C, all of Denmark

[21] Appl. No.: **261,235**

[22] Filed: **Jun. 14, 1994**

FOREIGN PATENT DOCUMENTS

0357003	3/1990	European Pat. Off.	623/900
1271508	11/1986	U.S.S.R.	623/2
1371701	2/1988	U.S.S.R.	623/2

OTHER PUBLICATIONS

Derwent Abstract No. 87-190867/27 (1987), SU 1271508 (Gorkii Kirov Medical Ins.).

Primary Examiner—David H. Willse
Attorney, Agent, or Firm—Watson, Cole, Grindle & Watson

FIGURE 3 | The Andersen patent. United States Patent Number 5,411,552.

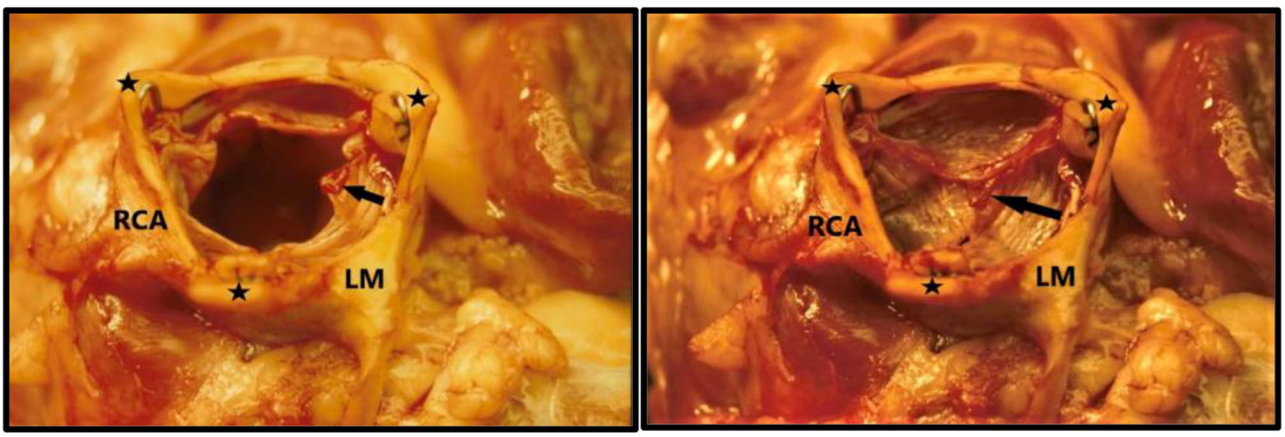

FIGURE 4 | TAVI valve implanted in the sub-coronary position in 1989. The aorta is nearly tri-angular as a result of the three small valvuloplasty balloons used for dilatation and implantation. The ostia of the left main coronary artery (LM) and right coronary artery RCA) are seen. **Left:** The leaflets are open like in systole. **Right:** leaflets are closed like in diastole. The three commissure supporting posts are indicated with black stars. Small thrombi (arrows) are seen on the leaflets because the pigs were not anticoagulated during the extensive abdominal surgery and experiment due to the high risk of bleeding.

gradients were measured using saline circulation at different flowrates from 5 to 8 L/min (**Figure 8A**). None of the valves became dislodged at these flow rates. In another 12 valves, the retrograde leakage volume was measured (**Figure 8B**). For this study, the aortic specimens with the implanted valves were hung up in a vertical position. A saline pressure of 100 mmHg was maintained above the closed valve by a fluid reservoir connected to a clinical blood pressure bag (d). Retrograde leakage was documented by measuring the fluid volume that leaked retrograde. None of the 12 valves dislodged during these experiments despite a retrograde pressure difference of 100 mmHg. Finally, the last 12 valves were tested for mechanical prosthesis stability to simulate dislodgement (**Figure 8C**).

SCIENTIFIC PRESENTATION

The TAVI invention was presented for the first time on May 19, 1990, at the 30-year anniversary symposium of the Danish Society of Cardiology in Odense, Denmark. In May 1990, we had submitted another abstract to the 12th Congress of the European Society of Cardiology meeting in Stockholm, Sweden. The abstract was not accepted for presentation. In June 1990, we submitted a manuscript to the Journal of the American College of Cardiology (JACC) which at that time had an impact factor of 5.9. Two of the four JACC reviewers had many concerns such as "*lack of long term-term follow-up, lack of information about long-term durability, risk of dislodgment, risk of larger clot formation with peripheral and central embolization including clot embolization*

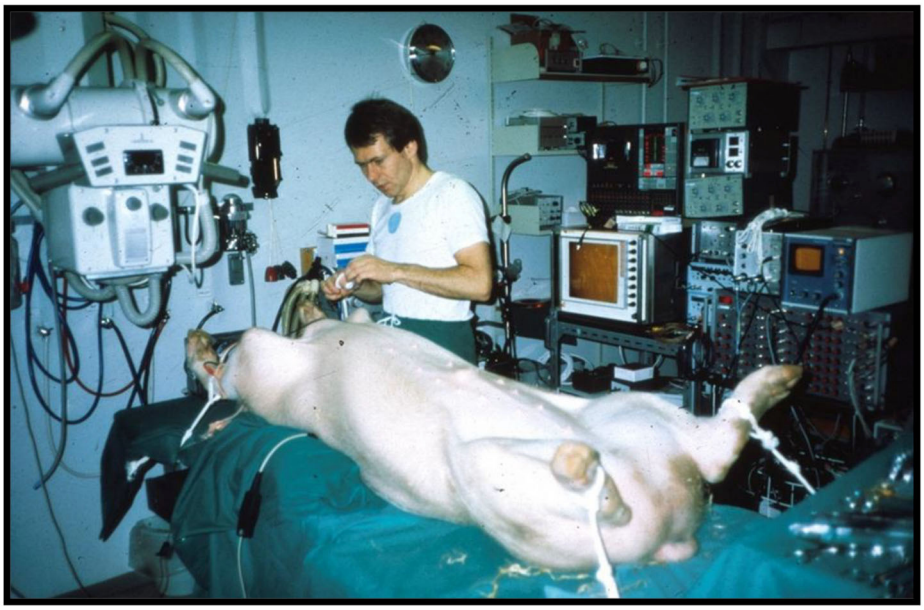

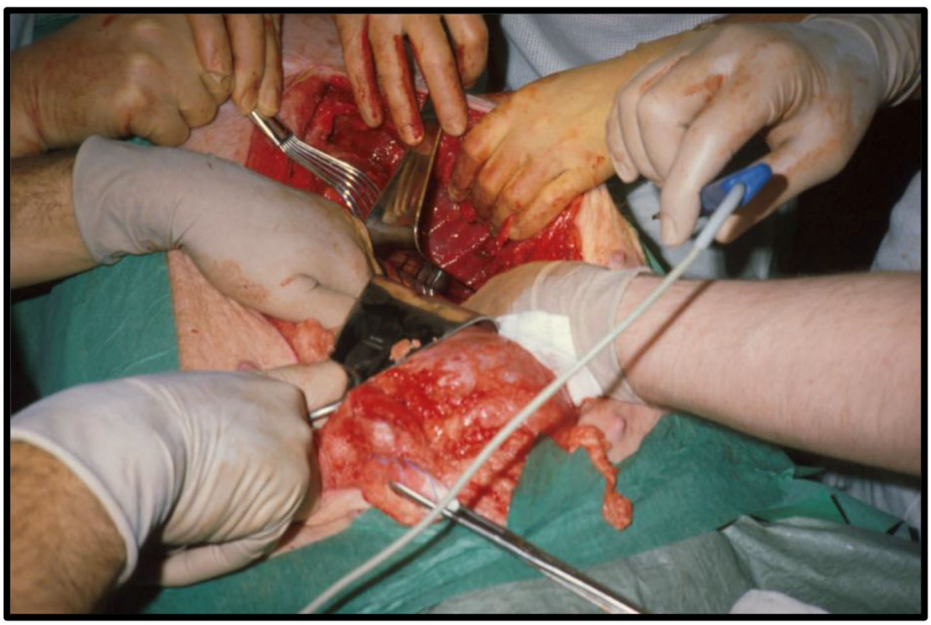

FIGURE 5 | Top: Henning Rud Andersen preparing an 80 kg pig for TAVI implantation in 1989. **Bottom:** Minimal invasive TAVI!! To get access to the abdominal aorta and obtain enough space to sew the large vascular graft end-to-side to the aorta, the abdomen was opened through a long laparotomy. The aorta is located very deep in the retroperitoneal space in front of the spine. Therefore, the two kidneys, the spleen, the bowel and most of the intestine was removed. It generated enough space to sew the large graft end-to-side to the aorta and insert the huge 75 cm long, 41 Fr. introducer sheath retrograde into the abdominal aorta. The 8 hands on the photo illustrate the importance of a good collaboration in our TAVI heart team in 1989.

to the coronary arteries, risk of gradual dilation or even necrosis of the portion of the aorta where the valve is implanted with subsequent distal migration, lack of hemodynamic measurements with calculation of the Gorlin valve area." Therefore, the two reviewers did not recommend publication in JACC. Then the Editor-in-Chief reviewed the manuscript together with a cardiologist. The Editor did not reveal the name of the cardiologist but wrote to us that he/she was *"a cardiologist skilled in interventional procedures."* The cardiologist responded quite differently from the two first reviewers. The Cardiologist wrote "*This is a most unusual manuscript, and the thinking is very creative and innovative. I think the manuscript is extremely well*

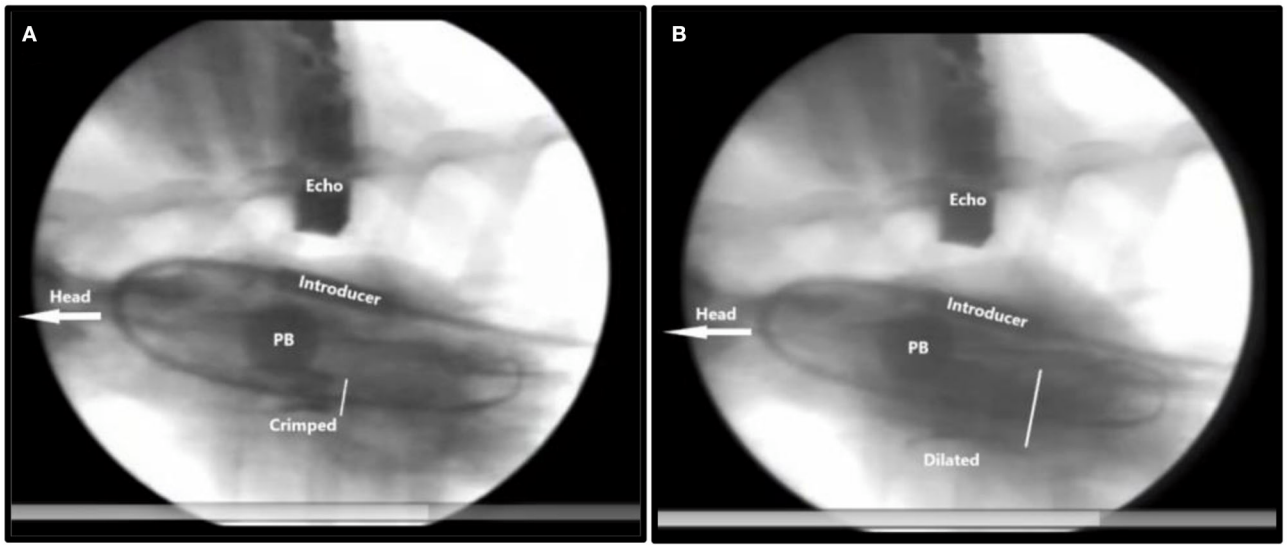

FIGURE 6 | X-ray of TAVI implantation in a pig. The head of the animal is to the left. Inflated pulmonary balloon (PB) occluding the pulmonary artery trunk stopping blood flow toward the lungs and the heart. **(A)** Crimped = The crimped TAVI valve in the aortic annulus. **(B)** Dilated = The balloon dilated TAVI valve. The white bar measures the diameter of the TAVI valve. Introducer = the 41Fr. introducer sheath. Echo = transthoracic echo transducer.

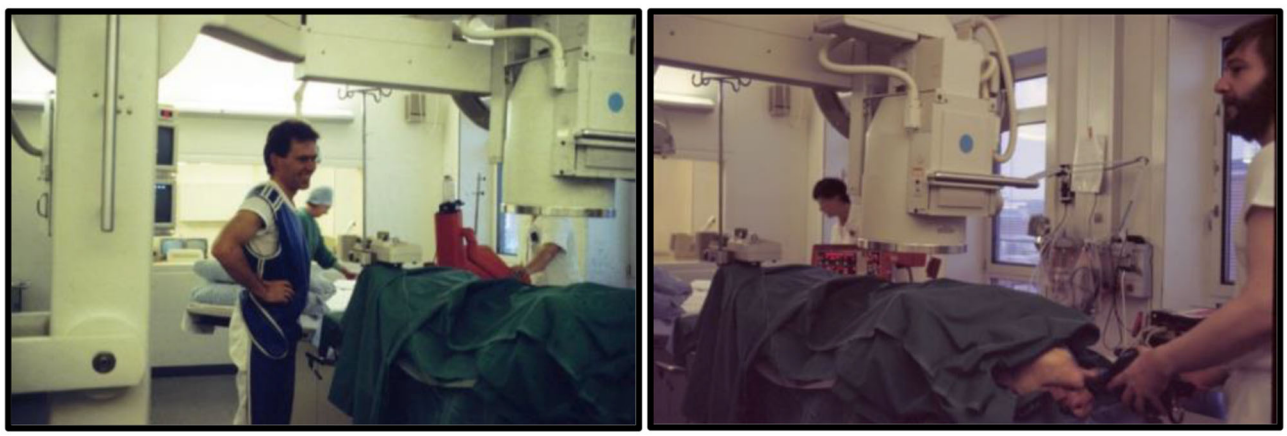

FIGURE 7 | TAVI pig in the clinical cardiac catheterization laboratory after all the patients had left, 1989. The X-ray equipment was much better compared with the equipment in the experimental animal laboratory. **Left:** Henning Rud Andersen. **Right:** J. Michael Hasenkam manually ventilating the pig during the visit in the laboratory.

written and the data carefully collected and presented. Because the subject of the report is extremely controversial, at first there might be some reluctance to publish this work in some of the surgical journals. However, I think this would be a mistake and the data should be published in a respected journal. Because of the quality of the work and the possibility of long-term importance, I feel that the manuscript should be published. I think the Journal of the American College of Cardiology is an appropriate place." Finally, the Editor-in-Chief reviewed the manuscript himself and concluded "*the deficiencies are such that publication now is premature. The authors need to provide a longer follow-up after placement of this valve under pulsatile condition.*" Therefore, he wrote back to us in July 1990 "*I am sorry to have to reject it, but my overall rating is that it has too low a priority for publication in JACC*" (**Figure 9**, left).

The next manuscript was submitted to Circulation in fall 1990 after we had performed additional animal implantations. At that time Circulation had an impact factor of 9.0. One of the Circulation reviewers wrote "*I do not see any possible use of it in patients with calcified aortic stenosis*" and another reviewer claimed, "*the current report is very crude*" and "*aortic stenosis is not a place where this could be used.*" Indeed, in our manuscript we had suggested "*patients with calcified aortic stenosis who are treated with balloon aortic valvuloplasty might also benefit from implantation of the stent-valve.*" It seemed that our suggestion provoked both reviewers. The second reviewer

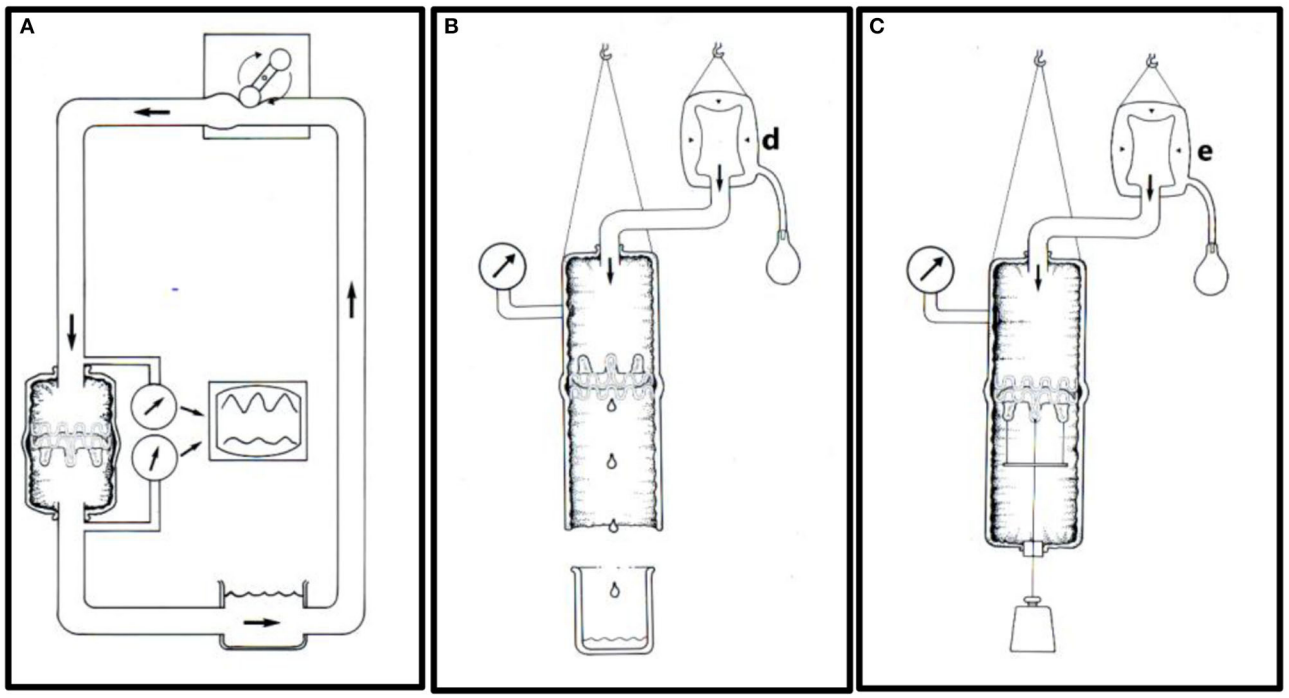

FIGURE 8 | *In-vitro* testing. **(A)** An aortic specimen with an implanted TAVI valve mounted in an open circulation driven by a roller pump. Pressures were measured on each side of the TAVI valve to determine the pressure drop. The flow's direction is indicated by thick arrows. **(B)** Experimental set-up for leakage flow measurements. A constant downstream saline pressure of 100 mmHg was maintained above the closed TAVI valve by a clinical blood pressure infusion bag (d). The retrograde saline volume was measured simulating a combination of paravalvular and transvalvular leak. **(C)** Experimental set-up for measuring prosthesis stability. The TAVI valve was implanted in a porcine thoracic aorta specimen and attached to a metallic disc and connected to an external axial load of increasing weight from 0.5 to 2.0 kg through a silicon occluder. The experiments started at 0.5 kg and were successively increased by 0.5 kg every 3 h. A constant intraluminal pressure of 100 mmHg was maintained by a pressure infusion bag (e).

continued "*questions regarding neointimalization, calcification, thrombogenicity, and dislodgement during long-term follow-up should be addressed.*" A third reviewer claimed, "*this paper is somewhat gimmicky. To simply state that you can do this on an acute basis is poor science and I think that it is giving the wrong message.*" Indeed, it was difficult for us to respond in a scientific way to these statements from the reviewers, so the manuscript was rejected, and the Editor wrote back to us in February 1991 "*its priority remains too low for publication in Circulation*" (**Figure 9**, right).

Finally, in March 1991 the manuscript was submitted to European Heart Journal, which at that time had a very low impact factor of only 1.6. The paper was accepted, and it was published in May 1992 (3). It was over 3 years after the idea sprang to life in Scottsdale.

The next paper was published in 1993, also in a journal with an extremely low impact factor (4). An abstract was accepted for a poster presentation in 1992 at the 14th European Society of Cardiology Scientific meeting in Barcelona, Spain (**Figure 10**, top) (5).

Another abstract was accepted for poster presentation in 1992 at the 65th American Heart Association Scientific meeting in New Orleans (**Figure 10**, bottom) (6). Neither of the two publications nor the two posters attracted much attention. It seemed that the TAVI invention could not be published in major prestigious international journals with high impact factors or presented as oral presentations at international conferences.

TAVI FROM 1989 AND BEYOND

Shortly after our first publication of balloon expandable valves in pigs, Professor Dusan Pavenik reported a percutaneous self-expandable mechanical valve which was successfully implanted in dogs (7). Pavenik's first-generation valve was a caged-ball design implanted in a two-step procedure. Later, Pavenik developed a mechanical disc valve which could be implanted in a one-step procedure (8). During the following years, several groups confirmed our concept using both balloon expandable and self-expandable biological valves in animal studies. Professor Philippe Bonhoeffer did preclinical evaluation with balloon implantation in the pulmonary artery in a lamb model (9), and in 2000 he performed the first-in-human percutaneous balloon implantation in a 12-year-old boy with stenosis and insufficiency of a prosthetic conduit from the right ventricle to the pulmonary artery (10). In 2001, Alain Cribier reported his experience with balloon implanted valves in sheep (11), and in 2002 he performed the FIM implantation in an adult patient with a severely calcified aortic stenosis (12). In 2004, Cribier

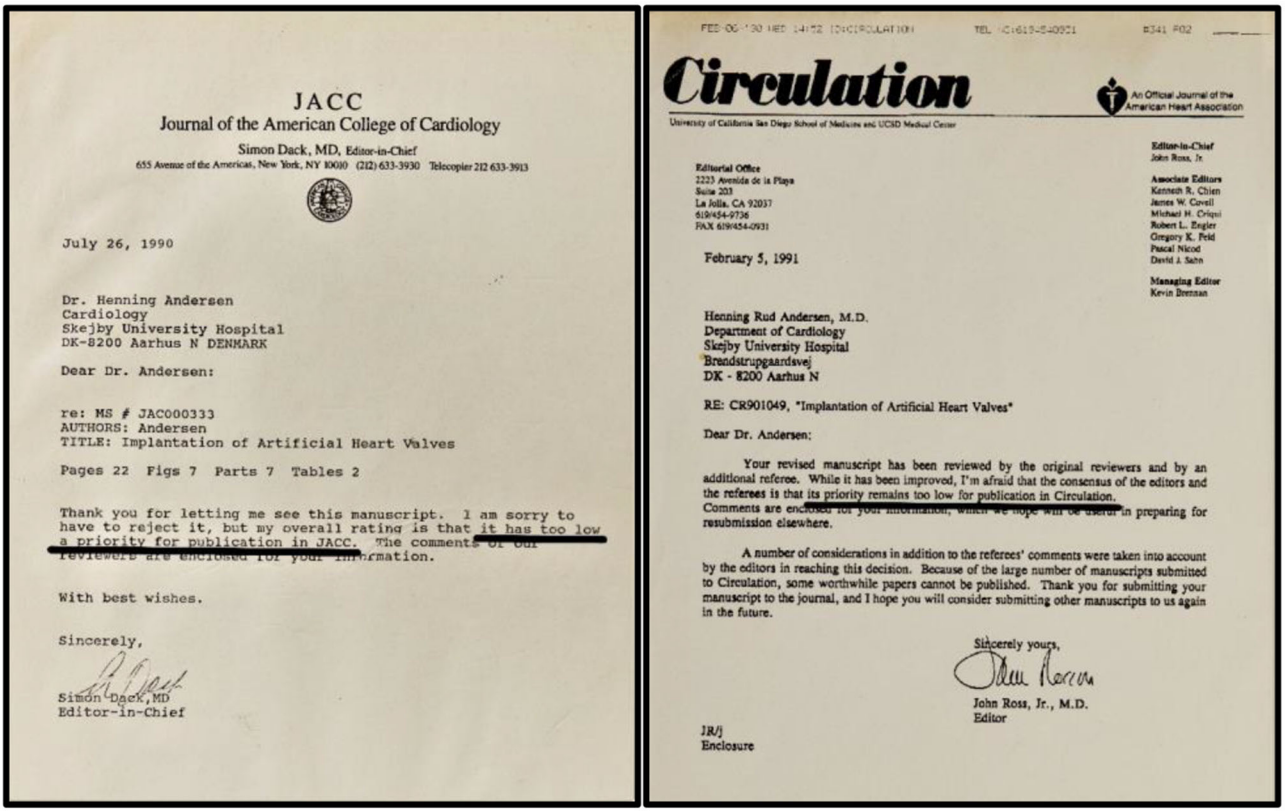

JACC
Journal of the American College of Cardiology
Simon Dack, MD, Editor-in-Chief
655 Avenue of the Americas, New York, NY 10010 (212) 633-3930 Telecopier 212 633-3913

July 26, 1990

Dr. Henning Andersen
Cardiology
Skejby University Hospital
DK-8200 Aarhus N DENMARK

Dear Dr. Andersen:

re: MS # JAC000333
AUTHORS: Andersen
TITLE: Implantation of Artificial Heart Valves

Pages 22 Figs 7 Parts 7 Tables 2

Thank you for letting me see this manuscript. I am sorry to have to reject it, but my overall rating is that it has too low a priority for publication in JACC. The comments of our reviewers are enclosed for your information.

With best wishes.

Sincerely,

Simon Dack, MD
Editor-in-Chief

Circulation
An Official Journal of the American Heart Association
University of California San Diego School of Medicine and UCSD Medical Center

Editorial Office
2223 Avenida de la Playa
Suite 203
La Jolla, CA 92037
619/454-9736
FAX 619/454-0931

Editor-in-Chief
John Ross, Jr.

Associate Editors
Kenneth R. Chien
James W. Covell
Michael H. Criqui
Robert L. Engler
Gregory K. Feld
Pascal Nicod
David J. Sahn

Managing Editor
Kevin Brennan

February 5, 1991

Henning Rud Andersen, M.D.
Department of Cardiology
Skejby University Hospital
Brendstrupgaardsvej
DK - 8200 Aarhus N

RE: CR901049, "Implantation of Artificial Heart Valves"

Dear Dr. Andersen:

Your revised manuscript has been reviewed by the original reviewers and by an additional referee. While it has been improved, I'm afraid that the consensus of the editors and the referees is that its priority remains too low for publication in Circulation. Comments are enclosed for your information, which we hope will be useful in preparing for resubmission elsewhere.

A number of considerations in addition to the referees' comments were taken into account by the editors in reaching this decision. Because of the large number of manuscripts submitted to Circulation, some worthwhile papers cannot be published. Thank you for submitting your manuscript to the journal, and I hope you will consider submitting other manuscripts to us again in the future.

Sincerely yours,

John Ross, Jr., M.D.
Editor

JR/j
Enclosure

FIGURE 9 | Left: Editorial letters from Journal of the American College of Cardiology, (1990). **Right:** Editorial letters from Circulation, (1991). Both journals declined publication with the argument that it had too low a priority for publication. The black underlining is made by the author.

reported implantation in six high risk inoperable patients using the antegrade atrial trans-septal approach (13). In the next series Cribier used both antegrade and retrograde approaches (14). These implantations were undertaken under mild sedation and in local anesthesia and without extracorporeal circulation. The studies were successful when we take into consideration that the patients were old, had multiple comorbidities, were in New York Heart Association (NYHA) functional class IV and several of them were in cardiogenic shock. All of them had been deemed inoperable and refused for surgery by two independent cardiac surgeons. It was said *"they had one foot in the grave and the other on a banana peel"* (15). A new self-expandable biological valve (CoreValve) was pioneered by the French cardiac surgeon Professor Jacques Seguin. Following initial implants in patients in India in 2002 (16), the first human implantation in Europe was performed by Professor Eberhard Grube in Germany in 2005 (17), followed by a registry study in 25 patients (18). These procedures were performed with the patient in general anesthesia and with percutaneous extracorporeal femoral-femoral bypass.

Initially, Cribier used the percutaneous femoral venous route, transseptal atrial puncture, balloon dilatation of the atrial septum, right atrium to left atrium access, mitral valve, left ventricle, and finally antegrade through the aortic valve where the 260-cm-long guidewire was advanced and snared from the femoral artery and externalized *via* the arterial sheath (12–14). The procedure was very complex and demanding and required extensive experience with cardiac catheterization and therefore complications were common. Consequently, the antegrade approach was largely abandoned with the advent of the transfemoral procedure in 2005 (19). Femoral, subclavian/transaxillary and transaortic access was developed (19–24). The first apical implantation in an animal was performed in 2000 by Professor John Webb in Vancouver, Canada (25, 26). Subsequently, the apical access was introduced in humans and soon became a preferred route for cardiac surgeons (27, 28). Recently, the carotid artery has been introduced as an alternative access route (29, 30). A few patients have also been treated with transcutaneous apical needle access through an intercostal space, and transcaval to abdominal aorta has been used in small series. In 2020 the first TAVI implantation in a porcine model through an interventricular septal approach was described (31).

Throughout the past 10 years, there have been tremendous development in valves, delivery systems, technical approaches and in experience of doctors to adapt the new technologies. New devices have been invented by creative doctors as well as industry who want to enter this new and very lucrative multi-billion-dollar market. It has led to many large randomized trials. The first such trial compared transfemoral TAVI with medical treatment including BAV in patients not suitable for surgery (32).

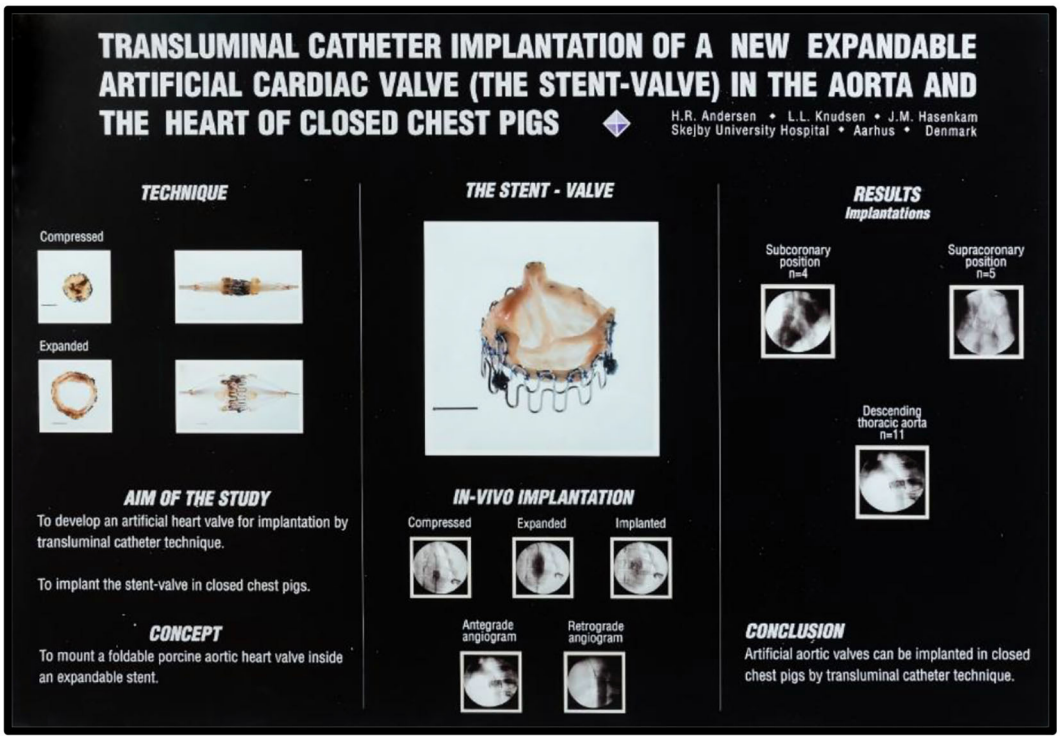

FIGURE 10 | Top: Henning Rud Andersen with his poster at the 14th Congress of the European Society of Cardiology (ESC) scientific meeting, Barcelona, Spain, August 1992. **Bottom:** Poster from the 65th American Heart Association scientific meeting in New Orleans, USA, November 1992.

TAVI significantly reduced the rates of death from any cause, but major strokes and major vascular events occurred more frequently in the TAVI group. After this first landmark study, a series of randomized trials comparing TAVI with cardiac surgery has been reported in patients at high risk (33, 34), intermediate risk (35, 36) and low risk (37–39) for cardiac surgery. The overall conclusion is that TAVI is superior or non-inferior to surgery, and 5-years follow-up confirmed these early results (40–43). Therefore, in patients ≥75 years of age, the totality of data demonstrated that TAVI should be the preferred treatment regardless of the degree of surgical risk (44).

Before TAVI was born, patients with severe aortic stenosis had only two treatment options, either surgical aortic valve replacement (SAVR) or medical treatment. This has changed significantly after the appearance of TAVI. Today, many more patients are referred for evaluation because TAVI might be an option for those who were previously declined for surgery. In many centers, including my own institution, first choice treatment for aortic stenosis is TAVI in 75–80% of patients, and SAVR in the remaining 20–25% of patients. The total number of patients treated for aortic stenosis has increased substantially since we can offer both SAVR and TAVI.

THE HEART TEAM APPROACH

The multidisciplinary TAVI heart team approach was established in the animal laboratory in 1989 with cooperation between interventional cardiologist, cardiac surgeons, anesthesiologist, doctors specialized in echocardiography and specially educated staff. This early collaboration between several specialties has proven to be a huge advantage for a very fruitful clinical collaboration. It has added tremendous benefit to the management of patients. In my institution it was natural for us to bring the heart team approach from the animal laboratory into the clinical setting. Therefore, many of the doctors who assisted me in the animal laboratory became members of our clinical TAVI heart team. Our first two clinical procedures were performed in 2006 with retrograde femoral artery technique and done in the cardiac catheterization laboratory. Unfortunately, both patients died during the procedure and our TAVI program was stopped. With a mortality rate of 100% for TAVI, we realized that we again had to learn from more experienced centers abroad. Therefore, we brought several of our doctors representing different specialties to USA and Canada to learn from experts. Additionally, we received on-site assistance from Professor John Webb, Vancouver, Canada when we successfully took-up the program again in 2007. Later, the TAVI team decided to move all TAVI procedures from the cardiac catheterization laboratory to the cardiac surgery department. A surgical suite was rebuilt into a huge hybrid room equipped with all modern facilities for TAVI. Today, our cardiac surgeons have been trained to perform femoral catheterization and valve implantations, and our cardiologist assists during the surgical TAVI procedures. Anesthesiologists are responsible for sedation, hemodynamic monitoring as well as the rapid- and back-up pacing. They also have the mandate to stop the procedure if low blood pressure or severe arrhythmias appear which need correction before the procedure can continue safely. The doctors and nurses from several specialties are now essentially transformed into hybrid doctors and hybrid nurses performing surgical and cardiology TAVI procedures together, thus eliminating the silos of the past.

TAVI CIRCLE CLOSED

In 2011, my 86-year-old father who was suffering from severe, symptomatic aortic stenosis was treated with a percutaneous transfemoral TAVI procedure (**Figure 11**). It was an enormous success for him. He was up walking around on the day of the procedure and discharged a few days later. He regained a normal life without any cardiac symptoms until he died 8 years later at age 95. For me, the circle was completed. My invention became a great personal achievement and the greatest gift I could ever give to my father.

THE BUSINESS WORLD: THE ANDERSEN PATENT

In 1989 we received assistance from the Danish Technology Institute (DTI) to draft a Danish patent application. DTI is an independent non-profit government institution with the goal to bring Danish inventions into production in Danish companies. DTI sought independent counseling from a Danish professor and interventional cardiologist. Based on his evaluation, DTI decided to grant sponsorship for a Danish and international patent application. The application covered the overriding fundamentals around a collapsible and expandable heart valve which included both balloon expandable as well as self-expandable valves. It described heart valve implantation in the aortic, pulmonic, mitral, and tricuspid positions. But the patent was not confined to heart valves. The title was "*Valve Prosthesis for implantation in the body and a catheter for implanting such valve prosthesis*" (**Figure 3**). Because it was so disruptive, it also included percutaneous catheter implantation of artificial valves in all places of the body where fluid is transported. The idea landed on virgin ground, and therefore it was easy to obtain a worldwide patent. It was so strong that it proved impossible to circumvent. It was later—unsuccessfully—challenged by attacks from large companies in patent courts. They tried to claim it was invalid and that it should be revoked because they wanted to enter the lucrative multi-billion market which was protected by the patent. However, the patent prevailed and survived in all patent fights in Europe and USA. It soon became known as "the Andersen patent" in the industry and in the world of patent lawyers.

With the Danish patent application in hand, we approached several Danish medical device companies. All the companies told us it was very interesting, but they declined to enter the project. They found that the development challenges and the costs would be too high. It would be a too risky investment and stretch over at least 10 years before a positive business might, or might not, materialize. We subsequently approached several other European companies with the same discouraging outcome. At that stage, DTI concluded that we would not be successful in finding a company in Europe, and therefore DTI could no longer sponsor our efforts to promote the invention

FIGURE 11 | Henning Rud Andersen with his farther Jørgen Rud Andersen a few hours after percutaneous transfemoral TAVI in 2011.

with resources granted from the Danish government. We were left to try ourselves without further assistance and support from DTI.

In 1992, after 41 *in-vivo* experiments, we realized that we had to find a non-European company with expertise in heart valves to develop the invention. We could no longer achieve more by building non-sterile valves and catheters with our own hands and performing only non-sterile acute feasibility studies. We needed serious sponsorship to continue the animal experiments with sterile heart valves and long-term follow-up studies.

With the international patent and our scientific results in hand, I contacted many of the big players on the market at that time; Johnson & Johnson (J&J), Medtronic, Baxter B.V. which at that time owned Edwards Lifesciences (Edwards), Boston Scientific, St. Jude Medical, USCI-Bard, SCIMED, Trimedyne, Meadox Surgimed, Pfizer, Astra Meditec and more. My efforts were all in vain. The response from the companies was always the same: *"Wow, that's interesting, I've never heard of a percutaneous heart valve before, We will look into it."* And who did the companies call to seek advice? Who were the experts in heart valves? The cardiac surgeons, of course! And what did the cardiac surgeons say? *"It is a silly idea, with very few patients who need it, after all there is no such thing as a nonsurgical patient. We can operate all the patients and have perfect outcomes. Here are the top eight reasons why this is never, ever going to work. It's a 'ridiculous' idea,"* (repeated eight times, authors comment). It was said that cardiologists know nothing about aortic stenosis and should not treat these patients, and *"It is the most stupid project ever heard of.…It will never work"* (15).

LICENSING THE PATENT TO STANFORD SURGICAL TECHNOLOGIES

In 1993, I could no longer afford to pay the yearly costs to maintain the patents. I had to find a sponsor to pay for maintaining the patents or lose them. A small company, Stanford Surgical Technologies (SST), from California had contacted me in 1992 during my poster presentation at the 65th American Heart Association Meeting (**Figure 10**). SST wanted to purchase the patent, but I would not sell it. Instead, in 1993 I decided to license it to SST in exchange for their payment of the patent fees which could keep the patent alive (**Figure 12**). We still owned the patent so we believed we could control the fate of it. It was a strategy I had learned from listening to Julio Palmaz's lecture in 1989. Palmaz licensed the rights to his patent to J&J, but he maintained ownership of it, a strategy which paid off for him.

During my visit to SST in California the same year we discussed how we could move forward together. My ultimate goal was to take my invention to much higher levels and finally develop it into a clinical treatment for patients, and at that time I judged that SST was capable of taking the first steps together with me. After returning to Denmark, SST wrote to me *"Our first goal is to send you sterilized valves for the 1–2-month chronic studies we discussed. I will keep you updated on the progress of this development."* I never received one single valve or catheter from SST for the years to come despite several inquiries which gradually became aggressive.

Due to our financial constraints, and our inexperience in the world of business and contract law, our position for negotiations

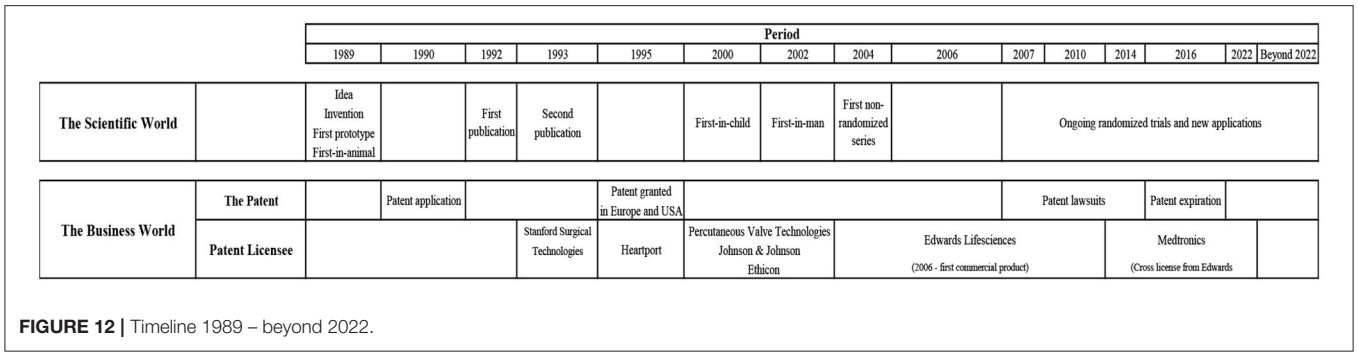

FIGURE 12 | Timeline 1989 – beyond 2022.

of the license agreement with SST in 1993 was very weak. Therefore, we ended up with a very flawed agreement. We could not afford to hire our own independent lawyers to assist us with negotiations. The patent applications nearly expired during my negotiations with SST. They delayed the writing and signing of the agreement until the very deadline for the next payment of the patent renewal applications and we nearly lost the patent. I had to raise private bank loans with a mortgage in my own home to ensure the survival of patent for 12 more months until the license agreement was finally formulated and signed, a situation which SST took great advantage of. Our very weak license agreement granted SST a worldwide exclusive license, including the right to grant sublicenses, and sell the license agreement to other companies without our engagement and without the obligation to share any income derived from that. The agreement did not include anything about the inventors' rights to be involved in the company and nothing about our participation in development, scientific research or academic publications. Furthermore, the license agreement did not include a clause about SST's obligation to develop the invention within a specific time frame. They were even free to do nothing, which turned out to be the case. We received an initial upfront payment of $20,000 to share between the three of us, and 5 years later we began to receive a fixed amount of $10,000 every year. The agreement also comprised a clause of 2.5% royalty from sales, but we never reached the point where we received royalty. It was very different from the decent deal Julio Palmaz negotiated with J&J when he licensed his stent patent in 1988. Palmaz received an initial down payment of $10 million plus royalty for 10 years which according to Shawn (45) amounted to "about $500 million" when Palmaz sold his patent to J&J in 1998.

TRANSFER OF THE LICENSE FROM STANFORD SURGICAL TECHNOLOGIES TO HEARTPORT

SST was founded by cardiac surgeons from Stanford University Hospital. They promised me to develop the technology and pay the fees for maintaining the patents. But SST did not reveal that they had already invented a new surgical technique, the minimally invasive Port Access Surgical Method for less invasive surgical aortic valve replacement. It turned out that SST wanted to develop their own invention rather than my device. SST soon changed their name to Heartport to reflect their own invention, Heart-Port-Access, and transferred the TAVI license agreement to the new company (**Figure 12**). Two years later Heartport announced they had also developed a new port-access technology for Coronary Artery Bypass Grafting (CABG) surgery. Now they owned a technology to perform both Port-Access-Valve Replacement combined with Port-Access-CABG. It became obvious to me why they did not develop the TAVI invention which was a potential competitor to their own invention and patents. In1995, Heartport and St. Jude Medical announced they had *"entered into a worldwide agreement including provisions for product development, patent licensing, and component supply, as well as the sale by St. Jude Medical of a new, jointly-developed product, the "St. Jude Medical Port-Access Mechanical Heart Valve System, incorporating Heartport Port-Access Technology.""* Now it was even more evident why TAVI was never developed in SST/Heartport and why they wanted to pay for the patent to make sure that other companies would not develop it. The license agreement survived deep in their archives. I complained aggressively to the CEO of SST/Heartport several times, but to no avail. He never responded. Heartport did pay the yearly patent fees which kept the patent alive, but my idea languished for 8 years and no development work was done despite their promise. In 2001, Heartport wrote to me, *"Heartport, Inc. had not pursued the development of licensed product based on the Licensed Patents. I like to hereby inform you that we signed a sublicense agreement with Percutaneous Valve Technologies in December 2000. The sublicense is in full compliance with the original Agreement. Enclosed please find a copy of the sublicense agreement. Also enclosed, please find two press releases."* So now, the license agreement had moved into a new company and the financial deal between the two companies had bypassed us.

TRANSFER OF THE LICENSE FROM HEARTPORT TO PERCUTANEOUS VALVE TECHNOLOGIES AND JOHNSON AND JOHNSON

Three weeks later Heartport was purchased by J&J for ∼$70 million, but at that time Heartport had already sold the cardiovascular part of the license agreement to Percutaneous Valve Technologies (PVT) for up-front $1.0 million followed by

$2.0 million 2 years later, and 3.5% equity in PVT. The rest of the license agreement was acquired by Ethicon, Inc., a J&J subsidiary, as was Heartport itself (**Figure 12**). Consequently, J&J had bought 3.5% equity in PVT, and therefore had a business interest in our TAVI license agreement. Paradoxically, it was J&J that had purchased the exclusive rights to file and prosecute new cardiovascular patent extension applications, not PVT. It led to much confusion when we found out that several new patent applications were filed in the name of us three patent owners but with Heartport wrongly assigned to the patent and without our knowledge. It also took me several communications with the different companies to find out who should now pay the yearly patents fees to ensure survival of our patents. It turned out to be Ethicon and not PVT or J&J.

When I realized that Heartport did not develop my invention, I contacted J&J and asked them if they were interested. At that time, they had already filed one of Alain Cribier's patent applications about TAVI valves, but so far, they did not develop it. J&J's Vice President of New Business Development called me and asked questions about our patent and the license. He was interested to discuss licensing the patent. I met with him and his co-Vice President in California together with a group of key persons from J&J. I wanted J&J to unbind the license from Heartport based on the fact that they did not develop it. My plan was to offer the license to J&J if they were seriously interested in developing it. Since they had already filed one of Cribiers patent applications I hoped they would say yes. The legal judgment from the J&J group was that it was not possible to unbind the license according to California laws. Then I suggested that J&J simply buy the whole company to get control of the license. The people from J&J liked the idea and went to the top management of the company and recommended it, but top management was not interested.

FOUNDATION OF PERCUTANEOUS VALVE TECHNOLOGIES

The two Vice Presidents from J&J became increasingly interested. They left J&J and began negotiations with Heartport to purchase our license agreement. They realized that if they were going to build a new successful company, they had to own the license to the Andersen patent. PVT was established by four people, the two previous Vice Presidents from J&J, Professor Marty Leon from New York and Professor Alain Cribier from Rouen in France. PVT raised ∼$19 million in funding capital to acquire the license and to develop the idea. Several U.S. companies such as Medtronic, Boston Scientific Corp., J&J and Oxford Bioscience together with two Israelian companies, Aran Research & Development and Medica Venture Partners invested in PVT and they all became members of the board of the company. I established a non-commercial partnership with PVT, but I had no money to invest. Much of the initial development was performed by Aran Research and Development Ltd. in Israel. Animal implantations were performed in Paris. The FIM implantation was performed by Professor Alain Cribier in Rouen, France in 2002 and was a great success (12).

TRANSFER OF THE LICENSE FROM PERCUTANEOUS VALVE TECHNOLOGIES TO EDWARDS LIFESCIENCES

In 2004, PVT and the license agreement were purchased by Edwards for $125 million in down payment and up to an additional $30 million upon achievement of key milestones (**Figure 12**). It was a difficult decision for Edwards to acquire PVT. Edwards was the world's leading manufacturer of surgical heart valves and their customers were cardiac surgeons. Several members of their advisory board were also cardiac surgeons. They were against it because TAVI was not about cardiac surgery but interventional cardiology and they did not recommend Edwards to engage in such a radical shift in business strategy. When Alain Cribier had performed the FIM and small series of implantation with the PVT valve (12–14), Edwards' CEO realized that his company was far behind with their own in-house TAVI development, and PVT was several years ahead of them. The Edwards' CEO acknowledged that PVT could undoubtedly sell their company for a considerable sum to one of Edwards' competitors which would outperform them and leave Edwards as a minor company in the heart valve market. The PVT's CEO deeply favored Edwards to develop their technology because Edwards was the leading heart valve company in the world. They had all the expertise needed, but he also realized that Medtronics, Boston Scientific and J&J, which were already members of the PVT board, had much stronger finances and could buy PVT for a huge amount and thereby outbid Edwards. Then, a very elegant strategy was orchestrated by the PVT's CEO. First, he called the Edwards' CEO and arranged a confidential meeting. The PVT's CEO suggested a strategy which could resolve the problem with overbidding from the much wealthier companies. The two CEOs agreed that Edwards make a bid of $125 million in cash without any term sheet. Both of them predicted that the other companies could not match such an offer in cash in such a short notice. It was all about timing and cash. After thorough planning, the PVT's CEO unexpectedly gave the other companies only 72 h to decide if they would give a higher bid in cash or leave it. He showed them the contract which Edwards had already signed. The other companies could predictably not make such a decision within 72 h, especially not in cash and without the opportunity to negotiate a term sheet agreement. Obviously the contract went to Edwards [**Figure 12**, (15)].

FURTHER DEVELOPMENT OF TAVI IN EDWARDS LIFESCIENCES

PVT now moved from their headquarter in New Jersey to the Edwards headquarters in Irvine, California together with key persons from PVT who all became integrated into Edwards. The PVT team established their own research and development unit inside the Edwards company where they got unrestricted hands

to develop TAVI. Much to my disappointment Edwards decided to name the valve "the Cribier-Edwards valve." That choice of name for the valve infuriated me because PVT and Edwards had on several occasions acknowledged that the TAVI valve was based on my invention and the Andersen patent (**Figure 13**).

After tough face-to-face meetings with Edwards where they argued that Cribier was very famous and I was not, which was actually correct, they finally accepted my point, and the name was soon changed to the more neutral Edwards SAPIEN valve. Edwards continued to invest, develop and refine the TAVI technology and made it into a lifesaving treatment for thousands of patients. It also became an enormous financial success for the company. I continued to be a partner in the non-commercial success story with Edwards. The original patent was still owned by us, but we got nothing from the deal between PVT and Edwards and no royalty from Edwards' annual sales of the SAPIEN valve which in 2021 alone is estimated to be $3.5 billion.

THE FIGHT FOR THE PATENTS: CORVALVE V. EDWARDS LIFESCIENCES

In 2007, a patent fight started between the French company CoreValve Inc. (CoreValve) and the Andersen patent. CoreValve had developed a self-expandable TAVI valve which infringed the Andersen patent because we owned the intellectual rights to the design. The patent fight initiated a legal battle with multiple court confrontations in Europe and USA for the next 7 years. First, CoreValve claimed that the Andersen patent was invalid and should be revoked. They filed a patent lawsuit against us patent owners in London. In 2005, I had been contacted by CoreValve, who at that time was located in Paris. They invited me to enter into a consulting agreement with them and they promised to compensate me amply for my services. But during this period I already had a partnership with Edwards and did animal implantations in Irvine, California, educational lectures in the company and scientific lectures at Edwards symposiums in Europe and USA. Therefore, I felt that I could not work with two competing companies. CoreValve did not inform me that they planned to file a patent case against us three patent owners in London. We first found out when we received a strict confidential personal letter from The High Court of Justice in London in 2007 where we were required to show up in London to defend our patent. I was in disbelief that, I was offered a consultancy position with CoreValve and shortly thereafter to be the target of a patent case. Shortly before the court hearings began in London, Edwards suggested that they could defend the patent with their lawyers free of charge for us three patent owners. We did not have our own lawyers and we could not afford to hire legal representation. Fortunately, we did not immediately accept Edwards wish to acquire ownership of the Andersen patents. At that time, Edwards had already invested a huge amount of money in development and clinical trials and had obtained approval for commercial sales in Europe in 2006 (**Figure 12**), so the patents was of extremely high value for them. Therefore, it was very much in their interest that the patents survived in litigation because they did not want to share the European and USA market with other companies.

At the same time, Edwards had filed litigation against CoreValve in Düsseldorf, Germany claiming that the CoreValve patent infringed upon the Andersen patents. CoreValve had moved from Paris to Irvine in California and the fight continued in the USA. In 2008, Edwards filed new patent infringement litigation against CoreValve in USA. The suit sought injunctive relief and damages for infringement of the Andersen family of patents.

THE FIGHT FOR THE PATENTS: MEDTRONIC V. EDWARDS LIFESCIENCES

In 2009, Medtronic purchased CoreValve for $700 million plus two $75 million milestone payments and continued the patent fight in USA even more aggressively (**Figure 12**). In 2010, a U.S. Federal jury ruled that the Andersen patent was valid, and that Medtronic willfully infringed it. The jury awarded Edwards $72 million in damages and $1.3 million as a reasonable royalty, and the willfulness finding allowed Edwards to seek increased damages of up to three times that amount (46). Medtronic appealed the ruling but in 2012 the U.S. Court of Appeals affirmed the decision. The Appeals Court also spontaneously ordered the Federal Court to reconsider Edwards' request for a preliminary injunction which would prohibit the manufacture and sale of the Medtronic's ReValving system in USA because the judge found *"There is evidence that Medtronics may have sought to stockpile infringing devices in the United States after the verdict* (2010 court ruling, authors comment) *as part of a greater plan to overtake Edwards in the THV market"* (46).

Several court meetings were held in USA, where J. Michael Hasenkam represented us three patent holders and appeared in the court in Wilmington, Delaware to support Edwards. In 2014 the Federal Court granted the injunction which required Medtronic to stop sales in USA within 7 days. The Court also ordered, *"The parties shall immediately enter upon discussions to jointly determine a mechanism by which a sufficient number of CoreValve Generation 3 devices can be provided to the hospitals and clinics that are currently already trained in use of the CoreValve Generation 3."* The Court ordered that within 36 days, *"the parties shall apprise the court via teleconference of the status of their discussions."* The Court did not expect that the discussions would end up with an overall settlement within such a short time, but the Court wanted to make sure that negotiations between the two companies had been initiated.

A PATENT CROSS-LICENSE AGREEMENT

On day 35, Edwards and Medtronic announced they had finalized a complete agreement to dismiss all pending cases worldwide in the field of both transcatheter and surgical valves for the 8 year duration of their agreement. Under the terms of a patent cross-license agreement, Edwards had granted Medtronic the right to manufacture and sell the Medtronic ReValving system

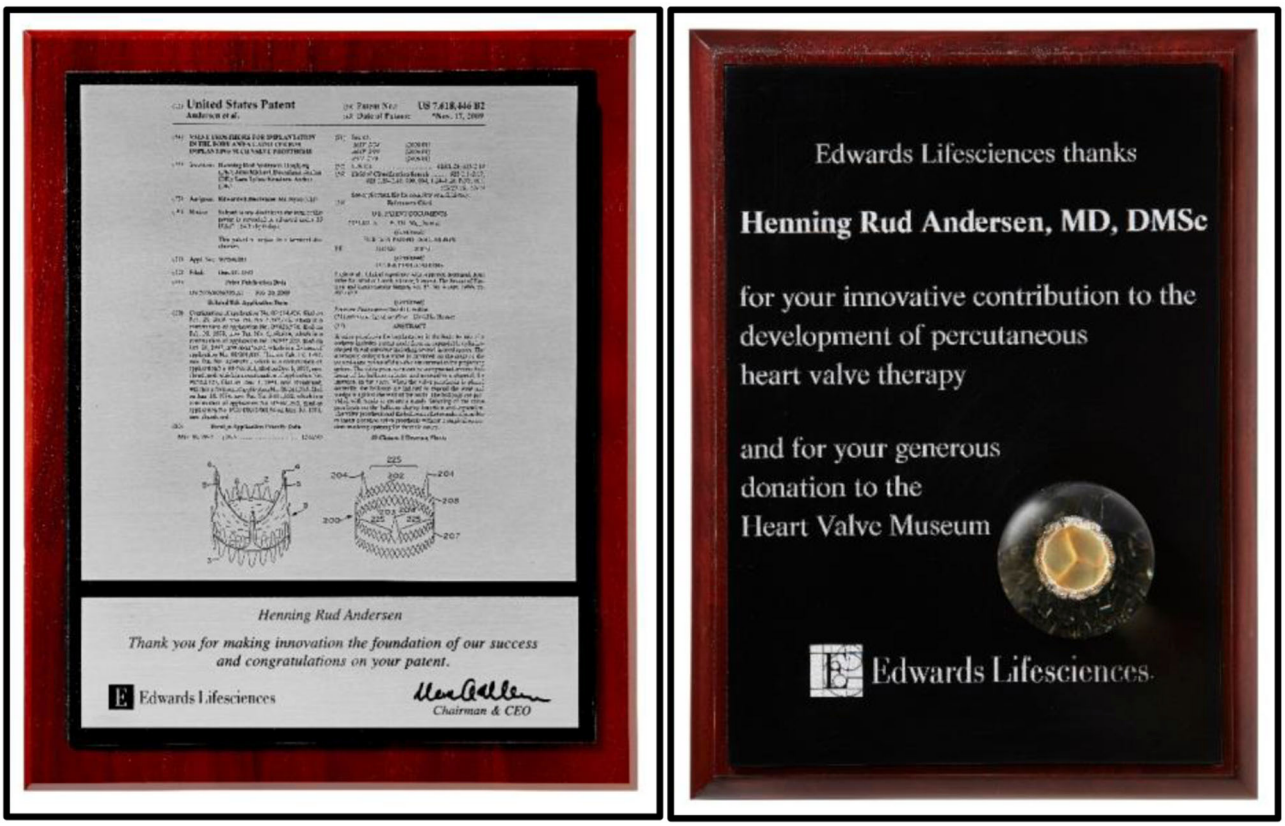

FIGURE 13 | Left: Acknowledgments from Edward for innovation of TAVI and foundation of Edwards' success. **Right:** Acknowledgments from Edwards for development of TAVI and for donating TAVI prototypes to the Edwards Heart Valve Museum in Irvine, California, USA.

under the Edwards' license (**Figure 12**). Medtronic made a one-time payment to Edwards of $750 million in cash. Additionally, Medtronic pays Edwards an ongoing royalty through April 2022. Royalty payments are based on a percentage of Medtronic's CoreValve sales, subject to a minimum annual payment of $40 million. So now, both Edwards and Medtronic benefited from their multi-billion-dollar business based on my invention and they had established a deal where Medtronic continues to pay royalty to Edwards until several years after the expiration of the Andersen patent. I was disappointed, because after all it was my invention and intellectual property the two companies were trading about. I had anticipated that they would be fair and reach out to us and rectify our flawed license agreement so the settlement also rewarded the innovators, but they did not. This is an important lesson for new inventors to learn from.

SURVIVAL OF THE ANDERSEN PATENTS

When the litigations began in 2007 nobody knew that TAVI would be such an enormous financial success. But we knew that financial success for Edwards and us, if any, depended on the value of my invention and the survival of the Andersen patent. Therefore, Edwards and we three patent owners formed a partnership to make sure that the Andersen patent prevailed in all litigations. If we turned out to be successful together with Edwards, we three patent owners should have a fair and substantial share of the outcome, if any, as long as our mutual partnership existed. Furthermore, we promised Edwards to participate in meetings with United States Patent and Trademark Office (USPTO) and help Edwards to ensure extension of the survival period of the Andersen patents beyond the timetabled expiration date. Our meetings with USPTO were successful and resulted in prolongation of the survival time of the patents by 2½ years into 2016. In the patent litigations we worked hard together with Edwards for 7 years in countless meetings in Europe and USA, and in 2014 the Andersen patents had finally prevailed and survived in all litigations in all countries. So far, both parties had fulfilled the obligations of our partnership. Edwards was granted a huge financial compensation of more than $1 billion. However, unexpectedly Edwards' compensation suddenly bypassed us and was never shared with us as they had promised. For new inventors, such a maneuver is important to remember and learn from.

After the 2012 ruling, Edwards had prevailed over Medtronic in all previous litigations. All USA judges had in unanimously declared that Medtronic willfully infringed the Andersen patents. In addition, the judges in several USA Courts were infuriated

with Medtronic when they found out that the company gave misleading evidence and a judge claimed that "*Medtronic was well aware that its representation in courts was false when made*" (46). Furthermore, the Supreme Court denied hearing Medtronic's appeal. This was the situation before the final 2014 court ruling. With such a legal position, the likelihood that Edwards would prevail, and Medtronic would lose the final court ruling must have been obvious to both companies. Furthermore, they were exhausted after 7 years with endless and costly patents fights in Europe and USA. Therefore, we speculate that the scene was set for an early voluntary settlement, and today we believe that such settlement negotiations about the Andersen patents were already secretly initiated long before the final 2014 ruling.

In 2014 we met with Edwards' Head of Legal affairs in Denmark a few weeks before the settlement with Medtronic unexpectedly for us went public. The lawyer told us that the litigation with Medtronic was still very much alive and that it was likely to drag out for years, and that the outcome was completely unpredictable. She said that if we and Edwards lost the ongoing litigation, we three innovators would not receive anything in accordance with our partnership agreement. When we questioned the lawyer, she said she had additional information, which she could not reveal to us due to US disclosure rules. Today we suspect that she knew very well that the settlement between Edwards and Medtronic was already completed and merely awaiting publication while negotiations with us could be consummated so Edwards could save a huge amount which was due to us according to our partnership agreement. She then suggested that we end our 7-years-long mutual partnership, so we three patent holders at least got some compensation from Edwards instead of waiting maybe several years and risk losing everything. We were against it because we had fought hard together with Edwards for 7 years and so far, we had prevailed in all similar litigations against CoreValve and Medtronic in both Europe and USA. Therefore, we predicted we would prevail again in the final litigation which could reward us with a huge share of Edwards' compensation. The lawyer telephoned the Edwards' Headquarters in USA several times during the meeting and then she started to threaten us with year-long and costly litigation in USA courts if we did not accept their suggestion. I had never imagined that I, the inventor of TAVI, would be threatened with litigation from the world's leading heart valve company, particularly after having worked so hard together for so many years to defend the Andersen patents and to bring the invention to clinical and financial fruition. However, the increasing legal pressure on us from the lawyer and the Edwards' Headquarters in California became so strong that we gave in to it. It ended our partnership with Edwards prematurely. To our amazement and consternation, a few weeks later, and not "years" later in contrast to what was explained to us by the lawyer, the settlement between Edwards and Medtronic suddenly went public. We then realized that we had been maneuvered out of a fair and substantial share of the $1 billion compensation to Edwards few weeks before the settlement was announced. We had lost both our partnership and fair compensation and Edwards had saved an enormous amount of money. Today, we believe that the Edwards' lawyer knew very well that the settlement with Medtronic was already finished when she traveled to Denmark to end our partnership prematurely. Such strategies from companies toward inventors is worth remembering for new inventors.

At the time when we entered the partnership with Edwards, we were not aware that we, the patent owners, had the right to settle the dispute between us and the counterpart (CoreValve and Medtronic) because it is normally the patent owner, not the licensee, who can negotiate a settlement with the counterpart in patent fights. Indeed, Edwards would not like it because they had invested a lot of money, but we could probably have negotiated a much better deal with both Medtronic and Edwards if we had offered Medtronic a cross-license settlement agreement where they would compensate us with a substantial amount. Because both companies were very much interested in the patent and the huge business opportunity the patent controlled, we could have negotiated a license agreement with both companies and received a lifelong double royalty income from both. But Edwards' lawyers did not inform us about our legal rights to settle the dispute with Medtronic, and we did not have our own independent lawyers to advise us. Instead, Edwards single-handedly negotiated a huge settlement with Medtronic and sold a cross-license to them which bypassed us. This is also worth remembering for new inventors. Keep ownership of your patent so you can control the fate of it and hire your own lawyers. This was the background for Julio Palmaz's success when he finally sold his patent to J&J in 1998 for a huge amount (45).

A DOCTOR IN PATENT COURTS

Instead of fame and fortune, I did however, get an incredibly unique experience in life from the invention of TAVI, which I would never have obtained in any other way. It was the life in patent courts in several countries around the world, all crowded with numerous lawyers and judges, many of them dressed in black medieval gowns and long white wigs, fighting and judging about my intellectual property. A deposition was also held here in Denmark where Medtronic/CoreValve sent a group of their lawyers to question the three Danish patent holders in a hotel conference room which was officially converted into a USA court room for the deposition. We were supported by a group of Edwards lawyers sitting on the opposite side of the table. All three of us were individually grilled for several hours and everything was video recorded during the hearings.

Afterwards, our partnership with Edwards was to participate in court hearings worldwide and in meetings with their lawyers and to hand over all relevant information and all raw data including early prototypes of the valves. The workspace for Edwards's law team—called "The War Room"—was a beehive of people, computers and documents set up in a hotel next to the court building in Wilmington, Delaware, USA (**Figure 14**).

In the Court room, the Medtronic lawyers twisted the wordings and claimed my idea, studies and publications were useless and therefore the Andersen patent was invalid. The Edwards lawyers on the other hand claimed the data, publications

FIGURE 14 | Left and Middle: "The War Room" for the patent fights, where all Edwards' legal preparations, meetings and storage of documentation were placed in one big, fully packed room in Wilmington, Delaware, USA in 2010. **Right**: After Edwards had prevailed in all patent cases, Edwards' CEO (left in the photo) was exited and gave me a warm hug. To the right in the photo is the CEO of PVT.

and patent were valid and that the Medtronic/CoreValve design was included in the Andersen patent because it clearly described both balloon expandable as well as self-expandable valves. Consequently, Edwards claimed that CoreValve infringed the Andersen patents and the courts agreed. After 7 years with court meetings the patent finally prevailed in 2014 which shortly after resulted in the cross-license agreement between Edwards and Medtronic which is still in force until 2022 (**Figure 12**).

DISCUSSION

In 1989 in Scottsdale, I had learned from listening to Julio Palmaz that an inventor must never ever give up. He must fight for his idea and his intellectual property, also if everything looks futile. That turned out to be sound advice because when an inventor comes up with a "crazy" disruptive idea, he must expect to be met with resistance and skepticism, even from his own peers and academic societies. A very disruptive invention like TAVI creates a paradigm shift and changes the world's concept of normality, and it creates resistance and annoyance when the inventor claims that the established rules no longer define the game (47). When the inventor announces that cardiac surgery is no longer needed to implant artificial heart valves many colleagues will not believe him, and some of them will even respond with anger. This response is widespread, even to the level of editors and review committees of scientific journals. In my case, disbelief and widespread rejection lasted 17 years before the first commercial valve reached market. This illustrates how much you must struggle and fight for your idea and during that time the clock is ticking on your patent.

ADVICE FOR INVENTORS

It is important for you to file a patent application before contacting a company. Otherwise, you have nothing to offer and nothing to negotiate with. The company can simply take your invention for free. Furthermore, the invention has a higher value for the company if you have already protected it with a patent application or a patent. You should insist that the company sign a confidentiality agreement. However, be aware that it might be of minor value for you. If the company breaks the confidentiality agreement, the only course of action is to pursue litigation that will be very time consuming and expensive. All the while, once again the patent clock is ticking. You should hire your own lawyers from the very beginning. If you cannot afford it, the company must agree to sponsor the costs of your independent representation. If they do not agree to that, you should not negotiate with them. Remember, they can be very cold-hearted and unscrupulous, and they do not want the inventor to be in a strong legal position during negotiations. Sad to say, but they want to take advantage of your relatively poor financial position, your inexperience in the world of business and contract law, and your desire to have your brainchild developed and ultimately deployed. You should also demand that the company invest and develop your invention within a specified time, otherwise the license should be returned to you free of charge so you can find another company, and you should not accept to compensate them for their expenses. It is their failure and problem if they are not successful in developing your idea. That is the risk they assume. You should insist on being compensated appropriately with initial down payment, milestones, royalties and equity in the company. If the company is a small start-up company like PVT, it is preferable to acquire equity than take money from the company since the start-up company needs the money for development of your invention. Equity will gain value if your invention turns out to be a financial success either in the company itself or from a bigger company which acquires it. That was the case with PVT when Edwards purchased them. Importantly, the license and the financial agreement should remain in effect lifelong, even after expiration of your patent. This can be illustrated with my own TAVI story. The time from patent application until commercial sales was long (**Figure 12**). Our Danish patent application was filed in 1990, the European application in 1991 and the USA application in 1993 and again in 1994. The European and the USA patents were granted in 1995. The first approval for commercial sales in Europe was granted to both Edwards and CoreValve in 2007 and for sales in USA to

Edwards in 2011 and to Medtronic in 2014. Consequently, the time from first patent application until first commercial sales in Europe was 17 years, and in USA 21 years, which is the lifespan of a patent. It is quite normal that transition from a ruling paradigm like cardiac surgery for treatment of aortic stenosis to a new paradigm like TAVI can last 15–20 years or more (47). It means that your patent can expire before commercial sales begin and you get no royalty from sales if the agreement is patent-related and not lifelong. However, your idea, invention and intellectual property remains lifelong and therefore the royalty should indeed also be lifelong as long as the company earns an income from your invention. In our case, we never received royalty from sales. However, still today in 2021, royalties are paid between Medtronic and Edwards based on sales of my invention. It demonstrates, that in the world of big multinational companies, royalty can be granted between companies long after the patents have expired. Therefore, the same rules should also apply for less privileged inventors.

ADVICE FOR COMPANIES

As opposed to us doctors and innovators, industries seem to employ a large contingent of lawyers whose job is to ensure that the company pays as little as possible or nothing on the original invention. Therefore, they can take advantage, or even cheat us if their leaders do not take responsibility for how their company treats inventors. Even in 1993, a small company like SST had retained their own Chief Patent Counsel. He was much sharper than me in formulating contract law and knew how to apply maximum financial pressure. Indeed, it may very well be his job description in a company, but it is ultimately always the responsibility of the CEO and the Board-of-Directors to control the lawyers and ensure that inventors are treated in a fair, respectful and correct manner. When a company buys a patent, a license or a sublicense and signs an agreement, they also buy the scientific research history. In the TAVI case it took us more than 6 years of hard work and fighting to create the huge value of the invention and the strong patent. Therefore, the license is not just a piece of paper which can be sold to the next company without recognizing the innovators hard work.

Initially, the commercial value of an invention and a patent/license is low because nobody knows if it can be developed into a business success. Therefore, the initial payment to the inventor can also be low. In our case it was $20,000 in down payment which was fair at that time. When Heartport sold the license to PVT, the value had increased to $3 million plus 3.5% equity in PVT, and when Edwards purchased PVT for $125 million plus $30 million, the value of the license had increased significantly, but it was not reflected in royalty to the patent holders. When Edwards had developed the invention and started commercial sales, the value of the patent and license had increased dramatically with our assistance. Therefore, it should also have been shared with the inventors. The same was the case when Edwards cross-licensed the invention to Medtronic several years after the patent had expired. None of the two companies rectified the original flawed license agreement and shared any of the device's value with the inventors.

ADVICE FOR INVENTORS AND COMPANIES

I hope my business story can be an inspiration and wake up call for new inventors, and for companies, too. Doctors are educated in natural and medical science, not in legal matters. We excel at coming up with new creative ideas and products which companies need and can benefit from by developing them beyond the early innovation stage. Inventors and companies simply must find a better way to work together in the future to develop new treatments and products. We need each other, and all good collaborations must be mutually beneficial. So far, the TAVI invention has been a disruptive clinical game changer which has generated great value for patients. It has created a major paradigm shift and has radically changed the way we treat patients with aortic stenosis worldwide. It has saved many thousand lives and it has rewarded several companies and investors with a multi-billion-dollar business, but the inventors and their academic institution where TAVI was invented did not gain anything near equivalent advantage from the success.

In the future, cooperation between academic inventors and companies should be transparent and made partly public to facilitate our academic freedom to teach and publish. Otherwise, academic inventors are tied hands, feet and mouth and cannot report the truth as they see it. Already back in 1993, SST's lawyers formulated confidentiality clauses and all the successive companies involved in the license and patents they forwarded new agreements with confidential clauses which we were required to sign. As doctors we hardly understood what it was all about. Our confidentially agreements with Edwards are life long, so the present business story about TAVI could never be told without breaking a few of the secret clauses in the agreement. For example, I am not allowed today to tell the truth that in 2007 we formed a partnership to defend our patent and I am not allowed to reveal how we assisted Edwards for many years in litigation in Europe and USA to make sure the Andersen patent prevailed and survived. Similarly, I am not allowed to disclose how we helped Edwards in USPTO meetings to successfully prolong the lifetime of the Andersen patent. Furthermore, I must not explain how our partnership with Edwards was manipulated so it suddenly ended prematurely and prevented us from receiving the huge compensation which we should have received according to the partnership agreement. However, such business information is crucial for new inventors to learn from and can only be told if we are not restricted by confidentiality clauses.

SUMMARY

When an academic inventor comes up with a new idea which has the potential to be disruptive and create a paradigm shift, he must be prepared to be met with skepticism, resistance and annoyance when he claims that the established rules no longer define the game. He will face ups and downs bringing his invention forward. Some of his colleagues will not believe him and sometimes even react with anger if it is their field he challenges. The response is widespread, even to the level of editors and review committees of scientific journals and even from powerful forces among his

own peers and academic societies. At the same time, he must fight for his intellectual property, even when it appears to be futile. Industry must understand that the individual academic inventor does not live in the world of attorneys and contract and patent law like the companies do. Therefore, the responsibility falls to the company to establish a decent code-of-conduct which ensures that the inventor gets a fair treatment. This business ethos will serve companies, inventors and patients best.

AUTHOR CONTRIBUTIONS

The author conceived the paper and received substantial factual, historical and linguistic input from J. Michael Hasenkam and Frederic Joyce (see acknowledgements).

ACKNOWLEDGMENTS

I gratefully thank Professor J. Michael Hasenkam, MD, DMSc, Department of Cardiothoracic Surgery, Aarhus University Hospital, Denmark for all his support and help with valve constructions and participation in animal experiments during the years. He also gave very important contribution to this paper. Dr. J. Michael Hasenkam is a co-holder of the Andersen patent and a co-author of Publications No. 3-6. I also gratefully thank Dr. Lars Lyhne Knudsen, MD. Regionshospitalet Herning, Denmark. During the development phase Lars was a medical student. He helped with valve constructions and participated in animal experiments during the early years. Dr. Lars Lyhne Knudsen is a co-holder of the Andersen patent and a co-author of Publications No. 3-6. Dr. Frederic Joyce, MD, FACC, now of Ascension Medical Group of Southeast Michigan, USA, lived in Denmark for 25 years, studied medicine at Aarhus University and subsequently pursued training in cardiac surgery at Copenhagen University's Rigshospitalet and the Cleveland Clinic Foundation. While at Aarhus University he did animal research in the very same experimental laboratories where TAVI was born (**Figure 5**). Frederic Joyce has contributed significantly with invaluable reviews and linguistic support. The manuscript has been forwarded to Edwards and Medtronic for information only after they signed a Confidentiality Agreement. None of the two companies have had any influence on the content of the paper which solely represents the experience of the author.

REFERENCES

1. Hufnagel CA, Harvey WP. The surgical correction of aortic regurgitation. *Prelim Rep Bull Georgetown Univ Center.* (1953) 6:3–6.
2. Hufnagel CA, Harvey WP, Rabil PJ, McDermott TF. Surgical correction of aortic insufficiency. *Surgery.* (1954) 35:285–300.
3. Andersen HR, Knudsen LL, Hasenkam JM. Transluminal implantation of artificial heart valves. Description of a new expandable aortic valve and initial results with implantation by catheter technique in closed chest pigs. *Eur Heart J.* (1992) 13:704–8. doi: 10.1093/oxfordjournals.eurheartj.a060238
4. Knudsen LL, Andersen HR, Hasenkam M. Catheter-implanted prosthetic valves. Transluminal catheter implantation of a new expandable artificial heart valve in the descending aorta in isolated vessels and closed chest pig.*s Int J Artif Organs.* (1993) 16:253–62. doi: 10.1177/039139889301600505
5. Knudsen LL, Andersen HR, Hasenkam JM. Transluminal catheter implantation of a new expandable artificial heart valve in the descending thoracic aorta in isolated vessels and closed chest pigs. *Eur Heart J.* (1992) 13:411.
6. Andersen HR, Knudsen LL, Hasenkam JM. A new expandable artificial heart valve for implantation by transluminal catheter technique. Initial results with implantation in closed chest pigs. *Circulation.* (1992) 86:I-698.
7. Pavenik D, Wright KE, Wallace S. Development and initial experimental evaluation of a prosthetic aorta valve for transcatheter placement. *Work Prog Radiol.* (1992) 183:151–4. doi: 10.1148/radiology.183.1.1549662
8. Sochman J, Peregrin JH, Rocek M, Timmermans HA, Pavcnik D, Rösch J. Percutaneous transcatheter one-step mechanical aorta disc valve prosthesis implantation: a preliminary feasibility study in swine. *Cardiovasc Intervent Radiol.* (2006) 29:114–9. doi: 10.1007/s00270-005-0029-9
9. Bonhoeffer P, Boudjemline Y, Saliba Z, Hausse AO, Aggoun Y, Bonnet D et al. Transcatheter implantation of a bovine valve in pulmonary position: a lamb study. *Circulation.* (2000) 102:813–6. doi: 10.1161/01.CIR.102.7.813
10. Bonhoeffer P, Boudjemline Y, Saliba Z, Merckx J, Aggoun Y, Bonnet D, et al. Percutaneous replacement of pulmonary valve in a right-ventricle to pulmonary-artery prosthetic conduit with valve dysfunction. *Lancet.* (2000) 356:1403–5. doi: 10.1016/S0140-6736(00)02844-0
11. Cribier A, Elchaninoff H, Borenstein N. Trans-catheter implantation of balloon-expandable prosthetic heart valves: early results in an animal model. *Circulation.* (2001) 104(Suppl. II):II-552.
12. Cribier A, Eltchaninoff H, Bash A, Borenstein N, Tron C, Bauer F, et al. Percutaneous transcatheter implantation of an aortic valve prosthesis for calcific aortic stenosis: first human case description. *Circulation.* (2002) 106:3006–8. doi: 10.1161/01.CIR.0000047200.36165.B8
13. Cribier A, Eltchaninoff H, Tron C, Bauer F, Agatiello C, Sebagh L, et al. Early experience with percutaneous transcatheter implantation of heart valve prosthesis for the treatment of end-stage inoperable patients with calcific aortic stenosis. *J Am Coll Cardiol.* (2004) 43:698–703. doi: 10.1016/j.jacc.2003.11.026
14. Cribier A, Eltchaninoff H, Tron C, Bauer F, Agatiello C, Nercolini D, et al. Treatment of calcified aortic stenosis with the percutaneous heart valve. Mid-term follow-up from the initial feasibility studies: the French Experience. *J Am Coll Cardiol.* (2006) 47:1214–23. doi: 10.1016/j.jacc.2006.01.049
15. Rowe S, Rabinovich S. *Launching the TAVR Revolution - The PVT Story*. Tel Aviv: MedTech Strategist (2014). p. 4–16.
16. Seth A, Rastogi V, Kumar V, Maqbool S, Mustaqueem A, Sekar VR. Transcatheter aortic valve implantation with Core Valve: first Indian experience of three high surgical risk patients with severe aortic stenosis. *Indian Heart J.* (2013) 65:395–9. doi: 10.1016/j.ihj.2013.06.003
17. Grube E, Laborde JC, Zickmann B, Gerckens U, Felderhoff T, Sauren B, et al. First report on a human percutaneous transluminal implantation of a self-expanding valve prosthesis for interventional treatment of aortic valve stenosis. *Catheter Cardiovasc Interv.* (2005) 66:465–9. doi: 10.1002/ccd.20544
18. Grube E, Laborde C, Gerckens U, Felderhoff T, Sauren B, Buellesfeld L, et al. Percutaneous implantation of the CoreValve self-expanding valve prosthesis in high-risk patients with aortic valve disease: the Siegburg first-in-man study. *Circulation.* (2006) 114:1616–24. doi: 10.1161/CIRCULATIONAHA.106.639450
19. Webb JG, Chandavimol M, Thompson CR, Ricci DR, Carere RG, Munt BI, et al. Percutaneous aortic valve implantation retrograde from the femoral artery. *Circulation.* (2006) 113:842–50. doi: 10.1161/CIRCULATIONAHA.105.582882
20. Ruge H, Lange R, Bleiziffer S, Hutter A, Mazzitelli D, Will A, et al. First successful aortic valve implantation with the CoreCalve revalving system *via* right subclavian artery access: a case report. *Heart Surg Forum.* (2008) 11(Suppl. 1):E323–4. doi: 10.1532/HSF98.20081021
21. Petronio AS, De Carlo M, Bedogni F, Marzocchi A, Klugmann S, Maisano F, et al. Safety and efficacy of the subclavian approach for transcatheter

aortic valve implantation with the CoreValve revalving system. *Cir Cardiovasc Interv*. (2010) 3:359–66. doi: 10.1161/CIRCINTERVENTIONS.109.930453
22. Asgar AW, Mullen MJ, Delahunty N, Davies SW, Dalby M, Petrou M, et al. Transcatheter aortic valve intervention through the axillary artery for the treatment of severe aortic stenosis. *J Thorac Cardiovasc Surg*. (2009) 137:773–5. doi: 10.1016/j.jtcvs.2007.12.084
23. Etienne PY, Papadatos S, El Khoury E, Pieters D, Price J, Glineur D. Transaortic transcatheter aortic valve implantation with the Edwards SAPIEN valve: feasibility, technical considerations, and clinical advantages. *Ann Thorac Surg*. (2011) 92:746–8. doi: 10.1016/j.athoracsur.2011.03.014
24. Bapat V, Khawaja MZ, Attia RA, Narayana A, Wilson K, Macgillivray K et al. Transaortic transcatheter aortic valve implantation using Edwards Sapien valve: a novel approach Catheter. *Cardiovasc Interv*. (2012) 79:733–40. doi: 10.1002/ccd.23276
25. Webb JG, Binder RK. Transcatheter aortic valve implantation: the evolution of prostheses, delivery systems and approaches. *Arch Cardiovasc Dis*. (2012) 105:153–9. doi: 10.1016/j.acvd.2012.02.001
26. Webb JG, Munt B, Makkar RR, Naqvi TZ, Dang N. Percutaneous stent-mounted valve for treatment of aortic or pulmonary valve disease. *Catheter Cardiovasc Interv*. (2004) 63:89–93. doi: 10.1002/ccd.20112
27. Ye J, Cheung A, Lichtenstein SV, Carere RG, Thompson CR, Pasupati S, et al. Transapical aortic valve implantations in humans. *J Thorac Cardiovasc Surg*. (2006) 131:1194–6. doi: 10.1016/j.jtcvs.2006.01.026
28. Walther T, Falk V, Borger MA, Dewey T, Wimmer-Greinecker G, Shuler G, et al. Minimally invasive transapical beating heart aortic valve implantation - proof of concept. *Eur J Cardiothorac Surg*. (2007) 31:9–15. doi: 10.1016/j.ejcts.2006.10.034
29. Azmoun A, Amabile N, Ramadan R, Ghostine S, Caussin C, Fradi S, et al. Transcatheter aortic valve implantation through carotic artery access under local anaesthesia. *Eur J Cardiothorac Surg*. (2014) 46:693–8. doi: 10.1093/ejcts/ezt619
30. Kirker EB, Hodson RW, Spinelli KJ, Korngold EC. The carotic artery as preferred alternative access route for transcatheter aortic valve replacement. *Ann Thorac Surg*. (2017) 104:621–9. doi: 10.1016/j.athoracsur.2016.12.030
31. Yan C, Wan L, Li L, Li H, Du B. Transfemoral transcatheter puncture of interventricular septum in a swine model: a novel transfemoral-venous access to left ventricle with the assistance of arterio-venous circuit. *Catheter Cardiovascular Interv*. (2020) 96:488–96. doi: 10.1002/ccd.28848
32. Leon MB, Smith CR, Mack M, Miller DC, Moses JW, Svensson LG, et al. Transcatheter aortic-valve implantation for aortic stenosis in patients who cannot undergo surgery. *N Engl J Med*. (2010) 363:1597–607. doi: 10.1056/NEJMoa1008232
33. Smith CR, Leon MB, Mack MJ, Miller DC, Moses JW, Svensson LG, et al. Transcatheter versus surgical aortic-valve replacement in high-risk patients. *N Engl J Med*. (2011) 364:2187–98. doi: 10.1056/NEJMoa1103510
34. Adams DH, Popma JJ, Reardon MJ, Yakubov SJ, Coselli JS, Deeb GM, et al. Transcatheter aortic-valve replacement with a self-expanding prosthesis. *N Eng J Med*. (2014) 370:1790–8. doi: 10.1056/NEJMoa1400590
35. Leon MB, Smith CR, Mack MJ, Makkar RR, Svensson LG, Kodali SK, et al. Transcatheter or surgical aortic-valve replacement in intermediate-risk patients. *N Engl J Med*. (2016) 374:1609–20. doi: 10.1056/NEJMoa1514616
36. Reardon MJ, Van Mieghem NM, Popma JJ, Kleiman NS, Søndergaard L, Mumtaz M, et al. Surgical or transcatheter aortic-valve replacement in intermediate-risk patients. *N Eng J Med*. (2017) 376:1321–31. doi: 10.1056/NEJMoa1700456
37. Mack MJ, Leon MB, Thourani VH, Makkar R, Kodali SK, Russo M, et al. Transcatheter aortic-valve replacement with a balloon-expandable valve in low-risk patients. *N Engl J Med*. (2019) 380:1695–705. doi: 10.1056/NEJMoa1814052
38. Popma JJ, Deeb GM, Yakubov SJ, Mumtaz M, Gada H, O'Hair D, et al. Transcatheter aortic-valve replacement with a self-expanding valve in low-risk patients. *N Eng J Med*. (2019) 380:1706–15. doi: 10.1056/NEJMoa1816885
39. Thyregod HGH, Steinbrüchel DA, Ihlemann N, Nissen H, Kjeldsen BJ, Petursson P, et al. Transcatheter versus surgical aortic valve replacement in patients with severe aortic valve stenosis: 1-year results from the all-comers NOTION randomized clinical trial. *J Am Coll Cardiol*. (2015) 65:2184–94. doi: 10.1016/j.jacc.2015.03.014
40. Thyregod HGH, Ihlemann N, Jørgensen TH, Nissen H, Kjeldsen BJ, Petursson P, et al. Five-years clinical and echocardiographic outcome from the NOTION randomized clinical trial in patients at lower surgical risk. *Circulation*. (2019) 139:2714–23. doi: 10.1161/CIRCULATIONAHA.118.036606
41. Makkar RR, Thourani VH, Mack MJ, Kodali SK, Kapadia S, Webb JG, et al. Five-year outcomes of transcatheter or surgical aortic-valve replacement. *N Engl J Med*. (2020) 382:799–809. doi: 10.1056/NEJMoa1910555
42. Mack MJ, Leon MB, Smith CR, Miller DC, Moses JW, Tuzcu EM, et al. 5-year outcomes of transcatheter aortic valve replacement or surgical aortic valve replacement for high surgical risk patients with aortic stenosis (PARTNER 1): a randomised controlled trial. *Lancet*. (2015) 385:2477–84. doi: 10.1016/S0140-6736(15)60308-7
43. Gleason TG, Reardon MJ, Popma JJ, Deeb GM, Yakubov SJ, Lee JS, et al. 5-year outcomes of self-expanding transcatheter versus surgical aortic valve replacement in high-risk patients. *J Am Coll Cardiol*. (2018) 72:2687–96. doi: 10.1016/j.jacc.2018.08.2146
44. Tang GHL, Verma S, Bhatt DL. Transcatheter aortic valve replacement in low-risk patients. A new era in the treatment of aortic stenosis. *Circulation*. (2019) 140:801–3. doi: 10.1161/CIRCULATIONAHA.119.041111
45. Shawn T. Blood feud this little piece of metal is worth $4.5 billion this year, generates more profits than a blockbuster drug, and has sparked one of the weirdest corporate battles ever. It could also save your life. *Fortune Magazine*. (2004) 149:11.
46. Sleet GM, *Chief District Judge for United States Court for the District of Delaware*. Wilmington: Edwards Lifesciences AG v. Medtronic CoreValve LLC (2014).
47. Kuhn TS. The resolutions of revolutions. In: Kuhn TS, editor. *The Structure of Scientific Revolutions*. 3rd ed. Chicago/London: The University of Chicago Press (1996). p. 144–59.

Conflict of Interest: The author declares that the research was conducted in the absence of any commercial or financial relationships that could be construed as a potential conflict of interest.

frontiers in Cardiovascular Medicine

ORIGINAL RESEARCH
published: 11 October 2021
doi: 10.3389/fcvm.2021.732784

Sealing Behavior in Transcatheter Bicuspid and Tricuspid Aortic Valves Replacement Through Patient-Specific Computational Modeling

Xianbao Liu[1†], Jiaqi Fan[1†], Peter Mortier[2], Yuxin He[1], Qifeng Zhu[1], Yuchao Guo[1], Xinping Lin[1], Huajun Li[1], Jubo Jiang[1], Giorgia Rocatello[2], Vanda Oliveira[2], Tim Dezutter[2], Lars Sondergaard[3] and Jian'an Wang[1]*

[1] Department of Cardiology, Second Affiliated Hospital, Zhejiang University School of Medicine, Hangzhou, China, [2] FEops, Ghent, Belgium, [3] Department of Cardiology, Rigshospitalet, Copenhagen, Denmark

OPEN ACCESS

Edited by:
Peter Zilla,
University of Cape Town, South Africa

Reviewed by:
Huseyin Cagatay Yalcin,
Qatar University, Qatar
Philippe Sucosky,
Kennesaw State University,
United States

***Correspondence:**
Jian'an Wang
wangjianan111@zju.edu.cn

[†] These authors have contributed equally to this work

Specialty section:
This article was submitted to Heart Valve Disease, a section of the journal Frontiers in Cardiovascular Medicine

Received: 01 July 2021
Accepted: 13 September 2021
Published: 11 October 2021

Citation:
Liu X, Fan J, Mortier P, He Y, Zhu Q, Guo Y, Lin X, Li H, Jiang J, Rocatello G, Oliveira V, Dezutter T, Sondergaard L and Wang J (2021) Sealing Behavior in Transcatheter Bicuspid and Tricuspid Aortic Valves Replacement Through Patient-Specific Computational Modeling. Front. Cardiovasc. Med. 8:732784. doi: 10.3389/fcvm.2021.732784

Background: Patient-specific computer simulation of transcatheter aortic valve replacement (TAVR) can provide unique insights in device-patient interaction.

Aims: This study was to compare transcatheter aortic valve sealing behavior in patients with bicuspid aortic valves (BAV) and tricuspid aortic valves (TAV) through patient-specific computational modeling.

Methods: Patient-specific computer simulation was retrospectively performed with FEops HEARTguide for TAVR patients. Simulation output was compared with postprocedural computed tomography and echocardiography to validate the accuracy. Skirt malapposition was defined by a distance larger than 1 mm based on the predicted device-patient interaction by quantifying the distance between the transcatheter heart valve (THV) skirt and the surrounding anatomical regions.

Results: In total, 43 patients were included in the study. Predicted and observed THV frame deformation showed good correlation ($R^2 \geq 0.90$) for all analyzed measurements (maximum diameter, minimum diameter, area, and perimeter). The amount of predicted THV skirt malapposition was strongly linked with the echocardiographic grading of paravalvular leakage (PVL). More THV skirt malapposition was observed for BAV cases when compared to TAV cases (22.7 vs. 15.5%, $p < 0.05$). A detailed analysis of skirt malapposition showed a higher degree of malapposition in the interleaflet triangles section for BAV cases as compared to TAV patients (11.1 vs. 5.8%, $p < 0.05$).

Conclusions: Patient-specific computer simulation of TAVR can accurately predict the behavior of the Venus A-valve. BAV patients are associated with more malapposition of the THV skirt as compared to TAV patients, and this is mainly driven by more malapposition in the interleaflet triangle region.

Keywords: transcatheter aortic valve replacement, bicuspid aortic valve, patient-specific computational modeling, sealing behavior, paravalvular leakage

INTRODUCTION

Transcatheter aortic valve replacement (TAVR) in patients with a bicuspid aortic valve (BAV) is becoming increasingly important due to expanding indications which include younger patients, as well as to global adoption. In many countries, TAVR has become the standard of care for high-risk patients, and is now expanding into younger, lower-risk patients, resulting in an increased amount of patients with BAV stenosis (1–4). On the other hand, the Chinese TAVR market is still relatively small but growing rapidly, and the prevalence of BAV cases in China is notably higher than in other countries (5). Several clinical studies have demonstrated the safety and efficacy of TAVR in BAV patients (3, 4), but there are still several challenges when treating BAV stenosis and patients should be carefully selected. Therefore, efforts to increase our knowledge of how TAVR devices interact with BAVs remain important.

The interaction of transcatheter heart valves with the aortic root is likely to be different between BAV and tricuspid aortic valve (TAV) patients. While device sizing for TAV cases is mainly based on the dimensions of the aortic annulus, an assessment of the supra-annular structure seems mandatory for BAV cases as this can be the primary location where the THV interacts with the aortic root (6, 7). This, however, depends on several anatomical factors such as BAV type, calcium burden, raphe length, and the ratio of the intercommissural diameter to the mean annular diameter (7).

Patient-specific computational modeling of TAVR with FEops HEARTguide (FEops, Ghent, Belgium) based on pre-procedural computed tomography (CT) has emerged as a promising technology capable of accurately predicting device-anatomy interaction, as well as paravalvular leakage and the risk on TAVR-induced conduction abnormalities for both TAV and BAV patients (8–12). Validation data are mainly available for the Medtronic self-expanding and the Boston Scientific mechanically expandable THVs. These three-dimensional computer models provide detailed insights that cannot be obtained through post-procedural imaging, and may also help to better understand the sealing behavior in BAV and TAV patients.

In this study, we aimed to validate a patient-specific computer simulation of TAVR in Chinese patients treated with the self-expandable Venus A-valve and use the validated computational model to explore potential differences in the sealing behavior between BAV and TAV patients.

METHODS

A retrospective single-center study was performed on patients who underwent transcatheter aortic valve replacement using a Venus A-valve (Venus Medtech). Both pre- and post-procedural CT imaging was available for all patients. All dual source computed tomography (DSCT) examinations were performed with the second generation dual-source CT (SOMATOM Definition Flash, Siemens Medical Solutions, Germany). The scan area was craniocaudal from the subclavian artery to the iliofemoral branches. Prospective ECG gating with a pitch of 2.4 was performed. Around 60–80 ml of iodine-containing contrast agent (Omnipaque 370 mg I/ml, GE Healthcare, Shanghai, China) was injected with a dual-head power injector (Mallinckrodt, American) at a flow rate of 4 ml/s followed by 60 ml of 0.9% saline solution at the same flow rate. A bolus tracking method was used in the descending aorta with a pre-set threshold of 180 Hounsfield units (HU) to achieve optimal synchronization. The tube voltage was 100 kV, with a reference tube current-time product of 280 mAs and a collimation of 38.4 mm (2*32*0.6 mm^3) with double sampling by a z-axis flying focal spot. All procedures were performed as reported in previous studies (13, 14). The study was approved by the medical ethics committee of Second Affiliated Hospital of Zhejiang University and carried out according to the principles of the Declaration of Helsinki. All patients provided written informed consent for TAVR and the use of anonymous clinical, procedural, and follow-up data for research.

Virtual Device Modeling

Accurate finite element models of the frames of all Venus A-valve sizes (23, 26, 29, and 32 mm) were generated based on CAD (Computer Aided Design) data provided by the device manufacturer. A virtual radial force test was performed to validate the virtual device models using the finite element analysis (FEA) software Abaqus (Abaqus v6.12, Dassault Systèmes, Paris, France). For this test, the device was crimped to a smaller diameter (loading) and then released (unloading) while the radial force in the crimper was measured. The model radial force was then compared with the experimental radial force data during unloading and within the relevant deployment range for each valve size. Model parameters were calibrated until excellent agreement was obtained. A mesh density analysis was performed on the device radial force to determine the optimal number of elements, which is around 4,000 elements for the different device sizes.

Patient-Specific Computational Modeling

Three-dimensional patient-specific geometries of the native aortic root (including the calcified native leaflets) were reconstructed from pre-operative contrast-enhanced CT scans, using the image segmentation software Mimics (Mimics v21.0, Materialise, Leuven, Belgium). The aortic wall and the calcified leaflets are modeled using ∼15,000 and 7,000 elements, respectively. Different material behavior was automatically assigned to the different tissue regions. Linear elastic models rather than more realistic but also more complex hyperelastic anisotropic models were adopted to describe the aortic root tissues. These simplified material models facilitated deriving the material parameters in a previous study with an iterative process of back-calculations using pre- and postoperative MSCT of 39 patients (8). For the aortic wall, an elastic modulus of 2 MPa and a uniform thickness of 2 mm was used, while for the aortic

Abbreviations: AS, aortic stenosis; BAV, bicuspid aortic valve; CAD, computer aided design; CT, computed tomography; FEA, finite element analysis; HU, Hounsfield unit; DSCT, dual source computed tomography; TAV, tricuspid aortic valve; TAVR, transcatheter aortic valve replacement; TTE, transthoracic echocardiography.

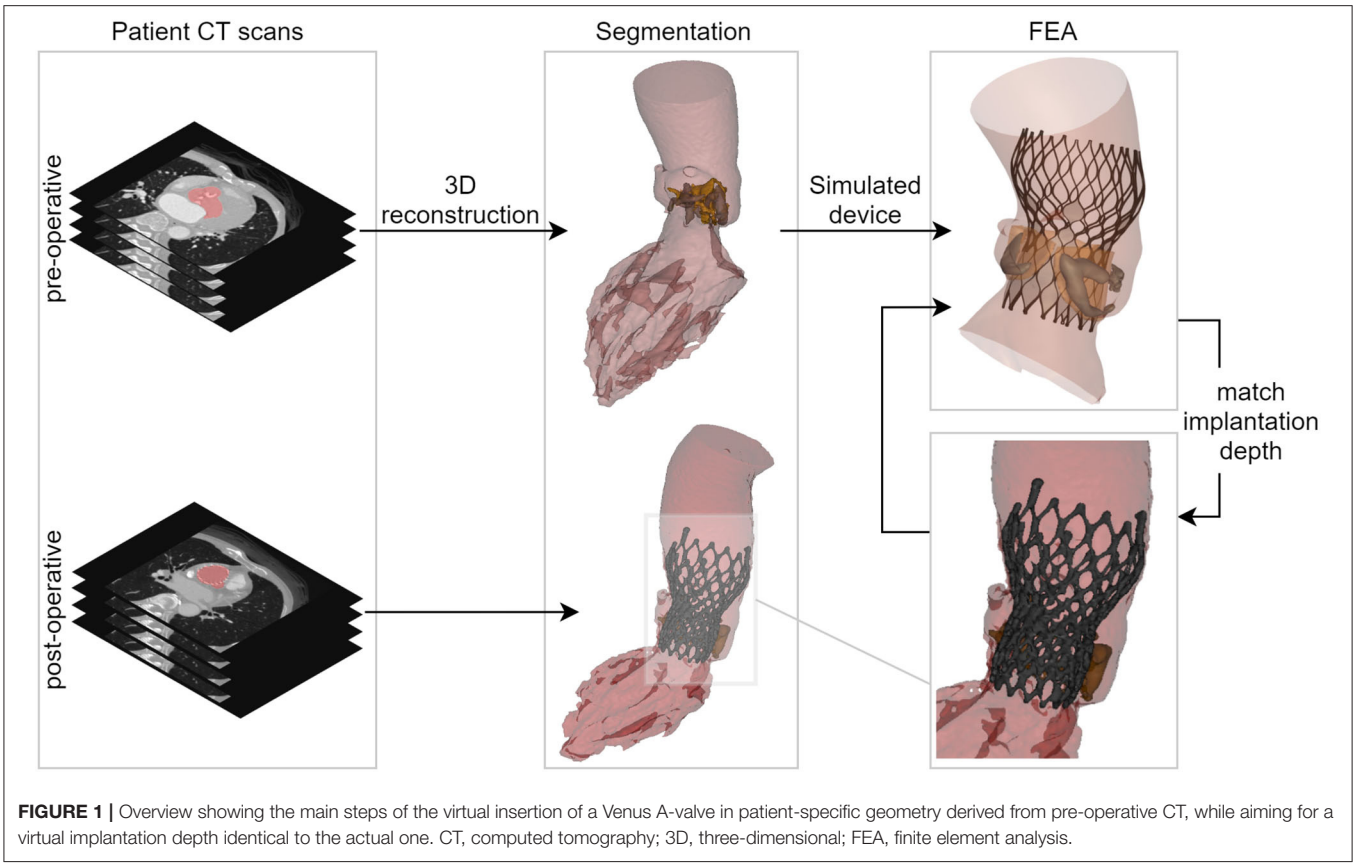

FIGURE 1 | Overview showing the main steps of the virtual insertion of a Venus A-valve in patient-specific geometry derived from pre-operative CT, while aiming for a virtual implantation depth identical to the actual one. CT, computed tomography; 3D, three-dimensional; FEA, finite element analysis.

leaflets, an elastic modulus of 0.6 MPa and uniform thickness of 1.5 mm was adopted. Calcifications were modeled using a stiffer elastic material with perfect plasticity (E = 4 MPa, yield stress = 0.6 MPa).

Venus A-valve models were then virtually deployed in these geometries using Abaqus (v6.12, Dassault Systemes, Simulia Corp, Johnson, RI). These simulations allow us to assess the device, native leaflet, and aortic wall deformation as previously described (8, 10, 11). The simulation strategy consists of a number of steps. The device is first crimped to a small diameter using a cylindrical surface. Then it is positioned nearly co-axially within the aortic root, and deployed by retracting a catheter. The default general contact with finite sliding between all the surfaces was used, assuming a coefficient of friction of 0.7 between the valve frame and the aortic model.

For each simulated implantation, the valve size selection and the depth of implantation were aligned with the clinical procedure. The simulated depth of implantation was iteratively adjusted to match the actual depth of implantation derived from the post-operative geometry, which was reconstructed from post-operative CT images using Mimics. This was done by overlaying the simulation results with the post-operative geometry using a manual geometrical registration method. In case the simulated device position differed from the observed position (post-op MSCT), an additional iteration was performed until a satisfactory match in terms of implantation depth was obtained. An overview of these different reconstruction and modeling steps is summarized in **Figure 1**.

Frame Deformation Comparison

For each patient, predicted frame deformation was both qualitatively and quantitatively compared to the post-operative device deformation (CT). A visual inspection was performed by overlaying the predicted and post-operative devices, and their dimensions (minimum and maximum diameter, perimeter, and area) were quantified at four relevant device levels (**Supplementary Figure 1**): commissures, central coaptation, nadir, and ventricular end (8).

Sealing Analysis

The regions of skirt apposition and malapposition were determined for all patients using the predicted device and aortic root deformation. Apposition was considered when the deformed device skirt was in contact with the anatomy, while malapposition was considered when the opposite was verified. The areas corresponding to the apposed and malapposed skirt were quantified in four different regions of the aortic root anatomy: left ventricular outflow tract (LVOT), leaflets, interleaflet triangles, and ascending aorta.

In order to obtain these regions, the deformation anatomy (after simulated device deployment) was firstly divided into the anatomical sections mentioned above. Then, each element of

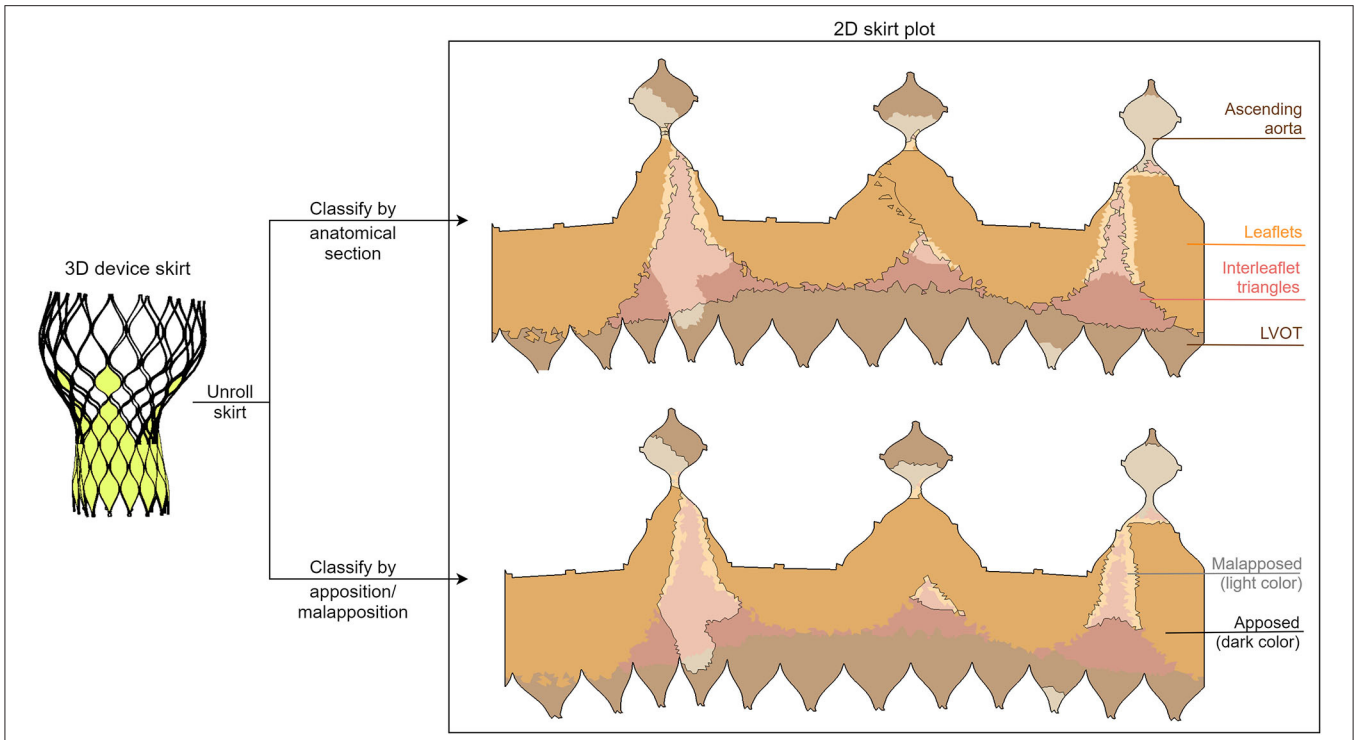

FIGURE 2 | Illustration of the division of the two-dimensional deformed device skirt into anatomical (top) and apposition/malapposition (bottom) sections. This division is evidenced both with a border line and with a color palette, as depicted in the legend.

the simulated skirt was attributed to one of these anatomical regions and the distance between the skirt and the anatomy was calculated. This was done by searching the anatomy element in the normal direction to each skirt element. Apposition and malapposition were then attributed to each element based on the distance (apposed if the distance was smaller than 1 mm, malapposed otherwise). Finally, the skirt was projected in 2D and the apposed and malapposed areas were computed for each anatomical section. A visual overview of the separation of the skirt into sections (both anatomical and apposition) is shown in **Figure 2**. The obtained area values were grouped according to the aortic valve morphology: tricuspid (TAV), bicuspid (all types, BAV), bicuspid type 0 (BAV0), and BAV type 1 (BAV1) using the Sievers classification (15).

PVL Comparison

Transthoracic Doppler echocardiography was used for the clinical PVL assessment. PVL was classified as none or trace, mild, or moderate based on the VARC-2 criteria. Observed PVL grades were compared to the predicted amount of skirt malapposition. The grades were also divided per valve morphology to detect possible patterns between the PVL severity and valve morphology.

Statistical Analysis

Continuous variables are expressed as mean ± SD. Correlation between predicted and observed continuous variables was analyzed using the coefficient of determination (R^2). Comparisons within the sealing analysis were carried out using the paired Student t-test or Mann–Whitney U-test depending on the variable distribution. Baseline characteristics and anatomic parameters were analyzed to explore the association with malapposition in interleaflet triangles. Only variables yielding a p-value < 0.1 were included in the stepwise multivariate linear regression analysis. Statistical significance was defined as a two-tailed $p < 0.05$. Statistical analysis was performed with SciPy Stats, a Python module for probability functions and statistical distributions.

RESULTS

A total of 43 patients were included in the study. There was no significant difference in age between BAV and TAV patients (BAV: 76.4 ± 7.1 years old vs. TAV: 79.4 ± 6.2 years old, $p = 0.164$) or other baseline characteristics (**Table 1**). Of these 43 patients, 26 patients were BAV patients of which 11 patients were type 0 and 15 were type 1. For the BAV patients, the sizing index (ratio of device size to perimeter-derived diameter) was lower when compared with TAV patients (BAV: 1.04 ± 0.09 vs. TAV: 1.11 ± 0.07, $p = 0.018$).

Comparison of Observed and Predicted Parameters

The mean differences and coefficients of determination between the measurements extracted from the post-operative and simulated device are summarized in **Table 2**. This is presented

TABLE 1 | Patient characteristics.

	BAV type 0	BAV type 1	BAV	TAV	
	***n* = 11**	***n* = 15**	***n* = 26**	***n* = 17**	***p*-value**
Age (yrs)	77.8 ± 5.6	75.4 ± 8.1	76.4 ± 7.1	79.4 ± 6.2	0.164
Male	5 (45.5)	12 (80.0)	17 (65.4)	9 (52.9)	0.528
Height (cm)	159.1 ± 6.5	165.7 ± 6.5	162.9 ± 7.2	162.2 ± 8.8	0.780
Weight (kg)	59.0 ± 8.0	64.9 ± 9.4	62.4 ± 9.1	60.4 ± 11.8	0.544
Body Mass Index (kg/m^2)	23.31 ± 3.01	23.59 ± 2.94	23.47 ± 2.91	22.85 ± 3.59	0.542
STS	5.29 ± 3.12	5.15 ± 2.56	5.21 ± 2.75	8.33 ± 5.95	0.124*
Echocardiography					
Left ventricular ejection fraction (%)	54.9 ± 14.9	55.0 ± 12.7	55.0 ± 13.3	54.8 ± 17.3	0.593*
Aortic valve area (cm^2)	0.53 ± 0.21	0.66 ± 0.15	0.60 ± 0.19	0.62 ± 0.21	0.726
Mean gradient (mmHg)	59.4 ± 19.4	56.5 ± 15.2	57.7 ± 16.8	52.9 ± 11.5	0.478*
Max velocity (m/s)	4.98 ± 0.90	4.67 ± 0.94	4.80 ± 0.92	4.70 ± 0.42	0.526*
Multi-slice computed tomography					
Max annulus diameter (mm)	27.4 ± 3.5	29.6 ± 3.0	28.7 ± 3.4	27.4 ± 3.2	0.240
Min annulus diameter (mm)	21.7 ± 3.5	22.7 ± 3.4	22.3 ± 3.4	21.1 ± 2.3	0.209
Mean annulus diameter (mm)	24.5 ± 3.4	26.2 ± 3.1	25.5 ± 3.3	24.3 ± 2.7	0.212
Perimeter derived diameter (mm)	24.7 ± 3.3	26.5 ± 3.1	25.8 ± 3.3	24.7 ± 3.0	0.312
Area derived diameter (mm)	24.3 ± 3.3	26.0 ± 3.1	25.3 ± 3.2	24.2 ± 2.9	0.285
Calcium volume (mm^3)	1210.7 ± 778.0	1213.5 ± 676.6	1212.4 ± 701.6	781.8 ± 576.6	0.094
Procedural characteristics					
Implanted depth (mm)	6.2 ± 3.3	6.1 ± 4.2	6.1 ± 3.7	7.4 ± 3.1	0.236
Device size					0.586
23 mm	3 (27.3)	1 (6.7)	4 (15.4)	1 (5.9)	
26 mm	7 (63.6)	8 (53.3)	15 (57.7)	11 (64.7)	
29 mm	0 (0.0)	5 (33.3)	5 (19.2)	2 (11.8)	
32 mm	1 (9.1)	1 (6.7)	2 (7.7)	3 (17.6)	
Sizing index§	1.05 ± 0.11	1.03 ± 0.09	1.04 ± 0.09	1.11 ± 0.07	0.018
Post-procedural outcomes					
Mortality	0 (0.0)	0 (0.0)	0 (0.0)	0 (0.0)	–
Stroke	0 (0.0)	0 (0.0)	0 (0.0)	0 (0.0)	–
MI	0 (0.0)	0 (0.0)	0 (0.0)	0 (0.0)	–
PVL III/IV	3 (27.3)	2 (13.3)	5 (19.2)	1 (5.9)	0.376
Pacemaker implantation	1 (9.1)	1 (6.7)	2 (7.7)	2 (11.8)	1.000

§*Sizing index, (device size)/(perimeter-based diameter).*

**Mann-Whitney U-test was used.*

Data are presented as no. (%) and mean ± SD.

BAV, bicuspid aortic valve; MI, myocardial infarction; PVL, paravalvular leakage; TAV, tricuspid aortic valve.

for each type of measurement for all levels of the device combined. A high coefficient of determination was obtained for all measurements ($\geq$0.90). All dimensions were slightly underestimated by the model, but the mean differences are negligible. Correlation and difference plots for each type of measurement are presented in **Figures 3A,B**.

Echocardiography showed none or trace post-operative PVL in 13 patients, mild PVL in 24, and moderate PVL in 6. **Figure 4** shows a comparison of predicted skirt malapposition for patients with none to trace, mild, and moderate PVL. The amount of skirt malapposition is higher for patients with a higher degree of clinically assessed PVL (**Supplementary Table 1**).

A comparison of post-operative PVL assessment for patients with different valve morphologies is shown in **Figure 5**. Moderate PVL was more frequent for BAV cases (19.2 vs. TAV 5.9%), with BAV0 having the highest incidence of moderate PVL (27.3% for BAV0 vs. 13.3% for BAV1, respectively).

TABLE 2 | Mean (±SD) difference between the measurements of the observed (post-operative) and simulated (model) devices and respective R-squared coefficient for the different levels of the devices.

Measurement	Mean difference (Post-op - Model)	R^2
Dmax (mm)	0.10 ± 1.42	0.90
Dmin (mm)	0.06 ± 1.55	0.90
Perimeter (mm)	0.34 ± 3.25	0.95
Area (mm^2)	0.96 ± 41.14	0.96

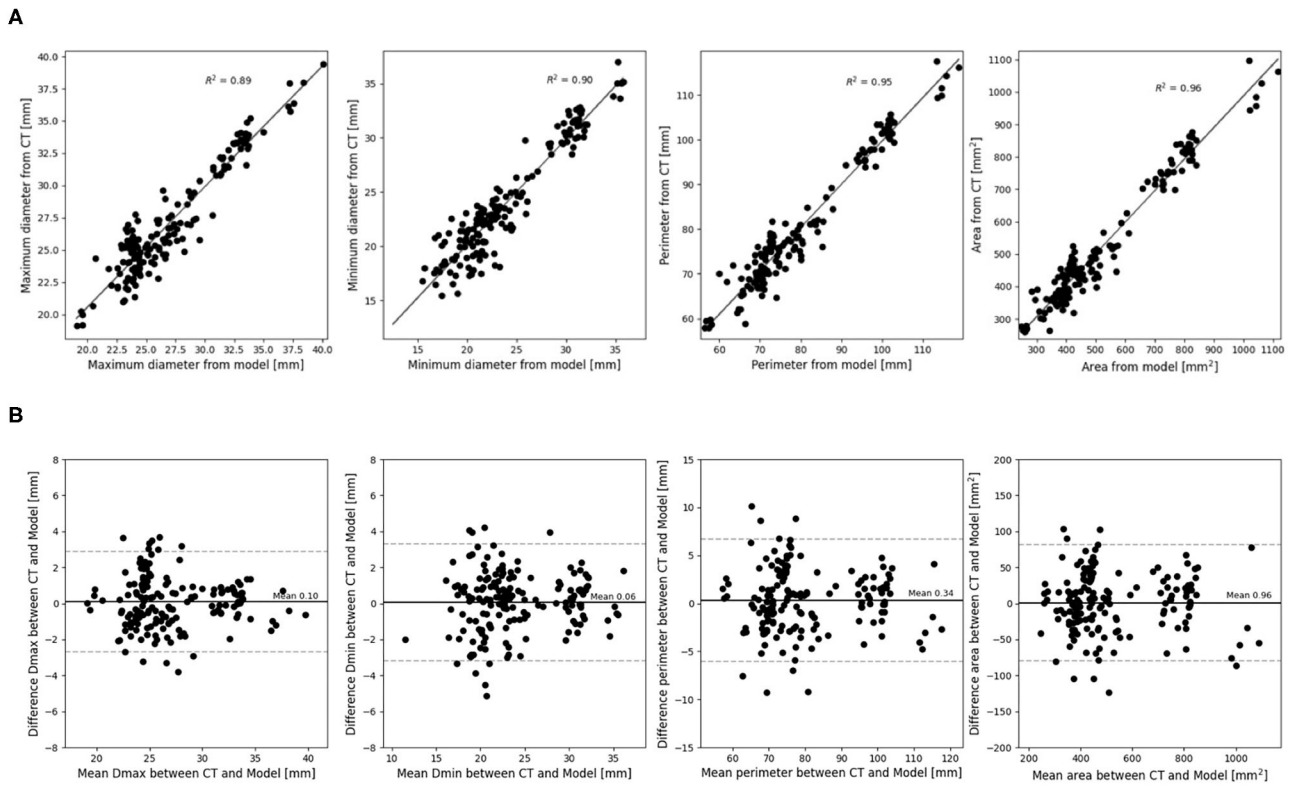

FIGURE 3 | (A) Correlation and **(B)** difference plots for obtained device measurements vs. predicted device measurements for all device levels.

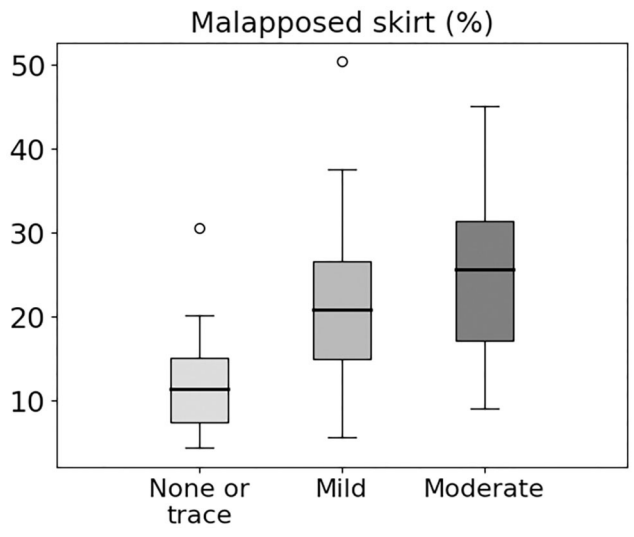

FIGURE 4 | Box and whiskers diagram showing predicted skirt malapposition for patients with none or trace, mild, and moderate PVL. Extreme values are presented as small circles (o).

Comparison of Sealing Behavior

Representative TAV (total skirt malapposition of 4.4%, no PVL) and BAV1 (total skirt malapposition of 20.9%, mild PVL) cases are depicted in **Figure 6**. A cross-section of the pre-operative CT scan at the aortic annular plane and a 3D reconstruction illustrate the morphology of the valves. For each valve, the 2D skirt is also shown with the apposition borders highlighted, evidencing the larger area of malapposition in the BAV1 case (relatively to TAV). For the BAV1 case, PVL channels are visible in the interleaflet triangles region.

An overview of all sealing analysis data for each valve morphology is provided in **Table 3**. The mean percentage of total skirt malapposition obtained for each anatomical section (LVOT, interleaflet triangles and leaflets) relatively to the total skirt is illustrated as bar plots for the different valve morphologies in **Figure 7A**. In this analysis, the values obtained for the ascending aorta section were not considered to simplify the analysis. More malapposition was obtained for BAV cases when compared to TAV cases (22.7 vs. 15.5%, $p < 0.05$), and this is also true when comparing TAV cases to BAV type 0 and BAV type 1 cases separately. This seems mainly driven by a higher degree of malapposition in the interleaflet triangles section: 5.8 and 11.1% for TAV and BAV ($p < 0.05$), respectively.

The percentage of apposed skirt obtained out of the apposed section of the total skirt is illustrated as pie charts for each anatomical section and valve morphology in **Figure 7B**. There is a trend for a higher contribution of the left ventricular outflow tract (LVOT) to the apposition in TAV (17.0%) as compared to BAV cases (11.7%), and this difference is most pronounced

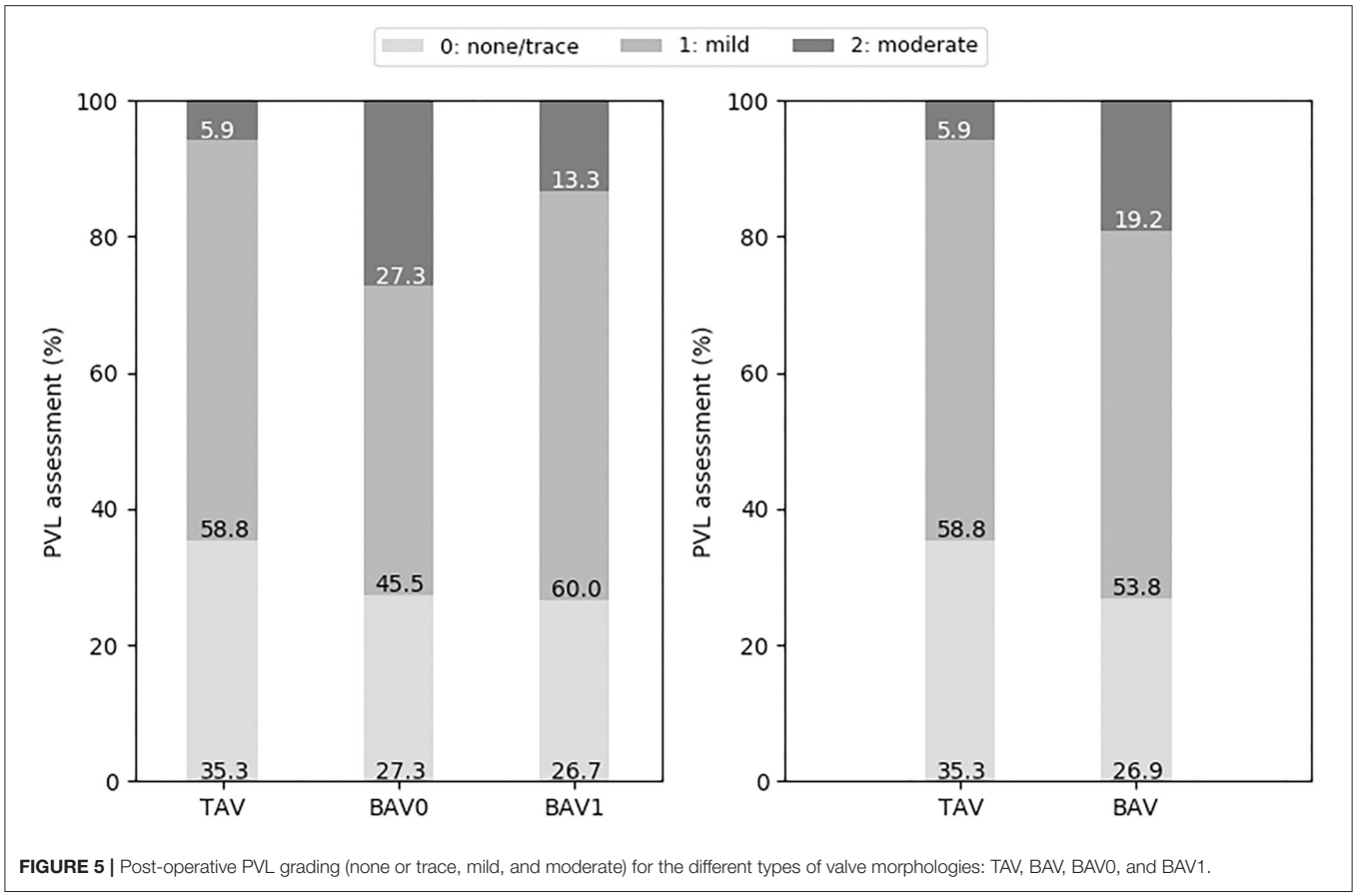

FIGURE 5 | Post-operative PVL grading (none or trace, mild, and moderate) for the different types of valve morphologies: TAV, BAV, BAV0, and BAV1.

for BAV type 0 patients (8.4%). In contrast, the leaflets seem to contribute more to apposition in BAV (73.6%) than in TAV cases (64.8%), and this is also true when looking at BAV type 0 and type 1 separately. However, no statistical significance was observed for these comparisons.

The multivariate linear regression analysis identified BAV ($p = 0.009$) and the sizing index ($p = 0.034$) as two independent predictors of malapposition in interleaflet triangles. The results of univariate and multivariate linear regression for association with malapposition in interleaflet triangles are presented in **Supplementary Table 2**.

DISCUSSION

In this study, we evaluated a patient-specific computer model of TAVR in Chinese BAV and TAV patients with the self-expanding Venus A-valve using FEops HEARTguide (FEops, Ghent, Belgium). We compared the predicted THV frame deformation with postprocedural CT and found excellent correlation. Moreover, we observed a good agreement between predicted THV skirt malapposition and postoperative PVL based on echocardiography. Finally, we conducted a detailed sealing analysis and found that more malapposition was obtained in BAV patients when compared to TAV patients which was mainly driven by more malapposition at the location of the interleaflet triangles. Interestingly, the leaflets seem to be the main contributor to device sealing (apposition) not only in BAV but also in TAV cases.

Validation of the Modeling

Patient-specific computer simulation of TAVR has been previously described and validated, not only in TAV patients but also in BAV cases (FEops, Ghent, Belgium) (8–12). These previous studies showed that computer simulation can accurately predict the THV frame deformation, severity of PVL, and potential occurrence of conduction abnormalities. However, these studies primarily focused on the Medtronic self-expanding and the Boston Scientific mechanically expandable THVs, and were all conducted by European hospitals. In this study, we employed the patient-specific computer simulation for the first time in a Chinese patient population with the self-expanding Venus A-valve. Despite the higher radial force of the Venus A-valve and the high calcium burden in this Chinese population, an excellent agreement between the predicted and observed dimensions of the valve frame was obtained (5, 16). Moreover, we compared predicted THV skirt malapposition and clinically assessed PVL, and found a good relationship.

These validated patient-specific computer simulations may help clinicians to better understand the risk of the procedure, and to optimize device sizing and positioning for each individual. This useful tool can also assist physicians recognizing patients

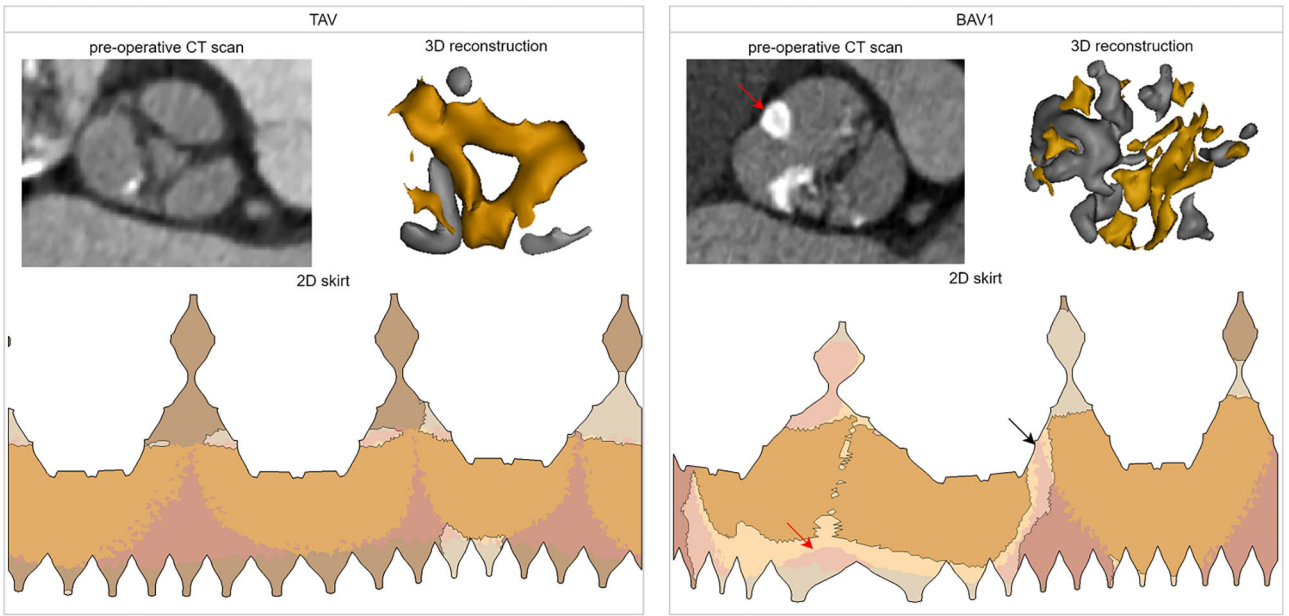

FIGURE 6 | Analysis of two cases of the cohort with different valve morphologies: TAV (total skirt malapposition of 4.4%, PVL grade 0) and BAV1 (total skirt malapposition of 20.9%, PVL grade 1). For each case, the following is shown: cross-section at the aortic annular plane in the pre-operative CT, three-dimensional reconstruction of the valve (and its calcifications), and distribution of the apposition/malapposition sections of the two-dimensional deformed device skirt. For the BAV1 case, the red arrow indicates the raphe and the black arrow the largest PVL channel. CT, computed tomography; 3D, three-dimensional; 2D, two-dimensional.

TABLE 3 | Overview of sealing analysis data for the different valve morphologies.

	BAV type 0	BAV type 1	BAV	TAV	
	***n* = 11**	***n* = 15**	***n* = 26**	***n* = 17**	***p*-value**
LVOT					
Apposed area (mm^2)	72.4 ± 68.4	133.1 ± 190.4	107.4 ± 152.0	157.4 ± 135.7	0.106*
Malapposed area (mm^2)	47.8 ± 87.0	81.6 ± 126.4	67.3 ± 110.7	52.0 ± 79.9	0.980*
Interleaflet triangles					
Apposed area (mm^2)	146.4 ± 95.2	123.8 ± 75.5	133.4 ± 83.4	175.1 ± 73.4	0.100
Malapposed area (mm^2)	146.1 ± 60.1	100.5 ± 45.7	119.8 ± 56.1	65.5 ± 36.4	0.001
Leaflets					
Apposed area (mm^2)	590.6 ± 84.2	628.3 ± 191.8	612.4 ± 154.3	611.5 ± 193.6	0.987
Malapposed area (mm^2)	69.1 ± 52.0	73.8 ± 30.6	71.8 ± 40.1	56.8 ± 30.1	0.195
Malapposition in total skirt (%)	24.1 ± 10.6	21.6 ± 10.5	22.7 ± 10.5	15.5 ± 9.8	0.030
Malapposition in LVOT (%)	3.6 ± 5.4	6.0 ± 8.2	4.9 ± 7.1	4.6 ± 7.1	0.960*
Malapposition in Interleaflet triangles (%)	14.0 ± 6.4	9.0 ± 4.0	11.1 ± 5.7	5.8 ± 2.8	0.001*
Malapposition in Leaflet (%)	6.5 ± 4.9	6.7 ± 3.1	6.6 ± 3.8	5.2 ± 2.9	0.200
Apposition in total skirt (%)	75.9 ± 10.6	78.4 ± 10.6	77.3 ± 10.5	84.5 ± 9.8	0.030
Apposition contribution LVOT (%)	8.4 ± 7.9	14.2 ± 19.8	11.7 ± 15.9	17.0 ± 16.0	0.124*
Apposition contribution Interleaflet triangles (%)	16.8 ± 8.7	13.1 ± 7.0	14.7 ± 7.9	18.0 ± 4.9	0.172*
Apposition contribution Leaflet (%)	74.8 ± 14.0	72.7 ± 20.0	73.6 ± 17.4	64.9 ± 17.6	0.120

**Mann-Whitney U-test was used.*
Data are presented as mean ± SD.
BAV, bicuspid aortic valve; LVOT, left ventricular outflow tract; TAV, tricuspid aortic valve.

who would benefit from TAVR and other patients for whom SAVR may be the preferred treatment. TAVR in mainland China is rapidly evolving, and the most widely used commercial THV is currently the Venus A-valve (17, 18). Therefore, the presented study may be an important step to bring this technology to Chinese physicians.

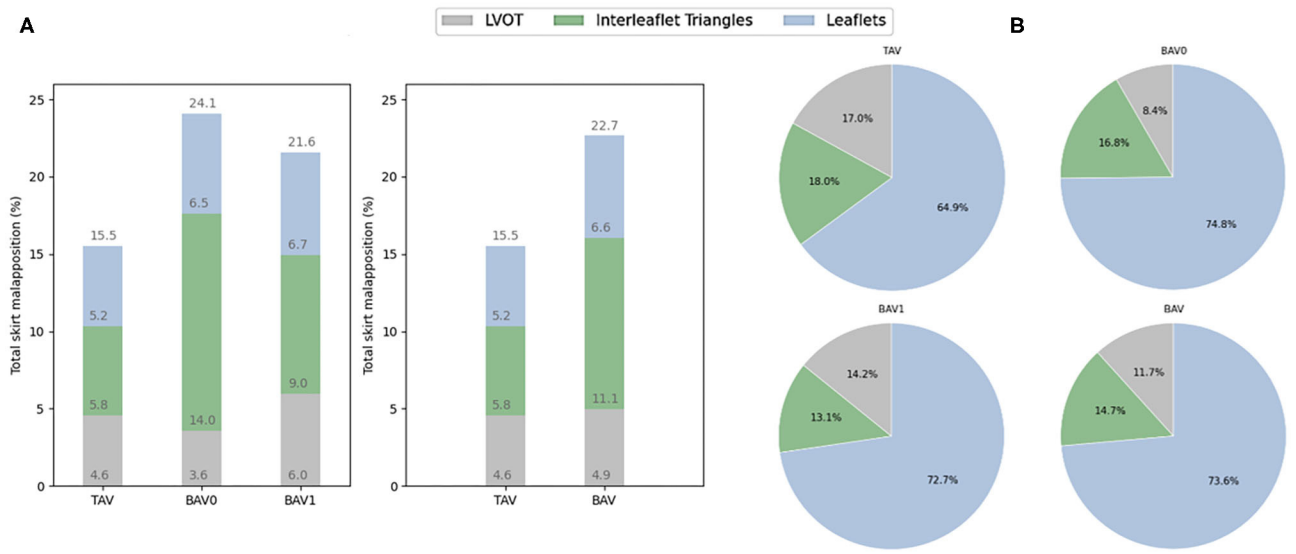

FIGURE 7 | (A) Contribution of each anatomical section to the malapposition (mean, %) of the total skirt. **(B)** Contribution of each anatomical section to the apposition (mean, %) for the apposed section of the skirt. All these values are presented for the different types of valve morphologies: TAV, BAV, BAV0, and BAV1. TAV, tricuspid aortic valve; BAV, bicuspid aortic valve; BAV0, type 0 bicuspid aortic valve; BAV1, type 1 bicuspid aortic valve.

Sealing Behavior in BAV and TAV Patients

TAVR in BAV patients has proven to be safe and effective, but patients need to be selected carefully and a widely accepted THV sizing strategy is still lacking. One key challenge of BAV disease is the increased anatomical heterogeneity as compared to TAV disease. In addition, there are important ethnic differences. In European populations, BAV type 1 with L-R coronary cusp fusion is most common, while in Asian populations, an unexpected high prevalence of type 0 was found (19, 20). As the deformed device skirt mainly interacts with three different regions of the aortic root anatomy, LVOT, leaflets, and interleaflet triangles, we performed a detailed analysis of the sealing behavior in these anatomical regions in BAV and TAV patients.

In the presented study, we found more malapposition in BAV patients when compared to TAV patients which was mainly driven by more malapposition in the interleaflet triangles. It should be emphasized that the pathologic landmark of BAV is always an absent or underdeveloped interleaflet triangle: a dysmorphic, underdeveloped interleaflet triangle is usually accompanied by a raphe, while the type 0 BAV is a valve with complete absence of one interleaflet triangle (21). Another factor is that TAVR in BAV might result in uneven bioprosthetic valve frame expansion after THV deployment, and the deformed device (skirt) may not touch the interleaflet triangle under the restricted stent-frame expansion (19, 22–24). This may explain the higher amount of malapposition that we observed in the interleaflet triangle region in type 0 and type 1 BAV cases compared with TAV.

Another finding is that the leaflets seem to be the main contributor to device sealing, not only in BAV but also in TAV cases. The importance of the interaction between the supra annular structure and THV has already been discussed in previous studies (7, 14, 25–27). Our present study based on patient-specific computer simulation further clarifies the crucial contribution of the leaflets to supra-annular sealing. Overall, these results confirm that an assessment of the supra-annular structure is important for the adequate planning of TAVR in BAV cases.

Moreover, in our present study, we found a trend for a higher contribution of the LVOT to the apposition in TAV as compared to BAV cases, and this difference was most pronounced for BAV type 0 patients. This result may be partially explained by the depth of implantation. As described in the baseline characteristics, BAV type 0 patients had a tendency of higher implantation than TAV. In addition, for BAV type 0 patients, the fish mouth-like shape of the valve may result in an under expansion of the THV frame in the annular and sub-annular (LVOT) region, and thus reduce the device-tissue interaction in this region.

Malapposition and PVL

The presented sealing analysis based on computational modeling may reflect the risk of PVL after TAVR. As showed in **Figure 4**, a higher amount of malapposition seems related to the echo-based PVL grading. In addition, we observed a higher prevalence of moderate echocardiographic-identified PVL in the BAV group which might be explained by the observed difference in sealing behavior between BAV and TAV cases. Understanding the sealing behavior of TAVR in BAV and TAV patients could assist physicians to comprehensively assess the risk of PVL and evaluate the interaction between supra-annular structure and THV stent frame.

LIMITATIONS

This study was a small and retrospective single-center study. Due to the low number of patients with more than moderate PVL, no formal statistical analysis was performed. More cases should be included to assess the sealing behavior on different leaflet fusion patterns. As a retrospective study, transthoracic echocardiography was used to assess the clinical PVL, and the location of PVL could not be evaluated due to the limitation of imaging quality.

CONCLUSIONS

Patient-specific computer simulation of TAVR can be used in Chinese patients with the self-expanding Venus A-valve. Transcatheter aortic valve sealing behavior is different between BAV and TAV patients with more malapposition at the location of the interleaflet triangles section for BAV cases.

IMPACT ON DAILY PRACTICE

BAV patients are associated with more malapposition of the transcatheter heart valve (THV) skirt as compared to TAV patients, and this is mainly driven by more malapposition in the interleaflet triangle region. More cases and studies are needed to confirm the results and related malapposition of the THV skirt to clinical echo-based paravalvular leakage grading. Patient-specific computational modeling of TAVR based on pre-procedural CT might be performed in BAV patients. Transcatheter heart valve size and ideal implanted depth could be recommended to reduce the malapposition and potential paravalvular leakage.

DATA AVAILABILITY STATEMENT

The data analyzed in this study is subject to the following licenses/restrictions: dataset can only be accessed after getting permission. Requests to access these datasets should be directed to jqfan@zju.edu.cn.

ETHICS STATEMENT

The studies involving human participants were reviewed and approved by the Medical Ethics Committee of Second Affiliated Hospital of Zhejiang University. The patients/participants provided their written informed consent to participate in this study. Written informed consent was obtained from the individual(s) for the publication of any potentially identifiable images or data included in this article.

AUTHOR CONTRIBUTIONS

JW, XLiu, and JF design the study. XLiu, JF, YH, QZ, YG, XLin, HL, and JJ conducted the study and performed the examinations. PM, GR, VO, TD, and JF performed the patient-specific computer simulation and statistical analysis. JF and PM performed the statistical analysis and wrote the manuscript. JW, LS, and PM revised the manuscript. All authors have read and approved the final version of the manuscript.

FUNDING

This study was part of a project that has received funding from the European Union's Horizon 2020 research and innovation program of Europe (No. 945698) and Zhejiang Province Science and Technology Department Key R&D Program of China (No. 2021C03097).

SUPPLEMENTARY MATERIAL

The Supplementary Material for this article can be found online at: https://www.frontiersin.org/articles/10.3389/fcvm.2021.732784/full#supplementary-material

REFERENCES

1. Popma JJ, Deeb GM, Yakubov SJ, Mumtaz M, Hemal Gada MD, O'Hair D, et al. Transcatheter aortic-valve replacement with a self-expanding valve in low-risk patients. *N Engl J Med.* (2019) 380:1706–15. doi: 10.1056/NEJMoa1816885
2. Mack MJ, Leon MB, Thourani VH, Makkar R, Kodali SK, Russo M, et al. Transcatheter aortic-valve replacement with a balloon-expandable valve in low-risk patients. *N Engl J Med.* (2019) 380:1695–705. doi: 10.1056/NEJMoa1814052
3. Makkar RR, Yoon S-H, Leon MB, Chakravarty T, Rinaldi M, Shah PB, et al. Association between transcatheter aortic valve replacement for bicuspid vs tricuspid aortic stenosis and mortality or stroke. *JAMA.* (2019) 321:2193–202. doi: 10.1001/jama.2019.7108
4. Yoon S, Bleiziffer S, Backer O De, Delgado V, Arai T, Ziegelmueller J, et al. Outcomes in transcatheter aortic valve replacement for bicuspid versus tricuspid aortic valve stenosis. *J Am Coll Cardiol.* (2017) 69:2579–89. doi: 10.1016/j.jacc.2017.10.006
5. Jilaihawi H, Wu Y, Yang Y, Xu L, Chen M, Wang J, et al. Morphological characteristics of severe aortic stenosis in China: imaging corelab observations from the first Chinese transcatheter aortic valve trial. *Catheter Cardiovasc Interv.* (2015) 85:752–61. doi: 10.1002/ccd.25863
6. Fan J, Fang X, Liu C, Zhu G, Hou CR, Jiang J, et al. Brain injury after transcatheter replacement of bicuspid versus tricuspid aortic valves. *J Am Coll Cardiol.* (2020) 76:2579–90. doi: 10.1016/j.jacc.2020.09.605
7. Tchetche D, De Biase C, Van Gils L, Parma R, Ochala A, Lefevre T, et al. Bicuspid aortic valve anatomy and relationship with devices: the Bavard multicenter Registry: a European picture of contemporary multidetector computed tomography sizing for bicuspid valves. *Circ Cardiovasc Interv.* (2019) 12:1–10. doi: 10.1161/CIRCINTERVENTIONS.118.007107
8. Schultz C, Rodriguez-Olivares R, Bosmans J, Lefèvre T, De Santis G, Bruining N, et al. Patient-specific image-based computer simulation for the prediction of valve morphology and calcium displacement after TAVI with the Medtronic CoreValve and the Edwards SAPIEN valve. *EuroIntervention.* (2016) 11:1044–52. doi: 10.4244/EIJV11I9A212
9. De Jaegere P, De Santis G, Rodriguez-Olivares R, Bosmans J, Bruining N, Dezutter T, et al. Patient-specific computer modeling to predict aortic regurgitation after transcatheter aortic valve replacement. *JACC Cardiovasc Interv.* (2016) 9:508–12. doi: 10.1016/j.jcin.2016.01.003
10. Rocatello G, El Faquir N, De Santis G, Iannaccone F, Bosmans J, De Backer O, et al. Patient-specific computer simulation to elucidate the role of contact

pressure in the development of new conduction abnormalities after catheter-based implantation of a self-expanding aortic valve. *Circ Cardiovasc Interv.* (2018) 11:e005344. doi: 10.1161/CIRCINTERVENTIONS.117.005344
11. Dowling C, Bavo AM, El Faquir N, Mortier P, De Jaegere P, De Backer O, et al. Patient-specific computer simulation of transcatheter aortic valve replacement in bicuspid aortic valve morphology. *Circ Cardiovasc Imaging.* (2019) 12:1–10. doi: 10.1161/CIRCIMAGING.119.009178
12. Dowling C, Firoozi S, Brecker SJ. First-in-human experience with patient-specific computer simulation of TAVR in bicuspid aortic valve morphology. *JACC Cardiovasc Interv.* (2020) 13:184–92. doi: 10.1016/j.jcin.2019.07.032
13. Liu XB, Jiang JB, Zhou QJ, Pu ZX, He W, Dong AQ, et al. Evaluation of the safety and efficacy of transcatheter aortic valve implantation in patients with a severe stenotic bicuspid aortic valve in a Chinese population. *J Zhejiang Univ Sci B.* (2015) 16:208–14. doi: 10.1631/jzus.B1500017
14. Liu X, He Y, Zhu Q, Gao F, He W, Yu L, et al. Supra-annular structure assessment for self-expanding transcatheter heart valve size selection in patients with bicuspid aortic valve. *Catheter Cardiovasc Interv.* (2018) 91:986–94. doi: 10.1002/ccd.27467
15. Sievers HH, Schmidtke C. A classification system for the bicuspid aortic valve from 304 surgical specimens. *J Thorac Cardiovasc Surg.* (2007) 133:1226–33. doi: 10.1016/j.jtcvs.2007.01.039
16. Liao YB, Zhao ZG, Wei X, Xu YN, Zuo ZL, Li YJ, et al. Transcatheter aortic valve implantation with the self-expandable venus A-Valve and CoreValve devices: preliminary experiences in China. *Catheter Cardiovasc Interv.* (2017) 89:528–33. doi: 10.1002/ccd.26912
17. Song G, Pan W, Zhou D, Wu Y. 2019 China structure week: a novel 5G internet-based training course for Structural Heart Disease is presented from China. *Eur Heart J.* (2020) 41:1325–7. doi: 10.1093/eurheartj/ehaa148
18. Hon JKF, Tay E. Transcatheter aortic valve implantation in Asia. *Ann Cardiothorac Surg.* (2017) 6:504–9. doi: 10.21037/acs.2017.08.05
19. Jilaihawi H, Chen M, Webb J, Himbert D, Ruiz CE, Rodés-cabau J, et al. A bicuspid aortic valve imaging classification for the TAVR Era A bicuspid aortic valve imaging classification for the TAVR era. *JACC Cardiovasc Imaging.* (2017) 9:1145–58. doi: 10.1016/j.jcmg.2015.12.022
20. Kong WKF, Delgado V, Poh KK, Regeer M V., Ng ACT, McCormack L, et al. Prognostic implications of raphe in bicuspid aortic valve anatomy. *JAMA Cardiol.* (2017) 2:285. doi: 10.1001/jamacardio.2016.5228
21. Amoretti F, Cerillo AG, Mariani M, Stefano P. A simple method to visualize the bicuspid aortic valve pathology by cardiac computed tomography. *J Cardiovasc Comput Tomogr.* (2020) 14:195–8. doi: 10.1016/j.jcct.2019.08.005
22. Rahhab Z, El Faquir N, Tchetche D, Delgado V, Kodali S, Mara Vollema E, et al. Expanding the indications for transcatheter aortic valve implantation. *Nat Rev Cardiol.* (2020) 17:75–84. doi: 10.1038/s41569-019-0254-6
23. Rotman OM, Bianchi M, Ghosh RP, Kovarovic B, Bluestein D. Principles of TAVR valve design, modelling, and testing. *Expert Rev Med Dev.* (2018) 15:771–91. doi: 10.1080/17434440.2018.1536427
24. Kamioka N, Lederman RJ, Khan JM, Lerakis S, Yousef A, Gleason PT, et al. BI-SILICA during transcatheter aortic valve replacement for noncalcific aortic insufficiency. *JACC Cardiovasc Interv.* (2018) 11:2237–9. doi: 10.1016/j.jcin.2018.08.015
25. Xiong TY, Li YJ, Feng Y, Liao YB, Zhao ZG, Mylotte D, et al. Understanding the interaction between transcatheter aortic valve prostheses and supra-annular structures from post-implant stent geometry. *JACC Cardiovasc Interv.* (2019) 12:1164–71. doi: 10.1016/j.jcin.2019.02.051
26. Jeger R, Reuthebuch O, Fahrni G, Laborde JC, Vogel R, Kaiser C. Supra-annular sizing for transcatheter valve implantation in bicuspid aortic stenosis. *Postep w Kardiol Interwencyjnej.* (2018) 14:187–90. doi: 10.5114/aic.2018.76411
27. Iannopollo G, Romano V, Buzzatti N, De Backer O, Søndergaard L, Merkely B, et al. A novel supra-annular plane to predict TAVI prosthesis anchoring in raphe-type bicuspid aortic valve disease: the LIRA plane. *EuroIntervention.* (2020) 16:259–61. doi: 10.4244/EIJ-D-19-00951

Conflict of Interest: This study received funding from Venus Medtech. The funder was not involved in the study design, collection, analysis, interpretation of data, the writing of this article, or the decision to submit it for publication.

The authors declare that the research was conducted in the absence of any commercial or financial relationships that could be construed as a potential conflict of interest.

frontiers in Cardiovascular Medicine

PERSPECTIVE
published: 02 November 2021
doi: 10.3389/fcvm.2021.740745

Societies of Futures Past: Examining the History and Potential of International Society Collaborations in Addressing the Burden of Rheumatic Heart Disease in the Developing World

Zachary Obinna Enumah[1], Percy Boateng[1], Ralph Morton Bolman[1,2], Friedhelm Beyersdorf[1,3,4], Liesl Zühlke[5,6,7,8], Maurice Musoni[9], Adriano Tivane[10] and Peter Zilla[1]**

[1] Cardiac Surgery Intersociety Alliance, Cape Town, South Africa, [2] University of Minnesota, Minneapolis, MN, United States, [3] Department of Cardiovascular Surgery, University Hospital Freiburg, Freiburg im Breisgau, Germany, [4] Faculty of Medicine, Albert-Ludwigs-University Freiburg, Freiburg im Breisgau, Germany, [5] Division of Paediatric Cardiology, Department of Paediatrics and Child Health, Red Cross War Memorial Children's Hospital, University of Cape Town, Cape Town, South Africa, [6] Division of Cardiology, Department of Medicine, Groote Schuur Hospital, University of Cape Town, Cape Town, South Africa, [7] Cape Heart Institute (CHI), Faculty of Health Sciences, University of Cape Town, Cape Town, South Africa, [8] Faculty of Health Sciences, Institute of Infectious Disease and Molecular Medicine (IDM), University of Cape Town, Cape Town, South Africa, [9] King Faisal Hospital Kigali, Kigali, Rwanda, [10] Hospital Central Maputo, Maputo, Mozambique

OPEN ACCESS

Edited by:
Kai Hang Yiu, The University of Hong Kong, Hong Kong SAR, China

Reviewed by:
Sasha A. Singh, Brigham and Women's Hospital and Harvard Medical School, United States
Adrien Lupieri, Brigham and Women's Hospital and Harvard Medical School, United States

***Correspondence:**
Zachary Obinna Enumah
zoe@jhmi.edu
Peter Zilla
peter.zilla@uct.ac.za

Specialty section:
This article was submitted to Heart Valve Disease, a section of the journal Frontiers in Cardiovascular Medicine

Received: *13 July 2021*
Accepted: *05 October 2021*
Published: *02 November 2021*

Citation:
Enumah ZO, Boateng P, Bolman RM, Beyersdorf F, Zühlke L, Musoni M, Tivane A and Zilla P (2021) Societies of Futures Past: Examining the History and Potential of International Society Collaborations in Addressing the Burden of Rheumatic Heart Disease in the Developing World. Front. Cardiovasc. Med. 8:740745. doi: 10.3389/fcvm.2021.740745

This paper explores the role and place of national, regional, and international society collaborations in addressing the major global burden of rheumatic heart disease (RHD). On the same order of HIV, RHD affects over 40 million people worldwide. In this article, we will outline the background and current therapeutic landscape for cardiac surgery in low- and middle-income countries (LMICs) including the resource-constrained settings within which RHD surgery often occurs. This creates numerous challenges to delivering adequate surgical care and post-operative management for RHD patients, and thus provides some context for a growing movement for and applicability of structural heart approaches, innovative valve replacement technologies, and minimally invasive techniques in this setting. Intertwined and building from this context will be the remainder of the paper which elaborates how national, regional, and international societies have collaborated to address rheumatic heart disease in the past (e.g., Drakensberg Declaration, World Heart Federation Working Group on RHD) with a focus on primary and secondary prevention. We then provide the recent history and context of the growing movement for how surgery has become front and center in the discussion of addressing RHD through the passing of the Cape Town Declaration.

Keywords: cardiac surgery, academic societies, rheumatic heart disease, registry, cardiac surgery intersociety alliance, CSIA

INTRODUCTION

Rheumatic heart disease (RHD) affects up to 40 million individuals globally (1). Caused by sequalae of skin or throat infection from streptococcal infection, RHD is endemic in low- and middle-income countries, and it is the most common cardiovascular pathology in young individuals aged 25 and younger (2, 3). Standing as a stark challenge to the international cardiac surgery community, the unmet need for cardiac surgery for rheumatic heart disease is estimated to be 300 to 400 operations per million population in low-income countries (4, 5). Recent global attention has addressed the burden of RHD with commitments to strengthening preventative efforts, as well as surgical efforts, with the adoption of the Drakensberg Declaration in 2006, the World Health Organization Resolution against rheumatic fever (RF) and RHD in 2018 and Cape Town Declaration on Access to Cardiac Surgery in the Developing World in 2018, respectively.

These efforts are commendable and will be elaborated upon further in this article. The current therapeutic landscape for addressing RHD is multidimensional and has many challenges. We will first provide a review of the therapeutic ecology of RHD treatment, specifically focusing on the current state of affairs of cardiac surgery for RHD in LMICs (6). This discussion will focus on the epidemiology of surgery for RHD, current challenges, and ongoing efforts to address these challenges, including an emerging environment for interventional techniques in resource poor settings (7–9). We will then focus on the history and roles of international medical and surgical societies, as well as global health agencies, in addressing the burden of RHD. Finally, and in the context of multisectoral collaboration, we will comment on the need and role of research and the lack of a robust, cardiac surgical registry for RHD patients (10).

Therapeutic Landscape of Surgical Treatment for RHD

Surgery is a cornerstone of any health care system. Nevertheless, it has been estimated that worldwide 5 billion people lack access to safe or affordable surgery and anesthesia (11). For cardiac surgery specifically, it is estimated that up to 6 billion people have inadequate, or insufficient access to cardiac surgery, if they have any access at all (12). Despite cardiovascular disease being the leading cause of death worldwide, enormous disparities exist between high-income countries and LMICs. Referral for adequate care and completion of care (e.g., surgery) is a major problem along the spectrum of management for RHD. For example, in the VALVAFRIC study by Kingue et al. (13), 1,200 patients were determined to be in need of surgery, yet only 27 patients (2.2%) were able to receive it. Even for those patients who can receive surgery, there are other challenges.

Mortality due to RHD is high in LMICs, especially among young individuals. For example, a recent study by Okello et. al. (14) reported a mortality rate of over 17% with a median age <30. Similarly, Gunther and colleagues have suggested up to a 12.5% mortality rate in Ethiopia (15). Post-operative care is a major challenge in the surgical management of RHD. Complications from surgery may be plentiful, such as stroke or bleeding. Some data suggest bleeding or thrombotic events may be low (16). Others, though, suggest that complications from thrombosis may be quite significant. For example, a recent study by Scherman et al. (17) showed that almost every fourth patient needing aortic valve replacement for RHD in a middle-income country like South Africa either had a stroke or had died of valve related complications 10 years after aortic valve replacement with a mechanical prosthesis. It is important to note that, in the context of access to cardiac surgery, in many resource-poor countries, reoperations are simply not offered, and some outcomes cannot be assessed without standard follow-up or mechanisms to capture patient outcomes.

In order for more patients to be able to receive treatment and to improve the safety of post-operative care for patients receiving surgery, the majority of these patients urgently require two major developments in replacement valves to address their needs. The first, and perhaps most pressing requirement is for improved valve design, incorporating long-lasting valve leaflet materials that will allow implantation into young patients without the need for anticoagulation. The other area in need of attention is to develop and implement simplified and reproducible transcatheter procedures that can deploy such valves cost-effectively, thereby significantly increasing the capacity of low-volume hospitals (7). A combination of easy-to-place trans-catheter technologies tailor-made for non-sophisticated medical facilities and suitable for the often compliant, non-calcified valves of patients with RHD, constructed with long-lasting leaflet material, promises to eventually introduce replacement valves that specifically address the "needs of the many" (8, 9). At the same time, advances in strengthening health systems to provide more access to sustainable cardiac surgical care is needed, as that will provide an avenue for valve repair in addition to minimally invasive valve replacement. Equally as important, a stronger health system will also provide avenues for improved medical management of heart failure for these vulnerable patients both pre and post-intervention.

There are many challenges to delivering sustainable cardiac surgical care in LMICs. On a broad scale, these include lack of health care infrastructure, critical gaps in the health care workforce, lack of training opportunities for critical providers, insufficient funding at the government level, competing health care priorities, and poor tracking of outcomes (18). Specifically, there is a lack of availability of multidisciplinary training including for perfusionists, anesthesiologists, and nurses, as well as surgeons and cardiologists. Additionally, the cost and labor intensive aspects of cardiac surgery pose substantial barriers, especially in the context of resource-poor countries having to consider and juxtapose health efforts to serve large populations (19). Research has been done on understanding the various cost models for cardiac surgery in resource-poor settings (20, 21) with estimates of approximately $6,000–11,000 per patient (22). Despite open heart surgery in a low- and middle-income

context costing approximately $10,000 per case (including the cost of cardiopulmonary bypass circuit and oxygenator, heart valves, intensive care and hospital associated costs, as well as other consumables such as drugs, blood gases, and other laboratory tests), cardiac surgery is often relegated to the back burner. There is a growing body of evidence that cardiac surgery may be more cost effective than previously understood (23).

Other challenges appear on a more local level in terms of advancing the cardiac surgical agenda. For example, there are few regional centers of excellence for cardiac surgery in sub-Saharan Africa. While centers throughout the continent do perform cardiac surgery, few pathways exist for collaboration. Furthermore, training of key providers, and the volume to support such training is still lacking (4).

The History of Attempts by Societies, Collaborations and Conferences to Address RHD

The concept of a role for international agencies and academic societies in collaborating to address capacity for cardiac surgery in the developing world is, in and of itself, a relatively recent initiative. Societies serve as an integral part of the academic and service community in terms of addressing and promoting clinical care, research, and education in cardiac surgery. In this section, we will provide a brief history of recent conferences with resultant publications and importantly policy documents which have been integral to the further advancement of the agenda to combat RHD.

In October 2005, delegates to the 1st All Africa Workshop on Rheumatic Fever and Rheumatic Heart Disease gathered in the Drakensberg mountains, South Africa and called out and acknowledged the large burden of RHD on the continent with an appreciation for the sociopolitical nature of its endemicity. The result was what has come to be known as the Drakensberg Declaration, with authors representing institutions from across the continent and the world including individuals representing the University of Cape Town, New York Medical College, University of Ibadan, University of Ghana Medical School, University of Melbourne, World Health Organization, University of Zimbabwe, Harare, University of Nairobi and the University of Libreville, to name a few (24). The result of this declaration was supporting the development of 1) public health awareness (both the lay public and health care workers) of RHD; 2) improving information quality vis-à-vis epidemiological surveillance; 3) advocacy; and 4) establishing national primary and secondary prevention programs for RHD (25). The underlying concept was a "bottoms up approach" with the central tenets being Awareness, Surveillance, Advocacy and Prevention, known as A.S.A.P and subsequently adopted across Africa.

In 2013, the World Heart Federation called for a reduction in premature RHD mortality by 25% by 2025 and the World Congress of Paediatric Cardiology and Cardiac Surgery brought together over 300 delegates at the 2nd RHD forum to discuss needs, opportunities and research in RHD, including the need for access to surgery in LMICs (26–28). One year later, in February 2014, the Second Rheumatic Fever/Rheumatic Heart Disease Workshop convened over 80 delegates in Zambia, from which emerged the Mosi-o-Tunya Call to Action. Again, representing institutions from 13 African countries and others, the message of this Mosi-o-Tunya Call to Action was to call for the elimination of RF and control of RHD in Africa in our lifetime (29). The Third All Africa Workshop on Rheumatic Fever and RHD occurred in February 2015. It was hosted by the Social Cluster of the African Union Commission and convened RHD experts in Addis Ababa, Ethiopia. These experts were both clinicians and researchers affiliated with the Pan-African Society of Cardiology (PASCAR) and also included representation from countries across the continent and the world. There were seven key recommendations from the Addis Ababa Communique: 1) establish prospective RHD registries; 2) ensure supplies of penicillin to promote primary and secondary prevention; 3) ensure access to reproductive health for women with RHD; 4) decentralize diagnostic capabilities to district hospitals including access to point-of-care technologies; 5) institute cardiac surgery centers of excellence for both sustainable care delivery and training; 6) promote national RHD control programs; and 7) foster partnerships to carry out the above recommendations (30). Other important events included the passing of the Cairo Accord (31, 32), the Khartoum Action Plan (33): culminating in a major milestone in May 2018 when all member states of the World Health Organization unanimously agreed to, and adopted, the Resolution on Rheumatic Fever and Rheumatic Heart Disease at the 71st World Health Assembly (34).

Local societies in endemic countries have played an important role in maintaining momentum, promoting partnerships, and outlining a clear and detailed path forward for curbing the burden of RHD e.g., Algerian Society of Cardiology. And, in the period between 1990 and 2015, deaths, disability-adjusted life years (DALYs) and years of life lost have all decreased. All this notwithstanding, however, new estimates of the prevalence of RHD are as high as 40 million, with stabilization of the mortality estimates in the 2019 Global burden of disease reports and it is estimated that as many as 300–400 operations per million population surgical procedures are needed for RHD patients in certain LMIC settings (4, 35). In light of this continued burden of disease, and especially the surgical aspects in addressing it, a major contribution on the international stage for RHD was the Cape Town Declaration on Access to Cardiac Surgery in the Developing World, launched at the 97th conference of the American Association of Thoracic Surgery in Boston (May 2017) and signed at the 50th anniversary of the 1st heart transplant at Groote Schuur Hospital, University of Cape Town.

Surgical Societies in Addressing the Burden of RHD

Convened by Professor Peter Zilla, the then-Chair of the Christiaan Barnard Division of Cardiothoracic Surgery, Faculty of Health Sciences, University of Cape Town, Cape Town, South Africa, delegates and signatories of the Cape Town

Declaration represented cardiothoracic/cardiovascular societies from across the globe, such as the Society of Thoracic Surgeons, American Association for Thoracic Surgery, Australian and New Zealand Society of Cardiac and Thoracic Surgeons, Society of Cardiothoracic Surgeons of South Africa, Pan-African Society of Cardiology, Brazilian Society of Cardiovascular Surgery, European Association for Cardio-Thoracic Surgery, World Heart Federation, Asian Society for Cardiovascular and Thoracic Surgery, Chinese Society for Thoracic and Cardiovascular Surgery, Pan-African Society for Cardiothoracic Surgery, and the South African Heart Association. Additionally, delegates represented many humanitarian organizations, governments, industry and academia (36).

The overarching theme of the Cape Town Declaration is unique to the previous multi-sectorial and international declarations and communiques. For perhaps the first time in modern history, surgery was front and center. The mission of the Cape Town Declaration was "to urge all relevant entities within the international cardiac surgery, industry and government sectors to commit to develop and implement an effective strategy to address the scourge of RHD in the developing world through increased access to life-saving cardiac surgery" (36). This was undertaken by two main aims including the formation of an international working group dedicated to this cause (henceforth known as the Cardiac Surgery Intersociety Alliance, CSIA) and the investment in training of cardiac surgeons and other important staff in LMICs. The announcement of the Cape Town Declaration was published in multiple (9) cardiovascular surgery journals simultaneously, signaling the commitment of the global cardiac surgery community to redoubling their efforts to reduce the burden of RHD.

The CSIA recently announced its endorsement of two pilot sites in Rwanda and Mozambique, including King Faisal Hospital Kigali (Rwanda) and Hospital Central Maputo (Mozambique) (37). International societies and conferences have maintained and increased the momentum necessary to address the burden of RHD. In important ways, the collaboration of these international societies holds forth the promise of finally addressing this formerly intractable problem of providing access to cardiac surgery for the countless millions who until now have been deprived of its benefits. Importantly, societies, aided and coordinated by the CSIA, may play an important role in furthering and facilitating regional collaborations between sites. For example, preliminary discussions between the cardiac surgery teams at King Faisal Hospital Kigali and Hospital Central Maputo have been facilitated, and planning is underway for regional cooperation between the two centers where staff may visit one another for mutual benefit. The CSIA will provide sponsorship for these trips.

Additionally, groups such as the CSIA can leverage and build upon previously existing efforts and strong networks of collaboration that have manifested from the All-Africa Workshops on Rheumatic Fever and RHD. The CSIA plans to partner and build on ongoing efforts in the region to build a robust, prospective, multicenter registry for RHD surgical patients, including following them in the post-operative period. Previous registry work, such as the REMEDY and VALVAFRIC, have made important contributions to our understanding of RHD in LMICs (13, 38). Smaller registries, such as the work of Ntaganda and colleagues, are laying important groundwork for future, robust, multi-center registries that the CSIA hopes to support (39). Again, surgical societies can and are playing a major role in addressing the massive global burden of RHD.

CONCLUSION

As we look to the future of cardiac surgery for RHD, it is clear it will continue to require a multisectoral and multidisciplinary effort. As part of that effort, we should not underestimate the role that collaborations between international societies, agencies, and other involved parties can play in furthering the agenda to reduce the enormous burden of RHD. Recent history has demonstrated that some trends for RHD mortality and morbidity have moved in the right direction, and international collaborations may have played a major role in achieving that. Nevertheless, the surgical burden of RHD remains high, and heretofore has been largely unaddressed. For many patients with symptomatic RHD and major valvular pathology, surgery remains the only effective treatment. Manifest through these new collaborations, we anticipate that cardiac surgical societies have a crucial role in ensuring increased access to life-saving cardiac surgery for RHD in the developing world. In doing so, we will begin to realize the vision of the Cape Town Declaration, the Addis Ababa Communique, and the many other declarations and hopes that have been laid bare to address and curb the burden of RHD for the most vulnerable populations.

DATA AVAILABILITY STATEMENT

The original contributions presented in the study are included in the article/supplementary material, further inquiries can be directed to the corresponding authors.

AUTHOR CONTRIBUTIONS

All authors listed have made a substantial, direct and intellectual contribution to the work, and approved it for publication.

REFERENCES

1. Peters F, Karthikeyan G, Abrams J, Muhwava L, Zühlke L. Rheumatic heart disease: current status of diagnosis and therapy. *Cardiovasc Diagnosis Therapy*. (2020) 10:305–15. doi: 10.21037/cdt.2019.10.07
2. Curry C, Zuhlke L, Mocumbi A, Kennedy N. Acquired heart disease in low-income and middle-income countries. *Arch Dis Child*. (2018) 103:73–7. doi: 10.1136/archdischild-2016-312521
3. *Rheumatic Heart Disease*. Available online at: https://www.who.int/health-topics/rheumatic-heart-disease#tab=tab_1 (accessed April 23, 2021).

4. Zilla P, Yacoub M, Zühlke L, Beyersdorf F, Sliwa K, Khubulava G, et al. Global unmet needs in cardiac surgery. *Glob Heart*. (2018) 13:293–303. doi: 10.1016/j.gheart.2018.08.002
5. Zilla P, Morton Bolman R, Boateng P, Sliwa K. A glimpse of hope: cardiac surgery in low-and middle-income countries (LMICs). *Cardiovasc Diagnosis Therapy*. (2020) 10:336–49. doi: 10.21037/cdt.2019.11.03
6. Scherman J, Zilla P. Poorly suited heart valve prostheses heighten the plight of patients with rheumatic heart disease. *Int J Cardiol*. (2020) 318:104–4. doi: 10.1016/j.ijcard.2020.05.073
7. Zilla P, Williams DF, Bezuidenhout D. TAVR for patients with rheumatic heart disease: opening the door for the many? *J Am Coll Cardiol*. (2021) 77:1714–6. doi: 10.1016/j.jacc.2021.02.044
8. Scherman J, Ofoegbu C, Myburgh A, Swanevelder J, van Breda B, Appa H, et al. Preclinical evaluation of a transcatheter aortic valve replacement system for patients with rheumatic heart disease. *EuroIntervention*. (2019) 15:E975–82. doi: 10.4244/EIJ-D-18-01052
9. Bezuidenhout D, Williams DF, Ofoegbu C, Scherman J, Zilla P. TAVI for low to middle income countries. *Eur Heart J*. (2017) 38:1182–4. doi: 10.1093/eurheartj/ehx169
10. Lin Y, Till BM, Yi S, Dahm JS, Taylor K, Lu N, et al. Cardiac surgery publications in Africa over the last 20 years: a literature review. *S Afr J Sci*. (2020) 116:1–6. doi: 10.17159/sajs.2020/6359
11. Meara JG, Leather AJM, Hagander L, Alkire BC, Alonso N, Ameh EA, et al. Global surgery 2030: evidence and solutions for achieving health, welfare, and economic development. *Lancet*. (2015) 386:569–624. doi: 10.1016/S0140-6736(15)60160-X
12. Vervoort D, Swain JBD, Pezzella AT, Kpodonu J. Cardiac surgery in low- and middle-income countries: a state-of-the-art review. *Ann Thorac Surg*. (2021) 111:1394–400. doi: 10.1016/j.athoracsur.2020.05.181
13. Kingué S, Ba SA, Balde D, Diarra MB, Anzouan-Kacou JB, Anisubia B, et al. The VALVAFRIC study: a registry of rheumatic heart disease in Western and Central Africa. *Arch Cardiovasc Dis*. (2016) 109:321–9. doi: 10.1016/j.acvd.2015.12.004
14. Okello E, Longenecker CT, Beaton A, Kamya MR, Lwabi P. Rheumatic heart disease in Uganda: predictors of morbidity and mortality one year after presentation. *BMC Cardiovasc Disord*. (2017) 17:1–10. doi: 10.1186/s12872-016-0451-8
15. Günther G, Asmera J, Parry E. Death from rheumatic heart disease in rural Ethiopia. *Lancet*. (2006) 367:391. doi: 10.1016/S0140-6736(06)68128-2
16. Rusingiza EK, El-Khatib Z, Hedt-Gauthier B, Ngoga G, Dusabeyezu S, Tapela N, et al. Outcomes for patients with rheumatic heart disease after cardiac surgery followed at rural district hospitals in Rwanda Healthcare delivery, economics and global health. *Heart*. (2018) 104:1707–13. doi: 10.1136/heartjnl-2017-312644
17. Scherman J, Manganyi R, Human P, Pennel T, Brooks A, Brink J, et al. Isolated mechanical aortic valve replacement in rheumatic patients in a low- to middle-income country. *J Thorac Cardiovasc Surg*. (2019) 157:886–93. doi: 10.1016/j.jtcvs.2018.06.083
18. Reichert HA, Rath TE. Cardiac surgery in developing countries. *J Extra-Corpor Technol*. (2017) 49:98–106.
19. Yacoub M, ElGuindy A, Afifi A, Yacoub L, Wright G. Taking cardiac surgery to the people. *J Cardiovasc Transl Res*. (2014) 7:797–802. doi: 10.1007/s12265-014-9598-9
20. Yankah C, Fynn-Thompson F, Antunes M, Edwin F, Yuko-Jowi C, Mendis S, et al. Cardiac surgery capacity in Sub—Saharan Africa: Quo Vadis? *Thorac Cardiovasc Surg*. (2014) 62:393–401. doi: 10.1055/s-0034-1383723
21. Mirabel M, Lachaud M, Offredo L, Lachaud C, Zuschmidt B, Ferreira B, et al. Chirurgie cardiaque: dix ans d'expérience dans deux pays en voie de développement. *Arch Cardiovasc Dis*. (2017) 110:82–90. doi: 10.1016/j.acvd.2016.05.006
22. Falase B, Sanusi M, Majekodunmi A, Ajose I, Idowu A, Oke D. The cost of open heart surgery in Nigeria. *Pan Afr Med J*. (2013) 14:61. doi: 10.11604/pamj.2013.14.61.2162
23. Coates MM, Sliwa K, Watkins DA, Zühlke L, Perel P, Berteletti F, et al. An investment case for the prevention and management of rheumatic heart disease in the African Union 2021–30: a modelling study. *Lancet Glob Heal*. (2021) 9:e957–66. doi: 10.1016/S2214-109X(21)00199-6
24. Mayosi B, Robertson K, Volmink J, Adebo W, Akinyore K, Amoah A, et al. The Drakensberg declaration on the control of rheumatic fever and rheumatic heart disease in Africa. *S Afr Med J*. (2006) 96(3 Pt 2):246.
25. ASAP. *Programme. ASAP. Programme – News – Pascar*. Available online at: https://www.pascar.org/news/entry/a.s.a.p.-programme1 (accessed April 23, 2021).
26. Remenyi B, Carapetis J, Wyber R, Taubert K, Mayosi BM. Position statement of the World Heart Federation on the prevention and control of rheumatic heart disease. *Nat Rev Cardiol*. (2013) 10:284–92. doi: 10.1038/nrcardio.2013.34
27. Zühlke L. Successes, failures, challenges and ground-breaking research: messages from the 6th world congress of paediatric cardiology and cardiac Surgery. *Cardiovasc J Afr*. (2013) 24:93–5.
28. Zühlke LJ, Engel ME, Remenyi B, Wyber R, Carapetis J, Committee RFMRW. The second rheumatic heart disease forum report. *Glob Heart*. (2013) 8:253–61. doi: 10.1016/j.gheart.2013.08.006
29. Mayosi BM, Gamra H, Dangou JM, Kasonde J, Abul-Fadl A, Adeoye MA, et al. Rheumatic heart disease in Africa: the Mosi-o-Tunya call to action. *Lancet Glob Health*. (2014) 2:e438–9. doi: 10.1016/S2214-109X(14)70234-7
30. Watkins D, Zuhlke L, Engel M, Daniels R, Francis V, Shaboodien G, et al. Seven key actions to eradicate rheumatic heart disease in Africa: the Addis Ababa communiqué. *Cardiovasc J Afr*. (2016) 27:184–7. doi: 10.5830/CVJA-2015-090
31. CAIRO ACCORD | AHC. Available online at: https://ahc-scienceandpractice.com/cairo-accord/ (accessed July 13, 2021).
32. *Rheumatic Heart Disease Congress, Cairo, Egypt: from Molecules to the Global Community – News – Pascar*. Available online at: https://www.pascar.org/news/entry/rheumatic-heart-disease-from-molecules-to-the-global-community (accessed July 13, 2021)
33. Sliwa K, Wood D, Suliman A, Yonga G, Eisele J-L, Millan P, et al. An African cardiology summit The World Heart Federation African Summit on best practices in policy and access to care in 2017 concluded with the Khartoum Action Plan, to improve cardiovascular on the African continent. *Eur Heart J*. (2018) 39:430–3. doi: 10.1093/eurheartj/ehx805
34. Sliwa K, White A, Milan P, Olga Mocumbi A, Zilla P, Wood D. Momentum builds for a global response to rheumatic heart disease. *Eur Heart J*. (2018) 39:4229–32. doi: 10.1093/eurheartj/ehy763
35. Roth GA, Mensah GA, Johnson CO, Addolorato G, Ammirati E, Baddour LM, et al. Global burden of cardiovascular diseases and risk factors, 1990-2019: update from the GBD 2019 study. *J Am Coll Cardiol*. (2020) 76:2982–3021. doi: 10.1016/j.jacc.2020.11.010
36. Zilla P, Bolman RM, Yacoub MH, Beyersdorf F, Sliwa K, Zühlke L, et al. The Cape Town Declaration on access to cardiac surgery in the developing world. *J Thorac Cardiovasc Surg*. (2018) 156:2206–9. doi: 10.1016/j.jtcvs.2018.06.002
37. Enumah ZO, Bolman RM, Zilla P, Boateng P, Wilson B, Kumar AS, et al. United in earnest: first pilot sites for increased surgical capacity for rheumatic heart disease announced by Cardiac Surgery Intersociety Alliance. *J Thorac Cardiovasc Surg*. (2021) 161:2108–13. doi: 10.1016/j.jtcvs.2020.11.183
38. Zühlke L, Karthikeyan G, Engel ME, Rangarajan S, Mackie P, Cupido-Katya Mauff B, et al. Clinical outcomes in 3343 children and adults with rheumatic heart disease from 14 low-and middle-income countries: two-year follow-up of the global rheumatic heart disease registry (the REMEDY Study). *Circulation*. (2016) 134:1456–66. doi: 10.1161/CIRCULATIONAHA.116.024769
39. Ntaganda E, Rusingiza E, Rukundo G, Ng'ang'a L, Hedt-Gauthier B, El-Khatib Z, et al. Postoperative rheumatic heart disease follow-up: creating a

national registry and first results from Rwanda. *Ann Glob Heal.* (2020) 86:1–9. doi: 10.5334/aogh.2719

Conflict of Interest: The authors declare that the research was conducted in the absence of any commercial or financial relationships that could be construed as a potential conflict of interest.

Publisher's Note: All claims expressed in this article are solely those of the authors and do not necessarily represent those of their affiliated organizations, or those of the publisher, the editors and the reviewers. Any product that may be evaluated in this article, or claim that may be made by its manufacturer, is not guaranteed or endorsed by the publisher.

frontiers in Cardiovascular Medicine

ORIGINAL RESEARCH
published: 08 December 2021
doi: 10.3389/fcvm.2021.738854

Vascular Access Site Complications Do Not Correlate With Large Sheath Diameter in TAVI Procedures With New Generation Devices

Birgid Gonska, Christopher Reuter, Johannes Mörike, Wolfgang Rottbauer and Dominik Buckert*

Department of Internal Medicine II–Cardiology, University of Ulm, Ulm, Germany

OPEN ACCESS

Edited by:
Peter Zilla,
University of Cape Town, South Africa

Reviewed by:
Fabrizio Buffolo,
University of Turin, Italy
Tanja Katharina Rudolph,
Heart and Diabetes Center North Rhine-Westphalia, Germany

****Correspondence:***
Birgid Gonska
birgid.gonska@uniklinik-ulm.de
orcid.org/0000-0002-1015-5853

Specialty section:
This article was submitted to Heart Valve Disease, a section of the journal Frontiers in Cardiovascular Medicine

Received: *09 July 2021*
Accepted: *10 November 2021*
Published: *08 December 2021*

Citation:
Gonska B, Reuter C, Mörike J, Rottbauer W and Buckert D (2021) Vascular Access Site Complications Do Not Correlate With Large Sheath Diameter in TAVI Procedures With New Generation Devices. Front. Cardiovasc. Med. 8:738854. doi: 10.3389/fcvm.2021.738854

Background: Vascular complications after transfemoral transcatheter aortic valve implantation (TAVI) are associated with morbidity and mortality. However, consistent predictors have not been identified yet. The size of the implantation sheath seems to play a role, though especially with new generation TAVI devices and their improved sheaths and delivery systems this remains uncertain.

Objectives: This study aimed to determine the incidence and predictors of access site-related vascular complications (VC) in the era of new generation TAVI devices.

Methods and Results: Four hundred consecutive patients receiving TAVI in an experienced tertiary care center were analyzed. VC occurred in 89 patients (22.25%) with the majority being minor VC (21%) and only 1.25% major VC. Possible predictors for VC were tested, and only peri-interventional dual antiplatelet therapy (DAPT) showed to be predictive for VC [OR 2.11 (95% CI 1.10–4.06, $p = 0.025$)]. The female gender [OR 0.75 (95% CI 0.44–1.3), $p = 0.31$], sheath to femoral artery ratio >1.05 [OR 1.18 (95% CI 0.66–2.08, $p = 0.58$)], calcification of the access site vessel [OR 0.83 (95% CI 0.48–1.42, $p = 0.48$)], known peripheral artery disease [OR 0.95 (95% CI 0.4–2.25, $p = 0.9$)], and BMI $\geq$ 25 kg/m² [OR 0.69 (95% CI 0.41–1.19, $p = 0–19$)] were not predictive of VC. The larger sheath with 20 French even showed less VC than the smaller sheath with 16 French [OR 0.43 (95% CI 0.25–0.74, $p = 0.002$)].

Conclusions: Overall, the rate of major and minor VC was low in this study population (for major VC: rate of 1.25%). Predefined risk factors were not associated with the occurrence of VC, except for peri-interventional treatment with DAPT. Especially, larger sheath size could not be identified as a predictor for VC in the setting of TAVI procedures performed with contemporary devices.

Keywords: transcatheter aortic valve implantation, vascular complications, bleeding, sheath size, calcification

INTRODUCTION

Since the first transcatheter aortic valve implantation (TAVI) in 2002 by Cribier et al. (1), it has become the standard of care for inoperable patients or patients at high risk for surgical valve implantation (2). It has grown into a rapidly evolving alternative for patients at intermediate risk and is even progressing toward low-risk patients (3, 4).

The preferred approach for TAVI is transfemoral access, which has been associated with a better outcome than non-transfemoral access (5). With the first-generation TAVI devices, major vascular complications (VC) occurred in ∼10% of patients (6–10). The occurrence of major VC proved to be associated with higher rates of morbidity and mortality (6, 11–13).

The growing experience with the management of percutaneous vascular access, development of new percutaneous suture devices, and improvements of the TAVI devices including implantation sheaths and delivery catheters have already led to a decline of VC compared with the beginning of TAVI. Nonetheless, VC is still one of the more common complications after transfemoral TAVI with incidences of 2 to 10% for major VC, and a wide range of 2 to 29% for minor VC (12, 14–16).

In previous studies, a variety of risk factors have been identified to influence the occurrence of VC after transfemoral TAVI, such as female gender, obesity, peripheral artery disease (PAD), femoral artery diameter, sheath size or sheath to (ilio-)femoral artery ratio (SIFAR; SFAR, respectively), and calcification of the access site vessel and center experience (7, 13, 17–20).

This study aimed to analyze the incidence of access site-related VC in an all-comers patient cohort treated with the newest generation TAVI devices and to evaluate whether risk factors can be identified that have an impact on the occurrence of VC. Therefore, we assessed access site-related VC as defined by the updated standardized endpoint definitions for TAVI according to the second Valve Academic Research Consortium- (VARC-2) criteria in patients treated with the newest generation TAVI devices (21). We chose to analyze TAVI devices with non-expandable sheaths to ensure consistent sheath diameters: the Boston Scientific Lotus Edge (BLE) valve (20 French) and the Medtronic Evolut Pro/R (MEV) valve with a low-profile delivery system (EnveoPro, 16 French).

METHODS

In this retrospective single-center study, 611 consecutive patients treated with transfemoral TAVI for aortic valve disease between January 2019 and May 2020 were screened for treatment with either the self-expandable MEV Pro (size 23/26 or 29 mm) and MEV R (size 34 mm) or with the mechanically expandable BLE.

The decision for transfemoral TAVI was made by the interdisciplinary heart team according to the 2017 European Society of Cardiology/ European Association for Cardio-Thoracic Surgery Guidelines for the management of valvular heart disease (22). The study was approved by the local ethics committee. All patients gave written informed consent.

All patients underwent preprocedural 256 multislice contrast-enhanced CT, which was evaluated with a dedicated software (3mensio Structural Heart 9.1 software, Pie Medical Imaging B.V., Maastricht, The Netherlands). Besides the decision for the valve size, there was also an evaluation of the vascular access. The slice thickness for the evaluation of vascular access was 0.7 to 1.0 mm. Routinely the access site was determined preprocedural and the size of the common femoral artery (CFA) was measured at the expected puncture position. Furthermore, calcification was semi-quantitatively classified in none, mild (calcification of not more than 25% of the circumference and not relevant protrusion into the lumen), or severe (calcification of more than 25% of the circumference, more than two spots, or relevant protrusion into the lumen) (**Figure 1**).

According to the hospital protocol, antiplatelet therapy was continued peri-interventionally whereas oral anticoagulation was stopped pre-procedurally. In these patients, single antiplatelet therapy was used peri-interventionally.

The decision for BLE or MEV device was made according to the experienced interventional cardiologist. Formally the BLE introducer set requires access vessel diameters of 6.5 mm or larger, the EnveoPro delivery system 5.5 mm or larger.

Transcatheter aortic valve implantation (TAVI) was performed in a hybrid catheterization laboratory under conscious sedation by an experienced operator team of four interventionalists with a standardized procedure protocol. First, the puncture of the non-access site CFA was performed under fluoroscopic control, and then the access site was cannulated under angiographic visualization *via* cross-over angiography from the non-access site, attempting for the puncture height predefined by the CT measurements. There was no use of ultrasound for the puncture. After the insertion of a 6 French sheath, angiography in an ipsilateral oblique view was performed to control the exact position of the puncture. Afterward, the vascular closure device was applied. For that matter, two Perclose ProGlide devices (Abbott Vascular, Santa Clara, California) were used at a 2-h angle (eleven o'clock and one o'clock). Then, the TAVI sheath was inserted over a stiff wire and heparin was administered to achieve an activated clotting time of 250–300 s. For the MEV Pro 23-, 26-, and 29-mm valve as well as for the MEV R 34 mm valve a 16 French Sheath (Cook Check-Flo Performer Introducer; Cook Medical, Limerick, Ireland) was used and later exchanged for the 16 French equivalent EnveoPro delivery system with an inline sheath, loaded with the valve. For the BLE the 20 French Boston Lotus Introducer sheath was inserted which remained in place throughout the procedure.

Before removal of the access site sheath, crossover access was obtained from the non-access femoral site with a 6 French pigtail catheter placed in the external iliac artery of the access site. Then, the access site sheath was removed and the ProGlides knots were pushed down and locked. Afterward, an angiography of the access site was performed. If necessary, dependent on the result of the angiogram and the discretion of the operator, either endovascular therapy (covered stent, percutaneous transluminal angioplasty) or manual compression was used to control the access site in case of a leak. Closure of the non-access site was achieved by 6 French Angio-Seal devices (Terumo Europe

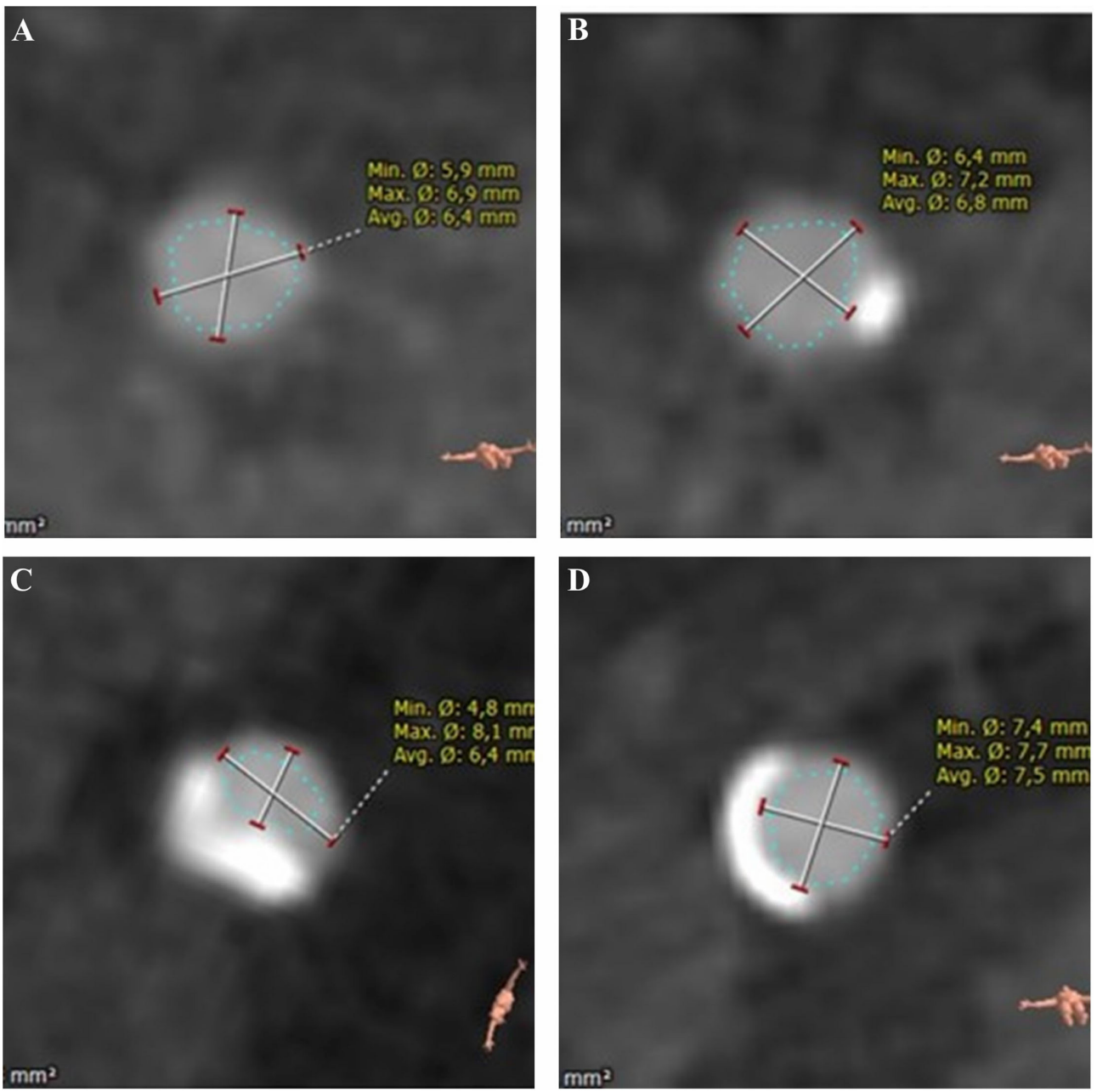

FIGURE 1 | Quantification of calcification of common femoral artery (derived from CT): none **(A)** mild **(B)** severe **(C,D)**.

N.V., Leuven, Belgium), or in case of use of a covered stent at the access site requiring a sheath size of 8–10 French by one ProGlide. Postprocedural, there was a clinical evaluation of the access and non-access site. Any hematoma of the access site was documented. Patients with periprocedural findings other than none or mild leak or patients with suspicious findings in the postprocedural clinical examination had Doppler-/Duplex ultrasound evaluation of access site and non-access site. If this showed pseudoaneurysm, either manual compression therapy was used or an injection of thrombin.

The last angiogram of the access site was evaluated retrospectively concerning any sign of leaks, dissection/endovascular flap, stenosis (lumen reduction of $\geq$50%), and total occlusion of the CFA (**Figure 2**).

The baseline characteristics of the patients, including medication and relevant medical history, were documented, as well as the clinically relevant periprocedural data. We assessed the sheath to femoral artery ratio (SFAR) by dividing the outer diameter of the sheath (6.667 mm for the Medtronic system and 7.9 mm for the Boston Lotus system) by the diameter of the CFA

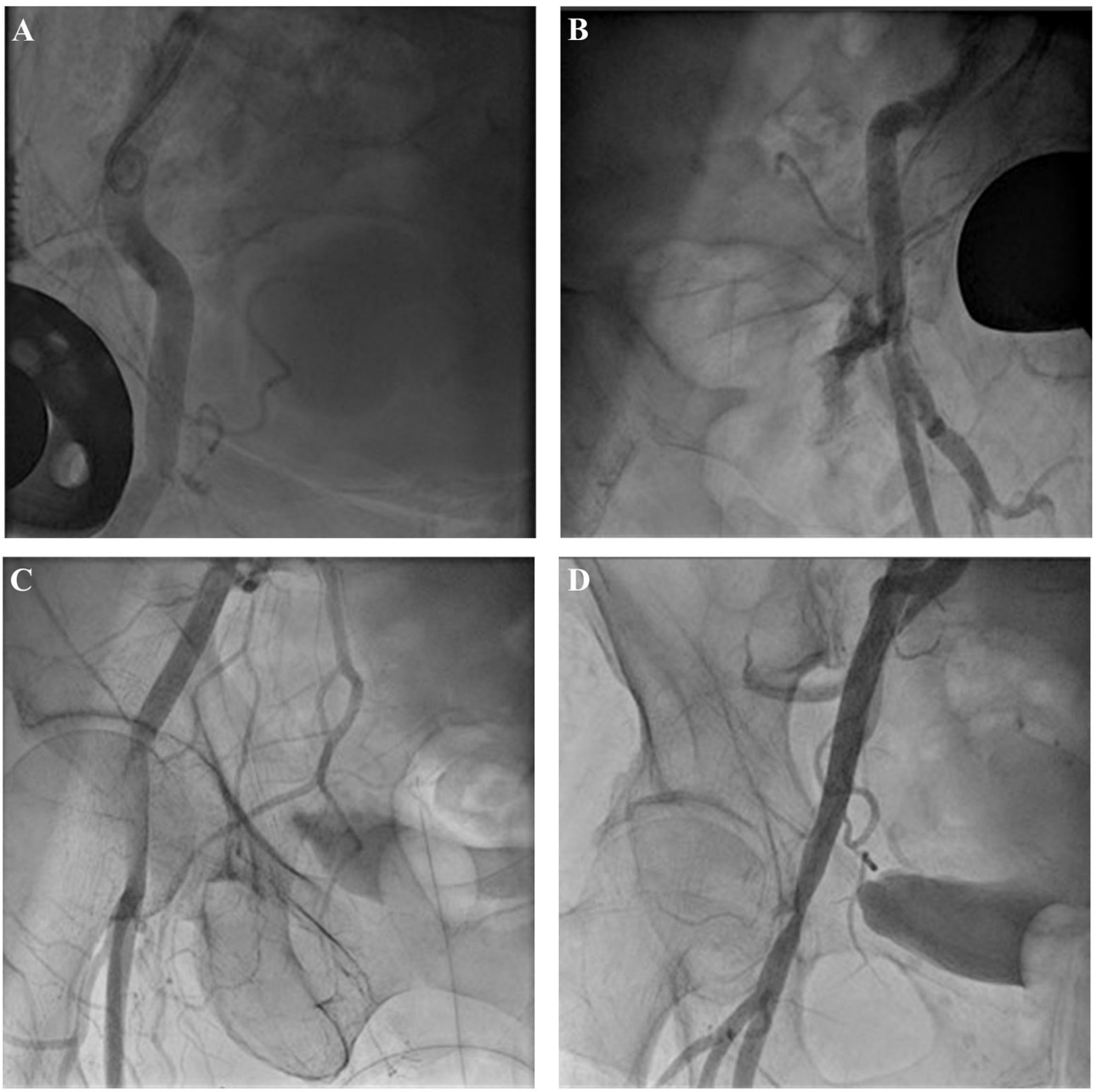

FIGURE 2 | Evaluation of angiogram after use of closure device: minor leak **(A)**, severe leak **(B)**, dissection **(C)**, and stenosis with minor leaks **(D)**.

at the expected puncture position of the access site, evaluating SFAR using the minimal diameter as well as the mean diameter.

The primary endpoint of this analysis was the predefined VARC-2 endpoints vascular access site and access-related complications with the focus on the access site itself. Major VCs at the access site were defined as vascular injuries such as perforation, bleeding, hematoma, dissection, stenosis, or pseudoaneurysm, leading to death, life-threatening or major bleeding. Minor VCs were assessed at the access and non-access site and defined as vascular injury as mentioned for the major VC however not leading to death, life-threatening, or major bleeding. Due to the small number of major VCs, patients with minor or major VC were combined and compared with patients without VC.

Furthermore, clinically relevant VARC-2 defined endpoints pacemaker, bleeding, peri-interventional stroke/transitory ischemic attack (TIA), and device success were assessed.

Statistical Analysis

We performed a sample size calculation based on assumed incidences for the small and the large sheath. Chen et al. had evaluated predictors for suture device failure and vascular

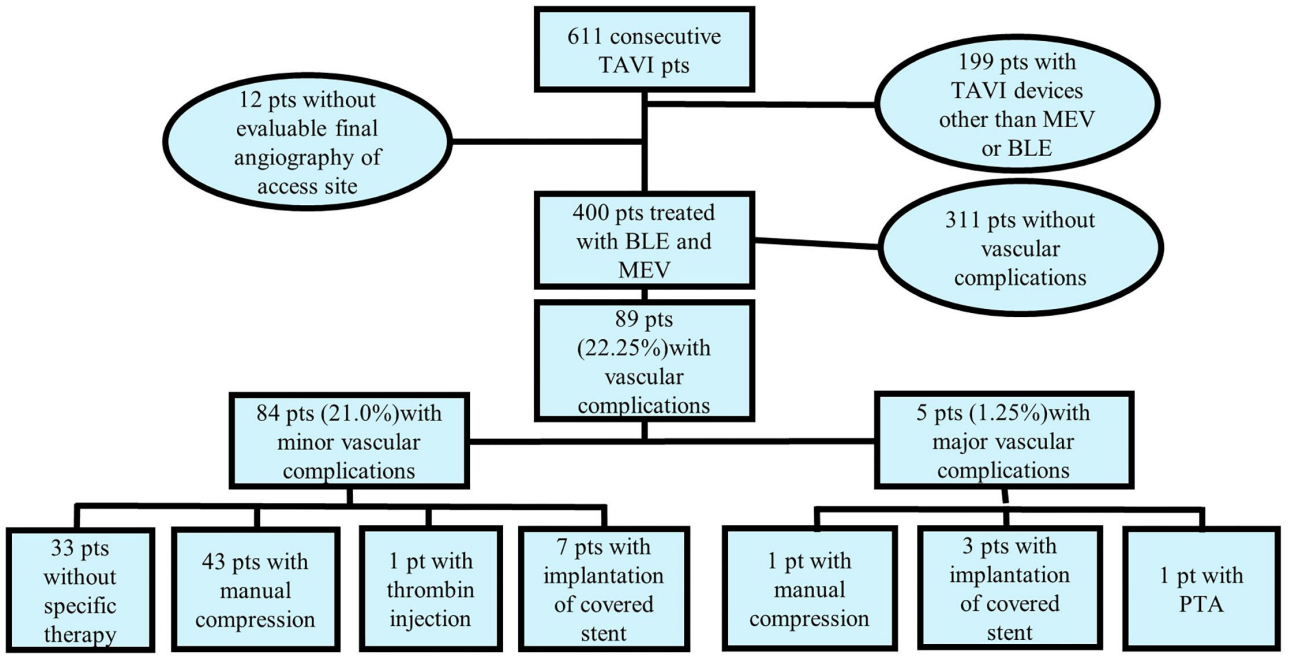

FIGURE 3 | Treatments for patients with minor and major access site vascular complications.

complications in a patient cohort of 458 patients with interventions with sheath sizes 16 to 26 French (18). The study showed a significantly higher incidence of suture device failure and following vascular complications with the use of >21 French sheath size than the ≤21 F sheath size with 17.2% vs. 4.9%, $p < 0.001$; using a receiver operating characteristic (ROC) curve sheath, size ≥19 French was found to be significantly associated with suture device failure. Barbanti et al. had experienced comparable results in their study on 375 patients (≥19 French rates of major VC 17.5 vs. 5.9%, $p < 0.001$) (20). Based on these results with expected event rates of 15% for the 20 French and 5% for the 16 French access and a power of 80% and an α-level of 0.05 group sizes of 141 patients each were found to be adequate. However, to achieve a sufficient safety margin we aimed for 200 consecutive patients with each valve type/sheath size. Statistical analysis was performed with the MedCalc software (MedCalc Version 19.6, MedCalc Software Ltd, Ostend; Belgium). Continuous variables are expressed as mean ± one SD and were compared with the *t*-test. Categorical variables are presented as counts and percentages and differences between proportions were calculated by using the χ^2 test. A logistic univariate and multivariate regression analysis were performed to identify predictors for VC after TAVI, results presented as odds ratio with 95% confidence interval (CI). A value of $p < 0.05$ was considered statistically significant.

RESULTS

In all 400 patients, an aortic valve prosthesis was successfully implanted, in 399 patients one valve, in one patient there was the implantation of a second valve due to an embolized MEV, without further complications. There was no conversion to surgery and there was no periprocedural death. The rate of major VC was low with only 1.25% (5 patients). Two of these patients showed severe leak and three showed severe leak and dissection of the CFA after use of the vascular closure devices. Three patients were treated with the implantation of a covered stent, one patient had percutaneous transluminal angioplasty (PTA) only of the CFA and one patient was treated with manual compression only (**Figure 3**). All of these patients met the criteria of major bleeding complications according to the VARC-2-criteria, even though only three of them showed hematoma of the access site afterward. Patients with major VC had a significantly larger drop in hemoglobin after the TAVI procedure (3.78 ± 1.93 vs. 1.34 ± 1.15 g/dl, $p = 0.048$), and received significantly more units of blood (0.75 ± 0.96 units of blood vs. 0.05 ± 0.34, $p < 0.001$). Minor vascular complications were more frequent with 21% (84 patients). Most of these patients had access site hematoma (66 patients), four patients developed pseudoaneurysm, and in 12 patients there was stenosis of at least 50% of the CFA by duplex ultrasound without need for further treatment. There were no major VC at the non-access site, only minor VC (69 patients, 17.25%), the majority having a hematoma (57 patients), nine developing pseudoaneurysms, which was treated with thrombin injection or manual compression (6 patients and 3 patients, respectively), and 3 patients with stenosis of at least 50% of the CFA by duplex ultrasound without need for further treatment.

Baseline Characteristics

The baseline characteristics of the patients with and without VC are displayed in **Table 1**. There was no statistically

TABLE 1 | Baseline clinical characteristics.

	No VC $n = 311$	VC $n = 89$	*P*-Value
Age, years	80.5 ± 6.3	79.6 ± 6.3	0.24
Female	159 (51.1%)	50 (56.2%)	0.40
BMI (kg/m^2)	27.4 ± 5.1	27.5 ± 4.5	0.86
Diabetes mellitus	79 (25.4%)	28 (31.5%)	0.26
Chronic renal failure with dialysis	5 (1.6%)	2 (2.2%)	0.70
Coronary artery disease	164 (52.9%)	54 (60.7%)	0.20
History of myocardial infarction	28 (9.0%)	10 (11.2%)	0.71
History of cardiac surgery	24 (7.7%)	10 (11.2%)	0.30
Known PAD	28 (9.0%)	8 (9.0%)	1.00
History of stroke or intracerebral bleeding	46 (14.8%)	11 (12.4%)	0.56
Pulmonary disease	126 (40.5%)	43 (48.3%)	0.20
NYHA class III/IV	207 (66.6%)	65 (73%)	0.25
Ejection fraction (%)	51.1 ± 11.0	52.6 ± 9.0	0.26
STS PROM	3.48 ± 2.37	3.52 ± 2.58	0.89
Medication at baseline			
ASA only	135 (43.4%)	42 (47.2%)	0.53
DAPT	43 (13.8%)	19 (21.3%)	0.08
Oral anticoagulation	109 (35.5%)	22 (24.7%)	0.06

Values are mean ± SD or n (%).
BMI, Body mass index; PAD, peripheral artery disease; NYHA, New York Heart Association; STS-PROM, Society of Thoracic Surgeons predicted risk of mortality; ASA, acetylsalicylic acid; DAPT, dual antiplatelet therapy.

TABLE 2 | Characteristics of access site common femoral artery.

	No VC $n = 311$	VC $n = 89$	*P*-Value
Minimal diameter of CFA, mm	6.73 ± 1.21	6.58 ± 1.69	0.36
Maximum diameter or CFA, mm	8.17 ± 1.47	8.08 ± 1.74	0.65
Mean diameter of CFA, mm	7.45 ± 1.29	7.33 ± 1.68	0.49
SFAR (mean diameter)	1.01 ± 0.20	1.02 ± 0.29	0.74
SFAR (minimal diameter)	1.13 ± 0.24	1.18 ± 0.55	0.18
SFAR≥1.05 (mean diameter)	120 (38.7%)	33 (37.5%)	0.84
SFAR≥1.05 (minimal diameter)	200 (64.5%)	50 (56.8%)	0.19
Calcification of CFA			
None	199 (64.0%)	61 (68.5%)	0.64
Moderate	78 (25.1%)	18 (20.2%)	
Severe	34 (10.9%)	10 (11.2%)	

Values are mean ± SD or n (%).
CFA, common femoral artery; SFAR, sheath to femoral artery ratio.

TABLE 3 | Procedural data.

	No VC $n = 311$	VC $n = 89$	*P*-Value
Valve type			
MVE	143 (46.0%)	57 (64.0%)	0.003
BLE	168 (54.0%)	32 (36.0%)	
Outer diameter of sheath/delivery catheter, mm	7.33 ± 0.62	7.11 ± 0.60	0.003
Angiography of access site			
Leak	159 (51.1%)	53 (59.6%)	0.16
Dissection/flap	45 (15.4%)	15 (17.2%)	0.26
Stenosis/occlusion	7 (2.3%)	4 (4.5%)	0.26

Values are mean ± SD or n (%).
MVE, Medtronic evolut; BLE, Boston lotus edge; SFAR, Sheath to common femoral artery ratio.

significant difference concerning their medical history or clinical presentation. There was especially no difference in gender (female 51.1% in no-VC vs. 56.2%, $p = 0.1$), in body mass index (27.4 ± 5.1 kg/m² in no-VC group vs. 27.5 ± 4.5 kg/m² in VC group, $p = 0.86$) or known history of PAD (9% in both groups). There was a trend of more patients being treated with peri-interventional dual antiplatelet therapy in the cohort of patients with VC (21.3 vs. 13.8%, $p = 0.08$).

CT Evaluation of Access Site Vessel

The evaluation of the preprocedural CT data revealed no significant difference in the diameter of the access vessel in patients treated with the BLE (7.5 ± 1.23 mm) or the MEV (7.36 ± 1.51 mm, $p = 0.30$). Seventeen patients (8.5%) treated with MEV had a vessel diameter smaller than the formally recommended 5.5 mm, 36 (18%) treated with BLE a had vessel diameter smaller than the recommended 6.5 mm. Patients with and without VC exhibited no relevant differences between the groups concerning access vessel characteristics as well (**Table 2**). Thirty-six percent of the patients without VC had calcification of the access vessel and 31.5% for the patients with VC ($p = 0.43$).

Procedural Data

The most frequently implanted size of BLE was 25 mm (43%), followed by 27 mm (38%), and 23 mm (19% of BLE). For the MEV, the most frequently implanted size was 29 mm (35.5%) followed by 26 mm (29%), 34 mm (28%), and 23 mm (7.5%). The procedural data with respect to VC are shown in **Table 3**. Patients receiving MEV had minor VC more often (64 vs. 36% $p = 0.003$), whereas major VC differed only numerically without statistical significance (2 vs.0.5%, $p = 0.18$). In relation to the difference in valve type distribution concerning VC outer sheath/delivery, the catheter diameter was smaller in patients with VC. SFAR however was not associated with VC in the study cohort ($p = 0.74$ for SFAR derived from mean CFA diameter; $p = 0.18$ for SFAR derived from minimal CFA diameter.) The results of the final angiography of the access site after use of the closure device (and before possible intervention are displayed in **Figure 4**. A leak of any sort was quite frequent with the 41.5%, however, the results of the angiography were not predictive for VC.

Postprocedural Data

Bleeding complications occurred in 50 patients (12.5%), most of them being minor bleedings (33 patients, 8.25%) due to access site or non-access site hematoma. Twelve patients developed major bleedings (3%) and five patients had life-threatening

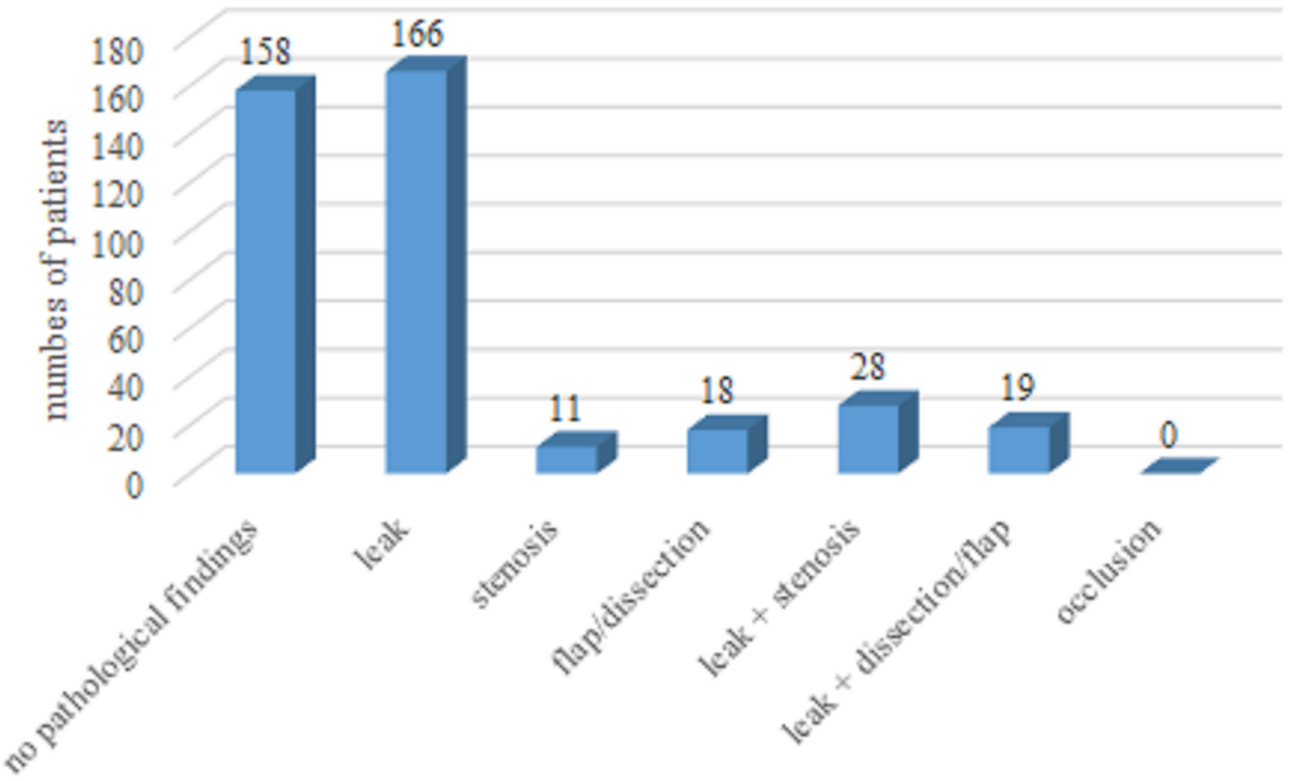

FIGURE 4 | Results of the angiogram of the access site after use of the closure device.

TABLE 4 | Procedural outcome.

	No VC $n = 311$	VC $n = 89$	*P*-Value
Device success	305 (98.1%)	87 (97.8%)	0.85
Periprocedural stroke/TIA	10 (3.3)	4 (4.5%)	0.56
Pacemaker implantation	67 (21.5%)	10 (11.2%)	0.03
Bleeding complications			
Minor bleeding	17 (5.5%)	16 (18.0%)	0.0002
Major bleeding	6 (1.9%)	6 (6.7%)	0.02
Life threatening bleeding	4 (1.2%)	1(1.1%)	0.90

Values are mean ± SD or n (%).
TIA, transitory ischemic attack.

bleedings, none of these access sites or non-access sites related there being two periprocedural intracerebral bleedings and three hemorrhagic pericardial effusions after pacemaker implantation after TAVI. Due to the definition of vascular complications minor and major bleeding complications occurred significantly more often in the group of patients with VC. The postprocedural pacemaker implantation rate was 19.25% for the overall population, significantly more frequent after treatment with the BLE (25%) compared with the MEV (13.5%, $p = 0.004$). The rate of device success was high at 98%. Data on postprocedural outcomes concerning VC are presented in **Table 4**.

Logistic Regression Analysis

The parameters that were distributed significantly different between groups or had been identified to be predictive of VC in previous studies such as age, gender, body mass index (BMI), PAD, large sheath size, SFAR, calcification, and DAPT were entered into a univariate and multivariate logistic regression analysis (**Table 5**). Peri-interventional treatment with DAPT showed to be an independent predictor for VC (OR 2.11, 95% CI 1.10–4.06, $p = 0.025$). Large sheath size was not independently associated with a higher rate of vascular complications.

DISCUSSION

With the use of the newest generation TAVI devices, MEV and BLE, we report a low rate of access site-related major VC with only 1.25%. Facing the low event rate, specific predictors of major VC could not be determined in this study. For the whole entity of VC combining major and minor VC peri-interventional treatment with DAPT showed to be an independent predictor for the occurrence of VC. We could not verify any of the other previous studies that identified predictors of VC.

The data on VC with the newer generation TAVI devices are still limited, most of the studies have evaluated the balloon-expandable valve with its expandable sheath. There are only a few studies on the MEV Pro valve: Major VC ranging from 0 to 10% in the first two studies, with only 60 and 74 patients, however,

TABLE 5 | Predictors of vascular complications.

	Univariate analysis		Multivariate analysis	
	OR (95% CI)	***P*-Value**	**OR (95% CI)**	***P*-Value**
Age	0.98 (0.94–1.01)	0.24	0.98 (0.94–1.02)	0.30
Gender (female)	0.82 (0.51–1.31)	0.40	0.75 (0.44–1.30)	0.31
BMI	1.00 (0.96–1.05)	0.86	–	–
BMI ≥25 kg/m²	0.69 (0.41–1.15)	0.14	0.69 (0.41–1.19)	0.19
SFAR (mean diameter)	1.19 (0.42–4.0)	0.74	–	–
SFAR > 1.05 (mean diameter)	0.95 (0.58–1.55)	0.84	1.18 (0.66–2.08)	0.58
Calcification of CFA	0.82 (0.49–1.35)	0.42	0.83 (0.48–1.42)	0.48
Known PAD	1.0 (0.44–2.28)	1.0	0.95 (0.40–2.25)	0.90
DAPT	1.69 (0.93–3.08)	0.09	2.11 (1.10–4.06)	0.025
20French sheath	0.48 (0.30–0.78)	0.0025	0.43 (0.25–0.74)	0.002

OR, odds ratio; CI, 95% confidence interval; BMI, body mass index; SFAR, sheath to femoral artery ratio; CFA, common femoral artery; PAD, peripheral artery disease; DAPT, dual antiplatelet therapy.

the largest published study cohort with 629 patients treated with the MEV Pro (and thus the EnveoPro delivery system) had a rate of only 3.3% major VC (15, 16, 23). Concerning the BLE valve there are no comparable data published yet, however, rates of major VC with its predecessor, the Boston Lotus valve were slightly higher ranging from 2.9 to 7.5% (23, 24). Our even lower rate of major VC in this study could be explained by the fact that the evaluated study cohort recently treated between 2019 and 2020, consisted of a lower risk cohort with a Society of Thoracic Surgeons–predicted risk of mortality (STS-PROM)-score <4%, furthermore, the study center being a high volume TAVI center with more than 400 procedures per year with a consistent team of experienced operators. In an analysis from the France TAVI Registry, Beurtheret et al. found a decline in major vascular complications between the period 2013–2015 and 2016/2017 of 1.44 to 1.02% ($p = 0.005$) and referring this to the increase in performed TAVI procedures from the first to the second period (25).

Despite the low rate of major VC, access site-related minor VC was still frequent with 21%., because of a high rate of minor VC, mainly due to local hematoma occurring in the postprocedural period. The incidence of minor VC varies widely in the literature from 2 to almost 30% if mentioned at all in publications. For studies with retrospective analysis, this could be explained by center-specific differences in thoroughness on documentation of clinically non-significant access site hematoma, which already accounts as minor VC according to the VARC-2 criteria. In contrast to the negative impact of major VC on mortality, there is no evidence, that minor VC is associated with increased mortality or increased length of hospital stay (8).

Vessel Size/Sheath Size

In TAVI studies or studies about large endovascular access for percutaneous procedures, a variety of parameters have been indicated to influence the occurrence of VC. The most obvious seems to be the size of the access vessel, respectively, sheath size, and sheath to access site vessel ratio. Especially the ratio of the sheath to the (ilio)-femoral vessel at the access site has been described as a predictor for major VC. In the study by Hayashida et al., an SFAR threshold of 1.05 was found to be predictive for major VC, in the study by Toggweiler et al., a threshold of 1.0 (7, 8). For the newer generation, TAVI devices S(I)FAR has been confirmed as a predictor for major VC by van Kesteren et al. for the balloon-expandable Edwards Sapien 3 valve and its expandable sheath [unadjusted OR 7.51 (1.61–34.95), $p = 0.01$)], though the area under the curve was much lower in comparison to studies describing S(I)FAR with older generation TAVI devices, indicating poorer accuracy (13). Potluri et al. also experienced SFAR as independently associated with VC, again, a study with the Edwards Sapien 3 as the most commonly used device with its expandable sheath (19). To our knowledge, there are no published data on predictors of VC concerning the ratio of the sheath to the access site vessel regarding new generation non-expandable sheaths. In contrast to previous studies, especially the large meta-analysis by Ueshima et al. we evaluated a recently treated low-risk patient cohort with low STS-PROM score, low rate of PAD, and use of new generation non-expandable sheaths, which might have led to the fact, that we did not experience higher rates of VC in patients with the use of the larger sheath or a higher SFAR (17). Furthermore, we only used the ProGlide vascular closure device, whereas, in older studies, other vascular closure devices as the Prostar (Abbott Vascular, Santa Clara, CA, USA) had still been in use. Mehilli et al. (12) and Seeger et al. (10) could both show in their studies that there were significantly fewer VC complications and bleeding complications with the use of ProGlide in comparison to the Prostar device.

A certain bias of not treating patients with more complex vascular access routes and smaller diameters with the larger sheath TAVI device cannot be completely excluded since the choice of the used TAVI device was not defined by a prospective randomized study design. However, there was no significant difference in vessel diameters concerning the CFA between the two valve types. Interestingly, the logistic regression analysis showed the larger sheath size to be associated with less VC, however, that statement has its limitations since this was contrary to the initial approach on this study and its power

calculation. A further explanation could lay within the necessity of removal of the sheath for the smaller sheath size (MEV) before insertion of the delivery system with subsequent intermittent manual compression.

Throughout the published studies on VC, the measurement of SFAR does not seem to be consistently defined. In some studies, the reference for the sheath diameter is the inner diameter, in others the outer diameter. This is correlated to the mean or the minimal diameter of the access vessel or even concerning the smallest diameter of the complete iliofemoral vessel length.

Calcification

There is no unified definition/quantification of access vessel calcification yet. We tried to construct a simple semi-quantitative definition based on the CT data. However, we failed to identify severe calcification or calcification in general of the CFA as a predictor for major or minor VC. Some older reports have demonstrated that iliofemoral calcification, assessed semi-quantitatively and slightly different in every report, is predictive of major VC (7). However, newer reports with more detailed CT evaluation of calcification, as Fonseca et al. who defined specific calcium thresholds, could not confirm this (14).

Periprocedural Medication

Dual antiplatelet therapy (DAPT) is known to increase bleeding risk in general and in TAVI, if that translates to a higher risk of VC is still not evident. Hioki et al. evaluated 540 TAVI patients and found DAPT to be a significant predictor for bleedings, however, this did not translate into a higher rate of VC, with only approximately one-third of bleedings being associated with the access site (26). In our study cohort, peri-interventional treatment with DAPT was independently associated with a higher rate of VC.

Peripheral Artery Disease

The presence of PAD seems to be an obvious parameter for the occurrence of VC, though existing data are not consistent. In previous studies, that have identified PAD as a predictor for VC, the rate of VC usually varied around 20% (13, 17). In our study, we could not confirm the influence of that parameter, however, we only saw a low rate of reported PAD with 9% in our study cohort, as well as Fonseca et al. who described a rate of 11.4% and could not identify PAD as a predictor for VC as well (14). The low reported incidence of reported PAD in our cohort may be attributed to the cohort being a low-risk cohort with a mean STS-PROM of <4%.

LIMITATIONS

Our study has several limitations. First, it is a retrospective single-center analysis. The lack of randomization may influence the selection of patients and outcomes. As for the documentation of minor vascular complications, not every patient had a duplex ultrasound of the access site post procedurally, only those with already clinically suspected pathological findings. Therefore, it is possible to have overlooked some minor VC complications.

The study was powered for the parameter sheath size and a difference of at least 10%. Therefore, we cannot derive definitive conclusions on other parameters, and cannot exclude, that smaller differences in predicting values of sheath diameter are present and are not detected for power limitations.

CONCLUSION

With the newest generation of TAVI devices, major VC seems to have reached the bottom line. The incidence of VC was low and most of the previously detected potential risk factors showed no relevant influence on the occurrence of VC in general in our study population of 400 patients, neither on major VC and thus did not offer potential angles for optimization. Only peri-interventional treatment with DAPT was associated with the occurrence of VC. Most likely, these low major VC rates are nowadays achieved by device improvements concerning sheaths and delivery systems, profound knowledge of performing percutaneous vascular access with large diameters, and well-established endovascular treatment options in case of need.

DATA AVAILABILITY STATEMENT

The raw data supporting the conclusions of this article will be made available by the authors, without undue reservation.

ETHICS STATEMENT

The studies involving human participants were reviewed and approved by Ethics Committee of the University of Ulm, Ulm Germany. The patients/participants provided their written informed consent to participate in this study.

AUTHOR CONTRIBUTIONS

BG: conceptualization, investigation, validation, methodology, formal analysis, and writing-original draft. CR and JM: investigation and data curation. WR: funding acquisition conceptualization, investigation, supervision, writing-review, and editing. DB: conceptualization, investigation, methodology, formal analysis, supervision, writing-review, and editing. All persons who meet the authorship criteria are listed as authors, certify that they have participated sufficiently in the work to take public responsibility for the content, including participation in the concept, design, analysis, writing, or revision of the manuscript, and provided critical feedback to the manuscript and approved the final version of the manuscript.

FUNDING

For the conduction of the study, the Department of Internal Medicine II, University of Ulm, received restricted funds from Medtronic (Medtronic Minneapolis, Minnesota, USA). The funder was not involved in the study design, collection, analysis, interpretation of data, the writing of this article, or the decision to submit it for publication.

REFERENCES

1. Cribier A, Eltchaninoff H, Bash A, Borenstein N, Tron C, Bauer F, et al. Percutaneous transcatheter implantation of an aortic valve prosthesis for calcific aortic stenosis: first human case description. *Circulation.* (2002) 106:3006–8. doi: 10.1161/01.CIR.0000047200.36165.B8
2. Makkar RR, Fontana GP, Jilaihawi H, Kapadia S, Pichard AD, Douglas PS, et al. Transcatheter aortic-valve replacement for inoperable severe aortic stenosis. *N Engl J Med.* (2012) 366:1696–704. doi: 10.1056/NEJMoa1202277
3. Reardon MJ, Van Mieghem NM, Popma JJ, Kleiman NS, Sondergaard L, Mumtaz M, et al. Surgical or transcatheter aortic-valve replacement in intermediate-risk patients. *N Engl J Med.* (2017) 376:1321–31. doi: 10.1056/NEJMoa1700456
4. Anantha-Narayanan M, Kandasamy VV, Reddy YN, Megaly M, Baskaran J, Pershad A, et al. Low-Risk transcatheter versus surgical aortic valve replacement - an updated meta-analysis of randomized controlled trials. *Cardiovasc Revasc Med.* (2020) 21:441–52. doi: 10.1016/j.carrev.2019.08.003
5. Pascual I, Carro A, Avanzas P, Hernandez-Vaquero D, Diaz R, Rozado J, et al. Vascular approaches for transcatheter aortic valve implantation. *J Thorac Dis.* (2017) 9 (Suppl. 6):S478–87. doi: 10.21037/jtd.2017.05.73
6. Genereux P, Head SJ, Van Mieghem NM, Kodali S, Kirtane AJ, Xu K, et al. Clinical outcomes after transcatheter aortic valve replacement using valve academic research consortium definitions: a weighted meta-analysis of 3,519 patients from 16 studies. *J Am Coll Cardiol.* (2012) 59:2317–26. doi: 10.1016/j.jacc.2012.02.022
7. Toggweiler S, Gurvitch R, Leipsic J, Wood DA, Willson AB, Binder RK, et al. Percutaneous aortic valve replacement: vascular outcomes with a fully percutaneous procedure. *J Am Coll Cardiol.* (2012) 59:113–8. doi: 10.1016/j.jacc.2011.08.069
8. Hayashida K, Lefevre T, Chevalier B, Hovasse T, Romano M, Garot P, et al. Transfemoral aortic valve implantation new criteria to predict vascular complications. *JACC Cardiovasc Interv.* (2011) 4:851–8. doi: 10.1016/j.jcin.2011.03.019
9. Gurvitch R, Toggweiler S, Willson AB, Wijesinghe N, Cheung A, Wood DA, et al. Outcomes and complications of transcatheter aortic valve replacement using a balloon expandable valve according to the valve academic research consortium (VARC) guidelines. *EuroIntervention.* (2011) 7:41–8. doi: 10.4244/EIJV7I1A10
10. Seeger J, Gonska B, Rodewald C, Rottbauer W, Wohrle J. Impact of suture mediated femoral access site closure with the prostar XL compared to the ProGlide system on outcome in transfemoral aortic valve implantation. *Int J Cardiol.* (2016) 223:564–7. doi: 10.1016/j.ijcard.2016.08.193
11. Ducrocq G, Francis F, Serfaty JM, Himbert D, Maury JM, Pasi N, et al. Vascular complications of transfemoral aortic valve implantation with the edwards SAPIEN prosthesis: incidence and impact on outcome. *EuroIntervention.* (2010) 5:666–72. doi: 10.4244/EIJV5I6A110
12. Mehilli J, Jochheim D, Abdel-Wahab M, Rizas KD, Theiss H, Spenkuch N, et al. One-year outcomes with two suture-mediated closure devices to achieve access-site haemostasis following transfemoral transcatheter aortic valve implantation. *EuroIntervention.* (2016) 12:1298–304. doi: 10.4244/EIJV12I10A213
13. van Kesteren F, van Mourik MS, Vendrik J, Wiegerinck EMA, Henriques JPS, Koch KT, et al. Incidence, predictors, and impact of vascular complications after transfemoral transcatheter aortic valve implantation with the SAPIEN 3 prosthesis. *Am J Cardiol.* (2018) 121:1231–8. doi: 10.1016/j.amjcard.2018.01.050
14. Fonseca P, Almeida J, Bettencourt N, Ferreira N, Carvalho M, Ferreira W, et al. Incidence and predictors of vascular access site complications following transfemoral transcatheter aortic valve implantation. *Rev Port Cardiol.* (2017) 36:747–53. doi: 10.1016/j.repc.2015.11.009
15. Hellhammer K, Piayda K, Afzal S, Kleinebrecht L, Makosch M, Hennig I, et al. The latest evolution of the medtronic CoreValve system in the era of transcatheter aortic valve replacement: matched comparison of the evolut PRO and evolut R. *JACC Cardiovasc Interv.* (2018) 11:2314–22. doi: 10.1016/j.jcin.2018.07.023
16. Forrest JK, Mangi AA, Popma JJ, Khabbaz K, Reardon MJ, Kleiman NS, et al. Early outcomes with the evolut PRO repositionable self-expanding transcatheter aortic valve with pericardial wrap. *JACC Cardiovasc Interv.* (2018) 11:160–8. doi: 10.1016/j.jcin.2017.10.014
17. Ueshima D, Barioli A, Nai Fovino L, D'Amico G, Fabris T, Brener SJ, et al. The impact of pre-existing peripheral artery disease on transcatheter aortic valve implantation outcomes: a systematic review and meta-analysis. *Catheter Cardiovasc Interv.* (2020) 95:993–1000. doi: 10.1002/ccd.28335
18. Chen IM, Lee TH, Chen PL, Shih CC, Chang HH. Factors in ProGlide(R) vascular closure failure in sheath arteriotomies greater than 16 french. *Eur J Vasc Endovasc Surg.* (2019) 58:615–22. doi: 10.1016/j.ejvs.2019.03.037
19. Potluri SP, Hamandi M, Basra SS, Shinn KV, Tabachnick D, Vasudevan A, et al. Comparison of frequency of vascular complications with ultrasound-guided versus fluroscopic roadmap-guided femoral arterial access in patients who underwent transcatheter aortic valve implantation. *Am J Cardiol.* (2020) 132:93–9. doi: 10.1016/j.amjcard.2020.07.013
20. Barbanti M, Binder RK, Freeman M, Wood DA, Leipsic J, Cheung A, et al. Impact of low-profile sheaths on vascular complications during transfemoral transcatheter aortic valve replacement. *EuroIntervention.* (2013) 9:929–35. doi: 10.4244/EIJV9I8A156
21. Kappetein AP, Head SJ, Genereux P, Piazza N, van Mieghem NM, Blackstone EH, et al. Updated standardized endpoint definitions for transcatheter aortic valve implantation: the valve academic research consortium-2 consensus document. *J Am Coll Cardiol.* (2012) 60:1438–54. doi: 10.1093/ejcts/ezs533
22. Baumgartner H, Falk V, Bax JJ, De Bonis M, Hamm C, Holm PJ, et al. 2017 ESC/EACTS guidelines for the management of valvular heart disease. *Eur Heart J.* (2017) 38:2739–91. doi: 10.1016/j.rec.2017.12.013
23. Reardon MJ, Feldman TE, Meduri CU, Makkar RR, O'Hair D, Linke A, et al. Two-Year outcomes after transcatheter aortic valve replacement with mechanical vs self-expanding valves: the REPRISE III randomized clinical trial. *JAMA Cardiol.* (2019) 4:223–9. doi: 10.1001/jamacardio.2019.0091
24. Seeger J, Gonska B, Rottbauer W, Wohrle J. New generation devices for transfemoral transcatheter aortic valve replacement are superior compared with last generation devices with respect to VARC-2 outcome. *Cardiovasc Interv Ther.* (2018) 33:247–55. doi: 10.1007/s12928-017-0477-6
25. Beurtheret S, Karam N, Resseguier N, Houel R, Modine T, Folliguet T, et al. Femoral versus nonfemoral peripheral access for transcatheter aortic valve replacement. *J Am Coll Cardiol.* (2019) 74:2728–39. doi: 10.1016/j.jacc.2019.09.054
26. Hioki H, Watanabe Y, Kozuma K, Nara Y, Kawashima H, Kataoka A, et al. Pre-procedural dual antiplatelet therapy in patients undergoing transcatheter aortic valve implantation increases risk of bleeding. *Heart.* (2017) 103:361–7. doi: 10.1136/heartjnl-2016-309735

Conflict of Interest: The authors declare that the research was conducted in the absence of any commercial or financial relationships that could be construed as a potential conflict of interest.

frontiers in Cardiovascular Medicine

ORIGINAL RESEARCH
published: 17 December 2021
doi: 10.3389/fcvm.2021.745370

Long-Term Outcomes of Bioprosthetic or Mechanical Valve Replacement in End-Stage Renal Disease: A Nationwide Population-Based Retrospective Study

Guan-Yi Li[1†], *Yun-Yu Chen*[1,2†], *Fa-Po Chung*[1,3*], *Kuo-Liong Chien*[2], *Chiao-Po Hsu*[3,4*] and *Yenn-Jiang Lin*[1,3]

[1] Division of Cardiology, Department of Medicine, Taipei Veterans General Hospital, Taipei, Taiwan, [2] Institute of Epidemiology and Preventive Medicine College of Public Health, National Taiwan University, Taipei, Taiwan, [3] Cardiovascular Research Center, Institute of Clinical Medicine, National Yang-Ming University, Taipei, Taiwan, [4] Division of Cardiovascular Surgery, Department of Surgery, Taipei Veterans General Hospital, Taipei, Taiwan

OPEN ACCESS

Edited by:
Peter Zilla,
University of Cape Town, South Africa

Reviewed by:
Simon Kraler,
University of Zurich, Switzerland
Paul Human,
University of Cape Town, South Africa

***Correspondence:**
Fa-Po Chung
marxtaiji@gmail.com
Chiao-Po Hsu
hsucp@vghtpe.gov.tw

[†]These authors have contributed equally to this work and share first authorship

Specialty section:
This article was submitted to Heart Valve Disease, a section of the journal Frontiers in Cardiovascular Medicine

Received: 21 July 2021
Accepted: 29 November 2021
Published: 17 December 2021

Citation:
Li G-Y, Chen Y-Y, Chung F-P, Chien K-L, Hsu C-P and Lin Y-J (2021) Long-Term Outcomes of Bioprosthetic or Mechanical Valve Replacement in End-Stage Renal Disease: A Nationwide Population-Based Retrospective Study. Front. Cardiovasc. Med. 8:745370. doi: 10.3389/fcvm.2021.745370

Background: Valve replacement is associated with worse outcomes in individuals who have end-stage renal disease (ESRD) and require a long-term renal replacement therapy. Prosthetic valve selection in patients with ESRD has remained controversial.

Objective: We aimed to investigate long-term outcomes of mechanical and bioprosthetic valve replacement in individuals with ESRD.

Methods: We conducted a population-based retrospective cohort study using data obtained from the Taiwan National Health Insurance Research Database. In total, 10,202 patients, including 912 ESRD and 9,290 non-ESRD patients, were selected after a 1:1 propensity-score matching based on the type of prosthetic valve used. The long-term mortality outcomes were then analyzed.

Results: During a median follow-up period of 59.6 months, the Kaplan–Meier survival analysis revealed that ESRD patients who underwent mechanical valve replacement had higher rates of all-cause mortality and CV deaths than those who underwent bioprosthetic valve replacement (Log-rank test, $p = 0.03$ and 0.02, respectively). Multivariable regression analyses demonstrated that ESRD patients who underwent bioprosthetic valve replacement had lower rates of all-cause mortality ($p < 0.001$, hazard ratio: 0.88, 95% confidence interval: 0.82–0.93) and cardiovascular (CV) death ($p < 0.001$, hazard ratio: 0.83, 95% confidence interval: 0.76–0.90) than those who had mechanical valve replacement.

Conclusion: Bioprosthetic valve replacement is significantly associated with lower rates of all-cause mortality and CV death in the ESRD population.

Keywords: bioprosthetic valve, cardiovascular event, end-stage renal disease, valve replacement, mechanical valve, mortality

INTRODUCTION

Choosing a prosthetic heart valve can be clinically challenging, and it is commonly based on several factors, such as age, underlying disease requiring the use of anticoagulants, risk of bleeding and thromboembolism, durability of the prosthesis, patients' preferences, and risk of structural deterioration requiring re-interventions (1, 2). Of note, the type of valve prosthesis that should be used in a specific population with comorbidity, including end-stage renal disease (ESRD), has been debated for decades (3–7).

It has long been established that the abnormal calcium and phosphate metabolism due to ESRD is related to calcification and degenerative valvular lesions, which may be explained by an active regulated process associated with an osteoblast-like phenotype (8–11). It results in a major concern regarding structural destruction of the bioprosthetic valves in ESRD. Thus, mechanical valves were previously recommended for ESRD patients (12).

In contrast, patients with ESRD receiving anticoagulants are at higher risk of bleeding, (13, 14) metastatic calcification, and even calciphylaxis (15, 16). In addition, ESRD patients have a short life expectancy. As a result, the increased durability of a mechanical valve may only benefit a small portion of ESRD patients (17–22).

The number of studies investigating the clinical outcome between dialysis patients who had bioprosthetic and mechanical valve replacement is increasing worldwide (23–25). However, owing to the limited sample size, non-uniform characteristics, and emerging advancements in prosthesis and clinical care of dialysis patients, previous studies had conflicting results, and some have shown a similar survival between dialysis patients who had mechanical and bioprosthetic valve replacement (26–30). Thus, the abovementioned findings were not validated in a large-scale nationwide population study. Furthermore, no specific recommendation regarding the selection of prosthetic valves for patients with ESRD was provided in the contemporary guideline (31).

This nationwide population-based study aimed to assess long-term outcomes and associated cardiovascular (CV) events in ESRD patients who underwent bioprosthetic and mechanical valve replacement. We believe that the abovementioned findings could provide insight on decision-making regarding the selection of prosthetic valves among ESRD patients.

MATERIALS AND METHODS

Study Design and Participants

We conducted a population-based retrospective cohort study, and data were collected from January 1, 2000 to December 31, 2011. The patients who underwent the first valve replacement surgery, without previous or concomitant valve repair, were identified using information from the National Health Insurance Research Database (NHIRD), and they were grouped based on the procedure code of the Specifications of the National Voluntary Consensus Standards for Cardiac Surgery: bioprosthetic valve replacement (procedure code: 35.21, 35.23, 35.25, and 35.27) and mechanical valve replacement (procedure code: 35.22, 35.24, 35.26, and 35.28).

This study was approved in accordance with the Good Clinical Practice Guidelines by the Research Ethics Committee C of the National Taiwan University Hospital.

Databases and Specifications of the Characteristics of the Participants

The Taiwan Collaboration Center of Health Information Application, Ministry of Health and Welfare, provided all the datasets of the NHIRD. The Taiwan's National Health Insurance (NHI) program enrolled 23 million people, which covered 99% of the country's population and included utilization of all NHI resources, including outpatient visits, hospital care, prescribed medications, and the National Death Registry. We obtained permission for the rights from the National Research Institute for the Department of Health and the Health Promotion Administration, Ministry of Health and Welfare. The underlying diseases were identified according to the International Classification of Diseases, 9th Revision—Clinical Modification (ICD 9-CM) codes. The diagnosis must be recorded twice in the outpatient records or at least once in the inpatient records. By linking to the NHIRD, we identified clinical variables, such as age (years), sex, type of valve replacement, number of valve replacements, and presence of chronic kidney disease, congestive heart failure, acute coronary diseases, chronic obstructive pulmonary disease, and thyroid diseases. The selection and grouping of medications were based on the guidelines of the Anatomical Therapeutic Chemical classification system by the World Health Organization.

Patients diagnosed with ESRD were identified using the order codes (**Supplementary Material**) of hemodialysis, peritoneal dialysis, and other types of dialysis for at least 3 months (32). In this study, we excluded individuals who were younger than 20 years, underwent both bioprosthetic and mechanical valve replacement, or presented with lethal ventricular arrhythmias before the procedures. In addition, no patient underwent kidney transplantation prior to enrollment.

Study Endpoints During the Long-Term Follow-Up

The primary endpoints were all-cause mortality and CV death (ICD 9-CM codes 390–429) during follow-up. Death was confirmed using data from the Taiwan's National Death Registry. Follow-up was terminated in case of death or if the patients lived beyond December 31, 2016.

Statistical Analysis

The normally distributed continuous variables are presented as mean values ± standard deviation, and non-normally distributed continuous variables are presented as medians with 25 and 75% interquartile ranges (IQRs). Student's *T*-test was utilized to compare two groups. For testing the distribution of general continuous variable such as age, the normality test was performed

Abbreviations: CI, confidence interval; CV, cardiovascular; ESRD, end-stage renal disease; HR, hazard ratio; IQR, interquartile range; NHIRD, National Health Insurance Research Database; PSM, propensity-score matching.

before the Student's *T*-test. Categorical variables were expressed as numbers and percentages and were compared using the chi-square test. The incidence rates of CV events were calculated as the number of cases per 1,000 person-years during follow-up. Propensity-score matching for patients receiving the mechanical valve replacement and the bioprosthetic valve replacement as exposures were performed to minimize the impact of the confounding factors on the clinical outcomes, including age, sex, hypertension, diabetes mellitus, chronic obstructive pulmonary disease, congestive heart failure, stroke, and total number of valves replaced. A one-to-one matching of pairs was conducted using identical propensity scores with a 0.15 caliper width.

The event-free survival curve was plotted using the Kaplan–Meier method with the statistical significance examined using the Log-rank test. The conditional Cox proportional-hazards regression model was utilized to compare the hazard ratios (HRs), with 95% confidence intervals (CIs), of the outcomes. The potential confounders were adjusted using three models (Model 1: age and sex; Model 2: Model 1 plus total number of valves replaced, hypertension, diabetes mellitus, congestive heart failure, coronary artery diseases, and chronic obstructive pulmonary disease; and Model 3: Model 2 plus the use of medications (antiarrhythmic agents of Ia Ib, Ic, III, calcium channel blockers, angiotensin receptor blockers, statins, insulin, and oral hypoglycemic agents). The level of statistical significance was set at a two-tailed alpha level <0.05. The analyses were performed with SAS software (version 9.4, SAS Institute, Cary, NC).

RESULTS

Selection and Characteristics of the Study Population

In total, 19,528 patients who had their first valve replacement were identified in the NHIRD. After excluding 883 patients according to the exclusion criteria, 18,645 were included in the original cohort (**Supplementary Table 1**), and 10,202 patients were selected after propensity-score matching (PSM) (**Supplementary Table 2**). After PSM, 9,290 and 912 patients were included in the non-ESRD group and ESRD group, respectively. Both groups had equal number of patients who had mechanical and bioprosthetic valve replacement (**Figure 1**, **Table 1**, **Supplementary Table 3**).

After PSM, a higher number of patients in the ESRD group underwent bioprosthetic valve replacement for the tricuspid valve (5.9 vs. 2.9%, $p = 0.02$; **Table 1**). In the ESRD group, the baseline characteristics were comparable between patients who had mechanical and bioprosthetic valve replacement, except that a high number of patients with mechanical valve replacement had a history of coronary artery disease (11.6 vs. 5.3%, $p < 0.001$). This could be a potential confounder and was further adjusted by the three models in the conditional Cox regression analysis.

Mortality and CV Events

Crude Incidence Rate

The median follow-up period was 59.6 months (25–75%, IQR: 22.8–108.9) after PSM. In patients without ESRD, the crude incidence rates of all-cause mortality were 80.2 and 80.3/1,000-person-years in patients who had mechanical and bioprosthetic valve replacement, respectively, and the crude incidence values of CV deaths were 43.4 and 41.4/1,000 person-years in patients who had mechanical and bioprosthetic valve replacement, respectively (**Supplementary Table 4**). In contrast, ESRD patients who underwent mechanical valve replacement had a higher rate of all-cause mortality (457.4/1,000 vs. 426.8/1,000 person-years) and CV death (262.0/1,000 vs. 218.7/1,000 person-years) than those who had bioprosthetic valve replacement (**Table 2**).

Kaplan–Meier Survival Analysis

The Kaplan–Meier survival analysis revealed that the all-cause mortality and CV deaths were comparable between non-ESRD patients who underwent mechanical and bioprosthetic valve replacement during the 5-year follow-up (Log-rank test, $p = 0.88$ and 0.58, respectively; **Supplementary Figures 1A,B**). Meanwhile, ESRD patients who underwent mechanical valve replacement had higher rates of all-cause mortality and CV deaths than those who underwent bioprosthetic valve replacement after the 5-year follow-up (Log-rank test, $p = 0.03$ and 0.02, respectively; **Figures 2A,B**).

Multivariable Regression Analysis

After adjusting for the effects of age, sex, total number of valves replaced, underlying disease, and use of medications via a multivariable regression analysis, results showed a comparable future risk of all-cause mortality in non-ESRD patients who had mechanical and bioprosthetic valve replacement ($p = 0.12$, HR: 0.89, 95% CI: 0.77–1.03; **Supplementary Table 4**). However, non-ESRD patients who had bioprosthetic valve replacement had a significant decrease in the rate of CV deaths ($p = 0.04$, HR: 0.82, 95% CI: 0.67–0.99; **Supplementary Table 4**). In contrast, in ESRD patients, bioprosthetic valve replacement was significantly associated with a lower rate of all-cause mortality and CV deaths after adjusting for the confounding variables during the 5-year follow-up ($p < 0.001$, HR: 0.88, 95% CI: 0.82–0.93 and $p < 0.001$, HR: 0.83, 95% CI: 0.76–0.90, respectively; **Table 2**).

Short-Term Mortality and the Impact of Total Number of Valves Replaced

Regarding the perioperative and short-term mortality, the mortality rate occurring within 30 days after valve replacement was 19.2%, while the 1-year mortality rate was 63.6% in the present study.

In addition, the increasing total number of valves replaced was significantly associated with a higher rate of all-cause mortality and CV deaths both before and after adjusting for the confounding variables (in all models 0–3) during the 5-year follow-up in patients with ESRD (**Supplementary Table 5**).

DISCUSSION

Major Findings

The current nationwide population-based study revealed the long-term outcome of ESRD and non-ESRD patients who underwent mechanical and bioprosthetic valve replacement.

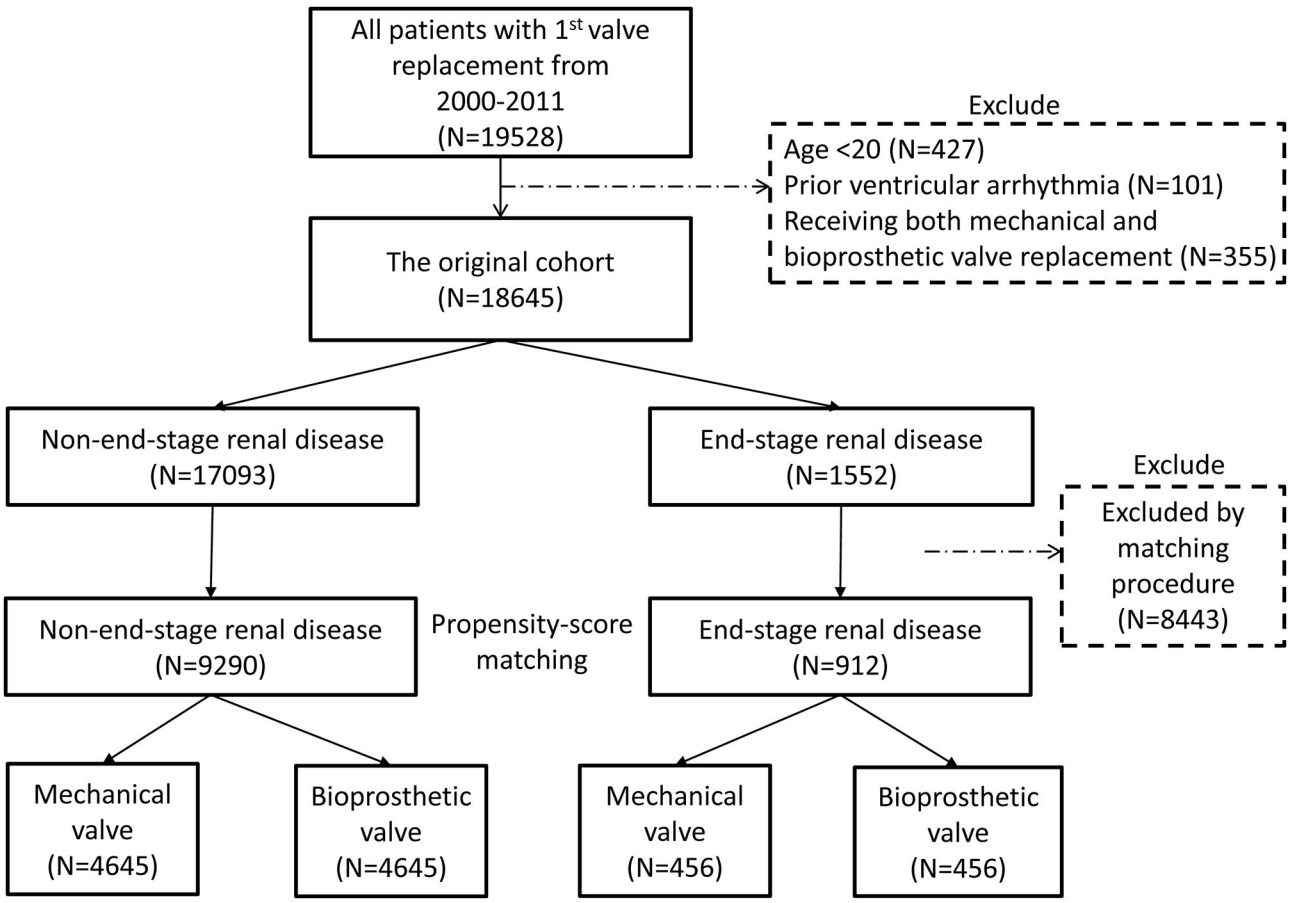

FIGURE 1 | Flow chart of the present study. The process of study population selection and propensity score matching is presented. After PSM, 9,290 and 912 patients were included in the non-ESRD group and ESRD group, respectively. Both groups had equal number of patients who had mechanical and bioprosthetic valve replacement. ESRD, end-stage renal disease; PSM, propensity score matching.

Firstly, despite the use of different types of valves for replacement, patients with ESRD before valvular surgery had a significantly worse outcome. Secondly, ESRD patients who had bioprosthetic valve replacement had a better long-term outcome in terms of all-cause mortality and CV deaths than those who underwent mechanical valve replacement.

Outcome of Valve Replacement in ESRD Patients

Based on the 2019 Annual Report on Kidney Disease in Taiwan, the overall survival at 1, 3, 5, and 10 years of ESRD patients in Taiwan are 88.7, 69.2, 54.3, and 29.8%, respectively. The present study demonstrated remarkably poorer survival outcomes in ESRD patients with surgical valve replacement. Previous studies have shown that ESRD patients who underwent valve replacement have poor long-term outcomes (17–21). Based on a pooled analysis of eight studies, Altarabsheh et al. (17) have revealed that the overall survival at 2, 4, and 6 years among ESRD patients who had valve replacement was 58, 38, and 29%, respectively (median survival = 2.61 years) (17). Williams et al. (18) have found that only about half of dialysis patients younger than 65 years survived beyond 2 years after valve replacement (18). Moreover, Böning et al. have reported that the median survival time of ESRD patients after aortic valve replacement is 24.7 months (20). All the aforementioned findings were consistent with our results which demonstrated that ESRD patients had a worse prognosis than non-ESRD patients after bioprosthetic and mechanical valve replacement. Nevertheless, the perioperative and short-term mortality rate was higher than most of the previous reports. Firstly, the possible explanation is the remarkably older age of both groups in the present study (mean age 67.4 for the mechanical valve and 66.8 for the bioprosthetic valve group). In addition, unlike previous trials which were mainly based on evidence from single tertiary or referral centers, this nationwide population-based study might have more scientific rigor and external validity to reflect the real-world prognosis of the general population and clinical practice.

The cause of the poor prognosis among ESRD patients who had valve replacement are complex and multifactorial. Firstly, the disturbance in mineral metabolism and increased calcium load due to calcium-based phosphorus binders in the ESRD population can result in vascular calcification, which plays a key role in CV death (33). Calcium and phosphorus dysregulation may accelerate the calcification and structural

TABLE 1 | Baseline characteristics of ESRD cohorts after propensity-score matching.

Variables	ESRD group (*N* = 912)		
	Mechanical valve (*N* = 456)	Bioprosthetic valve (*N* = 456)	*P* value
Age	67.4 ± 11.8	66.8 ± 11.9	0.51
Male gender	240 (52.6%)	254 (55.7%)	0.35
Valve location			
Aortic valve	242 (53.1%)	234 (51.3%)	0.60
Mitral valve	246 (53.9%)	254 (55.7%)	0.60
Tricuspid valve	13 (2.9%)	27 (5.9%)	0.02
Pulmonary valve	0 (0%)	3 (0.7%)	0.24
Total number of valves replaced	1.10 ± 0.30	1.14 ± 0.35	0.08
1	411 (90.1%)	395 (86.6%)	0.18
2	45 (9.9%)	59 (12.9%)	
3	0 (0%)	2 (0.44%)	
4	0 (0%)	0 (0%)	
Comorbidities			
ESRD (%)	456 (100%)	456 (100%)	>0.99
Diabetes mellitus (%)	16 (3.5%)	22 (4.8%)	0.32
Hypertension (%)	53 (11.6%)	62 (13.6%)	0.37
COPD (%)	4 (0.9%)	4 (0.9%)	>0.99
CHF (%)	118 (25.9%)	110 (24.1%)	0.54
Prior stroke (%)	16 (3.5%)	22 (4.8%)	0.32
Prior CAD (%)	53 (11.6%)	24 (5.3%)	0.001
Thyroid disease (%)	0 (0%)	0 (0%)	>0.99
Pharmacotherapy*			
AADs (%)	146 (32%)	175 (38.4%)	0.001
Class Ia	7 (1.5%)	8 (1.8%)	0.80
Class Ib	35 (7.7%)	42 (9.2%)	0.40
Class Ic	24 (5.3%)	29 (6.4%)	0.48
Class III	107 (23.5%)	138 (30.3%)	0.02
CCB (%)	203 (44.5%)	196 (42%)	0.64
ARB (%)	274 (60.1%)	322 (70.6%)	0.001
Statins (%)	184 (40.4%)	214 (46.9%)	0.045
Insulin (%)	134 (29.4%)	156 (34.2%)	0.12
OHA (%)	168 (36.8%)	192 (42.1%)	0.10

**Used from baseline till the end of follow-up.*

AAD, antiarrhythmic drugs; ARB, angiotensin receptor blockers; CAD, coronary artery disease; CCB, calcium channel blocker; CHF, congestive heart failure; COPD, chronic obstructive pulmonary disease; ESRD, end-stage renal disease; OHA, oral hypoglycemic agents.

destruction of valve bioprosthesis, which is mediated through a process of osteoblast-like differentiation on these structures (8–11). Moreover, several studies implicate that the host immune response is involved in a major pathogenesis of structural valve degeneration (34, 35). The persistent low-grade inflammation in patients with ESRD, which is associated with increased production and inadequate removal of pro-inflammatory cytokines, may accelerate the degeneration of bioprosthetic valves (36). On the other hand, a higher bleeding and thromboembolic risk has been observed in ESRD patients, (13, 14) particularly in those requiring anticoagulation therapy after mechanical valve replacement. Considering the abovementioned findings, the selection of valve for ESRD patients can be clinically challenging.

Long-Term Outcome of Mechanical and Bioprosthetic Valve Replacement Among ESRD Patients

To the best of our knowledge, this is the first large-scale study that compared the outcome of mechanical and bioprosthetic valve replacement in ESRD patients using data from a nationwide population-based database. Of note, in ESRD patients in this study, bioprosthetic valve replacement was found to be significantly associated with a lower rate of all-cause mortality and CV deaths compared to replacement with mechanical valves. However, this result was not in accordance with that of previous studies showing that ESRD patients who had mechanical vs. bioprosthetic valve replacement had a similar survival time (26–30). The heterogeneous results could be explained by the differences in sample size, follow-up duration, use of medications, presence of comorbidities, advances in the development of prosthetic devices, and improvement in clinical care for dialysis patients between this and the other studies. Notably, several drugs showed a greater distribution in the bioprosthetic valve group, including class III antiarrhythmic drugs, angiotensin receptor blockers, and statins. It suggests the higher prevalence of concealed comorbidities in ESRD patients. It also explains why the benefit of bioprosthetic valves in the ESRD patients could finally be revealed after all the probable bias was minimized in Model 3.

Clinically, the selection of different valves for replacement is based on several factors, and there is no randomized study that compared the long-term outcomes of ESRD patients who underwent different types of valve replacement. Conventionally, ESRD patients were thought to experience early structural deterioration of the bioprosthetic valve due to disturbance in calcium homeostasis (8, 9). However, some studies have reported that this phenomenon is relatively rare due to the limited life expectancy of this population (4, 25). In contrast, some studies have revealed that ESRD patients with mechanical valves more commonly present with bleeding or thromboembolic events than structural deterioration of bioprosthetic valves (17, 24, 27). Patients with ESRD receiving mechanical valve replacement require warfarin for stroke prevention, which is usually associated with a higher risk of bleeding event, metastatic calcification, and catastrophic calciphylaxis (15, 16). The aforementioned complications could increase the periprocedural mortality, as shown in the present findings. However, future prospective studies must be conducted to validate the findings of the current study and to identify ESRD patients who are eligible for bioprosthetic valve replacement.

Limitations

This study had some limitations. Firstly, this study is retrospective in nature, which might have caused inevitable

TABLE 2 | Incidence rates and effect sizes of outcomes by valve replacement status in ESRD group.

Outcomes	Variables	Total numbers	Event (%) / per 1,000 person-years	Models	Hazard ratios (95% CI)	*P* value
Total mortality	Patients with mechanical valve	456	412 (90.4%) / 457.4	0	1 (reference)	NA
				1		
				2		
				3		
	Patients with bioprosthetic valve	456	406 (89.0%) / 426.8	0	1.00 (0.95–1.06)	0.88
				1	0.98 (0.93–1.05)	0.55
				2	0.99 (0.93–1.05)	0.64
				3	0.88 (0.82–0.93)	<0.001
CV death	Patients with mechanical valve	456	236 (51.8%) / 262.0	0	1 (reference)	NA
				1		
				2		
				3		
	Patients with bioprosthetic valve	456	208 (45.6%) / 218.7	0	0.98 (0.90–1.06)	0.58
				1	0.96 (0.89–1.04)	0.29
				2	0.97 (0.89–1.05)	0.38
				3	0.83 (0.76–0.90)	<0.001

CI, confidence interval; CV, cardiovascular; ESRD, end-stage renal disease; NA, not available.
Model 0: crude effect size by the two groups.
Model 1: adjusted effect by age, sex.
Model 2: adjusted effect by age, sex, total number of valves replaced, hypertension, diabetes mellitus, congestive heart failure, coronary artery diseases, and chronic obstructive pulmonary disease.
Model 3: adjusted effect by age, sex, total number of valves replaced, hypertension, diabetes mellitus, congestive heart failure, coronary artery diseases, chronic obstructive pulmonary disease, and medications (antiarrhythmic agents of Ia Ib, Ic, III, calcium channel blockers, angiotensin receptor blockers, statins, insulin, oral hypoglycemic agents).

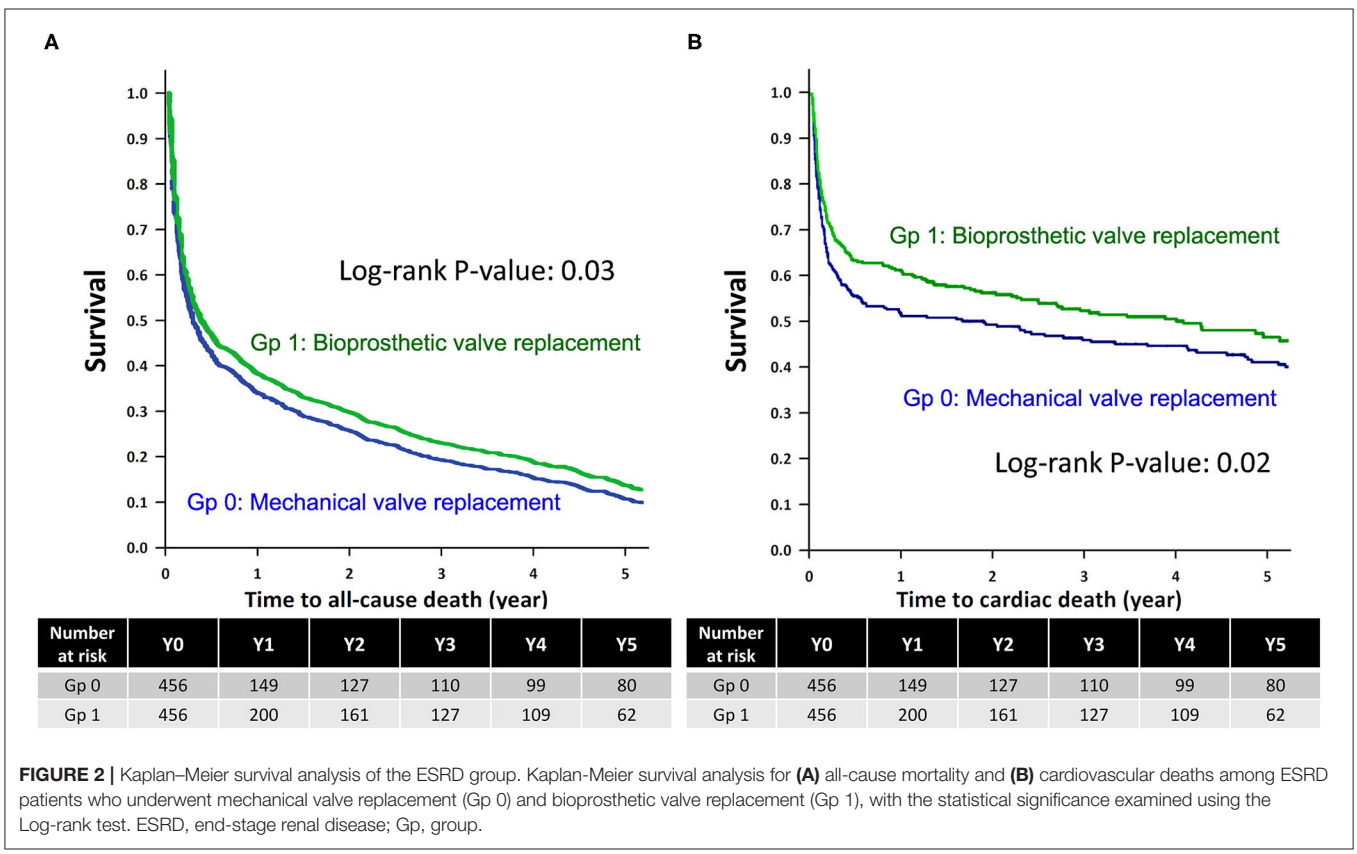

Number at risk	Y0	Y1	Y2	Y3	Y4	Y5
Gp 0	456	149	127	110	99	80
Gp 1	456	200	161	127	109	62

Number at risk	Y0	Y1	Y2	Y3	Y4	Y5
Gp 0	456	149	127	110	99	80
Gp 1	456	200	161	127	109	62

FIGURE 2 | Kaplan–Meier survival analysis of the ESRD group. Kaplan-Meier survival analysis for **(A)** all-cause mortality and **(B)** cardiovascular deaths among ESRD patients who underwent mechanical valve replacement (Gp 0) and bioprosthetic valve replacement (Gp 1), with the statistical significance examined using the Log-rank test. ESRD, end-stage renal disease; Gp, group.

bias. Given the entity of nationwide population-based study, additional information such as laboratory data, post-procedural complication and bleeding rate, causes of non-CV death, or causes of ESRD, cannot be retrieved from National Health Insurance Research Database. In addition, some detailed information was not available in the present study, including the presence of AF, concomitant CABG in valve replacement, specific cause of short-term mortality, or the survival data of ESRD patients without any valve replacement. However, our study can provide insight about clinical decision-making and can be used as a basis in further meta-analysis. Secondly, the baseline characteristics between the mechanical and bioprosthetic valve groups after PSM with potential covariates remained inconsistent. However, these potential confounders were all further adjusted by the three models in the conditional Cox regression analysis. We believe that the probable bias was minimized and assume that it's the reason why the benefit of bioprosthetic valves in the ESRD patients could finally be revealed. Third, diagnostic and procedure coding errors might exist. Nonetheless, the rate of coding error was supposed to be low because all data were double-checked by a professional coding team in each hospital before submission to the NHIRD. Fourth, this is a population-based study enrolling only people in Taiwan. It remains uncertain whether the findings are universal across various racial and ethnic groups in the world. In the end, based on the 2019 Annual Report on Kidney Disease in Taiwan, the majority of patients (around 90%) with ESRD received hemodialysis and <10% of ESRD patients undergoing peritoneal dialysis. Given the unbalanced distribution of hemodialysis vs. peritoneal dialysis and limited case numbers of study population, we didn't perform further analysis of the outcome between the above two groups. The further large cohort will be warranted for this investigation.

CONCLUSION

Preoperative ESRD was associated with a significantly worse outcome in patients who had valve replacement. Patients with ESRD who underwent bioprosthetic valve replacement had significantly better long-term outcomes, including a lower rate of all-cause mortality and CV deaths. However, to shed light on clinical decision-making in this specific population, future prospective cohort studies based on independent databases are warranted to validate the present findings.

DATA AVAILABILITY STATEMENT

The datasets presented in this study can be found in online repositories. The names of the repository/repositories and accession number(s) can be found in the article/**Supplementary Material**.

ETHICS STATEMENT

The studies involving human participants were reviewed and approved by Research Ethics Committee of the National Taiwan University Hospital. Written informed consent for participation was not required for this study in accordance with the national legislation and the institutional requirements.

AUTHOR CONTRIBUTIONS

All authors listed have made a substantial, direct, and intellectual contribution to the work and approved it for publication.

FUNDING

This work was supported by the Center for Dynamical Biomarkers and Translational Medicine, Ministry of Science and Technology (Grant Numbers 107-2314-B-010-061-MY2, MOST 106-2314-B-075-006-MY3, MOST 106-2314-B-010-046-MY3, and MOST 106-2314-B-075-073-MY3), Research Foundation of Cardiovascular Medicine, Szu-Yuan Research Foundation of Internal Medicine (Grant Number 107-02-036), and Taipei Veterans General Hospital (Grant Numbers V108C-032, V108C-107, V109C-113, V109D48-001-MY2-1, C17-095, V106C-158, V106C-104, V107B-014, V107C-060, and V107C-054).

SUPPLEMENTARY MATERIAL

The Supplementary Material for this article can be found online at: https://www.frontiersin.org/articles/10.3389/fcvm.2021.745370/full#supplementary-material

REFERENCES

1. Nishimura RA, Otto CM, Bonow RO, Carabello BA, Erwin JP 3rd, Fleisher LA, et al. 2017 AHA/ACC focused update of the 2014 AHA/ACC guideline for the management of patients with valvular heart disease: a report of the American College of Cardiology/American Heart Association task force on clinical practice guidelines. *Circulation*. (2017) 135:e1159–95. doi: 10.1161/CIR.0000000000000503
2. Baumgartner H, Falk V, Bax JJ, De Bonis M, Hamm C, Holm PJ, et al. 2017 ESC/EACTS guidelines for the management of valvular heart disease. *Rev Esp Cardiol.* (2018) 71:110. doi: 10.1016/j.rec.2017.12.013
3. Lucke JC, Samy RN, Atkins BZ, Silvestry SC, Douglas JM Jr, Schwab SJ, et al. Results of valve replacement with mechanical and biological prostheses in chronic renal dialysis patients. *Ann Thorac Surg.* (1997) 64:129–32; discussion 32–3. doi: 10.1016/S0003-497500342-1
4. Kaplon RJ, Cosgrove DM 3rd, Gillinov AM, Lytle BW, Blackstone EH, Smedira NG. Cardiac valve replacement in patients on dialysis: influence of prosthesis on survival. *Ann Thorac Surg.* (2000) 70:438–41. doi: 10.1016/S0003-497501544-7
5. Herzog CA, Ma JZ, Collins AJ. Long-term survival of dialysis patients in the United States with prosthetic heart valves: should ACC/AHA practice guidelines on valve selection be modified? *Circulation*. (2002) 105:1336–41. doi: 10.1161/hc1102.100075
6. Brinkman WT, Williams WH, Guyton RA, Jones EL, Craver JM. Valve replacement in patients on chronic renal dialysis: implications for valve prosthesis selection. *Ann Thorac Surg.* (2002) 74:37–42; discussion 42. doi: 10.1016/s0003-4975(02)03692-5

7. Chan V, Jamieson WR, Fleisher AG, Denmark D, Chan F, Germann E. Valve replacement surgery in end-stage renal failure: mechanical prostheses versus bioprostheses. *Ann Thorac Surg.* (2006) 81:857–62. doi: 10.1016/j.athoracsur.2005.09.009
8. Lamberti JJ, Wainer BH, Fisher KA, Karunaratne HB, Al-Sadir J. Calcific stenosis of the porcine heterograft. *Ann Thorac Surg.* (1979) 28:28–32. doi: 10.1016/S0003-497563387-5
9. Mao M, Madhavan M, Blauwet L, Schaff HV, Qian Q. Bioprosthetic tricuspid valve stenosis in end-stage renal failure. *Am J Med Sci.* (2012) 343:252–4. doi: 10.1097/MAJ.0b013e318238e92d
10. Bohbot Y, Candellier A, Diouf M, Rusinaru D, Altes A, Pasquet A, et al. Severe aortic stenosis and chronic kidney disease: outcomes and impact of aortic valve replacement. *J Am Heart Assoc.* (2020) 9:e017190. doi: 10.1161/JAHA.120.017190
11. Rajamannan NM, Subramaniam M, Rickard D, Stock SR, Donovan J, Springett M, et al. Human aortic valve calcification is associated with an osteoblast phenotype. *Circulation.* (2003) 107:2181–4. doi: 10.1161/01.CIR.0000070591.21548.69
12. Bonow RO, Carabello B, de Leon AC Jr., Edmunds LH Jr, Fedderly BJ, Freed MD, et al. Guidelines for the management of patients with valvular heart disease: executive summary a report of the American College of Cardiology/American Heart Association task force on practice guidelines (committee on management of patients with valvular heart disease). *Circulation*. (1998) 98:1949–84. doi: 10.1161/01.CIR.98.18.1949
13. Elliott MJ, Zimmerman D, Holden RM. Warfarin anticoagulation in hemodialysis patients: a systematic review of bleeding rates. *Am J Kidney Dis.* (2007) 50:433–40. doi: 10.1053/j.ajkd.2007.06.017
14. Holden RM, Harman GJ, Wang M, Holland D, Day AG. Major bleeding in hemodialysis patients. *Clin J Am Soc Nephrol.* (2008) 3:105–10. doi: 10.2215/CJN.01810407
15. Yu WY, Bhutani T, Kornik R, Pincus LB, Mauro T, Rosenblum MD, et al. Warfarin-associated nonuremic calciphylaxis. *JAMA Dermatol.* (2017) 153:309–14. doi: 10.1001/jamadermatol.2016.4821
16. Lehman JS, Chen TY, Lohse CM, El-Azhary RA. Evaluating the validity of subclassifying warfarin-associated nonuremic calciphylaxis: a retrospective cohort study. *Int J Dermatol.* (2018) 57:572–4. doi: 10.1111/ijd.13884
17. Altarabsheh SE, Deo SV, Dunlay SM, Obeidat YM, Erwin PJ, Rababa'h A, et al. Tissue valves are preferable for patients with end-stage renal disease: an aggregate meta-analysis. *J Card Surg.* (2016) 31:507–14. doi: 10.1111/jocs.12805
18. Williams ML, Bavaria JE, Acker MA, Desai ND, Vallabhajosyula P, Hargrove WC, et al. Valve selection in end-stage renal disease: should it always be biological? *Ann Thorac Surg.* (2016) 102:1531–5. doi: 10.1016/j.athoracsur.2016.04.092
19. Okada N, Tajima K, Takami Y, Kato W, Fujii K, Hibino M, et al. Valve selection for the aortic position in dialysis patients. *Ann Thorac Surg.* (2015) 99:1524–31. doi: 10.1016/j.athoracsur.2014.11.055
20. Böning A, Boedeker RH, Rosendahl UP, Niemann B, Haberer S, Roth P, et al. Long-term results of mechanical and biological heart valves in dialysis and non-dialysis patients. *Thorac Cardiovasc Surg.* (2011) 59:454–9. doi: 10.1055/s-0030-1271028
21. D'Alessandro DA, Skripochnik E, Neragi-Miandoab S. The significance of prosthesis type on survival following valve replacement in dialysis patients. *J Heart Valve Dis.* (2013) 22:743–50.
22. Vahanian A, Alfieri O, Andreotti F, Antunes MJ, Barón-Esquivias G, Baumgartner H, et al. Guidelines on the management of valvular heart disease (version 2012). *Eur Heart J.* (2012) 33:2451–96. doi: 10.1093/eurheartj/ehs109
23. Zhibing Q, Xin C, Ming X, Lele L, YingShuo J, LiMing W. Should bioprostheses be considered the valve of choice for dialysis-dependent patients? *J Cardiothorac Surg.* (2013) 8:42. doi: 10.1186/1749-8090-8-42
24. Umezu K, Saito S, Yamazaki K, Kawai A, Kurosawa H. Cardiac valvular surgery in dialysis patients: comparison of surgical outcome for mechanical versus bioprosthetic valves. *Gen Thorac Cardiovasc Surg.* (2009) 57:197–202. doi: 10.1007/s11748-008-0365-1
25. Pai VB, Tai CK, Bhakri K, Kolvekar S. Should we use mechanical valves in patients with end-stage renal disease? *Interact Cardiovasc Thorac Surg.* (2012) 15:240–3. doi: 10.1093/icvts/ivs115
26. Takemura H. Selection of artificial valve for the patients on hemodialysis. *Gen Thorac Cardiovasc Surg.* (2013) 61:314–9. doi: 10.1007/s11748-012-0173-5
27. Bianchi G, Solinas M, Bevilacqua S, Glauber M. Are bioprostheses associated with better outcome than mechanical valves in patients with chronic kidney disease requiring dialysis who undergo valve surgery? *Interact Cardiovasc Thorac Surg.* (2012) 15:473–83. doi: 10.1093/icvts/ivs236
28. Chan V, Chen L, Mesana L, Mesana TG, Ruel M. Heart valve prosthesis selection in patients with end-stage renal disease requiring dialysis: a systematic review and meta-analysis. *Heart.* (2011) 97:2033–7. doi: 10.1136/heartjnl-2011-300727
29. Thourani VH, Sarin EL, Keeling WB, Kilgo PD, Guyton RA, Dara AB, et al. Long-term survival for patients with preoperative renal failure undergoing bioprosthetic or mechanical valve replacement. *Ann Thorac Surg.* (2011) 91:1127–34. doi: 10.1016/j.athoracsur.2010.12.056
30. Phan K, Zhao DF, Zhou JJ, Karagaratnam A, Phan S, Yan TD. Bioprosthetic versus mechanical prostheses for valve replacement in end-stage renal disease patients: systematic review and meta-analysis. *J Thorac Dis.* (2016) 8:769–77. doi: 10.21037/jtd.2016.02.74
31. Otto CM, Nishimura RA, Bonow RO, Carabello BA, Erwin JP 3rd, Gentile F, et al. 2020 ACC/AHA guideline for the management of patients with valvular heart disease: a report of the American College of Cardiology/American Heart Association joint committee on clinical practice guidelines. *Circulation*. (2021) 143:e72–227. doi: 10.1161/CIR.0000000000000923
32. National Health Research Institutes. *Annual Report of Kidney Disease in Taiwan*. Taipei: National Health Research Institutes (2016).
33. Paloian NJ, Giachelli CM. A current understanding of vascular calcification in CKD. *Am J Physiol Renal Physiol.* (2014) 307:F891–900. doi: 10.1152/ajprenal.00163.2014
34. Kostyunin AE, Yuzhalin AE, Rezvova MA, Ovcharenko EA, Glushkova TV, Kutikhin AG. Degeneration of bioprosthetic heart valves: update 2020. *J Am Heart Assoc*. (2020) 9:e018506. doi: 10.1161/JAHA.120.018506
35. Gong G, Seifter E, Lyman WD, Factor SM, Blau S, Frater RW. Bioprosthetic cardiac valve degeneration: role of inflammatory and immune reactions. *J Heart Valve Dis*. (1993) 2:684–93.
36. Dai L, Golembiewska E, Lindholm B, Stenvinkel P. End-stage renal disease, inflammation and cardiovascular outcomes. *Contrib Nephrol*. (2017) 191:32–43. doi: 10.1159/000479254

Conflict of Interest: The authors declare that the research was conducted in the absence of any commercial or financial relationships that could be construed as a potential conflict of interest.

Publisher's Note: All claims expressed in this article are solely those of the authors and do not necessarily represent those of their affiliated organizations, or those of the publisher, the editors and the reviewers. Any product that may be evaluated in this article, or claim that may be made by its manufacturer, is not guaranteed or endorsed by the publisher.

frontiers in Cardiovascular Medicine

ORIGINAL RESEARCH
published: 25 January 2022
doi: 10.3389/fcvm.2021.743579

TAVI for Pure Non-calcified Aortic Regurgitation Using a Self-Expandable Transcatheter Heart Valve

Yvonne Schneeberger[1], Moritz Seiffert[2], Andreas Schaefer[1], Oliver D. Bhadra[1], Niklas Schofer[2], Simon Pecha[1], Dirk Westermann[2], Stefan Blankenberg[2], Hermann Reichenspurner[1] and Lenard Conradi[1]*

[1] Department of Cardiovascular Surgery, University Heart and Vascular Center Hamburg, Hamburg, Germany, [2] Department of Cardiology, University Heart and Vascular Center Hamburg, Hamburg, Germany

Objectives: Transcatheter aortic valve implantation (TAVI) is routinely performed in patients with severe aortic stenosis (AS). For patients with pure non-calcified aortic regurgitation (AR) who are not suitable for open heart surgery no clear recommendations exist and use of TAVI has been largely off-label. We herein report a series of patients treated with the self-expandable AcurateNeo and Neo2 (Boston Scientific Co., Marlborough, MS, USA) transcatheter heart valve (THV) for pure AR.

Methods: Between 05/2017 and 03/2021, 9 patients (88.8% female, 74.4 ± 7.1 years, logEuroSCORE II 5.5 ± 3.6%, STS PROM 6.2 ± 3.0%) received transfemoral (TF) TAVI for pure non-calcified AR following an adjusted valve sizing algorithm. Data were retrospectively analyzed according to updated Valve Academic Research Consortium (VARC-2) definitions.

Results: Device success was 100%. Early safety was 77.7% (7/10), due to two (22.2%) cases of acute kidney injury. Thirty-day mortality was 0%, in seven (77.7%) patients no or trace paravalvular leakage (PVL) was seen and mild PVL in two (22.2%) patients at 30-day follow-up. No permanent pacemaker (PPM) was required during 30-day follow-up.

Conclusion: In this series of selected patients using the Acurate neo THV for pure non-calcified AR, safety and efficacy were demonstrated. Thirty-day mortality as well as PPM implantation and PVL rates showed excellent results in this high-risk patient cohort. These results will have to be confirmed in larger patient cohorts.

Keywords: transcatheter aortic valve implantation, aortic valve, aortic regurgitation, self- expanding, transcatheter heart valve

OPEN ACCESS

Edited by:
Peter Zilla,
University of Cape Town, South Africa

Reviewed by:
Gabriele Tamagnini,
Villa Torri Hospital, Italy
Paul Human,
University of Cape Town, South Africa

****Correspondence:***
Yvonne Schneeberger
y.schneeberger@uke.de

Specialty section:
This article was submitted to Heart Valve Disease, a section of the journal Frontiers in Cardiovascular Medicine

Received: *18 July 2021*
Accepted: *08 December 2021*
Published: *25 January 2022*

Citation:
Schneeberger Y, Seiffert M, Schaefer A, Bhadra OD, Schofer N, Pecha S, Westermann D, Blankenberg S, Reichenspurner H and Conradi L (2022) TAVI for Pure Non-calcified Aortic Regurgitation Using a Self-Expandable Transcatheter Heart Valve. Front. Cardiovasc. Med. 8:743579. doi: 10.3389/fcvm.2021.743579

INTRODUCTION

Transcatheter aortic valve implantation (TAVI) is routinely performed in patients with severe aortic stenosis (AS) at intermediate or high risk for surgical aortic valve replacement (SAVR), when anatomical conditions for an interventional approach are adequate (1–3). Correspondingly, TAVI has been incorporated in international guidelines (4, 5). While extension of TAVI to low risk patients remains controversial, mainly due to a higher risk of postprocedural permanent pacemaker (PPM) implantation, residual paravalvular leakage (PVL) and lack of long-term durability data as

shown in registry analyses (6–8), evolution of transcatheter heart valves (THV) and corresponding delivery systems is continuing. Besides liberalization of TAVI indications, off-label use of THV for varying aortic valve diseases has been described, with broader clinical application in TAVI for pure non-calcified AR. Traditionally, pure AR is considered a contraindication for TAVI, since absence of aortic valve calcification can lead to insufficient anchoring of the stent frame with possible consecutive valve embolization or relevant PVL (9). However, patients with AR and high comorbidity burden may not be eligible for SAVR and the only THV certificated for AR due to a unique anchoring mechanism (JenaValve) has just very recently been commercially approved and is clinically not widely available (10). Patients with untreated severe AR and a left ventricular ejection fraction of $<$ 30% have an annular mortality of up to 20% and only few of these patients undergo SAVR. Since AR prevalence increases with age, an increasing number of patients with AR in need for TAVI can be anticipated (11). The most frequently utilized THV for treatment of AR are reported to be the self-expandable (SE) CoreValve EvolutR (Medtronic PLC., Minneapolis, MN, US) (12), the SE Acurate neo (Boston Scientific Co., Marlborough, MS, US) (13) and balloon-expandable (BE) THV of the Sapien family (Edwards Lifesciences Inc., Irvine, CA, US) (14). Since particular design features of the Acurate neo THV (distal stabilization arches and upper/lower stent crown inner/outer pericardium skirts) have the potential to protect against valve embolization and residual PVL in non-calcified aortic valves it has become our default THV for treatment of pure AR in patients with a prohibitive risk for SAVR. We herein present our experience with this THV platform for treatment of pure AR with a special emphasis on preprocedural planning and intraprocedural considerations.

MATERIALS AND METHODS

Patients

Between 05/2017 and 03/2021, 9 consecutive patients received transfemoral (TF) TAVI using the Acurate neo and neo2 THV for pure non-calcified AR following an adjusted valve sizing algorithm. Assessment of prohibitive risk for SAVR [3/9 patients with previous cardiac surgery, 4/9 due to age and comorbidities, 1/9 due to previous left ventricular assist device (LVAD) implantation and 1/9 due to malignant disease] and allocation to TAVI followed current international recommendations (4, 5) after consensus of the local dedicated heart team. Written informed consent was obtained from all patients. The study was approved by the local institutional review board.

Abbreviations: AR, Aortic regurgitation; AS, Aortic stenosis; BE, Balloon-expandable; LVAD, Left ventricular assist device; PPM, Permanent pacemaker; PVL, Paravalvular leakage; RVP, Rapid ventricular pacing; SAVR, Surgical aortic valve replacement; SE, Self-expandable; TAVI, Transcatheter aortic valve implantation; TEE, Transesophageal echocardiography; TF, Transfemoral; THV, Transcatheter heart valve.

Diagnostic Work-Up, Study Procedure, and Valve Sizing Algorithm

The preprocedural diagnostic work-up followed institutional standards and was described before (15): By routine, all patients received preoperative transthoracic and/or transesophageal echocardiography (TEE), a contrast-enhanced, electrocardiogram-gated MSCT for calculation for native aortic annulus dimensions and determination of adequate THV size as well as assessment of aortic root anatomy and morphology with the 3mensio Medical Imaging Software (3mensio, Medical Imaging, Bilthoven, Netherlands). Valve sizing followed an adjusted algorithm proposed by Kim et al. for aortic valve stenosis (16) with additional oversizing equivalent to 10.7 $\pm$ 2.7% of the THV diameter when compared to the native annulus diameter in this series (see **Table 1**). As a crude measure, an effective perimeter-derived annular diameter of 25.5 mm was considered the absolute technical maximum even though secondary measures such as annular eccentricity and diameter of the left ventricular outflow tract were also considered and may have contraindicated procedures below this value.

First line approach for all procedures was local anesthesia and/or analgosedation. All procedures were performed in a specially equipped hybrid operating suite by a dedicated team of cardiologists, cardiac surgeons and anesthesiologists. The first step of THV deployment was conducted on the beating heart using fast pacing while, during the second deployment step, rapid ventricular pacing (RVP) was used to ensure stable THV positioning. In the LVAD patient, the guidewire was placed adjacent to the LVAD inflow by fluoroscopy and TEE guidance and LVAD flow was minimized during THV deployment to avoid ventricular migration. THV function was assessed by invasive measurements of hemodynamics, aortic root angiography, and TTE.

Transcatheter Heart Valve

The Boston Scientific Acurate neo (Boston Scientific, Marlborough, MA, USA) THV has a SE nitinol frame carrying porcine pericardial leaflets in a supraannular position (**Figure 1**). The most important difference to other self-expanding platforms is the top-down deployment with minimal protrusion of the stent toward the left ventricular outflow tract. In addition, supraannular leaflet function provides very low gradients even in small anatomies (17) and the pericardial skirt in the new generation neo 2 design seals effectively against PVL. The transfemoral delivery system has a 18Fr outer diameter shaft. In detail, first the upper crown is opened, which guarantees stable positioning and supraannular anchoring of the valve. Then the flexible stabilization arches are opened, responsible for the self-aligning properties of the valve, thereby ensuring coaxial alignment. Finally, in step two the lower crown is deployed anchoring the device inside the annulus. The THV is available in three sizes for aortic annulus sizes from 20.0 to 26.3 mm and are labeled small (S: for aortic annulus sizes 20.0–22.4 mm), medium (M: for aortic annulus sizes 22.5–24.3 mm) and large (L: for aortic annulus sizes 24.4–26.3 mm) (16, 18) in AS patients.

TABLE 1 | Transcatheter heart valve sizes and corresponding oversizing values.

Pat. No	Perimeter (mm)	Area (mm^2)	Perimeter derived diameter (mm)	Area-derived diameter (mm)	Diameter min (mm)	Diameter max (mm)	Eccentricity index	LVOT diameter (mm)	SOV diameter (mm)	STJ diameter (mm)	STJ height (mm)	Ascending aorta diameter (mm)	THV size	Cover index*
1	78.1	476.7	24.9	24.6	22.6	26.7	0.2	26.2	43.2	32.2	34.9	32.0	L	7.8
2	66.2	337.7	21.1	20.7	18.1	23.7	0.2	24.6	23.3	19.7	19.7	20.9	S	8.3
3	68.8	370.0	21.9	21.7	19.4	23.7	0.2	27.4	33.9	33.8	25.5	35.4	M	12.4
4	74.9	434.4	23.8	23.5	20.8	26.9	0.2	28.1	36.8	31.4	25.6	33.9	L	11.9
5	71.7	404.1	22.8	22.7	20.9	24.5	0.1	25.9	36.2	32.5	23.7	35.2	M	8.8
6	70.5	390.3	22.4	22.3	20.6	24.1	0.1	29.5	30.6	27.9	20.3	32.7	M	10.4
7	76.9	460.6	24.5	24.2	21.4	26.6	0.2	28.8	39.8	35.6	24.1	42.5	L	9.3
8	73.2	406.7	23.3	22.8	19.7	26.9	0.3	27.0	35.5	27.9	24.0	33.6	L	13.7
9	66.9	344.5	21.3	20.9	18.1	23.0	0.2	22.9	30.6	26.7	23.5	30.7	M	14.8

*LVOT, Left ventricular outflow tract; SOV, Sinus of valsalva; STJ, Sinotubular junction; THV, Transcatheter heart valve. *[(nominal THV diameter-measured diameter)/nominal THV diameter)*100.*

FIGURE 1 | The self-expandable Acurate neo 2 THV. Latest generation self-expandable transcatheter heart valve consisting of a Nitinol stent carrying a porcine pericardial bioprosthesis in supra-annular position, deployment is carried out in a top-down fashion with opening of the upper crown and stabilization arches as first step for stable positioning and coaxial alignement and deployment of the lower valve stent for anchoring in the aortic annulus. Image provided courtesy of Boston Scientific. ©2021 Boston Scientific Corporation or its affiliates. All rights reserved. The usage of Acurate neo2^{TM} in aortic insufficiency is off-label use.

Statistics

Baseline, intraprocedural and acute follow-up data up to 30 days were retrospectively collected and entered into a standardized database and analyzed. Clinical endpoints were adjudicated in accordance with the updated standardized VARC-2 definitions (19). Data are presented as absolute numbers and percentages for categorical variables and mean values and standard deviation for continuous variables.

RESULTS

Baseline Demographics

All 9 consecutive patients (88.8% female, 74.4 ± 7.1 years) demonstrated an increased risk profile as reflected by common risk stratification tools (EuroSCORE II 5.5 ± 3.6%, STS PROM 6.2 ± 3.0%). Patients presented with a high comorbidity burden, including 3/9 (33.3%) with previous sternotomy, 3/9 (33.3%) patients with concomitant coronary artery disease, and 2/9

TABLE 2 | Baseline data.

	Study group ($n = 9$)
Age, years	74.4 ± 7.1
Female gender, % (*n*)	88.8 (8)
BMI, kg/m²	25.1 ± 5.9
EuroSCORE II, %	5.5 ± 3.6
STS PROM Score, %	6.2 ± 3.0
Diabetes, % (*n*)	22.2 (2)
Arterial hypertension, % (*n*)	55.5 (5)
Previous stroke, % (*n*)	11.1 (1)
Coronary artery disease, % (*n*)	33.3 (3)
Previous sternotomy, % (*n*)	33.3 (3)
s/p LVAD implantation, % (*n*)	11.1 (1)
Extracardiac atheropathy∞, % (*n*)	11.1 (1)
Arrhythmia, % (*n*)	55.5 (5)
COPD∞ > Gold II, % (*n*)	33.3 (3)
Creatinine, mg/dl	2.0 ± 2.3
NYHA ≥ III, % (*n*)	77.7 (7)
LVEF, >50%	44.4 (4)
LVEF, 50–30%	33.3 (3)
LVEF, >30%	22.2 (2)

BMI, Body mass index; logEuroSCORE, Logistic european system for cardiac operative risk evaluation; STS-PROM, Society of thoracic surgeons predicted risk of mortality; LVAD, Left ventricular assist device; COPD, Chronic obstructive pulmonary disease; NYHA, New York Heart Association functional class; ∞ extracardiac atheropathy; ∞ COPD according to EuroSCORE definitions.

TABLE 3 | Periprocedural data.

	Study group ($n = 9$)
Severe aortic regurgitation, % (*n*)	100 (9)
Baseline peak gradient, mmHg	21.3 ± 12.2
Baseline mean gradient, mmHg	9.9 ± 5.7
Invasive pre-implant peak gradient, mmHg	4.4 ± 3.5
Invasive pre-implant mean gradient, mmHg	9.4 ± 7.4
Acurate neo, % (*n*)	11.1 (1)
Acurate neo 2, % (*n*)	88.9 (8)
Procedure time, min	70.9 ± 32.4
Fluoroscopy time, min	23.2 ± 13.8
Contrast agent, ml	212.3 ± 105.8
Predilatation, % (*n*)	0 (0)
Postdilatation, % (*n*)	0 (0)
Anesthesia, % (*n*)	
General anesthesia	11.1 (1)
Local anesthesia/conscious sedation	88.8 (8)
Invasive post-implant peak gradient, mmHg	2.3 ± 2.7
Invasive post-implant mean gradient, mmHg	11.7 ± 7.1

(22.2%) patients with diabetes mellitus. 7/9 patients (77.7%) of the herein investigated patients were highly symptomatic with a New York Heart Association functional class ≥III. Baseline left ventricular ejection fraction was preserved in 44.4% (4/9), moderately reduced in 33.3% (3/9), and severely reduced in 22.2% (2/9). One patient suffered from end-stage heart failure and s/p left ventricular assist device (LVAD) implantation. Detailed patient demographics are summarized in **Table 2**.

Peripprocedural Data

Procedure time, fluoroscopy time, and volume of contrast agent used were 70.9 ± 32.4 min, 23.2 ± 13.8 min, and 212.3 ± 105.8 ml, respectively. The initial positioning of the THV differed from the standard procedure for AS. The THV was positioned ∼1 mm higher in the aortic annulus compared to interventions for AS. For final deployment (step two), rapid pacing was used for stable THV release. For implantation in the LVAD patient, LVAD flow was reduced prior to valve deployment.

The majority of the patients was treated under local anesthesia and/or analgosedation (8/9, 88.8%). Detailed periprocedural data are summarized in **Table 3**.

Clinical and Echocardiographic Outcome Data

All-cause 30-day mortality was 0% (0/9). Device success and early safety were 100% (0/9) and 77.7% (7/9), the latter due to two cases of acute kidney. The VARC-2 adjudicated clinical endpoints—stroke, myocardial infarction, or access site complication—did not occur. No postprocedural conduction disturbance or PPM implantation was observed. Intensive care unit and hospital stay were 1.7 ± 1.1 and 12.9 ± 8.8 days, respectively. Prolonged hospital stay was due to extensive preoperative diagnostic work-up because of planned off-label procedures. Echocardiography at 30 days revealed transvalvular peak/mean pressure gradients of 15.3 ± 12.3/7.2 ± 5.5 mmHg. PVL was ≤ trace in eight patients (77.7%, 7/9) and mild in two patients (22.2%, 2/9).

For detailed outcome parameter see **Table 4**.

DISCUSSION

Main Findings

Main findings of the herein conducted series using the Acurate neo or neo2 THV in TF TAVI for treatment of pure non-calcified AR are (I) the utilized device presents encouraging results in treatment of AR in patients not eligible for surgery, (II) clinical and echocardiographic results with no documented device migration/embolization and no PVL > mild suggest advantages of the particular design features of the THV for treatment of AR and (III) device success rate suggests that the herein recommended valve sizing algorithm may be especially appropriate for the Acurate neo 2 valve for this special subset of patients.

Over the last years, an increasing number of TAVI procedures for treatment of AR has been documented. Since prevalence of AR increases with age and physicians gather more experience with interventional treatment of this specific subset of patients, this trend is expected to continue. However, TAVI for AR represents certain pre- and intraprocedural challenges which are reflected by documented learning curves and uncertainty

TABLE 4 | Clinical outcome and echocardiographic results at 30 days.

	Study group ($n = 9$)
All-cause mortality (30 days), % (*n*)	0 (0)
Stroke (any), % (*n*)	0 (0)
Myocardial infarction, % (*n*)	0 (0)
Bleeding (major/life threatening), % (*n*)	0 (0)
Access site complications (major), % (*n*)	0.0 (0)
Acute kidney injury (AKIN* 2, 3), % (*n*)	22.2 (2)
PPM implantation, % (*n*)	0 (0)
Device success†, % (*n*)	100 (9)
Early safety‡, % (*n*)	77.7 (7)
Intensive care unit stay, days	1.7 ± 1.1
In hospital stay, days	12.9 ± 8.8
Peak gradient, mmHg	15.3 ± 12.3
Mean gradient, mmHg	7.2 ± 5.5
Mild PVL, % (*n*)	22.2 (2)
PVL > mild, % (*n*)	0 (0)

*PPM, Permanent pacemaker; PVL, Paravalvular leakage; *AKIN, Acute Kidney Injury Network; VARC-2 definitions: †Device success: absence of procedural mortality, correct positioning of a single prosthetic heart valve into the proper anatomical position, intended performance of the prosthetic heart valve (no prosthesis-patient mismatch and mean aortic valve gradient < 20 mmHg or peak velocity < 3 m/s and no moderate or severe prosthetic valve regurgitation), ‡Early safety at 30 days: all-cause mortality (at 30 days), all stroke (disabling and non-disabling), life-threatening bleeding, acute kidney injury stage 2 or 3 (including renal replacement therapy), coronary artery obstruction requiring intervention, major vascular complication, valve-related dysfunction requiring repeat procedure (Balloon aortic valvuloplasty, TAVI, or SAVR).*

regarding adequate valve selection and sizing algorithms (20). For the most frequently used THV systems for treatment of AR varying clinical outcomes and valve sizing algorithms are described. A review of 31 published manuscripts by Yousef et al. (21) evaluating a variety of THV (CoreValve, JenaValve, Direct Flow, Acurate TA, J-Valve, Sapien, Lotus) showed unfavorable clinical outcomes with high 30-day mortality (9.6%), high intraprocedural need for a second THV (11.3%), high PPM rate (10.7%), and a high incidence of more than moderate PVL (17.7%). Although different valve types were combined in this review, oversizing was $\leq$ 10% in two thirds (66.4%) of cases (21). However, with latest generation devices and increased experience improved outcomes were documented over the last few years. Registry data shows that the most frequently used THV for treatment of AR is the SE CoreValve Evolut/EvolutR (14). Although documented outcomes with this THV generation are significantly improved compared to the initial CoreValve system, mortality, PPM, and residual significant PVL rates are still remarkable with 9, 20, and 6.2% respectively (12). A series of 24 AR patients who received the Acurate neo THV achieved a device success rate of 87.5%, with moderate PVL in two patients, both when valve oversizing was >10%. Furthermore, mortality was 4.1% and PPM rate 21.1% (13). These reports and our herein described data, although comprising only a small series of patients, suggest that especially the Acurate neo2 THV may be particularly suitable for treatment of AR. Nevertheless, those cited previous reports presented significant higher rates of residual PVL and need for a second THV as compared to implantation of this THV for treatment of AS. Reasons for absence of valve migration/embolization and no PVL > mild in our series may be a combination of a modified sizing algorithm with an oversizing ratio of >10% in the majority of patients, the positioning ∼1 mm higher in the aortic annulus than in interventions for AS, the x-shaped stent frame preventing distal or proximal migration as well as extensive user experience with this type of THV. However, it has to be emphasized that the Acurate neo THV presented unfavorable results regarding residual significant PVL compared to a latest generation BE THV and inferiority regarding mortality and residual significant PVL compared to a latest generation SE THV in randomized controlled trials investigating TAVI in patients with AS (22, 23). Why these outcomes differ from the herein seen hemodynamic results remains speculative but may be founded in the valve sizing algorithm and the high implantation height. Reasons for the two cases of postoperative acute kidney injury remain speculative, but are highly likely attributable to preoperative existing reduced kidney function as reflected by preoperative creatinine values and preoperative reduced left ventricular function in the majority of the herein investigated patients.

Of note, in this AR patient cohort, the second deployment step was conducted under RVP to avoid THV dislocation. In one patient with status post LVAD implantation, LVAD flow was briefly reduced to a minimum during device deployment as an additional measure to avoid proximal embolization. The herein described more pronounced oversizing algorithm did not lead to conduction disturbances or postprocedural PPM implantation. This suggests that the documented high PPM rates with other THV systems may rather result from deep implantation height rather than oversizing alone. However, current THV systems are still used off-label and anchoring in non-calcified aortic annuli carries a certain risk for device migration. Therefore, for ideal results and patient safety, THV systems with modified anchoring mechanisms, like the only recently approved JenaValve with clipping of aortic valve cusps, might be advantageous (10).

These results will have to be confirmed in larger patient numbers for further clinical evaluation.

Study Limitations

Limitations are inherent in a single-center study design with limited patient numbers: patients were not randomized to a specific treatment or THV, therefore patient preselection with hidden confounders may apply. Furthermore, this is a purely descriptive study and conclusions regarding feasibility and especially regarding long-term safety should be drawn with caution.

CONCLUSIONS

In this limited series of TAVI using the Acurate neo THV for pure non-calcified AR, encouraging results were demonstrated. Thirty-day mortality as well as PPM implantation and significant PVL rates were 0% in this high-risk patient cohort. Whether these auspicious results are applicable in larger patient cohorts has yet

to be confirmed since PPM and PVL rates differ significantly compared to AS patients provided with this particular THV.

DATA AVAILABILITY STATEMENT

The raw data supporting the conclusions of this article will be made available by the authors, without undue reservation.

ETHICS STATEMENT

The studies involving human participants were reviewed and approved by UKE Ethics Committee. The patients/participants provided their written informed consent to participate in this study.

AUTHOR CONTRIBUTIONS

YS made substantial contributions to the conception and design of the work, the acquisition, analysis, interpretation of data for the work, and wrote the manuscript. OB made substantial contributions for the acquisition and analysis of the data. MS, AS, NS, SP, DW, SB, and HR were revising it critically for important intellectual content and made final approval of the version to be published. LC made substantial contributions to the conception and design of the work and the acquisition, analysis, interpretation of data for the work, and he was revising it critically for important intellectual content and made final approval of the version to be published. All authors contributed to the article and approved the submitted version.

REFERENCES

1. Smith CR, Leon MB, Mack MJ, Miller DC, Moses JW, Svensson LG, et al. Transcatheter versus surgical aortic-valve replacement in high-risk patients. *N Engl J Med.* (2011) 364:2187–98. doi: 10.1056/NEJMoa1103510
2. Reardon MJ, Van Mieghem NM, Popma JJ, Kleiman NS, Søndergaard L, Mumtaz M, et al. Surgical or transcatheter aortic-valve replacement in intermediate-risk patients. *N Engl J Med.* (2017) 376:1321–31. doi: 10.1056/NEJMoa1700456
3. Leon MB, Smith CR, Mack MJ, Makkar RR, Svensson LG, Kodali SK, et al. Transcatheter or surgical aortic-valve replacement in intermediate-risk patients. *N Engl J Med.* (2016) 374:1609–20. doi: 10.1056/NEJMoa1514616
4. Baumgartner H, Falk V, Bax JJ, De Bonis M, Hamm C, Holm PJ, et al. 2017 ESC/EACTS Guidelines for the management of valvular heart disease. *Eur Heart J.* (2017) 38:2739–91. doi: 10.1093/eurheartj/ehx391
5. Otto CM, Nishimura RA, Bonow RO, Carabello BA, Erwin JP III, Gentile F, et al. 2020 ACC/AHA guideline for the management of patients with valvular heart disease: executive summary: a report of the American College of Cardiology/American Heart Association joint committee on clinical practice guidelines. *Circulation.* (2021) 143:e35–71. doi: 10.1161/CIR.0000000000000932
6. Wendler O, Schymik G, Treede H, Baumgartner H, Dumonteil N, Ihlberg L, et al. SOURCE 3 registry: design and 30-day results of the European postapproval registry of the latest generation of the SAPIEN 3 transcatheter heart valve. *Circulation.* (2017) 135:1123–32. doi: 10.1161/CIRCULATIONAHA.116.025103
7. Grube E, Van Mieghem NM, Bleiziffer S, Modine T, Bosmans J, Manoharan G, et al. Clinical outcomes with a repositionable self-expanding transcatheter aortic valve prosthesis: the international FORWARD study. *J Am Coll Cardiol.* (2017) 70:845–53. doi: 10.1016/j.jacc.2017.06.045
8. Schaefer A, Schofer N, Goßling A, Seiffert M, Schirmer J, Deuschl F, et al. Transcatheter aortic valve implantation versus surgical aortic valve replacement in low-risk patients: a propensity score-matched analysis. *Eur J Cardiothorac Surg.* (2019) 56:1131–9. doi: 10.1093/ejcts/ezz245
9. Thielmann M, Tsagakis K, El Gabry M, Jakob H, Wendt D. Transcatheter aortic valve implantation (TAVI) in patients with aortic regurgitation. *Ann Cardiothorac Surg.* (2017) 6:558–60. doi: 10.21037/acs.2017.09.16
10. Treede H, Rastan A, Ferrari M, Ensminger S, Figulla HR, Mohr FW. JenaValve. *EuroIntervention.* (2012) 8(Suppl Q):Q88–93. doi: 10.4244/EIJV8SQA16
11. Arias EA, Bhan A, Lim ZY, Mullen M. TAVI for pure native aortic regurgitation: are we there yet? *Interv Cardiol.* (2019) 14:26–30. doi: 10.15420/icr.2018.37.1
12. Anwaruddin S, Desai ND, Szeto WY, Hermiller JB Jr, Sorajja P, Kodali S, et al. Self-expanding valve system for treatment of native aortic regurgitation by transcatheter aortic valve implantation (from the STS/ACC TVT Registry). *Am J Cardiol.* (2019) 124:781–8. doi: 10.1016/j.amjcard.2019.05.045
13. Purita PAM, Tahoces LS, Fraccaro C, Nai Fovino L, Kim WK, Espada-Guerreiro C, et al. Transcatheter treatment of native aortic valve regurgitation: results from an international registry using the transfemoral ACURATE *neo* valve. *Int J Cardiol Heart Vasc.* (2020) 27:100480. doi: 10.1016/j.ijcha.2020.100480
14. Yoon SH, Schmidt T, Bleiziffer S, Schofer N, Fiorina C, Munoz-Garcia AJ, et al. Transcatheter aortic valve replacement in pure native aortic valve regurgitation. *J Am Coll Cardiol.* (2017) 70:2752–63. doi: 10.1016/j.jacc.2017.10.006
15. Schaefer A, Linder M, Treede H, Deuschl F, Schofer N, Seiffert M, et al. Applicability of next generation balloon-expandable transcatheter heart valves in aortic annuli exceeding formally approved dimensions. *Clin Res Cardiol.* (2016) 105:585–91. doi: 10.1007/s00392-015-0954-9
16. Kim WK, Hengstenberg C, Hilker M, Schäfer U, Rudolph TK, Toggweiler S, et al. CollaboratorsTranscatheter aortic valve implantation with the ACURATE neo valve: indications, procedural aspects and clinical outcomes. *EuroIntervention.* (2020) 15:e1571–79. doi: 10.4244/EIJ-D-19-H00908
17. Mauri V, Kim WK, Abumayyaleh M, Walther T, Moellmann H, Schaefer U, et al. Short-term outcome and hemodynamic performance of next-generation self-expanding versus balloon-expandable transcatheter aortic valves in patients with small aortic annulus: a multicenter propensity-matched comparison. *Circ Cardiovasc Interv.* (2017) 10:e005013. doi: 10.1161/CIRCINTERVENTIONS.117.005013
18. Schäfer U, Conradi L, Diemert P, Deuschl F, Schofer N, Seiffert M, et al. Symetis ACURATE TAVI: review of the technology, developments and current data with this self-expanding transcatheter heart valve. *Minerva Cardioangiol.* (2015) 63:359–69.
19. Kappetein AP, Head SJ, Généreux P, Piazza N, van Mieghem NM, Blackstone EH, et al. Updated standardized endpoint definitions for transcatheter aortic valve implantation: the Valve Academic Research Consortium-2 consensus document. *J Thorac Cardiovasc Surg.* (2013) 145:6–23. doi: 10.1016/j.jtcvs.2012.09.002
20. Takagi H, Hari Y, Kawai N, Ando T; ALICE (All-Literature Investigation of Cardiovascular Evidence) Group. Meta-analysis and meta-regression of transcatheter aortic valve implantation for pure native aortic regurgitation. *Heart Lung Circ.* (2020) 29:729–41. doi: 10.1016/j.hlc.2019.04.012
21. Yousef A, MacDonald Z, Simard T, Russo JJ, Feder J, Froeschl MV, et al. Transcatheter Aortic Valve Implantation (TAVI) for native aortic valve regurgitation - a systematic review. *Circ J.* (2018) 82:895–902. doi: 10.1253/circj.CJ-17-0672
22. Lanz J, Kim WK, Walther T, Burgdorf C, Möllmann H, Linke A, et al. Safety and efficacy of a self-expanding versus a balloon-expandable bioprosthesis for transcatheter aortic valve replacement in patients with symptomatic severe

aortic stenosis: a randomised non-inferiority trial. *Lancet.* (2019) 394:1619–28. doi: 10.1016/S0140-6736(19)32220-2

23. Tamburino C, Bleiziffer S, Thiele H, Scholtz S, Hildick-Smith D, Cunnington M, et al. Comparison of self-expanding bioprostheses for transcatheter aortic valve replacement in patients with symptomatic severe aortic stenosis: SCOPE 2 randomized clinical trial. *Circulation.* (2020) 142:2431–42. doi: 10.1161/CIRCULATIONAHA.120.051547

Conflict of Interest: MS reports lecture fees and travel expenses from Boston Scientific. LC is advisory board member for Boston Scientific.

The remaining authors declare that the research was conducted in the absence of any commercial or financial relationships that could be construed as a potential conflict of interest.

Publisher's Note: All claims expressed in this article are solely those of the authors and do not necessarily represent those of their affiliated organizations, or those of the publisher, the editors and the reviewers. Any product that may be evaluated in this article, or claim that may be made by its manufacturer, is not guaranteed or endorsed by the publisher.

frontiers in Cardiovascular Medicine

ORIGINAL RESEARCH
published: 27 January 2022
doi: 10.3389/fcvm.2022.686208

Prevalence and Prognostic Importance of Massive Tricuspid Regurgitation in Patients Undergoing Tricuspid Annuloplasty With Concomitant Left-Sided Valve Surgery: A Study on Rheumatic Valvular Heart Disease

*Yan Chen[1,2,3], Yap-Hang Chan[3], Mei-Zhen Wu[3], Yu-Juan Yu[3], Yui-Ming Lam[3], Ko-Yung Sit[4], Daniel Tai-Leung Chan[4], Cally Ka-Lai Ho[4], Lai-Ming Ho[5], Chu-Pak Lau[3], Wing-Kuk Au[4], Hung-Fat Tse[3] and Kai-Hang Yiu[2,3]**

[1] Department of Ultrasound, Shenzhen Hospital, Southern Medical University, Shenzhen, China, [2] Division of Cardiology, Department of Medicine, The University of Hong Kong Shen Zhen Hospital, Shenzhen, China, [3] Division of Cardiology, Department of Medicine, The University of Hong Kong, Queen Mary Hospital, Hong Kong, Hong Kong SAR, China, [4] Department of Cardiothoracic Surgery, The University of Hong Kong, Queen Mary Hospital, Hong Kong, Hong Kong SAR, China, [5] School of Public Health, The University of Hong Kong, Hong Kong, Hong Kong SAR, China

Background: The presence of tricuspid regurgitation (TR) is very common in patients with concomitant left-sided valve disease. Recent studies have advocated an additional grading of massive TR that is beyond severe. The present study sought to characterize the spectrum of TR in patients undergoing tricuspid annuloplasty (TA) and to evaluate the prognostic value of TR severity for post-operative outcome following TA.

Methods: A total of 176 patients who underwent TA with combined left-sided valve surgery, secondary to rheumatic valvular heart disease, were prospectively evaluated. The severity of TR was quantified by effective regurgitant orifice area (EROA) using the proximal isovelocity surface area method. Patients were categorized as having non-massive TR (EROA < 0.6 cm^2) or massive TR (EROA ≥ 0.6 cm^2). Adverse outcome was defined as all-cause mortality or heart failure requiring hospital admission following TA.

Results: A total of 55 (31%) patients were considered to have massive TR. Patients with massive TR had a greater right ventricular dimension but a smaller left ventricular dimension compared with those with non-massive TR. After a median follow-up of 39 months, 35 adverse events occurred. Cox-regression analysis showed that both continuous EROA and dichotomized EROA (massive vs. non-massive TR) were independently associated with adverse events even after multivariable adjustment. Further, Harrell C index demonstrated that the addition of massive TR provided better discrimination ability of a prediction model to known prognosticators following TA.

OPEN ACCESS

Edited by:
Peter Zilla,
University of Cape Town, South Africa

Reviewed by:
Tanja Katharina Rudolph,
Heart and Diabetes Center North Rhine-Westphalia, Germany
Alexander Sedaghat,
University Hospital Bonn, Germany
Andreina Carbone,
University of Campania Luigi Vanvitelli, Italy
Hiroyuki Kamiya,
Asahikawa Medical University, Japan

***Correspondence:**
Kai-Hang Yiu
khkyiu@hku.hk

Specialty section:
This article was submitted to Heart Valve Disease, a section of the journal Frontiers in Cardiovascular Medicine

Received: *26 March 2021*
Accepted: *04 January 2022*
Published: *27 January 2022*

Citation:
Chen Y, Chan Y-H, Wu M-Z, Yu Y-J, Lam Y-M, Sit K-Y, Chan DT-L, Ho CK-L, Ho L-M, Lau C-P, Au W-K, Tse H-F and Yiu K-H (2022) Prevalence and Prognostic Importance of Massive Tricuspid Regurgitation in Patients Undergoing Tricuspid Annuloplasty With Concomitant Left-Sided Valve Surgery: A Study on Rheumatic Valvular Heart Disease. Front. Cardiovasc. Med. 9:686208. doi: 10.3389/fcvm.2022.686208

Conclusions: Massive TR is common and up to 31% of study population had massive TR. Massive TR was associated with adverse outcome in patients undergoing TA. Classification of the severity of TR by quantitative measures and identification of massive TR in patients with concomitant left-sided valve disease are essential when considering the optimal timing of corrective surgery.

Keywords: tricuspid regurgitation (TR), tricuspid annuloplasty, effective regurgitant orifice area (EROA), adverse outcome, left-sided valve disease, rheumatic valvular heart disease

INTRODUCTION

Tricuspid regurgitation (TR) is a very common condition (1) that is closely associated with decreased survival (2). Traditionally, the severity of TR is classified as mild, moderate or severe assessed by transthoracic echocardiography. The measurement of effective regurgitant orifice area (EROA) has been advocated as a quantifiable assessment of TR grade and can provide superior prognostic value compared with qualitative and semi-quantitative assessment (3). Recent experience from patients referred for transcather tricuspid valve procedure has revealed that long-standing TR and regurgitant volume can double the conventional criteria for severe TR measured by EROA (4). Consequently, recent recommendation has further classified an extreme type of TR beyond severe, expanding the TR grading scheme to include "massive TR" and "torrential TR" (5).

Current guidelines (6, 7) recommend that tricuspid annuloplasty (TA) to correct TR is concomitant with left-side valve surgery, based on the clinical status of the left-sided valve lesion. The severity of TR in these patients is nonetheless not a consideration when determining timing of surgery. Indeed, TR is considered to run an indolent natural course and is not uncommon in patients with left-sided heart disease. Compared with severe TR, extreme severity of TR has recently been proven to be a strong predictor of adverse outcome, further supporting the need for another classification of extreme risk (8, 9). Nonetheless the prevalence of extreme TR, beyond severe, in patients undergoing TA during concomitant left-sided valve surgery is uncertain. In addition, the prognostic implication of extreme severity of TR in patients who underwent TA has not been evaluated. The present study aimed to characterize the spectrum of TR severity measured by EROA, in particular massive TR, in patients who underwent TA during concomitant left-sided valve surgery. The prognostic implication of TR severity for post-operative course following TA was also evaluated.

MATERIALS AND METHODS

Study Population

This was a single-center prospective cohort study. The study was part of the Chinese Valvular Heart Disease Study (CVATS) to evaluate the pattern of disease, pathophysiology, and clinical outcome in Chinese patients (10). A total of 308 consecutive patients undergoing elective TA during left-sided valve surgery at Queen Mary Hospital between January 2013 and January 2019 were recruited. Patients were excluded if they had history of congenital heart disease ($n = 7$), pacemaker implantation ($n = 9$), or previous tricuspid valve surgery ($n = 20$). Patients were excluded if major lesion of the left-sided heart valve was recorded as non-rheumatic valvular heart disease ($n = 84$). Patients with poor-quality echocardiographic images ($n = 12$) that were unsuitable for further measure were also excluded. Accordingly, only 176 patients who underwent TA with combined left-sided valve surgery, secondary to rheumatic valvular heart disease, were included in the final analysis. Patients were followed up by one clinical investigator and details of adverse events were obtained from the electronic Clinical Management System. Adverse outcome was defined as all-cause mortality or heart failure requiring hospital admission following TA. Hospitalization for heart failure was defined as admission due to dyspnea with chest radiographic evidence of pulmonary congestion and treatment with intravenous diuretics. If patients had multiple adverse events, the first one was coded and recorded as study end point. For the study end points, patients who experienced adverse outcome were followed until the first episode of adverse event, the other patients were followed until February 2020. The study was approved by the institutional review board of Hospital Authority Hong Kong West Cluster and all participants gave written informed consent.

Clinical Parameters

Baseline clinical information and laboratory blood tests for preoperative parameters were gathered at the time of recruitment. Conventional cardiovascular risk factors including diabetes mellitus, hypertension, hyperlipidemia and smoking status were recorded. New York Heart Association (NYHA) classification was recorded as class I/II or class III/IV, and the status of valvular atrial fibrillation (AF) was also retrieved for each subject from Hospital Authority records. Detailed surgery type including coronary artery bypass grafting and combined left-sided valve surgery during TA surgery was recorded. Data on prescription of angiotensin converting enzyme inhibitor (ACEI) or angiotensin receptor blocker (ARB), calcium-channel, blocker beta-blocker and statin were also collected. The European System for Cardiac Operative Risk Evaluation (EuroSCORE II) was employed to estimate operative mortality risk.

Echocardiography Parameters

Comprehensive transthoracic echocardiography was performed before valvular surgery using GE Vivid E9 echocardiography system. All image acquisitions were recorded over three

consecutive cycles. Left ventricular (LV) and right ventricular (RV) echocardiographic parameters including left ventricular end-diastolic volume (LVEDV), left ventricular end-systolic volume (LVESV), left ventricular ejection fraction (LVEF), right ventricular end-diastolic area (RVEDA), right ventricular end-systolic area (RVESA), and right ventricular fractional area change (RVFAC) were measured according to the current recommendations (11). Tricuspid annulus diameter was measured from the insertion of the septal leaflet to the insertion of the anterior leaflet at end-diastole. Tricuspid annular plane systolic excursion (TAPSE), a measure of RV systolic function, was obtained from the M-mode apical four-chamber view. Pulmonary arterial systolic pressure (PASP) was estimated from peak TR velocity by continuous-wave Doppler using the modified Bernoulli equation: PASP $= 4(V)^2 +$ right atrial pressure value (12).

The severity of TR was quantified by effective regurgitant orifice area (EROA) using the proximal isovelocity surface area (PISA) method (13, 14). The PISA method was used to calculate EROA by combining the measurement of TR flow and its velocity by continuous-wave Doppler, as previously described (13, 14). As shown in our previous study (15): color Doppler images of TR proximal flow convergence were obtained from apical 4-chamber views and zoomed to the region of interest, the color-flow velocity scale was maximized and the baseline was shifted downwards until the flow convergence region was visualized clearly. The Nyquist limit (aliasing velocity) was controlled at 0.28–0.34 m/s in order to optimize visualization and avoid overestimation or underestimation under color Doppler. Radial distance between the first aliasing velocity (blue/yellow interface) and the center of the tricuspid orifice was measured in mid-systole to calculate regurgitant flow, and the EROA was then calculated as the ratio of regurgitant flow to the peak velocity of the TR jet (15). Patients were divided into two groups based on their TR severity according to the recommendation (5): 121 patients with non-massive TR (EROA < 0.6 cm^2) and 55 patients with massive TR (EROA ≥ 0.6 cm^2). Residual significant TR was defined as moderate or severe TR according to transthoracic echocardiography examination results before discharge after TA surgery.

Statistical Analysis

Continuous variables are expressed as mean $\pm$ SD if normally distributed or median (25–75th percentiles) if non-normally distributed. Categorical variables are described as numbers (percentages). Student *t*-test and Mann-Whitney *U*-test were used to compare continuous variables between two groups. Categorical variables were compared using Chi-square test or Fisher's exact test. Univariate Cox regression analysis was performed to evaluate the potential predictors of long-term adverse outcome. Multivariable Cox regression analysis was subsequently performed to determine the independent predictive ability of EROA for long-term adverse outcome. The Harrell C statistic was calculated using Stata 14.0 to assess the prediction value of each primary model and comparison model for long-term adverse outcome. The higher Harrell C index indicated that the better the model can discriminate the adverse outcome. The incremental prognostic value of massive TR was subsequently assessed in nested Cox regression model that includes the other risk factors. To compare the adverse outcome for massive and non-massive TR, Kaplan-Meier curve was constructed and the percentage of adverse events compared using the log-rank test. All statistical analyses were performed using the statistical package SPSS (Version 22.0, SPSS, Chicago, USA) and *P*-values reported are 2-sided for consistency. A *P*-value < 0.05 was considered statistically significant.

RESULTS

Baseline Characteristics

The baseline characteristics of the entire study cohort and patients with and without massive TR are shown in **Table 1**. All the patients had functional TR secondary to left-sided rheumatic valvular heart disease, and underwent TA with ring annuloplasty. For the entire study population, up to 85% of study population had AF. The median EuroSCORE II was 3.2% (interquartile range: 1.9–5.4%). Pre-operative mean LVEF and RVFAC were respectively 60 and 48%, suggesting a preserved LV and RV function in the study population. Further, the median EROA was 0.40 cm^2 (interquartile range: 0.25–0.66 cm^2) and 55 (31%) patients were considered to have massive TR. The mean tricuspid annulus diameter and PASP was 3.7 ± 0.6 cm and 47.9 ± 12.6 mmHg, respectively. The most common combined left-sided valve procedure during TA was mitral valve replacement. All patients experienced cardiopulmonary bypass and 10 patients who had significant coronary artery disease, underwent simultaneous coronary artery bypass grafting.

Patients with massive TR had lower hemoglobin and estimated glomerular filtration rate, higher EuroSCORE II (all $P < 0.05$). As expected, patients with massive TR had larger RVEDA [19.4 (15.8–23.4) vs. 12.9 (11.1–15.8) cm^2, $P < 0.01$], RVESA [10.3 (7.9–12.9) vs. 6.6 (5.4–8.3) cm^2, $P < 0.01$], and tricuspid annulus diameter (4.2 ± 0.6 vs. 3.5 ± 0.5 cm, $P < 0.01$), and lower RVFAC (46.2 ± 8.8 vs. 49.1 ± 6.8%, $P = 0.04$) and TAPSE (1.5 ± 0.2 vs. 1.7 ± 0.3 cm, $P < 0.01$) compared with those with non-massive TR. In contrast, LVEDV [72.0 (55.0–94.0) vs. 83.0 (68.5–106.0) ml, $P = 0.03$] was significantly smaller in patients with massive TR compared with those with non-massive TR. The other clinical parameters were nonetheless similar between the two groups (**Table 1**).

Predictors Associated With Long-Term Adverse Outcome

Median follow-up following TA was 39 months (range 1–86 months). A total of 35 adverse events happened: including 19 hospitalizations for heart failure (nine in non-massive TR and 10 in massive TR, 7.7 vs. 23.3%, Log-rank test $P = 0.015$) and 16 deaths (four in non-massive and 12 in massive TR, 3.6 vs. 26.7%, Log-rank test $P < 0.001$). Univariate Cox regression analysis of baseline characteristics associated

TABLE 1 | Baseline characteristics of the study population.

Variables	Overall ($n = 176$)	Non-massive TR (EROA < 0.6 cm^2, $n = 121$)	Massive TR (EROA ≥ 0.6 cm^2, $n = 55$)	*P*-value
Age (years)	64.4 ± 8.2	63.8 ± 8.5	65.9 ± 7.3	0.10
Male, *n* (%)	44 (25.0)	25 (20.7)	19 (34.5)	0.05
Diabetes mellitus, n (%)	33 (18.8)	20 (16.5)	13 (23.6)	0.26
Hypertension, *n* (%)	28 (15.9)	18 (14.9)	10 (18.0)	0.58
Hyperlipidemia, *n* (%)	33 (18.8)	22 (18.2)	11 (20.0)	0.78
Smoking, *n* (%)	24 (13.6)	16 (13.2)	8 (14.5)	0.81
Atrial fibrillation, *n* (%)	150 (85.2)	102 (84.3)	48 (87.3)	0.61
NYHA class III/IV, *n* (%)	75 (42.6)	49 (40.5)	26 (47.3)	0.40
Hemoglobin (g/dL)	12.3 ± 1.8	12.6 ± 1.7	11.8 ± 1.9	0.01
eGFR (mL/min/1.73 m^2)	71.4 ± 18.7	73.6 ± 17.4	66.4 ± 20.5	0.02
Combined valvular surgery with TA, *n* (%)				
Mitral valve repair	15 (8.5)	11 (9.1)	4 (7.3)	0.78
Mitral valve replacement	78 (44.3)	53 (43.8)	25 (45.5)	0.84
Aortic valve replacement	17 (9.7)	9 (7.4)	8 (14.5)	0.14
Dual valvular surgery	66 (37.5)	48 (39.7)	18 (32.7)	0.38
Concomitant CABG, *n* (%)	10 (5.7)	5 (4.1)	5 (9.1)	0.29
Medications, *n* (%)				
ACEI/ARB	64 (36.4)	42 (34.7)	22 (40.0)	0.50
Beta blocker	67 (38.1)	44 (36.4)	23 (41.8)	0.49
Calcium-channel blockers	41 (23.3)	29 (24.0)	12 (21.8)	0.76
Statins	51 (29.0)	36 (29.8)	15 (27.3)	0.74
EuroSCORE II (%)	3.2 (1.9–5.4)	3.0 (1.8–5.1)	4.0 (2.4–7.0)	0.02
Echocardiographic parameters				
LVEDV (ml)	80.0 (62.0–101.8)	83.0 (68.5–106.0)	72.0 (55.0–94.0)	0.03
LVESV (ml)	31.0 (23.0–43.0)	32.0 (25.0–44.0)	27.0 (20.0–41.0)	0.09
LVEF (%)	59.6 ± 8.0	59.7 ± 8.1	59.5 ± 7.8	0.93
RVEDA (cm^2)	14.5 (11.9–19.0)	12.9 (11.1–15.8)	19.4 (15.8–23.4)	<0.01
RVESA (cm^2)	7.4 (5.7–9.7)	6.6 (5.4–8.3)	10.3 (7.9–12.9)	<0.01
RVFAC (%)	48.2 ± 7.6	49.1 ± 6.8	46.2 ± 8.8	0.04
TAPSE (cm)	1.6 ± 0.3	1.7 ± 0.3	1.5 ± 0.2	<0.01
Tricuspid annulus diameter (cm)	3.7 ± 0.6	3.5 ± 0.5	4.2 ± 0.6	<0.01
PASP (mmHg)	47.9 ± 12.6	48.4 ± 12.2	46.7 ± 13.4	0.41
EROA (cm^2)	0.40 (0.25–0.66)	0.29 (0.21–0.40)	0.76 (0.68–1.20)	<0.01
Residual significant TR, *n* (%)	14 (8.0)	9 (7.4)	5 (9.1)	0.77

Values are mean ± SD or median (25–75th percentiles), or n (%).

ACEI, angiotensin converting enzyme inhibitor; ARB, angiotensin receptor blocker; CABG, coronary artery bypass graft; eGFR, estimated glomerular filtration rate; LVEDV, Left ventricular end-diastolic volume; LVEF, left ventricular ejection fraction; LVESV, Left ventricular end-systolic volume; NYHA, New York Heart Association; PASP, pulmonary artery systolic pressure; RVEDA, right ventricular end-diastolic area; RVESA, right ventricular end-systolic area; RVFAC, right ventricular fractional area change; TA, tricuspid annuloplasty; TAPSE, tricuspid annular plane systolic excursion; TR, tricuspid regurgitation; EROA, effective regurgitant orifice area; EuroSCORE, European System for Cardiac Operative Risk Evaluation.

with long-term adverse events are shown in **Table 2**. Clinical parameters including older age, male gender, diabetes mellitus, hypertension, advanced NYHA class, lower hemoglobin and estimated glomerular filtration rate, higher EuroSCORE II were associated with adverse events. Regarding echocardiographic parameters, a larger RVEDA, RVESA, tricuspid annulus diameter, a higher RVFAC and lower TAPSE were associated with adverse outcome (**Table 2**). Importantly, both EROA (as a continuous variable) and categorical variable of EROA (massive TR vs. non-massive TR) were correlated with adverse outcome. Nonetheless LV volume and ejection fraction showed no such relationship.

Independent Predictive Ability of EROA for Long-Term Adverse Events

As shown in **Table 3**, multivariable Cox regression analysis showed that EROA (as a continuous variable) was independently associated with adverse events, even after adjusting for the other potential risk factors. In addition, patients with massive TR had a 3-fold risk of developing adverse events compared with patients with non-massive TR. Importantly, Harrell C index demonstrated that adding dichotomized EROA assessment provided better discrimination of a prediction model in each comparison model (**Table 4**). Furthermore,

TABLE 2 | Factors associated with long-term adverse events by univariate Cox regression analysis.

Variables	Univariate analysis		
	HR	95% CI	*P*
Age	1.06	1.02–1.11	<0.01
Male	2.84	1.46–5.54	<0.01
Diabetes mellitus	2.08	1.02–4.25	0.04
Hypertension	3.20	1.59–6.44	<0.01
Hyperlipidemia	1.38	0.63–3.03	0.43
Smoking	1.84	0.80–4.22	0.15
Atrial fibrillation	1.43	0.50–4.05	0.50
NYHA class III/IV	2.08	1.06–4.07	0.03
Hemoglobin	0.73	0.61–0.86	<0.01
eGFR	0.97	0.95–0.99	<0.01
Combined valvular surgery with TA			
Mitral valve repair	1.93	0.75–4.97	0.17
Mitral valve replacement	0.84	0.43–1.65	0.61
Aortic valve replacement	1.15	0.41–3.25	0.79
Dual valvular surgery	0.87	0.43–1.74	0.68
Concomitant CABG	0.91	0.22–3.79	0.89
Medications			
ACEI/ARB	1.92	0.99–3.73	0.06
Beta blocker	1.06	0.54–2.08	0.87
Calcium-channel blockers	0.68	0.30–1.56	0.36
Statins	0.80	0.38–1.71	0.57
EuroSCORE II	1.10	1.06–1.14	<0.01
LVEDV	1.01	0.99–1.01	0.23
LVESV	1.01	0.99–1.02	0.40
LVEF	1.01	0.96–1.05	0.83
RVEDA	1.08	1.03–1.14	<0.01
RVESA	1.13	1.05–1.21	<0.01
RVFAC	0.96	0.92–0.99	0.02
TAPSE	0.28	0.08–0.98	<0.05
Tricuspid annulus diameter	1.93	1.22–3.06	<0.01
PASP	1.01	0.99–1.04	0.25
EROA (per 0.1 cm^2 increase)	1.59	1.29–1.96	<0.01
Massive TR vs. non-massive TR	4.05	2.04–8.03	<0.01
Residual significant TR	1.64	0.58–4.65	0.35

ACEI, angiotensin converting enzyme inhibitor; ARB, angiotensin receptor blocker; CABG, coronary artery bypass graft; eGFR, estimated glomerular filtration rate; LVEDV, Left ventricular end-diastolic volume; LVEF, left ventricular ejection fraction; LVESV, Left ventricular end-systolic volume; NYHA, New York Heart Association; PASP, pulmonary artery systolic pressure; RVEDA, right ventricular end-diastolic area; RVESA, right ventricular end-systolic area; RVFAC, right ventricular fractional area change; TA, tricuspid annuloplasty; TAPSE, tricuspid annular plane systolic excursion; TR, tricuspid regurgitation; EROA, effective regurgitant orifice area; EuroSCORE, European System for Cardiac Operative Risk Evaluation.

nested Cox regression analysis showed that the addition of massive TR provided incremental prognostic value beyond demographic parameters, traditional cardiovascular risk factors, clinical data and important echocardiographic parameters (**Figure 1**).

TABLE 3 | Prognostic value of TR severity.

	TR-EROA (per 0.1 cm^2 increase)		Massive TR vs. non-massive TR	
	HR (95% CI)	*P*-value	HR (95% CI)	*P*-value
Model 1	1.35 (1.08–1.69)	<0.01	3.16 (1.57–6.37)	<0.01
Model 2	1.69 (1.36–2.11)	<0.01	3.67 (1.84–7.32)	<0.01
Model 3	1.36 (1.09–1.70)	<0.01	2.94 (1.44–6.02)	<0.01
Model 4	1.62 (1.29–2.03)	<0.01	3.89 (1.94–7.82)	<0.01
Model 5	1.52 (1.06–2.18)	0.02	3.09 (1.40–6.79)	<0.01
Model 6	1.59 (1.11–2.26)	0.01	3.26 (1.49–7.12)	<0.01
Model 7	1.49 (1.10–2.01)	0.01	3.30 (1.44–7.55)	<0.01

Model 1 = adjusted for demographic parameters including age, male.
Model 2 = adjusted for traditional cardiovascular risk factors including diabetes mellitus, hypertension.
Model 3 = adjusted for blood biochemical parameters including hemoglobin, eGFR.
Model 4 = adjusted for NYHA class III/IV, EuroSCORE II.
Model 5 = adjusted for echocardiographic parameters including RVEDA, RVFAC, TAPSE.
Model 6 = adjusted for echocardiographic parameters including RVESA, RVFAC, TAPSE.
Model 7 = adjusted for echocardiographic parameters including tricuspid annulus diameter, RVFAC and TAPSE.
RVEDA, RVESA and tricuspid annulus diameter were collinearity. To avoid bias from multicollinearity and follow the statistical rules, RVEDA, RVESA, and tricuspid annulus diameter were entered into multivariable analysis individually.
CI, confidence interval; eGFR, estimated glomerular filtration rate; HR, hazard ratio; NYHA, New York Heart Association; RVEDA, right ventricular end-diastolic area; RVESA, right ventricular end-systolic area; RVFAC, right ventricular fractional area change; TAPSE, tricuspid annular plane systolic excursion; TR, tricuspid regurgitation; EROA, effective regurgitant orifice area; EuroSCORE, European System for Cardiac Operative Risk Evaluation.

Comparison of Adverse Events for Massive TR and Non-massive TR

The Kaplan-Meier survival curve analysis showed that patients with massive TR had a significantly higher percentage of adverse outcome than those with non-massive TR (**Figure 2**). The incidence of adverse outcome was 15% at 1 year, 30% at 2 years, and 36% at 3 years for patients with massive TR, significantly higher compared with that for patients with non-massive TR (6% at 1 year, 8% at 2 years, and 10% at 3 years).

DISCUSSION

Our study demonstrates that in patients undergoing TA during concomitant left-sided valve surgery, the prevalence of massive TR, defined as an EROA $\geq$ 0.6 cm^2, is not uncommon and present in nearly a third of patients. Of interest, despite having a greater RV dimension and more impaired RV function, patients with massive TR had a smaller LV dimension, and a similar LV ejection fraction and NYHA functional class compared with those with non-massive TR. Importantly, patients with massive TR had a worse outcome following TA than those with non-massive TR. The Harrell C index analysis further revealed that the addition of massive TR provided better discrimination power of perdition model for adverse events compared with other known prognostic factors.

TABLE 4 | Better discrimination of a prediction model after including dichotomized EROA.

	Harrell C index (95% CI)	
	Primary model	Comparison model
Model 1 vs. Model 1+ dichotomized EROA*	0.68 (0.58–0.79)	0.74 (0.67–0.82)
Model 2 vs. Model 2+ dichotomized EROA*	0.72 (0.60–0.83)	0.79 (0.71–0.86)
Model 3 vs. Model 3+ dichotomized EROA*	0.73 (0.65–0.82)	0.76 (0.69–0.84)
Model 4 vs. Model 4+ dichotomized EROA*	0.71 (0.63–0.80)	0.78 (0.72–0.85)
Model 5 vs. Model 5+ dichotomized EROA*	0.68 (0.60–0.77)	0.71 (0.62–0.79)
Model 6 vs. Model 6+ dichotomized EROA*	0.67 (0.59–0.76)	0.70 (0.61–0.80)
Model 7 vs. Model 7+ dichotomized EROA*	0.67 (0.59–0.75)	0.70 (0.61–0.79)

Model 1 = age, male.
Model 2 = diabetes mellitus, hypertension.
Model 3 = hemoglobin, eGFR.
Model 4 = NYHA class III/IV, EuroSCORE II.
Model 5 = RVEDA, RVFAC, TAPSE.
Model 6 = RVESA, RVFAC, TAPSE.
Model 7 = Tricuspid annulus diameter, RVFAC and TAPSE.
Dichotomized EROA: Massive TR vs. non-massive TR (EROA ≥ 0.6 cm^2 vs. EROA < 0.6 cm^2).*
CI, confidence interval; eGFR, estimated glomerular filtration rate; NYHA, New York Heart Association; RVEDA, right ventricular end-diastolic area; RVESA, right ventricular end-systolic area; RVFAC, right ventricular fractional area change; TAPSE, tricuspid annular plane systolic excursion; TR, tricuspid regurgitation; EROA, effective regurgitant orifice area; EuroSCORE, European System for Cardiac Operative Risk Evaluation.

Prevalence of Massive TR

The presence of TR is often an incidental finding during echocardiographic assessment. A trivial or mild degree is generally regarded as benign. In contrast, those with moderate and severe TR have an increased risk of adverse outcome (2). In the Framingham Heart Study, the prevalence of moderate and severe TR was up to 1.5 and 5.6% in men and women aged >70 years, respectively (1). In another study that evaluated over 5,000 adults at three Veterans Affairs medical centers, moderate or severe TR was present in 15.7% (2). In the OxVALVE population cohort study that included 2,500 individuals aged ≥65 years with no known valvular disease, moderate/severe TR was present in 2.9% and was the most common valvular lesion detected (16). Collectively, these studies suggest that significant TR is not uncommon in clinical practice and undoubtedly deserves more attention (17). Recent studies have demonstrated that late in the natural history of the disease, patients may further develop an extreme form of TR, beyond the current definition of severe grade (18). As a result, there has been a move to revise the current TR grading, expanding the spectrum beyond severe to include massive and torrential (5). Further, symptoms in patients with TR, such as ankle oedema, are usually well-tolerated and generally respond to diuretic therapy. It is only at a later stage that TR may cause symptoms of right-sided heart failure such as weight loss, ascites and cachexia. Because of these insidious and non-specific symptoms, the presence of significant TR can sometimes be overlooked. In our present study, we determined that massive TR can occur in nearly a third of patients with concomitant left-sided valve disease. Indeed, massive TR is even more frequent in patients undergoing percutaneous tricuspid valve intervention who are considered too high risk for conventional surgery (4). These findings highlight the increasing prevalence of massive TR that will place a significant health burden on society parallel to our aging population. Large epidemiological studies are required to further evaluate the prevalence of extreme forms of TR that perhaps are asymptomatic and remain unidentified or underestimated.

Characteristics of Patients With Massive TR

In our present study, patients with massive TR exhibited a higher EuroSCORE II compared with those with non-massive TR. This illustrates that patients with massive TR are more likely to have advanced diseases with clustering of comorbidities. Nonetheless the NYHA class was similar between the two groups of patients, indicating that subjective functional assessment cannot accurately describe the complex risk profile. This finding further underscores that the timing of surgery, driven partly by symptoms, cannot distinguish the composite risk of patients with and without massive TR.

In addition, our finding reveals that although RV dimension was larger, patients with massive TR had a smaller LV dimension compared with those with non-massive TR. This intriguing observation is consistent with another study that revealed LV dimension to be inversely correlated with severity of TR in a cohort of patients with LV systolic dysfunction (19). One possible explanation could be that pre-load of the LV is smaller in patients with massive TR, leading to smaller LV. Another reason could speculate that the smaller LV dimension observed in those with more severe TR was due to compression by the enlarged RV within a confined pericardial space. As a result, the paradoxically smaller LV dimension may create a false impression to the clinician that patients with massive TR have a preserved LV dimension, despite having a higher EuroSCORE II. Given that LV dilatation is a key factor that determines the timing of surgery, the misinterpretation of a preserved LV dimension in patients with massive TR may further delay surgery. Studies to evaluate the optimal cut-off value of LV dimension or the LV eccentricity index (20), an index that reflects abnormal motion of the interventricular septum due to RV volume overload, to predict adverse outcome in patients with massive TR would nonetheless require clarification by future studies.

Prognostic Implication of Massive TR

The TR has often been considered a forgotten entity of valve disease, in part due to its secondary nature in left-sided valve disease and long latent asymptomatic period. Increasingly, studies have now demonstrated that TR is not a benign entity and the presence of moderate and severe TR is correlated with adverse outcome (2, 19). A recent study further demonstrated that patients with an extreme degree of TR with an EROA > 0.7 cm^2 exhibited poorer survival than those with severe TR (EROA >0.4 and <0.7 cm^2) (8). Similarly, in a study that recruited consecutive severe TR patients, massive TR (EROA ≥ 0.6 cm^2) was associated with mortality and heart failure re-hospitalization (9). These studies reiterate the need to

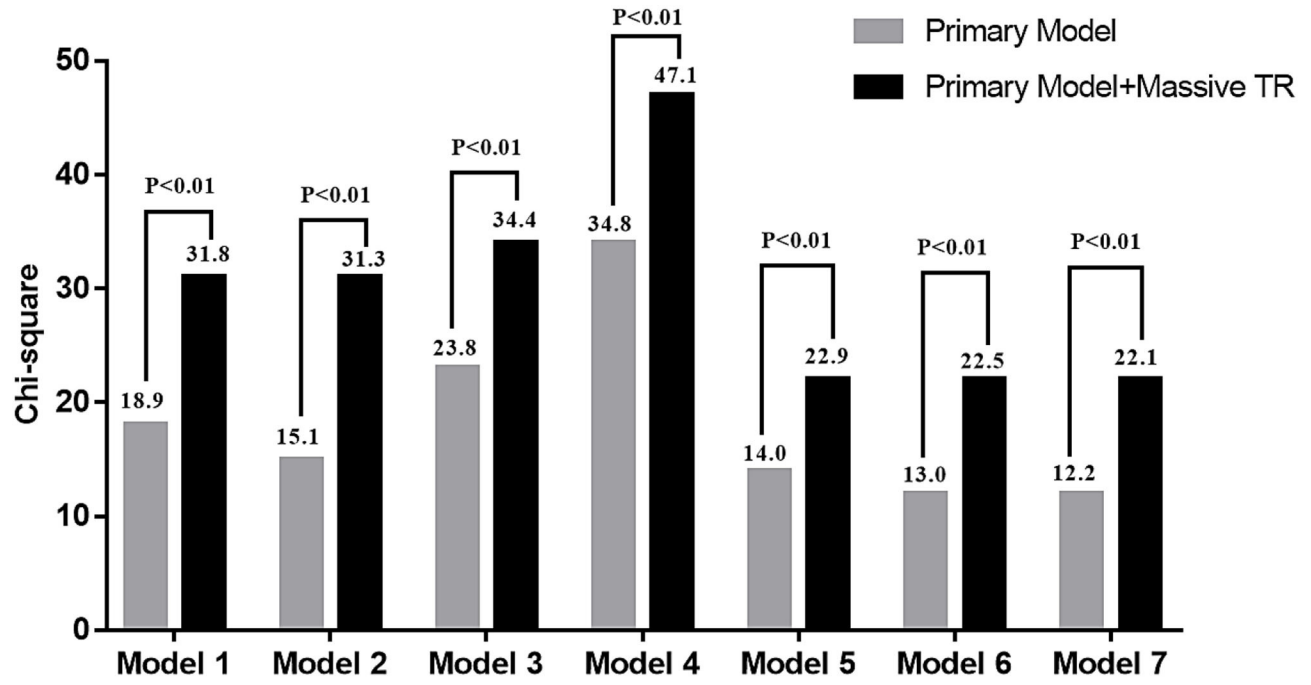

FIGURE 1 | Change in model Chi square with addition of massive tricuspid regurgitation (TR) to the other risk factors. The including parameters of each primary model was same as **Table 3**.

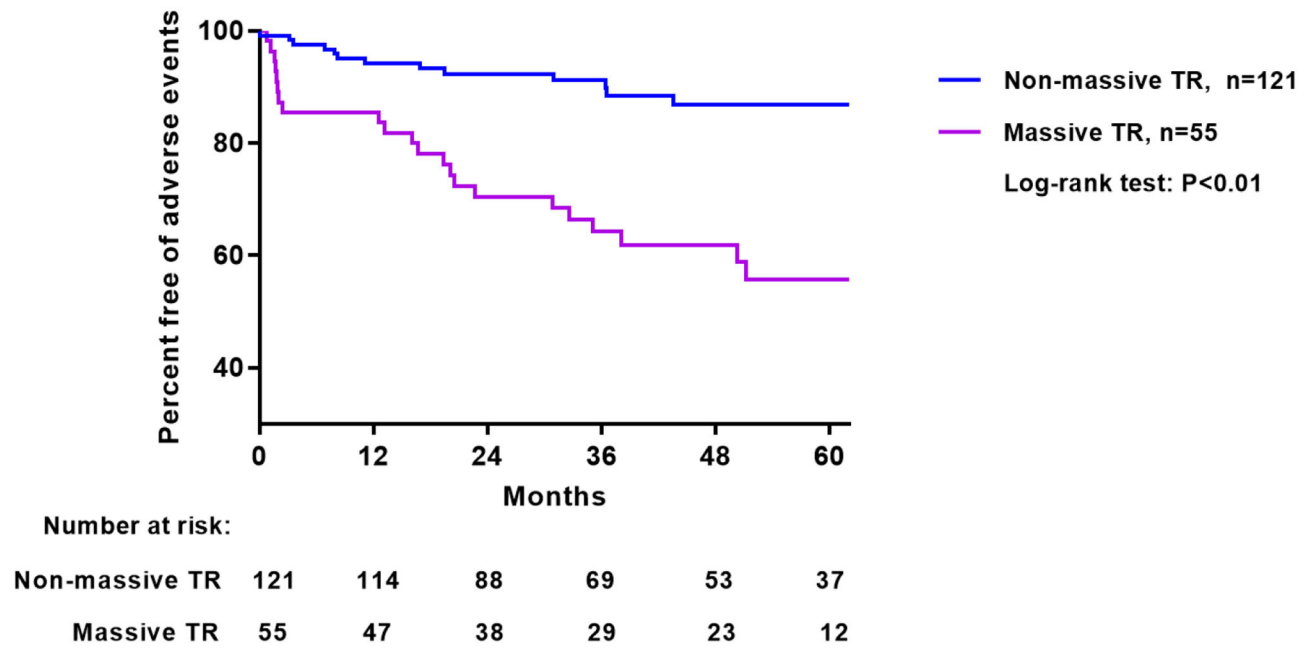

FIGURE 2 | Kaplan-Meier analysis according to tricuspid regurgitation (TR) severity.

revise TR grading. The current definition of severe TR cannot completely accentuate the dismal outcome for those with an extreme form of TR. Our present findings further demonstrate that patients with massive TR experience an adverse outcome following TA. It is clear that early surgical correction before the development of massive TR is warranted as well as intense clinical surveillance following surgery in order to improve clinical performance.

Clinical Implications

The prevalence of TR is increasing, with an estimated prevalence of around 1.6 million patients with significant TR in the USA. Nonetheless fewer than 8,000 patients undergo tricuspid valve surgery per year (21). One reason for this relatively small number of corrective surgeries is perhaps the controversial optimal timing of surgical intervention for TR, mostly due to the limited data available and their heterogeneous nature (6). Another reason may be the poor outcomes following surgery due to late referrals that are often associated with a high risk condition such as hepatic or renal dysfunction. Delayed surgical correction for patients with significant TR may explain their poor long-term postoperative mortality with 5- and 10-year survival rates of 62–72 and 49–51%, respectively (22–24).

According to the current guidelines, TA should be performed during concomitant left-sided valve surgery in patients with TR or dilated tricuspid annulus (6, 7). Recent research further showed that the inclusion of TA at the time of mitral valve surgery resulted in a lower risk of a primary-end-point event at 2 years than those who underwent mitral-valve surgery alone (25). Nonetheless the severity of TR, in particular massive TR, is not one of the indications for surgical correction. Our study highlights that a significant proportion of patients who undergo TA during concomitant left-sided valve surgery have already developed massive TR that is strongly associated with adverse events. Surgeons should consider earlier TA before the development of massive TR, even when LV remodeling has not reached a level that warrants left-sided valve surgery, in order to optimize clinical outcome. Future studies are warranted to provide confirmatory evidence and to support the assessment of TR severity as a factor determining timing of surgery.

Limitations

There are several limitations in this study. Because of the single center study and small number of patients with extreme TR, we used only EROA $\geq$ 0.6 cm^2 to define massive TR. A larger study population is required to further characterize the prognostic risk for those with torrential TR (EROA $\geq$ 0.8 cm^2) according to the recommendation (5). Further, a larger sample size is required to better discriminate the adverse outcome and define the cut-off value of EROA to predict adverse outcome. The present study only included patients who underwent TA with combined left-sided valve surgery; future study should be verified in patients undergoing isolated TA and in a control group. The advent of three-dimensional assessment-derived EROA or vena contracta area may improve the quantification of TR severity (26), and advanced speckle tracking analysis derived right ventricular strain may provide additional predictive information. Therefore, their prognostic value in patients undergoing TA will require future evaluation. Post-operative detailed echocardiography was not systematically performed and post-intervention EROA would require evaluation by future prospective study. In order to confirm the clinical benefits of early TA prior to the development of massive TR, a prospective, randomized multicenter trial is required. In addition, right heart catheter was not performed routinely in our locality and thus invasive measurement of pulmonary hypertension cannot be systematically evaluated. Furthermore, the present study mainly represents Chinese rheumatic valvular heart disease and thus these findings should be confirmed by European/US patients, who may experience functional TR due to non-rheumatic left-sided valve disease.

CONCLUSION

This study provides novel evidence that massive TR is common in patients who underwent TA during concomitant left-sided valve surgery. Importantly, massive TR is independently associated with a dismal outcome. Our observations provide evidence to support the notion that as a coexisting entity, TR severity should be considered to determine the optimal timing for surgery in patients with concomitant left-sided valve disease.

DATA AVAILABILITY STATEMENT

The original contributions presented in the study are included in the article/supplementary material, further inquiries can be directed to the corresponding author/s.

ETHICS STATEMENT

The studies involving human participants were reviewed and approved by the Ethics Committee of the West Cluster Hospital Authority of Hong Kong. The patients/participants provided their written informed consent to participate in this study.

AUTHOR CONTRIBUTIONS

YC and K-HY contributed to conception and design of the study, collection, analysis and interpretation of the data, and drafting and revising of the manuscript. Y-HC, M-ZW, Y-JY, Y-ML, K-YS, DC, CH, and L-MH contributed to patients' recruitment, data collection, and data analysis. C-PL, W-KA, and H-FT contributed to conception of the study and revising of the manuscript. All authors have significant contribution to the manuscript and have approved the final version for submission.

ACKNOWLEDGMENTS

We thank the medical and nursing staff of the Division of Cardiology, Queen Mary Hospital, for their help and support in this study.

REFERENCES

1. Singh JP, Evans JC, Levy D, Larson MG, Freed LA, Fuller DL, et al. Prevalence and clinical determinants of mitral, tricuspid, and aortic regurgitation (the Framingham Heart Study). *Am J Cardiol.* (1999) 83:897–902. doi: 10.1016/S0002-9149(98)01064-9
2. Nath J, Foster E, Heidenreich PA. Impact of tricuspid regurgitation on long-term survival. *J Am Coll Cardiol.* (2004) 43:405–9. doi: 10.1016/j.jacc.2003.09.036

3. Topilsky Y, Nkomo VT, Vatury O, Michelena HI, Letourneau T, Suri RM, et al. Clinical outcome of isolated tricuspid regurgitation. *JACC Cardiovasc Imaging.* (2014) 7:1185–94. doi: 10.1016/j.jcmg.2014.07.018
4. Taramasso M, Hahn RT, Alessandrini H, Latib A, Attinger-Toller A, Braun D, et al. The international multicenter trivalve registry: which patients are undergoing transcatheter tricuspid repair? *JACC Cardiovasc Interv.* (2017) 10:1982–90.
5. Hahn RT, Zamorano JL. The need for a new tricuspid regurgitation grading scheme. *Eur Heart J Cardiovasc Imaging.* (2017) 18:1342–3. doi: 10.1093/ehjci/jex139
6. Vahanian A, Beyersdorf F, Praz F, Milojevic M, Baldus S, Bauersachs J, et al. 2021 ESC/EACTS guidelines for the management of valvular heart disease. *Eur Heart J.* (2021) 2021:ehab395. doi: 10.1093/eurheartj/ehab395
7. Otto CM, Nishimura RA, Bonow RO, Carabello BA, Erwin JP 3rd, Gentile F, et al. 2020 ACC/AHA guideline for the management of patients with valvular heart disease: a report of the American College of Cardiology/American Heart Association Joint Committee on Clinical Practice Guidelines. *Circulation.* (2021) 143:e72–227. doi: 10.1161/CIR.0000000000000923
8. Peri Y, Sadeh B, Sherez C, Hochstadt A, Biner S, Aviram G, et al. Quantitative assessment of effective regurgitant orifice: impact on risk stratification, and cut-off for severe and torrential tricuspid regurgitation grade. *Eur Heart J Cardiovasc Imaging.* (2019) 21:768–76. doi: 10.1093/ehjci/jez267
9. Santoro C, Marco Del Castillo A, González-Gómez A, Monteagudo JM, Hinojar R, Lorente A, et al. Mid-term outcome of severe tricuspid regurgitation: are there any differences according to mechanism and severity? *Eur Heart J Cardiovasc Imaging.* (2019) 20:1035–42. doi: 10.1093/ehjci/jez024
10. Yiu KH, Wong A, Pu L, Chiang MF, Sit KY, Chan D, et al. Prognostic value of preoperative right ventricular geometry and tricuspid valve tethering area in patients undergoing tricuspid annuloplasty. *Circulation.* (2014) 129:87–92. doi: 10.1161/CIRCULATIONAHA.113.003811
11. Lang RM, Badano LP, Mor-Avi V, Afilalo J, Armstrong A, Ernande L, et al. Recommendations for cardiac chamber quantification by echocardiography in adults: an update from the American Society of Echocardiography and the European Association of Cardiovascular Imaging. *J Am Soc Echocardiogr.* (2015) 28:1–39.e14. doi: 10.1016/j.echo.2014.10.003
12. Rudski LG, Lai WW, Afilalo J, Hua L, Handschumacher MD, Chandrasekaran K, et al. Guidelines for the echocardiographic assessment of the right heart in adults: a report from the American Society of Echocardiography endorsed by the European Association of Echocardiography, a registered branch of the European Society of Cardiology, and the Canadian Society of Echocardiography. *J Am Soc Echocardiogr.* (2010) 23:685–713. doi: 10.1016/j.echo.2010.05.010
13. Rivera JM, Mele D, Vandervoort PM, Morris E, Weyman AE, Thomas JD. Effective regurgitant orifice area in tricuspid regurgitation: clinical implementation and follow-up study. *Am Heart J.* (1994) 128:927–33. doi: 10.1016/0002-8703(94)90591-6
14. Zoghbi WA, Adams D, Bonow RO, Enriquez-Sarano M, Foster E, Grayburn PA, et al. Recommendations for noninvasive evaluation of native valvular regurgitation: a report from the American Society of Echocardiography developed in collaboration with the society for cardiovascular magnetic resonance. *J Am Soc Echocardiogr.* (2017) 30:303–71. doi: 10.1016/j.echo.2017.01.007
15. Chen Y, Seto WK, Ho LM, Fung J, Jim MH, Yip G, et al. Relation of tricuspid regurgitation to liver stiffness measured by transient elastography in patients with left-sided cardiac valve disease. *Am J Cardiol.* (2016) 117:640–6. doi: 10.1016/j.amjcard.2015.11.030
16. d'Arcy JL, Coffey S, Loudon MA, Kennedy A, Pearson-Stuttard J, Birks J, et al. Large-scale community echocardiographic screening reveals a major burden of undiagnosed valvular heart disease in older people: the OxVALVE Population Cohort Study. *Eur Heart J.* (2017) 37:3515–22. doi: 10.1093/eurheartj/ehw229
17. Bruce CJ, Connolly HM. Right-sided valve disease deserves a little more respect. *Circulation.* (2009) 119:2726–34. doi: 10.1161/CIRCULATIONAHA.108.776021
18. Hahn RT, Meduri CU, Davidson CJ, Lim S, Nazif TM, Ricciardi MJ, et al. Early feasibility study of a transcatheter tricuspid valve annuloplasty: SCOUT trial 30-day results. *J Am Coll Cardiol.* (2017) 69:1795–806. doi: 10.1016/j.jacc.2017.01.054
19. Topilsky Y, Inojosa JM, Benfari G, Vaturi O, Maltais S, Michelena H, et al. Clinical presentation and outcome of tricuspid regurgitation in patients with systolic dysfunction. *Eur Heart J.* (2018) 39:3584–92. doi: 10.1093/eurheartj/ehy434
20. Ryan T, Petrovic O, Dillon JC, Feigenbaum H, Conley MJ, Armstrong WF. An echocardiographic index for separation of right ventricular volume and pressure overload. *J Am Coll Cardiol.* (1985) 5:918–27. doi: 10.1016/S0735-1097(85)80433-2
21. Stuge O, Liddicoat J. Emerging opportunities for cardiac surgeons within structural heart disease. *J Thorac Cardiovasc Surg.* (2006) 132:1258–61. doi: 10.1016/j.jtcvs.2006.08.049
22. Pfannmuller B, Doenst T, Eberhardt K, Seeburger J, Borger MA, Mohr FW. Increased risk of dehiscence after tricuspid valve repair with rigid annuloplasty rings. *J Thorac Cardiovasc Surg.* (2012) 143:1050–5. doi: 10.1016/j.jtcvs.2011.06.019
23. Marquis-Gravel G, Bouchard D, Perrault LP, Page P, Jeanmart H, Demers P, et al. Retrospective cohort analysis of 926 tricuspid valve surgeries: clinical and hemodynamic outcomes with propensity score analysis. *Am Heart J.* (2012) 163:851–8.e1. doi: 10.1016/j.ahj.2012.02.010
24. Gatti G, Dell'Angela L, Morosin M, Maschietto L, Pinamonti B, Forti G, et al. Tricuspid annuloplasty for tricuspid regurgitation secondary to left-sided heart valve disease: immediate outcomes and risk factors for late failure. *Can J Cardiol.* (2016) 32:760–6. doi: 10.1016/j.cjca.2015.09.007
25. Gammie JS, Chu MWA, Falk V, Overbey JR, Moskowitz AJ, Gillinov M, et al. Concomitant tricuspid repair in patients with degenerative mitral regurgitation. *N Engl J Med.* (2021). doi: 10.1056/NEJMoa2115961. [Epub ahead of print].
26. de Agustin JA, Viliani D, Vieira C, Islas F, Marcos-Alberca P, Gomez de Diego JJ, et al. Proximal isovelocity surface area by single-beat three-dimensional color Doppler echocardiography applied for tricuspid regurgitation quantification. *J Am Soc Echocardiogr.* (2013) 26:1063–72. doi: 10.1016/j.echo.2013.06.006

Conflict of Interest: The authors declare that the research was conducted in the absence of any commercial or financial relationships that could be construed as a potential conflict of interest.

Publisher's Note: All claims expressed in this article are solely those of the authors and do not necessarily represent those of their affiliated organizations, or those of the publisher, the editors and the reviewers. Any product that may be evaluated in this article, or claim that may be made by its manufacturer, is not guaranteed or endorsed by the publisher.

frontiers in Cardiovascular Medicine

ORIGINAL RESEARCH
published: 07 February 2022
doi: 10.3389/fcvm.2022.750634

Prevalence and Prognostic Value of Mesenteric Artery Stenosis in Patients Undergoing Transcatheter Aortic Valve Implantation

Henri Lu[1], David Rotzinger[2], Pierre Monney[1], Olivier Muller[1], Michael Egea[2], Matthieu Grange[3], Eric Eeckhout[1], Matthias Kirsch[4] and Salah D. Qanadli[2]*

[1] Service of Cardiology, Lausanne University Hospital and University of Lausanne, Lausanne, Switzerland, [2] Cardiothoracic and Vascular Unit, Department of Radiology, Lausanne University Hospital, Lausanne, Switzerland, [3] Department of Medical Imaging, Neuchâtel Cantonal Hospital, Neuchâtel, Switzerland, [4] Service of Cardiovascular Surgery, Lausanne University Hospital and University of Lausanne, Lausanne, Switzerland

OPEN ACCESS

Edited by:
Peter Zilla,
University of Cape Town, South Africa

Reviewed by:
Antonino S. Rubino,
University of Campania Luigi Vanvitelli, Italy
Andreina Carbone,
University of Campania Luigi Vanvitelli, Italy

***Correspondence:**
Henri Lu
henri.lu@chuv.ch

Specialty section:
This article was submitted to Heart Valve Disease, a section of the journal Frontiers in Cardiovascular Medicine

Received: *12 August 2021*
Accepted: *17 January 2022*
Published: *07 February 2022*

Citation:
Lu H, Rotzinger D, Monney P, Muller O, Egea M, Grange M, Eeckhout E, Kirsch M and Qanadli SD (2022) Prevalence and Prognostic Value of Mesenteric Artery Stenosis in Patients Undergoing Transcatheter Aortic Valve Implantation. Front. Cardiovasc. Med. 9:750634. doi: 10.3389/fcvm.2022.750634

Introduction: Data regarding the prevalence of mesenteric artery stenosis in patients undergoing transcatheter aortic valve implantation (TAVI) are scarce. Whether patients with high-risk features for acute mesenteric ischemia (AMesI) have a worse prognosis compared with those without high-risk features is unknown. We aimed to address these questions.

Methods: We included 361 patients who underwent TAVI between 2015 and 2019. Using pre-TAVI computed tomography exams, the number of stenosed arteries in each patient and the degree of stenosis for the coeliac trunk (CTr), SMA and inferior mesenteric artery (IMA) were analyzed. High-risk features for AMesI were defined as the presence of ≥2 arteries presenting with ≥50% stenosis. Patient demographic and echocardiographic data were collected. Endpoints included 30-day all-cause mortality, mortality and morbidity related to mesenteric ischemia.

Results: 22.7% of patients had no arterial stenosis, while 59.3% had 1 or 2 stenosed arteries, and 18.0% presented stenoses in 3 arteries. Prevalence of significant stenosis (≥50%) in CTr, SMA, and IMA were respectively 11.9, 5.5, 10.8%. Twenty patients at high-risk for AMesI were identified: they had significantly higher all-cause mortality (15.0 vs. 1.2%, $p < 0.001$) and higher mortality related to AMesI (5.0 vs. 0.3%, $p = 0.004$), compared with non-high-risk patients.

Conclusions: Patients at high-risk for AMesI presented with significantly higher 30-day all-cause mortality and mortality related to AMesI following TAVI. Mesenteric revascularization before TAVI interventions may be beneficial in these patients. Prospective studies are needed to clarify these questions.

Keywords: transcatheter aortic valve implantation, TAVI, TAVR, mesenteric artery stenosis, acute mesenteric ischemia

INTRODUCTION

Mesenteric artery stenosis (MAS) is a frequent incidental finding on abdominal imaging, with more than 90% of cases believed to be of atherosclerotic origin (1). The indications for revascularization in patients presenting with symptomatic MAS are well-established and codified (2), but the management of those with asymptomatic MAS is subject to debate. Although there is consensus that revascularization is not needed in patients with asymptomatic single-vessel stenosis, a decision not to intervene is less clear in those presenting with asymptomatic stenosis of 2 or more mesenteric arteries, as these patients may be at high risk for developing acute mesenteric ischemia (AMesI) (3). This is all the more important as the prevalence of asymptomatic MAS increases with age, being reported as 3% in patients under 65 years and up to 18% in those older than 65 years (4). Patients with aortic stenosis eligible for transcatheter aortic valve implantation (TAVI) are frequently diagnosed with asymptomatic MAS on routine pre-intervention aortic computed tomography (CT) imaging (5). The indication for mesenteric revascularization before TAVI procedures in this particular population is of special interest because TAVI by itself may induce transient hypotension and peripheral hypoperfusion via rapid ventricular pacing, thus theoretically increasing the risk of post-intervention digestive ischemia and digestive ischemia-reperfusion injury (6). To our knowledge, prognosis after TAVI of patients having MAS at baseline has never been studied. Therefore, we performed this single-center study using prospectively collected clinical and imaging data in patients undergoing TAVI to: (1) describe the prevalence and characteristics of asymptomatic MAS, (2) compare patients at high-risk for AMesI, vs. those not at high-risk, with regard to baseline clinical and echocardiographic characteristics, (3) compare the same patients with regard to 30-day all-cause mortality, mortality related to mesenteric ischemia, and incidence of AMesI.

METHODS

Study Population

From January 1st 2015 to December 31st 2019, all patients who underwent TAVI interventions in our institution (Lausanne University Hospital, or CHUV), with available pre-intervention CT imaging data, were included. The CHUV serves as an academic tertiary-care hospital for a major part of the French-speaking population of Switzerland.

Ethical Statement

All patients belonged to the SWISS TAVI Registry and provided written informed consent for the use of their data for research purposes. The study was conducted in accordance with the Declaration of Helsinki. Ethical approval was given by the local ethics commission (*Commission cantonale d'éthique de la recherche sur l'être humain*), decision CER-VD 211/13, dated May 10th, 2013.

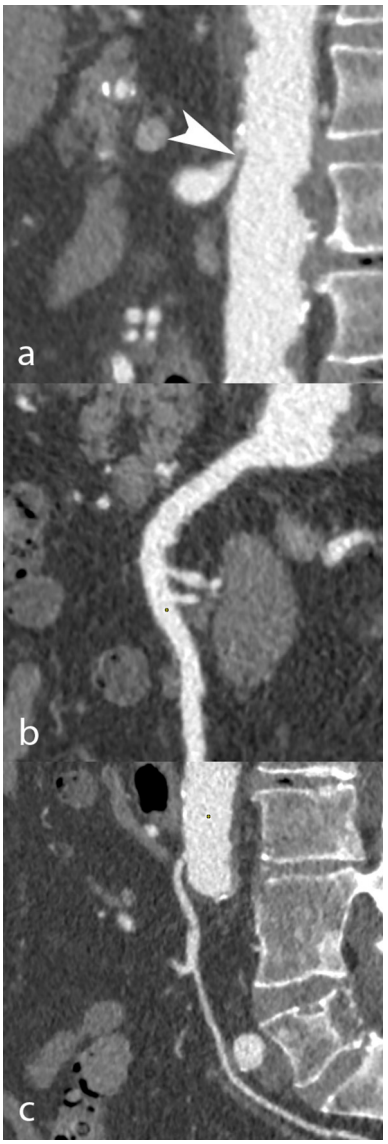

FIGURE 1 | CT angiography in an 85-year-old man scheduled to undergo TAVI. Curvilinear reconstructions show the coeliac trunk **(a)**, superior **(b)**, and inferior mesenteric artery **(c)**. While the coeliac trunk was occluded due to the combination of an arcuate ligament and a mixed plaque (white arrowhead), the mesenteric arteries had no occlusive disease.

CT Image Acquisition and Analysis

CT imaging acquisitions were performed on a 256-row multidetector CT system (Revolution CT, GE Healthcare), with patients lying on their back, arms raised above their head, in a single breath-hold. Cardiac ECG-gated non-contrast images were first acquired to compute the aortic valve calcium score (these series were not analyzed as part of this study). In a second step, ECG-gated CT angiography of the carotid arteries, aorta, and iliac arteries was performed in the craniocaudal direction, following 100 mL of 350 mg/mL of iodinated contrast medium (Accupaque 350, GE Healthcare) injected into an antecubital vein

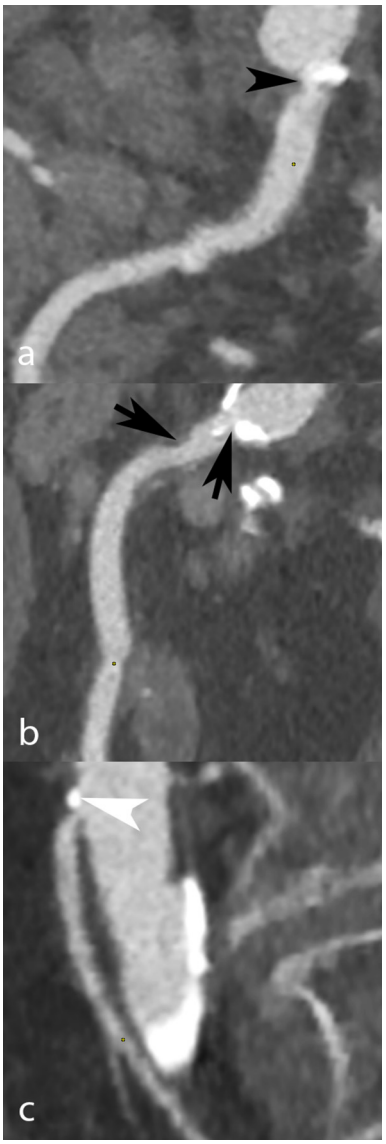

FIGURE 2 | CT angiography in a 90-year-old woman scheduled to undergo TAVI. Curvilinear reconstructions show the coeliac trunk **(a)**, superior **(b)**, and inferior mesenteric artery **(c)**. All three arteries had significant ostial occlusive disease, due to mixed plaques at the coeliac (black arrowhead) and inferior mesenteric (white arrowhead) arteries' ostium, and to a mixed ostial plaque associated with a non-calcified post-ostial plaque (black arrows) in the superior mesenteric artery.

(on the right side whenever possible). Images were analyzed by two radiologists, with any disagreement resolved by consensus or with the help of a third senior radiologist. Interrater variability for superior mesenteric artery (SMA) stenosis assessment has been evaluated previously (7). Data were prospectively collected in a dedicated file.

Data Collection and Analysis

Imaging Data

The coeliac trunk (CTr), superior mesenteric artery (SMA) and inferior mesenteric artery (IMA) were analyzed in all patients. Each artery was classified according to lumen narrowing expressed in percentage of the reference diameter: normal (0%), mild stenosis (<50%), moderate stenosis (50 to 69%), severe stenosis (70 to 99%), or occlusion (100%). The total number of stenosed arteries (0, 1, 2, or 3) in each patient, regardless of stenosis severity, was also collected. Patients at high-risk for AMesI were defined as those presenting with at least 2 arteries out of 3 presenting each with ≥50% stenosis (8). **Figures 1**, **2** show examples of CT-angiography with reconstructions of the CTr, SMA, and IMA, in patients undergoing pre-TAVI assessment.

TABLE 1 | Repartition of patients by number of stenosed arteries, regardless of stenosis severity.

Number of stenosed arteries	Number of patients (%)
0	82 (22.7)
1	109 (30.2)
2	105 (29.1)
3	65 (18.0)

TABLE 2 | Repartition of patients by degree of stenosis for each artery.

CT findings	Coeliac trunk	Superior mesenteric artery	Inferior mesenteric artery
Normal	164 (45.4)	218 (60.4)	226 (62.6)
Mild (1–49%)	152 (42.2)	123 (34.1)	84 (23.3)
Moderate (50–69%)	35 (9.7)	19 (5.3)	35 (9.7)
Severe (70–99%)	8 (2.2)	1 (0.2)	4 (1.1)
Occlusion (100%)	2 (0.5)	0 (0.0)	12 (3.3)

Values are expressed as n (%).

Patient Data

Baseline patient demographic characteristics, including gender, age, body mass index (BMI), major comorbidities (such as diabetes mellitus and coronary artery disease), and echocardiographic data (left ventricular ejection fraction [LVEF]) were collected. Post-operative endpoints included 30-day all-cause mortality, 30-day mortality related to AMesI (as assessed by reviewing of medical files), all cases of AMesI within 30 days after TAVI. Only cases where the diagnosis of AMesI was confirmed based on an abdominal CT exam or perioperatively if the patient directly underwent abdominal surgery, were counted.

Statistical Analysis

Categorical variables were expressed as frequencies and percentages and compared using Pearson's χ^2 test. Continuous variables were reported as means with standard deviations (SDs) or medians with interquartile ranges (IQRs) and were tested for normality distribution using the Shapiro-Wilk test. Student's *t*-test was used to compare normally distributed continuous variables, whereas the Mann-Whitney test was used to compare non-normally distributed ones. Thirty-day survival curves were

TABLE 3 | Baseline clinical and echocardiographic characteristics of patients at high-risk for mesenteric ischemia, vs. patients non at high-risk.

	High-risk ($n = 20$)	Non-high risk ($n = 341$)	*p*-value
Clinical characteristics			
Age, years, median (IQR)	82.0 (76.0, 87.0)	83.0 (79.0, 87.0)	0.950
Male	7 (35.0)	159 (46.6)	0.311
BMI, kg/m^2, median (IQR)	23.8 (20.8, 26.0)	25.6 (23.0, 29.7)	0.060
NYHA Functional class			
• I–II	4 (20.0)	114 (33.4)	0.239
• III–IV	16 (80.0)	227 (66.6)	
Euroscore II, median (IQR)	5.31 (3.86, 16.45)	3.87 (2.23, 6.42)	0.030
Chronic obstructive pulmonary disease	7 (35.0)	55 (16.1)	0.030
Diabetes mellitus	4 (20.0)	89 (26.1)	0.544
Dyslipidemia	15 (75.0)	182 (53.4)	0.059
Previous cardiac surgery	5 (25.0)	56 (16.4)	0.320
Coronary artery disease	12 (60.0)	171 (50.1)	0.392
Previous PCI	3 (15.0)	48 (14.1)	0.908
Hypertension	16 (80.0)	255 (74.8)	0.600
Stroke or TIA	4 (20.0)	47 (13.8)	0.438
Moderate to severe CKD	15 (75.0)	194 (56.9)	0.111
Echocardiographic characteristics			
LVEF			
• >50%	15 (75.0)	245 (71.8)	0.775
• 30–50%	4 (20.0)	73 (21.4)	0.876
• <30%	2 (10.0)	22 (6.4)	0.536

Patients were considered high-risk if they had at least 2 arteries out of 3 presenting each with ≥50% stenosis. Values are expressed as n (%), unless specified otherwise.TAVI, transcatheter aortic valve replacement; IQR, interquartile range; BMI, body mass index; PCI, percutaneous coronary intervention; NYHA, New York Heart Association; TIA, transient ischemic attack; CKD, chronic kidney disease; LVEF, left ventricle ejection fraction.

modeled using the Kaplan-Meier method and were analyzed using a log-rank test. Values with a $p < 0.05$ were considered statistically significant. The SPSS 27.0 software (SPSS Inc., Chicago, Illinois, USA) was used for all statistical analyses.

RESULTS

A total of 361 patients were included in our study. The distribution of the patients according to the number of stenosed arteries, regardless of stenosis severity, is presented in **Table 1**: 82 (22.7%) did not present any arterial stenosis, while 109 (30.2%) had 1 stenosed artery, 105 (29.1%) had 2 stenosed arteries, and 65 (18.0%) presented stenosis in all 3 arteries. Among the 361 patients, 20 at high-risk for AMesI were identified. **Table 2** shows the repartition of patients by degree of stenosis for each artery. Overall, 197 patients (54.6%) presented with CTr stenosis of any degree, or occlusion, while 143 (39.6%) had SMA stenosis of any degree or occlusion, and 135 (37.4%) IMA stenosis of any degree or occlusion. Prevalence of moderate and severe stenosis associated with CTr, SMA, and IMA were, respectively 11.9, 5.5, 10.8%; the prevalence of occlusion was, respectively 0.5, 0.0, and 3.3%.

Baseline patient demographic, clinical, and echocardiographic characteristics are presented in **Table 3**. Compared with patients not at high-risk for AMesI, those at high-risk had significantly higher surgical risk, as assessed by the Euroscore II (5.31 [IQR, 3.86–16.45] vs. 3.87, [IQR, 2.23–6.42], $p = 0.030$) and higher prevalence of chronic obstructive pulmonary disease (35.0 vs. 16.1%, $p = 0.030$). No significant difference was found regarding the other baseline patient characteristics, although a trend toward lower BMIs and higher prevalence of dyslipidemia was found in high-risk patients.

Post-operative Outcomes

Thirty-day outcomes are presented in **Table 4**. Patients at high-risk for AMesI had significantly higher all-cause mortality (15.0 vs. 1.2%, $p < 0.001$) and higher mortality related to AMesI (5.0 vs. 0.3%, $p = 0.004$). Among the three patients at high-risk for AMesI who died, one died of AMesI, while two died of extra-digestive causes (acute respiratory failure in both cases). There was a non-significant trend toward a higher incidence of AMesI in high-risk patients (5.0 vs. 0.9%, $p = 0.065$). Kaplan-Meier survival curves for 30-day all-cause mortality and mortality related to AMesI are presented in **Figure 3**.

DISCUSSION

Our results can be summarized as follows: (1) among the 361 patients undergoing pre-TAVI routine CT screening, 279

TABLE 4 | Postoperative endpoints of patients at high-risk for mesenteric ischemia, vs. patients non at high-risk.

	High-risk ($n = 20$)	Non-high risk ($n = 341$)	p-value
All-cause 30-day mortality	3 (15.0)	4 (1.2)	<0.001
30-day mortality related to digestive ischemia	1 (5.0)	1 (0.3)	0.004
Digestive ischemia (all cases)	1 (5.0)	3 (0.9)	0.065

Values are expressed as n (%).

(77.3%) presented with at least one stenosed mesenteric artery and 20 (5.5%) were at high-risk for AMesI, (2) patients at high-risk for AMesI had significantly more comorbidities and higher surgical risk, compared with those not at high-risk, (3) patients at high-risk for AMesI at baseline presented with increased risks of 30-day all-cause mortality and 30-day mortality related to AMesI following TAVI.

Routine CT exams performed in patients eligible for TAVI constitute an important database to analyze asymptomatic MAS. This is all the more interesting as available data in the literature on asymptomatic MAS is very scarce. A previous retrospective study compared the prevalence of MAS in 73 patients planned for TAVI interventions who underwent routine CT imaging against 111 control patients who had CT imaging for other reasons (5). Stenoses with a lumen reduction of at least 50% were considered significant. 45.2% of TAVI patients had significant stenosis in at least 1 artery, and 8.2% of TAVI patients had significant stenosis in multiple arteries: these results are similar to our data. Interestingly, although the TAVI patients and control patients had no significant difference regarding demographic and clinical characteristics, the prevalence of MAS in control patients was lower (22.5% had at least 1 stenosed artery, and 1.8% had multiple stenosed arteries). This observation suggests that candidates for TAVI may present a higher atherosclerotic burden than the general population and is in agreement with previous reports (9, 10).

Although an increased risk of all-cause 30-day mortality was observed in patients at high-risk for AMesI compared with those not at high-risk, the two population groups were not comparable, as patients at high-risk for AMesI had a significantly higher surgical risk and more comorbidities. To which extent these differences regarding baseline characteristics have biased our results is unclear. Likewise, it is not possible to conclude if high-risk features for AMesI are mere markers of overall frailty or are independent predictors of mortality. In that sense, considering mortality related to AMesI may be more relevant, as potential confounding factors may less influence this endpoint. Concerning mortality related to AMesI in all our patients, it is worth noting that one previous study analyzing vascular complications in 102 patients undergoing TAVI found five major vascular complications, of which one was AMesI, with a fatal outcome at day 7. This rate of approximately 1% lies in the same range as our data (11).

One physio-pathological mechanism behind the increased mortality rate in patients at high-risk for AMesI may be the transient hypotension and peripheral hypoperfusion induced by rapid ventricular pacing. Briefly, the latter is necessary to implant balloon-expandable transcatheter heart valves (THVs) to reduce cardiac output and achieve cardiac standstill, thus allowing optimal positioning of the THVs (12). Rapid ventricular pacing may also be used with self-expandable THVs when pre- or post-dilatation of the aortic valve is needed. Patients at high-risk for AMesI at baseline may be more prone to developing overt digestive ischemia following rapid ventricular pacing. The same mechanism has been used to explain, among others, the pathogenesis of acute kidney injury after TAVI (13). Supporting this hypothesis, Fefer and colleagues, using a cohort of 412 patients undergoing TAVI, showed that patients who had three or more pacing episodes during TAVI procedures, compared with those who had no pacing, or 1 to2 pacing episodes, were significantly more likely to present prolonged procedural hypotension (respectively 25, 0, and 16%, $p < 0.001$) and suffered greater in-hospital mortality (6.5, 1.7, and 1.7%, $p = 0.045$) (6). From a physio-pathological standpoint, other factors that might precipitate overt AMesI in patients presenting high-risk features include embolic events, massive periprocedural bleeding, and anesthesia modality (local with sedation or general). However, these were not analyzed in our study.

The number of patients at high-risk for AMesI was relatively low (20 out of 361), yet the risk of 30-day mortality (all-cause and AMesI-related) was significantly increased. In our opinion, this highlights the importance of adequately screening and following these patients. The indication for pre-TAVI mesenteric revascularization should be tailored to each situation, and, in the absence of clear recommendations, it should be discussed on a case-by-case basis. This is all the more important as MAS is now easily treatable in most cases via an endovascular approach (percutaneous transluminal angioplasty and stenting). This approach has become the gold standard in most centers in the past decade and may be associated with significantly lower morbidity and mortality compared with open surgical revascularization (4, 14). After TAVI, the threshold to screen for AMesI should be particularly low in high-risk patients, especially since AMesI often presents with non-specific abdominal symptoms (postprandial abdominal pain, nausea/vomiting, diarrhea) (15). In all cases, cardiovascular secondary prevention measures are recommended to limit the progression of atherosclerotic disease (16).

LIMITATIONS

Our study is subject to some limitations. First, patients at high-risk for AMesI and those not at high-risk for AMesI had significantly different baseline surgical risk and comorbidities;

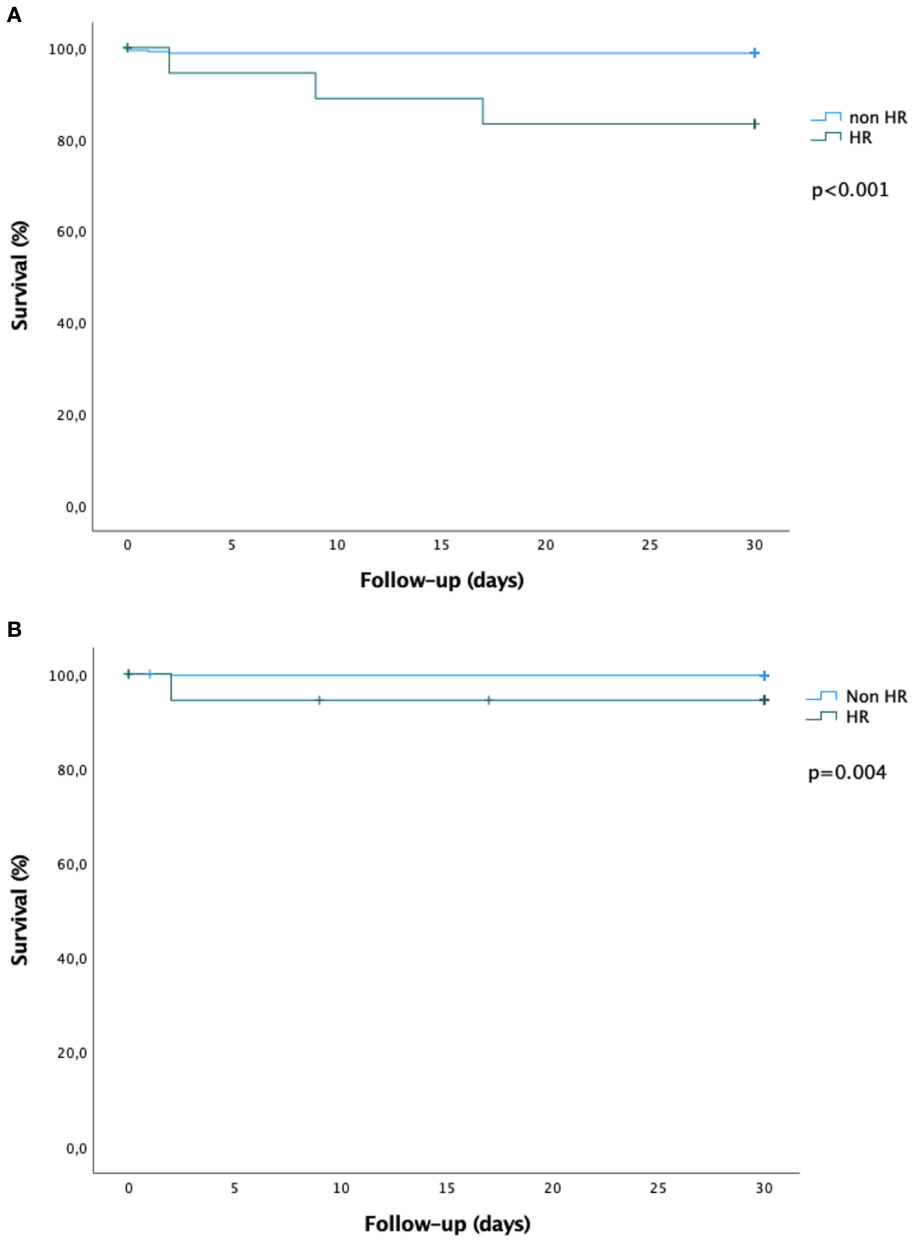

FIGURE 3 | Kaplan-Meier survival curves at 30 days. **(A)** All-cause mortality. **(B)** Mortality related to digestive ischemia. The green curves represent the high-risk group, the blue curves represent the non-high-risk group. Survival curves were compared using the log-rank test.

to which extent this may have affected the outcomes of interest is unclear. We tried to overcome this issue by adjusting for differences in comorbidities at baseline, but because of the small sample of patients with high-risk features and the relatively low overall mortality rate, statistical power was insufficient to consider a multivariable analysis. However, despite this limitation, our findings are hypothesis-generating. Secondly, we only compared 30-day outcomes after TAVI, but a more extended analysis period may be interesting. Finally, the results reported here are those of a single Swiss tertiary center and may not be transposable to other populations and centers.

CONCLUSIONS

To our knowledge, this study is the first report evaluating the prognosis of patients at high-risk for AMesI after TAVI interventions. These patients presented with higher 30-day all-cause mortality and mortality related to AMesI, provided they had more comorbidities and higher surgical risk

compared with those not at high-risk for AMesI. Although these results need to be confirmed with larger cohorts, they are hypothesis-generating in so far as mesenteric revascularization before TAVI interventions may be beneficial in patients presenting with high-risk features for AMesI. Further prospective studies are needed to clarify this question.

DATA AVAILABILITY STATEMENT

The raw data supporting the conclusions of this article will be made available by the authors, without undue reservation.

ETHICS STATEMENT

The studies involving human participants were reviewed and approved by CER-VD 211/13. The patients/participants provided their written informed consent to participate in this study.

AUTHOR CONTRIBUTIONS

HL: data curation, formal analysis, methodology, and writing (original draft). DR, PM, and SQ: supervision, validation, and writing (review and editing). OM, ME, MG, EE, and MK: validation. All authors contributed to the article and approved the submitted version.

REFERENCES

1. Clair DG, Beach JM. Mesenteric ischemia. *N Engl J Med.* (2016) 374: 959-68. doi: 10.1056/NEJMra1503884
2. Hohenwalter EJ. Chronic mesenteric ischemia: diagnosis and treatment. *Semin Intervent Radiol.* (2009) 26: 345-51. doi: 10.1055/s-0029-1242198
3. Terlouw LG, Moelker A, Abrahamsen J, Acosta S, Bakker OJ, Baumgartner I, et al. European guidelines on chronic mesenteric ischaemia – joint United European gastroenterology, European association for gastroenterology, endoscopy and ntrition, European society of gastrointestinal and abdominal radiology, netherlands association of hepatogastroenterologists, hellenic society of gastroenterology, cardiovascular and interventional radiological society of Europe, and dutch mesenteric ischemia study group clinical guidelines on the diagnosis and treatment of patients with chronic mesenteric ischaemia. *United Eur Gastroenterol J.* (2020) 8:371–95. doi: 10.1177/2050640620916681
4. van Dijk LJ, van Noord D, de Vries AC, Kolkman JJ, Geelkerken RH, Verhagen HJ, et al. Clinical management of chronic mesenteric ischemia. *United Eur Gastroenterol J.* (2019) 7:179–88. doi: 10.1177/2050640618817698
5. Idil Soylu A, Avcioglu U, Uzunkaya F, Soylu K. Evaluation of mesenteric artery disease in patients with severe aortic valve stenosis. *J Investig Med.* (2021) 69:719–23. doi: 10.1136/jim-2020-001549
6. Fefer P, Bogdan A, Grossman Y, Berkovitch A, Brodov Y, Kuperstein R, et al. Impact of rapid ventricular pacing on outcome after transcatheter aortic valve replacement. *J Am Heart Assoc.* (2018) 7:e009038. doi: 10.1161/JAHA.118.009038
7. Lundin N, Lehti L, Ekberg O, Acosta S. Validation of computed tomography angiography using mean arterial pressure gradient as a reference in stented superior mesenteric artery. *Abdom Radiol.* (2021) 46:792diol, Acosta S. Validation of compu
8. Bj46:7 M, Koelemay M, Acosta S, Bastos Goncalves F, KF, Kl T, Kolkman JJ, et al. EditorJJnchoice - management of the diseases of mesenteric arteries and veins: clinical practice guidelines of the european society of vascular surgery (ESVS). *Eur J Vasc Endovasc Surg.* (2017) 53:460 SurggSurg 10.1016/j.ejvs.2017.01.010
9. Fusini L, Mirea O, Tamborini G, Muratori M, Gripari P, Cefale C, et al. Incidence and severity of atherosclerotic cardiovascular artery disease in patients undergoing TAVI. *Int J Cardiovasc Imaging.* (2015) 31:975sc Imaginginging7/s10554-015-0651-9
10. Fanaroff AC, Manandhar P, Holmes DR, Cohen DJ, Harrison JK, Hughes GC, et al. Peripheral artery disease and transcatheter aortic valve replacement outcomes: a report from the society of thoracic surgeons/american college of cardiology transcatheter therapy registry. *Circ Cardiovasc Interv.* (2017) 10:e005456. doi: 10.1161/CIRCINTERVENTIONS.117.005456
11. Perrin N, Ellenberger C, Licker M, Hachulla AL, Cikirikcioglu M, Frei A, et al. Management of vascular complications following transcatheter aortic valve implantation. *Arch Cardiovasc Dis.* (2015) 108:491c Disc Discular complications followi
12. Faurie B, Souteyrand G, Staat P, Godin M, Caussin C, Van Belle E, et al. Left ventricular rapid pacing via the valve delivery guidewire in transcatheter aortic valve replacement. *JACC Cardiovasc Interv.* (2019) 12:2449–449:9vasc Intervntervic valve repla
13. Cheungpasitporn W, Thongprayoon C, Kashani K. Transcatheter aortic valve replacement; a kidney's perspective. *J Ren Inj Prev.* (2016) 5:1–7. doi: 10.15171/jrip.2016.01
14. Fioole B, van de Rest HJM, Meijer JRM, van Leersum M, van Koeverden S, Moll FL, et al. Percutaneous transluminal angioplasty and stenting as first-choice treatment in patients with chronic mesenteric ischemia. *J Vasc Surg.* (2010) 51:386-91. doi: 10.1016/j.jvs.2009.08.055
15. Wilkins LR, Stone JR. Chronic Mesenteric Ischemia. *Tech Vasc Interv Radiol.* (2015) 18:31–7. doi: 10.1053/j.tvir.2014.12.005
16. Zeller T, Rastan A, Sixt S. Chronic atherosclerotic mesenteric ischemia (CMI). *Vasc Med.* (2010) 15:333nic doi: 10.1177/1358863X10372437

Conflict of Interest: The authors declare that the research was conducted in the absence of any commercial or financial relationships that could be construed as a potential conflict of interest.

frontiers in Cardiovascular Medicine

ORIGINAL RESEARCH
published: 03 March 2022
doi: 10.3389/fcvm.2022.796447

Prevalence and Mortality of Moderate or Severe Mitral Regurgitation Among Patients Undergoing Percutaneous Coronary Intervention With or Without Heart Failure: Results From CIN Study With 28,358 Patients

Haozhang Huang[1†], Jin Liu[1†], Kunming Bao[2†], Xiaoyu Huang[3], Dehua Huang[3], Haiyan Wei[4], Nuerbahaer Remutula[4], Tilakezi Tuersun[4], Wenguang Lai[1,5], Qiang Li[1], Bo Wang[1], Yibo He[1], Heyin Yang[4], Shiqun Chen[1], Jiyan Chen[1,5], Kaihong Chen[2], Ning Tan[1,5], Xiaoyan Wang[6,7], Liling Chen[2]* and Yong Liu[1,5]**

[1] Department of Guangdong Provincial Key Laboratory of Coronary Heart Disease Prevention, Guangdong Cardiovascular Institute, Guangdong Provincial People's Hospital, Guangdong Academy of Medical Sciences, Guangzhou, China, [2] Department of Cardiology, Longyan First Hospital Affiliated With Fujian Medical University, Longyan, China, [3] People's Hospital of Yangjiang, Yangjiang, China, [4] Department of Cardiology, First People's Hospital of Kashgar, Kashgar, China, [5] Guangdong Provincial People's Hospital, School of Medicine, South China University of Technology, Guangzhou, China, [6] The First Affiliated Hospital, Sun Yat-sen University, Guangzhou, China, [7] Department of Nuclear Medicine, The First Affiliated Hospital of Sun Yat-sen University, Guangzhou, China

Aim: This study investigated the prevalence and mortality associated with moderate or severe mitral regurgitation (MR) among patients undergoing percutaneous coronary intervention (PCI), with or without heart failure (HF).

Methods: We analyzed patients undergoing PCI without mitral valve surgery from the Cardiorenal ImprovemeNt (CIN) study (ClinicalTrials.gov NCT04407936). Patients without echocardiography to determine MR occurrence or lacking follow-up death data were excluded. Primary endpoints were 1-year and long-term all-cause mortality, with a median follow-up time of 5 years (interquartile range: 3.1–7.6).

Results: Of 28,358 patients undergoing PCI treatment [mean age: 62.7 ± 10.7; women: 6,749 (25.6%)], 3,506 (12.4%) had moderate or severe MR, and there was a higher rate of moderate or severe MR in HF group than non-HF group (28.8 vs. 5.6%, respectively). Regardless of HF conditions, patients with moderate or severe MR were older and had worse cardio-renal function and significantly increased 1-year mortality [adjusted hazard ratio (aHR): 1.82, 95% confidence interval (CI): 1.51–2.2], and long-term mortality [aHR: 1.43, 95% CI: 1.3–1.58]. There was no significant difference between patients with HF and those with non-HF (*P* for interaction > 0.05).

OPEN ACCESS

Edited by:
Peter Zilla,
University of Cape Town, South Africa

Reviewed by:
Ailan Chen,
First Affiliated Hospital of Guangzhou Medical University, China
Antonio Miceli,
Istituto Clinico Sant'Ambrogio, Italy

***Correspondence:**
Yong Liu
liuyong@gdph.org.cn
Liling Chen
chenliling19790206@163.com
Xiaoyan Wang
wangxy7@mail.sysu.edu.cn

[†]These authors have contributed equally to this work

Specialty section:
This article was submitted to Heart Valve Disease, a section of the journal Frontiers in Cardiovascular Medicine

Received: *16 October 2021*
Accepted: *03 February 2022*
Published: *03 March 2022*

Citation:
Huang H, Liu J, Bao K, Huang X, Huang D, Wei H, Remutula N, Tuersun T, Lai W, Li Q, Wang B, He Y, Yang H, Chen S, Chen J, Chen K, Tan N, Wang X, Chen L and Liu Y (2022) Prevalence and Mortality of Moderate or Severe Mitral Regurgitation Among Patients Undergoing Percutaneous Coronary Intervention With or Without Heart Failure: Results From CIN Study With 28,358 Patients. Front. Cardiovasc. Med. 9:796447. doi: 10.3389/fcvm.2022.796447

Conclusion: One-eighth of the patients undergoing PCI had moderate or severe MR. Furthermore, one-third and one-seventeenth experienced moderate or severe MR with worse cardiorenal function in the HF and non-HF groups, and increased consistent mortality risk. Further studies should explore the efficacy of mitral interventional procedures for moderate or severe MR after PCI treatment, regardless of HF.

Keywords: moderate or severe mitral regurgitation, percutaneous coronary intervention, heart failure, coronary artery disease, prevalence, mortality

INTRODUCTION

Mitral regurgitation (MR) is a common valvular disease and serves as a worse prognosis predictor, especially in patients with coronary artery disease (CAD) (1–3), and up to 50% of moderate or severe MR pathological remodeling was attributed to chronic CAD (4).

Percutaneous coronary intervention (PCI) has become the most common revascularization strategy for patients with obstructive CAD; it can reduce the area of myocardial ischemia and reflux of MR (5, 6). There were several studies indicating a lower survival rate of moderate or severe MR among patients undergoing PCI, but these were limited to small samples or CAD subtypes (7, 8). Therefore, large-scale cohort studies on prevalence and outcomes of moderate or severe MR among patients with CAD undergoing PCI are still lacking.

With improvement in management, the treatment rate of PCI is increasing in patients with CAD with HF, but the prognosis remains poor because of complicated clinical features (9). Previous studies have demonstrated that moderate or severe MR is common among patients with HF and associated with poor prognosis (10–12), while the role of moderate or severe MR in patients with HF undergoing PCI has been poorly addressed. Furthermore, whether there is higher incidence and mortality of moderate or severe MR among PCI with HF compared to those without has not been previously reported.

To address some of these knowledge gaps, we aimed to systematically explore the prevalence and outcomes of moderate or severe MR compared with normal or mild MR among patients with CAD undergoing PCI. Most importantly, we intended to test the hypothesis that these patients, with or without HF, would have significant differences in mortality risk in moderate or severe MR.

METHODS

Study Design and Patient Selection

The Cardiorenal ImprovemeNt (CIN) Registry is a retrospective, single-center, observational cohort study that enrolled patients undergoing PCI treatment according to standardized clinical practice guidelines at Guangdong Provincial People's Hospital, China, from January 2007 to December 2018 (ClinicalTrials.gov NCT04407936) (13, 14). Among these patients, 8,275 were complicated by HF. The exclusion criteria were (1) age < 18 years ($n = 12$); (2) life expectancy < 1 year due to malignancy or other end-stage diseases ($n = 346$); (3) subsequent mitral valve surgery ($n = 74$); and (4) lack of follow-up data ($n = 3,235$). Finally, 28,358 patients undergoing PCI treatment complicated by MR, with or without HF, were included in our study (**Figure 1**). The study population was divided into four groups according to MR severity and cardiac function as follows: Group 1 experienced HF and was classified as normal or mild MR; Group 2 experienced HF with moderate or severe MR; Group 3 did not experience HF (non-HF) and was classified as normal or mild MR; Group 4 did not experience HF with moderate or severe MR.

Data Extraction

The presence of MR was determined according to the results of first echocardiography examination, and the severity of MR was derived from the echocardiogram report and classified according to two levels (normal or mild vs. moderate or severe). MR severity was evaluated by visual assessment integrating Doppler data from multiple acoustic windows and incorporating qualitative and semi-quantitative methods. Senior echocardiography physicians were responsible for data quality control and periodic database verification.

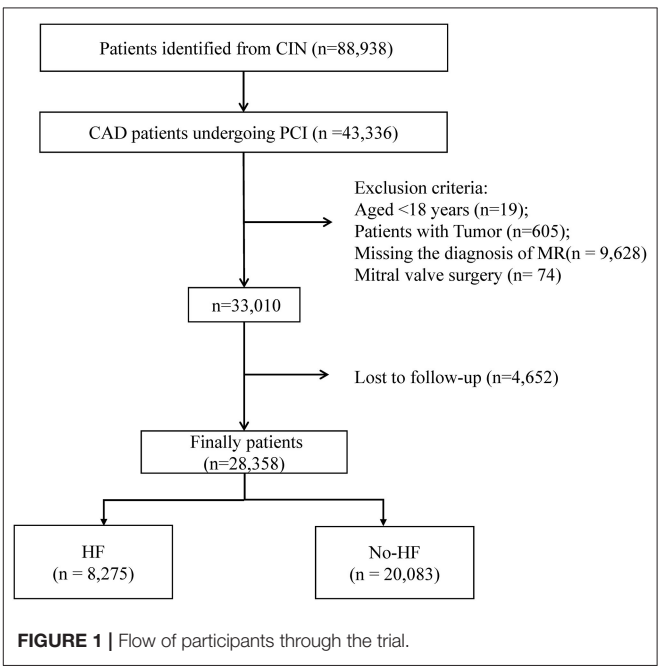

FIGURE 1 | Flow of participants through the trial.

Outcomes and Definitions

The primary endpoints were 1-year and long-term all-cause mortality. The follow-up data were obtained from the Guangdong Provincial Public Security database, which was matched against the electronic Clinical Management System of the Guangdong Provincial People's Hospital records based on the unique ID number for each patient.

Heart failure (HF) status was assessed according to signs, symptoms, and guideline-based laboratory tests (15, 16). Comorbidities included hypertension (HT), diabetes mellitus (DM), acute myocardial infarction (AMI), atrial fibrillation(AF), chronic kidney disease (CKD, defined as eGFR $\leq$ 60 ml/min/1.73 m^2), anemia (defined as hematocrit $<$ 36% for women and $<$ 39% for men) (17), hyperlipidemia (defined according to 2016 ESC guidelines for treating dyslipidemias) (18), and chronic obstructive pulmonary disease.

Statistical Analysis

Descriptive statistics for baseline variables are presented as the mean [standard deviation (SD)], median [interquartile range (IQR)], or number and percentage as appropriate. Differences in baseline characteristics between two groups were analyzed by Student's *t*-test and Pearson's Chi-squared test. Comparison among multiple groups was assessed by analysis of variance (ANOVA) (for continuous variables) and chi-square test (for categorical variables) as appropriate. Type I errors were minimized using the Bonferroni correction (Bonferroni correction = 0.05/6).

Kaplan–Meier (KM) analyses with stratified log-rank tests were performed to assess survival among the four groups. A Cox proportional hazards model with multivariable analysis was used to compare 1-year and long-term all-cause mortality risk according to the prevalence of moderate or severe MR among the HF and non-HF groups. Variables known to be associated with mortality according to clinical experience were controlled further by multivariable Cox regression using different models. Model 1 was unadjusted; Model 2 was adjusted for age and sex; and Model 3 included age, gender, hypertension, CKD, AMI, stroke, AF, DM, hyperlipidemia, anemia, in-hospital dialysis, angiotensin-converting enzyme inhibitors (ACEI)/angiotensin receptor blockers (ARB), β-blockers, statins, antiplatelet, calcium channel blocker, mineralocorticoid receptor antagonists (MRA), loop diuretics, and oral anticoagulants.

We also performed eight pre-specified subgroup analyses to assess the effects of moderate or severe MR on long-term all-cause mortality among patients undergoing PCI with or without HF, including male vs. female; age $>$ 65 years vs. $\leq$ 65 years; AMI vs. non-AMI; and left ventricular dysfunction (LVD) vs. non-LVD. All statistical tests were two-sided, and a threshold of *p*-value $<$ 0.05 was set for significance. All the statistical analyses were performed using R v 4.0.3 (R Institute for Statistical Computing, Vienna, Austria).

RESULTS

Baseline Characteristics

Overall Characteristics of the Whole Population

From January 2007 to December 2018, a total of 28,358 PCI patients were enrolled in the final analysis [mean age: 62.6 $\pm$ 10.7 years, 6,749 (23.8%) women], and 53.9% of patients undergoing PCI suffered from MR. The prevalence of moderate or severe MR was 12.4% (n = 3,506). A total of 8,275 patients undergoing PCI experienced HF [mean age: 63.04 $\pm$ 11.1 years, 2,029 (24.5%) were women].

Baseline Characteristics of Patients Undergoing PCI With HF

Overall, among the patients undergoing PCI with HF, 28.8% (n = 2,386) were classified as experiencing moderate or severe MR (**Table 1**). Patients with moderate or severe MR were more likely to be older ($P < 0.001$), and the prevalence of complications increased, such as anemia, CKD, and atrial fibrillation ($P < 0.001$) compared with the normal and mild MR groups. In contrast, the prevalence of hypertension, stroke, COPD, hyperlipidemia, and previous coronary artery bypass graft (CABG) did not differ significantly among the different groups. Higher prevalence of prior PCI was reported among the patients with moderate or severe MR (P = 0.08) compared with the normal and mild MR groups. Higher prevalence of DM was also observed among patients undergoing PCI with moderate or severe MR compared with the normal and mild MR groups.

The distribution of cardiac indicators among patients undergoing PCI with HF, stratified by MR severity, was also significantly different. With increase in MR severity, left ventricular end-diastolic dimension (LEVDD), left ventricular end-systolic diameter; LA size (LVESD), left atrial size (LA size), E/A, and N-terminal pro-brain natriuretic peptide (NT-proBNP) gradually increased ($P < 0.001$), whereas left ventricular ejection fraction (LVEF) gradually decreased ($P < 0.001$). In addition, among the patients with HF and moderate or severe MR, ACEI/ARB, beta-blockers, and MRA were used in 54.2, 81.7, and 17.3% of cases, respectively. Among these, beta-blockers were most commonly used in the patients with moderate or severe MR compared with the patients classified as with normal or mild MR.

Baseline Characteristics of Patients Undergoing PCI Without HF

A total of 20,083 patients undergoing PCI without HF were enrolled in this study, including 5.6% (n = 1,120) diagnosed with moderate or severe MR. Patients undergoing PCI with moderate or severe MR were significantly older and had lower LVEF, and higher LVEDD, LVESD, LA size, and E/A than patients undergoing PCI diagnosed as normal or with mild MR The prevalence of complications, such as DM, anemia, CKD, atrial fibrillation, and AMI ($P < 0.001$), increased among patients with moderate or severe MR compared with those who were normal or with mild MR. In addition, patients diagnosed with moderate or severe MR were more likely to use MRA and loop

TABLE 1 | Baseline characteristics of the patients undergoing percutaneous coronary intervention (PCI) with different levels of mitral regurgitation severity stratified by heart failure (HF).

Characteristic	HF				Non-HF				*P*-value*
	Overall (*n* = 8,275)	Normal/mild (*n* = 5,889)	Moderate/severe (*n* = 2,386)	*P*-value	Overall (*n* = 20,083)	Normal/mild (*n* = 18,963)	Moderate/severe (*n* = 1,120)	*P*-value	
Demographic characteristics									
Age, years	63.0 (11.1)	62.5 (11.2)	64.4 (10.8)	<0.001	62.4 (10.6)	62.2 (10.5)	65.6 (10.6)	<0.001	<0.001
Age group, *n* (%)			<0.001				<0.001	<0.001	
<60	2,939 (35.5)	2,201 (37.4)	738 (30.9)		7,814 (38.9)	7,497 (39.5)	317 (28.3)		
60–75	4,070 (49.2)	2,865 (48.7)	1,205 (50.5)		9,512 (47.4)	8,970 (47.3)	542 (48.4)		
≥75	1,266 (15.3)	823 (14.0)	443 (18.6)		2,757 (13.7)	2,496 (13.2)	261 (23.3)		
Women, *n* (%)	2,029 (24.5)	1,416 (24.0)	613 (25.7)	0.121	4,720 (23.5)	4,423 (23.3)	297 (26.5)	0.016	0.096
Medical history					11,339 (56.5)	10,701 (56.4)	638 (57.0)	0.75	>0.99
Anemia, *n* (%)	3,758 (46.4)	2,547 (44.2)	1,211 (51.9)	<0.001	5,556 (28.8)	5,128 (28.1)	428 (40.1)	<0.001	<0.001
HT, *n* (%)									>0.99
AMI, *n* (%)	3,914 (47.3)	2,996 (50.9)	918 (38.5)	<0.001	3,978 (19.8)	3,613 (19.1)	365 (32.6)	<0.001	<0.001
DM, *n* (%)	2,767 (33.4)	1,913 (32.5)	854 (35.8)	0.004	7,252 (28.0)	6,397 (27.5)	855 (32.4)	<0.001	<0.001
CKD, *n* (%)	2,798 (33.8)	1,805 (30.7)	993 (41.6)	<0.001	2,580 (12.8)	2,347 (12.4)	233 (20.8)	<0.001	<0.001
AF, *n* (%)	333 (4.0)	162 (2.8)	171 (7.2)	<0.001	270 (1.3)	202 (1.1)	68 (6.1)	<0.001	<0.001
Stroke, *n* (%)	592 (7.2)	408 (6.9)	184 (7.7)	0.228	1,047 (5.2)	997 (5.3)	50 (4.5)	0.275	<0.001
COPD, *n* (%)	95 (1.1)	69 (1.2)	26 (1.1)	0.839	130 (0.6)	118 (0.6)	12 (1.1)	0.103	<0.001
Hyperlipidemia, *n* (%)	5,726 (71.3)	4,055 (70.8)	1,671 (72.5)	0.136	13,269 (68.1)	12,533 (68.1)	736 (68.1)	0.986	<0.001
Laboratory tests									
LDLC, mmol/L	2.88 (0.99)	2.88 (0.99)	2.88 (1.00)	0.996	2.85 (0.98)	2.85 (0.98)	2.86 (0.96)	0.956	>0.99
HDLC, mmol/L	0.96 (0.25)	0.96 (0.25)	0.93 (0.25)	<0.001	0.99 (0.25)	0.99 (0.25)	0.98 (0.26)	0.139	<0.001
CMV, ml	167.6 (78.4)	166.0 (76.5)	171.4 (82.8)	0.006	166.0 (75.8)	165.8 (75.5)	169.5 (80.0)	0.12	0.036
ALB, g/L	34.0 (4.6)	34.3 (4.6)	33.4 (4.6)	<0.001	36.9 (3.9)	37.0 (3.8)	34.9 (4.4)	<0.001	<0.001
eGFR, mL/min/1.73 m^2	67.8 (27.4)	70.0 (27.7)	62.6 (25.9)	<0.001	81.2 (22.7)	81.5 (22.6)	76.4 (24.4)	<0.001	<0.001
Cardiac indicators									
ProBNP, pg/ml	1,895 [1,047, 3,932]	1,611 [951, 3,155]	2,906 [1,563, 5,821]	<0.001	134 [54, 339]	126 [52, 319]	413 [208, 669]	<0.001	<0.001
LVEDD, mm	52.7 (8.0)	50.9 (7.2)	57.2 (8.2)	<0.001	46.6 (4.9)	46.4 (4.7)	50.7 (5.8)	<0.001	<0.001
LVESD, mm	38.5 (10.1)	36.2 (9.0)	44.2 (10.4)	<0.001	29.50 (5.27)	29.26 (5.07)	34.14 (6.76)	<0.001	<0.001
LA size, mm	37.8 (6.4)	36.7 (6.1)	40.4 (6.4)	<0.001	35.42 (5.60)	35.21 (5.51)	39.10 (5.73)	<0.001	<0.001
LVEF, %	47.7 (13.3)	50.2 (12.7)	41.6 (12.8)	<0.001	62.9 (7.7)	63.2 (7.6)	57.6 (8.8)	<0.001	<0.001
E/A	0.76 (0.33)	0.73 (0.31)	0.84 (0.39)	<0.001	0.71 (0.26)	0.71 (0.26)	0.77 (0.30)	<0.001	<0.001
Medications									
ACEI/ARB, *n* (%)	4,426 (55.3)	3,173 (55.5)	1,253 (54.7)	0.519	10,925 (54.7)	10,298 (54.6)	627 (56.5)	0.218	>0.99
Beta-blocker, *n* (%)	6,805 (85.0)	4,915 (86.0)	1,890 (82.5)	<0.001	16,953 (84.9)	16,022 (84.9)	931 (83.9)	0.395	<0.001
CCB, *n* (%)	1,255 (15.7)	925 (16.2)	330 (14.4)	0.052	4,210 (21.1)	3,994 (21.2)	216 (19.5)	0.191	<0.001
Statins, *n* (%)	7,743 (96.8)	5,559 (97.3)	2,184 (95.4)	<0.001	19,601 (98.1)	18,525 (98.2)	1,076 (97.0)	0.006	<0.001
Antiplatelet, *n* (%)	7,973 (99.6)	5,692 (99.6)	2,281 (99.6)	0.999	19,920 (99.7)	18,813 (99.7)	1,107 (99.8)	0.814	>0.99
loop diuretic, *n* (%)	2,635 (32.9)	1,455 (25.5)	1,180 (51.5)	<0.001	821 (4.1)	646 (3.4)	175 (15.8)	<0.001	<0.001
MRA, *n* (%)	2,690 (33.6)	1,501 (26.3)	1,189 (51.9)	<0.001	950 (4.8)	758 (4.0)	192 (17.3)	<0.001	<0.001

ACEI/ARB, angiotensin-converting enzyme inhibitor/angiotensin receptor blocker; ALB, albumin; AMI, acute myocardial infarction; CCB, calcium channel blocker; CKD, chronic kidney disease; COPD, chronic obstructive pulmonary disease; DM, diabetes mellitus; HT, hypertension; eGFR, estimated glomerular filtration rate; LDL-C, low-density lipoprotein cholesterol; LVEDD, left ventricular end-diastolic dimension; LVESD, left ventricular end-systolic diameter; LA size, left atrial size; LVEF, left ventricular ejection fraction; MRA, mineralocorticoid receptor antagonist; PCI, percutaneous coronary intervention.

**Bonferroni correction for multiple comparisons.*

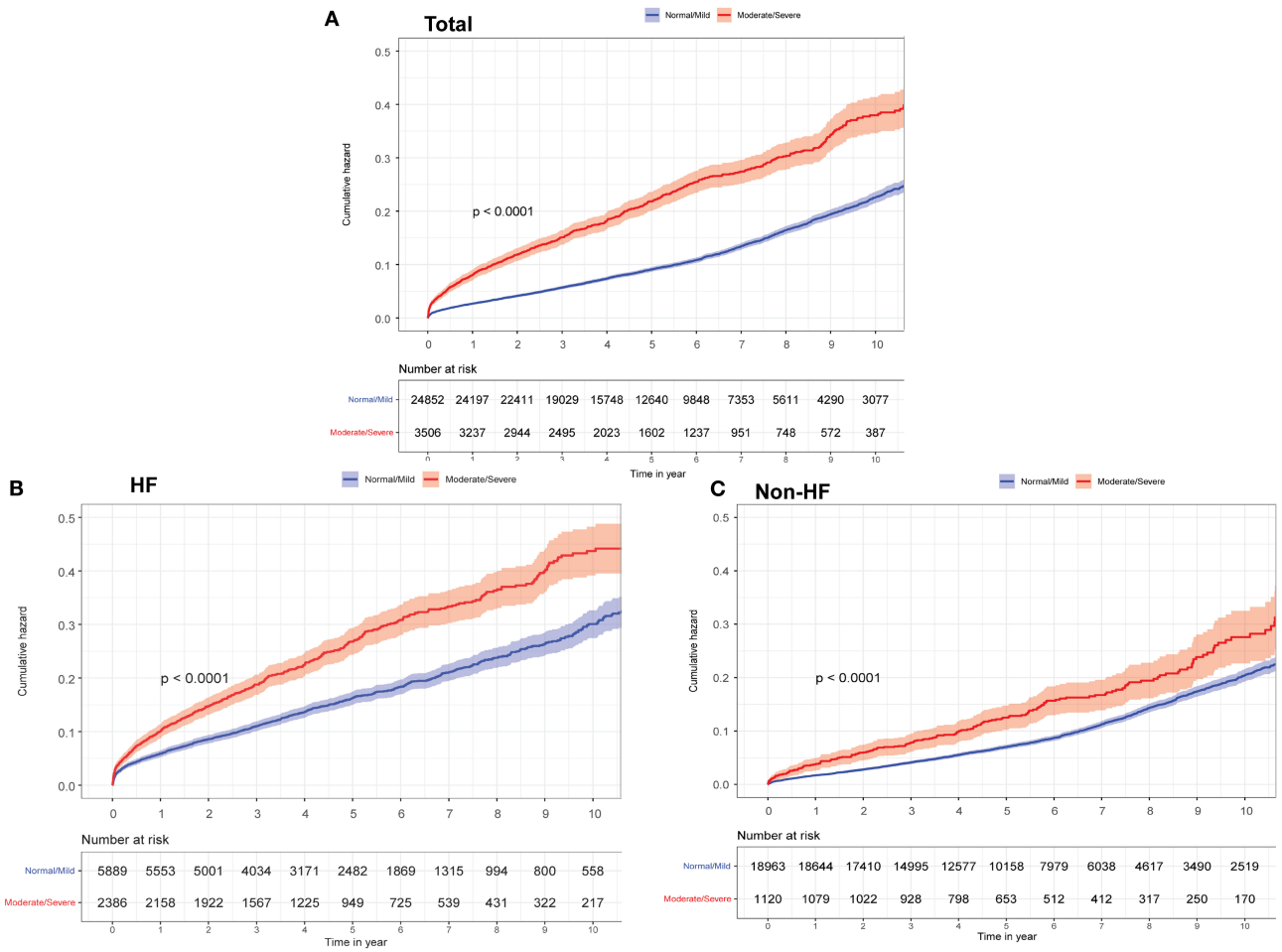

FIGURE 2 | Kaplan-Meier curves for long-term all-cause mortality among different groups according to heart failure (HF) and mitral regurgitation (MR) severity. **(A)** Total. **(B)** HF. **(C)** Non-HF.

diuretics compared with those who were normal or with mild MR (**Table 1**).

Mortality

1-Year Mortality

During the 1-year follow-up, a total of 360 (1.8%) and 564 (6.8%) patients died from all causes among patients undergoing PCI with and without HF, respectively. As determined by Kaplan–Meier survival curves (**Figure 2**), moderate or severe MR was associated with increased risk of 1-year mortality among patients who underwent PCI. A greater proportion of patients who underwent PCI with HF had all causes of mortality compared to the other group without HF (9.6 vs. 3.7%).

Among patients undergoing PCI with or without HF, relationships between 1-year all-cause mortality and MR severity were evaluated using Cox proportional hazards models (moderate or severe vs. normal or mild). The results indicated that the patients with moderate or severe MR had higher 1-year all-cause mortality risk (total: adjusted hazard ratio (aHR): 1.82, 95% confidence interval (CI): 1.51–2.2; $P < 0.001$; HF group: aHR: 1.57, 95% CI: 1.26–1.96; $P < 0.001$; non-HF group: aHR: 1.63, 95% CI: 1.11–2.4; $P = 0.012$; P for interaction $= 0.33$; **Table 2**).

Long-Term Mortality

The median follow-up time was 5 years (interquartile range: 3.1–7.6). The long-term prognosis results indicated that moderate or severe MR was positively associated with mortality in patients undergoing PCI with or without HF. Patients with moderate or severe MR were found to experience a nearly 40% increase in mortality risk compared with patients classified as with normal or mild MR (total, aHR: 1.43, 95% CI: 1.3–1.58; $P < 0.001$; HF group, aHR: 1.35, 95% CI: 1.2–1.52; $P < 0.001$; non-HF group, aHR: 1.27, 95% CI: 1.07–1.52; $P = 0.006$; P for interaction $= 0.81$).

Subgroup Analyses

In the subgroup analyses, Cox regression analysis demonstrated that MR severity was associated with a consistent risk of mortality across dichotomized subgroups, even between the AMI and LVD

TABLE 2 | Cox proportional hazard ratios for 1-year and long-term all-cause mortality in different models.

	Model 1* (HR, 95% CI)	*P*-value	Model 2# (HR, 95% CI)	*P*-value	Model 3§ (HR, 95% CI)	*P*-value
1-year all-cause mortality						
Total	2.19 (1.89–2.54)	<0.001	2.02 (1.74–2.34)	<0.001	1.57 (1.34–1.84)	<0.001
Non-HF	1.67 (1.24–2.25)	0.001	1.57 (1.16–2.11)	0.003	1.46 (1.07–1.99)	0.018
HF	1.42 (1.19–1.69)	<0.001	1.34 (1.13–1.60)	0.001	1.26 (1.05–1.52)	0.015
P-interaction	0.36		0.38		0.42	
Long-term all-cause mortality						
Total	1.80 (1.66–1.96)	<0.001	1.66 (1.53–1.81)	<0.001	1.48 (1.35–1.61)	<0.001
Non-HF	1.38 (1.20–1.60)	<0.001	1.28 (1.10–1.48)	0.001	1.26 (1.08–1.48)	0.003
HF	1.47 (1.32–1.63)	<0.001	1.39 (1.25–1.54)	<0.001	1.31 (1.17–1.46)	<0.001
P-interaction	0.44		0.28		0.48	

**Unadjusted.*

#Adjusted for age and gender.

§Adjusted for age, gender, hypertension, CKD, AMI, stroke, AF, DM, hyperlipidemia, anemia, in-hospital dialysis, angiotensin-converting enzyme inhibitors (ACEI)/angiotensin receptor blockers (ARB), β-blockers, statins, antiplatelet, calcium channel blocker, mineralocorticoid receptor antagonists (MRA), loop diuretics, and oral anticoagulants.

Central Illustration. Prevalence and prognostic significance of mitral regurgitation in patients undergoing percutaneous coronary intervention with or without heart failure.

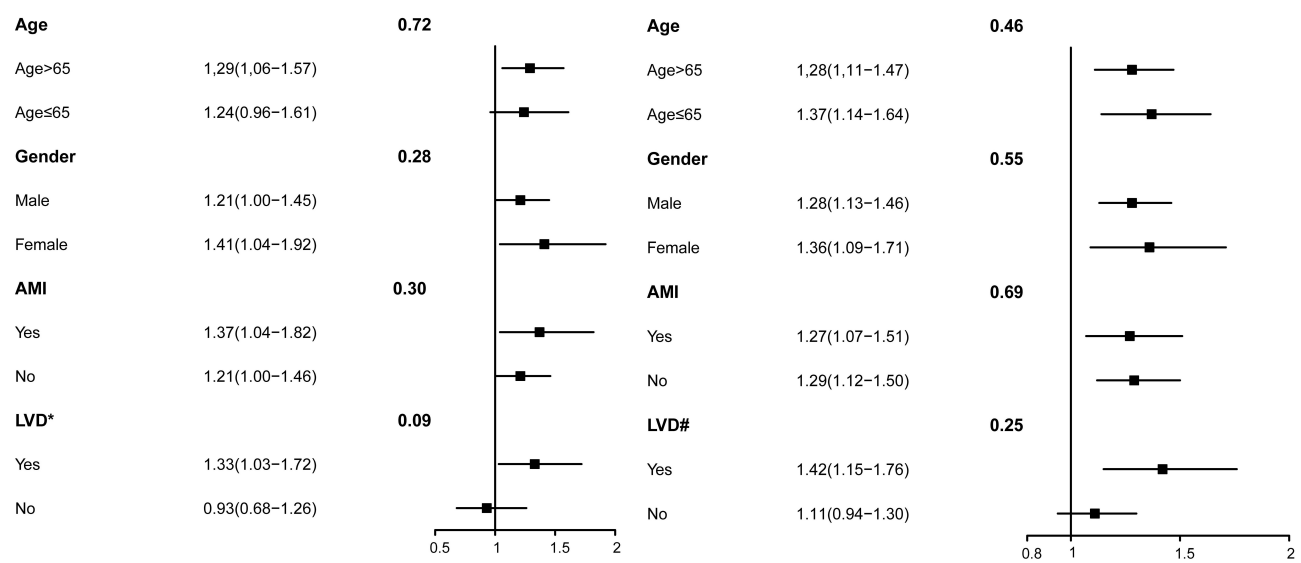

FIGURE 3 | Subgroup analysis of moderate or severe MR among in patients undergoing percutaneous coronary intervention (PCI) without mitral valve surgery. Model 3 for long-term mortality. *LVEF < 64(median among non-HF); #LVEF < 47(median among HF).

subgroups (**Figure 3**). A summary of this study is shown in the central illustration (**Figure 4**).

DISCUSSION

To our knowledge, this is the first large cohort study to systematically identify the prevalence and mortality of moderate or severe MR among patients undergoing PCI without mitral valve surgery. Our data showed that moderate or severe MR was common among patients undergoing PCI (1/17 and 1/3 of patients without and with HF, respectively). Additional risks of 1-year and long-term mortality of ∼80 and 40%, respectively, were attributable to moderate or severe MR among patients undergoing PCI with or without HF.

Coronary artery disease (CAD) remains a major clinical and public health challenge, with a huge economic burden worldwide (2, 19), and PCI has become the main strategy for the treatment of obstructive CAD (20, 21). Pastorius et al. indicated that patients with MR undergoing PCI have significantly decreased survival rates, while this study was limited by a small sample, with only 711 patients (7). Uddin et al. indicated that higher grades of MR in 4,005 patients with STEMI undergoing primary PCI are associated with worse short- and long-term outcomes, but they only analyzed patients with STEMI (8). Currently, large-scale cohort studies on prevalence and outcomes of moderate or severe MR among patients with CAD undergoing PCI without mitral valve surgery are still lacking. Several previous cohort studies have also reported an

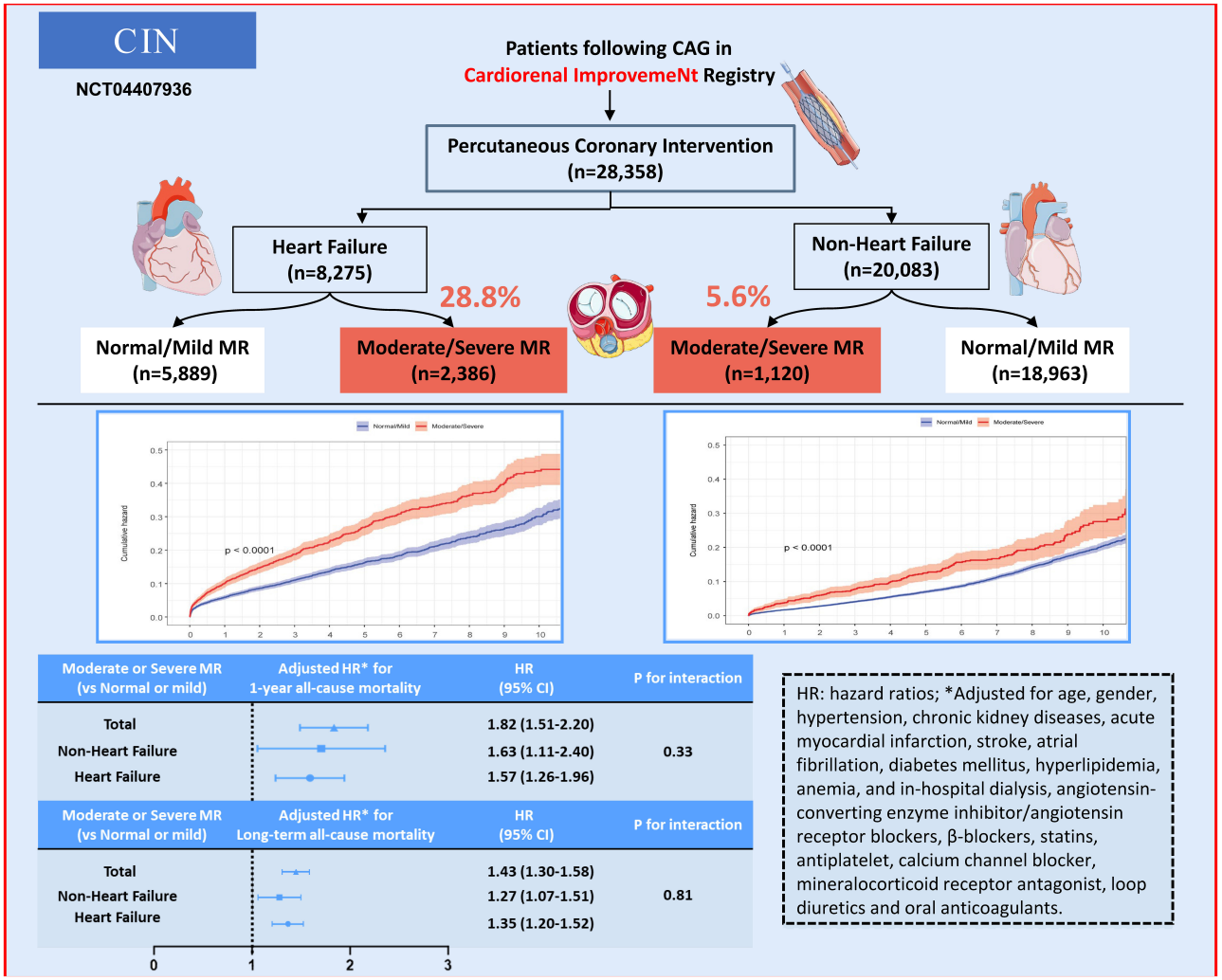

FIGURE 4 | Central illustration.

association between MR and mortality among patients with HF (10, 22, 23).

An article published by the Journal of the American College of Cardiology (JACC) demonstrated that moderate or severe MR was not independently associated with 1-year mortality among patients with acute decompensated HF (ADHF) who had LVEF $\geq$ 50% (12). Another study demonstrated that MR has a negative effect on prognosis only in patients with severely reduced LVEF (11). The relationship between MR and PCI with or without HF has not been fully clarified. Therefore, we hypothesized that MR negatively impacts prognosis only in patients with HF but not in those without HF.

However, in our study, contrary to our hypothesis, moderate or severe MR was an independent risk factor in patients with and without HF. Several possible mechanisms may underlie the relationship between MR and PCI with or with HF. MR in patients with HF and left ventricular dilation occurs because of distortion of the valve apparatus, including apical and posterior displacement of the papillary muscles and annular dilation, which may lead to incomplete closure of the mitral leaflets (22, 24). In addition, the destructive influence of CAD on left ventricle function is well-known, and patients with CAD may experience improved left ventricular function after PCI treatment, which might explain why moderate or severe MR increased the mortality risk of patients undergoing PCI, regardless of HF prevalence. Moderate or severe MR may also increase the risk of poor prognosis independent of HF and other important survival predictors because of increased LV filling pressure, activation of neurohumoral systems, and cellular modifications (25). The relevant mechanisms require further study.

The 2021 European Society of Cardiology (ESC) guidelines for the management of secondary MR in patients with HF recommended that patients undergoing PCI with HF complicated by moderate or severe MR should be considered for further treatment to improve the current poor prognosis (12). However, current CAD management guidelines do not provide

convincing evidence in patients undergoing PCI with or without HF (26–30).

In conclusion, we report that moderate or severe MR may increase the risk of poor prognosis, independent of HF occurrence and other important predictors of survival. This finding supports clinicians in the utilization of more aggressive treatments for moderate or severe MR among patients who undergo PCI, even in the absence of HF. These findings also provide an avenue for further improvements in existing guidelines. However, we were unable to establish a causal relationship in the present analysis because of the observational nature of this study. Further studies remain necessary to confirm our findings and to better understand the mechanisms that underlie the association between moderate or severe MR and mortality among patients undergoing PCI with or without HF.

Our investigation is not without limitations. First, the data were extracted from a single-center retrospective study, which hampered our ability to control confounders in the analyses; however, sizeable quantities of the data extracted from medical records allowed us to control some confounders. Second, all of the patients included in the study were from Guangdong Provincial People's Hospital, which represents the largest cardiovascular medical center in South China, and more than half of the subjects were referred from non-teaching and community hospitals in both urban and rural areas. Third, we used echocardiography data from 1-year follow-up without regular monitoring of dynamic changes in MR, which may be important. However, our admission ultrasound was performed by professional cardiac ultrasound experts with a small measurement bias. Fourth, information on cause-specific death was not available in this study, and examining correlations between MR and cause-specific death was difficult. Finally, although we excluded baseline surgical or percutaneous approach of MR, we could not analyze the influence of MR evolution and subsequent surgical or percutaneous approach because of the absence of follow-up data. The above variables are very meaningful for the analysis and interpretation of the results, and we will further collect and analyze the above variables in future studies.

Our cohort suggested that moderate or severe MR was a common event among patients undergoing PCI without mitral valve surgery, with one-third of all the patients experiencing HF and 1-17th of all the patients without HF experiencing moderate or severe MR. Patients with moderate or severe MR were more likely to be older and had worse cardio-renal function; and moderate or severe MR was associated with an over 40% increase in long-term mortality among patients undergoing PCI, regardless of HF occurrence. Our findings supported the idea of conducting further studies to test interventional procedures for moderate or severe MR during PCI, regardless of HF.

DATA AVAILABILITY STATEMENT

The original contributions presented in the study are included in the article/supplementary materials, further inquiries can be directed to the corresponding authors.

ETHICS STATEMENT

The studies involving human participants were reviewed and approved by Guangdong Provincial People's Hospital Ethics Committee. The Ethics Committee waived the requirement of written informed consent for participation.

AUTHOR CONTRIBUTIONS

YL, LC, NT, KC, JC, and SC: designed the study. SC, HY, YH, and BW: collected and reviewed the clinical and laboratory data. WL, TT, QL, and NR: analyzed the data. SC, HH, HW, and DH: performed the statistical analysis. HH, KB, JL, and XH: drafted or revised the manuscript. YL, LC, NT, KC, and JC: reviewed, interpreted, and checked the clinical data. All authors contributed to the article and approved the submitted version.

FUNDING

This study was supported by grants from the Natural Science Foundation of Fujian Provincial Science and Technology Department (2018J01405 and 2019J01617). The study was not funded by any industry sponsors.

ACKNOWLEDGMENTS

Special thank to Younan Yao (Fuwai Hospital, Chinese Academy of Medical Sciences, and Peking Union Medical College, China) for helping with the study design and precious comments.

REFERENCES

1. Valuckiene Ž, Urbonaite D, Jurkevičius R. Functional (ischemic) mitral regurgitation in acute phase of myocardial infarction: associated clinical factors and in-hospital outcomes. *Medicina.* (2015) 51:92–9. doi: 10.1016/j.medici.2015.02.003
2. Dai H, Much AA, Maor E, Asher E, Younis A, Xu Y, et al. Global, regional, and national burden of ischemic heart disease and its attributable risk factors, 1990-2017: results from the global Burden of Disease Study 2017. *Eur Heart J Qual Care Clin Outcomes.* (2020) 8:50–60. doi: 10.1093/ehjqcco/qcaa076
3. Tcheng JE, Jackman JD Jr, Nelson CL, Gardner LH, Smith LR, Rankin JS, et al. Outcome of patients sustaining acute ischemic mitral regurgitation during myocardial infarction. *Ann Intern Med.* (1992) 117:18–24. doi: 10.7326/0003-4819-117-1-18
4. Samad Z, Shaw LK, Phelan M, Glower DD, Ersboll M, Toptine JH, et al. Long-term outcomes of mitral regurgitation by type and severity. *Am Heart J.* (2018) 203:39–48. doi: 10.1016/j.ahj.2018.05.001
5. Kawashima H, Serruys PW, Ono M, Hara H, O'Leary N, Mack MJ, et al. Impact of optimal medical therapy on 10-year mortality after coronary revascularization. *J Am Coll Cardiol.* (2021) 78:27–38. doi: 10.1016/j.jacc.2021.04.087
6. Tu Y, Zeng QC, Huang Y, Li JY. Percutaneous coronary intervention for acute myocardial infarction with mitral regurgitation. *J Geriatr Cardiol.* (2016) 13:521–7. doi: 10.11909/j.issn.1671-5411.2016.06.010

7. Pastorius CA, Henry TD, Harris KM. Long-term outcomes of patients with mitral regurgitation undergoing percutaneous coronary intervention. *Am J Cardiol.* (2007) 100:1218–23. doi: 10.1016/j.amjcard.2007.05.050
8. Mentias A, Raza MQ, Barakat AF, Hill E, Youssef D, Krishnaswamy A, et al. Prognostic significance of ischemic mitral regurgitation on outcomes in acute ST-elevation myocardial infarction managed by primary percutaneous coronary intervention. *Am J Cardiol.* (2017) 119:20–6. doi: 10.1016/j.amjcard.2016.09.007
9. Parikh PB, Bhatt DL, Bhasin V, Anker SD, Skopicki HA, Claessen BE, et al. Impact of percutaneous coronary intervention on outcomes in patients with heart failure: JACC state-of-the-art review. *J Am Coll Cardiol.* (2021) 77:2432–47. doi: 10.1016/j.jacc.2021.03.310
10. Bursi F, Barbieri A, Grigioni F, Reggianini L, Zanasi V, Leuzzi C, et al. Prognostic implications of functional mitral regurgitation according to the severity of the underlying chronic heart failure: a long-term outcome study. *Eur J Heart Fail.* (2010) 12:382–8. doi: 10.1093/eurjhf/hfq014
11. Pecini R, Thune JJ, Torp-Pedersen C, Hassager C, Køber L. The relationship between mitral regurgitation and ejection fraction as predictors for the prognosis of patients with heart failure. *Eur J Heart Fail.* (2011) 13:1121–5. doi: 10.1093/eurjhf/hfr114
12. Arora S, Sivaraj K, Hendrickson M, Chang PP, Weickert T, Qamar A, et al. Prevalence and prognostic significance of mitral regurgitation in acute decompensated heart failure: the ARIC study. *JACC Heart Fail.* (2021) 9:179–89. doi: 10.1016/j.jchf.2020.09.015
13. Jneid H, Anderson JL, Wright RS, Adams CD, Bridges CR, Casey DE Jr, et al. 2012 ACCF/AHA focused update of the guideline for the management of patients with unstable angina/Non-ST-elevation myocardial infarction (updating the 2007 guideline and replacing the 2011 focused update): a report of the American College of Cardiology Foundation/American Heart Association Task Force on practice guidelines. *Circulation*. (2012) 126:875–910. doi: 10.1161/CIR.0b013e318256f1e0
14. Levine GN, Bates ER, Blankenship JC, Bailey SR, Bittl JA, Cercek B, et al. 2015 ACC/AHA/SCAI focused update on primary percutaneous coronary intervention for patients with ST-elevation myocardial infarction: an update of the 2011 ACCF/AHA/SCAI guideline for percutaneous coronary intervention and the 2013 ACCF/AHA guideline for the management of ST-elevation myocardial infarction. *J Am Coll Cardiol.* (2016) 67:1235–50. doi: 10.1016/j.jacc.2015.10.005
15. Bozkurt B, Coats AJS, Tsutsui H, Abdelhamid CM, Adamopoulos S, Albert N, et al. Universal definition and classification of heart failure: a report of the Heart Failure Society of America, Heart Failure Association of the European Society of Cardiology, Japanese Heart Failure Society and Writing Committee of the Universal Definition of Heart Failure: Endorsed by the Canadian Heart Failure Society, Heart Failure Association of India, Cardiac Society of Australia and New Zealand, and Chinese Heart Failure Association. *Eur J Heart Fail.* (2021) 23:352–80. doi: 10.1002/ejhf.2115
16. Ponikowski P, Voors AA, Anker SD, Bueno H, Cleland JGF, Coats AJS, et al. 2016 ESC Guidelines for the diagnosis and treatment of acute and chronic heart failure: The Task Force for the diagnosis and treatment of acute and chronic heart failure of the European Society of Cardiology (ESC)Developed with the special contribution of the Heart Failure Association (HFA) of the ESC. *Eur Heart J.* (2016) 37:2129–200. doi: 10.1093/eurheartj/ehw128
17. Aguiar-Souto P, Ferrante G, Del Furia F, Barlis P, Khurana R, Di Mario C. Frequency and predictors of contrast-induced nephropathy after angioplasty for chronic total occlusions. *Int J Cardiol.* (2010) 139:68–74. doi: 10.1016/j.ijcard.2008.10.006
18. Catapano AL, Graham I, De Backer G, Wiklund O, Chapman MJ, Drexel H, et al. 2016 ESC/EAS guidelines for the management of dyslipidaemias. *Eur Heart J.* (2016) 37:2999–3058. doi: 10.1093/eurheartj/ehw272
19. Rodriguez-Leyva D, Dupasquier CM, McCullough R, Pierce GN. The cardiovascular effects of flaxseed and its omega-3 fatty acid, alpha-linolenic acid. *Can J Cardiol.* (2010) 26:489–96. doi: 10.1016/S0828-282X(10)70455-4
20. Sousa JE, Serruys PW, Costa MA. New frontiers in cardiology: drug-eluting stents: part I. *Circulation.* (2003) 107:2274–9. doi: 10.1161/01.CIR.0000069330.41022.90
21. Epstein AJ, Polsky D, Yang F, Yang L, Groeneveld PW. Coronary revascularization trends in the United States, 2001-2008. *J Am Med Assoc.* (2011) 305:1769–76. doi: 10.1001/jama.2011.551
22. Koelling TM, Aaronson KD, Cody RJ, Bach DS, Armstrong WF. Prognostic significance of mitral regurgitation and tricuspid regurgitation in patients with left ventricular systolic dysfunction. *Am Heart J.* (2002) 144:524–9. doi: 10.1067/mhj.2002.123575
23. Samad Z, Shaw LK, Phelan M, Ersboll M, Risum N, Al-Khalidi HR, et al. Management and outcomes in patients with moderate or severe functional mitral regurgitation and severe left ventricular dysfunction. *Eur Heart J.* (2015) 36:2733–41. doi: 10.1093/eurheartj/ehv343
24. Boltwood CM, Tei C, Wong M, Shah PM. Quantitative echocardiography of the mitral complex in dilated cardiomyopathy: the mechanism of functional mitral regurgitation. *Circulation.* (1983) 68:498–508. doi: 10.1161/01.CIR.68.3.498
25. Behr TM, Wang X, Aiyar N, Coatney RW, Li X, Koster P, et al. Monocyte chemoattractant protein-1 is upregulated in rats with volume-overload congestive heart failure. *Circulation.* (2000) 102:1315–22. doi: 10.1161/01.CIR.102.11.1315
26. Baumgartner H, Falk V, Bax JJ, De Bonis M, Hamm C, Holm PJ, et al. 2017 ESC/EACTS Guidelines for the management of valvular heart disease. *Eur Heart J.* (2017) 38:2739–91. doi: 10.1093/eurheartj/ehx391
27. Collet JP, Thiele H, Barbato E, Barthélémy O, Bauersachs J, Bhatt DL, et al. 2020 ESC Guidelines for the management of acute coronary syndromes in patients presenting without persistent ST-segment elevation. *Eur Heart J.* (2021) 42:1289–367. doi: 10.1093/eurheartj/ehaa575
28. Coats AJS, Anker SD, Baumbach A, Alfieri O, von Bardeleben RS, Bauersachs J, et al. The management of secondary mitral regurgitation in patients with heart failure: a joint position statement from the Heart Failure Association (HFA), European Association of Cardiovascular Imaging (EACVI), European Heart Rhythm Association (EHRA), and European Association of Percutaneous Cardiovascular Interventions (EAPCI) of the ESC. *Eur Heart J.* (2021) 42:1254–69. doi: 10.1093/eurheartj/ehab086
29. Knuuti J, Wijns W, Saraste A, Capodanno D, Barbato E, Funck-Brentano C, et al. 2019 ESC Guidelines for the diagnosis and management of chronic coronary syndromes. *Eur Heart J.* (2020) 41:407–77. doi: 10.1093/eurheartj/ehz425
30. Ibanez B, James S, Agewall S, Antunes MJ, Bucciarelli-Ducci C, Bueno H, et al. 2017 ESC Guidelines for the management of acute myocardial infarction in patients presenting with ST-segment elevation: the Task Force for the management of acute myocardial infarction in patients presenting with ST-segment elevation of the European Society of Cardiology (ESC). *Eur Heart J.* (2018) 39:119–77. doi: 10.1093/eurheartj/ehx393

Conflict of Interest: The authors declare that the research was conducted in the absence of any commercial or financial relationships that could be construed as a potential conflict of interest.

frontiers in Cardiovascular Medicine

ORIGINAL RESEARCH
published: 03 March 2022
doi: 10.3389/fcvm.2022.791949

The Technological Basis of a Balloon-Expandable TAVR System: Non-occlusive Deployment, Anchorage in the Absence of Calcification and Polymer Leaflets

*Harish Appa[1], Kenneth Park[1], Deon Bezuidenhout[1,2], Braden van Breda[1], Bruce de Jongh[1], Jandré de Villiers[1], Reno Chacko[1], Jacques Scherman[2,3], Chima Ofoegbu[2,3], Justiaan Swanevelder[4], Michael Cousins[1], Paul Human[2,3], Robin Smith[1], Ferdinand Vogt[5,6], Bruno K. Podesser[7], Christoph Schmitz[8,9], Lenard Conradi[10], Hendrik Treede[11], Holger Schröfel[12], Theodor Fischlein[6], Martin Grabenwöger[13], Xinjin Luo[14], Heather Coombes[1], Simon Matskeplishvili[15], David F. Williams[1,16] and Peter Zilla[1,2,3,17]**

[1] Strait Access Technologies (SAT), University of Cape Town, Cape Town, South Africa, [2] Cardiovascular Research Unit, University of Cape Town, Cape Town, South Africa, [3] Chris Barnard Division for Cardiothoracic Surgery, University of Cape Town, Cape Town, South Africa, [4] Department of Anaesthesia and Perioperative Medicine, University of Cape Town, Cape Town, South Africa, [5] Deparment of Cardiac Surgery, Artemed Clinic Munich South, Munich, Germany, [6] Department of Cardiac Surgery, Klinikum Nürnberg, Paracelsus Medical University, Nuremberg, Germany, [7] Center for Biomedical Research, Medical University of Vienna, Vienna, Austria, [8] Auto Tissue Berlin, Berlin, Germany, [9] Department of Cardiac Surgery, University of Munich, Munich, Germany, [10] Department of Cardiovascular Surgery, University Heart Center, Hamburg, Germany, [11] Department of Cardiac and Vascular Surgery, University Hospital, Mainz, Germany, [12] Department of Cardiovascular Surgery, University Heart Center, Freiburg, Germany, [13] Department of Cardiovascular Surgery, Vienna North Hospital, Vienna, Austria, [14] Department of Cardiac Sugery, Fu Wai Hospital, Peking Union Medical College, Beijing, China, [15] Lomonosov Moscow State University Medical Center, Moscow, Russia, [16] Wake Forest Institute of Regenerative Medicine, Wake Forest School of Medicine, Winston-Salem, NC, United States, [17] Cape Heart Centre, University of Cape Town, Cape Town, South Africa

OPEN ACCESS

Edited by:
Maria Nunes,
Federal University of Minas Gerais, Brazil

Reviewed by:
Alessandro Iadanza,
University of Siena, Italy
David Chistian Reineke,
Inselspital, Switzerland

***Correspondence:**
Peter Zilla
peter.zilla@uct.ac.za

Specialty section:
This article was submitted to Heart Valve Disease, a section of the journal Frontiers in Cardiovascular Medicine

Received: 09 October 2021
Accepted: 18 January 2022
Published: 03 March 2022

Citation:
Appa H, Park K, Bezuidenhout D, van Breda B, de Jongh B, de Villiers J, Chacko R, Scherman J, Ofoegbu C, Swanevelder J, Cousins M, Human P, Smith R, Vogt F, Podesser BK, Schmitz C, Conradi L, Treede H, Schröfel H, Fischlein T, Grabenwöger M, Luo XJ, Coombes H, Matskeplishvili S, Williams DF and Zilla P (2022) The Technological Basis of a Balloon-Expandable TAVR System: Non-occlusive Deployment, Anchorage in the Absence of Calcification and Polymer Leaflets. Front. Cardiovasc. Med. 9:791949. doi: 10.3389/fcvm.2022.791949

Leaflet durability and costs restrict contemporary trans-catheter aortic valve replacement (TAVR) largely to elderly patients in affluent countries. TAVR that are easily deployable, avoid secondary procedures and are also suitable for younger patients and non-calcific aortic regurgitation (AR) would significantly expand their global reach. Recognizing the reduced need for post-implantation pacemakers in balloon-expandable (BE) TAVR and the recent advances with potentially superior leaflet materials, a trans-catheter BE-system was developed that allows tactile, non-occlusive deployment without rapid pacing, direct attachment of both bioprosthetic and polymer leaflets onto a shape-stabilized scallop and anchorage achieved by plastic deformation even in the absence of calcification. Three sizes were developed from nickel-cobalt-chromium MP35N alloy tubes: Small/23 mm, Medium/26 mm and Large/29 mm. Crimp-diameters of valves with both bioprosthetic (sandwich-crosslinked decellularized pericardium) and polymer leaflets (triblock polyurethane combining siloxane and carbonate segments) match those of modern clinically used BE TAVR. Balloon expansion favors the wing-structures of the stent thereby creating supra-annular anchors whose diameter exceeds the outer diameter at the waist level by a quarter. In the pulse duplicator, polymer and bioprosthetic TAVR showed equivalent fluid dynamics with excellent EOA,

pressure gradients and regurgitation volumes. Post-deployment fatigue resistance surpassed ISO requirements. The radial force of the helical deployment balloon at different filling pressures resulted in a fully developed anchorage profile of the valves from two thirds of their maximum deployment diameter onwards. By combining a unique balloon-expandable TAVR system that also caters for non-calcific AR with polymer leaflets, a powerful, potentially disruptive technology for heart valve disease has been incorporated into a TAVR that addresses global needs. While fulfilling key prerequisites for expanding the scope of TAVR to the vast number of patients of low- to middle income countries living with rheumatic heart disease the system may eventually also bring hope to patients of high-income countries presently excluded from TAVR for being too young.

Keywords: balloon-expandable, plastic deformation, aortic regurgitations, polymer leaflets, rheumatic heart disease

INTRODUCTION

During several decades of development, transcatheter aortic valve replacement almost exclusively focused on the treatment of calcific aortic stenosis (AS) (1–4). Being the most common heart valve pathology in the Western World, it provided the patient numbers needed for non-inferiority studies in comparison with an established low-mortality procedure such as surgical aortic valve replacement (SAVR). Since in high-income countries (HIC) where TAVR was pioneered (1, 5), pure aortic regurgitation (AR) occurs less frequently than AS (4, 6, 7) pure AR did not have enough traction to influence developments. This is still reflected in contemporary TAVR designs whose simple mesh structures are sufficient to anchor the stents in the rigid calcific deposits of AS. However, given the huge global burden of rheumatic heart disease (RHD) in emerging economies (8–10) with its predominance of AR (9–13) and the growing number of patients with pure AR in industrialized countries, it seems timely to extend transcatheter procedures to patients with non-calcified regurgitant aortic valves (14–17).

Initial attempts to treat non-calcific pure AR with TAVR were directed at patients in HICs who were typically old, with reasonably preserved ventricular function (18). To compensate for the absence of calcification for anchoring, devices were distinctly oversized (19). The few newer generation devices with dedicated anchoring systems improved the success rates (18) but also highlighted how deployment requirements vary between AS and AR.

Further extending the indication for TAVR from patients with degenerative AR to those with RHD in low- to middle-income countries (LMICs) introduces additional challenges. These patients are significantly younger (20) and often present at a later stage of ventricular remodeling when they are past conventional operability. Severe volume overload, eccentric hypertrophy and excessive left ventricular (LV) wall stress cause progressive LV dysfunction, making it desirable to avoid rapid pacing during implantation (21). The hyperdynamic nature of eccentric hypertrophy also makes stabilization during deployment even more essential than in AS.

Thus, TAVRs that cater for this sizable but vulnerable group must address aspects that go beyond those of patients in industrialized countries that were hitherto also outside the spectrum of TAVR indications. The avoidance of rapid-pacing (21), of costly secondary procedures such as post-implant balloon dilatations (22) and of permanent pacemaker implantations (22, 23) are the foremost additional constraints in LMICs.

Guided by these considerations, we have developed a balloon-expandable (BE) TAVR system with several critical features. An hourglass shape was designed to ease the pressure on the conduction system. Expansion-linked plastic deformation of the stent was utilized to enable firm supra-annular anchorage in non-calcified roots. The stent has a continuous scallop design to allow the seamless attachment of degradation resistant polyurethane leaflets promising durability in younger patients through their fatigue- and calcification resistance. To avoid rapid pacing a helical hollow balloon was developed for the deployment system protecting against backflow through a temporary valve. Invaginating balloon trunks were added to stabilize the hyperdynamic hearts while accurately positioning the TAVR in the absence of an X-ray footprint.

MATERIALS AND METHODS

Balloon-Expandable TAVR Stent for Bioprosthetic and Polymer Leaflets

The design of the TAVR stent was based on three principles: (1) continual stent-scallops for leaflet attachment that are crimpable and restored to their original shape upon balloon expansion; (2) self-elevating inter-commissural anchoring arms based on geometric changes due to plastic deformation occurring after crimping during deployment and (3) an hourglass shape with the waist seated in the annulus plane resulting in a concavity around the bulge of the crest of the muscular ventricular septum, easing the pressure on the crest (24, 25).

Stents of three sizes (Small "S," Medium "M," and Large "L" were cut from 23, 26, and 29 mm OD nickel-cobalt-chromium alloy MP35N tubes (Minitubes, Grenoble, France), respectively, using a Tube-Fiber Laser cutter (wavelength 900–1250 nm;

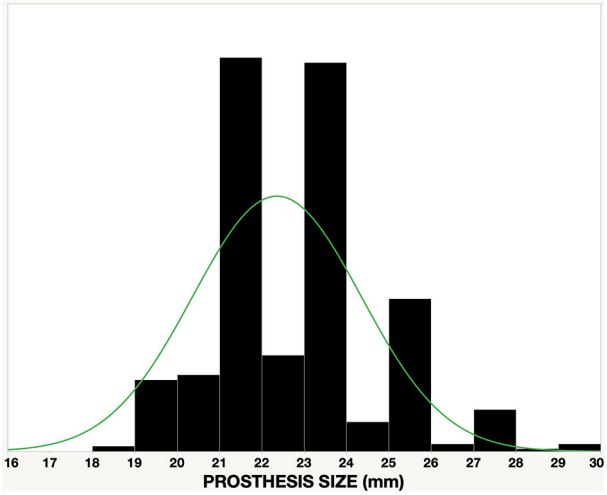

FIGURE 1 | Size distribution of surgically implanted valves in a cohort of 350 patients with mainly rheumatic aortic regurgitation at Groote Schuur Hospital, University of Cape Town.

StarCut; Rofin/Coherent Inc., Plymouth, MI, USA). Sizes were based on the size distribution of surgically implanted prostheses for rheumatic AR at the University of Cape Town (**Figure 1**). Scallop-struts were designed smooth to accommodate polymer (PU) leaflets and with stitching holes for bioprosthetic (BP) leaflets (**Figures 2A,B**).

ABAQUS (Dassault Systèmes Simulia Corp, Providence, Rhode Island, USA) was used for the Finite Element Analysis (FEA) assuming isotropic elasto-plastic materials. Stent fatigue was tested at 25 Hz for 400 million cycles at 6–8.5% compliance at ΔP 120 mmHg, 37°C (BDC Laboratories RDTL-0200-3600i, Wheat Ridge, CO, USA).

Second Generation: "Universal" TAVR Stent

A prototype universal stent was developed for sizes M and L, providing one stent design for both BP and PU leaflets while reducing the crimp-size to allow both transapical (TA) and transfemoral (TF) delivery. The gap between two horizontal struts of the upper spacer-arm was increased to facilitate future coronary access in the unlikely event that the left coronary artery (LCA) was below the upper stent strut (**Figure 2C**).

Valve Leaflets and Skirt

The leaflet design was based on Bézier curves. Stresses were optimized using FEA on the basis of isotropic hyperelastic materials (**Figure 3**). Decellularized, sandwich-crosslinked Namibian bovine pericardium (porcine for the "universal" stent) was processed as previously described (26). The potential longevity of leaflets was assessed in the rat subcutaneous model. Leaflet discs were implanted into 5-week-old Long–Evans male rats for 6 weeks. Decellularized and sandwich-crosslinked bovine and porcine pericardium as well as Carbosil (100% pre-strained on Co-Cr lattice frames to simulate the contact of the leaflets with valve stents) were compared with standard 0.7% glutaraldehyde fixed bovine pericardium. Calcium contents were analyzed by Inductively Coupled Plasma Optical Emission Spectroscopy (ICP-OES; Spectro Arcos, Kleve, Germany) and expressed as μg/mg of dry mass. Pre-strained 25 week implants of Pellethane and carbosil film-strips (4 × 1 cm, 150 μm thick) were analyzed by scanning electron microscopy to visualize any degradation of the sample surface.

BP-leaflets were stitched onto the stent *via* suture holes using 5-0 Ticron sutures. PU valves were manufactured by a robotic arm in a combination spray process using different hardnesses of CarboSil (DSM Engineering Materials Inc., Evansville, IN, USA). Electrospun polymer skirts (thickness: 110–140 μm; pore size: 20–100 μm^2) were externally heat-welded onto the stent.

Dimensions During Deployment

BP and PU valves were assessed in conjunction with the SAT non-occlusive TA deployment system. "Universal" SAT TAVR were assessed using conventional deployment balloons for TF delivery. Since the different sizes of the system represent scaled versions of one basic design, detailed dimensional analyses were obtained for the M system. Dimensional changes during balloon inflation were recorded against increasing filling pressures at 1 bar increments. The diameters were measured at the level of the distal end of the stent, at the levels of maximal expansion of the top ("spacer") and bottom ("supra-annular") arms, at the narrowest waist (beneath the nadir of the scallops) and at the proximal end ("ventricular flare"). Stent recoil was assessed from the dimensions at each point with the balloon inflated and deflated.

Fluid Dynamics, Crush-Force and Fatigue-Testing

Hydrodynamic testing to determine gradients (ΔP), effective orifice areas (EOA) and regurgitant fractions was performed in a pulse duplicator (Cardiac Output: 5 L/min; 37°C; 70 bpm; Stroke Volume: 32 ± 5 ml; Systolic Phase Duration of 35 ± 5%) (ViVitro Labs Inc; Victoria, BC, Canada). The radial crush force was determined by using a radial expansion tester (RX650 Radial Expansion Equipment, F033919 Head) and a conditioning chamber (Machine Solutions Inc. [MSI], AZ, USA). Accelerated durability testing was conducted using a BDC Laboratories VDT-3600i Valve Fatigue Tester (BDC Laboratories, Wheat Ridge, CO, USA) for up to 500 million fatigue cycles at 15 Hz in 0.9% saline (containing 0.2–1.5% Biguanide 20 bactericide) at 37°C. After every 50 million cycles, the valves were evaluated for structural damage and hydrodynamic testing.

Non-occlusive TA Deployment System

The delivery device had four requirements: (1) a non-occlusive balloon; (2) tactile placement in and stabilization of hyper-dynamic hearts with unpinchable retractable feelers; (3) a back-flow valve that permits protracted delivery (4) and an atraumatic retrieval system.

The hollow-balloon was based on a helical tube held by a fine-meshed Nitinol frame. The locator/stabilizing arms were based on balloon tubes that could be retracted through invagination.

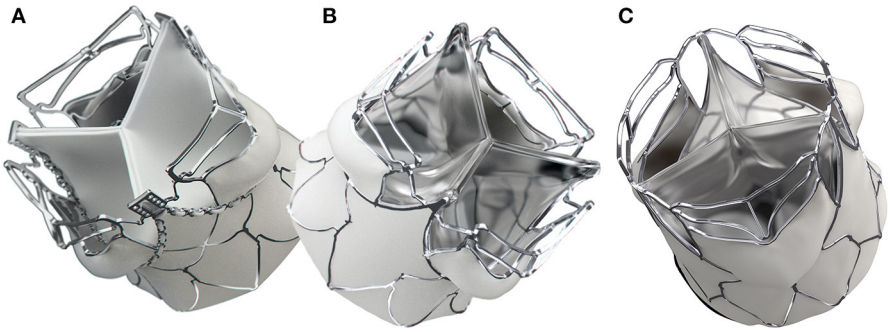

FIGURE 2 | SAT balloon-expandable TAVR valve. The direct bonding to the MP35N-scallop allows an optimal attachment of polymer leaflets to the stent. Both the supra-annular anchorage arms and the spacer arms are structures that are self-elevating on the basis of plastic deformation. The first generation SAT TAVRs show minor differences between the bioprosthetic **(A)** and the polymer version **(B)**. The second generation "universal" stent **(C)** supports both bioprosthetic and polymer leaflets and allows crimp-diameters for trans-femoral access.

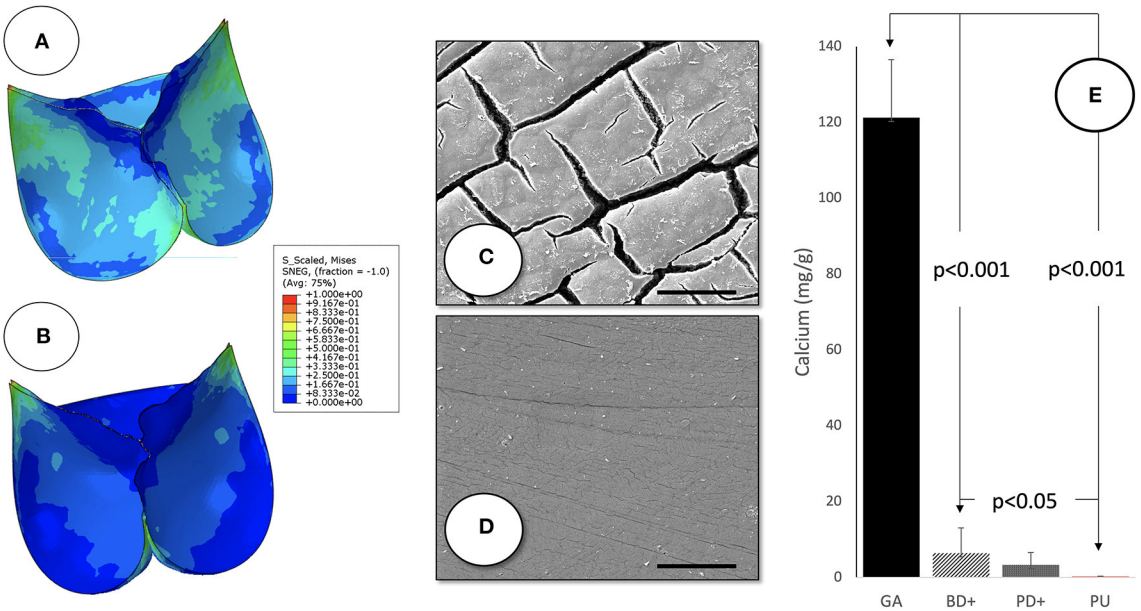

FIGURE 3 | Leaflet characteristics of SAT TAVR: normalized Von Mises stress of the PU **(A)** and BP **(B)** leaflets in the closed position shown as a contour plot of FEA results. Scanning electron micrographs of 100% pre-strained polyurethane leaflet films after 25 weeks of subcutaneous implantation in long-Evans rats demonstrating the degradation resistance of the SAT Carbosil leaflets **(D)** compared to significant surface degradation visible on the Pellethane control samples **(C)** (5,000×; Scale bar = 10 μm). While calcification **(E)** was distinctly reduced in the decellularized, sandwich-crosslinked bioprosthetic leaflets **(D)** both in bovine (−95%; left) and porcine (−97% right) pericardium compared to the control group (GA), Calcium levels were almost undetectable in the group of pre-strained Carbosil samples.

The retrieval sheath rolls over the crimped valve and the distal end of the delivery device, thus eliminating shear between the sheath and the device. Both helical and trunk balloons use thin walled, high UTS polyethylene terephthalate (PET) (wall thickness: 25–33 μm) while the retrieval "rolling" sheath uses Nylon 12. End points of trunk-balloon optimization were the maintenance of stability in the extended state, torque resistance and prevention of buckling during retraction. Test systems were based on 3D printed jigs and fixtures, a force gauge (FG-6005SD, Lutron Electronic Enterprise Co., Ltd.), Torque Gauge (BTG26CN, Tohnichi Mfg. Co., Ltd.) and a tensile testing machine (Instron 5544, Instron® Norwood, MA United States).

Balloon performance testing established the rated burst pressure and the safety factor based on functionality or as guided by ISO 25539-1 using a custom-made burst pressure rig. This was also used to evaluate the ability of the balloons to withstand repeated cycles/inflations as guided by ISO 25539-1 and for specific creep testing to determine the safety factor before time dependent deformation affects functionality during use. Tensile (water bath, Instron 5544) and torsional tests were performed to evaluate the respective peak forces at each

junction of incremental diameter increases as guided by ISO 10555-1. Radial force measurements (RX650 Radial Expansion Equipment, F033919 Head, Machine Solutions Inc. [MSI], AZ, USA) determined per unit length of the helical balloon were related to inflation diameters and pressures. Occlusiveness of the helical balloon in relation to filling pressures was established for the M-size system.

Dilatation Balloon Catheter

A TF dilatation balloon catheter for aortic pre-dilatation was developed following the same non-occlusive principle as the deployment balloon but designed to minimize inflation and deflation times, thereby minimizing the occlusive phase in the absence of rapid ventricular pacing (RVP). Pressure gradients across the expanded balloon and radial forces were determined. A wall thickness of 14 μm (Nordson Medical) was chosen to minimize the catheter crossing profile while still maintaining device safety and performance. Simulated use and burst pressure, fatigue performance and tensile tests were carried out in accordance with ISO 10555-1 and ISO 10555-4.

Simulated TAVR Placement and Anchorage Testing

To evaluate the ability to access, deploy and withdraw the devices, an ex vivo porcine heart (XH) loop system was used to simulate cardiac flow, using a software-controlled piston pump with variable stroke volume and heart rate. An adjustable atrial reservoir provided constant positive pressure to the atrium, a flow resistor adjusted the arterial pressure and a Windkessel provided shape-modulation of the pulse-wave and diastolic back-pressure (27). The deployment procedure was endoscopically visualized after insertion through the stump of the brachiocephalic artery. The mock-circulation was used in combination with a Philips angio-permissible C-Arm (Philips BV Pulsera mobile C-arm system, Philips Medical Systems, NL). The deployment process commenced with trunk-inflation in the ascending aorta (at 12 bar) and tactile trunk-location in the nadirs of the native leaflets. The TAVR was then deployed at 18 bar followed by the retrieval of the deployment system using the pressurized rolling-sheath. The correct position of the TAVR was confirmed through an oblique ventriculotomy. Pull-out resistance of the valve was tested with a Lutron FG-60055D force gauge.

A second test system used a Pulse Duplicator loop that simulates flow through a 3D printed annular ring, with a crush force of 3 N when expanded to the maximum waist diameter corresponding with the landing site for the trunks during the deployment process. This commenced with trunk-inflation above the ring (at 12 bar) and tactile trunk-location on the landing site, followed by retrieval through the pressurized rolling-sheath.

RESULTS

The BE TAVR system met all requirements for which it was developed: the expansion-linked shape-change of the stent resulted in the profile differences required for anchorage in non-calcified aortic roots; the scallop-design allowed for the direct, fatigue-resistant attachment of both elastomeric and bioprosthetic leaflets and the deployment device permitted

TABLE 1 | Dimensional and hemodynamic characteristics of SAT TAVR [transapical (TA) and universal (Univ)] comparing bioprosthetic (BP) with polymer (PU) leaflets, in combination with the non-occlusive trans-apical delivery system (TA-DD) or a conventional trans-femoral (TF) delivery balloon.

		BP/TA	PU/TA	BP/Univ.	PU/Univ.
Non-occlusive DD	Stent top	27.03 ± 0.17	27.19 ± 0.39	25.32 ± 0.08	26.52 ± 0.33
(TA delivery) (diameter at 18 bar in mm)	Spacer arm	29.45 ± 0.19	28.08 ± 0.53	29.31 ± 0.56	29.39 ± 0.11
	Supra-annular arm	30.14 ± 0.13	30.69 ± 0.54	29.72 ± 0.81	30.69 ± 0.25
	Nadir/landing zone	24.42 ± 0.20	24.50 ± 0.35	24.65 ± 0.12	24.67 ± 0.16
	Bottom flare	29.54 ± 0.49	28.18 ± 0.98	28.16 ± 0.06	28.48 ± 0.26
	EOA/cm^2 (ISO limit: 1.58)	2.39 ± 0.03	2.34 ± 0.09	2.43 ± 0.04	2.38 ± 0.10
	ΔP (mm/Hg)	6.17 ± 0.14	6.72 ± 0.20	5.93 ± 0.13	6.40 ± 0.35
	Regurgitant fraction (%)	7.60 ± 0.77	7.25 ± 0.60	11.97 ± 0.35	6.92 ± 0.76
	Crimp diameter (mm)	9.17 ± 0.06	9.24 ± 0.47	8.94 ± 0.09	9.21 ± 0.12
Conventional TAVR balloon	Stent top			25.02 ± 0.30	25.78 ± 0.17
(TF delivery) (Diameter at 5 bar)	Spacer arm			28.30 ± 0.53	28.19 ± 0.41
	Supra-annular arm			31.49 ± 0.28	31.55 ± 0.67
	Nadir/landing zone			24.57 ± 0.09	24.46 ± 0.21
	Bottom flare			29.27 ± 0.26	29.52 ± 0.16
	EOA/cm^2 (ISO limit: 1.58)			2.41 ± 0.01	2.31 ± 0.11
	ΔP (mm/Hg)			6.03 ± 0.01	6.59 ± 0.47
	Regurgitant fraction (%)			10.65 ± 0.15	6.25 ± 0.97
	Crimp diameter (mm)			6.45 ± 0.11	6.55 ± 0.06

Only the Universal design is suitable for both TA and TF delivery (measurements in millimeters).

root stabilization and tactile placement during uninterrupted cardiac output.

Stents

The BP stents (S and M) were fatigue-tested to 400 million cycles; no strut breakage occurred. Radial Crush Force was 102.45 ± 4.63 N (S), 116.42 ± 4.20 N (M) and 115.00 ± 5.00 (L) for the BP stent and 124.47 ± 16.70 N (S), 103.04 ± 5.83 N (M) for the PU stent, respectively. Design modifications and strut width reductions with the goal of a "universal" stent for both TF and TA delivery only modestly reduced the crush resistance by 9.6% when compared to the BP stent (M).

Leaflets and Skirt

FEA modeling of leaflets defined the extra length of the free edge to accommodate top-flaring of the stent. Decellularised, sandwich-crosslinked tissue showed markedly and significantly less calcification (6.4 ± 6.6 and 3.3 ± 3.2 μg/mg for bovine and porcine respectively) than GA-fixed non-decellularized pericardium (121.2 ± 15.3 μg/mg; $p < 0.001$). The polyurethane implants (Carbosil) showed practically no calcification at all (0.28 ± 0.07 μg/mg), significantly less than even the decellularised tissue ($p < 0.05$) (**Figure 3**). After 25 weeks of subcutaneous impantation the pre-strained Carbosil samples showed hardly any surface degradation while the Pellethane samples were visibly and heavily degraded on their surfaces.

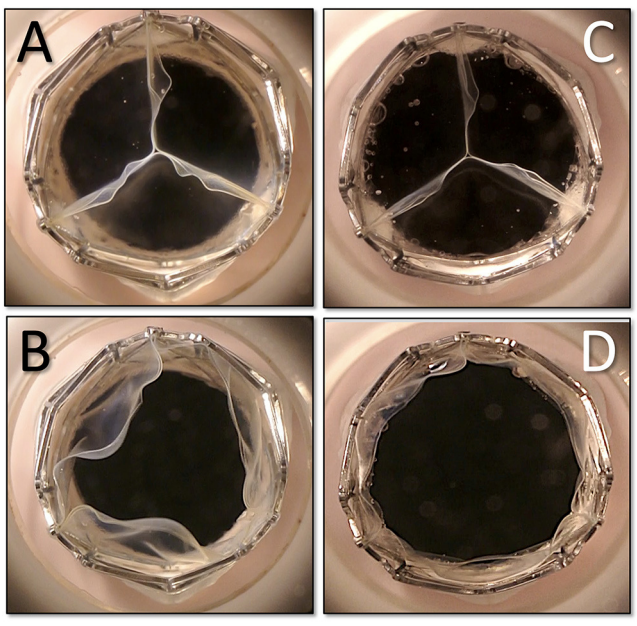

FIGURE 4 | Fine-tuning of the thickness of the polymer leaflets in the pulse duplicator. With twice the cusp thickness on the left side **(A,B)** end-diastolic coaptation is identical **(A,C)** but endsystolic opening shows a more complete hinge-motion in the thinner leaflets **(D)** eliminating some areas with a potentially lower wash-out effect. The flaring of the top of the stent and the diameter increase is visibly compensated by the clam-shell design of the leaflets.

Leaflet thickness was 340 ± 31 μm for BP and 150 ± 14 μm for PU leaflets. Both materials reached the predetermined 400 million cycles, neither leaflet type showing signs of macro-degradation such as delamination of the free leaflet edge. In the pulse duplicator, PU and BP leaflets showed equal fluid dynamics with excellent EOA, pressure gradients and regurgitation volumes (**Table 1**). For the universal stent, leaflet thickness of treated porcine pericardium was 137 ± 22 μm and that of PU leaflets was 52 ± 8 μm. While fatigue testing and regurgitation-fraction have not been finalized, fluid dynamics were improved (**Table 1**). Thinner polymer leaflets also led to reduced zones of incomplete hinging during systole (**Figure 4**). Across the three TAVR sizes, crimping was shown to expose the electrospun skirts to a strain of up to 67%. No tearing or detachment from the welding lines occurred in the crimping and re-expansion tests (**Figure 5**). Skirt permeability was shown to be 1,616 ± 1,344 ml/min/cm^2 sufficient to allow transmural capillary ingrowth (**Figure 6**)(17). The lowest point of the skirt was always the lowest point of the void between commissural posts and stent arms (**Figures 2**, **5**).

TAVR Dimensions and Deployment Dynamics

Crimped onto a conventional 26 mm trans-femoral TAVR deployment balloon, the diameters of the M-size BP

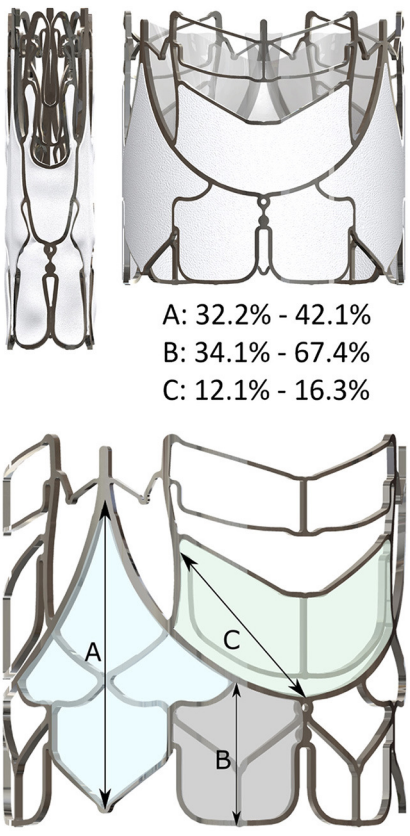

FIGURE 5 | Crimping of a scalloped stent leads to distinct elongations of the skirt. Stretching is most pronounced along the indicated vectors **(A)** at the commissures; **(B)** at the infra-annular flare and **(C)** on the supra-annular arm.

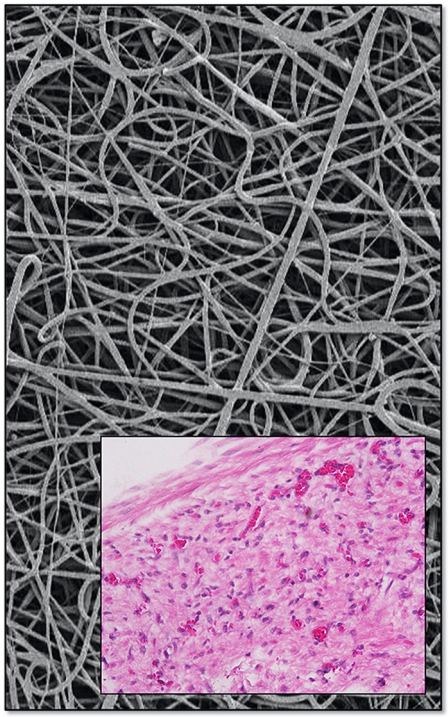

FIGURE 6 | Skirts are electrospun from the same material used for the polymer leaflets. Porosity was shown to allow transmural capillarization [bottom, from (17) with permission].

and PU-TAVR measured 6.45 ± 0.11 mm and 6.55 ± 0.06 mm, respectively, compared with 9.17 ± 0.06 mm and 9.24 ± 0.47 mm when crimped onto the 26 mm non-occlusive trans-apical SAT hollow-balloon. Dimensions of TAVR valves (stents plus leafets and skirts) are listed in **Table 1**.

Longitudinal shortening of the valve during expansion after crimping was initially distinct but then flattened out non-linearly (**Figure 7A**). At 14 bar inflation pressure the crimped valves shortened from 31.53 ± 0.02 mm for BP and 31.34 ± 0.01 mm for PU to a post-deployment length of 24.87 ± 0.31 mm and 24.69 ± 0.02 mm respectively. Further pressure-increases to 18 bar had little additional effect on shortening.

Radial expansion favored the wing-structures (**Figures 7B,C**), which, together with flaring of the bottom end of the stent, resulted in an hourglass-shape (**Figure 8**). The waist (corresponding with the landing zone) was in immediate proximity beneath the nadir of the scallops, right below the supra-annular anchoring arms. When fully deployed, a circle defined by the outermost points of the anchoring arms exceeded the outer diameter at the waist level by 26.5 ± 0.4/29.5 ± 0.6% (**Figures 7–9**; **Table 1**) introducing the distinct anchoring principle of the mid-portion of an hourglass against the limited distensibility of the annulus. The elevation of the stent arms was already fully developed at 6 bar inflation pressure [diameter-difference 21.9% BP/ 16.4% PU] when the OD of the stent-waist was only 18.21 ± 0.22 mm (BP) and 17.40 ± 0.12 mm (PU), respectively (**Figures 7B,C**). While the waist increased from 20.69 ± 0.42 mm/20.04 ± 0.12 mm to 23.77 ± 0.09 mm/23.51 ± 0.09 mm between 8 and 14 bar it only minimally increased further from 14 to 18 bar (24.54 ± 0.50 mm/24.48 ± 0.07 mm). From 6 bar onwards, corresponding with two thirds of the diameter at full expansion, the OD of the anchoring arms exceeded that of the waist by one quarter. Incremental inflations and deflations led to only 0.52 mm bigger waist diameter at 18 bar compared to single inflation. Over the entire range of non-occlusive inflation pressures, average post-deployment recoil was less than 2.47%/3.17% for the waist and 5.03%/6.29% for the wings of BP and PU valves.

Non-occlusive Deployment System

Rated burst pressures were 18.4/18.3/5.6 bar for the trunk balloon, helical balloon and retrieval balloon, respectively. Each inflation was safely repeatable with a fatigue factor of 2 and a creep safety factor of 3/6/5. **Figure 10** shows the main components. During the tensile and torsional tests, each bond exceeded the predetermined tensile and torsional load required to withstand component embolism. Radial force measurements of the helical balloon are shown in **Figure 11A** and the EOA during deployment in relation to filling pressure in **Figure 11B**. In the XH tests, the supra-annular arms anchored the stent on the rim of the annulus sufficiently below the LCA ostium (**Figure 8**) without diminished coronary outflow or obstruction.

Simulated Use Testing

Endoscopic visualization during simulated *ex-vivo* placement (n = 21 S) and (n = 30 M) of BP and PU valves confirmed first attempt engagement of all three leaflets in 81 and 77 % respectively. The native commissure to TAVR commissure was rotationally in congruent alignment in 67 and 87 %. The anchoring arms were tightly snuggling supra-annularly onto the annulus in 76 and 90%. Post implant pull-out force was 23.50 ± 2.52 N for both stent sizes.

Dilatation Balloon Catheter

The dilatation balloon catheter is shown in **Figure 12**. Safety was satisfactorily demonstrated for the 20 mm balloon: each sample was inflated at least 10 times to RBP of 9 bar without device failure. Inflation time ranged between 0.27 and 0.35 s between different users and deflation time was 2.74 ± 0.58 s. When inflated, the mean gradient across the device during physiological pulse-duplicator generated flow was 32.68 ± 7.64 mmHg. Inflation-pressure dependent radial force measurements of the 20 mm balloon catheter are shown in **Figure 13**.

DISCUSSION

Utilizing differential plastic deformation rather than shape memory, with a dimensionally stable scallop design and the radial force of helical balloons, we have developed a fundamentally new concept of balloon-expandable TAVR that may greatly broaden its clinical use.

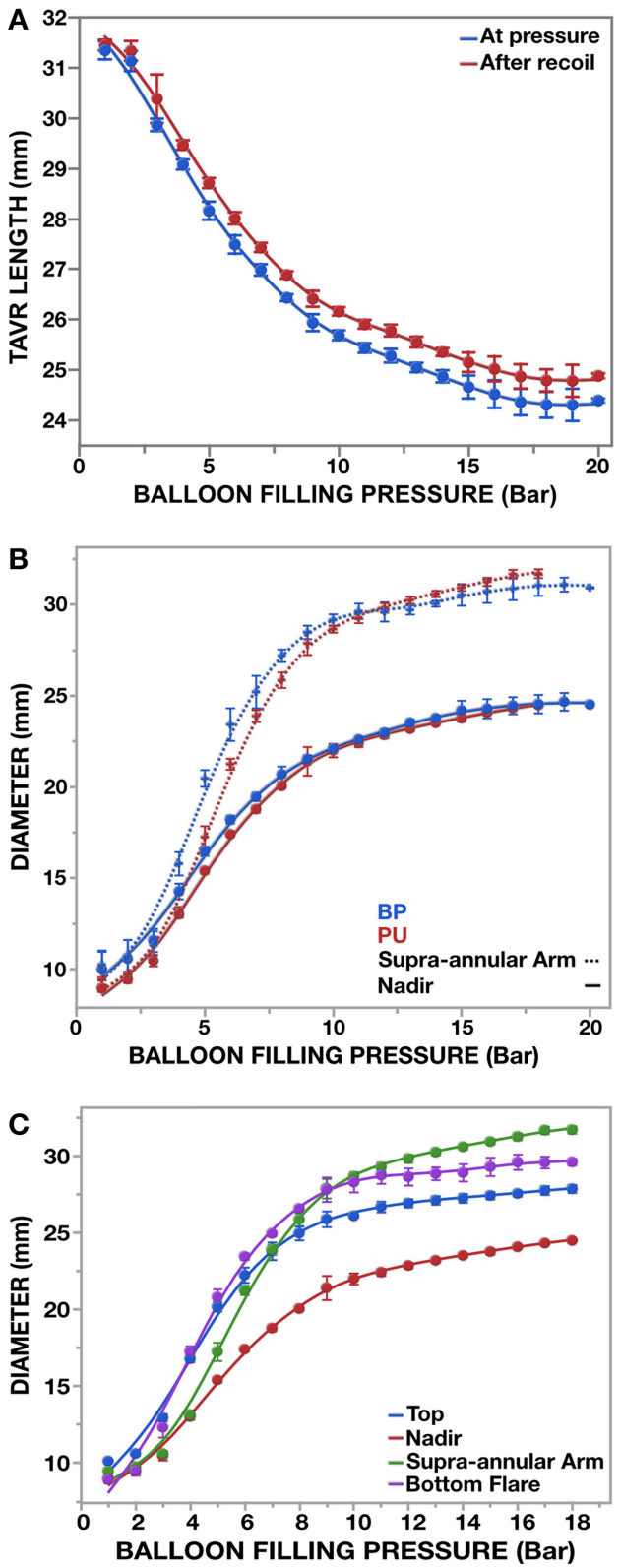

FIGURE 7 | Outer dimensions of (M)-size pericardial (BP; $n = 3$) and polymer (PU; $n = 3$) SAT valves during expansion with a 26 mm non-occlusive SAT

(Continued)

FIGURE 7 | delivery device ($n = 6$). Measurements were taken at inflation increments of the balloon of 1 bar. **(A)** Overall shortening of the crimped valve during deployment. **(B)** A main feature of the SAT TAVR is that anchoring arms made of a non-shape memory alloy elevate on the basis of plastic deformation during expansion. The resulting diameter difference between waist and anchoring arms is already fully developed when the valve has only reached 60% of its maximum diameter. **(C)** With the supra-anular arms and the bottom flare having the biggest diameter difference to the "waist (nadir)," anchorage in compliant aortic roots is secured in both directions.

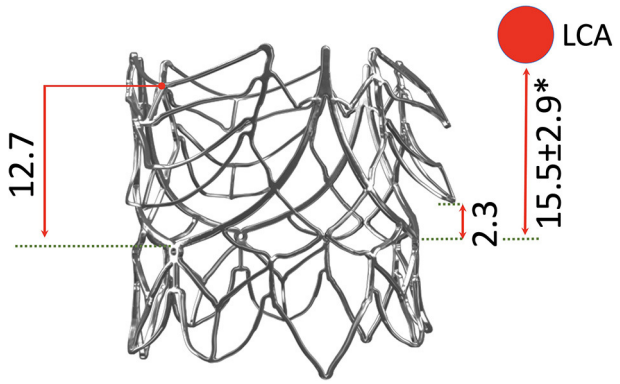

FIGURE 8 | Profile view of the SAT TAVR stent relating key parts to the annular plain and showing the extent of arm-elevation achieved purely by the expansion force of the balloon. The average distance of the left coronary ostium (LCA) is shown in relation to the stent (*) (28–30).

Balloon-Expandable (BE) vs. Self Expanding (SE) TAVR and Permanent Pacemaker (PPM)

For almost two decades it has been presumed that SE TAVRs would supplant BE systems, even though the latter remained the unchallenged preference of clinicians. After 20 years experience, two-thirds of implanted TAVR in the USA are BE (32). In Europe, SE TAVR devices together account for less than half of the market (32) and the situation is even more extreme in Japan where three quarters of TAVRs are BE (33). The perception that the future belongs to SE TAVR is self-perpetuating, which is astonishing with respect to clinical realities. Huge cohort studies repeatedly showed key advantages of BE (33–37) the most prominent being the persistently higher need for a permanent pacemaker (PPM) with SE devices (33–35, 38–42), even if used for valve-in-valve procedures (43). The acceptance of these drawbacks by many clinicians in HICs is partly because the implantation of a pacemaker is affordable. This higher need for PPMs in SE devices can be related to their radial force profiles (44). SE valves exert less radial force than BE counterparts during deployment and therefore result in a higher degree of PVLs (41) and initial micro-dislodgement (45). However, they maintain a relatively high radial force beyond their nominal diameter while that of BE valves is limited to the diameter at deployment. Therefore, once a BE TAVR has healed in, the pressure on the conduction system has eased, whereas SE TAVRs continue to push against

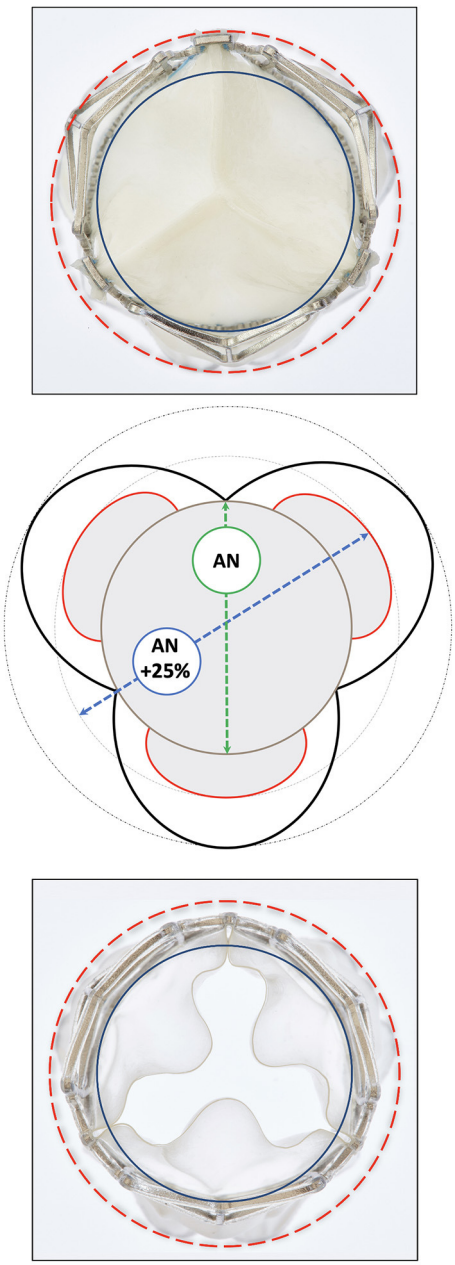

FIGURE 9 | Top view of a deployed SAT bioprosthetic (top) and polymer (bottom) TAVR showing the radius of the supra-annular anchoring-arms (red) *vis a vis* that at the waist level corresponding with the annular landing zone (blue). The schematic drawing (middle) shows that the supra-annular diameter is 25% bigger than the annular landing zone of the TAVR firmly securing anchorage (pull-out resistance >23 N) even in the absence of calcification. There is still ample space between the arms and the sinus wall in average sinuses of Valsalva.

the surrounding tissue. Use of a shallower implantation depth (46) and non-flaring designs (47) have attempted to mitigate this, but recent studies confirmed continual contact pressure independent of implant depth as the key predictor for conduction abnormalities with SE TAVR (48). Moreover, as the PARTNER 3 trial showed, the disadvantage of a larger crimping diameter of BE systems has been minimized with expandable sheaths and when extending TAVR to low-risk patients (3).

Another perceived advantage of SE systems is their ability to be re-sheathed during deployment. Although appealing, this does not solve a general problem of transcatheter implantations but one that specifically concerns SE TAVR. The rate of re-sheating maneuvers required was 24% with the Portico system (47) and 23% in the Evolut-R US registry (49) but in modern comparative studies hardly any of the patients receiving BE TAVR would have required it (50). While the combination of affluence, local experience and skill-profiles may make a case for either BE or SE in HICs, the avoidance of expensive adjunct procedures would make BE devices more affordable and suitable for the vast number of potential patients in LMICs.

TAVR Needs in AR Patients: More Than a Fringe Group

The specific needs of MICs, including their high proportion of relatively young patients with AR and often the lower level of skills and equipment available, has slowly begun to challenge the unwavering bet on the unlimited growth trajectory of Western products in these regions (9, 10, 20, 31, 51). A majority of symptomatic patients in countries such as China, India, Brazil and South Africa require AVR for rheumatic regurgitation (9, 10, 13, 31, 52). While often concealed by the fact that the leading heart centers in these countries disproportionally cater for an aging urban population that partially mirrors HIC pathologies these data have long been available. In a study from Shanghai's Zhongshan Hospital that assessed 315,884 patients with moderate to severe aortic valve disease, only 27% were above 65 years of age and even in this subgroup AR outweighed AS by a factor three (13). Shanghai's Changhai hospital confirmed that the proportion of patients undergoing SAVR was significantly higher for AR than AS (11). The 2020 up-date of the "Chinese Expert Consensus on TAVR" confirms the high proportion of rheumatic etiology in Chinese patients with aortic valve disease (53).

Clearly, TAVR suitable for pure, non-calcific AR in younger patients would therefore not only be for a fringe-indication but of relevance for a dominant pathology in MICs (9, 10, 15, 31). Recent publications on the use of TAVR for RHD can be regarded as important harbingers of this development (14–17, 31) particularly since TAVR was shown to have a profound, durable impact on heart remodeling in patients with severe AR. Within the first 3 days, a significant decrease in LV end-diastolic pressure, a significant reduction in LV size and mass index (54) and a sharp reduction in systolic pulmonary arterial pressure were seen (55), confirming that in patients undergoing valve replacement for severe AR, cardiac function often recovers faster than in AS. In many areas with a high incidence of RHD, patients are breadwinners for extended families, so that symptomatic relief would critically affect livelihoods even in the absence of significantly extended life expectancy. Even then, minimizing the ischaemic myocardial injury associated with open heart surgery

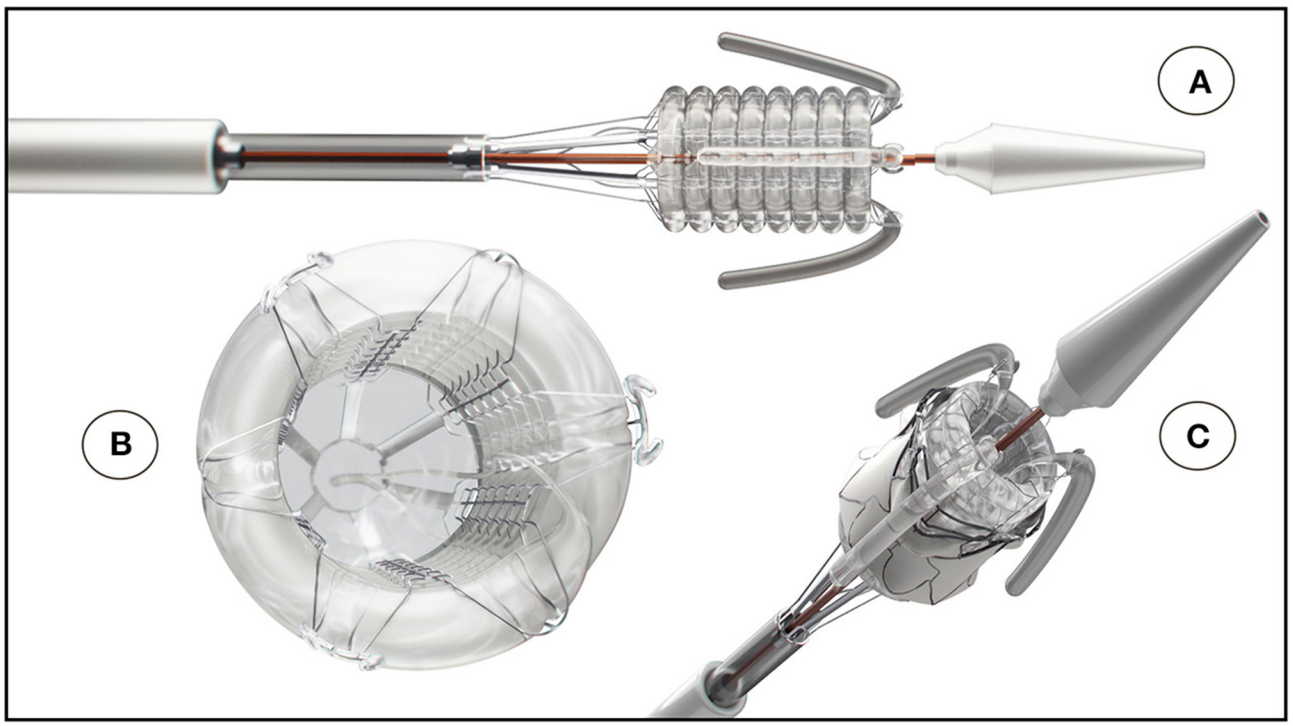

FIGURE 10 | The SAT non-occlusive balloon-delivery system consisting of a helical balloon is prevented from toppling by a Nitinol frame; **(B)** positioning- and stabilizer-trunks that are invaginating upon retraction; **(A,C)** a back-flow valve and **(B)** a pressurized rolling sleeve for device retrieval [**(A)** Reproduced from (31) with permission].

(OHS) by using trans-catheter procedures would increase the likelihood of remodeling, and thus of a longer life expectancy.

The scope for TAVR is also changing in HICs. According to the Euro Heart Survey (56) the treatment of severe pure AR clearly represents an unmet clinical need. For this reason, TAVR is being increasingly performed "off label" for pure AR in patients excluded by surgery (18). Already, TAVR patients transapically treated for AR had better in-hospital outcome compared with SAVR patients (39, 57). With TAVR increasingly being considered for patients with bicuspid aortic valves (58) the demand for devices suitable for AR will also grow, since 10–15% of these patients need AVR for pure AR (59). This particular indication would create an overlap between HICs and MICs as patients with such valves are prevalent in China (11). It is therefore foreseeable that TAVR designs will need to cater for both (57) AS and AR in order to have a true global appeal.

Leaflet Durability: The Next Horizon for Both AR and AS Patients

The need for improved valve durability in younger patients is growing globally. Currently, TAVRs are largely restricted to patients in their seventies and older. As long as TAVR was confined to high risk patients, the vast majority of patients fell into this age category. This has changed with the approval of TAVR for lower risk patients (3, 41) but as these patients are usually younger many do not qualify for a TAVR. Therefore while "low operative risk" is now treatable by TAVR, "younger age" becomes the new reason for not qualifying. When all AVRs were performed through conventional cardiac surgery, there were no procedural choices, just formulaic decision of mechanical valves for the young or tissue valves for the old. The advent of TAVR for all risk categories has turned this situation into an exclusive privilege for some: non-invasive TAVR reserved for elderly patients while the need for a durable mechanical prosthesis still condemns young patients to open heart surgery.

In MICs the situation is even more extreme. Since RHD patients are often in their early fourties at the time of surgery (31, 60, 61) valve durability would need to be markedly improved to permit a trans-catheter approach. Since access to open heart surgery and post-implant control of anticoagulation is often severely limited, simple transcatheter approaches would provide hope for many (9, 10, 15, 31). Therefore, the highest bar for leaflet longevity is defined by the needs of patients with RHD in MICs. Achieving this would also profoundly address the needs of patients with degenerative AS in HICs who are currently deemed too young for a tissue valve and therefore for TAVR (62). Recent developments suggest that such improved leaflet durability is a real possibility as both major degeneration modes of soft-leaflet materials have been identified and successfully addressed: remnant immunogenicity in bioprosthetic materials (63) and biodegradation in polymers (28). The SAT TAVR implemented the most recent features in both its pericardial and polymeric leaflets. For the BP version

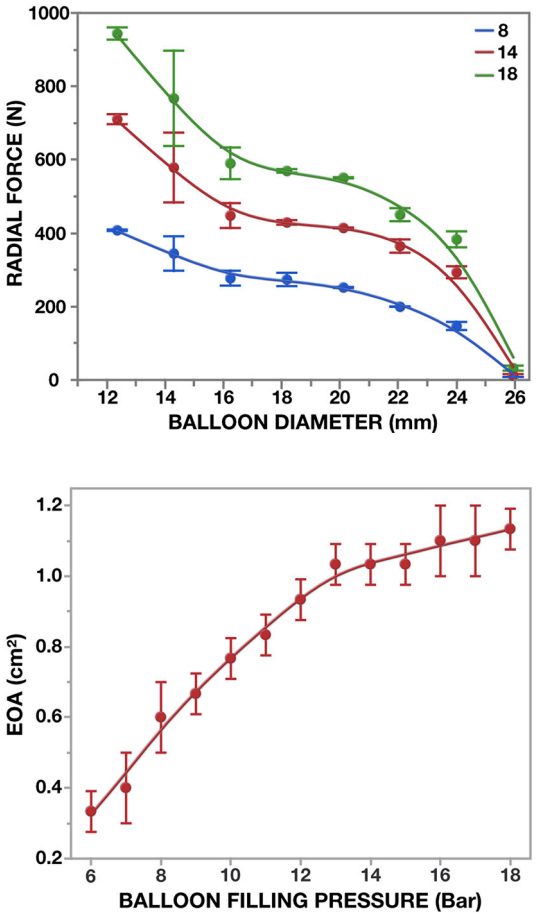

FIGURE 11 | Radial force of the 26 mm non-occlusive delivery device for [M]-size TAVR. Three different inflation pressures were blotted against balloon-diameters (top): 8 bar (onset of non-occlusiveness); 14 and 18 bar ($n = 3 \times 3$). In the pulse duplicator, effective orifice areas were determined against restricted balloon inflation (bottom).

the leaflets consist of decellularized, sandwich-crosslinked pericardium that completely suppressed calcific degeneration both in the rat (26) and the sheep model (17). At the same time, degradation-resistant polymers (64) promise to be a realistic alternative with potentially significantly longer lasting soft-leaflet heart valves. Recent first-in-man studies with polymeric surgical valves (65) have strengthened the belief that polymer leaflets represent an important opportunity for heart valve technology. Therefore, the SAT TAVR stent was specifically designed to provide optimal support for polymer cusps. The choice of Carbosil® for the leaflets was based on excellent biostability (66) combined with mechanical properties, and wide clinical use in other high-performance applications such as drug eluting stents (67). Carbosil 2080A TSiPCU is a segmented triblock polyurethane which combines siloxane segments for biostability and carbonate segments for processability and toughness. Its excellent biostability has been confirmed both *in-vitro* (68, 69) and *in-vivo* (70). *In-vitro* experiments under both hydrolytic and oxidative conditions showed preservation of material properties in contrast to earlier generations of polyurethanes (71–73). Moreover, the surface properties of Carbosil also provided excellent biocompatibility, including haemocompatibilty (74–76). It does not induce conformational changes in any attached fibrinogen thereby preventing triggering the coagulation cascade and subsequent thrombus formation (77, 78). Moreover, the low intrinsic capacity of segmented polyurethane leaflets to calcify *in vivo* (79) has been confirmed by our results. Both the fatigue resistance with leaflets as thin as 50μm and the excellent preliminary *in-vivo* performance vindicate this material choice.

Leaflet Thrombus and Valve Design

While leaflet durability is a prerequisite for the longevity of heart valves in younger patients, valve thrombogenicity and the potential consequences of subsequent leaflet immobilization and embolization (80) may also threaten valve endurance, particularly in the absence of anti-coagulation (81). Subclinical thrombus formation on valve leaflets following TAVR is increasingly recognized (82) ranging from 4 to 40% after 1 year (83). The most plausible explanation for this phenomenon is the largely absent vortex formation due to the small neo-sinuses between the prosthetic leaflets and the displaced diseased native leaflet or skirt, leading to increased blood stasis (84). Vortices generated by the sinuses of Valsalva during early systole and persisting into early diastole play a crucial role in reducing thrombus formation on the outflow-side of native aortic valves (82, 85, 86). Increasing the neo-sinus size by higher deployment of conventional TAVR was shown to reduce the stagnation zone seven-fold (87) but such a higher implantation level would need to be balanced with the risk of coronary occlusion (82).

In the SAT valve the external skirt follows the shape of the supra-annular arms, creating spacious neo-sinuses. Furthermore, the direct insertion of the prosthetic leaflets into the scallops of the stent avoids spatial separation between the TAVR leaflet and the neo-sinus, creating a continuous physiologically shaped space intended to facilitate sufficient vortex formation (**Figure 14**).

At the same time, leaflet mobility and the degree of bending at the hinges of the leaflet insertion (**Figure 4**) add to the elimination of low-vortex zones. Our ability to produce thin, mechanically durable polymer leaflets has validated this concept in the challenging pig model, where thrombus formations previously seen at the nadir of thicker leaflets could be avoided by reducing their thickness.

Ingrowth-permissible skirt porosity further reduces the likelihood of thrombus formation in the neo-sinuses, as confined non-porous intra-vascular spaces increase that risk. Although poorly understood, non-porous vascular prostheses have a distinctly higher thrombosis rate than porous ones (88). Also, while most TAVR publications refer to delicate and functional endothelialisation on explanted leaflets in animal models (89), the actual tissue outgrowth onto the leaflet surfaces in humans consists of fibrotic transanastomotic pannus tissue (90). This pseudo-neointima with its "endothelial-like" surface layer does not have the non-thrombogenic properties of true endothelium and is likely to eventually consolidate hypoattenuated leaflet thickening (HALT) seen in TAVR (91). As described by Berger et al. (90) as early as in the 1960s this tissue response

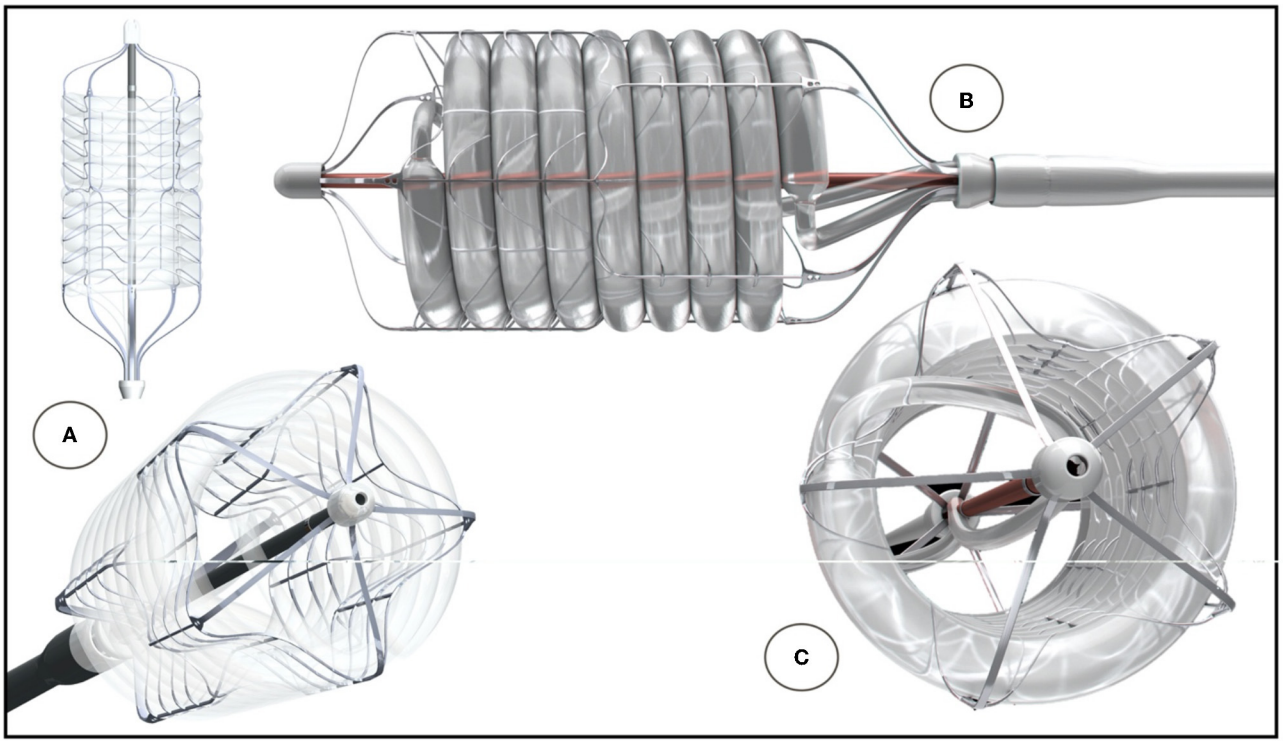

FIGURE 12 | SAT helical dilatation balloon. The helix is prevented from toppling by a fine-meshed Nitinol frame **(C)**. A directional change at mid-level allows mirror-imaging of the proximal and distal ends **(A)**. Profile of combined helical balloon and support frame **(B)**. Dual inflation from both sides and relatively large feeding lines allow rapid inflation **(C)**.

represents the typical prosthetic fibrosis-mode in humans and is initiated by the deposition of surface thrombi. While diminished vortex formation explains the fluid-dynamic trigger for these thrombi, the absence of a functional endothelium allows platelet aggregation and fibrinogen conversion to unfold uninhibited. Recent experimental work indicates that transmural capillarization may compensate for the deranged trans-anastomotic neo-intima outgrowth typically seen in humans (88, 92). In contrast to the densely woven PET and PTFE skirts of contemporary TAVR, the electrospun SAT skirt provides sufficient porosity for this healing mode (17, 88, 92). Therefore, the successful capillary ingrowth seen across the entire skirt thickness in long-term sheep implants (17) encourages the belief that the SAT TAVR valve may allow functional endothelialization in patients.

A Balloon-Expandable TAVR for Non-calcified AR

The second main focus of SAT was to develop the first BE TAVR that also caters for non-calcified pure AR, the predominant pathology in RHD patients (9, 10, 13, 31, 52) which is also a prevalent occurrence in other pathologies including bicuspid aortic valves (59). Two major challenges face the use of TAVR in pure AR: anchorage in the absence of calcification and correct positioning in cases of excessive stroke volumes. Lack of calcium in the annulus and leaflets makes delineation of the annular plane difficult, requiring greater contrast exposure with a potentially elevated risk of acute kidney injury (93). Moreover, this lack of calcium conglomerates for anchoring requires considerable oversizing in conventional TAVR (to prevent migration or embolization) leading to a higher risk of pacemaker implantation (94) and annular rupture (93).

Of the SE valves which address anchorage in the absence of calcification (JenaValve, J-Valve, the discontinued Engager and Symetis/Boston Scientific Acurate) the first three featured supra-cuspal arms resting outside the leaflets in the sinuses. In contrast, the Acurate valve anchors with supra-annular arms on the ventricular side of the leaflets. Accordingly, the embolization rate of the Acurate TAVR was negligible in a "pure AR" study while conventional SE valves had a 50–58% embolization rate if they were <10% oversized but still 31–60% if they were >20% larger (95). Others have recommended oversizing at 15–25% or more for conventional SE devices or using up to 3 ml additional balloon-inflation volume for BE valves in AR patients (96). Alternative dedicated TAVR systems for AR improved outcomes but still had higher than acceptable procedural complications and mortality rates (18). While a dedicated SE-TAVR system for AR such as the JenaValve prevented embolization into the ventricle it still had the typical shortcomings of SE TAVR, with almost 10% needing a second valve implantation and 16% requiring a PPM (18). In two pure AR studies with the "Acurate Neo" valve, embolization could be prevented with moderate annular

oversizing of 9% (54) but a PPM was still required in 15% of cases. This acceptable performance in AR was offset by failure to achieve non-inferiority with the Sapien 3 in patients with AS due to higher rates of severe PVL (97).

The SAT TAVR uses a supra-annular anchoring system in conjunction with a BE concept. Boston Scientific's Acurate is an SE TAVR that shares the principle of supra-annular anchorage. Both rely on a stent profile that prevents slippage through the annulus with an immediate supra-annular diameter exceeding that at the annular level by >20% resulting in a pull-out resistance of >23 N. However, while the supra-annular stent-expansion is only mildly wider in the SAT valve than in the "Acurate Neo" (26 vs. 20%), the difference in infra-annular flare is distinct (20 vs. 12%) (54). Since a significant proportion of TAVR embolization in patients with native valve AR is due to a forward dislodgement into the aorta (95) the inferior flare is crucial. In a TAVR study in patients with pure AR using predominantly Core- and Evolut-Valves, modest undersizing led to 50% of the embolizations occurring in antegrade direction. Even with oversizing, every 5th dislodged valve still did so toward the aorta (95).

In the SAT valve the infra-valvular flare is combined with a concavity intended to "contour-snuggle" along the septum beyond the muscular crest, even in a sigmoid septum. This combination of the restricted expansion of a BE stent with an anatomy-following shape resulted in the absence of conduction disturbances in 263 consecutive pig and sheep implants. This complete avoidance of heart block in two different animal models in spite of a distinct flare and an implantation depth that was previously identified as a risk factor for conduction damage (46, 98) supports the argument that it is the continual contact pressure exerted beyond the intended diameter by SE stents (48) rather than implantation depth or flaring that increases the risk of needing a PPM.

Most importantly, the plastic deformation of the stent during expansion does not only occur at full deployment but creates the distinct profile that anchors the valve from two thirds of the nominal diameter onwards (**Figure 7**) allowing measured sizing that further reduces the risk of conduction disturbances.

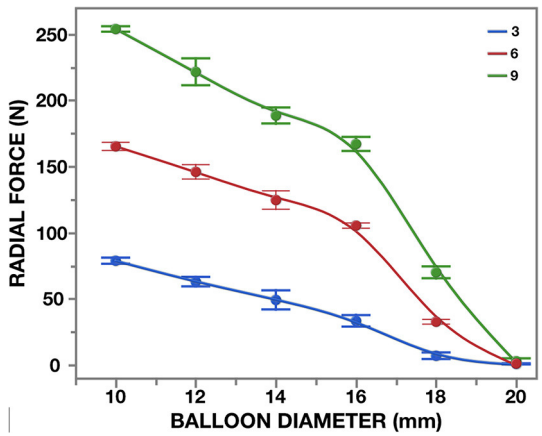

FIGURE 13 | Radial force of the 20 mm dilatation balloon at three different inflation pressures (in Bar).

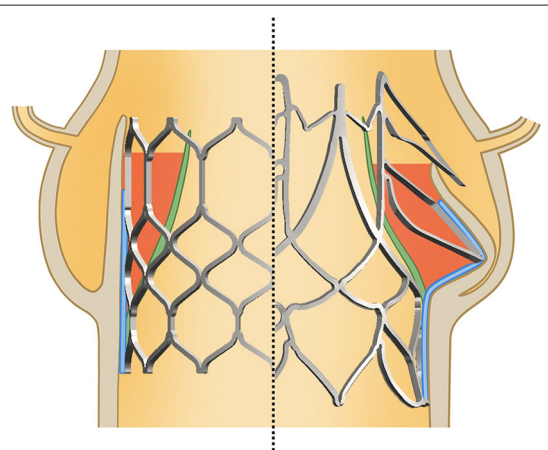

FIGURE 14 | Difference between a conventional cylindrical TAVR and the SAT design: by skirting the supra-annular anchorage arms a spaceous neo-sinus is created between skirt (blue) and prosthesis leaflet (green) intended to facilitate sufficient vortex formation for the prevention of thrombus. This is opposed by the relatively narrow space of the neo-sinuses in cylindrical designs.

Mitral Valve, Skirt and Coronaries

The mildly deeper implantation depth of the SAT TAVR may give rise to concerns regarding the mitral valve. While injuries to the anterior mitral leaflet are extremely rare, they have happened in TAVR valves with relatively sharp crowns (99). In contrast, the SAT stent has predominantly flat, round crowns; furthermore, modeling studies indicate that, counterintuitively, a lower stent position may have a lower risk for mitral tissue damage (100, 101) or even SAM (systolic anterior motion) of the anterior mitral leaflet (102).

Skirting a stent that comprises diverse design elements creates greater challenges than covering stents that predominantly consist of repetitive elements. For example, crimping of our scallop-based stent leads to areas where the skirt elongates up to 67%, which considerably exceed the maximum estimated strain of 50% for the skirt of the Sapien 3 Ultra [based on Yudi et al. (103)] and 42% for the Evolut Pro [based on Jubran et al. (104)]. Electrospinning the skirt from the same polymer as used for the leaflets provided both the required viscoelasticity and an ingrowth-permissible porosity. By fully covering each supra-annular arm, the skirt becomes an integral part of the physiologically shaped neo-sinuses. The concern that the skirt-covered commissural area may be potentially occlusive in relation to coronary ostia was recently put into perspective in a study using post-implantation CT after both SE and BE TAVR. Although 51% of cases showed severe overlap of the neo-commissures with either or both coronary ostia due to rotational misalignment, no impediment of coronary blood flow occurred (105). Instead, coronary obstruction seems to occur due to displacement of the native valve leaflets by the TAVR stents or by displaced calcium in patients with a low LCA (106). In our XH tests, two features of the SAT stent have

been confirmed to increase the safety-space between the edge of the native leafelets and the LCA: the supra-annular arms cause a "downward-tenting" of the native leaflet at the rim of the annulus, thereby lowering the edge of the native leaflets, and the nonagonal cross-sectional footprint created by the stent arms, by countering the congruency in shape that cylindrical stents cause opposite the sinus wall. With a height of 7 mm above the stent-waist (and therefore the annulus), the SAT skirt lies somewhere between the 8–10 mm in the Evolut R/Pro (103, 107) and the 5.7 mm reported for the Sapien 3 Ultra (if implanted in an 80%:20% aorto:ventricular ratio) (108, 109). This lies well below the coronary height of 10.3 ± 1.6 mm that was identified as risk factor for coronary obstruction (106). Furthermore, the three uncovered upper "spacer arms" potentially increase the inflow space even in effaced sinuses of Valsalva that fall into the high-risk group when diameters are less than 27.8 ± 2.8 mm (106). The inward-tilt of the upper part of the SAT as well as the Acurate skirts, compared to an outward-tilt in the Evolut and a zero-tilt in the Sapien further increases the distance to the coronary ostia. Additionally, the upper spacer arms point downwards with their struts in a V-shape. As the lowest point of the "V" lies below the average position of the LCA ostium, this shape should facilitate potential coronary interventions (29, 30, 110).

Non-occlusive TA Deployment Without Rapid Ventricular Pacing (RVP)

A major feature of the SAT system is the non-occlusive TA balloon-based delivery device. In view of the narrow focus in HICs on predominantly AS patients, any effort to develop an innovative TA deployment system for AR patients may seem anachronistic. Yet, the transapical access had allowed general surgeons to successfully treat RHD making it the commonest heart operation performed in the beginning of the second half of the twentieth century especially in countries of the southern hemisphere. This highlighted the potential of this route to treat valvular heart disease in the absence of open heart surgery (111) making it one of the backbones of our concept.

In TAVR, TF delivery has continually emerged as the dominant access route in AS patients, epitomized in the PARTNER 3 trial where the lack of TF access was an exclusion criterium (3). Nonetheless, this shift was only possible under socioeconomic circumstances that allowed the regular use of another costly secondary device, as TF access requires a vascular closure device at the conclusion of the procedure in practically all patients (112). However, while in calcific AS this trend increasingly restricted TA access to patients with unsuitable iliofemoral vessel size or significant vessel tortuosity (113, 114) the rational for an antegrade approach is entirely different for AR with its high stroke volumes and often significantly decreased ventricular function. Moreover, given the natural history of AR, with its long asymptomatic period and the relatively short transition into decompensated excentric volume-overloaded failure, RVP is unlikely to be tolerated in a significant proportion of these patients. Although an integral part of conventional TAVR procedures for AS, RVP is known for its detrimental effect on the myocardium (21). Every episode of RVP increases the incidence of new atrial fibrillation, acute kidney injury, in-hospital mortality and 1-year mortality (21). In a 2021 study, the significant decrease of cerebral oxygenation observed during RVP was a predictor for the occurrence of neurological complications such as TIA/stroke and post-intervention delirium (115). The Chinese consensus on TAVR recognizes this danger by stating that "the total pacing time should be <15 s to avoid serious complications caused by prolonged hypoperfusion" (53).

While clinical results suggest that in AS, with its concentric hypertrophy, the overall benefits of TAVR still outweigh the harm caused by RVP, this is unlikely to be the case for many patients with symptomatic AR. Once high-volume remodeling has led to endsystolic dimensions of more than 25 mm/m^2, together with ejection fractions of <35% (116) these patients are considered very high risk. According to a European Heart Study, up to one-fifth of patients with pure AR are in this category (56) with an annual mortality of 10–20% associated with conservative therapy (56) and a 59% post-operative 10 year mortality (116) if operated. The 14% intraoperative mortality of this sizeable patient group highlights the vulnerability of the thinned-out myocardium in response to the ischaemia associated with open heart surgery, even with modern cardioplegia. At the same time, it is unlikely that TAVR that require RVP will cause less damage to an already weakend myocardium. Given the myocardial injury associated with RVP in the concentric hypertrophy of AS (21) rapid ventricular pacing can be expected to have a particularly detrimental effect on the borderline myocardial capacity of the excentric, volume-overloaded ventricles of late diagnosed AR. While some attempts to insert SE TAVR without RVP were successful in patients with AS (117) the need to stabilize the aortic root during deployment seems to be essential for AR. Although patients in HICs usually present for valve replacement well before AR has led to the hallmark hyperdynamic, jerking motion of the aortic root, TAVR could not be performed without RVP with the same procedural success rate as in AS (117). Although 20% of patients receiving an Acurate Neo for native valve AR were rapid-paced, a second TAVR using a balloon-expandable valve was necessary in every 8th patient (54, 118).

Avoidance of RVP during deployment of a BE TAVR can only be achieved if the balloon does not obstruct bloodflow. Hollow-balloons, developed with multiple longitudinal tube structures have recently been used for predilatation of AS (117). However, a helical balloon not only delivers the very high radial force (almost 1,000 N) needed to deploy a BE TAVR (**Figure 11**) but also has a significantly larger luminal area at comparable outer diameter, as well as half the pressure gradient when fully deployed (unpublished data). During a series of pre-clinical implants of the SAT PU TAVR, the mean gradients during the deployment were 19.4 ± 9.3 mmHg, with peak gradients of 32.0 ± 6.5 mmHg (119). By incorporating the location and stabilization components into the balloon system rather than the valve stent (120), all functions of a sophisticated deployment system for hyperdynamic AR were combined in one device and all were activated by pressure-controlled inflation. Unlike AS, where the TA access route largely reflected the chronology of development,

this SAT system was designed for the hyperdynamic AR that is so prevalent in LMICs. Apart from enabling tactile location even with less sophisticated imaging facilities, it stabilizes a hyperdynamic root during unmitigated ventricular contraction. Both these requirements can be easily realized *via* a direct TA access route compared to a long and multiply bent TF system. With the locator/stabilization trunks on the balloon, their pull-line system allows individual height adjustment if required as well as retraction through invagination, making it impossible for the stent to pinch the trunks and get dislodged after deployment, even in very narrow sinuses. The temporary nature of the trunks during deployment allows building them at a diameter of >4 mm, minimizing the risk of leaflet perforation, while keeping generous inflow spaces between the valve and the sinus wall during deployment.

A further feature of this deployment device is the temporary backflow valve. The combination of a large lumen with a temporary backflow valve allows for a slow controlled implantation of the TAVR prosthesis while maintaining physiological aortic pressures throughout (119).

TF Access and Pre-dilatation for Aortic Stenosis

The SAT system was primarily designed to address the needs of patients with pure AR, even at a late stage of the disease; however, the polymer leaflets represent a potential quantum leap for all recipients of TAVR including patients with AS currently deemed to young. Nonetheless, a transcatheter valve that can only be delivered trans-apically would not be considered for the vast majority of patients in HICs. A universal polymer TAVR, therefore, needs to be also deliverable trans-femorally. While conventional TF delivery devices have been perfected for highly accurate deployment and even integrated rotational alignment (121) the *sine qua non* for this access route is crimpability of the valve to a diameter that can pass through the iliac vessels without detriment. Although the crimp diameter of SE TAVR has been continually reduced, expandable introducer sheaths have overcome the natural disadvantage of BE TAVR which retain a minimum crimp diameter of 20 to 23 Fr (122, 123). Expandable sheaths not only overcome psychological barriers by having diameters as low as 14 Fr while actually expanding to as much as 24.3 ± 1.7 Fr during passage (124, 125), but also have reduced vascular complications. With <20 Fr for the medium-size TAVR the SAT universal stent allows for similar crimp diameters as the most widely implanted TAVR valve and as such is compatible with TF delivery.

Although the combined need for pre- and post-dilatation in patients with AS is still moderately lower in BE than in SE valves (126), modern TAVR systems have lowered the proportion of patients undergoing an additional balloon procedure to one in four (127). Recognizing the detrimental effect of RVP, partially non-occlusive dilatation balloons were used for pre-dilatation in beating hearts (117). Expanding the helical balloon concept of the SAT delivery device to a TF dilatation balloon further extends the system to potential use in patients with AS. Apart from a robust radial force, the main advantage of a helical balloon is it's 44% larger lumen than that of its longitudinal counterpart (Bard Vascular Brochure 2018).

CONCLUSIONS

Middle income countries are catching up fast with TAVR. However, as contemporary products have been conceptualized for the needs of the affluent regions of the world, their use will remain confined to an aging urban population. With so many relatively young patients of emerging economies suffering from AR, there is a need to expand the often limited capabilities to replace heart valves and the next TAVR era will have to address global needs and not just those of the high income countries.

The approach presented in this paper is based on the belief that global needs are better addressed by BE TAVR. The resulting design provided a scallop-shaped core which allows the direct attachment of leaflets, including polymeric leaflets. Elevating arms, extending exclusively on the basis of plastic deformation, secure the anchorage in non-calcified and regurgitant valves. The use of an electrospun skirt allows trans-mural capillary ingrowth, facilitating accelerated surface enothelialization of the neo-sinuses. The back-flow-protected hollow-balloon system of the delivery device with its retractable balloon locator and stabilization-trunks allows slow deployment in a beating heart. Preclinical experience suggests that the avoidance of expensive secondary procedures has been addressed. The tactile non-occlusive delivery system not only makes RVP unnecessary, but also allows implantation in the absence of sophisticated imaging equipment. The stent design allows a crimp diameter that is even smaller than that of the most widely implanted conventional TAVR, also opening the door to TF delivery.

By combining this universal system with polymer leaflets, a powerful disruptive technology for heart valve disease has been incorporated into a TAVR that addresses global needs.

As such, this SAT system fulfills all prerequisites to expand the scope of TAVR to the many more patients living in low- to middle-income countries, while also bringing hope to the patients of high-income countries that are presently excluded from TAVR.

DATA AVAILABILITY STATEMENT

The raw data supporting the conclusions of this article will be made available by the authors, without undue reservation.

ETHICS STATEMENT

The animal study was reviewed and approved by the Animal Research Ethics Committee of the Faculty of Health Science at the University of Cape Town.

AUTHOR CONTRIBUTIONS

HA and KP introduced and executed the novel idea of plastic deformation in a BE stent. PZ and DW wrote the manuscript. BvB, BdJ, JdV, RC, MC, and RS: development. PZ, DB, DW, and HC involved in the daily R&D and production. PH: statistical oversight and design of animal verification experiments. JSc, CO, JSw, FV, BP, CS, LC, HT, HS, TF, MG, XL, and SM actively provided clinician feed-back with involvement in tests, animal experiments and modifications. All authors contributed to the article and approved the submitted version.

REFERENCES

1. Andersen HR. How transcatheter aortic valve implantation (TAVI) was born: the struggle of a new invention. *Front Cardiovasc Medicine.* (2021) 8:722693. doi: 10.3389/fcvm.2021.722693
2. Voigtlander L, Seiffert M. Expanding TAVI to low and intermediate risk patients. *Front Cardiovasc Med.* (2018) 5:92. doi: 10.3389/fcvm.2018.00092
3. Mack MJ, Leon MB, Thourani VH, Makkar R, Kodali SK, Russo M, et al. Transcatheter aortic-valve replacement with a balloon-expandable valve in low-risk patients. *N Engl J Med.* (2019) 380:1695–705. doi: 10.1056/NEJMoa1814052
4. Osnabrugge RL, Mylotte D, Head SJ, Van Mieghem NM, Nkomo VT, LeReun CM, et al. Aortic stenosis in the elderly: disease prevalence and number of candidates for transcatheter aortic valve replacement: a meta-analysis and modeling study. *J Am Coll Cardiol.* (2013) 62:1002–12. doi: 10.1016/j.jacc.2013.05.015
5. Andersen HR, Knudsen LL, Hasenkam JM. Transluminal implantation of artificial heart valves. Description of a new expandable aortic valve and initial results with implantation by catheter technique in closed chest pigs. *Eur Heart J.* (1992) 13:704–8. doi: 10.1093/oxfordjournals.eurheartj.a060238
6. Danielsen R, Aspelund T, Harris TB, Gudnason V. The prevalence of aortic stenosis in the elderly in Iceland and predictions for the coming decades: the AGES-Reykjavik study. *Int J Cardiol.* (2014) 176:916–22. doi: 10.1016/j.ijcard.2014.08.053
7. Nkomo VT, Gardin JM, Skelton TN, Gottdiener JS, Scott CG, Enriquez-Sarano M. Burden of valvular heart diseases: a population-based study. *Lancet.* (2006) 368:1005–11. doi: 10.1016/S0140-6736(06)69208-8
8. Roth GA, Mensah GA CO J. Global burden of cardiovascular diseases and risk factors, 1990–2019: update from the GBD 2019 study. *J Am Coll Cardiol.* (2019) 76:2982–3021. doi: 10.1016/j.jacc.2020.11.010
9. Zilla P, Yacoub M, Zuhlke L, Beyersdorf F, Sliwa K, Khubulava G, et al. Global unmet needs in cardiac surgery. *Glob Heart.* (2018) 13:293–303. doi: 10.1016/j.gheart.2018.08.002
10. Zilla P, Bolman RM. 3rd, Boateng P, Sliwa K. A glimpse of hope: cardiac surgery in low- and middle-income countries (LMICs). *Cardiovasc Diagn Ther.* (2020) 10:336–49. doi: 10.21037/cdt.2019.11.03
11. Zhang HMX. Transcatheter treatment of aortic stenosis and regurgitation. In: *Advances in Complex Valvular Disease*. London: IntechOpen.
12. Pan W, Zhou D, Cheng L, Shu X, Ge J. Candidates for transcatheter aortic valve implantation may be fewer in China. *Int J Cardiol.* (2013) 168:e133–4. doi: 10.1016/j.ijcard.2013.08.028
13. Pan W, Zhou D, Cheng L, Ge J. Aortic regurgitation is more prevalent than aortic stenosis in Chinese elderly population: implications for transcatheter aortic valve replacement. *Int J Cardiol.* (2015) 201:547–8. doi: 10.1016/j.ijcard.2014.10.069
14. Mentias A, Saad M, Desai MY, Krishnaswamy A, Menon V, Horwitz PA, et al. Transcatheter versus surgical aortic valve replacement in patients with rheumatic aortic stenosis. *J Am Coll Cardiol.* (2021) 77:1703–13. doi: 10.1016/j.jacc.2021.02.032
15. Zilla P, Williams DF, Bezuidenhout D. TAVR for patients with rheumatic heart disease: opening the door for the many? *J Am Coll Cardiol.* (2021) 77:1714–6. doi: 10.1016/j.jacc.2021.02.044
16. Scherman J, van Breda B, Appa H, Heerden C, Ofoegbu C, Bezuidenhout D, et al. Transcatheter valve with a hollow balloon for aortic valve insufficiency. *Multimed Man Cardiothorac Surg.* (2018) 2018. doi: 10.1510/mmcts.2018.012
17. Scherman J, Ofoegbu C, Myburgh A, Swanevelder J, van Breda B, Appa H, et al. Preclinical evaluation of a transcatheter aortic valve replacement system for patients with rheumatic heart disease. *EuroIntervention.* (2019) 15:e975–82. doi: 10.4244/EIJ-D-18-01052
18. Yoon SH, Schmidt T, Bleiziffer S, Schofer N, Fiorina C, Munoz-Garcia AJ, et al. Transcatheter aortic valve replacement in pure native aortic valve regurgitation. *J Am Coll Cardiol.* (2017) 70:2752–63. doi: 10.1016/j.jacc.2017.10.006
19. Arias E, Bhan A, Lim Z, Mullen M, TAVI. for pure native aortic regurgitation: are we there yet? *Interv Cardiol Rev.* (2019) 14:26–30. doi: 10.15420/icr.2018.37.1
20. Scherman J, Manganyi R, Human P, Pennel T, Brooks A, Brink J, et al. Isolated mechanical aortic valve replacement in rheumatic patients in a low- to middle-income country. *J Thorac Cardiovasc Surg.* (2019) 157:886–93. doi: 10.1016/j.jtcvs.2018.06.083
21. Fefer P, Bogdan A, Grossman Y, Berkovitch A, Brodov Y, Kuperstein R, et al. Impact of rapid ventricular pacing on outcome after transcatheter aortic valve replacement. *J Am Heart Assoc.* (2018) 7:e009038. doi: 10.1161/JAHA.118.009038
22. Winter MP, Bartko P, Hofer F, Zbiral M, Burger A, Ghanim B, et al. Evolution of outcome and complications in TAVR: a meta-analysis of observational and randomized studies. *Sci Rep.* (2020) 10:15568. doi: 10.1038/s41598-020-72453-1
23. Goldsweig AM, Al-Ani A, Almomani A. Pacemaker requirements following self-expanding transcatheter aortic valve replacement. *Cardiology.* (2020) 145:35–7. doi: 10.1159/000503380
24. Park K, Appa H, Visagie C, Bezuidenhout D, Zilla P. *Prosthetic Heart Valve.* (2017). US Patent Office US20050222688.
25. Nelson GL, Park KS, Van Breda BSC, Bezuidenhout D, Zilla P, et al. Expandable Stent and Methods of Crimping and Expanding Such Stent (2016). US Patent Office Published PCT/ZA2017/050025 27.4.2016. Washington, DC: U.S. Patent and Trademark Office.
26. Human P, Ofoegbu C, Ilsley H, Bezuidenhout D, de Villiers J, Williams DF, et al. Decellularization and engineered crosslinking: a promising dual approach toward bioprosthetic heart valve longevity. *Eur J Cardiothorac Surg.* (2020) 58:1192–200. doi: 10.1093/ejcts/ezaa257
27. Schima H, Tsangaris S, Zilla P, Kadletz M, Wolner E. Mechanical simulation of shear stress on the walls of peripheral arteries. *J Biomech.* (1990) 23:845–51. doi: 10.1016/0021-9290(90)90031-W
28. Bezuidenhout D, Williams DF, Zilla P. Polymeric heart valves for surgical implantation, catheter-based technologies and heart assist devices. *Biomaterials.* (2015) 36:6–25. doi: 10.1016/j.biomaterials.2014.09.013
29. Delgado V, Ng AC, Schuijf JD, van der Kley F, Shanks M, Tops LF, et al. Automated assessment of the aortic root dimensions with multidetector row computed tomography. *Ann Thorac Surg.* (2011) 91:716–23. doi: 10.1016/j.athoracsur.2010.09.060
30. Tops LF, Wood DA, Delgado V, Schuijf JD, Mayo JR, Pasupati S, et al. Noninvasive evaluation of the aortic root with multislice computed tomography implications for transcatheter aortic valve replacement. *JACC Cardiovasc Imaging.* (2008) 1:321–30. doi: 10.1016/j.jcmg.2007.12.006
31. Scherman J, Zilla P. Poorly suited heart valve prostheses heighten the plight of patients with rheumatic heart disease. *Int J Cardiol.* (2020) 318:104–14. doi: 10.1016/j.ijcard.2020.05.073
32. Tamara M. *Edwards, Medtronic Heart Valve Systems Prove Worth in Low-Risk Patient Studies*. London: Reuters Health Care and Pharma March 16 (2019).
33. Fukuda H, Kiyohara K, Sato D, Kitamura T, Kodera S, A. Real-world comparison of 1-year survival and expenditures for transcatheter aortic valve

replacements: SAPIEN 3 versus corevalve versus evolut R. *Value Health.* (2021) 24:497–504. doi: 10.1016/j.jval.2020.10.022
34. Deharo P, Bisson A, Herbert J, Lacour T, Saint Etienne C, Grammatico-Guillon L, et al. Impact of sapien 3 balloon-expandable versus evolut R self-expandable transcatheter aortic valve implantation in patients with aortic stenosis: data from a nationwide analysis. *Circulation.* (2020) 141:260–8. doi: 10.1161/CIRCULATIONAHA.119.043971
35. Bisson A, Bodin A, Herbert J, Lacour T, Saint Etienne C, Pierre B, et al. Pacemaker implantation after balloon- or self-expandable transcatheter aortic valve replacement in patients with aortic stenosis. *J Am Heart Assoc.* (2020) 9:e015896. doi: 10.1161/JAHA.120.015896
36. Van Belle E, Vincent F, Labreuche J, Auffret V, Debry N, Lefevre T, et al. Balloon-expandable versus self-expanding transcatheter aortic valve replacement: a propensity-matched comparison from the FRANCE-TAVI registry. *Circulation.* (2020) 141:243–59. doi: 10.1161/CIRCULATIONAHA.119.043785
37. Lanz J, Kim WK, Walther T, Burgdorf C, Mollmann H, Linke A, et al. Safety and efficacy of a self-expanding versus a balloon-expandable bioprosthesis for transcatheter aortic valve replacement in patients with symptomatic severe aortic stenosis: a randomised non-inferiority trial. *Lancet.* (2019) 394:1619–28. doi: 10.1016/S0140-6736(19)32220-2
38. El-Sabawi B, Welle GA, Cha YM, Espinosa RE, Gulati R, Sandhu GS, et al. Temporal incidence and predictors of high-grade atrioventricular block after transcatheter aortic valve replacement. *J Am Heart Assoc.* (2021) 10:e020033. doi: 10.1161/JAHA.120.020033
39. Vlastra W, Chandrasekhar J, Munoz-Garcia AJ, Tchetche D, de Brito FS Jr., et al. Comparison of balloon-expandable vs self-expandable valves in patients undergoing transfemoral transcatheter aortic valve implantation: from the CENTER-collaboration. *Eur Heart J.* (2019) 40:456–65. doi: 10.1093/eurheartj/ehy805
40. Rogers T, Steinvil A, Buchanan K, Alraies MC, Koifman E, Gai J, et al. Contemporary transcatheter aortic valve replacement with third-generation balloon-expandable versus self-expanding devices. *J Interv Cardiol.* (2017) 30:356–61. doi: 10.1111/joic.12389
41. Popma JJ, Deeb GM, Yakubov SJ, Mumtaz M, Gada H, O'Hair D, et al. Transcatheter aortic-valve replacement with a self-expanding valve in low-risk patients. *N Engl J Med.* (2019) 380:1706–15. doi: 10.1056/NEJMoa1816885
42. Nazif TM, Chen S, George I, Dizon JM, Hahn RT, Crowley A, et al. New-onset left bundle branch block after transcatheter aortic valve replacement is associated with adverse long-term clinical outcomes in intermediate-risk patients: an analysis from the PARTNER II trial. *Eur Heart J.* (2019) 40:2218–27. doi: 10.1093/eurheartj/ehz227
43. Lee HA, Chou AH, Wu VC, Chen DY, Lee HF, Lee KT, et al. Balloon-expandable versus self-expanding transcatheter aortic valve replacement for bioprosthetic dysfunction: A systematic review and meta-analysis. *PLoS ONE.* (2020) 15:e0233894. doi: 10.1371/journal.pone.0233894
44. Almeida JG, Ferreira SM, Fonseca P, Dias T, Guerreiro C, Barbosa A, et al. Comparison of self-expanding and balloon-expandable transcatheter aortic valves morphology and association with paravalvular regurgitation: Evaluation using multidetector computed tomography. *Catheter Cardiovasc Interv.* (2018) 92:533–41. doi: 10.1002/ccd.27401
45. Hellhammer K, Piayda K, Afzal S, Veulemans V, Hennig I, Makosch M, et al. Micro-dislodgement during transcatheter aortic valve implantation with a contemporary self-expandable prosthesis. *PLoS ONE.* (2019) 14:e0224815. doi: 10.1371/journal.pone.0224815
46. Hamdan A, Guetta V, Klempfner R, Konen E, Raanani E, Glikson M, et al. Inverse relationship between membranous septal length and the risk of atrioventricular block in patients undergoing transcatheter aortic valve implantation. *JACC Cardiovasc Interv.* (2015) 8:1218–28. doi: 10.1016/j.jcin.2015.05.010
47. Manoharan G, Linke A, Moellmann H, Redwood S, Frerker C, Kovac J, et al. Multicentre clinical study evaluating a novel resheathable annular functioning self-expanding transcatheter aortic valve system: safety and performance results at 30 days with the Portico system. *EuroIntervention.* (2016) 12:768–74. doi: 10.4244/EIJV12I6A125
48. Rocatello G, El Faquir N, De Santis G, Iannaccone F, Bosmans J, De Backer O, et al. Patient-specific computer simulation to elucidate the role of contact pressure in the development of new conduction abnormalities after catheter-based implantation of a self-expanding aortic valve. *Circ Cardiovasc Interv.* (2018) 11:e005344. doi: 10.1161/CIRCINTERVENTIONS.117.005344
49. Popma JJ, Reardon MJ, Khabbaz K, Harrison JK, Hughes GC, Kodali S, et al. Early clinical outcomes after transcatheter aortic valve replacement using a novel self-expanding bioprosthesis in patients with severe aortic stenosis who are suboptimal for surgery: results of the evolut R US study. *JACC Cardiovasc Interv.* (2017) 10:268–75. doi: 10.1016/j.jcin.2016.08.050
50. Kefer J, Maes F, Renkin J, Kautbally S, De Meester C, Delacour M, et al. Resheathing of self-expanding bioprosthesis: impact on procedural results, clinical outcome and prosthetic valve durability after transcatheter aortic valve implantation. *Int J Cardiol Heart Vasc.* (2020) 26:100462. doi: 10.1016/j.ijcha.2019.100462
51. Enumah ZO, Bolman RM, Zilla P, Boateng P, Wilson B, Kumar AS, et al. United in earnest: First pilot sites for increased surgical capacity for rheumatic heart disease announced by Cardiac Surgery Intersociety Alliance. *J Thorac Cardiovasc Surg.* (2021) 161:2108–13. doi: 10.1016/j.jtcvs.2020.11.183
52. Hu P, Liu XB, Liang J, Zhu QF, Pu CX, Tang MY, et al. A hospital-based survey of patients with severe valvular heart disease in China. *Int J Cardiol.* (2017) 231:244–7. doi: 10.1016/j.ijcard.2016.11.301
53. Jun-Bo G. Structural Heart Disease Professional Committee, Cardiovascular Branch, Chinese Physicians' Association. Chinese expert consensus on transcatheter aortic valve replacement (2020 Update). *Cardiol Plus.* (2020) 5:71–80. doi: 10.4103/cp.cp_11_20
54. Toggweiler S, Cerillo AG, Kim WK, Biaggi P, Lloyd C, Hilker M, et al. Transfemoral implantation of the acurate neo for the treatment of aortic regurgitation. *J Invasive Cardiol.* (2018) 30:329–33.
55. Graziani F, Menzarelli E, Burzotta F, Paraggio L, Aurigemma C, Romagnoli E, et al. Early heamodynamic and structural impact of transcatheter aortic valve replacement in pure aortic regurgitation. *Eur Heart J.* (2020) 41:ehaa946-1919. doi: 10.1093/ehjci/ehaa946.1919
56. Iung B, Baron G, Butchart EG, Delahaye F, Gohlke-Barwolf C, Levang OW, et al. A prospective survey of patients with valvular heart disease in Europe: the Euro Heart Survey on Valvular Heart Disease. *Eur Heart J.* (2003) 24:1231–43. doi: 10.1016/S0195-668X(03)00201-X
57. Tarantini G, Fabris T. Pure aortic valve regurgitation: SAVR is the gold standard, but TAVR is another gun. *Catheter Cardiovasc Interv.* (2020) 95:817–8. doi: 10.1002/ccd.28787
58. Vincent F, Ternacle J, Denimal T, Shen M, Redfors B, Delhaye C, et al. Transcatheter aortic valve replacement in bicuspid aortic valve stenosis. *Circulation.* (2021) 143:1043–61. doi: 10.1161/CIRCULATIONAHA.120.048048
59. Egbe AC, Luis SA, Padang R, Warnes CA. Outcomes in moderate mixed aortic valve disease: is it time for a paradigm shift? *J Am Coll Cardiol.* (2016) 67:2321–9. doi: 10.1016/j.jacc.2016.03.509
60. de Aquino Xavier RM, Azevedo VMP, Godoy PH, Migowski A, Ribeiro ALP, Chaves RBM, et al. Medium-term outcomes of 78,808 patients after heart valve surgery in a middle-income country: a nationwide population-based study. *BMC Cardiovasc Disord.* (2017) 17:302. doi: 10.1186/s12872-017-0725-9
61. Sliwa K, Carrington M, Mayosi BM, Zigiriadis E, Mvungi R, Stewart S. Incidence and characteristics of newly diagnosed rheumatic heart disease in urban African adults: insights from the heart of Soweto study. *Eur Heart J.* (2010) 31:719–27. doi: 10.1093/eurheartj/ehp530
62. Delesalle G, Bohbot Y, Rusinaru D, Delpierre Q, Marechaux S, Tribouilloy C. Characteristics and prognosis of patients with moderate aortic stenosis and preserved left ventricular ejection fraction. *J Am Heart Assoc.* (2019) 8:e011036. doi: 10.1161/JAHA.118.011036
63. Human P, Zilla P. Characterization of the immune response to valve bioprostheses and its role in primary tissue failure. *Ann Thorac Surg.* (2001) 71:S385–8. doi: 10.1016/S0003-4975(01)02492-4
64. Jenney C, Millson P, Grainger DW, Grubbs R, Gunatillake P, McCarthy SJ, et al. Assessment of a Siloxan(urethane-urea) Elastomer designed for impantable Heart Valve Leaflets. *Adv NanoBiomed Res.* (2020). doi: 10.1002/anbr.202000032

65. Clinical Trials USFG. *Early Feasibility Study for the Foldax TRIA Mitral Heart Valve Replacement (FOLDAX).* Bethesda, MD: NIH, US National Library of Medicine (2021).
66. Gunatillake PA. D'andeniyage LS, Adhikari R, Brown M, Shanks R, Adhikari BA, et al. Advances in the development of biostable polyurethanes. *Polym Rev.* (2019) 59:391–417. doi: 10.1080/15583724.2018.1493694
67. Savvoulidis P, Perlman G, Bagur R. The EluNIR(TM) ridaforolimus eluting coronary stent system. *Expert Rev Med Devices.* (2019) 16:71–6. doi: 10.1080/17434440.2018.1549986
68. Dempsey DK, Carranza C, Chawla CP, Gray P, Eoh JH, Cereceres S, et al. Comparative analysis of *in vitro* oxidative degradation of poly(carbonate urethanes) for biostability screening. *J Biomed Mater Res A.* (2014) 102:3649–65. doi: 10.1002/jbm.a.35037
69. Kutuzova L. In vitro bio-stability screening of novel implantable polyurethane elastomers. *Curr Dir Biomed Eng.* (2018) 4:535–8. doi: 10.1515/cdbme-2018-0128
70. Christenson EM, Dadsetan M, Hiltner A. Biostability and macrophage-mediated foreign body reaction of silicone-modified polyurethanes. *J Biomed Mater Res A.* (2005) 74:141–55. doi: 10.1002/jbm.a.30317
71. Wiggins MJ, Wilkoff B, Anderson JM, Hiltner A. Biodegradation of polyether polyurethane inner insulation in bipolar pacemaker leads. *J Biomed Mater Res.* (2001) 58:302–7. doi: 10.1002/1097-4636(2001)58:3<302::AID-JBM1021>3.0.CO;2-Y
72. Ward R, Anderson J, McVenes R, Stokes K. In vivo biostability of polysiloxane polyether polyurethanes: resistance to biologic oxidation and stress cracking. *J Biomed Mater Res A.* (2006) 77:580–9. doi: 10.1002/jbm.a.30555
73. Ward R, Anderson J, McVenes R, Stokes K. In vivo biostability of shore 55D polyether polyurethanes with and without fluoropolymer surface modifying endgroups. *J Biomed Mater Res A.* (2006) 79:836–45. doi: 10.1002/jbm.a.30800
74. Wo Y, Brisbois EJ, Wu J, Li Z, Major TC, Mohammed A, et al. Reduction of thrombosis and bacterial infection via controlled nitric oxide (NO) release from S-nitroso-N-acetylpenicillamine (SNAP) impregnated carbosil intravascular catheters. *ACS Biomater Sci Eng.* (2017) 3:349–59. doi: 10.1021/acsbiomaterials.6b00622
75. Handa H, Major TC, Brisbois EJ, Amoako KA, Meyerhoff ME, Bartlett RH. Hemocompatibility comparison of biomedical grade polymers using rabbit thrombogenicity model for preparing nonthrombogenic nitric oxide releasing surfaces. *J Mater Chem B.* (2014) 2:1059–67. doi: 10.1039/C3TB21771J
76. Wo Y, Li Z, Brisbois EJ, Colletta A, Wu J, Major TC, et al. Origin of long-term storage stability and nitric oxide release behavior of carbosil polymer doped with S-nitroso-N-acetyl-D-penicillamine. *ACS Appl Mater Interfaces.* (2015) 7:22218–27. doi: 10.1021/acsami.5b07501
77. Wo Y, Brisbois EJ, Bartlett RH, Meyerhoff ME. Recent advances in thromboresistant and antimicrobial polymers for biomedical applications: just say yes to nitric oxide (NO). *Biomater Sci.* (2016) 4:1161–83. doi: 10.1039/C6BM00271D
78. Clarke ML, Wang J, Chen Z. Conformational changes of fibrinogen after adsorption. *J Phys Chem B.* (2005) 109:22027–35. doi: 10.1021/jp054456k
79. Daebritz SH, Fausten B, Hermanns B, Schroeder J, Groetzner J, Autschbach R, et al. Introduction of a flexible polymeric heart valve prosthesis with special design for aortic position. *Eur J Cardiothorac Surg.* (2004) 25:946–52. doi: 10.1016/j.ejcts.2004.02.040
80. Ruile P, Jander N, Blanke P, Schoechlin S, Reinohl J, Gick M, et al. Course of early subclinical leaflet thrombosis after transcatheter aortic valve implantation with or without oral anticoagulation. *Clin Res Cardiol.* (2017) 106:85–95. doi: 10.1007/s00392-016-1052-3
81. Makkar RR, Fontana G, Jilaihawi H, Chakravarty T, Kofoed KF, De Backer O, et al. Possible subclinical leaflet thrombosis in bioprosthetic aortic valves. *N Engl J Med.* (2015) 373:2015–24. doi: 10.1056/NEJMoa1509233
82. Ng ACT, Holmes DR, Mack MJ, Delgado V, Makkar R, Blanke P, et al. Leaflet immobility and thrombosis in transcatheter aortic valve replacement. *Eur Heart J.* (2020) 41:3184–97. doi: 10.1093/eurheartj/ehaa542
83. Brown RA, Reid AB, Turaga M, Huang AL, Maggiore PL, Sellers SL, et al. Subclinical leaflet thrombosis post transcatheter aortic valve replacement—an update for 2020. *Struct Heart.* (2020) 4:369–81. doi: 10.1080/24748706.2020.1805534
84. Vahidkhah K, Azadani AN. Supra-annular valve-in-valve implantation reduces blood stasis on the transcatheter aortic valve leaflets. *J Biomech.* (2017) 58:114–22. doi: 10.1016/j.jbiomech.2017.04.020
85. Kvitting JP, Ebbers T, Wigstrom L, Engvall J, Olin CL, Bolger AF. Flow patterns in the aortic root and the aorta studied with time-resolved, 3-dimensional, phase-contrast magnetic resonance imaging: implications for aortic valve-sparing surgery. *J Thorac Cardiovasc Surg.* (2004) 127:1602–7. doi: 10.1016/j.jtcvs.2003.10.042
86. Oechtering TH, Hons CF, Sieren M, Hunold P, Hennemuth A, Huellebrand M, et al. Time-resolved 3-dimensional magnetic resonance phase contrast imaging. (4D Flow MRI) analysis of hemodynamics in valve-sparing aortic root repair with an anatomically shaped sinus prosthesis. *J Thorac Cardiovasc Surg.* (2016) 152:418–427 e1. doi: 10.1016/j.jtcvs.2016.04.029
87. Midha PA, Raghav V, Sharma R, Condado JF, Okafor IU, Rami T, et al. The fluid mechanics of transcatheter heart valve leaflet thrombosis in the neosinus. *Circulation.* (2017) 136:1598–609. doi: 10.1161/CIRCULATIONAHA.117.029479
88. Zilla P, Bezuidenhout D, Human P. Prosthetic vascular grafts: wrong models, wrong questions and no healing. *Biomaterials.* (2007) 28:5009–27. doi: 10.1016/j.biomaterials.2007.07.017
89. Gallo M, Bonetti A, Poser H, Naso F, Bottio T, Bianco R, et al. Decellularized aortic conduits: could their cryopreservation affect post-implantation outcomes? A morpho-functional study on porcine homografts. *Heart Vessels.* (2016) 31:1862–73. doi: 10.1007/s00380-016-0839-5
90. Berger K, Sauvage LR, Wood SJ, Wesolowski SA. Sewing ring healing of cardiac valve prostheses. *Surgery.* (1967) 61:102–17.
91. Hamadanchi A, Bäz L, Möbius-Winkler S, Teichgräber U, Schulze PC, Franz M. Basal leaflet thickening and color paucity in the echocardiographic evaluation of subclinical leaflet thrombosis after transcatheter aortic valve replacement. *Int J Cardiovasc Imaging.* (2019) 35:119–20. doi: 10.1007/s10554-018-1439-5
92. Zilla P, Deutsch M, Bezuidenhout D, Davies NH, Pennel T. Progressive reinvention or destination lost? Half a century of cardiovascular tissue engineering. *Front Cardiovasc Med.* (2020) 7:159. doi: 10.3389/fcvm.2020.00159
93. Khera S. Dangas G. TAVR for aortic regurgitation: not as straightforward! *Catheter Cardiovasc Interv.* (2021) 97:486–7. doi: 10.1002/ccd.29520
94. Zaid S, Sengupta A, Okoli K, Tsoi M, Khan A, Ahmad H, et al. Novel anatomic predictors of new persistent left bundle branch block after evolut transcatheter aortic valve implantation. *Am J Cardiol.* (2020) 125:1222–9. doi: 10.1016/j.amjcard.2020.01.008
95. De Backer O, Pilgrim T, Simonato M, Mackensen GB, Fiorina C, Veulemanns V, et al. Usefulness of transcatheter aortic valve implantation for treatment of pure native aortic valve regurgitation. *Am J Cardiol.* (2018) 122:1028–35. doi: 10.1016/j.amjcard.2018.05.044
96. Urena M, Himbert D, Ohlmann P, Capretti G, Goublaire C, Kindo M, et al. Transcatheter aortic valve replacement to treat pure aortic regurgitation on noncalcified native valves. *J Am Coll Cardiol.* (2016) 68:1705–6. doi: 10.1016/j.jacc.2016.07.746
97. Okuno T, Lanz J, Pilgrim T, ACURATE. neo: How is this TAVR valve doing to fit into an increasingly crowded field? *Curr Cardiol Rep.* (2020) 22:107. doi: 10.1007/s11886-020-01364-4
98. Du F, Zhu Q, Jiang J, Chen H, Liu X, Wang J. Incidence and predictors of permanent pacemaker implantation in patients who underwent transcatheter aortic valve replacement: observation of a Chinese population. *Cardiology.* (2020) 145:27–34. doi: 10.1159/000502792
99. Miura M, Isotani A, Murata K, Kawaguchi T, Hayashi M, Arai Y, et al. Perforation of anterior mitral leaflet due to mechanical stimulation late after transcatheter aortic valve replacement. *JACC Cardiovasc Interv.* (2016) 9:e233–4. doi: 10.1016/j.jcin.2016.10.009
100. Bianchi M, Marom G, Ghosh RP, Fernandez HA, Taylor JR Jr., et al. Effect of balloon-expandable transcatheter aortic valve replacement positioning: a patient-specific numerical model. *Artif Organs.* (2016) 40:E292–304. doi: 10.1111/aor.12806

101. Caballero A, Mao W, McKay R, Sun W. The impact of balloon-expandable transcatheter aortic valve replacement on concomitant mitral regurgitation: a comprehensive computational analysis. *J R Soc Interface.* (2019) 16:20190355. doi: 10.1098/rsif.2019.0355
102. Marchel M, Szczerba E, Pedzich-Placha E, Huczek Z, Kochman J, Kochanowski J, et al. Left ventricular outflow obstruction after TAVR due to systolic anterior motion successfully treated with cardiac pacing. *J Cardiothorac Vasc Anesth.* (2020) 34:2718–21. doi: 10.1053/j.jvca.2020.04.042
103. Yudi MB, Sharma SK, Tang GHL, Kini A. Coronary angiography and percutaneous coronary intervention after transcatheter aortic valve replacement. *J Am Coll Cardiol.* (2018) 71:1360–78. doi: 10.1016/j.jacc.2018.01.057
104. Jubran A, Flugelman MY, Zafrir B, Shiran A, Khader N, Rubinshtein R, et al. Intraprocedural valve-in-valve deployment for treatment of aortic regurgitation following transcatheter aortic valve replacement: an individualized approach. *Int J Cardiol.* (2019) 283:73–7. doi: 10.1016/j.ijcard.2018.12.079
105. Tang GHL, Zaid S, Ahmad H, Undemir C, Lansman SL. Transcatheter valve neo-commissural overlap with coronary orifices after transcatheter aortic valve replacement. *Circ Cardiovasc Interv.* (2018) 11:e007263. doi: 10.1161/CIRCINTERVENTIONS.118.007263
106. Ribeiro HB, Nombela-Franco L, Urena M, Mok M, Pasian S, Doyle D, et al. Coronary obstruction following transcatheter aortic valve implantation: a systematic review. *JACC Cardiovasc Interv.* (2013) 6:452–61. doi: 10.1016/j.jcin.2012.11.014
107. Piayda K, Hellhammer K, Veulemans V, Sievert H, Gafoor S, Afzal S, et al. Navigating the "optimal implantation depth" with a self-expandable TAVR device in daily clinical practice. *JACC Cardiovasc Interv.* (2020) 13:679–88. doi: 10.1016/j.jcin.2019.07.048
108. Moriyama N, Lehtola H, Miyashita H, Piuhola J, Niemela M, Laine M. Hemodynamic comparison of transcatheter aortic valve replacement with the SAPIEN 3 Ultra versus SAPIEN 3: the HomoSAPIEN registry. *Catheter Cardiovasc Interv.* (2021) 97:E982–91. doi: 10.1002/ccd.29281
109. Sammour Y, Banerjee K, Kumar A, Lak H, Chawla S, Incognito C, et al. Systematic approach to high implantation of SAPIEN-3 valve achieves a lower rate of conduction abnormalities including pacemaker implantation. *Circ Cardiovasc Interv.* (2021) 14:e009407. doi: 10.1161/CIRCINTERVENTIONS.120.009407
110. Buellesfeld L, Stortecky S, Kalesan B, Gloekler S, Khattab AA, Nietlispach F, et al. Aortic root dimensions among patients with severe aortic stenosis undergoing transcatheter aortic valve replacement. *JACC Cardiovasc Interv.* (2013) 6:72–83. doi: 10.1016/j.jcin.2012.09.007
111. Antunes M. Closed mitral commissurotomy—a cheap, reproducible and successful way to treat mitral stenosis. *J Thorac Cardiovasc Surg.* (2019) 11:3659–71.
112. Abbott JD, Bavishi C. In search of an ideal vascular closure device for transcatheter aortic valve replacement. *JACC Cardiovasc Interv.* (2021) 14:158–60. doi: 10.1016/j.jcin.2020.10.046
113. Murdock JE, Jensen HA, Thourani VH. Nontransfemoral approaches to transcatheter aortic valve replacement. *Interv Cardiol Clin.* (2015) 4:95–105. doi: 10.1016/j.iccl.2014.09.006
114. Thourani VH, Li C, Devireddy C, Jensen HA, Kilgo P, Leshnower BG, et al. High-risk patients with inoperative aortic stenosis: use of transapical, transaortic, and transcarotid techniques. *Ann Thorac Surg.* (2015) 99:817–23; discussion 823–5. doi: 10.1016/j.athoracsur.2014.10.012
115. Seppelt PC, Mas-Peiro S, De Rosa R, Murray IM, Arsalan M, Holzer L, et al. Dynamics of cerebral oxygenation during rapid ventricular pacing and its impact on outcome in transfemoral transcatheter aortic valve implantation. *Catheter Cardiovasc Interv.* (2021) 97:E146–53. doi: 10.1002/ccd.28975
116. Chaliki HP, Mohty D, Avierinos JF, Scott CG, Schaff HV, Tajik AJ, et al. Outcomes after aortic valve replacement in patients with severe aortic regurgitation and markedly reduced left ventricular function. *Circulation.* (2002) 106:2687–93. doi: 10.1161/01.CIR.0000038498.59829.38
117. Toggweiler S, Loretz L, Brinkert M, Bossard M, Wolfrum M, Moccetti F, et al. Simplifying transfemoral ACURATE neo implantation using the TrueFlow nonocclusive balloon catheter. *Catheter Cardiovasc Interv.* (2020) 96:E640–5. doi: 10.1002/ccd.28741
118. Purita PAM, Tahoces LS, Fraccaro C, Nai Fovino L, Kim WK, Espada-Guerreiro C, et al. Transcatheter treatment of native aortic valve regurgitation: results from an international registry using the transfemoral ACURATE neo valve. *Int J Cardiol Heart Vasc.* (2020) 27:100480. doi: 10.1016/j.ijcha.2020.100480
119. Scherman J, Bezuidenhout D, Ofoegbu C, Williams DF, Zilla P. TAVI for low to middle income countries. *Eur Heart J.* (2017) 38:1182–4. doi: 10.1093/eurheartj/ehx169
120. Figulla H, Ferrari M, Carr-Brendel V, Lauten A. The jenavalve program for transcatheter aortic valve implantation. In: Giordano A, Biondi-Zoccai G, Frati G (editors). *Transcatheter Aortic Valve Implantation.* Cham: Springer (2019).
121. Medicine NUSNLo. *The Align-AR Pivotal Trial: JenaValve Pericardial TAVR Aortic Regurgitation Study (ALIGN-AR).* Clinical Trialsgov. (2020) Identifyer: NCT04415047.
122. Rheude T, Blumenstein J, Mollmann H, Husser O. Spotlight on the SAPIEN 3 transcatheter heart valve. *Med Devices.* (2018) 11:353–60. doi: 10.2147/MDER.S143897
123. Binder RK, Rodes-Cabau J, Wood DA, Mok M, Leipsic J, De Larochelliere R, et al. Transcatheter aortic valve replacement with the SAPIEN 3: a new balloon-expandable transcatheter heart valve. *JACC Cardiovasc Interv.* (2013) 6:293–300. doi: 10.1016/j.jcin.2012.09.019
124. Koehler T, Buege M, Schleiting H, Seyfarth M, Tiroch K, Vorpahl M. Changes of the eSheath outer dimensions used for transfemoral transcatheter aortic valve replacement. *Biomed Res Int.* (2015) 2015:572681. doi: 10.1155/2015/572681
125. Taramasso M, Denegri A, Kuwata S, Rickli H, Haager PK, Sutsch G, et al. Feasibility and safety of transfemoral sheathless portico aortic valve implantation: preliminary results in a single center experience. *Catheter Cardiovasc Interv.* (2018) 91:533–9. doi: 10.1002/ccd.27100
126. Toutouzas K, Benetos G, Voudris V, Drakopoulou M, Stathogiannis K, Latsios G, et al. Pre-dilatation versus no pre-dilatation for implantation of a self-expanding valve in all comers undergoing TAVR: the DIRECT trial. *JACC Cardiovasc Interv.* (2019) 12:767–77. doi: 10.1016/j.jcin.2019.02.005
127. Saia F, Gandolfo C, Palmerini T, Berti S, Doshi SN, Laine M, et al. In-hospital and thirty-day outcomes of the SAPIEN 3 ultra balloon-expandable transcatheter aortic valve: the S3U registry. *EuroIntervention.* (2020) 15:1240–7. doi: 10.4244/EIJ-D-19-00541

Conflict of Interest: "Strait Access Technologies" (SAT) is a start-up company of the University of Cape Town. HA, DB, JSc, HC, DW, and PZ own shares in SAT. JV, RC, and RS are employed by SAT. KP, BB, and MC are former employees and shareholders of SAT. BJ is a former employee of SAT. CS is employed by Auto Tissue Berlin.

The remaining authors declare that the research was conducted in the absence of any commercial or financial relationships that could be construed as a potential conflict of interest.

Publisher's Note: All claims expressed in this article are solely those of the authors and do not necessarily represent those of their affiliated organizations, or those of the publisher, the editors and the reviewers. Any product that may be evaluated in this article, or claim that may be made by its manufacturer, is not guaranteed or endorsed by the publisher.

frontiers in Cardiovascular Medicine

ORIGINAL RESEARCH
published: 22 March 2022
doi: 10.3389/fcvm.2022.774189

Introduction of the Rapid Deployment Aortic Valve System Use in Elderly Patients With Endocarditis

*Alper Öner[1], Christoph Hemmer[2], Anthony Alozie[3], Benjamin Löser[4] and Pascal M. Dohmen[3,5]**

[1] Department of Cardiology, Heart Center Rostock, University of Rostock, Rostock, Germany, [2] Department of Tropical Medicine and Infectious Diseases, University of Rostock, Rostock, Germany, [3] Department of Cardiac Surgery, Heart Center Rostock, University of Rostock, Rostock, Germany, [4] Department of Anesthesiology and Intensive Care Medicine, University of Rostock, Rostock, Germany, [5] Department of Cardiothoracic Surgery, Faculty of Health Science, University of the Free State, Bloemfontein, South Africa

Introduction: The rapid-deployment valve system (RDVS) was introduced to facility minimally invasive aortic valve replacement. In this study we evaluate the potential benefits of RDVS in elderly high-risk patients with endocarditis of the aortic valve.

Materials and Methods: Since the introduction of RDVS in our institution in December 2017 through October 2021, EDWARDS INTUITY rapid-deployment prosthesis (Model 8300A, Edwards Lifesciences, Irvine, CA, USA) has been implanted in a total of 115 patients for different indications by a single surgeon. Out of one-hundred and fifteen cases of RDVS implantation, seven patients with a median age of 77 yrs. (range 62–84yrs.), suffered from active infective endocarditis of the aortic valve. The median EuroSCORE II of these highly selected patient cohort was 77% (range 19–80%). Patient data were evaluated perioperatively including intra-operative data as well as in-hospital morbidity/mortality and follow-up after discharge from hospital.

Results: Three patients underwent previous cardiac surgery. Concomitant procedures were performed in six patients including, ascending aorta replacement ($n = 3$), mitral valve repair ($n = 1$), pulmonary valve replacement ($n = 1$), bypass surgery ($n = 1$), left atrial appendix resection ($n = 1$) and anterior mitral valve repair ($n = 1$). Median aortic cross-clamp and cardiopulmonary bypass time was 56 min (range 29–122 min) and 81 min (range 45–162 min.), respectively. Post-operative complications in these elderly high-risk patients were atrial fibrillation ($n = 3$) and re-exploration for pericardial effusion ($n = 1$). One pacemaker implantation was required on postoperative day 6 due to sick sinus syndrome. There was one in-hospital death (14%) and one during follow-up (14%).

Conclusion: Rapid-deployment aortic valve system seems to be a viable option with acceptable morbidity and mortality in elderly high-risk patients with active infective endocarditis of the aortic valve.

Keywords: active infective endocarditis, rapid-deployment valve system, heart valve surgery, aortic valve, aortic valve endocarditis

OPEN ACCESS

Edited by:
Peter Zilla,
University of Cape Town, South Africa

Reviewed by:
Faizus Sazzad,
National University of Singapore, Singapore
Ameli Yates,
Medical University of Graz, Austria

****Correspondence:***
Pascal M. Dohmen
pascal.dohmen@med.uni-rostock.de

Specialty section:
This article was submitted to Heart Valve Disease, a section of the journal Frontiers in Cardiovascular Medicine

Received: *11 September 2021*
Accepted: *14 February 2022*
Published: *22 March 2022*

Citation:
Öner A, Hemmer C, Alozie A, Löser B and Dohmen PM (2022) Introduction of the Rapid Deployment Aortic Valve System Use in Elderly Patients With Endocarditis. Front. Cardiovasc. Med. 9:774189. doi: 10.3389/fcvm.2022.774189

INTRODUCTION

Active infective aortic valve endocarditis (AI-AVE) is still associated with high morbidity and mortality, especially in the elderly and multimorbid patients (1–5).

Early surgery in addition to immediate appropriate antimicrobial therapy was proposed in these elderly AI-AVE patients to reduce mortality and embolic events (6, 7). In the study by Lalani et al. (8) early surgery was associated with lower in-hospital and 1-year mortality in the unadjusted analysis and after controlling for treatment selection bias. However, these results could not be replicated after adjustment for survivor bias. The subgroup analysis indicated a lower in-hospital mortality with early surgery in the highest (fifth) surgical propensity quintile. At one year follow-up the lower mortality associated with early surgery was retained both in the fourth and fifth quintiles of surgery propensity group (8). All these indicate an urgent need for further investigations into the effects and timing of surgery in infective endocarditis in patient with indication for surgery.

Another important tool that has been associated with reduction of mortality in patients with AI-AVE is strict implementation of multidisciplinary approach as reported by Botelho-Nevers et al. (9). Due to the highly significant reduction in mortality, this important tool has recently been incorporated into the published European Society of Cardiology guidelines (10).

Regardless of these impressive results, the implementation of surgery recommendations has been suffered a significant setback due to non-referral of patients for surgery. In this context Iung et al. (11) reported that although these guidelines were available and surgery was recommended in 75% of the patients with active infective endocarditis, only half of the patients were operated upon. Prohibitive operative risk due to general status of the patients was cited as reason for non-referral for surgery in 62% of the cases.

New operative techniques are required for the increasing number of elderly patients in need of surgery, including those patients suffering from transcatheter aortic valve endocarditis (12, 13). Sutureless or rapid-deployment aortic bioprostheses were introduced to increase implementation of minimally invasive surgery for aortic valve replacement (MIS-AVR) making it simpler and faster, thereby reducing surgery time and need for blood transfusion, which ultimately facilitates faster recovery and improved survival (14–16). In this context, indications for survival advantage with the use of sutureless bioprostheses in high-risk patients over transcatheter aortic valve intervention has been previously demonstrated by some studies (17–19). Currently, use of sutureless aortic valves are not only limited to MIS-AVR but also in combined cardiac procedures due to shorter implantation time (20–22). This study aimed to evaluate the implementation of rapid-deployment bioprostheses in elderly high-risk patients with AI-AVE.

MATERIALS AND METHODS

Between December 2017 and October 2021, 115 patients were treated with EDWARDS INTUITY rapid-deployment prosthesis (Model 8300A, Edwards Lifesciences, Irvine, CA, USA) for different indications by a single surgeon. According to the modified Duke criteria, seven patients were identified with AI-AVE (23). Data were prospectively collected and approved by the local ethical committee. In-hospital mortality was defined as death occurring within 30-days of surgery.

TABLE 1 | Pre-operative clinical characteristics.

Factors		
Age (y)	77	(62–84)
Male gender	6	(86)
NYHA class III-IV	7	(100)
Critical preoperative status	3	(29)
Hyperlipidaemia	4	(57)
Arterial hypertension	7	(100)
Pulmonary hypertension	3	(43)
COPD	4	(57)
Previous cardiac surgery	3	(43)
Recent acute myocardial infarction	2	(29)
Peripheral artery disease	4	(57)
Chronic renal failure	5	(71)
IDDM	1	(14)
LV ejection fraction (%)	50	(30-55)
EuroSCORE II (%)	77	(32-80)

Continuous data are presented as median (range) and categorical data as n (%). BMI, body mass index; COPD, chronic obstructive pulmonary disease; IDDM, insulin depending diabetes mellitus; LV, left ventricular; EuroSCORE, European system for cardiac operative risk evaluation.

Patient's Characteristics

The median age of the studied patients was 77 years (range 62–84 years). Six patients were males, one patient female. Essential pre-operative characteristics are summarized in **Table 1**. The predicted mortality was calculated using the EuroSCORE II (median 77%; range 32–80 %). Three patients had moderate pulmonary hypertension (30–55 mm Hg). The pathogen was known in all patients except one, namely *Staphylococcus epidermidis* ($n = 2$), *Aggregatibacter aphrophilus* ($n = 1$), *Rothia dentocariosa* ($n = 1$), *Enterococcus faecalis* ($n = 1$) and *Streptococcus salivarius* ($n = 1$), which were identified by blood cultures. Adequate antimicrobial therapy was initiated in all patients preoperatively followed by regular controls of the infective parameters alongside serial echocardiography evaluations (**Figure 1**). Despite these measures, all seven patients experienced clinical deterioration and fulfill the modified Duke criteria, warranting consultation of our endocarditis team. Following the team's recommendation of expedited surgery, informed consent was obtained from patient and relatives. Preoperative whole body computed tomography was performed in all patients to identify the entry site for endocarditis as well as previous embolization (**Figure 2**). Surgical debridement was then scheduled and carried out successfully in all seven patients.

Surgery Details

A RDVS was implanted successfully in all seven patients. The implantation technique has been extensively described in the past

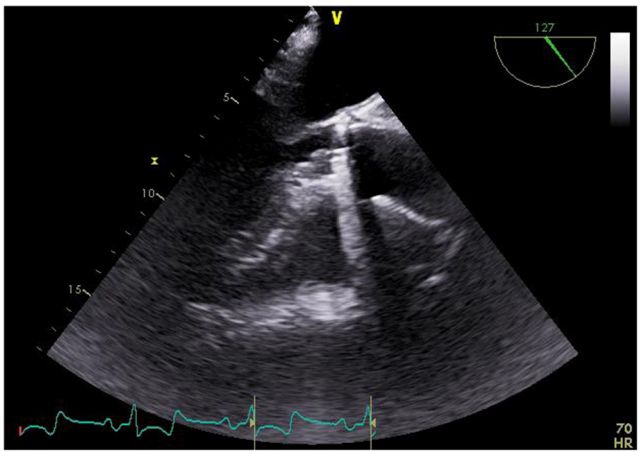

FIGURE 1 | Echocardiographic finding of the vegetation at the annulus of the implanted valve prosthesis.

(24). The average implanted valve size was 25 mm (range 23–27 mm). Additional procedures were performed in six patients including, ascending aortic replacement ($n = 3$) (**Figure 3**), mitral valve repair ($n = 1$), pulmonary valve replacement ($n = 1$), bypass surgery ($n = 1$), left atrial appendix resection ($n = 1$) and anterior mitral leaflet repair (**Table 2**). Median aortic cross-clamping time was 56 min (range 29–122 min) and median cardiopulmonary bypass time was 81 min (range 45–162 min).

Three patients underwent re-aortic valve replacement due to infective endocarditis of the aortic bioprosthesis (**Figure 4**). In one patient, previous surgery was due to type-A aortic dissection, treated with a Bentall-procedure and partial arch replacement. Only this patient was cannulated peripheral using the left femoral vein and right subclavian artery. One patient suffered from pulmonary and aortic valve endocarditis after a Ross procedure. The third patient was re-operated on the aortic bioprosthesis after previous triple coronary bypass surgery with aortic valve replacement. At the time of surgery, all bypasses were patent. An additional aneurysm of the ascending aorta was also treated. On the native and prosthetic valves, large vegetations were noticed in all explants as identified by transesophageal echocardiography. The annulus were in all patients intact and endocarditis was limited to the native aortic leaflets or the valve prosthesis. There were no abscess seen in any of these treated patients.

Intra-operative transesophageal echocardiography showed absence of para- and transvalvular leak in all patients on the end of surgery.

RESULTS

There was one in-hospital death and one patient died during follow-up. This patient had an initially uneventful postoperative follow-up, without recurrence of endocarditis. He died during follow-up due to respiratory failure. The other patient died of multi-organ failure as sepsis could

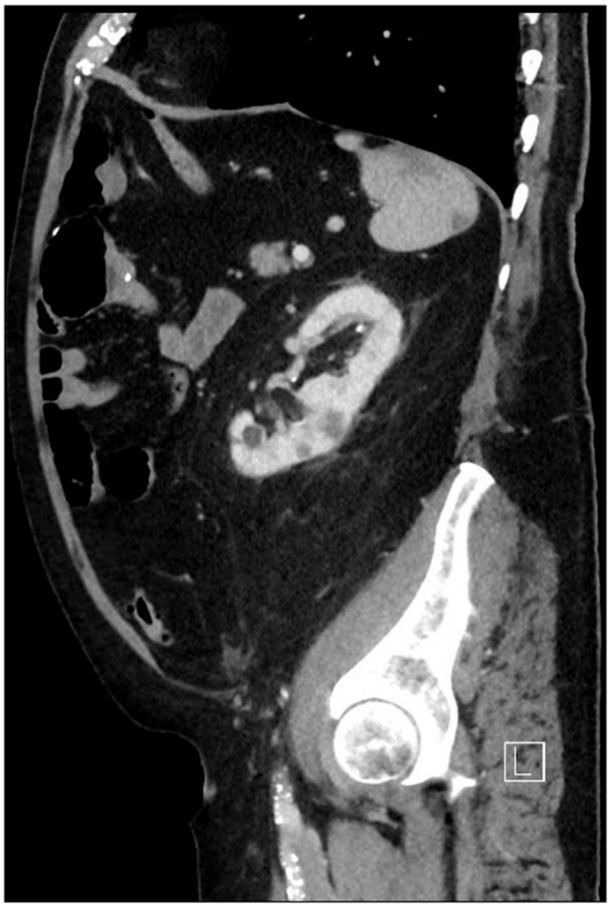

FIGURE 2 | Computed tomography of the chest and abdomen showing septic embolism of the spleen and kidneys.

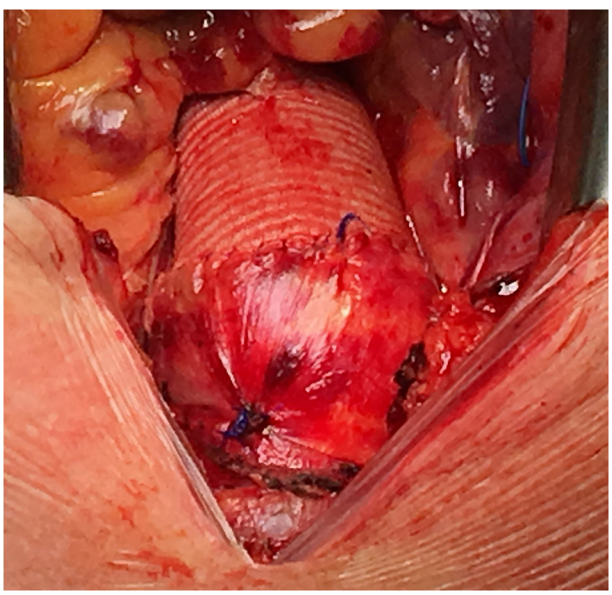

FIGURE 3 | Post-operative finding after aortic valve implantation and ascending aorta replacement.

TABLE 2 | Surgical details.

Patient no.	Concomitant procedure	Previous cardiac surgery	CC time (min)	CPB time (min)	Op time (min)	Complications
1	None	No	29	45	135	Pacemaker implantation
2	AAR and anterior mitral valve leaflet repair	No	52	69	173	Pericardial effusion
3	Mitral valve repair	No	66	81	194	Atrial fibrillation, respiratory failure, died
4	Re-pulmonary valve replacement	Ross operation	122	162	341	Atrial fibrillation
5	Re-AAR	Bentall-operation for TAAD	56	138	227	Acute renal failure
6	Single bypass surgery, LAA	Single bypass surgery, LAA	39	70	158	Multi-organ failure, died
7	AAR	AVR and ACB	57	84	239	no

AAR, ascending aorta replacement; ACB, aortocoronary bypass; AVR, aortic valve replacement; CA, circulatory arrest; CC, cross clamping; CPB, cardiopulmonary bypass; LAA, left atrial appendix; LV, left ventricle; min, minutes; no, number; Op, operation; TAAD, Type-A aortic dissection.

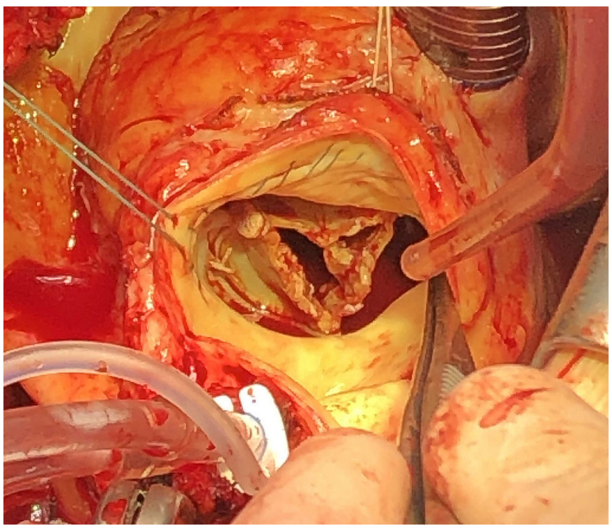

FIGURE 4 | Intraoperative finding of the vegetations at a bioprosthesis.

not be controlled under appropriate antibiotic therapy. One patient was re-explored for pericardial effusion. Another patient required permanent pacemaker due to sick sinus syndrome on day 6 post-surgery. One patient developed acute renal failure which was managed conservatively until recovery of renal function prior to discharge from the hospital. The median intensive-care unit stay was 1 day (range, 1–4 days). Echocardiographic evaluation at discharge demonstrated absence of central- or paravalvular leak with correct position of the rapid-deployment aortic bioprostheses. The average median pressure gradient was 8 mm Hg (rang 5–14 mm Hg). During hospitalization, interdisciplinary examination was undertaken to evaluate clinical and hemodynamics of each patient. All patients received a 6 week antibiogram-guided antimicrobial therapy in accordance with treatment of infective endocarditis guidelines. At median follow-up period of 29 months (range 1–47 months), there was no incidence of re-operation, reinfection, structural/non-structural prosthetic dysfunction, thrombosis, embolism or bleeding events.

DISCUSSION

Active infective endocarditis remains a uncommon serious disease with considerable morbidity and mortality. Given the proper indications, surgery together with adequate antibiotic therapy can cure the infective pathology of the cardiac tissue and should be comprehensively implemented. Indication for surgery include: cardiac abscess and failure to improve appropriate antibiotic therapy. In older patients, this equally indicates a substantial increase in risk of adverse perioperative outcome (25, 26).

Regardless of the heart valve pathology, recent improvements in conventional valve replacement have demonstrated promise in minimizing cardiac operative risk, especially in high-risk patients. In the aortic position, this includes percutaneous valve implantations as well as sutureless valve prosthesis, and rapid-deployment valve prosthesis (27–29).

The rapid-deployment valve system demonstrated significantly shorter aortic cross-clamp and cardiopulmonary bypass times, which should have a positive effect on morbidity and mortality also in older high-risk patients. Moriggia et al. (30) compared traditional aortic valve surgery with RDVS, demonstrated significant shorter cross-clamp and cardiopulmonary bypass times in patients undergoing full sternotomy. This makes such valve prosthesis even more appealing in special situations as redo-surgeries, combined procedures and high-risk patient unsuitable for transcatheter aortic valve replacement. Moreover, several work groups reported the use of rapid-deployment in special situations such as minimally invasive aortic valve replacement, anomalous coronary arteries, small aortic roots and heavily calcified aortic roots, demonstrating safety and feasibility with potential advantage over conventional aortic valve replacement (31–35).

Another emerging special patient group comprise patients developing endocarditis of the transcatheter aortic valve, as conventional heart surgery was contraindicated in the first place by the heart team. For this reason, experts still debate whether surgery is the treatment of choice in such cases (36, 37). Four reports (38–40) presented such cases, which were treated

surgically and showed no 30-day mortality. These findings are further reinforced by the outcome of the results in our series.

In this case series, we present our initial experience with the RDVS in another special situation; active aortic valve endocarditis without abscess formation. We believe conventional aortic valve replacement should be standard for most patients, except in elderly population with prohibitive surgical risk constellation. On the other hand, implementation of sutureless or rapid-deployment valves is quite common in our practice, and the presented patient group comprised highly selected patients with a EuroSCORE II as high as 80%. In patients with additional abscess formation and destruction of the aortic annulus we prefer the self-expandable sutureless aortic valve as previously published (34).

The major postoperative complication encountered was mortality in two cases, which occurred early and later during the postoperative course and was not related to the valve prosthesis. The first patient was multi-morbid, with end-stage renal failure, severe peripheral vascular disease and preoperative stroke. It is noteworthy that transesophageal examination of the aortic valve prosthesis did not reveal valve pathology. The second patients was an octogenarian, which developed multi-organ failure under optimal intensive care support. This mortality rate represents 28% of our "patient population"; however, which we deem acceptable given the very high predicted operative risk, low patient number, and the generally higher mortality in endocarditis patients, who often have chronic renal failure or chronic hemodialysis (11).

Although several studies reported frequent postoperative conduction disorders with need for permanent pacemaker after RDVS, this was not necessary in our patients (25). One patient needed a pacemaker on postoperative day 6, however due to sick sinus syndrome.

One patient needed to be re-explored by pericardial effusion, which is common seen in endocarditis. Youssef et al. found an incidence of 26%, showing a significant correlation in patients by age, left-sided vegetation and splenic infarction/abscesses (41). A similar aspect had our patient.

Although the number of patients presented in this case series is too small to draw a comprehensive conclusion, we have documented encouraging results, especially in terms of the efficacy and safety in the presented patients, who were elderly high-risk patients suffering from acute infection aortic valve endocarditis.

CONCLUSION

Rapid-deployment aortic valve prosthesis is effective and practical in surgical treatment in older high-risk patients with aortic valve endocarditis. Available reports provide initial evidence of low morbidity and acceptable mortality, particularly in the elderly high-risk patients.

STUDY LIMITATIONS

The main limiting factor in this case series the very small number of patients. Our results are in line with those of Lio et al. who also presented a small number (5) of patients (40).

Another limiting factor is the retrospective analysis of the data. To improve the results, prospective studies are encouraged, even though we would discourage from randomization in such cases, so that each patient should get the valve prosthesis that most suits his/her particular anatomical and pathological features.

DATA AVAILABILITY STATEMENT

The original contributions presented in the study are included in the article/supplementary material, further inquiries can be directed to the corresponding author/s.

ETHICS STATEMENT

The studies involving human participants were reviewed and approved by Ethikkommission an der Medizinischen Fakultät der Universität Rostock. The Ethics Committee waived the requirement of written informed consent for participation.

AUTHOR CONTRIBUTIONS

AÖ, CH, AA, BL, and PD drafted and edited the manuscript. All authors contributed to the article and approved the submitted version.

REFERENCES

1. Thuny F, Grisoli D, Collart F, Habib G, Raoult D. Management of infective endocarditis: challenges and perspectives. *Lancet.* (2012) 379:965–75. doi: 10.1016/S0140-6736(11)60755-1
2. Hoen B, Chirouze C, Cabell CH, Selton-Suty C, Duchêne F, Olaison L, et al. Emergence of endocarditis due to group D streptococci: findings derived from the merged database of the International Collaboration on Endocarditis. *Eur J Clin Microbiol Infect Dis.* (2005) 24:12–6. doi: 10.1007/s10096-004-1266-6
3. Thuny F, Di Salvo G, Belliard O, Avierinos JF, Pergola V, Rosenberg V, et al. Risk of embolism and death in infective endocarditis: prognostic value of echocardiography: a prospective multicenter study. *Circulation.* (2005) 112:69–75. doi: 10.1161/CIRCULATIONAHA.104.493155
4. Lee S, Chang B-C, Park HK. Surgical experience with infective endocarditis and aortic root abscess. *Yonsei Med J.* (2014) 55:1253–9. doi: 10.3349/ymj.2014.55.5.1253
5. Misfeld M, Girrbach F, Etz CD, Binner C, Aspern KV, Dohmen PM, et al. Surgery for infective endocarditis complicated by cerebral embolism: a consecutive series of 375 patients. *J Thorac Cardiovasc Surg.* (2014) 147:1837–44. doi: 10.1016/j.jtcvs.2013.10.076
6. Kang DH, Kim YJ, Kim SH, Sun BJ, Kim DH, Yun SC, et al. Early surgery versus conventional treatment for infective endocarditis. *N Engl J Med.* (2012) 366:2466–73. doi: 10.1056/NEJMoa1112843
7. Chu VH, Park LP, Athan E, Delahaye F, Freiberger T, Lamas C, et al. Association between surgical indications, operative risk, and clinical outcome in infective endocarditis: a prospective study from the International Collaboration on Endocarditis. *Circulation.* (2015) 131:131–40. doi: 10.1161/CIRCULATIONAHA.114.012461

8. Lalani T, Chu VH, Park LP, Cecchi E, Corey GR, Durante-Mangoni E, et al. In-hospital and 1-year mortality in patients undergoing early surgery for prosthetic valve endocarditis. *JAMA Intern Med.* (2013) 173:1495–504. doi: 10.1001/jamainternmed.2013.8203
9. Botelho-Nevers E, Thuny F, Casalta JP, Richet H, Gouriet F, Collart F, et al. Dramatic reduction in infective endocarditis-related mortality with a management-based approach. *Arch Intern Med.* (2009) 169:1290–8. doi: 10.1001/archinternmed.2009.192
10. Habib G, Lancellotti P, Antunes MJ, et al. 2015 ESC Guidelines for the management of infective endocarditis: The Task Force for the Management of Infective Endocarditis of the European Society of Cardiology (ESC). Endorsed by: European Association for Cardio-Thoracic Surgery (EACTS), the European. *Eur Heart J.* (2015) 36:3075–128. doi: 10.1093/eurheartj/ehv319
11. Iung B, Doco-Lecompte T, Chocron S, Strady C, Delahaye F, Le Moing V, et al. Cardiac surgery during the acute phase of infective endocarditis: discrepancies between European Society of Cardiology guidelines and practices. *Eur Heart J.* (2016) 37:840–8. doi: 10.1093/eurheartj/ehv650
12. Puls M, Eiffert H, Hunlich M, Schöndube F. Hasenfuß Gerd, Seiperlt R, Schillinger W. Prosthetic valve endocarditis after transcatheter aortic valve implantation: the incidence in a single-centre cohort and reflections on clinical, echocardiographic and prognostic features EuroIntervention. *J Eur Collab with Work Gr Interv Cardiol Eur Soc Cardiol.* (2013) 8:1407–18. doi: 10.4244/EIJV8I12A214
13. Amat-Santos IJ, Messika-Zeitoun D, Eltchaninoff H, Kapadia S, Lerakis S, Cheema AN, et al. Infective endocarditis after transcatheter aortic valve implantation: results from a large multicenter registry. *Circulation.* (2015) 131:1566–74. doi: 10.1161/CIRCULATIONAHA.114.014089
14. Borger MA, Dohmen P, Misfeld M, Mohr FW. Current trends in aortic valve replacement: development of the rapid deployment EDWARDS INTUITY valve system. *Expert Rev Med Devices.* (2013) 10:461–70. doi: 10.1586/17434440.2013.811828
15. Merk DR, Lehmann S, Holzhey DM, Dohmen P, Candolfi P, Misfeld M, et al. Minimal invasive aortic valve replacement surgery is associated with improved survival: a propensity-matched comparison. *Eur J Cardiothorac Surg.* (2015) 47:11–7. doi: 10.1093/ejcts/ezu068
16. Dohmen PM. Use of the perceval sutureless valve in active prosthetic aortic valve endocarditis (Commentary). *Ann Thorac Surg.* (2018) 105:1174–75. doi: 10.1016/j.athoracsur.2017.11.029
17. Santarpino G, Pfeiffer S, Jessl J, Dell'Aquila A, Vogt F, von Wardenburg C, et al. Clinical outcome and cost analysis of sutureless versus transcatheter aortic valve implantation with propensity score matching analysis. *Am J Cardiol.* (2015) 116:1737–43. doi: 10.1016/j.amjcard.2015.08.043
18. Biancari F, Barbanti M, Santarpino G, Deste W, Tamburino C, Gulino S, et al. Immediate outcome after sutureless versus transcatheter aortic valve replacement. *Heart Vessels.* (2016) 31:427–33. doi: 10.1007/s00380-014-0623-3
19. Muneretto C, Bisleri G, Moggi A, Di Bacco L, Tespili M, Repossini A, et al. Treating the patients in the "grey-zone" with aortic valve disease: a comparison among conventional surgery, sutureless valves and transcatheter aortic valve replacement. *Interact Cardiovasc Thorac Surg.* (2015) 20:90–5. doi: 10.1093/icvts/ivu340
20. Minh TH, Mazine A, Bouhout I, El-Hamamsy I, Carrier M, Bouchard D. Demers Ph. Expanding the indication for sutureless aortic valve replacement to patients with mitral disease. *J Thorac Cardiovasc Surg.* (2014) 148:1354–9. doi: 10.1016/j.jtcvs.2013.12.061
21. Parlar AI, Hanedan MO, Mataraci I, Yuruk M, Sayer U, Arslan A, et al. Immediate outcomes of aortic valve replacement with sutureless versus stentless bioprosthesis. *J Heart Valve Dis.* (2016) 25:21–7.
22. Dohmen PM. Benefits of sutureless aortic valves may not be limited to reduced crossclamp time. *J Thorac Cardiovasc Surg.* (2015) 149:395. doi: 10.1016/j.jtcvs.2014.09.032
23. Li JS, Sexton DJ, Mick N, Nettles R, Fowler VG Jr, Ryan TM, et al. Proposed modifications to the Duke criteria for the diagnosis of infective endocarditis. *Clin Infect Dis.* (2000) 30:633–8. doi: 10.1086/313753
24. Borger MA, Dohmen P, Misfeld M, Mohr FW. Minimal invasive implantation of an EDWARDS INTUITY rapid deployment aortic valve. *Multimed Man Cardiothorac Surg.* (2013) 2013:mmt011. doi: 10.1093/mmcts/mmt011
25. Zannis K, Folliguet T, Laborde F. New sutureless aortic valve prosthesis: another tool in less invasive aortic valve replacement. *Curr Opin Cardiol.* (2012) 27:125–9. doi: 10.1097/HCO.0b013e3283501a11
26. Villa E, Messina A, Cirillo M, Brunelli F, Mhagna Z, Dalla Tombo M, et al. Perceval sutureless valve in freestyle root: new surgical valve-in-valve therapy. *Ann Thorac Surg.* (2013) 96:e155–7. doi: 10.1016/j.athoracsur.2013.06.125
27. Folliguet TA, Laborde F. Sutureless Perceval aortic valve replacement in aortic homograft. *Ann Thorac Surg.* (2013) 96:1866–8. doi: 10.1016/j.athoracsur.2013.02.056
28. Santarpino G, Pfeiffer S, Fischlein T. Perceval sutureless approach in a patient with porcelain aorta unsuitable for transcatheter aortic valve implantation. *Int J Cardiol.* (2012) 155:168–70. doi: 10.1016/j.ijcard.2011.09.025
29. Shrestha M, Maeding I, Hoffler K, Koigeldiyev N, Marsch G, Siemeni T, et al. Aortic valve replacement in geriatric patients with small aortic roots: are sutureless valves the future? *Interact Cardiovasc Thorac Surg.* (2013) 17:778–82. doi: 10.1093/icvts/ivt291
30. Moriggia S, Trumello C, Buzzatti N, Iaci G, Di Giannuario G, Alfieri O. Aortic sutureless Perceval valve for small root in concomitant mitral valve replacement. *J Heart Valve Dis.* (2015) 24:187–9.
31. Giuseppe Cerillo A, Haxhiademi D, Berti S, Solinas M. Sutureless aortic valve replacement: an easy and safe approach for patients with anomalous left circumflex coronary artery. *J Heart Valve Dis.* (2016) 25:145–8.
32. Dohmen PM, Lehmkuhl L, Borger MA, Misfeld M, Mohr FW. Valve-in-valve replacement using a sutureless aortic valve. *Am J Case Rep.* (2016) 17:699–702. doi: 10.12659/AJCR.899374
33. Dohmen PM, Binner C, Mende M, Daviewala P, Etz CD, Borger MA, et al. Gender-based long-term surgical outcome in patients with active infective aortic valve endocarditis. *Med Sci Monit.* (2016) 22:2520–7. doi: 10.12659/MSM.899360
34. Weymann A, Konertz J, Laule M, Stangl K, Dohmen PM. Are sutureless aortic valves suitable for severe high-risk patients suffering from active infective aortic valve endocarditis? *Med Sci Monit.* (2017) 23:2782–7. doi: 10.12659/MSM.902785
35. Olsen NT, De Backer O, Thyregod HGH, Vejlstrup N, Bundgaard H, Sondergaard L, et al. Prosthetic valve endocarditis after transcatheter aortic valve implantation. *Circ Cardiovasc Interv.* (2015) 8:e001939. doi: 10.1161/CIRCINTERVENTIONS.114.001939
36. Garcia-Pardo H, Revilla A, Sevilla T, Lopez J, Ortiz C, San Roman JA. Staphylococcus aureus endocarditis on transcatheter aortic valves. *Rev Esp Cardiol.* (2012) 65:771–3. doi: 10.1016/j.rec.2011.11.004
37. Rafiq I, Parthasarathy H, Tremlett C, Freeman LJ, Mullin M. Infective endocarditis caused by Moraxella nonliquefaciens in a percutaneous aortic valve replacement. *Cardiovasc Revasc Med.* (2011) 12:184–6. doi: 10.1016/j.carrev.2010.03.082
38. Comoglio C, Boffini M, El Qarra S, Sansone F, D'Amico M, Marra S, et al. Aortic valve replacement and mitral valve repair as treatment of complications after percutaneous core valve implantation. *J Thorac Cardiovasc Surg.* (2009) 138:1025–7. doi: 10.1016/j.jtcvs.2008.11.005
39. Sanchez E, Corrales JA, Fantidis P, Tarhini IS, Khan I, Pineda T, et al. Thrombocytopenia after aortic valve replacement with Perceval S sutureless bioprosthesis. *J Heart Valve Dis.* (2016) 25:75–81.
40. Konertz J, Kastrup M, Treskatsch S, Dohmen PM, A. perceval valve in active infective bioprosthetic valve endocarditis: Case report. *J Heart Valve Dis.* (2016) 25:512–4.
41. Youssef GS, Mashaal MS, El Remisy DR, Sorour KA, Rizk HH. Pericardial effusion in prosthetic and native valve infective endocarditis. *Indian Heart J.* (2019) 71:80–4. doi: 10.1016/j.ihj.2018.12.002

Conflict of Interest: The authors declare that the research was conducted in the absence of any commercial or financial relationships that could be construed as a potential conflict ofinterest.

this article, or claim that may be made by its manufacturer, is not guaranteed or endorsed by the publisher.

Advantages of publishing in Frontiers

OPEN ACCESS
Articles are free to read for greatest visibility and readership

FAST PUBLICATION
Around 90 days from submission to decision

HIGH QUALITY PEER-REVIEW
Rigorous, collaborative, and constructive peer-review

TRANSPARENT PEER-REVIEW
Editors and reviewers acknowledged by name on published articles

Frontiers
Avenue du Tribunal-Fédéral 34
1005 Lausanne | Switzerland

Visit us: www.frontiersin.org
Contact us: frontiersin.org/about/contact

REPRODUCIBILITY OF RESEARCH
Support open data and methods to enhance research reproducibility

DIGITAL PUBLISHING
Articles designed for optimal readership across devices

FOLLOW US
@frontiersin

IMPACT METRICS
Advanced article metrics track visibility across digital media

EXTENSIVE PROMOTION
Marketing and promotion of impactful research

LOOP RESEARCH NETWORK
Our network increases your article's readership